NEURONAL POLARITY: ESTABLISHMENT AND MAINTENANCE

EDITED BY: Froylan Calderon de Anda and Annette Gaertner
PUBLISHED IN: Frontiers in Cellular Neuroscience

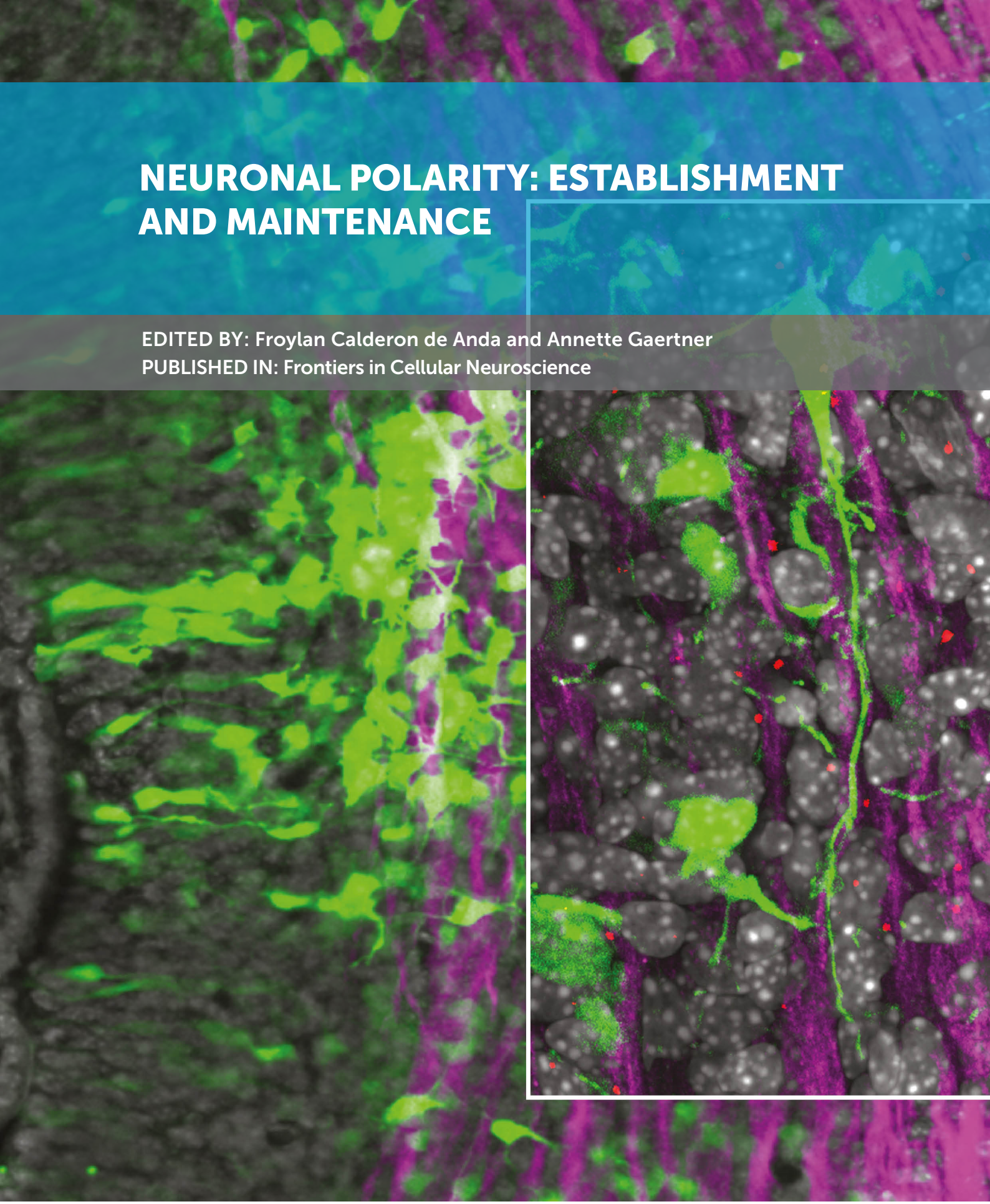

frontiers Research Topics

frontiers

ISSN 1664-8714
ISBN 978-2-88945-517-1
DOI 10.3389/978-2-88945-517-1

About Frontiers

Frontiers is more than just an open-access publisher of scholarly articles: it is a pioneering approach to the world of academia, radically improving the way scholarly research is managed. The grand vision of Frontiers is a world where all people have an equal opportunity to seek, share and generate knowledge. Frontiers provides immediate and permanent online open access to all its publications, but this alone is not enough to realize our grand goals.

Frontiers Journal Series

The Frontiers Journal Series is a multi-tier and interdisciplinary set of open-access, online journals, promising a paradigm shift from the current review, selection and dissemination processes in academic publishing. All Frontiers journals are driven by researchers for researchers; therefore, they constitute a service to the scholarly community. At the same time, the Frontiers Journal Series operates on a revolutionary invention, the tiered publishing system, initially addressing specific communities of scholars, and gradually climbing up to broader public understanding, thus serving the interests of the lay society, too.

Dedication to Quality

Each Frontiers article is a landmark of the highest quality, thanks to genuinely collaborative interactions between authors and review editors, who include some of the world's best academicians. Research must be certified by peers before entering a stream of knowledge that may eventually reach the public - and shape society; therefore, Frontiers only applies the most rigorous and unbiased reviews.
Frontiers revolutionizes research publishing by freely delivering the most outstanding research, evaluated with no bias from both the academic and social point of view. By applying the most advanced information technologies, Frontiers is catapulting scholarly publishing into a new generation.

What are Frontiers Research Topics?

Frontiers Research Topics are very popular trademarks of the Frontiers Journals Series: they are collections of at least ten articles, all centered on a particular subject. With their unique mix of varied contributions from Original Research to Review Articles, Frontiers Research Topics unify the most influential researchers, the latest key findings and historical advances in a hot research area! Find out more on how to host your own Frontiers Research Topic or contribute to one as an author by contacting the Frontiers Editorial Office: researchtopics@frontiersin.org

NEURONAL POLARITY: ESTABLISHMENT AND MAINTENANCE

Topic Editors:
Froylan Calderon de Anda, University Medical Center Hamburg-Eppendorf, Germany
†**Annette Gaertner,** KU Leuven, Belgium
†Current address: Evotec, Hamburg, Germany

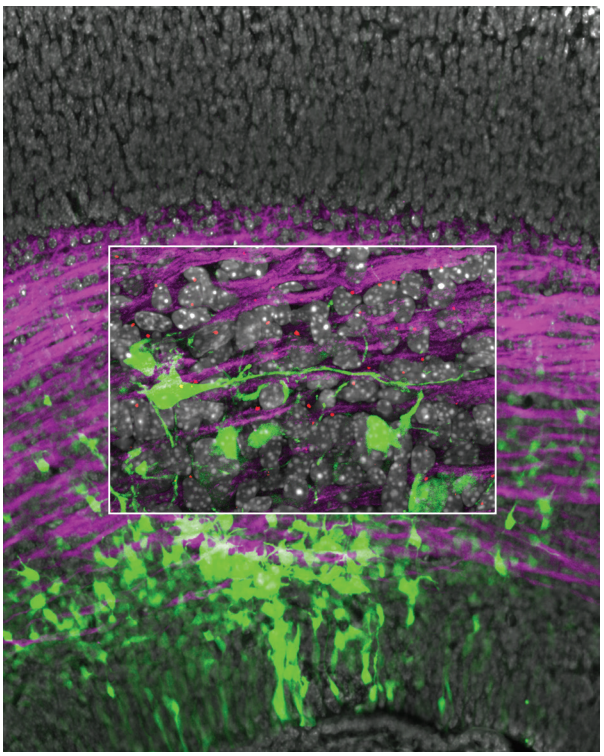

Image overlay of E15 in utero electroporated mouse neocortex transfected with green fluorescent protein and analyzed at E17 (Nuclei: white, axons: magenta). Center image: Multipolar neuron (green) from the intermediate zone with the centrosome (yellow) oriented towards the midline at the time of axon initiation (nuclei: white, axons: magenta, centrosomes: red).
Image: Froylan Calderon de Anda.

The term polarity in a biological context is used to describe an asymmetry in morphology and distribution of molecules. In neurons, their complex shape with typically one axon and several dendrites reflects this asymmetry. Although neurons assume many different shapes and sizes they always maintain these two domains, which are essential for neuronal function. In the most simple view, neurons use their axon to transmit signals over long distances due to its capacity to extend to enormous lengths. Dendrites, on the other hand, are shorter and receive and integrate signals from different locations. The selection of the site where the axon and dendrites initially emerge during embryonic development is a tightly regulated event, eventually important for the correct formation of neuronal circuits, and disturbances of these processes can have pathological consequences due to circuit malformation. An important question is which mechanisms neurons utilize to specify the sites where

axonal and dendrite outgrowth occurs and how their identities are maintained during and after development. The formation of these functionally diverse domains is the result of polarized differences of membrane and protein delivery, mitochondria transport, actin dynamics and microtubule stability. However how and in which temporal order all those events which coordinate the selection and maintenance of axons and dendrites is still under investigation. This selection of articles shall highlight new findings, which help to unravel all molecular and cellular events important for neuronal polarity establishment and maintenance.

Citation: Calderon de Anda, F., Gaertner, A., eds. (2018). Neuronal Polarity: Establishment and Maintenance. Lausanne: Frontiers Media. doi: 10.3389/978-2-88945-517-1

Table of Contents

frontiers in Cellular Neuroscience

EDITORIAL
published: 23 May 2018
doi: 10.3389/fncel.2018.00137

Editorial: Neuronal Polarity: Establishment and Maintenance

Froylan Calderon de Anda[1]*† *and Annette Gaertner*[2]*†

[1] Center for Molecular Neurobiology Hamburg, Research Group Neuronal Development, University Medical Center Hamburg-Eppendorf, Hamburg, Germany, [2] Department of Development and Regeneration, Faculty of Medicine, KU Leuven, Leuven, Belgium

Keywords: neuronal polarization, neuronal migration disorders, axon, dendrites, neuronal differentiation

Editorial on the Research Topic

Neuronal Polarity: Establishment and Maintenance

The term neuronal polarization denotes cellular compartmentalization, which leads to an asymmetric cellular morphology. This compartmentalization is depicted by the morphological and functional separation of axons and dendrites. The axon transmits signals over long distances while dendrites are shorter and receive information. One fundamental question in neurobiology is how neurons form one axon and several dendrites. This issue has been tackled for several years using neurons growing in culture. However, neurons develop in a complex and changing environment that is not easy to reproduce *in vitro*; thus, in the recent years, different animal models and organotypic cultures were used to investigate neuronal differentiation *in situ*. This research topic on the establishment and maintenance of neuronal polarity brings together important scientific contributions that help to better understand several aspects of neuronal development in vertebrates.

NEURONAL POLARIZATION *IN SITU*: FROM GENESIS TO MIGRATION

Studying neuronal development *in situ* is instrumental to understand how external cues help to sculpt neuronal morphology during polarization. This issue is analyzed in reviews and original research articles on this topic. With a global perspective, Hansen et al. provided an extensive overview of the extrinsic and intrinsic molecular mechanisms currently associated with neuronal differentiation in the developing cortex. In the developing cortex, the differentiation and development of neurons start with neuronal progenitors. Arai and Taverna summarized the current knowledge regarding cellular polarity in neuronal progenitors. The intracellular polarized architecture of neuronal progenitors dictates their behavior and thus the type of cellular divisions they undergo. This ultimately might determine the number and type of neurons produced, and the organization of the inherited cytoplasm to their progeny. Ong and Solecki reviewed the latest results, which support the role of seven in absentia homolog (Siah) ubiquitin ligases controlling the onset of neuronal polarization in the developing cerebellum. Siah is involved in post-translational regulation of cellular polarity and regulates neuron migration through cellular adhesion and the cytoskeleton. Moreover, the authors speculate on additional targets and interactors found in non-neuronal cells.

OPEN ACCESS

Edited and reviewed by:
Laura Cancedda, Fondazione Istituto Italiano di Technologia, Italy

***Correspondence:**
Froylan Calderon de Anda
froylan.calderon@zmnh.uni-hamburg.de
Annette Gaertner
annette.gaertner@gmail.com

†Present Address:
Annette Gaertner, Evotec, Hamburg, Germany

Received: *04 April 2018*
Accepted: *02 May 2018*
Published: *23 May 2018*

Citation:
Calderon de Anda F and Gaertner A (2018) Editorial: Neuronal Polarity: Establishment and Maintenance. Front. Cell. Neurosci. 12:137. doi: 10.3389/fncel.2018.00137

NEURONAL MIGRATION AND AXON FORMATION: THE TRANSITION TOWARD THE FINAL POLARIZATION

In the developing cortex, newly formed neurons migrate to their final destination to eventually find their location where they will form connections. Importantly, neuronal polarization occurs while neurons migrate (Noctor et al., 2004; de Anda et al., 2010; Namba et al., 2014; Sakakibara et al., 2014). Kon et al. analyzed different cellular, morphological changes and underlying molecular mechanisms during initial steps of neuronal polarization. The review by Frotscher et al. summarized the role of Reelin signaling during neuronal migration in the developing cortex. Reelin is important for the orientation and maintenance of the leading process of migrating neurons by phosphorylating and inactivation of Cofilin, an actin-binding protein.

Gorelik et al. exemplified how molecules such as *Serping1* (C1 inhibitor, a member of the complement cascade), known for very distinct biological functions, are "hijacked" for regulating cortical development. Knockdown or knockout of *Serping1* delayed migration of neurons in mice suggesting it's importance in cortical development at several stages of neuronal differentiation. Similarly, Laguesse et al. identified a molecular pathway, which regulates the acetylation of Connexin-43 (Cx43), that might modulate neuronal motility in the developing cortex. Elp3 acetylates Cx43 while histones deacetylase 6 (HDAC6) controls levels of acetylated Cx43.

Finally, during migration neurons initiate axon formation—a morphological landmark of neuronal polarization. Lee et al. investigated the role of Calsyntenin-1 (Clstn-1), which is a kinesin adaptor, in organizing microtubule polarity during axon development. Using a zebrafish model and high-speed *in vivo* imaging, Lee et al. imaged sensory neurons during axon formation and branching. Their results suggest an important role for Clstn-1 in the regulation of microtubule polarity in actively branching axons.

DENDRITE FORMATION: THE FINAL STEP BEFORE CONNECTIVITY

Once neurons arrive at their final destination they form dendrites, spines, and establish connections. In addition, the compartmentalization of axon and dendrites is defined at the subcellular level. At this stage, the selective sorting into axons and dendrites becomes crucial for differentiating their distinct function (Zollinger et al., 2015). A sorting barrier, the axon initial segment (AIS), assembled at this developmental time point (Zollinger et al., 2015), and the selective recruitment of cargo by different motor proteins supports the polarized transport (Rasband, 2010). Janssen et al. illustrated the involvement of myosin-V, a dendritic transporter, in the clustering of kinesin-driven cargoes at the AIS, precisely in actin-rich hotspots. The cargo retrieval from these hotspots is taken over by a yet unidentified protein. To understand how neurite formation takes place, Wang et al. investigated the role of microRNA-189 (miR-182) in neurite outgrowth. Interestingly, they found that miR-182 plays a role in axon and dendrite extension through a molecular pathway, which involves AKT phosphorylation and inhibition of BCAT2. With a cellular and mathematical approach, Tomba et al. analyzed the contribution of actin-rich structures (actin waves), which travel along the neurite shaft from the cell body to the neurite tip (Ruthel and Banker, 1999; Winans et al., 2016; Mortal et al., 2017), in supporting neurite outgrowth. Their mathematical modeling leads to a quantitative characterization of the generation of actin waves. In dendrites, actin was mainly described to be important for spine morphology and dynamics. Konietzny et al. provided an interesting overview of recent findings showing the role of dendritic actin in dendrite morphology and protein traffic and the regulation of dendritic actin dynamics. Finally, once neurons initiate building networks, the specialization of subcellular domains allow for proper connections. The insertion of ion channels in proper places ensures adequate propagation of electrical impulses—a crucial step in the development of a fully differentiated neuron. Duménieu et al. reviewed recent data on the organization and mechanisms behind the segregation of voltage-gated Potassium and Sodium channels in dendrites.

Our knowledge regarding neuronal polarization and maintenance *in situ* is limited. However, in recent years we have advanced our understanding of this matter. This research topic reunites studies to emphasize the importance of studying neuronal differentiation *in situ*. Overall, it helps to better understand the cellular and molecular mechanism underlying neuronal polarization in a complex environment, different from the culture conditions. It is our hope that this knowledge will pave the way for future contributions in the field.

AUTHOR CONTRIBUTIONS

FCdA and AG wrote the Editorial and coordinated the Topic.

FUNDING

FCdA is supported by Deutsche Forschungsgemeinschaft (DFG) Grant (FOR 2419; CA1495/1-1; and CA 1495/4-1), ERA-NET Neuron Grant (Bundesministerium für Bildung und Forschung, BMBF, 01EW1410 ZMNH AN B1), Landesforschungsförderung Hamburg (Z-AN LF), and University Medical Center Hamburg-Eppendorf (UKE).

ACKNOWLEDGMENTS

We thanks Durga Praveen Meka for critical reading of the manuscript.

REFERENCES

de Anda, F. C., Meletis, K., Ge, X., Rei, D., and Tsai, L. H. (2010).Centrosome motility is essential for initial axon formation in the neocortex. *J. Neurosci.* 30, 10391–10406. doi: 10.1523/JNEUROSCI.0381-10.2010

Mortal, S., Iseppon, F., Perissinotto, A., D'Este, E., Cojoc, D., Napolitano, L. M. R. et al. (2017). Actin waves do not boost neurite outgrowth in the early stages of neuron maturation. *Front. Cell Neurosci.* 11:402. doi: 10.3389/fncel.2017.00402

Namba, T., Kibe, Y., Funahashi, Y., Nakamuta, S., Takano, T., Ueno T., et al. (2014). Pioneering axons regulate neuronal polarization in the developing cerebral cortex. *Neuron* 81, 814–829. doi: 10.1016/j.neuron.2013.12.015

Noctor, S. C., Martínez-Cerdeño, V., Ivic, L., and Kriegstein, A. R. (2004).Cortical neurons arise in symmetric and asymmetric division zones and migrate through specific phases. *Nat. Neurosci.* 7, 136–144. doi: 10.1038/nn1172

Rasband, M. N. (2010). The axon initial segment and the maintenance of neuronal polarity. *Nat. Rev. Neurosci.* 11, 552–562. doi: 10.1038/nrn2852

Ruthel, G., and Banker, G. (1999). Role of moving growth cone-like "wave" structures in the outgrowth of cultured hippocampal axons and dendrites. *J. Neurobiol.* 39, 97–106. doi: 10.1002/(SICI)1097-4695(199904)39:1<97::AID-NEU8>3.0.CO;2-Z

Sakakibara, A., Sato, T., Ando, R., Noguchi, N., Masaoka, M., Miyata, T. (2014). Dynamics of centrosome translocation and microtubule organization in neocortical neurons during distinct modes of polarization. *Cereb. Cortex* 24, 1301–1310. doi: 10.1093/cercor/bhs411

Winans, A. M., Collins, S. R., and Meyer, T. (2016). Waves of actin and microtubule polymerization drive microtubule-based transport and neurite growth before single axon formation. *Elife* 5:e12387. doi: 10.7554/elife

Zollinger, D. R., Baalman, K. L., and Rasband, M. N. (2015). The ins and outs of polarized axonal domains. *Annu. Rev. Cell Dev. Biol.* 31, 647–667. doi: 10.1146/annurev-cellbio-100913-013107

Conflict of Interest Statement: The authors declare that the research was conducted in the absence of any commercial or financial relationships that could be construed as a potential conflict of interest.

frontiers in Cellular Neuroscience

REVIEW
published: 28 June 2017
doi: 10.3389/fncel.2017.00176

Cell Polarity in Cerebral Cortex Development—Cellular Architecture Shaped by Biochemical Networks

Andi H. Hansen†, Christian Duellberg†, Christine Mieck†, Martin Loose and Simon Hippenmeyer**

Institute of Science and Technology Austria, Klosterneuburg, Austria

The human cerebral cortex is the seat of our cognitive abilities and composed of an extraordinary number of neurons, organized in six distinct layers. The establishment of specific morphological and physiological features in individual neurons needs to be regulated with high precision. Impairments in the sequential developmental programs instructing corticogenesis lead to alterations in the cortical cytoarchitecture which is thought to represent the major underlying cause for several neurological disorders including neurodevelopmental and psychiatric diseases. In this review article we discuss the role of cell polarity at sequential stages during cortex development. We first provide an overview of morphological cell polarity features in cortical neural stem cells and newly-born postmitotic neurons. We then synthesize a conceptual molecular and biochemical framework how cell polarity is established at the cellular level through a break in symmetry in nascent cortical projection neurons. Lastly we provide a perspective how the molecular mechanisms applying to single cells could be probed and integrated in an *in vivo* and tissue-wide context.

Keywords: cerebral cortex, polarity, neurogenesis, neuronal migration, axon, dendrite, break in symmetry, GTPases

OPEN ACCESS

Edited by:
Annette Gaertner, Evotec (Germany), Germany

Reviewed by:
Anthony Paul Barnes, Oregon Health & Science University, United States
Yves Jossin, Université catholique de Louvain, Belgium

****Correspondence:***
Martin Loose
martin.loose@ist.ac.at
Simon Hippenmeyer
simon.hippenmeyer@ist.ac.at

†These authors have contributed equally to this work.

Received: *30 March 2017*
Accepted: *12 June 2017*
Published: *28 June 2017*

Citation:
Hansen AH, Duellberg C, Mieck C, Loose M and Hippenmeyer S (2017) Cell Polarity in Cerebral Cortex Development—Cellular Architecture Shaped by Biochemical Networks. Front. Cell. Neurosci. 11:176. doi: 10.3389/fncel.2017.00176

ESTABLISHMENT OF CELLULAR POLARITY IN SEQUENTIAL STAGES OF CORTICAL DEVELOPMENT

Neural Stem Cell Polarity

The mammalian cerebral cortex emerges from the neuroectoderm. At the end of neurulation and neural tube closure, occurring from embryonic day (E) 7 to E9 in mice, the early neuroepithelium is composed of neuroepithelial stem cells (NESCs) from which all subsequent neural progenitor cells and their neuron lineages derive (**Figure 1**). NESCs are highly polarized and their nuclei exhibit interkinetic nuclear migration whereby they translocate from the ventricular (apical) side to the more basal side in concert with the cell cycle (Lee and Norden, 2013). NESC polarity correlates with the asymmetric distribution of cell fate determinants which are thought to control the fine balance between symmetric and asymmetric progenitor divisions (Shitamukai and Matsuzaki, 2012). Such balance is critical for the generation of the correct number of radial glia progenitor cells (RGPCs), which are not only lineally related to NESCs but exhibit even more polarized cellular morphology with an extended basal process (Taverna et al., 2014). In the initial stages of neurogenesis, NESCs arrange the mitotic spindle in parallel (division plane perpendicular) to the ventricular zone (VZ) and divide mostly symmetrically, thereby expanding the progenitor pool (Postiglione and Hippenmeyer, 2014; Taverna et al., 2014). The disruption of the mitotic spindle, anchored

to the lateral walls of NESCs, results in the precocious generation of neurons and apoptosis (Yingling et al., 2008). Thus the correct cellular polarization of the earliest neural progenitor cells in the developing cerebral cortex is absolutely essential for the correct lineage progression and eventual neuron production. While it has been well established that components of the planar cell polarity signaling pathway play critical roles in establishing and maintaining progenitor polarity (Knoblich, 2008; Homem et al., 2015), the signaling cues and molecular mechanisms that instruct polarization and the break of symmetry in NESCs are not well understood *in vivo*.

Radial glia progenitors (RGPs) have been demonstrated to be the major neural progenitors in the developing cortex responsible for producing the vast majority of cortical excitatory neurons (Malatesta et al., 2000; Noctor et al., 2001; Anthony et al., 2004; Lui et al., 2011; Franco and Muller, 2013; Borrell and Götz, 2014; Taverna et al., 2014). The RGP division patterns and dynamics determine the number of neurons in the mature cortex. RGP cell division during mitosis occurs at the surface of the embryonic VZ and can be either symmetric or asymmetric, which is defined by the fate of the two daughter cells (Lui et al., 2011; Gao et al., 2014; Taverna et al., 2014; Homem et al., 2015). The extrinsic and intracellular signaling cues that instruct the mode of cell division are not well understood. The directional segregation of cell fate determinants such as Notch, components of the planar cell polarity signaling module, or entire centrosomes (i.e., duplicated centrioles) in dividing neural stem cells indicates however that polarized secretion and/or trafficking is a key mechanism (Wang et al., 2009; Lui et al., 2011; Paridaen et al., 2013; Taverna et al., 2014). Symmetric RGP divisions generate two RGPs to amplify the progenitor pool or two postmitotic neurons. In contrast, asymmetric divisions produce a renewing RGP and a neuron or an intermediate progenitor (IP). IPs can further divide symmetrically in the subventricular zone (SVZ) to produce neurons (Noctor et al., 2004; Kowalczyk et al., 2009). Interestingly, IPs adopt a multipolar morphology (Noctor et al., 2004; Kowalczyk et al., 2009) and it is currently not known whether the transition from bipolar (RGP) to multipolar (IP) state could correlate with, or even be instructive, for the neurogenic potential in dividing IPs. RGPs may also produce other types of transient amplifying progenitors, such as short neural precursors (SNPs; Stancik et al., 2010) and outer SVZ radial glial progenitors (oRGs aka basal RGs or bRGs; Fietz et al., 2010; Hansen et al., 2010; Shitamukai et al., 2011; Wang X. et al., 2011; Kelava et al., 2012; Betizeau et al., 2013; Florio et al., 2015; Johnson et al., 2015; Pollen et al., 2015). Although oRGs like RGPs are bipolar, they have been shown to adopt different morphological states and thus likely exhibit distinct cellular polarity since they lack apical attachment at the ventricle. Distinct oRG morphologies may reflect distinct competence states with respect to the number and types of neurons which are generated (Betizeau et al., 2013). Although the above studies provide a framework of stem cell polarity and lineage progression at the cellular level (**Figure 1**), the underlying molecular and biochemical mechanisms of progenitor cell polarization are still poorly defined.

Polarity in Nascent Postmitotic Neurons—Implications for Neuronal Migration

The basal processes of RGPs serve as a scaffold for nascent cortical neurons, which migrate from the VZ/SVZ through the intermediate zone (IZ), in order to reach the cortical plate (CP; Rakic, 1972; Evsyukova et al., 2013). Cortical layering occurs in an "inside-out" fashion whereby earlier born neurons populate deep layers and later born neurons occupy progressively upper layers (Angevine and Sidman, 1961; Rakic, 1974). Newly-born cortical neurons migrate, in a step-wise fashion coupled with changes in cell polarity, from the VZ/SVZ through IZ zone in order to reach the CP where they position themselves at their final location (**Figure 1**; Rakic, 1972; Nadarajah and Parnavelas, 2002; Noctor et al., 2004; Tsai et al., 2005; Marín et al., 2010; Hippenmeyer, 2014). Timelapse and videomicroscopy approaches (Tabata and Nakajima, 2008; Noctor, 2011; Tsai and Vallee, 2011) with the goal to trace the migration paths of individual cortical projection neurons have impressively revealed that: (1) radially migrating neurons proceed though several distinct migratory phases; (2) change their morphology and polarize along the way; and (3) adjust their mode of migration while transiting through the different zones along the radial migratory path (Nadarajah et al., 2001; Tabata and Nakajima, 2003; Noctor et al., 2004; Tsai et al., 2005; Sekine et al., 2011; **Figure 1**). From these observations through live-imaging, it is evident that nascent migrating neurons undergo a series of morphological changes including the depolarization and repolarization within the SVZ/IZ. The molecular mechanisms controlling these morphological transitions are poorly defined but if they are perturbed or delayed, the development of the cortical cytoarchitecture may be compromised. This is in particular relevant in humans that suffer from e.g., Lissencephaly (a severe cortical malformation disorder) where the loss of *LIS1* activity results in a defect to repolarize migrating neurons which in turn accumulate in ectopic positions instead of properly migrating into the developing CP (Tsai et al., 2005; Wynshaw-Boris et al., 2010). LIS1 is only one of many molecules which are involved in more than one cellular polarization process. As such LIS1 plays a role in neural progenitor polarization and in the establishment of polarity in postmitotic neurons. It will thus be important to precisely dissect the sequential and/or distinct functions of proteins orchestrating cellular polarity during development.

Establishment of Axon and Dendrite Compartments in Cortical Projection Neurons

After nascent cortical projection neurons, exhibiting bipolar (BP) morphology, have delaminated from the neuroepithelium at the ventricular surface they move radially away to the SVZ. Within

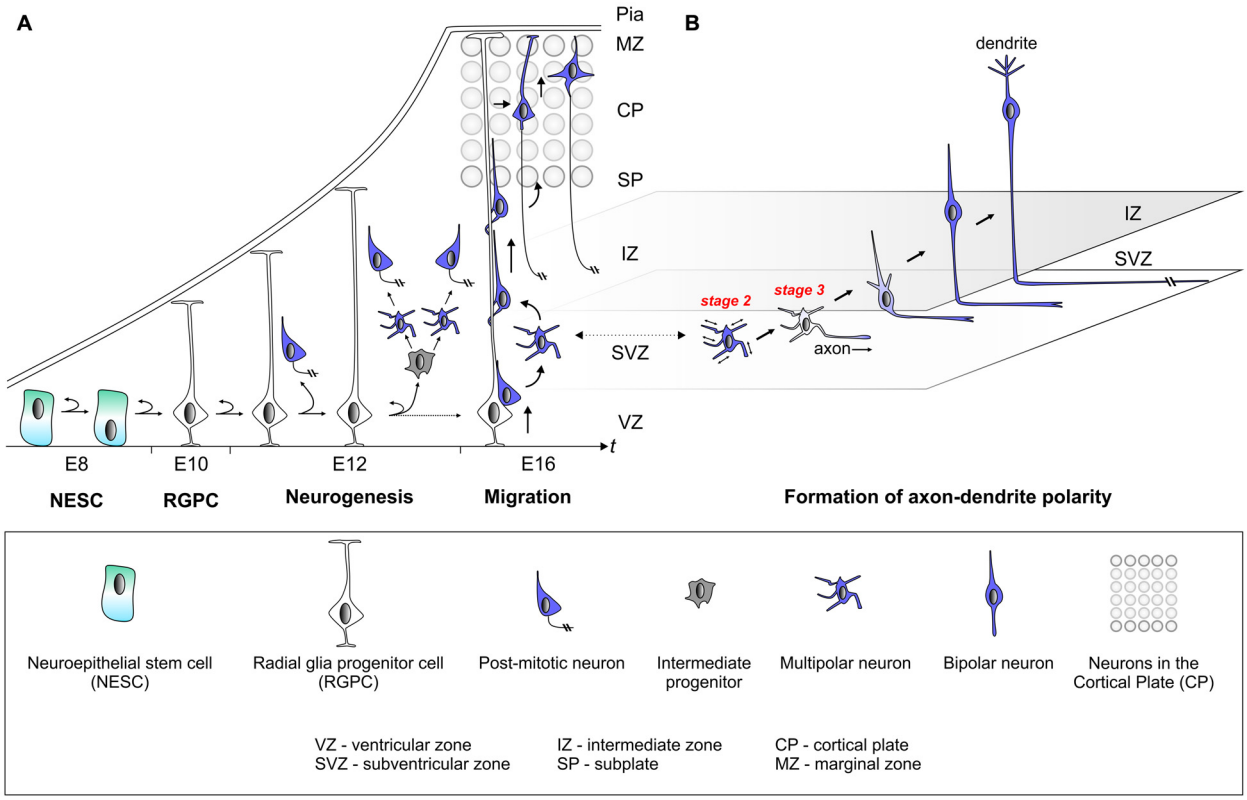

FIGURE 1 | Establishment of cell polarity in cerebral cortex development. **(A)** The early neuroepithelium is composed of highly polarized neuroepithelial stem cells (NESCs, apical-basal polarity is indicated). NESCs give rise to radial glia progenitor stem cells (RGPCs) which exhibit even more polarized cellular morphology with an extended basal process. During neurogenesis symmetric radial glia progenitor (RGP) divisions may generate two RGPs but asymmetric divisions produce a renewing RGP and a neuron or an intermediate progenitor (IP). IPs further divide symmetrically in the subventricular zone (SVZ) to produce neurons. The basal processes of RGPs serve as a scaffold for nascent post-mitotic neurons, which migrate in a step-wise fashion coupled with changes in cell polarity, from the ventricular zone (VZ)/SVZ through the intermediate zone (IZ) in order to reach the cortical plate (CP). After nascent cortical projection neurons have delaminated from the neuroepithelium at the ventricular surface they move radially away to the SVZ exhibiting bipolar (BP) morphology. Within the SVZ/IZ, neurons "sojourn" for about 24 h or longer and most adopt a multipolar (MP) morphology, extending and retracting processes in all directions. At one point fundamental cellular polarization events take place that predetermine the future axon of the neuron before the neuron again adopts a bipolar morphology and starts locomoting along the radial glial fiber through the IZ. Once reaching the subplate (SP), neurons enter the CP and migrate towards the marginal zone (MZ) where they detach from the radial glial fiber. Finally, neurons settle in their appropriate position in the CP and the leading process will eventually become the dendrite. **(B)** This panel depicts the migrating neuron from panel **(A)** in higher detail with the leading and trailing processes which eventually become the dendrite and axon, respectively.

the SVZ neurons "sojourn" for about 24 h or longer and most adopt a multipolar (MP) morphology, extending and retracting processes in all directions (Tabata and Nakajima, 2003; Noctor et al., 2004). While this stage is critical for the progression of the sequential migration program it is also essential for establishing the cellular compartments that later transform into axonal and dendritic processes. During this phase, multipolar (MP) neurons tend to migrate tangentially in an apparent random fashion (Noctor et al., 2004; Jossin and Cooper, 2011). At one point however, fundamental cellular polarization events take place that predetermine the future axon of the neuron (Barnes and Polleux, 2009) before the neuron again adopts a bipolar morphology (**Figure 1**). In the remainder of this review we synthesize a framework of neuronal polarization based upon *in vitro* biochemical, cell culture and genetic loss of function experiments *in vivo*. We reflect upon the relative contribution of extrinsic cues and cell-intrinsic molecular and biochemical signaling modules that dictate the break in symmetry and control polarization of cortical projection neurons.

EXTRACELLULAR CUES CONTROLLING PROJECTION NEURON POLARITY IN CORTEX DEVELOPMENT

Developing cortical neurons can break symmetry in the absence of external cues suggesting that the role of the extracellular signals in the *in vivo* context is solely to activate/trigger an intrinsic symmetry-breaking pathway. The intrinsic signaling pathways on the other hand are dependent on the internal biochemical state of the cell (**Figures 2**, **3** and see below for detailed discussion). Albeit cell intrinsic mechanisms have received much more attention than extracellular regulatory cues it is clear that in the developing cortex, cell-to-cell interactions,

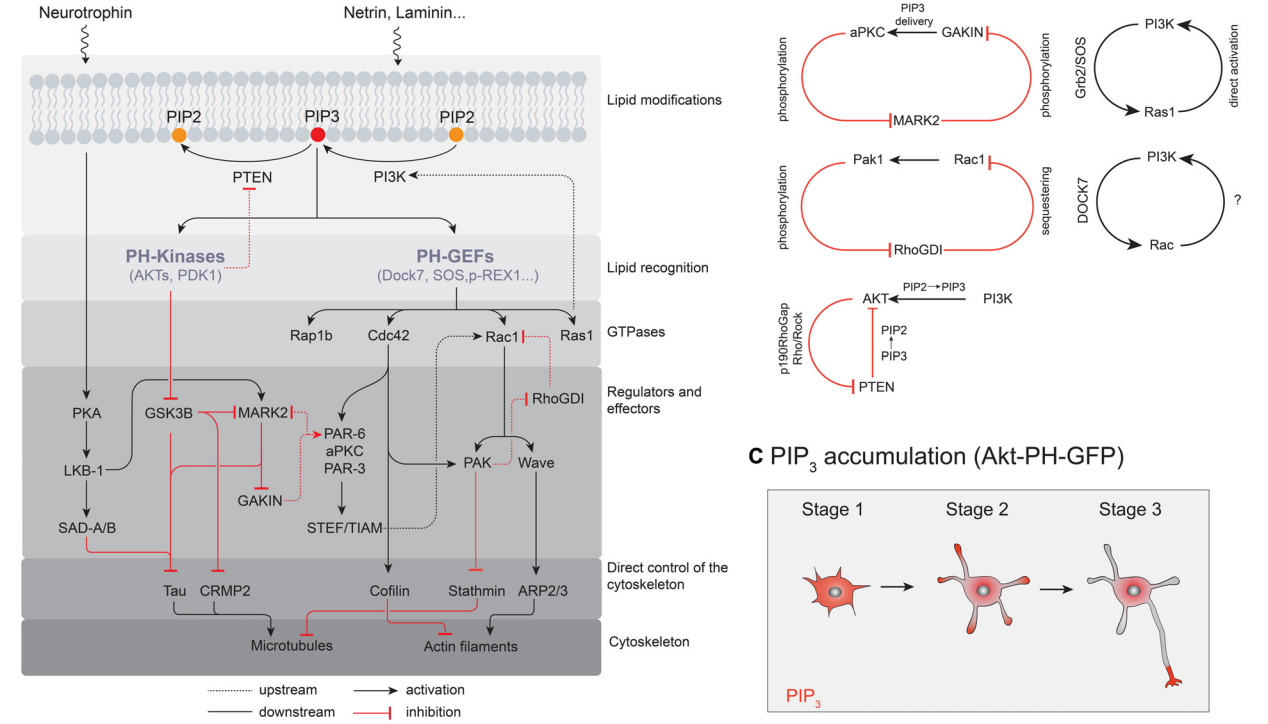

FIGURE 2 | Molecular signaling pathways controlling neuronal polarization. **(A)** A simplified illustration of the biochemical network of axon determination. Only interactions localized to the nascent axon are shown. **(B)** Positive feedback loops in the process of axon determination. **(C)** Probing PIP_3 localization and accumulation in polarizing neurons with Akt-pleckstrin-homology (PH)-GFP as a probe for PIP_3.

the local microenvironment and long-range signaling constitute essential factors for the establishment of projection neuron polarity *in vivo*.

Cell-Cell Interactions

Nascent projection neurons are embedded in a heterogeneous environment and cell-cell interactions are likely to play an important role in neuronal polarization (Jossin, 2011; Gartner et al., 2015; Namba et al., 2015). It has been suggested that the radial glial scaffold, on which neurons perform locomotion in the IZ, could be involved in the MP-to-BP transition. Experiments inhibiting the cell-adhesion molecule N-cadherin have shown that newly-born neurons expressing a dominant-negative form of N-cadherin establish abnormal leading processes (Gartner et al., 2012, 2015). These experiments have also indicated that radial glial-neuron interactions mediated by N-cadherin play an essential role in the initial radial alignment of nascent neurons and thus possibly (albeit in an indirect manner) in the subsequent MP-to-BP transition. Interestingly, polarized N-cadherin localization has been shown to occur in a single neurite during MP-to-BP transition and thus likely represents one of the earliest consequences of the symmetry-break (Gartner et al., 2012). In such context, it has been proposed that the interaction of multipolar cells and RGPs mediated by N-cadherin leads to the establishment of axon-dendrite polarity through polarized distribution of active RhoA in the neurite contacting the RGC and active Rac1 on the opposite side where the axon is formed (Xu et al., 2015). Physical interactions between pioneering axons from earlier generated neurons and the dynamic neurites from newly born neurons have been shown to contribute to polarization in MP neurons (Namba et al., 2014, 2015). These interactions involve the cell adhesion molecule transient axonal glycoprotein 1 (TAG-1). The highest expression of TAG-1 has been observed in the lower IZ (Namba et al., 2014), exactly where nascent neurons switch from MP-to-BP morphology. Current models propose that TAG-1 is expressed in both MP cells and pioneering axons and thus could mediate homophilic cell-cell contacts. Indeed, shRNA-mediated knockdown of TAG-1 results in the disruption of the MP-to-BP transition and axon specification. The underlying mechanism of TAG-1 action in polarization may involve: (1) an increase in physical tension in the immature neurite leading to axon induction and formation; and (2) contact-mediated activation of signaling molecules that instruct axon specification (Namba et al., 2015). Interestingly, N-cadherin is mainly expressed in the upper IZ (Xu et al., 2015) but TAG-1 in the lower IZ (Namba et al., 2014). Thus N-cadherin and TAG-1 could act as two separate polarity inducing cues which might work complementary in axon-dendrite formation as proposed by the Kaibuchi laboratory (Xu et al., 2015). Whether the induction of cellular polarization within these

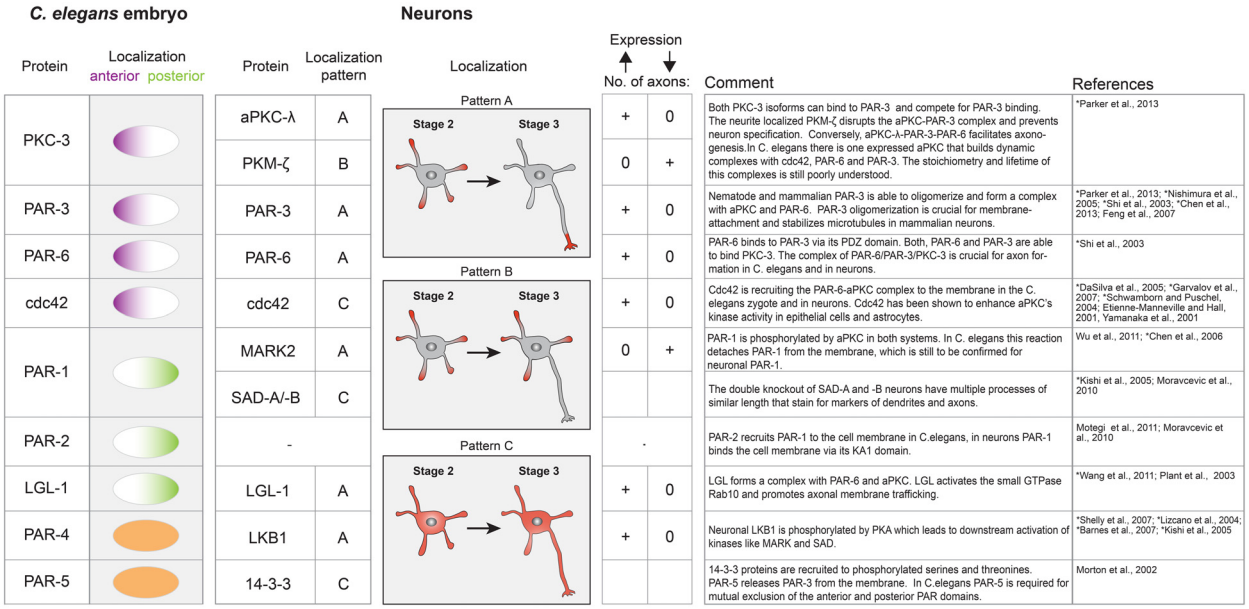

FIGURE 3 | Table of key polarity proteins in *C. elegans* and their neuronal homologs. The localization of the nematode proteins is illustrated according to their anterior or posterior domain affiliation. In neurons the respective localization is classified according to the indicated patterns (A–C). A supernumerary axon phenotype is indicated by a plus sign, while 0 represents the absence of an axon upon overexpression or downregulation of the respective polarity protein. References describing neuronal protein systems are marked with an asterisk.

two distinct zones correlates with a certain neuron type (e.g., derived from either RGCs or IPs) remains to be determined.

Secreted Factors

Reelin

Newly born cortical projection neurons migrate from the VZ to the CP in order to reach their final target area (Marín et al., 2010; Hippenmeyer, 2014). A key regulatory module controlling neuronal migration includes the Reelin pathway (Honda et al., 2011). The function of Reelin in neuronal migration has been studied extensively for decades and several hypotheses concerning the mechanism of Reelin action have been put forward (Honda et al., 2011). However, it has also become clear recently that Reelin fulfills an important role in the polarization of nascent projection neurons (Jossin and Cooper, 2011; Jossin, 2011). Reelin is mainly expressed by Cajal-Retzius cells in the marginal one (MZ) in the developing cortex (Ogawa et al., 1995). The Reelin protein primarily binds to its two cognate receptors, very low density lipoprotein receptor (VLDLR) and apolipoprotein E receptor 2 (ApoER2/LRP8; D'Arcangelo et al., 1999), which are mainly expressed in RGPs and nascent migrating neurons (Perez-Garcia et al., 2004). Binding of Reelin to its receptors triggers the activation of a Src family kinase (SFK) called Fyn which in turn phosphorylates the adaptor protein disabled-1 (DAB1; Howell et al., 1997, 1999). Phosphorylated DAB1 functions as a hub for several downstream intracellular signals and has been shown to activate the effectors CRK, C3G and PI3K which in turn regulate the activity of Limk1, Akt and Rap1 to eventually modulate the dynamic cytoskeleton (Honda et al., 2011; Sekine et al., 2014). Thus the Reelin-DAB1 pathway translates extracellular cues into cytoskeletal changes in migrating neurons (Frotscher, 2010; Forster et al., 2010). How Reelin might regulate dynamic polarization events in nascent cortical projection neurons is less well understood. Interestingly however, it has been shown that while VLDLR is mainly localized on the leading processes of migrating neurons in the MZ, ApoER2 is primarily localized to neuronal processes and the cell membranes of multipolar neurons in the SVZ and lower IZ. In addition to strong expression of Reelin in the MZ, it was also demonstrated that Reelin is also expressed in the IZ at early developmental stages (Hirota et al., 2015). *Ex vivo* experiments where exogenous Reelin was added to cultured brain slices have shown an effect on the morphology and dynamic behavior of nascent neurons in the IZ (Britto et al., 2014). Thus, based on the expression pattern of Reelin and its cognate receptors it is conceivable that Reelin could play a prominent role during the polarization process of nascent cortical projection neurons. Indeed, Jossin and Cooper propose a three step model (Jossin and Cooper, 2011) how Reelin controls the radial orientation of multipolar neurons in SVZ/IZ. First, multipolar neurons migrate tangentially in a stochastic manner in the SVZ/IZ until they encounter Reelin which leads to the activation of the small GTPase RAP1, likely via pDAB1-CRK/CRKL-C3G signaling (Ballif et al., 2004; Voss et al., 2008). Next, active RAP1 triggers an increase of the surface level of N-Cadherin in multipolar neurons. These increased cell surface levels of N-Cadherin could then allow the multipolar neurons to sample local

microenvironmental cues which then could initiate the break in symmetry and induce polarization. The cortical projection neurons then progressively exit the multipolar stage and adopt a bipolar morphology (Jossin, 2011; Jossin and Cooper, 2011). Altogether, the above data and model indicates that Reelin acts as a critical cue for the directional movement of nascent migrating cortical projection neurons and could serve as a critical extracellular cue for modulating polarization of nascent migrating cortical projection neurons. It will be intriguing to decipher the precise intracellular and biochemical signaling pathways controlling RAP1-dependent N-Cadherin trafficking and how N-Cadherin-dependent signaling triggers the break in symmetry.

Neurotrophins

Brain derived neurotrophic factor (BDNF) and neurotrophin-3 (NT-3) are highly expressed in the developing brain and have been shown to stimulate axon specification and elongation (Morfini et al., 1994; Nakamuta et al., 2011). Both, BDNF and NT-3 as extracellular regulators of neuronal polarity are of special interest since they act in an autocrine and/or paracrine manner in cell-culture (Nakamuta et al., 2011). This feature indicates that neurons are able to produce extracellular stimuli (in form of secreted neurotrophins) that activate the intrinsic machinery for axon-dendrite specification in a cell-autonomous and non-cell-autonomous manner. BDNF and NT-3 bind to tropomyosin related kinases receptors (TRK), TRK-B and TRK-C respectively (Chao, 2003). Upon TRK receptor binding, the small GTPase Ras and PI3K are activated. This leads to the production of phosphatidylinositol (3,4,5)-trisphosphate (PIP_3) and the activation of its downstream signaling pathways (Reichardt, 2006). Neurotrophin signaling through TRK receptors also leads to increased levels of inositol triphosphate (IP3)-induced calcium release which in turn activates the calmodulin-dependent protein kinase kinase (CaMKK) and calmodulin-dependent protein kinase I (CamKI; Nakamuta et al., 2011). The activation of CaMKK and CamKI triggers the phosphorylation of microtubule affinity regulating kinase 2 (MARK2). This leads to the phosphorylation of downstream microtubule associated proteins (MAPs) MAP2/4, Tau and DCX which reduces microtubule stability (Drewes et al., 1997; Schaar et al., 2004; Nakamuta et al., 2011). Interestingly, acute knockdown of MARK2 has been shown to stall MP-to-BP transition in the IZ in mice (Sapir et al., 2008). Thus, proper regulation of MARK2 appears to be essential for neuronal polarization *in vivo*.

BDNF signaling via TrkB has been demonstrated in culture experiments to lead to the activation of LKB1 (liver kinase b1 in mammals and PAR-4 in *C. elegans* (**Figures 2**, **3**; Shelly et al., 2007). Loss of function of LKB1 either by genetic knockout or knockdown by shRNA in nascent cortical projection neurons results in striking phenotypes: axon specification is completely abolished while the dendrite appears to still be specified (Barnes et al., 2007; Shelly et al., 2007). In contrast, overexpression of LKB1 in neural progenitors and postmitotic neurons lead to formation of multiple axons. In a biochemical pathway downstream of BDNF/TrkB, LKB1 is phosphorylated by protein kinase A (PKA) or ribosomal S6 kinase (p90RSK) at Serine 431 (Collins et al., 2000; Sapkota et al., 2001). Phosphorylated LKB1 leads to downstream activation of MARK2 (Shelly et al., 2007) and the SAD kinases which in turn phosphorylate Tau-1 (Kishi et al., 2005; Barnes et al., 2007). Remarkably, SAD-A/B double knockout precisely mimic the LKB1 loss of function phenotype with complete absence of the axon (Kishi et al., 2005). In summary, the above studies established a model whereby BDNF signaling via TrkB results in the activation of LKB1 which is translated into an intracellular symmetry break in multipolar cortical projection neurons while sojourning in the SVZ/IZ. Phosphorylated LKB1 localizes into the nascent axon and is required for axon extension and development. It will be interesting to determine the extent of specificity and functional redundancy of individual downstream components along the BDNF/TrkB-LKB1-SAD-A/B signaling module while executing the break in symmetry.

Semaphorins

Semaphorins consist of a large family of membrane bound or secreted proteins (Nakamura et al., 2000). The secreted semaphorin, Sema3A have been shown to act as a chemotactic factor for migrating cortical projection neurons (Polleux et al., 2000; Chen et al., 2008). Sema3A expression is highest near the pial surface in the developing cortex and the Sema3A expression domain establishes a descending gradient across the emerging cortical layers (Polleux et al., 2000; Chen et al., 2008). Sema3A binds its co-receptors Plexin and Neuropilin (Negishi et al., 2005) and it has been suggested that Sema3A may actively control the process of symmetry breaking and cellular polarization. Sema3A activates a number of downstream cascades resulting in the tuning of relative levels of cGMP and cyclic adenosine 3′,5′-monophosphate (cAMP) which negatively affects axon formation by downregulation of PKA-dependent phosphorylation of LKB1 (Shelly et al., 2011). Interestingly, exposure of undifferentiated neurites to local sources of Sema3A in hippocampal neuron cell culture leads to the suppression of axon-formation but promotion of dendrite formation in culture conditions (Shelly et al., 2011). Strikingly, *in vivo* knockdown of the Sema3A receptor neuropilin-1 in rat embryonic cortical progenitors results in severe polarization defects. Furthermore, Sema4D inactivates Ras (Oinuma et al., 2004) while it activates RhoA (Swiercz et al., 2002) which prevents axon formation and/or outgrowth via reduced actin dynamics and actin contraction. Thus, Sema3A acting via the neuropilin-1 receptor and semaphorins in general are critically involved in the symmetry break and polarization of nascent projection neurons in the developing cortex (Shelly et al., 2011).

TGF-β

The transforming growth factor β (TGF-β) has been reported to play an important role in the polarization of nascent cortical projection neurons in the developing cerebral cortex (Yi et al., 2010). Upon binding of one of the three TGF-β ligands (TGF-β1-3) to the type II TGF-β receptor (TβR2), this receptor

is recruited to the type I TGF-β receptor (TβR1) to form a complex which triggers the phosphorylation of the two receptors by the serine/threonine kinase domain (Shi and Massagué, 2003). The TβR2-TβR1 receptor complex has been shown to phosphorylate Par-6 which in turn regulates Cdc42/Rac1 activity by recruiting the ubiquitin ligase Smurf1 which promotes proteasomal degradation of the RhoA GTPase. This results in reduced activity of RhoA in the nascent axon thereby stimulating its outgrowth (Gonzalez-Billault et al., 2012). Thus, RhoA activity can be precisely regulated in response to TGF-β signaling thereby controlling the dynamics of the local actin organization which is essential for axon specification and thus cellular polarization (Yi et al., 2010). Interestingly, TGF-β2-3 is highly expressed near the VZ/SVZ. Thus nascent developing neurons could be exposed to a gradient which delivers a uniform stimuli for axon specification (Yi et al., 2010). However, the majority of MP neurons extend their axons tangentially (Hatanaka and Yamauchi, 2013) rather than towards the ventricular side. It is thus conceivable that TGF-β might only act as a stimulus for axon specification rather than an axon guidance cue (Yi et al., 2010). Bone morphogenic protein (BMP), also a member of the TGF-β superfamily appears to play important functions in the MP-to-BP transition as well. BMPs are known to signal via the intracellular downstream mediator SMAD which leads to the suppression of collapsin response mediator protein 2 (CRMP2), a transcription factor known to promote microtubule assembly (Shi and Massagué, 2003; Sun et al., 2010). Strikingly, upon suppression of CRMP2 or overexpression of dominant negative forms of CRMP2 multipolar cells accumulate in the SVZ/IZ in the developing cortex. While these findings suggest that a BMP-SMAD signaling pathway, via CRMP2, regulates the polarization of cortical projection neurons the precise molecular and biochemical mechanisms remain to be determined (Sun et al., 2010). Altogether, different members of the TFG-β superfamily play important roles in multipolar cortical neurons and direct neuronal polarization through distinct signaling pathways.

INTRINSIC BIOCHEMICAL NETWORKS THAT MEDIATE NEURONAL POLARITY

While the above sections illustrated the role of extracellular cues for triggering and/or execution of neuronal polarization, the intrinsic molecular mechanisms involved in symmetry breaking will be discussed in the sections below with a focus on *in vitro* and cell culture experiments. Isolated neurons in cell culture form one axon and several dendrites. External chemical or physical cues of instructive or antagonistic nature that determine axon formation have been identified (Lamoureux et al., 2002; Gomez et al., 2007; Shelly et al., 2011). However, cultured neuronal cells are able to polarize even in the absence of any external cue (Dotti et al., 1988) suggesting that cells have intrinsic ability to break symmetry, which is solely activated externally. What are the functional cell-intrinsic networks that underlie cell polarization and determine the biochemical state of the cell? Based on Turing's idea of a reaction-diffusion mechanism to explain how spatial order during embryogenesis may arise (Turing, 1990), Gierer and Meinhardt developed a conceptual framework for pattern formation, which is based on the local activation in the form of self-enhancing feedback, which amplifies and reinforces spatially asymmetric distributions of molecules, coupled to long-range inhibitory processes (Meinhardt and Gierer, 2000). While this concept was originally developed to explain spatial patterning during morphogenesis, it also provides a framework to understand cell polarity. Accordingly, cell polarization is seen as a self-organized process (Wennekamp et al., 2013), which involves local symmetry breaking, signal amplification and long-range inhibition (Wang, 2009; Chau et al., 2012).

Previous work was able to identify many molecular players involved in the processes that allow a neuron to choose the one neurite to become an axon (Barnes and Polleux, 2009). While cell polarization can theoretically arise from a single molecular species that features a positive feedback (Altschuler et al., 2008), symmetry breaking in neurons likely reflects interactions among multiple, partially redundant pathways with crosstalk among them (Namba et al., 2015). This network can be subdivided into several, partially overlapping modules, each of which comprises a subset of molecular players that encode for specific cellular functions. To a rough approximation, the output of one module can serve as the input for a module downstream. Here, we want to illustrate how these functional modules orchestrate neuronal polarization and how they are embedded in a more complex biochemical network giving rise to axon specification. Importantly, individual modules are often evolutionarily conserved among species and pathways that regulate cell polarization in seemingly distinct tissues and contexts are remarkably similar. Accordingly we can to some degree take advantage of known cell polarization concepts in yeast, *C. elegans* and migrating cells (Iden and Collard, 2008), with the goal to anticipate a better understanding of the molecular processes that underlie axon specification.

PIP/PI_3K Module

Molecules involved in the initial symmetry breaking event are commonly localized to the plasma membrane, where not only integral membrane proteins receive extracellular signals, but where also peripherally binding membrane proteins bind reversibly to the membrane (Cho and Stahelin, 2005). This restricts the diffusion of these proteins, increases the efficiency of protein-protein interactions and/or modulates their catalytic activity (Vaz et al., 1984; Leonard and Hurley, 2011; Ebner et al., 2017). As a result, the membrane can be interpreted as a computational platform where transient protein clusters integrate, interpret and amplify incoming biochemical signals (Groves and Kuriyan, 2010).

One component of membrane-based signaling pathways that was found to be essential for the establishment of intracellular organization include phosphoinositides (PIPs). Even though they represent only about 1% of membrane phospholipids (Di Paolo and De Camilli, 2006), the associated signaling pathways control cell growth, division, survival and

differentiation, and allow to generate highly polarized neuronal morphologies such as growth cones and synapses (Sasaki et al., 2007). Cells use a precisely defined spatiotemporal distribution of PIPs to control the activity of intracellular signaling pathways. For cell polarity, it is the asymmetry of phosphatidylinositol-3,4,5-phosphate ($PI(3,4,5)P_3$ = PIP_3) at the plasma membrane that is used to establish a polarity axis in the cell. The intramembranous PIP_3 concentration is controlled by activation of the phosphoinositide-3-kinase (PI3K; Whitman et al., 1985) as well as phosphatases such as phosphatase and tensin homolog (PTEN; Lee et al., 1999) that directly antagonize PI3K by dephosphorylating PIP_3 to $PI(4,5)P_2$ (PIP_2) (Carracedo and Pandolfi, 2008). Overexpression of PTEN or inhibition of the PI3K were both found to abolish cell polarization and axon specification (Shi et al., 2003; Jiang et al., 2005). In contrast, reduction of PTEN expression results in neurons with multiple axons (Jiang et al., 2005). Together, these results demonstrate that the activities of these enzymes need to be tightly balanced to produce one and only one axon.

Since polarization is a dynamic spatiotemporal process, not only the total amount of phosphoinositides but also their distribution in space and time needs to be precisely regulated. In cells, the intracellular distribution of PIP_3 can be visualized using a fluorescent reporter protein that specifically binds to PIP_3; e.g., GFP fused to the Pleckstrin-homology (PH) domain of the serine/threonine kinase Akt (Gray et al., 1999). This probe visualized PIP_3 accumulation at the tip of a neurite contributing to neuronal polarity and axon specification (Ménager et al., 2004). In contrast, EGFP-PLCd1-PH, which binds to PI(4, 5)P2 or IP3 showed a homogeneous distribution in cultured neuronal cells (Ménager et al., 2004).

The localized accumulation of PIP_3 likely represents the first spatial landmark that establishes the polarity axes of the cell. *In vivo*, activity of PI3K and PIP_3 production is most likely regulated by asymmetric distribution of extracellular factors (Namba et al., 2015), still, neurons polarize in cell culture without obvious asymmetries in their environment (Dotti et al., 1988). This suggest that starting from a homogeneous distribution of signaling molecules, dedicated biochemical circuits are able to amplify small fluctuations of signaling lipids in the plasma membrane. These interactions eventually break the symmetry of the cell and control cell morphogenesis (Wennekamp et al., 2013). The biochemical network underlying phosphoinositide polarity was studied in detail in other model systems. For example, *Dictyostelium discoideum* cells (Malchow et al., 1973), leukocytes and neutrophils (Trepat et al., 2012) polarize in response to a gradient of the chemoattractant cAMP or a variety of chemokines respectively by establishing domains of different phosphoinositides: PIP_3 at the leading edge of the cell and PIP_2 at its tail (Petrie et al., 2009). Importantly, and similar to neurons, the ability to break symmetry is independent from directional sensing, as cells that are placed in a uniform distribution of chemoattractant are still able to polarize (Petrie et al., 2009). Again, this illustrates the intrinsic ability of biochemical networks to polarize the cell in the absence of exogenous spatial signals (Wedlich-Soldner and Li, 2003). While phosphoinositide signaling was found to spatially organize the actin cytoskeleton, the initial symmetry breaking event itself does not depend on actin filaments. Fluorescently-labeled PH_{Akt} and PTEN, which acted as probes for PIP_3 and PIP_2 respectively, were found to self-organize into traveling waves in *Dictyostelium discoideum* cells even in the presence of the actin polymerization inhibitor latrunculin A (Gerisch et al., 2012). Importantly, this finding indicates that the ability to break symmetry in the membrane is established upstream and independent of the cytoskeleton. Instead, a PIP_3-dependent negative regulation of PTEN recruitment to the membrane was suggested to allow PIP_3 to accumulate. In addition, PTEN localization and activity has been found to be dependent on the small GTPase RhoA, which was found to restrict PTEN to the rear of chemotaxing leukocytes (Li et al., 2005) and *Dictyostelium* cells. Arai et al. (2010) further suggest a Ras-dependent positive feedback of PI3K activity to stabilize the polarized state of the cell. In addition, negative regulation of PTEN activity downstream of the PIP_3 activated AKT kinase has been reported, which constitutes a parallel mechanism to maintain and stabilize polarity (Papakonstanti et al., 2007).

While phosphoinositides are the most important lipid species for cellular signaling there are also other lipid species involved in neuronal polarization: plasma membrane ganglioside sialidase (PMGS), which controls the ganglioside content in the plasma membrane of neurons was also found to show an asymmetric distribution of its activity: it is enriched in one of the stage 2 neurites and facilitates axon outgrowth by enhancing Rac and PI3K activity (Da Silva et al., 2005). Thus, the asymmetric distribution of two different kinds of lipid species appears to control the polarity of the cell.

GEFs and Small GTPases

Which biochemical circuits underlie signal amplification in neurons? By now, the identity of several PI3K-dependent GTPases involved in neuronal polarization is known, such as H-Ras (Yoshimura et al., 2006b), Cdc42 (Garvalov et al., 2007) or Rap1B (Schwamborn and Püschel, 2004; Nakamura et al., 2013). Similar to PI3K (Shi et al., 2003) their overexpression results in supernumerary axons (see **Figure 3**), while their knock down prevents axon formation (Schwamborn and Püschel, 2004; Yoshimura et al., 2006b; Garvalov et al., 2007; Nakamura et al., 2013), however, these proteins do not interact with PIP_3 themselves. Instead, the phosphorylation state of phosphoinositides in the plasma membrane is recognized by soluble guanine nucleotide exchange factors (GEFs) that contain PIP3 binding domains, such as GEFs of the Dbl and DOCK180 families (Rossman et al., 2005; Laurin and Côté, 2014). These protein families in turn activate GTPases while recruiting them to the membrane (Cherfils and Zeghouf, 2013). Though a systematic characterization of GEFs that directly interact with PIP_3 and control cell polarization is not complete yet, candidate proteins include SOS and RasGFR, both members of the Dbl family of GEFs that contain a canonical DH-PH domain structure (Zheng, 2001). The PH (Pleckstrin homology) domain binds to phosphoinositides and

thereby controls localization and the DH (Dbl homology) domain is responsible for catalyzing nucleotide exchange (Zheng, 2001). Dock7, a Dock180 related protein that catalyzes the nucleotide exchange of Rac1 (Watabe-Uchida et al., 2006), was found to specifically bind PIP_3 via its DHR-1 domain (Kobayashi et al., 2001; Cote et al., 2005). Importantly, Dock7 is enriched in one of the stage 2 neurites—potentially the designated axon—supposedly controlling polarization and morphogenesis of the neuron (Watabe-Uchida et al., 2006). Controlled by these regulators, small GTPases can show phosphoinositide dependent activity patterns and a characteristic spatial distribution in the cell. However, direct evidence that GEF enrichment is a direct consequence of elevated PIP_3 levels in a stage 2 neurite is largely missing. Accordingly, the spatial distribution of GEFs could also depend on another PIP_3 binding protein which is recruited to and initiates a nascent axon.

As a result of their activation, GTP-bound GTPases engage in specific protein-protein interactions. By recruiting so-called effector proteins to the plasma membrane small GTPases determining the spatiotemporal activation pattern of other protein systems in the cell (Cherfils and Zeghouf, 2013). Effector proteins can be categorized in two classes: first, they can control cell morphology by directly acting on regulators of the actin or microtubule cytoskeleton, namely by increasing actin dynamicity and microtubule stabilization in the axon while stabilizing actin filaments in dendrites (Neukirchen and Bradke, 2011). For example, activation of Rac1 leads to a stabilization of axon microtubules via the stathmin pathway (Watabe-Uchida et al., 2006) while triggering actin remodeling (Hall et al., 2001; Gonzalez-Billault et al., 2012). In contrast, active RhoA promotes actin stabilization and contraction in dendrites as revealed by fluorescent activity sensors (Gonzalez-Billault et al., 2012). Second, effector proteins can be involved in the regulation of other small GTPases (DerMardirossian et al., 2004) or constituents of supramolecular complexes with various functions (Joberty et al., 2000; Lin et al., 2000). For example, they can act as coincidence detector for multiple binding partners (Carlton and Cullen, 2005) or signal to additional levels of regulation. For example, a common theme for the activation of small GTPases is that they comprise positive feedback loops. These self-amplifying circuits may not only lead to a local enrichment of GTPases on the membrane, but can also lead to collective, switch-like activation of proteins (Mizuno-Yamasaki et al., 2012). Accordingly, these kind of interactions can give rise to nonlinear signaling circuits with emergent properties, which can be crucial for breaking the symmetry and spatially organizing the cell (Yoshimura et al., 2006a).

The importance of positive feedback regulation for the symmetry breaking is probably best characterized in single-cell organisms such as yeast (Johnson et al., 2011). Despite the much lower complexity of this model organism, the general architecture of the biochemical network leading to cell polarization is most probably similar. In yeast, Cdc42 is the main spatial organizer of the cell as it regulates asymmetric cell division. Active, GTP-bound Cdc42 binds to the plasma membrane via its prenylated C-terminus, while GDP-bound Cdc42 is kept soluble in the cytoplasm via its interaction with its Guanosine nucleotide dissociation inhibitor (GDI) Rdi1. Cdc42-GTP is thought to form a locally confined protein cluster on the membrane by a local amplification of spontaneous asymmetries. The positive feedback is thought to arise from an effector-GEF complex, where the activated GTPase recruits an effector protein that in turn interacts with its activator. In yeast, a small, transient patch of Cdc42-GTP would recruit the scaffolding protein Bem-1 to the membrane, which interacts with the Cdc42 GEF Cdc24. Bem-1 not only binds to Cdc24 but also boosts its GEF activity. Thus Bem-1 efficiently catalyzes proximal Cdc42-GDP to exchange their nucleotide to Cdc42-GTP which again is able to recruit more Bem-1-Cdc24 complex (Nern and Arkowitz, 1998; Gulli et al., 2000; Johnson et al., 2011). Effector-GEF interactions have been found to be involved for the regulation of many different small GTPases (Mizuno-Yamasaki et al., 2012) and might be generally required for collective, switch-like activation of GTPases. These kind of decisive signaling reactions are of crucial importance for the cell, as they not only lead to cell polarization, but also regulate other fundamental processes such as membrane trafficking and the dynamic properties of the actin and microtubule cytoskeletons, thereby controlling the morphogenesis of the cell.

While the role of many proteins involved in neuronal polarity has been studied in neuronal cell culture, the function of Cdc42 has also been studied *in vivo* (Garvalov et al., 2007). Only about 30% of neurons derived from Cdc42 null mice were able to form a Tau-1 positive axon and the activity levels of the actin regulator cofilin were disturbed. However, when axon formation in Cdc42 null cells was initiated by cytochalasin, axons formed even if the drug was washed away. This indicates that Cdc42 is needed for the initial steps of axon specification but is dispensable for axon outgrowth (Garvalov et al., 2007).

The PAR System

During cell polarization, the asymmetric distribution of phosphoinositides provides an initial signal to a number of protein systems that together control cell morphogenesis. One of those protein systems is the PAR system, which is recruited downstream of activated Cdc42 (Etienne-Manneville and Hall, 2001; Yamanaka et al., 2001; Nishimura et al., 2005). The PAR system is a set of highly conserved proteins that organize cell polarity in all metazoan cells. In neurons, it was found that the PAR system is required for axon dendrite polarity (Shi et al., 2003; Chen et al., 2006), migration (Sapir et al., 2008) and dendrite development (Terabayashi et al., 2007). However, a complete mechanistic characterization of how these proteins regulate axon formation is missing.

The PAR system is probably best studied in the nematode *Caenorhabditis elegans*, where it controls the first division. In a single cell embryo, the PAR proteins self-organize into two non-overlapping domains (anterior and posterior domain) to govern asymmetric spindle positioning and ultimately the generation of daughter cells with different fate (Kemphues et al., 1988; Gönczy and Rose, 2005). The PAR proteins have been

categorized in anterior PARs (aPARs; PAR-3, PAR-6, PKC-3, cdc42) and posterior PARs (pPARs; PAR-2, PAR-1, LGL-1), all of which are peripheral membrane proteins. Their mutual exclusion is thought to arise from cross-phosphorylation by the two kinases PKC-3 and PAR-1, which leads to membrane detachment, controls oligomerization state and hence their diffusivity (Feng et al., 2007; Hoege and Hyman, 2013; Arata et al., 2016). PKC-3 can phosphorylate all posterior PARs (Hao et al., 2006; Hoege et al., 2010), in return, PAR-1 phosphorylates PAR-3 (Guo and Kemphues, 1995; Benton and St Johnston, 2003; Motegi et al., 2011). A network of regulatory biochemical interactions between aPARs and pPARs is thought to finely tune the activity of these kinases, leading to two dynamically stable cellular domains that govern a plethora of downstream events (Goehring, 2014).

Apart from PAR-2, the PAR system is conserved among most multicellular organisms and defines polarity via mutual exclusion in different contexts such as anterior-posterior polarity in *Drosophila* oocytes and apical-basal polarity in epithelial tissues (Morton et al., 2002; Goldstein and Macara, 2007; Thompson, 2013). The overall importance of the PAR system for axon dendrite polarity was firmly established in dissociated hippocampal cell culture system and enrichment of anterior PARs at the tip of the outgrowing axon has been observed (Shi et al., 2003). Subsequent knock down or overexpression studies of several PAR members showed that genetic manipulation of the PAR system either results in no or supernumerary axons (**Figure 3**). If mutual exclusion among aPARs and pPARs is a universal feature of the PAR system one would expect the posterior PAR-1 homolog MARK2 to be absent from the tip of the axon. Surprisingly, fluorescence sensors to measure MARK2 activity in the developing axon of cortical neurons showed highest kinase activity in the growing axon tip (Moravcevic et al., 2010; Timm et al., 2011). This indicates that both active PAR-1 kinases and aPARs are co-localizing at tip of the outgrowing axon and mutual exclusion of the "opposing" PAR complexes is not a requirement for axon dendrite polarity establishment. On a functional level, antagonism between MARK2 and the aPAR complex has been suggested (Chen et al., 2006). Analog to the *C. elegans* system, aPKC phosphorylates MARK2, which results in membrane detachment and most likely in reduced activity. Overexpression of MARK2 in hippocampal neurons prevented axon formation while knock down caused multiple axons (Chen et al., 2006; Wu et al., 2011). The opposite was seen for aPKC overexpression, which resulted in multiple axons (**Figure 3**; Parker et al., 2013). The overexpression phenotype of MARK2 was rescued by simultaneous overexpression of aPARs. No rescue was observed with a non phosphorylatable MARK2, indicating that direct inhibition of MARK2 by aPKC is responsible for the observed rescue. In a simple view, this could mean that MARK2 is a negative regulator of axon formation which is specifically inhibited by axon enriched aPARs via aPKC phosphorylation. However, *in vivo* knock out of the other PAR-1 homologs (SAD-kinases) also inhibited axon formation (see also above), indicating that a fine balance between these activities is needed (Kishi et al., 2005). Both, MARK2 and SAD kinases have to be activated by LKB1/PAR-4 (Lizcano et al., 2004; Shelly and Poo, 2011), which itself is downstream of cAMP/PKA signaling (Shelly et al., 2007). Thus, the PAR system not only translates PIP_3 dependent signaling into altered cytoskeleton dynamics but also integrates the input of heterotrimeric G protein receptor ligands. Interestingly and in contrast to *C. elegans*, LKB1/PAR-4 is enriched in the axon (Shelly et al., 2007) while it is homogenously distributed in the *C. elegans* zygote (Goehring, 2014). Knockdown of LGL-1 prevents axon formation but the precise role of LGL-1 in axon development is still poorly understood (Plant et al., 2003; Wang T. et al., 2011).

Another fundamental difference between the neuronal and nematode PAR system is their dependence on a previous symmetry breaking event. In *C. elegans*, the sperm entry marks a single symmetry breaking event that starts actomyosin based flows and facilitates PAR domain establishment whereas no asymmetries of PIP_3 have been reported. The PAR system in neurons is clearly downstream of regulators that directly control or are controlled by PIP_3, such as PI3K or ATK/GSK3b, Cdc42 and Rap1B (Insolera et al., 2011), whereas initial polarity formation in *C. elegans* does not depend on these PIP_3 controlled proteins (Schlesinger et al., 1999; Insolera et al., 2011). A possible explanation for this difference could be that neurons have to screen their environment during development (open systems) to remain a certain degree of plasticity while communication with the extracellular space is less important in the early stages of worm development. Thus, the PAR system is integrated into a more complex signaling network in neurons while it constitutes a rather autonomous polarity system in *C. elegans*. Since many PAR system intrinsic reactions (like phosphorylation events) seem to be conserved, it is still not clear how these reactions have to occur in space and time in neurons for faithful axon dendrite polarity establishment. Super resolution microscopy and higher temporal resolution of simultaneous activity monitoring of PARs and PIP_3 may be required to solve the question of how PARs fulfil their functions during neuronal development.

Closing the Loop

So far, we have only considered biochemical reactions downstream of an initial asymmetry of PIP_3. For robust symmetry breaking, a self-enforcing loop is required, which would give rise to a local accumulation of PIP_3 despite its rapid diffusion in the plasma membrane and the proteins in the cytoplasm. One possible functional network could originate from PIP_3 and at the same time further increase its local concentration on the membrane. Therefore, the described functional modules need to talk to each other and eventually feed back to the activity of PI3K.

The molecular players involved for this regulatory network could for example be GTPases or their GEFs and effector proteins, which would not only translate local PIP_3 enrichment into altered cytoskeleton dynamics and transport, but themselves further enhance the activity of PI3K. For example, Ras-GTP (Sasaki et al., 2004) and Rac1-GTP (Srinivasan et al., 2003) in combination with actin polymerization (Peyrollier et al., 2000; Wang et al., 2002) or via additional players like the Par6/Par3 aPKC complex where found to activate PI3K

(Motegi et al., 2011; Laurin and Côté, 2014). Indeed, these proteins were all found to be required for axon formation (Shi et al., 2003; Yoshimura et al., 2006b; Tahirovic et al., 2010). H-Ras is a direct activator of PI3K and is also activated downstream of PI3K (Rodriguez-Viciana et al., 1994; Yang et al., 2012). Interestingly, this feedback loop results in H-Ras translocation via vesicle based transport into the future axon, which depletes H-RAS from the other neurites, presumably leading to reduced PI3K activity in other neurites and subsequently to inhibition of their outgrowth (Fivaz et al., 2008). While the idea of this amplifying circuit is at least partially based on experimentally verified protein-protein interactions, the emergent properties of this network have not been tested yet. For example, the role of PTEN localization and activity for phosphoinositide polarization in neurons is not yet clear (Kreis et al., 2014) and there might be functional networks that involve either less or a different set of molecular players. Furthermore, the connectivity of those circuits could even change with time, different extracellular inputs or in different subcellular locations.

Another layer of regulation can also be performed on the level of GDP dissociation inhibitors (GDIs), whose main function is to maintain their target, lipid-modified GTPases in an inactive, soluble state (Cherfils and Zeghouf, 2013). There is evidence that the affinity of RhoGDIs for different GTPases can be modulated by phosphorylation. For example, the kinase PAK1 is an effector protein of Rac1 that was found to phosphorylate RhoGDIs (DerMardirossian et al., 2004). Phosphorylation of these GDIs can enhance the dissociation of Rac1 from the GDI complex, thereby increasing the rate of Rac1 activation. As this leads to further stimulation of PAK1 activity such interaction may give rise to another positive feedback and symmetry breaking in neurons (**Figure 2B**).

Finally, and in addition to molecular processes that depend on locally confined phosphorylation and dephosphorylation of PIPs, PIP_3 can also accumulate in the outgrowing axon with the help of directed microtubule-based transport. For example, the plus-end directed kinesin-like motor Gakin transports PIP_3-containing vesicles through the interaction with the adaptor protein α-centaurin (Horiguchi et al., 2006). MARK2, a homolog of PAR-1, inhibits this transport by phosphorylating Gakin thereby preventing the development of axons (Yoshimura et al., 2010). MARK2 itself is deactivated by the PIP_3-regulated kinase aPKC (Chen et al., 2006; Ivey et al., 2014). Thus a high local PIP_3 concentration could inhibit MARK2 in the axon shaft, further enhancing directed transport of PIP_3-containing vesicles to the growth cone. Accordingly, this could result in a self-perpetuating feedback loop supporting axon outgrowth (Yoshimura et al., 2010).

Collectively, these feedback loops stabilize polarity that can arise from short-lived local concentration fluctuations of external signals, temporal fluctuations in the output signal strength of receptors (Ladbury and Arold, 2012) or subtle heterogeneities on a coverslip. These small differences then lead to high and persistent activity of modulators that favor actin dynamicity and microtubule stability in the designated axon. Studies using drugs that either stabilized microtubules (Witte et al., 2008) or destabilized actin filaments (Bradke and Dotti, 1999) are sufficient to induce the formation of multiple axons, consistent with the view that the effects of the above mentioned circuits are transmitted via selective modulation of the cytoskeleton. In particular, these are the MARK2/SAD target and microtubule stabilizing tau proteins, microtubule destabilizers such as stathmin, actin dynamics modulators cofilin and WAVE and/ or inactivation of regulators that prevent axon outgrowth such as the RhoA/Rock module. This ultimately gives rise to a permanent molecular difference between axon and dendrites that will later on be manifested in a functional/electrophysiological difference of the two compartments, axon and dendrites. How this compartmentalization is maintained is not well understood and probably also relies on long range inhibitory signals, but future research will be needed to entangle the exact communications of these compartments during neuronal development.

CONCLUSION AND PERSPECTIVES

The phenomenon of neuronal polarization has been extensively studied in the last decades. Many of the analyses used the elegant cell culture system developed by Dotti et al. (1988). Thus the current model of neuronal polarization is to a large extent based on single hippocampal cells in an isolated system. Still, these extensive *in vitro* biochemical and cell biological analyses have provided a solid understanding of the general principles of cell polarization. A key question however remains: what are the cell-intrinsic biophysical and molecular mechanisms that induce the initial break in symmetry in cortical progenitor cells and developing cortical projection neurons *in vivo*? In order to address this question it will be essential to establish tools that allow the visualization and/or manipulation of the precise localization of molecular markers at high resolution in an *in situ* tissue context. The CRISPR-Cas9-dependent SLENDR method promises a high-throughput platform to visualize the endogenous localization of candidate proteins at high micro- to nanometer resolution (Mikuni et al., 2016). Given that a number of "polarity signaling systems" seem quite sensitive to perturbation and not particularly resilient, the precise determination of "polarity gene" function at distinct stages in development represents a current challenge in the field. In order to probe the function of genes encoding regulators of neuronal polarity *in vivo*, the genetic mosaic analysis with double markers (MADM) technology (Zong et al., 2005; Hippenmeyer et al., 2010; Hippenmeyer, 2013) offers an experimental opportunity. By exploiting MADM, one can induce sparse genetic mosaics with wild-type and mutant cells labeled in two distinct colors at high resolution. In combination with live-imaging such an experimental MADM paradigm enables: (1) the dissection of the cell-autonomous gene function; and (2) determination of the relative contribution of non-cell-autonomous effects *in situ* at the global tissue level (Beattie et al., 2017). Altogether, the experimental platforms above promise a robust approach to determine the so far unknown functions of regulators implicated in the polarization process of progenitor cells and nascent cortical projection neurons. A key open question in a functional context is: what is the level of redundancy and specificity in extracellular cues and intracellular amplification mechanisms? Interestingly,

the process of MP-to-BP transition appears to involve not only dynamic cytoskeletal-associated processes but also regulation at the transcriptional level (Hippenmeyer, 2014; Ohtaka-Maruyama and Okado, 2015). It will be important to analyze transcriptional responses at high temporal resolution and evaluate the influence on the general biochemical cell state. In future experiments it will be also important to establish biochemical and biophysical methods and assays that should allow the precise analysis of the break in symmetry at high molecular and/or structural resolution. In a broader context it will be important to address the question whether cell-type diversity may imply the necessity for adaptation in the mechanisms controlling polarization? In other words, how conserved is the process of symmetry break and polarization in distinct classes of neurons with different morphologies? The future analysis of the core signaling modules controlling cell polarity in a variety of brain areas and at high cellular and molecular resolution promises great conceptual advance.

AUTHOR CONTRIBUTIONS

AHH, CD, CM, ML and SH contributed equally to the writing of the initial draft. All authors revised the manuscript.

ACKNOWLEDGMENTS

This work was supported by IST Austria institutional funds; the European Union (FP7-CIG618444 to SH) and a program grant from the Human Frontiers Science Program (RGP0053/2014 to SH). CD was supported by a postdoctoral ISTFELLOW fellowship and CM was a postdoctoral fellow of the FWF Herta Firnberg programme.

REFERENCES

Altschuler, S. J., Angenent, S. B., Wang, Y., and Wu, L. F. (2008). On the spontaneous emergence of cell polarity. *Nature* 454, 886–889. doi: 10.1038/nature07119

Angevine, J. B. Jr., and Sidman, R. L. (1961). Autoradiographic study of cell migration during histogenesis of cerebral cortex in the mouse. *Nature* 192, 766–768. doi: 10.1038/192766b0

Anthony, T. E., Klein, C., Fishell, G., and Heintz, N. (2004). Radial glia serve as neuronal progenitors in all regions of the central nervous system. *Neuron* 41, 881–890. doi: 10.1016/s0896-6273(04)00140-0

Arai, Y., Shibata, T., Matsuoka, S., Sato, M. J., Yanagida, T., and Ueda, M. (2010). Self-organization of the phosphatidylinositol lipids signaling system for random cell migration. *Proc. Natl. Acad. Sci. U S A* 107, 12399–12404. doi: 10.1073/pnas.0908278107

Arata, Y., Hiroshima, M., Pack, C. G., Ramanujam, R., Motegi, F., Nakazato, K., et al. (2016). Cortical polarity of the RING protein PAR-2 is maintained by exchange rate kinetics at the cortical-cytoplasmic boundary. *Cell rep.* 17:316. doi: 10.1016/j.celrep.2016.09.044

Ballif, B. A., Arnaud, L., Arthur, W. T., Guris, D., Imamoto, A., and Cooper, J. A. (2004). Activation of a Dab1/CrkL/C3G/Rap1 pathway in Reelin-stimulated neurons. *Curr. Biol.* 14, 606–610. doi: 10.1016/j.cub.2004.03.038

Barnes, A. P., Lilley, B. N., Pan, Y. A., Plummer, L. J., Powell, A. W., Raines, A. N., et al. (2007). LKB1 and SAD kinases define a pathway required for the polarization of cortical neurons. *Cell* 129, 549–563. doi: 10.1016/j.cell.2007.03.025

Barnes, A. P., and Polleux, F. (2009). Establishment of axon-dendrite polarity in developing neurons. *Annu. Rev. Neurosci.* 32, 347–381. doi: 10.1146/annurev.neuro.31.060407.125536

Beattie, R., Postiglione, M. P., Burnett, L. E., Laukoter, S., Streicher, C., Pauler, F. M., et al. (2017). Mosaic analysis with double markers reveals distinct sequential functions of lgl1 in neural stem cells. *Neuron* 94, 517.e3–533.e3. doi: 10.1016/j.neuron.2017.04.012

Benton, R., and St Johnston, D. (2003). *Drosophila* PAR-1 and 14–3-3 inhibit Bazooka/PAR-3 to establish complementary cortical domains in polarized cells. *Cell* 115, 691–704. doi: 10.1016/s0092-8674(03)00938-3

Betizeau, M., Cortay, V., Patti, D., Pfister, S., Gautier, E., Bellemin-Ménard, A., et al. (2013). Precursor diversity and complexity of lineage relationships in the outer subventricular zone of the primate. *Neuron* 80, 442–457. doi: 10.1016/j.neuron.2013.09.032

Borrell, V., and Götz, M. (2014). Role of radial glial cells in cerebral cortex folding. *Curr. Opin. Neurobiol.* 27, 39–46. doi: 10.1016/j.conb.2014.02.007

Bradke, F., and Dotti, C. G. (1999). The role of local actin instability in axon formation. *Science* 283, 1931–1934. doi: 10.1126/science.283.5409.1931

Britto, J. M., Tait, K. J., Lee, E. P., Gamble, R. S., Hattori, M., and Tan, S. S. (2014). Exogenous Reelin modifies the migratory behavior of neurons depending on cortical location. *Cereb. Cortex* 24, 2835–2847. doi: 10.1093/cercor/bht123

Carlton, J. G., and Cullen, P. J. (2005). Coincidence detection in phosphoinositide signaling. *Trends Cell Biol.* 15, 540–547. doi: 10.1016/j.tcb.2005.08.005

Carracedo, A., and Pandolfi, P. P. (2008). The PTEN-PI3K pathway: of feedbacks and cross-talks. *Oncogene* 27, 5527–5541. doi: 10.1038/onc.2008.247

Chao, M. V. (2003). Neurotrophins and their receptors: a convergence point for many signalling pathways. *Nat. Rev. Neurosci.* 4, 299–309. doi: 10.1038/nrn1078

Chau, A. H., Walter, J. M., Gerardin, J., Tang, C., and Lim, W. A. (2012). Designing synthetic regulatory networks capable of self-organizing cell polarization. *Cell* 151, 320–332. doi: 10.1016/j.cell.2012.08.040

Chen, S., Chen, J., Shi, H., Wei, M., Castaneda-Castellanos, D. R., Bultje, R. S., et al. (2013). Regulation of microtubule stability and organization by mammalian Par3 in specifying neuronal polarity. *Dev. Cell* 24, 26–40. doi: 10.1016/j.devcel.2012.11.014

Chen, G., Sima, J., Jin, M., Wang, K. Y., Xue, X. J., Zheng, W., et al. (2008). Semaphorin-3A guides radial migration of cortical neurons during development. *Nat. Neurosci.* 11, 36–44. doi: 10.1038/nn2018

Chen, Y. M., Wang, Q. J., Hu, H. S., Yu, P. C., Zhu, J., Drewes, G., et al. (2006). Microtubule affinity-regulating kinase 2 functions downstream of the PAR-3/PAR-6/atypical PKC complex in regulating hippocampal neuronal polarity. *Proc. Natl. Acad. Sci. U S A* 103, 8534–8539. doi: 10.1073/pnas.0509955103

Cherfils, J., and Zeghouf, M. (2013). Regulation of small GTPases by GEFs, GAPs and GDIs. *Physiol. Rev.* 93, 269–309. doi: 10.1152/physrev.00003.2012

Cho, W., and Stahelin, R. V. (2005). Membrane-protein interactions in cell signaling and membrane trafficking. *Annu. Rev. Biophys. Biomol. Struct.* 34, 119–151. doi: 10.1146/annurev.biophys.33.110502.133337

Collins, S. P., Reoma, J. L., Gamm, D. M., and Uhler, M. D. (2000). LKB1, a novel serine/threonine protein kinase and potential tumour suppressor, is phosphorylated by cAMP-dependent protein kinase (PKA) and prenylated *in vivo*. *Biochem. J.* 345, 673–680. doi: 10.1042/0264-6021:3450673

Cote, J. F., Motoyama, A. B., Bush, J. A., and Vuori, K. (2005). A novel and evolutionarily conserved PtdIns(3,4,5)P3-binding domain is necessary for DOCK180 signalling. *Nat. Cell Biol.* 7, 797–807. doi: 10.1038/ncb1280

D'Arcangelo, G., Homayouni, R., Keshvara, L., Rice, D. S., Sheldon, M., and Curran, T. (1999). Reelin is a ligand for lipoprotein receptors. *Neuron* 24, 471–479. doi: 10.1016/s0896-6273(00)80860-0

Da Silva, J. S., Hasegawa, T., Miyagi, T., Dotti, C. G., and Abad-Rodriguez, J. (2005). Asymmetric membrane ganglioside sialidase activity specifies axonal fate. *Nat. Neurosci.* 8, 606–615. doi: 10.1038/nn1442

DerMardirossian, C., Schnelzer, A., and Bokoch, G. M. (2004). Phosphorylation of RhoGDI by Pak1 mediates dissociation of Rac GTPase. *Mol. Cell* 15, 117–127. doi: 10.1016/j.molcel.2004.05.019

Di Paolo, G., and De Camilli, P. (2006). Phosphoinositides in cell regulation and membrane dynamics. *Nature* 443, 651–657. doi: 10.1038/nature05185

Dotti, C. G., Sullivan, C. A., and Banker, G. A. (1988). The establishment of polarity by hippocampal neurons in culture. *J. Neurosci.* 8, 1454–1468.

Drewes, G., Ebneth, A., Preuss, U., Mandelkow, E. M., and Mandelkow, E. (1997). MARK, a novel family of protein kinases that phosphorylate microtubule-associated proteins and trigger microtubule disruption. *Cell* 89, 297–308. doi: 10.1016/s0092-8674(00)80208-1

Ebner, M., Lucic, I., Leonard, T. A., and Yudushkin, I. (2017). PI(3,4,5)P3 engagement restricts Akt activity to cellular membranes. *Mol. Cell* 65, 416.e6–431.e6. doi: 10.1016/j.molcel.2016.12.028

Etienne-Manneville, S., and Hall, A. (2001). Integrin-mediated activation of Cdc42 controls cell polarity in migrating astrocytes through PKCζ. *Cell* 106, 489–498. doi: 10.1016/s0092-8674(01)00471-8

Evsyukova, I., Plestant, C., and Anton, E. S. (2013). Integrative mechanisms of oriented neuronal migration in the developing brain. *Annu. Rev. Cell Dev. Biol.* 29, 299–353. doi: 10.1146/annurev-cellbio-101512-122400

Feng, W., Wu, H., Chan, L. N., and Zhang, M. (2007). The Par-3 NTD adopts a PB1-like structure required for Par-3 oligomerization and membrane localization. *EMBO J.* 26, 2786–2796. doi: 10.2210/pdb2ns5/pdb

Fietz, S. A., Kelava, I., Vogt, J., Wilsch-Brauninger, M., Stenzel, D., Fish, J. L., et al. (2010). OSVZ progenitors of human and ferret neocortex are epithelial-like and expand by integrin signaling. *Nat. Neurosci.* 13, 690–699. doi: 10.1038/nn.2553

Fivaz, M., Bandara, S., Inoue, T., and Meyer, T. (2008). Robust neuronal symmetry breaking by Ras-triggered local positive feedback. *Curr. Biol.* 18, 44–50. doi: 10.1016/j.cub.2007.11.051

Florio, M., Albert, M., Taverna, E., Namba, T., Brandl, H., Lewitus, E., et al. (2015). Human-specific gene *ARHGAP11B* promotes basal progenitor amplification and neocortex expansion. *Science* 347, 1465–1470. doi: 10.1126/science.aaa1975

Forster, E., Bock, H. H., Herz, J., Chai, X., Frotscher, M., and Zhao, S. (2010). Emerging topics in Reelin function. *Eur. J. Neurosci.* 31, 1511–1518. doi: 10.1111/j.1460-9568.2010.07222.x

Franco, S. J., and Muller, U. (2013). Shaping our minds: stem and progenitor cell diversity in the mammalian neocortex. *Neuron* 77, 19–34. doi: 10.1016/j.neuron.2012.12.022

Frotscher, M. (2010). Role for Reelin in stabilizing cortical architecture. *Trends Neurosci.* 33, 407–414. doi: 10.1016/j.tins.2010.06.001

Gao, P., Postiglione, M. P., Krieger, T. G., Hernandez, L., Wang, C., Han, Z., et al. (2014). Deterministic progenitor behavior and unitary production of neurons in the neocortex. *Cell* 159, 775–788. doi: 10.1016/j.cell.2014.10.027

Gartner, A., Fornasiero, E. F., and Dotti, C. G. (2015). Cadherins as regulators of neuronal polarity. *Cell Adh. Migr.* 9, 175–182. doi: 10.4161/19336918.2014.983808

Gartner, A., Fornasiero, E. F., Munck, S., Vennekens, K., Seuntjens, E., Huttner, W. B., et al. (2012). N-cadherin specifies first asymmetry in developing neurons. *EMBO J.* 31, 1893–1903. doi: 10.1038/emboj.2012.41

Garvalov, B. K., Flynn, K. C., Neukirchen, D., Meyn, L., Teusch, N., Wu, X., et al. (2007). Cdc42 regulates cofilin during the establishment of neuronal polarity. *J. Neurosci.* 27, 13117–13129. doi: 10.1523/jneurosci.3322-07.2007

Gerisch, G., Schroth-Diez, B., Muller-Taubenberger, A., and Ecke, M. (2012). PIP3 waves and PTEN dynamics in the emergence of cell polarity. *Biophys. J.* 103, 1170–1178. doi: 10.1016/j.bpj.2012.08.004

Goehring, N. W. (2014). PAR polarity: from complexity to design principles. *Exp. Cell Res.* 328, 258–266. doi: 10.1016/j.yexcr.2014.08.009

Goldstein, B., and Macara, I. G. (2007). The PAR proteins: fundamental players in animal cell polarization. *Dev. Cell* 13, 609–622. doi: 10.1016/j.devcel.2007.10.007

Gomez, N., Chen, S., and Schmidt, C. E. (2007). Polarization of hippocampal neurons with competitive surface stimuli: contact guidance cues are preferred over chemical ligands. *J. R. Soc. Interface* 4, 223–233. doi: 10.1098/rsif.2006.0171

Gönczy, P., and Rose, L. S. (2005). "Asymmetric cell division and axis formation in the embryo," in *WormBook*, ed. The *C. elegans* Research Community, 1–20. doi: 10.1895/wormbook.1.30.1

Gonzalez-Billault, C., Muñoz-Llancao, P., Henriquez, D. R., Wojnacki, J., Conde, C., and Caceres, A. (2012). The role of small GTPases in neuronal morphogenesis and polarity. *Cytoskeleton* 69, 464–485. doi: 10.1002/cm.21034

Gray, A., Van Der Kaay, J., and Downes, C. P. (1999). The pleckstrin homology domains of protein kinase B and GRP1 (general receptor for phosphoinositides-1) are sensitive and selective probes for the cellular detection of phosphatidylinositol 3,4-bisphosphate and/or phosphatidylinositol 3,4,5-trisphosphate *in vivo*. *Biochem. J.* 344, 929–936. doi: 10.1042/0264-6021:3440929

Groves, J. T., and Kuriyan, J. (2010). Molecular mechanisms in signal transduction at the membrane. *Nat. Struct. Mol. Biol.* 17, 659–665. doi: 10.1038/nsmb.1844

Gulli, M. P., Jaquenoud, M., Shimada, Y., Niederhauser, G., Wiget, P., and Peter, M. (2000). Phosphorylation of the Cdc42 exchange factor Cdc24 by the PAK-like kinase Cla4 may regulate polarized growth in yeast. *Mol. Cell* 6, 1155–1167. doi: 10.1016/s1097-2765(00)00113-1

Guo, S., and Kemphues, K. J. (1995). par-1, a gene required for establishing polarity in *C. elegans* embryos, encodes a putative Ser/Thr kinase that is asymmetrically distributed. *Cell* 81, 611–620. doi: 10.1016/0092-8674(95)90082-9

Hall, C., Brown, M., Jacobs, T., Ferrari, G., Cann, N., Teo, M., et al. (2001). Collapsin response mediator protein switches RhoA and Rac1 morphology in N1E-115 neuroblastoma cells and is regulated by Rho kinase. *J. Biol. Chem.* 276, 43482–43486. doi: 10.1074/jbc.c100455200

Hansen, D. V., Lui, J. H., Parker, P. R., and Kriegstein, A. R. (2010). Neurogenic radial glia in the outer subventricular zone of human neocortex. *Nature* 464, 554–561. doi: 10.1038/nature08845

Hao, Y., Boyd, L., and Seydoux, G. (2006). Stabilization of cell polarity by the *C. elegans* RING protein PAR-2. *Dev. Cell* 10, 199–208. doi: 10.1016/j.devcel.2005.12.015

Hatanaka, Y., and Yamauchi, K. (2013). Excitatory cortical neurons with multipolar shape establish neuronal polarity by forming a tangentially oriented axon in the intermediate zone. *Cereb. Cortex* 23, 105–113. doi: 10.1093/cercor/bhr383

Hippenmeyer, S. (2013). Dissection of gene function at clonal level using mosaic analysis with double markers. *Front. Biol.* 8, 557–568. doi: 10.1007/s11515-013-1279-6

Hippenmeyer, S. (2014). Molecular pathways controlling the sequential steps of cortical projection neuron migration. *Adv. Exp. Med. Biol.* 800, 1–24. doi: 10.1007/978-94-007-7687-6_1

Hippenmeyer, S., Youn, Y. H., Moon, H. M., Miyamichi, K., Zong, H., Wynshaw-Boris, A., et al. (2010). Genetic mosaic dissection of Lis1 and Ndel1 in neuronal migration. *Neuron* 68, 695–709. doi: 10.1016/j.neuron.2010.09.027

Hirota, Y., Kubo, K., Katayama, K., Honda, T., Fujino, T., Yamamoto, T. T., et al. (2015). Reelin receptors ApoER2 and VLDLR are expressed in distinct spatiotemporal patterns in developing mouse cerebral cortex. *J. Comp. Neurol.* 523, 463–478. doi: 10.1002/cne.23691

Hoege, C., Constantinescu, A. T., Schwager, A., Goehring, N. W., Kumar, P., and Hyman, A. A. (2010). LGL can partition the cortex of one-cell *Caenorhabditis elegans* embryos into two domains. *Curr. Biol.* 20, 1296–1303. doi: 10.1016/j.cub.2010.05.061

Hoege, C., and Hyman, A. A. (2013). Principles of PAR polarity in *Caenorhabditis elegans* embryos. *Nat. Rev. Mol. Cell Biol.* 14, 315–322. doi: 10.1038/nrm3558

Homem, C. C., Repic, M., and Knoblich, J. A. (2015). Proliferation control in neural stem and progenitor cells. *Nat. Rev. Neurosci.* 16, 647–659. doi: 10.1038/nrn4021

Honda, T., Kobayashi, K., Mikoshiba, K., and Nakajima, K. (2011). Regulation of cortical neuron migration by the Reelin signaling pathway. *Neurochem. Res.* 36, 1270–1279. doi: 10.1007/s11064-011-0407-4

Horiguchi, K., Hanada, T., Fukui, Y., and Chishti, A. H. (2006). Transport of PIP3 by GAKIN, a kinesin-3 family protein, regulates neuronal cell polarity. *J. Cell Biol.* 174, 425–436. doi: 10.1083/jcb.200604031

Howell, B. W., Hawkes, R., Soriano, P., and Cooper, J. A. (1997). Neuronal position in the developing brain is regulated by mouse disabled-1. *Nature* 389, 733–737. doi: 10.1038/39607

Howell, B. W., Herrick, T. M., and Cooper, J. A. (1999). Reelin-induced tyrosine [corrected] phosphorylation of disabled 1 during neuronal positioning. *Genes Dev.* 13, 643–648. doi: 10.1101/gad.13.6.643

Iden, S., and Collard, J. G. (2008). Crosstalk between small GTPases and polarity proteins in cell polarization. *Nat. Rev. Mol. Cell Biol.* 9, 846–859. doi: 10.1038/nrm2521

Insolera, R., Chen, S., and Shi, S. H. (2011). Par proteins and neuronal polarity. *Dev. Neurobiol.* 71, 483–494. doi: 10.1002/dneu.20867

Ivey, R. A., Sajan, M. P., and Farese, R. V. (2014). Requirements for pseudosubstrate arginine residues during autoinhibition and phosphatidylinositol 3,4,5-$(PO_4)_3$-dependent activation of atypical PKC. *J. Biol. Chem.* 289, 25021–25030. doi: 10.1074/jbc.M114.565671

Jiang, H., Guo, W., Liang, X., and Rao, Y. (2005). Both the establishment and the maintenance of neuronal polarity require active mechanisms: critical roles of GSK-3beta and its upstream regulators. *Cell* 120, 123–135. doi: 10.1016/s0092-8674(04)01258-9

Joberty, G., Petersen, C., Gao, L., and Macara, I. G. (2000). The cell-polarity protein Par6 links Par3 and atypical protein kinase C to Cdc42. *Nat. Cell Biol.* 2, 531–539. doi: 10.1038/35019573

Johnson, J. M., Jin, M., and Lew, D. J. (2011). Symmetry breaking and the establishment of cell polarity in budding yeast. *Curr. Opin. Genet. Dev.* 21, 740–746. doi: 10.1016/j.gde.2011.09.007

Johnson, M. B., Wang, P. P., Atabay, K. D., Murphy, E. A., Doan, R. N., Hecht, J. L., et al. (2015). Single-cell analysis reveals transcriptional heterogeneity of neural progenitors in human cortex. *Nat. Neurosci.* 18, 637–646. doi: 10.1038/nn.3980

Jossin, Y. (2011). Polarization of migrating cortical neurons by Rap1 and N-cadherin: revisiting the model for the reelin signaling pathway. *Small GTPases* 2, 322–328. doi: 10.4161/sgtp.18283

Jossin, Y., and Cooper, J. A. (2011). Reelin, Rap1 and N-cadherin orient the migration of multipolar neurons in the developing neocortex. *Nat. Neurosci.* 14, 697–703. doi: 10.1038/nn.2816

Kelava, I., Reillo, I., Murayama, A. Y., Kalinka, A. T., Stenzel, D., Tomancak, P., et al. (2012). Abundant occurrence of basal radial glia in the subventricular zone of embryonic neocortex of a lissencephalic primate, the common marmoset Callithrix jacchus. *Cereb. Cortex* 22, 469–481. doi: 10.1093/cercor/bhr301

Kemphues, K. J., Priess, J. R., Morton, D. G., and Cheng, N. S. (1988). Identification of genes required for cytoplasmic localization in early *C. elegans* embryos. *Cell* 52, 311–320. doi: 10.1016/s0092-8674(88)80024-2

Kishi, M., Pan, Y. A., Crump, J. G., and Sanes, J. R. (2005). Mammalian SAD kinases are required for neuronal polarization. *Science* 307, 929–932. doi: 10.1126/science.1107403

Knoblich, J. A. (2008). Mechanisms of asymmetric stem cell division. *Cell* 132, 583–597. doi: 10.1016/j.cell.2008.02.007

Kobayashi, S., Shirai, T., Kiyokawa, E., Mochizuki, N., Matsuda, M., and Fukui, Y. (2001). Membrane recruitment of DOCK180 by binding to PtdIns(3,4,5)P3. *Biochem. J.* 354, 73–78. doi: 10.1042/0264-6021:3540073

Kowalczyk, T., Pontious, A., Englund, C., Daza, R. A., Bedogni, F., Hodge, R., et al. (2009). Intermediate neuronal progenitors (basal progenitors) produce pyramidal-projection neurons for all layers of cerebral cortex. *Cereb. Cortex* 19, 2439–2450. doi: 10.1093/cercor/bhn260

Kreis, P., Leondaritis, G., Lieberam, I., and Eickholt, B. J. (2014). Subcellular targeting and dynamic regulation of PTEN: implications for neuronal cells and neurological disorders. *Front. Mol. Neurosci.* 7:23. doi: 10.3389/fnmol.2014.00023

Ladbury, J. E., and Arold, S. T. (2012). Noise in cellular signaling pathways: causes and effects. *Trends Biochem. Sci.* 37, 173–178. doi: 10.1016/j.tibs.2012.01.001

Lamoureux, P., Ruthel, G., Buxbaum, R. E., and Heidemann, S. R. (2002). Mechanical tension can specify axonal fate in hippocampal neurons. *J. Cell Biol.* 159, 499–508. doi: 10.1083/jcb.200207174

Laurin, M., and Côté, J.-F. (2014). Insights into the biological functions of Dock family guanine nucleotide exchange factors. *Genes Dev.* 28, 533–547. doi: 10.1101/gad.236349.113

Lee, H. O., and Norden, C. (2013). Mechanisms controlling arrangements and movements of nuclei in pseudostratified epithelia. *Trends Cell Biol.* 23, 141–150. doi: 10.1016/j.tcb.2012.11.001

Lee, J. O., Yang, H., Georgescu, M. M., Di Cristofano, A., Maehama, T., Shi, Y., et al. (1999). Crystal structure of the PTEN tumor suppressor: implications for its phosphoinositide phosphatase activity and membrane association. *Cell* 99, 323–334.

Leonard, T. A., and Hurley, J. H. (2011). Regulation of protein kinases by lipids. *Curr. Opin. Struct. Biol.* 21, 785–791. doi: 10.1016/j.sbi.2011.07.006

Li, Z., Dong, X., Wang, Z., Liu, W., Deng, N., Ding, Y., et al. (2005). Regulation of PTEN by Rho small GTPases. *Nat. Cell Biol.* 7, 399–404. doi: 10.1038/ncb1236

Lin, D., Edwards, A. S., Fawcett, J. P., Mbamalu, G., Scott, J. D., and Pawson, T. (2000). A mammalian PAR-3-PAR-6 complex implicated in Cdc42/Rac1 and aPKC signalling and cell polarity. *Nat. Cell Biol.* 2, 540–547. doi: 10.1038/35019582

Lizcano, J. M., Göransson, O., Toth, R., Deak, M., Morrice, N. A., Boudeau, J., et al. (2004). LKB1 is a master kinase that activates 13 kinases of the AMPK subfamily, including MARK/PAR-1. *EMBO J.* 23, 833–843. doi: 10.1038/sj.emboj.7600110

Lui, J. H., Hansen, D. V., and Kriegstein, A. R. (2011). Development and evolution of the human neocortex. *Cell* 146, 18–36. doi: 10.1016/j.cell.2011.06.030

Malatesta, P., Hartfuss, E., and Götz, M. (2000). Isolation of radial glial cells by fluorescent-activated cell sorting reveals a neuronal lineage. *Development* 127, 5253–5263.

Malchow, D., Fuchila, J., and Jastorff, B. (1973). Correlation of substrate specificity of cAMP-phosphodiesterase in Dictyostelium discoideum with chemotactic activity of cAMP-analogues. *FEBS Lett.* 34, 5–9. doi: 10.1016/0014-5793(73)80690-8

Marín, O., Valiente, M., Ge, X., and Tsai, L.-H. (2010). Guiding neuronal cell migrations. *Cold Spring Harb. Perspect. Biol.* 2:a001834. doi: 10.1101/cshperspect.a001834

Meinhardt, H., and Gierer, A. (2000). Pattern formation by local self-activation and lateral inhibition. *Bioessays* 22, 753–760. doi: 10.1002/1521-1878(200008)22:8<753::AID-BIES9>3.0.CO;2-Z

Ménager, C., Arimura, N., Fukata, Y., and Kaibuchi, K. (2004). PIP_3 is involved in neuronal polarization and axon formation. *J. Neurochem.* 89, 109–118. doi: 10.1046/j.1471-4159.2004.02302.x

Mikuni, T., Nishiyama, J., Sun, Y., Kamasawa, N., and Yasuda, R. (2016). High-throughput, high-resolution mapping of protein localization in mammalian brain by *in vivo* genome editing. *Cell* 165, 1803–1817. doi: 10.1016/j.cell.2016.04.044

Mizuno-Yamasaki, E., Rivera-Molina, F., and Novick, P. (2012). GTPase networks in membrane traffic. *Annu. Rev. Biochem.* 81, 637–659. doi: 10.1146/annurev-biochem-052810-093700

Moravcevic, K., Mendrola, J. M., Schmitz, K. R., Wang, Y. H., Slochower, D., Janmey, P. A., et al. (2010). Kinase associated-1 domains drive MARK/PAR1 kinases to membrane targets by binding acidic phospholipids. *Cell* 143, 966–977. doi: 10.1016/j.cell.2010.11.028

Morfini, G., DiTella, M. C., Feiguin, F., Carri, N., and Cáeres, A. (1994). Neurotrophin-3 enhances neurite outgrowth in cultured hippocampal pyramidal neurons. *J. Neurosci. Res.* 39, 219–232. doi: 10.1002/jnr.490390212

Morton, D. G., Shakes, D. C., Nugent, S., Dichoso, D., Wang, W., Golden, A., et al. (2002). The *Caenorhabditis elegans* par-5 gene encodes a 14–3-3 protein required for cellular asymmetry in the early embryo. *Dev. Biol.* 241, 47–58. doi: 10.1006/dbio.2001.0489

Motegi, F., Zonies, S., Hao, Y., Cuenca, A. A., Griffin, E., and Seydoux, G. (2011). Microtubules induce self-organization of polarized PAR domains in *C. elegans* zygotes. *Nat. Cell Biol.* 13, 1361–1367. doi: 10.1038/ncb2354

Nadarajah, B., Brunstrom, J. E., Grutzendler, J., Wong, R. O., and Pearlman, A. L. (2001). Two modes of radial migration in early development of the cerebral cortex. *Nat. Neurosci.* 4, 143–150. doi: 10.1038/83967

Nadarajah, B., and Parnavelas, J. G. (2002). Modes of neuronal migration in the developing cerebral cortex. *Nat. Rev. Neurosci.* 3, 423–432. doi: 10.1038/nrn845

Nakamura, F., Kalb, R. G., and Strittmatter, S. M. (2000). Molecular basis of semaphorin-mediated axon guidance. *J. Neurobiol.* 44, 219–229. doi: 10.1002/1097-4695(200008)44:2<219::AID-NEU11>3.0.CO;2-W

Nakamura, T., Yasuda, S., Nagai, H., Koinuma, S., Morishita, S., Goto, A., et al. (2013). Longest neurite-specific activation of Rap1B in hippocampal neurons contributes to polarity formation through RalA and Nore1A in addition to PI3-kinase. *Genes Cells* 18, 1020–1031. doi: 10.1111/gtc.12097

Nakamuta, S., Funahashi, Y., Namba, T., Arimura, N., Picciotto, M. R., Tokumitsu, H., et al. (2011). Local application of neurotrophins specifies axons through inositol 1,4,5-trisphosphate, calcium, and Ca^{2+}/calmodulin-dependent protein kinases. *Sci. Signal.* 4:ra76. doi: 10.1126/scisignal.2002011

Namba, T., Funahashi, Y., Nakamuta, S., Xu, C., Takano, T., and Kaibuchi, K. (2015). Extracellular and intracellular signaling for neuronal polarity. *Physiol. Rev.* 95, 995–1024. doi: 10.1152/physrev.00025.2014

Namba, T., Kibe, Y., Funahashi, Y., Nakamuta, S., Takano, T., Ueno, T., et al. (2014). Pioneering axons regulate neuronal polarization in the developing cerebral cortex. *Neuron* 81, 814–829. doi: 10.1016/j.neuron.2013.12.015

Negishi, M., Oinuma, I., and Katoh, H. (2005). Plexins: axon guidance and signal transduction. *Cell. Mol. Life Sci.* 62, 1363–1371. doi: 10.1007/s00018-005-5018-2

Nern, A., and Arkowitz, R. A. (1998). A GTP-exchange factor required for cell orientation. *Nature* 391, 195–198. doi: 10.1038/34458

Neukirchen, D., and Bradke, F. (2011). Neuronal polarization and the cytoskeleton. *Semin. Cell Dev. Biol.* 22, 825–833. doi: 10.1016/j.semcdb.2011.08.007

Nishimura, T., Yamaguchi, T., Kato, K., Yoshizawa, M., Nabeshima, Y., Ohno, S., et al. (2005). PAR-6-PAR-3 mediates Cdc42-induced Rac activation through the Rac GEFs STEF/Tiam1. *Nat. Cell Biol.* 7, 270–277. doi: 10.1038/ncb1227

Noctor, S. C. (2011). Time-lapse imaging of fluorescently labeled live cells in the embryonic mammalian forebrain. *Cold Spring Harb. Protoc.* 2011, 1350–1361. doi: 10.1101/pdb.prot066605

Noctor, S. C., Flint, A. C., Weissman, T. A., Dammerman, R. S., and Kriegstein, A. R. (2001). Neurons derived from radial glial cells establish radial units in neocortex. *Nature* 409, 714–720. doi: 10.1038/35055553

Noctor, S. C., Martínez-Cerdeño, V., Ivic, L., and Kriegstein, A. R. (2004). Cortical neurons arise in symmetric and asymmetric division zones and migrate through specific phases. *Nat. Neurosci.* 7, 136–144. doi: 10.1038/nn1172

Ogawa, M., Miyata, T., Nakajima, K., Yagyu, K., Seike, M., Ikenaka, K., et al. (1995). The reeler gene-associated antigen on Cajal-Retzius neurons is a crucial molecule for laminar organization of cortical neurons. *Neuron* 14, 899–912. doi: 10.1016/0896-6273(95)90329-1

Ohtaka-Maruyama, C., and Okado, H. (2015). Molecular pathways underlying projection neuron production and migration during cerebral cortical development. *Front. Neurosci.* 9:447. doi: 10.3389/fnins.2015.00447

Oinuma, I., Ishikawa, Y., Katoh, H., and Negishi, M. (2004). The Semaphorin 4D receptor Plexin-B1 is a GTPase activating protein for R-Ras. *Science* 305, 862–865. doi: 10.1126/science.1097545

Papakonstanti, E. A., Ridley, A. J., and Vanhaesebroeck, B. (2007). The p110delta isoform of PI 3-kinase negatively controls RhoA and PTEN. *EMBO J.* 26, 3050–3061. doi: 10.1038/sj.emboj.7601763

Paridaen, J. T., Wilsch-Bräuninger, M., and Huttner, W. B. (2013). Asymmetric inheritance of centrosome-associated primary cilium membrane directs ciliogenesis after cell division. *Cell* 155, 333–344. doi: 10.1016/j.cell.2013.08.060

Parker, S. S., Mandell, E. K., Hapak, S. M., Maskaykina, I. Y., Kusne, Y., Kim, J. Y., et al. (2013). Competing molecular interactions of aPKC isoforms regulate neuronal polarity. *Proc. Natl. Acad. Sci. U S A* 110, 14450–14455. doi: 10.1073/pnas.1301588110

Perez-Garcia, C. G., Tissir, F., Goffinet, A. M., and Meyer, G. (2004). Reelin receptors in developing laminated brain structures of mouse and human. *Eur. J. Neurosci.* 20, 2827–2832. doi: 10.1111/j.1460-9568.2004.03733.x

Petrie, R. J., Doyle, A. D., and Yamada, K. M. (2009). Random versus directionally persistent cell migration. *Nat. Rev. Mol. Cell Biol.* 10, 538–549. doi: 10.1038/nrm2729

Peyrollier, K., Hajduch, E., Gray, A., Litherland, G. J., Prescott, A. R., Leslie, N. R., et al. (2000). A role for the actin cytoskeleton in the hormonal and growth-factor-mediated activation of protein kinase B. *Biochem. J.* 352, 617–622. doi: 10.1042/0264-6021:3520617

Plant, P. J., Fawcett, J. P., Lin, D. C., Holdorf, A. D., Binns, K., Kulkarni, S., et al. (2003). A polarity complex of mPar-6 and atypical PKC binds, phosphorylates and regulates mammalian Lgl. *Nat. Cell Biol.* 5, 301–308. doi: 10.1038/ncb948

Pollen, A. A., Nowakowski, T. J., Chen, J., Retallack, H., Sandoval-Espinosa, C., Nicholas, C. R., et al. (2015). Molecular identity of human outer radial glia during cortical development. *Cell* 163, 55–67. doi: 10.1016/j.cell.2015.09.004

Polleux, F., Morrow, T., and Ghosh, A. (2000). Semaphorin 3A is a chemoattractant for cortical apical dendrites. *Nature* 404, 567–573. doi: 10.1038/35007001

Postiglione, M. P., and Hippenmeyer, S. (2014). Monitoring neurogenesis in the cerebral cortex: an update. *Fut. Neurol.* 9, 323–340. doi: 10.2217/fnl.14.18

Rakic, P. (1972). Mode of cell migration to the superficial layers of fetal monkey neocortex. *J. Comp. Neurol.* 145, 61–83. doi: 10.1002/cne.901450105

Rakic, P. (1974). Neurons in rhesus monkey visual cortex: systematic relation between time of origin and eventual disposition. *Science* 183, 425–427. doi: 10.1126/science.183.4123.425

Reichardt, L. F. (2006). Neurotrophin-regulated signalling pathways. *Philos. Trans. R. Soc. Lond. B Biol. Sci.* 361, 1545–1564. doi: 10.1098/rstb.2006.1894

Rodriguez-Viciana, P., Warne, P. H., Dhand, R., Vanhaesebroeck, B., Gout, I., Fry, M. J., et al. (1994). Phosphatidylinositol-3-OH kinase as a direct target of Ras. *Nature* 370, 527–532. doi: 10.1038/370527a0

Rossman, K. L., Der, C. J., and Sondek, J. (2005). GEF means go: turning on RHO GTPases with guanine nucleotide-exchange factors. *Nat. Rev. Mol. Cell Biol.* 6, 167–180. doi: 10.1038/nrm1587

Sapir, T., Sapoznik, S., Levy, T., Finkelshtein, D., Shmueli, A., Timm, T., et al. (2008). Accurate balance of the polarity kinase MARK2/Par-1 is required for proper cortical neuronal migration. *J. Neurosci.* 28, 5710–5720. doi: 10.1523/JNEUROSCI.0911-08.2008

Sapkota, G. P., Kieloch, A., Lizcano, J. M., Lain, S., Arthur, J. S., Williams, M. R., et al. (2001). Phosphorylation of the protein kinase mutated in Peutz-Jeghers cancer syndrome, LKB1/STK11, at Ser431 by p90(RSK) and cAMP-dependent protein kinase, but not its farnesylation at Cys(433), is essential for LKB1 to suppress cell growth. *J. Biol. Chem.* 276, 19469–19482. doi: 10.1074/jbc.M009953200

Sasaki, A. T., Chun, C., Takeda, K., and Firtel, R. A. (2004). Localized Ras signaling at the leading edge regulates PI3K, cell polarity, and directional cell movement. *J. Cell Biol.* 167, 505–518. doi: 10.1083/jcb.200406177

Sasaki, T., Sasaki, J., Sakai, T., Takasuga, S., and Suzuki, A. (2007). The physiology of phosphoinositides. *Biol. Pharm. Bull.* 30, 1599–1604. doi: 10.1248/bpb.30.1599

Schaar, B. T., Kinoshita, K., and McConnell, S. K. (2004). Doublecortin microtubule affinity is regulated by a balance of kinase and phosphatase activity at the leading edge of migrating neurons. *Neuron* 41, 203–213. doi: 10.1016/s0896-6273(03)00843-2

Schlesinger, A., Shelton, C. A., Maloof, J. N., Meneghini, M., and Bowerman, B. (1999). Wnt pathway components orient a mitotic spindle in the early *Caenorhabditis elegans* embryo without requiring gene transcription in the responding cell. *Genes Dev.* 13, 2028–2038. doi: 10.1101/gad.13.15.2028

Schwamborn, J. C., and Püschel, A. W. (2004). The sequential activity of the GTPases Rap1B and Cdc42 determines neuronal polarity. *Nat. Neurosci.* 7, 923–929. doi: 10.1038/nn1295

Sekine, K., Honda, T., Kawauchi, T., Kubo, K., and Nakajima, K. (2011). The outermost region of the developing cortical plate is crucial for both the switch of the radial migration mode and the Dab1-dependent "inside-out" lamination in the neocortex. *J. Neurosci.* 31, 9426–9439. doi: 10.1523/JNEUROSCI.0650-11.2011

Sekine, K., Kubo, K., and Nakajima, K. (2014). How does Reelin control neuronal migration and layer formation in the developing mammalian neocortex? *Neurosci. Res.* 86, 50–58. doi: 10.1016/j.neures.2014.06.004

Shelly, M., Cancedda, L., Heilshorn, S., Sumbre, G., and Poo, M. M. (2007). LKB1/STRAD promotes axon initiation during neuronal polarization. *Cell* 129, 565–577. doi: 10.1016/j.cell.2007.04.012

Shelly, M., Cancedda, L., Lim, B. K., Popescu, A. T., Cheng, P. L., Gao, H., et al. (2011). Semaphorin3A regulates neuronal polarization by suppressing axon formation and promoting dendrite growth. *Neuron* 71, 433–446. doi: 10.1016/j.neuron.2011.06.041

Shelly, M., and Poo, M. M. (2011). Role of LKB1-SAD/MARK pathway in neuronal polarization. *Dev. Neurobiol.* 71, 508–527. doi: 10.1002/dneu.20884

Shi, S. H., Jan, L. Y., and Jan, Y. N. (2003). Hippocampal neuronal polarity specified by spatially localized mPar3/mPar6 and PI 3-kinase activity. *Cell* 112, 63–75. doi: 10.1016/s0092-8674(02)01249-7

Shi, Y., and Massagué, J. (2003). Mechanisms of TGF-β signaling from cell membrane to the nucleus. *Cell* 113, 685–700. doi: 10.1016/s0092-8674(03)00432-x

Shitamukai, A., Konno, D., and Matsuzaki, F. (2011). Oblique radial glial divisions in the developing mouse neocortex induce self-renewing progenitors outside the germinal zone that resemble primate outer subventricular zone progenitors. *J. Neurosci.* 31, 3683–3695. doi: 10.1523/JNEUROSCI.4773-10.2011

Shitamukai, A., and Matsuzaki, F. (2012). Control of asymmetric cell division of mammalian neural progenitors. *Dev. Growth Differ.* 54, 277–286. doi: 10.1111/j.1440-169X.2012.01345.x

Srinivasan, S., Wang, F., Glavas, S., Ott, A., Hofmann, F., Aktories, K., et al. (2003). Rac and Cdc42 play distinct roles in regulating PI(3,4,5)P3 and polarity during neutrophil chemotaxis. *J. Cell Biol.* 160, 375–385. doi: 10.1083/jcb.200208179

Stancik, E. K., Navarro-Quiroga, I., Sellke, R., and Haydar, T. F. (2010). Heterogeneity in ventricular zone neural precursors contributes to neuronal fate diversity in the postnatal neocortex. *J. Neurosci.* 30, 7028–7036. doi: 10.1523/JNEUROSCI.6131-09.2010

Sun, Y., Fei, T., Yang, T., Zhang, F., Chen, Y. G., Li, H., et al. (2010). The suppression of CRMP2 expression by bone morphogenetic protein (BMP)-SMAD gradient signaling controls multiple stages of neuronal development. *J. Biol. Chem.* 285, 39039–39050. doi: 10.1074/jbc.M110.168351

Swiercz, J. M., Kuner, R., Behrens, J., and Offermanns, S. (2002). Plexin-B1 directly interacts with PDZ-RhoGEF/LARG to regulate RhoA and growth cone morphology. *Neuron* 35, 51–63. doi: 10.1016/s0896-6273(02)00750-x

Tabata, H., and Nakajima, K. (2003). Multipolar migration: the third mode of radial neuronal migration in the developing cerebral cortex. *J. Neurosci.* 23, 9996–10001.

Tabata, H., and Nakajima, K. (2008). Labeling embryonic mouse central nervous system cells by *in utero* electroporation. *Dev. Growth Differ.* 50, 507–511. doi: 10.1111/j.1440-169x.2008.01043.x

Tahirovic, S., Hellal, F., Neukirchen, D., Hindges, R., Garvalov, B. K., Flynn, K. C., et al. (2010). Rac1 regulates neuronal polarization through the WAVE complex. *J. Neurosci.* 30, 6930–6943. doi: 10.1523/JNEUROSCI.5395-09.2010

Taverna, E., Götz, M., and Huttner, W. B. (2014). The cell biology of neurogenesis: toward an understanding of the development and evolution of the neocortex. *Annu. Rev. Cell Dev. Biol.* 30, 465–502. doi: 10.1146/annurev-cellbio-101011-155801

Terabayashi, T., Itoh, T. J., Yamaguchi, H., Yoshimura, Y., Funato, Y., Ohno, S., et al. (2007). Polarity-regulating kinase partitioning-defective 1/microtubule affinity-regulating kinase 2 negatively regulates development of dendrites on hippocampal neurons. *J. Neurosci.* 27, 13098–13107. doi: 10.1523/JNEUROSCI.3986-07.2007

Thompson, B. J. (2013). Cell polarity: models and mechanisms from yeast, worms and flies. *Development* 140, 13–21. doi: 10.1242/dev.083634

Timm, T., von Kries, J. P., Li, X., Zempel, H., Mandelkow, E., and Mandelkow, E. M. (2011). Microtubule affinity regulating kinase activity in living neurons was examined by a genetically encoded fluorescence resonance energy transfer/fluorescence lifetime imaging-based biosensor: inhibitors with therapeutic potential. *J. Biol. Chem.* 286, 41711–41722. doi: 10.1074/jbc.M111.257865

Trepat, X., Chen, Z., and Jacobson, K. (2012). Cell migration. *Compr. Physiol.* 2, 2369–2392. doi: 10.1002/cphy.c110012

Tsai, J. W., Chen, Y., Kriegstein, A. R., and Vallee, R. B. (2005). LIS1 RNA interference blocks neural stem cell division, morphogenesis and motility at multiple stages. *J. Cell Biol.* 170, 935–945. doi: 10.1083/jcb.200505166

Tsai, J. W., and Vallee, R. B. (2011). Live microscopy of neural stem cell migration in brain slices. *Methods Mol. Biol.* 750, 131–142. doi: 10.1007/978-1-61779-145-1_9

Turing, A. M. (1990). The chemical basis of morphogenesis. *Bull. Math. Biol.* 52, 153–197; discussion 119–152. doi: 10.1007/BF02459572

Vaz, W. L. C., Goodsaid-Zalduondo, F., and Jacobson, K. (1984). Lateral diffusion of lipids and proteins in bilayer membranes. *FEBS Lett.* 174, 199–207. doi: 10.1016/0014-5793(84)81157-6

Voss, A. K., Britto, J. M., Dixon, M. P., Sheikh, B. N., Collin, C., Tan, S. S., et al. (2008). C3G regulates cortical neuron migration, preplate splitting and radial glial cell attachment. *Development* 135, 2139–2149. doi: 10.1242/dev.016725

Wang, F. (2009). The signaling mechanisms underlying cell polarity and chemotaxis. *Cold Spring Harb. Perspect. Biol.* 1:a002980. doi: 10.1101/cshperspect.a002980

Wang, F., Herzmark, P., Weiner, O. D., Srinivasan, S., Servant, G., and Bourne, H. R. (2002). Lipid products of PI(3)Ks maintain persistent cell polarity and directed motility in neutrophils. *Nat. Cell Biol.* 4, 513–518. doi: 10.1038/ncb810

Wang, T., Liu, Y., Xu, X. H., Deng, C. Y., Wu, K. Y., Zhu, J., et al. (2011). Lgl1 activation of rab10 promotes axonal membrane trafficking underlying neuronal polarization. *Dev. Cell* 21, 431–444. doi: 10.1016/j.devcel.2011.07.007

Wang, X., Tsai, J. W., LaMonica, B., and Kriegstein, A. R. (2011). A new subtype of progenitor cell in the mouse embryonic neocortex. *Nat. Neurosci.* 14, 555–561. doi: 10.1038/nn.2807

Wang, X., Tsai, J. W., Imai, J. H., Lian, W. N., Vallee, R. B., and Shi, S. H. (2009). Asymmetric centrosome inheritance maintains neural progenitors in the neocortex. *Nature* 461, 947–955. doi: 10.1038/nature08435

Watabe-Uchida, M., John, K. A., Janas, J. A., Newey, S. E., and Van Aelst, L. (2006). The Rac activator DOCK7 regulates neuronal polarity through local phosphorylation of stathmin/Op18. *Neuron* 51, 727–739. doi: 10.1016/j.neuron.2006.07.020

Wedlich-Soldner, R., and Li, R. (2003). Spontaneous cell polarization: undermining determinism. *Nat. Cell Biol.* 5, 267–270. doi: 10.1038/ncb0403-267

Wennekamp, S., Mesecke, S., Nédélec, F., and Hiiragi, T. (2013). A self-organization framework for symmetry breaking in the mammalian embryo. *Nat. Rev. Mol. Cell Biol.* 14, 452–459. doi: 10.1038/nrm3602

Whitman, M., Kaplan, D. R., Schaffhausen, B., Cantley, L., and Roberts, T. M. (1985). Association of phosphatidylinositol kinase activity with polyoma middle-T competent for transformation. *Nature* 315, 239–242. doi: 10.1038/315239a0

Witte, H., Neukirchen, D., and Bradke, F. (2008). Microtubule stabilization specifies initial neuronal polarization. *J. Cell Biol.* 180, 619–632. doi: 10.1083/jcb.200707042

Wu, P. R., Tsai, P. I., Chen, G. C., Chou, H. J., Huang, Y. P., Chen, Y. H., et al. (2011). DAPK activates MARK1/2 to regulate microtubule assembly, neuronal differentiation and tau toxicity. *Cell Death Differ.* 18, 1507–1520. doi: 10.1038/cdd.2011.2

Wynshaw-Boris, A., Pramparo, T., Youn, Y. H., and Hirotsune, S. (2010). Lissencephaly: mechanistic insights from animal models and potential therapeutic strategies. *Semin. Cell Dev. Biol.* 21, 823–830. doi: 10.1016/j.semcdb.2010.07.008

Xu, C., Funahashi, Y., Watanabe, T., Takano, T., Nakamuta, S., Namba, T., et al. (2015). Radial glial cell-neuron interaction directs axon formation at the opposite side of the neuron from the contact site. *J. Neurosci.* 35, 14517–14532. doi: 10.1523/jneurosci.1266-15.2015

Yamanaka, T., Horikoshi, Y., Suzuki, A., Sugiyama, Y., Kitamura, K., Maniwa, R., et al. (2001). PAR-6 regulates aPKC activity in a novel way and mediates cell-cell contact-induced formation of the epithelial junctional complex. *Genes Cells* 6, 721–731. doi: 10.1046/j.1365-2443.2001.00453.x

Yang, H. W., Shin, M. G., Lee, S., Kim, J. R., Park, W. S., Cho, K. H., et al. (2012). Cooperative activation of PI3K by Ras and Rho family small GTPases. *Mol. Cell* 47, 281–290. doi: 10.1016/j.molcel.2012.05.007

Yi, J. J., Barnes, A. P., Hand, R., Polleux, F., and Ehlers, M. D. (2010). TGF-β signaling specifies axons during brain development. *Cell* 142, 144–157. doi: 10.1016/j.cell.2010.06.010

Yingling, J., Youn, Y. H., Darling, D., Toyo-Oka, K., Pramparo, T., Hirotsune, S., et al. (2008). Neuroepithelial stem cell proliferation requires LIS1 for precise spindle orientation and symmetric division. *Cell* 132, 474–486. doi: 10.1016/j.cell.2008.01.026

Yoshimura, T., Arimura, N., and Kaibuchi, K. (2006a). Signaling networks in neuronal polarization. *J. Neurosci.* 26, 10626–10630. doi: 10.1523/jneurosci.3824-06.2006

Yoshimura, T., Arimura, N., Kawano, Y., Kawabata, S., Wang, S., and Kaibuchi, K. (2006b). Ras regulates neuronal polarity via the PI3-kinase/Akt/GSK-3beta/CRMP-2 pathway. *Biochem. Biophys. Res. Commun.* 340, 62–68. doi: 10.1016/j.bbrc.2005.11.147

Yoshimura, Y., Terabayashi, T., and Miki, H. (2010). Par1b/MARK2 phosphorylates kinesin-like motor protein GAKIN/KIF13B to regulate axon formation. *Mol. Cell. Biol.* 30, 2206–2219. doi: 10.1128/mcb.01181-09

Zheng, Y. (2001). Dbl family guanine nucleotide exchange factors. *Trends Biochem. Sci.* 26, 724–732. doi: 10.1016/s0968-0004(01)01973-9

Zong, H., Espinosa, J. S., Su, H. H., Muzumdar, M. D., and Luo, L. (2005). Mosaic analysis with double markers in mice. *Cell* 121, 479–492. doi: 10.1016/j.cell.2005.02.012

Conflict of Interest Statement: The authors declare that the research was conducted in the absence of any commercial or financial relationships that could be construed as a potential conflict of interest.

frontiers in Cellular Neuroscience

REVIEW
published: 05 December 2017
doi: 10.3389/fncel.2017.00384

Neural Progenitor Cell Polarity and Cortical Development

Yoko Arai[1] *and Elena Taverna*[2]*

[1]Centre for Interdisciplinary Research in Biology (CIRB), Collège de France, CNRS UMR 7241/INSERM U1050, PSL Research University, Paris, France, [2]Department of Evolutionary Genetics, Max Planck Institute for Evolutionary Anthropology (MPG), Leipzig, Germany

Neurons populating the cerebral cortex are generated during embryonic development from neural stem and progenitor cells in a process called neurogenesis. Neural stem and progenitor cells are classified into several classes based on the different location of mitosis (apical or basal) and polarity features (bipolar, monopolar and non-polar). The polarized architecture of stem cells is linked to the asymmetric localization of proteins, mRNAs and organelles, such as the centrosome and the Golgi apparatus (GA). Polarity affects stem cell function and allows stem cells to integrate environmental cues from distinct niches in the developing cerebral cortex. The crucial role of polarity in neural stem and progenitor cells is highlighted by the fact that impairment of cell polarity is linked to neurodevelopmental disorders such as Down syndrome, Fragile X syndrome, autism spectrum disorders (ASD) and schizophrenia.

Keywords: brain development, epithelial polarity, apical progenitors, basal progenitors, neural stem and progenitor cells, polarity, epithelial to mesenchymal transition (EMT), neurodevelopmental disorders

OPEN ACCESS

Edited by:
Annette Gaertner, Faculty of Medicine, KU Leuven, Belgium

Reviewed by:
Gonzalo Alvarez-Bolado, Universität Heidelberg, Germany
Froylan Calderon De Anda, University of Hamburg, Germany
Christian Lange, Technische Universität Dresden, Germany

***Correspondence:**
Elena Taverna
elena_taverna@eva.mpg.de

Received: *23 May 2017*
Accepted: *17 November 2017*
Published: *05 December 2017*

Citation:
Arai Y and Taverna E (2017) Neural Progenitor Cell Polarity and Cortical Development. Front. Cell. Neurosci. 11:384. doi: 10.3389/fncel.2017.00384

INTRODUCTION

The cerebral cortex is the center of higher cognitive functions. Neurons and glial cells populating the cerebral cortex arise sequentially during embryonic development from the division of neural stem and progenitor cells.

Polarity, that is the asymmetric spatial organization of cellular components and subcellular structures, is one of the main criteria used to classify and distinguish different types of stem and progenitor cells (Fietz and Huttner, 2011; Taverna et al., 2014). In actively dividing cells, such as neural stem cells, the polarity cues of the mother cells are used to generate different types of daughter cells: polarity is therefore instrumental in increasing cell type diversity (Fietz and Huttner, 2011). This is a crucial aspect in the central nervous system (CNS), particularly for cerebral cortex development and evolution, as enhanced cognitive functions in mammals are thought to arise from an increase in the diversity of cell types; in particular neural progenitor cell types in the developing cerebral cortex (Wilsch-Bräuninger et al., 2016; Arai and Pierani, 2014).

In this review article, we will focus on: (i) neural stem and progenitor cells and their polarity features; (ii) molecular mechanisms underlying neural stem and progenitor cell polarity; (iii) cell polarity and cell identity; and (iv) how the impairment of cellular polarity impacts cortical development.

NEUROGENESIS IN MAMMALS: CELL TYPES AND THEIR POLARITY FEATURES

Neural stem cells compared to neural progenitor cells differ with regards to their multipotency state: while neural stem cells are multipotent, neural progenitor cells are unipotent and fate restricted. They are classified based on several criteria, such as the location where they undergo mitosis, polarity features, and proliferation vs. differentiation potential (Taverna et al., 2014). Based on the location of their mitoses, neural stem and progenitor cells fall into two groups: apically-dividing and basally-dividing progenitor cells apical progenitors (APs) and basal progenitors (BPs), respectively (**Figure 1**; note that unless specified otherwise, the findings reported here refer to the developing dorsal telencephalon of rodents).

Apical Progenitors

The term apical stem and progenitor cells (APs) refer to cells undergoing mitosis at the apical surface of the ventricular zone (VZ; **Figure 1**). This category is comprised of cells which have a wide range of mitotic capacity and proliferation/differentiation potential. In the subsequent sections, we will describe the different AP subtypes in order from the most multipotent down to unipotent cells.

Neuroepithelial Cells

Before the onset of neurogenesis, the developing brain is formed mostly by neuroepithelial cells (NECs). They are highly polarized epithelial cells exhibiting apico-basal polarity (**Figure 1**). Their apical plasma membrane is integrated into the adherens junctional (AJ) belt and lines the lumen of the neural tube, which is filled with lipoprotein- and membrane particle-rich embryonic cerebrospinal fluid (Lehtinen et al., 2011). The AJs are cell junctions surrounding the cell, they are linked to the actin cytoskeleton and they separate the apical and the basal domain of NECs (for an historical perspective on AJs refer to Franke, 2009; and references therein; see also Farquhar and Palade, 1963; Takeichi, 1977; Stocker and Chenn, 2015). The basal plasma membrane of NECs spans the neuroepithelium and reaches the basal lamina, a rich source of extracellular molecules (Vaccarino et al., 1999a,b; Raballo et al., 2000; Götz and Huttner, 2005; Fietz et al., 2010). This highly dynamic and rich micro-environment provides a "stem cell niche" to the NECs during development (Lehtinen et al., 2011) that is crucial for the regulation of neurogenesis. NECs undergo interkinetic nuclear migration (INM), that is, they move their nuclei in the VZ in concert with the cell cycle: after completing mitosis at the ventricular surface, their nuclei undergo apical-to-basal migration during G1. After exiting from S-phase at the basal part of the VZ the nuclei undergo basal-to-apical migration, so that their successive mitosis will occur again at the ventricular surface (see Taverna and Huttner, 2010; Lee and Norden, 2013 and references therein). The NECs mitosis is confined to the ventricular surface, as the apical plasma membrane harbors the primary cilium that is nucleated by the centrosomes that also builds the mitotic spindle (see Taverna and Huttner, 2010; and references therein). NECs undergo proliferative divisions to expand the NEC pool. Ultimately, they develop into radial glial cells. Although it is not the main topics of this review article, it is important to mention that a proportion of NECs are embryonic neural stem cells from which adult neural stem cells originate (Furutachi et al., 2015). Using a strategy to follow the cell cycle progression of NECs, it has been shown that a subpopulation of NECs at early developmental stage gives rise to adult neural stem cells. This NECs subpopulation can be therefore considered as an embryonic neural stem cell (Furutachi et al., 2015). Embryonic neural stem cells slow down their cell-cycle speed allowing cells remain in a quiescence state. It still remains unclear how this embryonic neural stem cell population is determined during development and if adult neural stem cells can have also a radial glial origin.

Apical Radial Glial Cells

With the onset of neurogenesis, NECs differentiate into apical radial glial cells (aRGCs; Malatesta et al., 2003; Götz and Huttner, 2005). aRGCs are even more elongated than NECs. Their basolateral plasma membrane is divided in two sub-compartments: the apical and the basal process (**Figures 1**, **2**). The apical process is the portion of the basolateral plasma membrane residing in the VZ and it accommodates the nucleus during the different phases of INM. The basal process is the portion of the cell that traverses the sub-ventricular zone (SVZ) and the forming neuronal layers and reaches the basal lamina. Of note, as neurogenesis proceeds and neuronal layers are formed, the width of the cortical wall increases radially: therefore, the basal process elongates. The basal process functions as a guide for radial neuronal migration, allowing newborn excitatory cortical neurons to translocate from the place of birth to their final destination. In addition to providing a migratory scaffold for neurons in their journey to the cortical plate (CP), the basal process is a subcellular compartment involved in signaling and fate specification (Stenzel et al., 2014). Furthermore, live imaging has revealed that the basal process is a very dynamic entity, with the basal end changing from highly branched to club-like during cortical development (Yokota et al., 2010; **Figure 2**).

aRGCs have been extensively studied in the last decades and it is now clear that they contribute to neurogenesis mainly via the generation of a second type of neural progenitor cells: the BPs (Pontious et al., 2008; Kowalczyk et al., 2009). Interestingly, one of the main difference between apical and BPs is the absence of apical polarity cues in the latter.

Short Neural Precursors

Short neural precursors (SNPs, also known as apical intermediate progenitors) were first described in the mouse developing neocortex, where they exhibit several features in common with aRGCs, such as the bipolar morphology and the integration into the AJ belt (Gal et al., 2006; Tyler and Haydar, 2013). Unlike aRGCs, SNPs feature a basal process that does not traverse the neuronal layer, but it is confined to the VZ (**Figure 1**). A potentially similar cell type was reported to be present in the mouse ventral telencephalon, where aRGCs

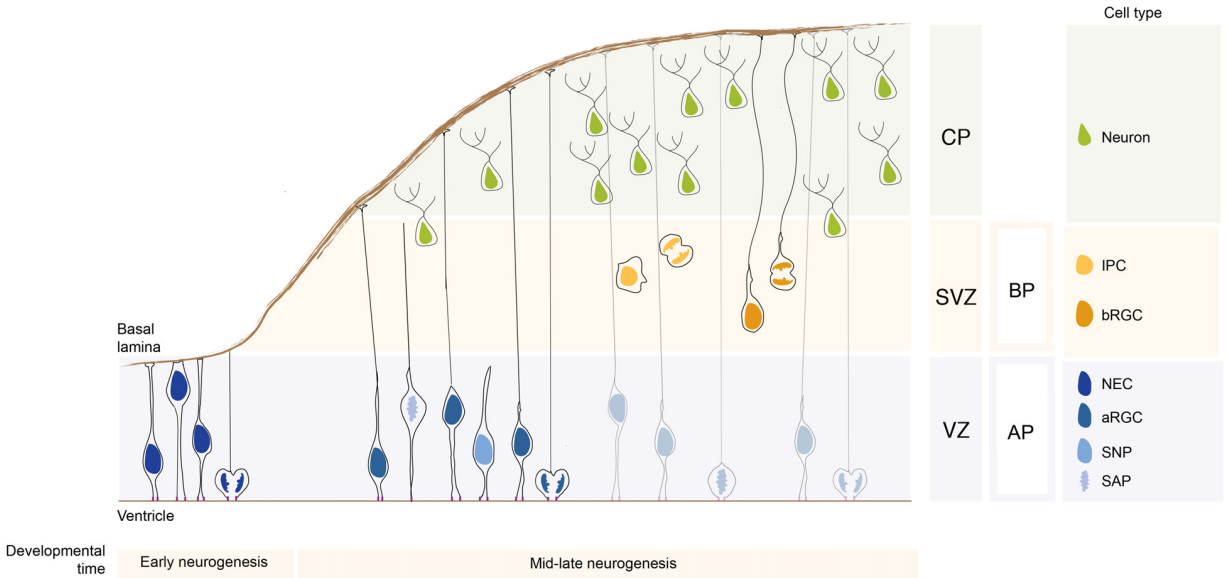

FIGURE 1 | Neural stem and progenitor cell types in the developing neocortex. During early neurogenesis, neuroepithelial cells (NECs) form the ventricular zone (VZ) and are responsible for the lateral expansion of the neocortex. During mid-late neurogenesis, apical progenitors (APs) divide and give rise to basal progenitors (BPs), which form a new proliferative zone, the subventricular zone (SVZ). The APs pool is mainly composed of apical radial glial cells (aRGCs) and a lower proportion of short neural precursors (SNPs) and sub-apical progenitors (SAPs). The BPs pool is composed by intermediate progenitor cells (IPCs) and basal radial glial cells (bRGCs). APs and BPs give rise to neurons that migrate basally and settle in the forming cortical plate (CP). The relative proportion of the different neural stem and progenitor cells changes greatly in species with different encephalyzation and gyrification. APs and BPs generate in a tightly controlled temporal order the pyramidal neurons populating the 6-layered neocortex (not depicted here for simplicity).

give rise to interneurons (Tan et al., 2016). As development proceed, the aRGCs in the ventral telencephalon grow radial glial fibers that no longer reach the basal lamina, but rather contact periventricular vessels (Tan et al., 2016). The vessel-anchored aRGCs undergo INM, divide apically (as SNPs do) and maintain the radial fiber throughout mitosis (unlike SNPs). Furthermore, a recent paper (Nowakowski et al., 2016) shows that in the human developing neocortex, during the mid-neurogenesis stage, aRGCs transform into "truncated" aRGCs, with a basal process that no longer reaches the basal lamina, but terminates in the depth of the cortical wall. Several interesting questions remain: are SNPs, vessel-anchored aRGCs in the mouse ventral telencephalon and truncated aRGCs in human related? Is the lack of basal attachment affecting the radial migration of the daughter cell after division? Is the daughter cell migrating for shorter distances?

Subapical Progenitors

Subapical progenitors (SAPs) were identified in the mouse ventral telencephalon and in the dorsal telencephalon of gyrencephalic species (Pilz et al., 2013). SAPs are anchored to the ventricle with an apical process. However, they undergo mitosis at a subapical location (Pilz et al., 2013; **Figure 1**). Most likely, in SAPs the centrosome is not docked at the apical plasma membrane and is therefore free to move basally to nucleate the mitotic spindle, as opposed to what happens in NECs where the centrosome is restricted to the apical side (see above).

Basal Progenitors

The term BPs indicates cells which undergo mitosis in the SVZ, the secondary germinal zone located basally compared to the VZ (**Figure 1**). BPs are generated by divisions of aRGCs and move basally via a process known as delamination. BPs are further divided into two classes: the intermediate progenitors (IPCs) and the basal radial glial cells (bRGCs).

Intermediate Progenitor Cells

IPCs represent the main class of BPs in rodents, as originally described independently by three different groups (Haubensak et al., 2004; Noctor et al., 2004; Miyata et al., 2004). IPCs are non-polar cells, as they lack both apical and basal polarity cues (**Figure 1**). The process of delamination of an IPC from the apical junctional belt very much resembles an epithelial-to-mesenchimal transition (EMT; Wilsch-Bräuninger et al., 2016), in which an epithelial cell gives rise to an unpolarized, highly motile cell (reviewed in Acloque et al., 2009; Itoh et al., 2013b). EMT is a process by which a polarized epithelial cell transforms into an unpolarized and highly motile mesenchymal cell. EMT occurs extensively during embryogenesis and it is crucial for gastrulation and neural crest formation. In pathological conditions, EMT is associated with in the initiation of metastasis and with cancer progression (Acloque et al., 2009; Itoh et al., 2013b; Wilsch-Bräuninger et al., 2016).

Basal Radial Glial Cells

Basal radial glial cells were first described in the developing neocortex of gyrencephalic species, namely in humans and

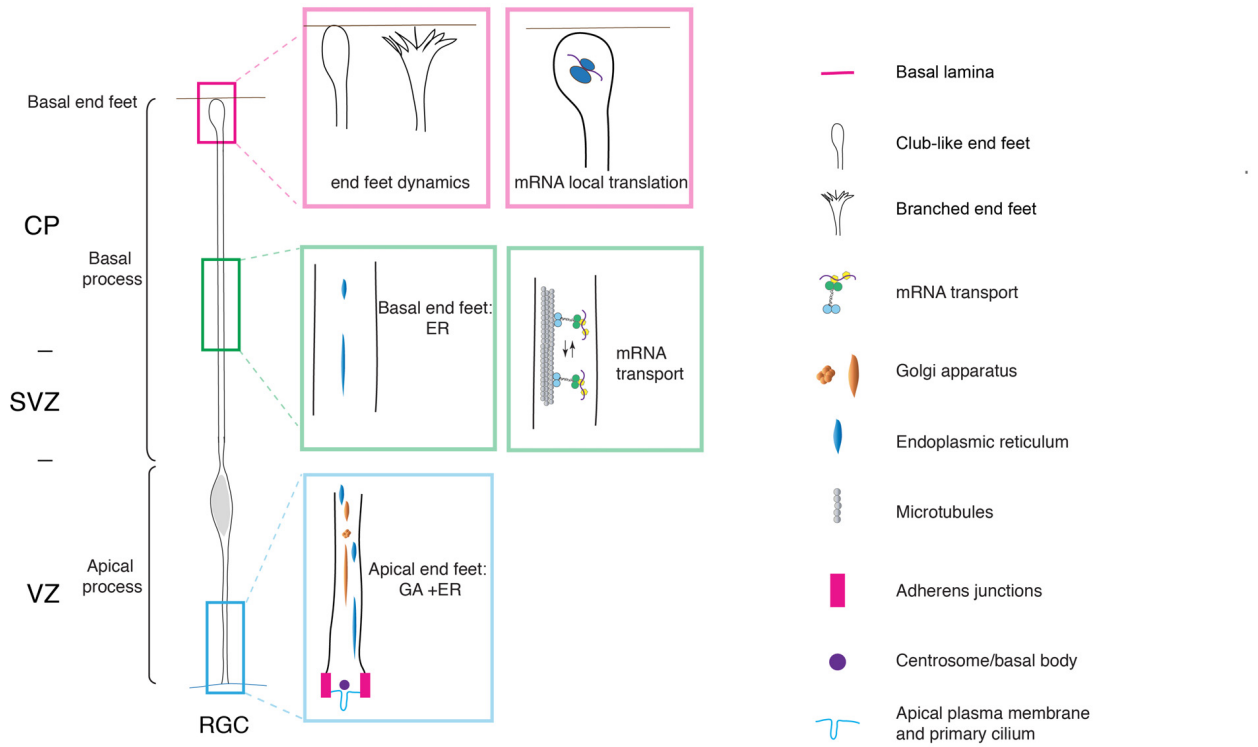

FIGURE 2 | Cell polarity and subcellular dynamics in apical radial glial cells. Apical radial glial cells (aRGCs) are highly polarized along their apico-basal axis. The adherens junctions maintain aRGC architecture and tissue integrity at the apical end feet. The basal process contacts the basal lamina with the basal end foot, where several mRNAs are transported and locally translated. The morphology of the basal end feet changes dynamically during neurogenesis. An organelle such as Golgi apparatus (GA) is distributed in the apical process exclusively. On the other hand, the endoplasmic reticulum (ER) is distributed globally in basal and apical processes. aRGC, apical radial glial cell; CP, cortical plate; SVZ, sub-ventricular zone and VZ, ventricular zone (the drawing is adapted from Taverna et al., 2016, licensed under a Creative Commons Attribution 4.0 International License).

ferrets, and were subsequently found, albeit at a much lower abundance, also in the lissencephalic developing rodent brain (Fietz et al., 2010; Hansen et al., 2010; Reillo et al., 2011; Wang et al., 2011; Reillo and Borrell, 2012; Sauerland et al., 2016). From an evolutionary perspective, the pool of bRGCs greatly expanded in humans and other gyrencephalic species, leading to the generation of two separate basal germinal zones: the inner and outer sub VZ (ISVZ and OSVZ, respectively; Smart et al., 2002). Recently, bRGCs have attracted great interest, as their abundance seems to correlate with the extent of brain expansion across species and with gyrification (Reillo et al., 2011; Kelava and Huttner, 2013). Several lines of evidence, including wide occurrence of bRGs in the marsupials and wallaby, suggest that bRGs might have been present in the ancestor of all mammals (Kelava et al., 2012; Sauerland et al., 2016). From a cell biological point of view, bRGCs are monopolar cells lacking an apical attachment (**Figure 1**). Interestingly, bRGCs still maintain an attachment to the basal lamina via a basal process (Hansen et al., 2010; Florio et al., 2015; Nowakowski et al., 2016). Functional manipulation has shown that the basal process is crucial for the maintenance of the proliferative capacity of bRGCs (Fietz et al., 2010). bRGCs appear to be a rather heterogeneous cell population, as shown by high resolution live imaging of the developing macaque neocortex (Betizeau et al., 2013). The heterogeneity was found to be both morphological and transcriptional. In particular, macaque bRGCs differ in term of presence vs. absence of apical-directed and basal-directed processes (Betizeau et al., 2013).

In summary, APs and BPs show striking differences in cell polarity. Evidences are accumulating that polarity influences the behavior of neural stem and progenitor cells during brain development.

MOLECULAR MECHANISMS OF NEURAL PROGENITOR CELL POLARITY

Key players of the maintenance of aRGCs polarity were found to be localized at the apical and basal end foot. The apical end foot of aRGCs is composed of the apical plasma membrane and the AJ belt (**Figure 2**). The apical plasma membrane represents a minor fraction of the total plasma membrane (1%–2%) and features the primary cilium that protrudes in the lumen of the ventricle and receives signals generated therein. The apical plasma membrane is delimited by the AJ, a subcellular structure

that plays a crucial role in maintaining aRGCs architecture and function at the apical pole. At the cellular level, the AJ separates the apical and basolateral plasma membrane, while at the tissue level it maintains the integration of aRGCs in the neuroepithelium, securing tissue integrity. Consistent with this notion, perturbation of AJ components and polarity proteins localized at the apical end foot results in severe changes in APs morphology and function (Chenn and Walsh, 2002, 2003; Cappello et al., 2006, 2012; Katayama et al., 2011; Durak et al., 2016).

Among the polarity proteins regulating aRGCs function, Cdc42 represents a very interesting case, as it regulates the structure and function of aRGCs both at the apical and the basal pole. Indeed, the loss of function of Cdc42 results in the gradual loss of AJs and retraction of the apical processes, ultimately leading to an increase in the generation of IPCs and in turn premature neuronal differentiation (Cappello et al., 2006). Interestingly, the manipulation of Arp2/3 complex, a downstream effector of Cdc42, shows a phenotype similar to the Cdc42 mutant mouse, with altered aRGCs polarity, defective adhesion and an increased number of IPCs. Arp2/3 is an actin nucleator producing branched actin networks, suggesting a possible involvement of the actin cytoskeleton in maintaining aRGCs polarity. The actin cytoskeleton was found to be involved in the G1 apical-to-basal phase of INM in aRGCs and the pharmacological inhibition of actin contractility led to an increase in basal mitoses in the developing mouse neocortex (Schenk et al., 2009), suggesting a role for actin in maintaining a progenitor pool. The actin cytoskeleton is also crucial for vesicle trafficking, exocytosis and endocytosis. The formation of AJs requires the transport of cadherins and apical polarity proteins from trans-Golgi networks to the plasma membrane (Sheen et al., 2004). Furthermore, endocytosis may allow for the recycling of cadherins and the dynamic remodeling of the AJs in response to a change in aRGCs activity and function.

Cdc42 was found to be localized at the aRGCs basal pole, where it regulates the dynamics of the basal end feet (Yokota et al., 2010). As revealed by live imaging experiments, the basal end foot is a very dynamic structure, with small protrusions emanating from the basal process shaft, possibly engaging in cell-to-cell communication between aRGCs. The expression of the Cdc42 dominant negative results in morphological changes in the basal end feet, with a concomitant reduction in inter-radial glia interaction (Yokota et al., 2010). Of note, and consistent with the fact that Arp2/3 is a downstream effector of Cdc42, Arp2/3 was found to have an effect on the dynamics of the basal process. Upon conditional ablation of the Arp2/3 complex in aRGCs, the dynamics of basal process extension is altered and this ultimately results in an overall change in organization, orientation and length of the basal process (Wang et al., 2016).

CELL POLARITY AND SUBCELLULAR DYNAMICS

The extreme elongation of aRGCs and the division of the basolateral plasma membrane in apical and basal process pose very interesting questions. Is the subcellular organization different between the apical and the basal process? How do intracellular organelles, in particular the biosynthetic pathway, help build the apical and basal process? Using a panel of morphological approaches, it was recently shown that in aRGCs the Golgi apparatus (GA) is strongly polarized along the cell's apico-basal axis, and is confined to the apical process (Taverna et al., 2016; **Figure 2**). In contrast, the endoplasmic reticulum (ER) was found to be present in both the apical and the basal process. The confinement of the GA to the apical process of aRGCs impacts on the composition of the apical and basal process plasma membrane: the basal process plasma membrane was found to contain almost exclusively ER-derived glycans, whereas the apical process contains both ER- and Golgi-derived glycans. These observations prompted the authors to propose that the biosynthesis of the apical and basal process could rely on two different mechanisms: the delivery to the apical process plasma membrane is thought to largely occur via the canonical biosynthetic route (ER → GA–plasma membrane), whereas the delivery to the basal process plasma membrane has been proposed to occur via an unconventional route that bypasses the GA (ER → plasma membrane; Taverna et al., 2016; **Figure 2**).

What underlies the confinement of Golgi-derived glycans to the apical process? In neurons, the axon initial segment confines proteins and lipids to the axonal plasma membrane, thus contributing to maintain the identity of the axo-dendritic compartments (Rasband, 2010). One can speculate that a similar macromolecular complex could be involved in creating a boundary between the apical and the basal process, creating a diffusion barrier for membrane-bound and cytoplasmic molecules.

The enrichment of ER-derived glycans in the basal process plasma membrane may provide a specific environment for neuronal migration. Several questions remain to be answered. Do the particular glycans present in the membrane of the aRGCs have an influence on the behavior of the IPCs? Are ER-derived glycans influencing the migratory kinetics of neurons in their long journey along the basal process? Do early-born neurons, generated from less elongated aRGCs through IPCs, containing less ER-derived glycans than late-born neurons, generated from more elongated aRGCs? What is the glycan composition of the bRGC basal process?

Another important question is if any other organelle is asymmetrically distributed between apical and basal process. Interestingly, recent data has shown that mitochondria undergo extensive morphological changes in the developing neural tube of chick and mouse embryos. This study showed that mitochondria are thick and short in interphase APs, while they are thin and strongly connected in networks in neuronal cells (Mils et al., 2015).

Not only intracellular organelles but also *mRNAs* are distributed in a highly-polarized fashion along the apico-basal axis in aRGCs, a finding that opens an exciting avenue in the field of neural stem cell biology. In particular, it was first demonstrated that the *CyclinD2 mRNA* is highly enriched at the basal end foot (Tsunekawa et al., 2012), where it is

locally translated into protein (Pilaz et al., 2016; **Figure 2**). This finding reveals that local translation can take place far away from the VZ, the germinal zone where the cell body and nucleus resides, even for proteins exerting their action in the nucleus, as is the case for CyclinD2. Possibly, the local translation of *CyclinD2* serves as a mechanism to strictly confine in space and time the function of CyclinD2 itself. Recently, FMRP were identified as the molecular motor responsible for *mRNA* transport to and localization at the basal end foot (Pilaz et al., 2016; Pilaz and Silver, 2017; **Figure 2**). The authors conducted an elegant and thorough characterization of the *mRNAs* localized at the basal end foot and showed that transcripts are locally translated (Pilaz et al., 2016). The local translation is somehow reminiscent of the local translation of *mRNA* in dendrites and axons (Bramham and Wells, 2007; Lin and Holt, 2008). In the case of neurons, transcripts can be translated on demand and in an activity-dependent manner. To push the parallel further, it would be extremely interesting to understand to which extent the transport and local translation of *mRNA* in the aRGCs basal end foot is regulated in a spatiotemporal manner by cell-to-cell interaction, either between neighbors aRGCs, or between aRGCs and the surrounding basal niche formed by meninges, basal lamina and Cajal-Retzius cells.

CELL BIOLOGICAL MECHANISMS OF APs TO BPs TRANSITION

Research in the last decade has focused on the fine cell biological mechanisms underlying APs-to-BPs fate transition and delamination (Acloque et al., 2009; Itoh et al., 2013b; Wilsch-Bräuninger et al., 2016), a process that very much resembles an epithelial-to-mesenchymal transition. Consistent with that parallel, the AJ components cadherins and catenins were found to have a role in the delamination of post-mitotic cell from aRGC and in the generation of bRGCs (Kadowaki et al., 2007; Stocker and Chenn, 2009, 2015; Itoh et al., 2013a; Martínez-Martínez et al., 2016). Conditional or focal reduction of N-Cadherin and αE-catenin, respectively, resulted in severe disruption in NECs structure and in turn affect cortical lamination (Kadowaki et al., 2007; Stocker and Chenn, 2009, 2015). Furthermore, a functional link between AJ complex and Wnt/β-catenin pro-proliferative signaling was observed in cortical progenitor cells (Hirabayashi et al., 2004; Stocker and Chenn, 2009).

One of the first detectable differences during fate transition and BP delamination is the change in the location of ciliogenesis. Cilia in APs are localized apically and they protrude in the ventricle from the apical plasma membrane, where they are tethered via the basal body (**Figure 2**). Elegant electron microscopy studies showed that in nascent BPs the cilium/basal body is located abventricularly, above the AJ belt (Wilsch-Bräuninger et al., 2012). The change in location of the cilium could favor cellular delamination either by favoring the "extrusion" of the apical plasma membrane from the AJ belt, or by increasing the endocytosis of the apical membrane components (though the two explanations are not mutually exclusive; Wilsch-Bräuninger et al., 2016). From a functional point of view, the relocation of the cilium could remove nascent BPs from the exposure to certain signals originating in the ventricle in favor of a signal originating in the VZ proper. An obvious question is if any other organelle undergoes reorganization upon fate transition. A good candidate in that respect is the GA, owing to the tight physical and functional link between the GA and the centrosome. Indeed, the GA in the aRGC's apical process was found to be neither perinuclear nor pericentrosomal. Interestingly, the GA was shown to become pericentrosomal in BPs upon delamination (Taverna et al., 2016). This data suggests that upon fate transition, the lack of polarity cues induces a reorganization at the centrosome-Golgi interface.

Another organelle involved in AP-to-BP fate transition is the ER. Recent findings show a role of the ER stress and unfolded protein response (UPR) in fate transition and neurogenesis (Laguesse et al., 2015). The authors focus on Elp3, a Elongator complex protein expressed in APs, where it maintains translational fidelity through the regulation of tRNA modification. Disruption of Elp3 decreases the speed of translation, promoting ER stress response and UPR upregulation. The knockout of Elp3 shows a progressive downregulation of UPR in APs and an amplification of IPCs leading to microcephaly (Laguesse et al., 2015). In a recent report, the authors also showed a role of Elp3 in the regulation of acetylation and membrane distribution of connexin-43 (Cx-43, Gja1; Laguesse et al., 2015). Cx-43 is a gap junction component expressed in APs where it plays a crucial role in cell-to-cell communication, INM and radial migration of neurons (Pearson et al., 2004; Sutor and Hagerty, 2005; Elias et al., 2007; Liu et al., 2010).

CELL POLARITY AND CELL FATE SPECIFICATION: RELEVANCE OF POLARITY FOR NEURAL STEM CELL FUNCTION

Cell polarity has important implications for neural stem cell fate for two main reasons: (i) the polarized organization allows progenitors to differentially respond to signals from the ventricle and/or from the basal pole; and (ii) the apical-basal polarity of aRGCs is the structural basis for their symmetric vs. asymmetric division, as defined by an equal vs. unequal distribution of cellular components to the daughter cells. Polarity is therefore instrumental in generating neural stem cell diversity.

Polarity and Differential Responses to Apical and Basal Niches

The organization of aRGCs along their apico-basal axis somehow mirrors the histological organization of the cortical wall. In that context, the basal and apical extensions of aRGCs could allow the aRGCs to sense, integrate and respond to different signals generated in different niches, either at the apical or at the basal pole. The apical plasma membrane delimits the ventricle, which is filled with cerebrospinal fluid, and contains different signaling molecules including morphogens (Lehtinen et al., 2011, 2013).

At the basal pole, the basal end feet are physically in contact with meninges, extracellular matrix and Cajal-Retzius cells which are sources for morphogens promoting proliferation and/or differentiation (Siegenthaler et al., 2009; Griveau et al., 2010). The basal end foot is therefore in a privileged position to sense and respond to basal extracellular signals. These signals could regulate local biological processes such as *mRNA* translation (Tsunekawa et al., 2012; Pilaz et al., 2016). It is interesting to note that due to their cellular organization, different neural stem cell subtypes have different level of access to signaling niches localized along the apico-basal axis of the cell and of the tissue. Since during development and evolution there is a progressive shift from apical to basal mitosis, it is tempting to speculate that this shift also represents a shift in signaling, with stem cells being regulated by basal and apical polarity cues during early development, and then being regulated mainly by basal polarity cues (Stenzel et al., 2014). This could also represent a way to restrict the expansion of the ventricular surface and favor the expansion of the basal part of the developing neocortex.

Polarity and Cell Division

The cell polarity of APs is the structural basis for symmetric vs. asymmetric division as it allows the equal vs. unequal distribution of cellular components to the daughter cells (Huttner and Kosodo, 2005). Several findings support the idea that the apical pole and subcellular structure therein are asymmetrically partitioned and influence cell fate. The apical plasma membrane constitutes a minor proportion of the total plasma membrane and can be either bisected or bypassed by the cleavage plane, resulting in only one daughter cell inheriting a portion of the apical plasma membrane (Kosodo et al., 2004). The cell inheriting the apical plasma membrane was reported to maintain proliferative potential (Kosodo et al., 2004). Not all the apical plasma membrane is partitioned based on the cleavage plane orientation: it was shown that the ciliary membrane, a specialized domain of the apical plasma membrane, is endocytosed at the onset of mitosis (Paridaen et al., 2013). The ciliary membrane preferentially associates with the mother centriole, is conserved throughout mitosis in association with one spindle pole and is asymmetrically inherited by one of the two daughter cells (Paridaen et al., 2013). The cell inheriting the ciliary membrane re-establishes the cilium faster and tend to maintain stem cell-like characteristics. These findings strongly suggest a role for the apical pole and subcellular structures therein in maintaining and influencing the choice between proliferation and differentiation.

It has also been shown that the basal process can be asymmetrically inherited by one of the two daughter cells, with the cell inheriting the basal process tending to maintain proliferative capacities (Konno et al., 2008; Shitamukai et al., 2011). How is the inheritance of the basal process linked to the choice between proliferation and differentiation? The inherited basal process could maintain aRGCs in a proliferative state thanks to the inheritance of the basal process-localized *mRNAs* and/or receptors for growth factors. Furthermore, data showed that both aRGCs and bRGCs are able to re-grow their basal process (Hansen et al., 2010; Shitamukai and Matsuzaki, 2012; Betizeau et al., 2013; Subramanian et al., 2017). What are the differences between an inherited vs. a regrown basal process? Is the re-growth of the basal process a mechanism to bypass the limitation imposed by the asymmetric inheritance of the basal process, so that both daughter cells are equally able to respond to extracellular signals? Is the re-grown basal process featuring different receptors compared to the inherited basal process? One might speculate that the newly delivered receptors in a re-grown basal process features different post-translational modifications and/or has a different desensitization status, allowing the two daughter cells to respond differentially to the same extracellular stimuli. Further research will be required to obtain a coherent picture on the interplay between polarity, asymmetric division and cell fate specification. It would also be extremely interesting to extend the pioneering work performed on aRGCs to other polarized progenitor cells, such as bRGCs, in order to understand to which extent similar cell biological principles are used in different cell types and how they act in generating neural stem cell diversity.

IMPAIRED CELL POLARITY AS A CAUSE OF NEURODEVELOPMENTAL DISORDERS

Neurodevelopmental defects comprise a substantial proportion of neuropsychiatric diseases and the general consensus is that they originate from early events in brain development (Feng et al., 2000; Bond et al., 2002; Chenn and Walsh, 2002; Tsai et al., 2005; Shu et al., 2006; Xie et al., 2007; Singh et al., 2010; Birnbaum et al., 2014). We here focus on neurodevelopmental disorders that are reported to be associated with polarity defects in neural stem and progenitor cells (Chenn and Walsh, 2003; Hirabayashi et al., 2004; Sheen et al., 2004; Mao et al., 2009; Katayama et al., 2011; Durak et al., 2015, 2016).

Down Syndrome

Down syndrome is the most common genetic cause of mental retardation. Patients diagnosed with Down syndrome showed an overall reduction of cerebrum gray matter volume (Weitzdoerfer et al., 2002) as well as a disorganized cortical lamination (Pinter et al., 2001). The reduction of Arp2/3 complex was reported in fetal Down syndrome brain and the conditional ablation of Arp2/3 complex in mice showed a reduction in neuronal number and highly disorganized cortical lamination (Wang et al., 2016). It would be important to understand to which extent the effects of Arp2/3 on the overall brain functions are due to the early effects of Arp2/3 on neural stem and progenitor cells, in particular on aRGCs (Tyler and Haydar, 2013).

Fragile X Syndrome and Autism Spectrum Disorders

Fragile-X syndrome (FXS) is the most common form of inherited intellectual disability and it is caused by mutations in *Fragile X Mental Retardation 1* (*FMR1*) gene. Loss-of-functions of FMR protein (FMRP) showed: (i) a switch from AP to BP fate, indicating the depletion of aRGCs pool (Saffary and Xie, 2011); (ii) defects in neuronal positioning due to the misregulation of

N-cadherin levels (La Fata et al., 2014); and (iii) early postnatal circuitry impairments possibly linked to abnormalities in the projection fibers (La Fata et al., 2014). Of interest, *FMR1* is also the most common single genetic cause of autism spectrum disorders (ASD; Hagerman et al., 2011; Bagni et al., 2012). In line with that, clinical crosstalk has been reported between FXS and ASD (Hagerman et al., 2011; Bagni et al., 2012). Considering the involvement of FMRP in *mRNA* transport in aRGCs (Pilaz et al., 2016; Pilaz and Silver, 2017), it would be interesting to understand if and how impaired *mRNA* transport in aRGCs contribute to the etiology of FXS and ASD (for an extensive discussion on the link between FXS, ASD, neural progenitors and cortical neurogenesis refer to Callan and Zarnescu, 2011; Packer, 2016; Marchetto et al., 2017 and references therein).

Ciliopathies

Ciliopathies are genetic disorders of ciliary structure or function. Joubert syndrome (JS) and related disorders are ciliopathies clinically characterized by ataxia, psychomotor delay and cognitive impairment (Cantagrel et al., 2008). The classical form of JS is caused by mutations in *Arl13b*, a cilia-specific small GTPase. *Arl13b* mutations lead to an inverted apico-basal polarity of aRGCs and impair the ability of primary cilia to convey extracellular signals such as insulin-like growth factor (Igf; Higginbotham et al., 2013). Igf is highly enriched in the CSF. It would be interesting to understand if the relocation of the primary cilium from the apical to the basolateral plasma membrane upon APs to BPs fate transition (Wilsch-Bräuninger et al., 2012) changes the degree of exposure to extracellular signals generated from the CSF.

Schizophrenia

Schizophrenia shares several common characteristics with ASD in term of behavioral, social and cognitive disturbances and also in term of genes implicated in the disease etiology (Carroll and Owen, 2009). *Disrupted In Schizophrenia* (*DISC1*) is a common susceptibility gene for those disorders and it is also associated with bipolar and mood disorders (Khanzada et al., 2017). Mutations in DISC1 gene lead to schizophrenic or depressive behavior (Clapcote et al., 2007; Mao et al., 2009; Dachtler et al., 2016). DISC1 is highly expressed in aRGCs during development and a knock-down of DISC1 showed a decreased proliferation of aRGCs and premature neurogenesis (Mao et al., 2009; De Rienzo et al., 2011; Ishizuka et al., 2011; Ye et al., 2017). The neuronal phenotypes observed are reminiscent of Cdc42 loss-of-functions (Yokota et al., 2010; Ishizuka et al., 2011). Consistent with that, DISC1 regulates aRGC proliferation through GSK3β, a downstream effector of Cdc42 (Clapcote et al., 2007; Ishizuka et al., 2011; Dachtler et al., 2016).

Taken together, these data suggest that alteration of aRGCs polarity can trigger neurodevelopmental and psychiatric disorders.

CONCLUDING REMARKS

In this review article, we discussed the polarity features of neural stem and progenitor cells in the developing cerebral cortex and their functional implications. Research in the last decades clearly showed that polarity affects neural stem and progenitor cells, including their architecture and shape, INM, proliferation vs. differentiation potential and asymmetric cell division. Nowadays concepts derived from work in mice are finally applied in an evolutionary perspective: one notable example is provided by aRGCs in humans, where their extreme elongation matches the massive growth of the cerebral cortex. In the future, it is likely that the functions of the basal process will receive increasing attention, both in aRGCs and bRGCs. Here are few questions that in our opinion deserve attention: which are the differences between a aRGC and a bRGC basal process? How is the growth of the basal process in a single RGC coordinated with the global tissue growth? Which is the role of intracellular traffic in the basal process elongation? How are the biological functions of the basal process (e.g., mRNA translation) affected by extracellular stimuli, and how are they coordinated with the rest of the cell? We are now witnessing a very exciting time, when thanks to several technological breakthroughs we can reasonably expect that several of these questions will be answered, leading to a better understanding of cerebral cortex development and evolution.

AUTHOR CONTRIBUTIONS

ET and YA wrote the manuscript.

ACKNOWLEDGMENTS

We thank Veronique Dubreuil, Nicola Maghelli, Jeanette Nardelli, Judith Paridaean and Jeremy Pulvers for their helpful comments and input on the manuscript.

REFERENCES

Acloque, H., Adams, M. S., Fishwick, K., Bronner-Fraser, M., and Nieto, M. A. (2009). Epithelial-mesenchymal transitions: the importance of changing cell state in development and disease. *J. Clin. Invest.* 119, 1438–1449. doi: 10.1172/jci38019

Arai, Y., and Pierani, A. (2014). Development and evolution of cortical fields. *Neurosci. Res.* 86, 66–76. doi: 10.1016/j.neures.2014.06.005

Bagni, C., Tassone, F., Neri, G., and Hagerman, R. (2012). Fragile X syndrome: causes, diagnosis, mechanisms, and therapeutics. *J. Clin. Invest.* 122, 4314–4322. doi: 10.1172/jci63141

Betizeau, M., Cortay, V., Patti, D., Pfister, S., Gautier, E., Bellemin-Ménard, A., et al. (2013). Precursor diversity and complexity of lineage relationships in the outer subventricular zone (OSVZ) of the primate. *Neuron* 80, 442–457. doi: 10.1016/j.neuron.2013.09.032

Birnbaum, R., Jaffe, A. E., Hyde, T. M., Kleinman, J. E., and Weinberger, D. R. (2014). Prenatal expression patterns of genes associated with neuropsychiatric disorders. *Am. J. Psychiatry* 171, 758–767. doi: 10.1176/appi.ajp.2014.13111452

Bond, J., Roberts, E., Mochida, G. H., Hampshire, D. J., Scott, S., Askham, J. M., et al. (2002). ASPM is a major determinant of cerebral cortical size. *Nat. Genet.* 32, 316–3120. doi: 10.1038/ng995

Bramham, C. R., and Wells, D. G. (2007). Dendritic mRNA: transport, translation and function. *Nat. Rev. Neurosci.* 8, 776–789. doi: 10.1038/nrn2150

Callan, M. A., and Zarnescu, D. C. (2011). Heads-up: new roles for the fragile X mental retardation protein in neural stem and progenitor cells. *Genesis* 49, 424–440. doi: 10.1002/dvg.20745

Cantagrel, V., Silhavy, J. L., Bielas, S. L., Swistun, D., Marsh, S. E., Marsh, S. E., et al. (2008). Mutations in the cilia gene ARL13B lead to the classical form of Joubert syndrome. *Am. J. Hum. Genet.* 83, 170–179. doi: 10.1016/j.ajhg.2008.06.023

Cappello, S., Attardo, A., Wu, X., Iwasato, T., Itohara, S., Wilsch-Bräuninger, M., et al. (2006). The Rho-GTPase cdc42 regulates neural progenitor fate at the apical surface. *Nat. Neurosci.* 9, 1099–1107. doi: 10.1038/nn1744

Cappello, S., Böhringer, C. R., Bergami, M., Conzelmann, K. K., Ghanem, A., Tomassy, G. S., et al. (2012). A radial glia-specific role of RhoA in double cortex formation. *Neuron* 73, 911–924. doi: 10.1016/j.neuron.2011.12.030

Carroll, L. S., and Owen, M. J. (2009). Genetic overlap between autism, schizophrenia and bipolar disorder. *Genome Med.* 1:102. doi: 10.1186/gm102

Chenn, A., and Walsh, C. A. (2002). Regulation of cerebral cortical size by control of cell cycle exit in neural precursors. *Science* 297, 365–369. doi: 10.1126/science.1074192

Chenn, A., and Walsh, C. A. (2003). Increased neuronal production, enlarged forebrains and cytoarchitectural distortions in β-catenin overexpressing transgenic mice. *Cereb. Cortex* 13, 599–606. doi: 10.1093/cercor/13.6.599

Clapcote, S. J., Lipina, T. V., Millar, J. K., Mackie, S., Christie, S., Ogawa, F., et al. (2007). Behavioral phenotypes of Disc1 missense mutations in mice. *Neuron* 54, 387–402. doi: 10.1016/j.neuron.2007.04.015

Dachtler, J., Elliott, C., Rodgers, R. J., Baillie, G. S., and Clapcote, S. J. (2016). Missense mutation in DISC1 C-terminal coiled-coil has GSK3β signaling and sex-dependent behavioral effects in mice. *Sci. Rep.* 6:18748. doi: 10.1038/srep18748

De Rienzo, G., Bishop, J. A., Mao, Y., Pan, L., Ma, T. P., Moens, C. B., et al. (2011). Disc1 regulates both β-catenin-mediated and noncanonical Wnt signaling during vertebrate embryogenesis. *FASEB J.* 25, 4184–4197. doi: 10.1096/fj.11-186239

Durak, O., de Anda, F. C., Singh, K. K., Leussis, M. P., Petryshen, T. L., Sklar, P., et al. (2015). Ankyrin-G regulates neurogenesis and Wnt signaling by altering the subcellular localization of β-catenin. *Mol. Psychiatry* 20, 388–397. doi: 10.1038/mp.2014.42

Durak, O., Gao, F., Kaeser-Woo, Y. J., Rueda, R., Martorell, A. J., Nott, A., et al. (2016). Chd8 mediates cortical neurogenesis via transcriptional regulation of cell cycle and Wnt signaling. *Nat. Neurosci.* 19, 1477–1488. doi: 10.1038/nn.4400

Elias, L. A., Wang, D. D., and Kriegstein, A. R. (2007). Gap junction adhesion is necessary for radial migration in the neocortex. *Nature* 448, 901–907. doi: 10.1038/nature06063

Farquhar, M. G., and Palade, G. E. (1963). Junctional complexes in various epithelia. *J. Cell Biol.* 17, 375–412. doi: 10.1083/jcb.17.2.375

Feng, Y., Olson, E. C., Stukenberg, P. T., Flanagan, L. A., Kirschner, M. W., and Walsh, C. A. (2000). LIS1 regulates CNS lamination by interacting with mNudE, a central component of the centrosome. *Neuron* 28, 665–679. doi: 10.1016/s0896-6273(00)00145-8

Fietz, S. A., and Huttner, W. B. (2011). Cortical progenitor expansion, self-renewal and neurogenesis—a polarized perspective. *Curr. Opin. Neurobiol.* 21, 23–35. doi: 10.1016/j.conb.2010.10.002

Fietz, S. A., Kelava, I., Vogt, J., Wilsch-Bräuninger, M., Stenzel, D., Fish, J. L., et al. (2010). OSVZ progenitors of human and ferret neocortex are epithelial-like and expand by integrin signaling. *Nat. Neurosci.* 13, 690–699. doi: 10.1038/nn.2553

Florio, M., Albert, M., Taverna, E., Namba, T., Brandl, H., Lewitus, E., et al. (2015). Human-specific gene ARHGAP11B promotes basal progenitor amplification and neocortex expansion. *Science* 347, 1465–1470. doi: 10.1126/science.aaa1975

Franke, W. W. (2009). Discovering the molecular components of intercellular junctions—a historical view. *Cold Spring Harb. Perspect. Biol.* 1:a003061. doi: 10.1101/cshperspect.a003061

Furutachi, S., Miya, H., Watanabe, T., Kawai, H., Yamasaki, N., Harada, Y., et al. (2015). Slowly dividing neural progenitors are an embryonic origin of adult neural stem cells. *Nat. Neurosci.* 18, 657–665. doi: 10.1038/nn.3989

Gal, J. S., Morozov, Y. M., Ayoub, A. E., Chatterjee, M., Rakic, P., and Haydar, T. F. (2006). Molecular and morphological heterogeneity of neural precursors in the mouse neocortical proliferative zones. *J. Neurosci.* 26, 1045–1056. doi: 10.1523/jneurosci.4499-05.2006

Götz, M., and Huttner, W. B. (2005). The cell biology of neurogenesis. *Nat. Rev. Mol. Cell Biol.* 6, 777–788. doi: 10.1038/nrm1739

Griveau, A., Borello, U., Causeret, F., Tissir, F., Boggetto, N., Karaz, S., et al. (2010). A novel role for Dbx1-derived Cajal-Retzius cells in early regionalization of the cerebral cortical neuroepithelium. *PLoS Biol.* 8:e1000440. doi: 10.1371/journal.pbio.1000440

Hagerman, R., Au, J., and Hagerman, P. (2011). FMR1 premutation and full mutation molecular mechanisms related to autism. *J. Neurodev. Disord.* 3, 211–224. doi: 10.1007/s11689-011-9084-5

Hansen, D. V., Lui, J. H., Parker, P. R., and Kriegstein, A. R. (2010). Neurogenic radial glia in the outer subventricular zone of human neocortex. *Nature* 464, 554–561. doi: 10.1038/nature08845

Haubensak, W., Attardo, A., Denk, W., and Huttner, W. B. (2004). Neurons arise in the basal neuroepithelium of the early mammalian telencephalon: a major site of neurogenesis. *Proc. Natl. Acad. Sci. U S A* 101, 3196–3201. doi: 10.1073/pnas.0308600100

Higginbotham, H., Guo, J., Yokota, Y., Umberger, N. L., Su, C. Y., Li, J., et al. (2013). Arl13b-regulated cilia activities are essential for polarized radial glial scaffold formation. *Nat. Neurosci.* 16, 1000–1007. doi: 10.1038/nn.3451

Hirabayashi, Y., Itoh, Y., Tabata, H., Nakajima, K., Akiyama, T., Masuyama, N., et al. (2004). The Wnt/β-catenin pathway directs neuronal differentiation of cortical neural precursor cells. *Development* 131, 2791–2801. doi: 10.1242/dev.01165

Huttner, W. B., and Kosodo, Y. (2005). Symmetric versus asymmetric cell division during neurogenesis in the developing vertebrate central nervous system. *Curr. Opin. Cell Biol.* 17, 648–657. doi: 10.1016/j.ceb.2005.10.005

Ishizuka, K., Kamiya, A., Oh, E. C., Kanki, H., Seshadri, S., Robinson, J. F., et al. (2011). DISC1-dependent switch from progenitor proliferation to migration in the developing cortex. *Nature* 473, 92–96. doi: 10.1038/nature09859

Itoh, Y., Moriyama, Y., Hasegawa, T., Endo, T. A., Toyoda, T., and Gotoh, Y. (2013a). Scratch regulates neuronal migration onset via an epithelial-mesenchymal transition-like mechanism. *Nat. Neurosci.* 16, 416–425. doi: 10.1038/nn.3336

Itoh, Y., Tyssowski, K., and Gotoh, Y. (2013b). Transcriptional coupling of neuronal fate commitment and the onset of migration. *Curr. Opin. Neurobiol.* 23, 957–964. doi: 10.1016/j.conb.2013.08.003

Kadowaki, M., Nakamura, S., Machon, O., Krauss, S., Radice, G. L., and Takeichi, M. (2007). N-cadherin mediates cortical organization in the mouse brain. *Dev. Biol.* 304, 22–33. doi: 10.1016/j.ydbio.2006.12.014

Katayama, K., Melendez, J., Baumann, J. M., Leslie, J. R., Chauhan, B. K., Nemkul, N., et al. (2011). Loss of RhoA in neural progenitor cells causes the disruption of adherens junctions and hyperproliferation. *Proc. Natl. Acad. Sci. U S A* 108, 7607–7612. doi: 10.1073/pnas.1101347108

Kelava, I., and Huttner, W. B. (2013). "Neural progenitors and evolution of mammalian neocortex," in *Stem Cells*, eds F. Calegari and C. Waskow (Enfield, NH: Science Publishers, Edenbridge Ltd., CRC Press/Taylor and Francis Group).

Kelava, I., Reillo, I., Murayama, A. Y., Kalinka, A. T., Stenzel, D., Tomancak, P., et al. (2012). Abundant occurrence of basal radial glia in the subventricular zone of embryonic neocortex of a lissencephalic primate, the common marmoset *Callithrix jacchus*. *Cereb. Cortex* 22, 469–481. doi: 10.1093/cercor/bhr301

Khanzada, N. S., Butler, M. G., and Manzardo, A. M. (2017). GeneAnalytics pathway analysis and genetic overlap among autism spectrum disorder, bipolar disorder and schizophrenia. *Int. J. Mol. Sci.* 18:E527. doi: 10.3390/ijms18030527

Konno, D., Shioi, G., Shitamukai, A., Mori, A., Kiyonari, H., Miyata, T., et al. (2008). Neuroepithelial progenitors undergo LGN-dependent planar divisions to maintain self-renewability during mammalian neurogenesis. *Nat. Cell Biol.* 10, 93–101. doi: 10.1038/ncb1673

Kosodo, Y., Röper, K., Haubensak, W., Marzesco, A.-M., Corbeil, D., and Huttner, W. B. (2004). Asymmetric distribution of the apical plasma membrane during neurogenic divisions of mammalian neuroepithelial cells. *EMBO J.* 23, 2314–2324. doi: 10.1038/sj.emboj.7600223

Kowalczyk, T., Pontious, A., Englund, C., Daza, R. A., Bedogni, F., Hodge, R., et al. (2009). Intermediate neuronal progenitors (basal progenitors) produce pyramidal-projection neurons for all layers of cerebral cortex. *Cereb. Cortex* 19, 2439–2450. doi: 10.1093/cercor/bhn260

La Fata, G., Gärtner, A., Domínguez-Iturza, N., Dresselaers, T., Dawitz, J., Poorthuis, R. B., et al. (2014). FMRP regulates multipolar to bipolar transition affecting neuronal migration and cortical circuitry. *Nat. Neurosci.* 17, 1693–1700. doi: 10.1038/nn.3870

Laguesse, S., Creppe, C., Nedialkova, D. D., Prévot, P. P., Borgs, L., Huysseune, S., et al. (2015). A dynamic unfolded protein response contributes to the control of cortical neurogenesis. *Dev. Cell* 35, 553–567. doi: 10.1016/j.devcel.2015.11.005

Lee, H. O., and Norden, C. (2013). Mechanisms controlling arrangements and movements of nuclei in pseudostratified epithelia. *Trends Cell Biol.* 23, 141–150. doi: 10.1016/j.tcb.2012.11.001

Lehtinen, M. K., Bjornsson, C. S., Dymecki, S. M., Gilbertson, R. J., Holtzman, D. M., and Monuki, E. S. (2013). The choroid plexus and cerebrospinal fluid: emerging roles in development, disease, and therapy. *J. Neurosci.* 33, 17553–17559. doi: 10.1523/JNEUROSCI.3258-13.2013

Lehtinen, M. K., Zappaterra, M. W., Chen, X., Yang, Y. J., Hill, A. D., Lun, A. D., et al. (2011). The cerebrospinal fluid provides a proliferative niche for neural progenitor cells. *Neuron* 69, 893–905. doi: 10.1016/j.neuron.2011.01.023

Lin, A. C., and Holt, C. E. (2008). Function and regulation of local axonal translation. *Curr. Opin. Neurobiol.* 18, 60–68. doi: 10.1016/j.conb.2008.05.004

Liu, X., Hashimoto-Torii, K., Torii, M., Ding, C., and Rakic, P. (2010). Gap junctions/hemichannels modulate interkinetic nuclear migration in the forebrain precursors. *J. Neurosci.* 30, 4197–4209. doi: 10.1523/JNEUROSCI.4187-09.2010

Malatesta, P., Hack, M. A., Hartfuss, E., Kettenmann, H., Klinkert, W., Kirchhoff, F., et al. (2003). Neuronal or glial progeny: regional differences in radial glia fate. *Neuron* 37, 751–764. doi: 10.1016/S0896-6273(03)00116-8

Mao, Y., Ge, X., Frank, C. L., Madison, J. M., Koehler, A. N., Doud, M. K., et al. (2009). Disrupted in schizophrenia 1 regulates neuronal progenitor proliferation via modulation of GSK3β/β-catenin signaling. *Cell* 136, 1017–1031. doi: 10.1016/j.cell.2008.12.044

Marchetto, M. C., Belinson, H., Tian, Y., Freitas, B. C., Fu, C., Vadodaria, K., et al. (2017). Altered proliferation and networks in neural cells derived from idiopathic autistic individuals. *Mol. Psychiatry* 22, 820–835. doi: 10.1038/mp.2016.95

Martínez-Martínez, M. Á., De Juan Romero, C., Fernández, V., Cárdenas, A., Götz, M., and Borrell, V. (2016). A restricted period for formation of outer subventricular zone defined by Cdh1 and Trnp1 levels. *Nat. Commun.* 7:11812. doi: 10.1038/ncomms11812

Mils, V., Bosch, S., Roy, J., Bel-Vialar, S., Belenguer, P., Pituello, F., et al. (2015). Mitochondrial reshaping accompanies neural differentiation in the developing spinal cord. *PLoS One* 10:e0128130. doi: 10.1371/journal.pone.0128130

Miyata, T., Kawaguchi, A., Saito, K., Kawano, M., Muto, T., and Ogawa, M. (2004). Asymmetric production of surface-dividing and non-surface-dividing cortical progenitor cells. *Development* 131, 3133–3145. doi: 10.1242/dev.01173

Noctor, S. C., Martínez-Cerdeño, V., Ivic, L., and Kriegstein, A. R. (2004). Cortical neurons arise in symmetric and asymmetric division zones and migrate through specific phases. *Nat. Neurosci.* 7, 136–144. doi: 10.1038/nn1172

Nowakowski, T. J., Pollen, A. A., Sandoval-Espinosa, C., and Kriegstein, A. R. (2016). Transformation of the radial glia scaffold demarcates two stages of human cerebral cortex development. *Neuron* 91, 1219–1227. doi: 10.1016/j.neuron.2016.09.005

Packer, A. (2016). Neocortical neurogenesis and the etiology of autism spectrum disorder. *Neurosci. Biobehav. Rev.* 64, 185–195. doi: 10.1016/j.neubiorev.2016.03.002

Paridaen, J. T., Wilsch-Bräuninger, M., and Huttner, W. B. (2013). Asymmetric inheritance of centrosome-associated primary cilium membrane directs ciliogenesis after cell division. *Cell* 155, 333–344. doi: 10.1016/j.cell.2013.08.060

Pearson, R. A., Catsicas, M., Becker, D. L., Bayley, P., Lüneborg, N. L., and Mobbs, P. (2004). Ca^{2+} signalling and gap junction coupling within and between pigment epithelium and neural retina in the developing chick. *Eur. J. Neurosci.* 19, 2435–2445. doi: 10.1111/j.0953-816x.2004.03338.x

Pilaz, L. J., Lennox, A. L., Rouanet, J. P., and Silver, D. L. (2016). Dynamic mRNA transport and local translation in radial glial progenitors of the developing brain. *Curr. Biol.* 26, 3383–3392. doi: 10.1016/j.cub.2016.10.040

Pilaz, L. J., and Silver, D. L. (2017). Moving messages in the developing brain-emerging roles for mRNA transport and local translation in neural stem cells. *FEBS Lett.* 591, 1526–1539. doi: 10.1002/1873-3468.12626

Pilz, G. A., Shitamukai, A., Reillo, I., Pacary, E., Schwausch, J., Stahl, R., et al. (2013). Amplification of progenitors in the mammalian telencephalon includes a new radial glial cell type. *Nat. Commun.* 4:2125. doi: 10.1038/ncomms3125

Pinter, J. D., Eliez, S., Schmitt, J. E., Capone, G. T., and Reiss, A. L. (2001). Neuroanatomy of Down's syndrome: a high-resolution MRI study. *Am. J. Psychiatry* 158, 1659–1665. doi: 10.1176/appi.ajp.158.10.1659

Pontious, A., Kowalczyk, T., Englund, C., and Hevner, R. F. (2008). Role of intermediate progenitor cells in cerebral cortex development. *Dev. Neurosci.* 30, 24–32. doi: 10.1159/000109848

Raballo, R., Rhee, J., Lyn-Cook, R., Leckman, J. F., Schwartz, M. L., and Vaccarino, F. M. (2000). Basic fibroblast growth factor (Fgf2) is necessary for cell proliferation and neurogenesis in the developing cerebral cortex. *J. Neurosci.* 20, 5012–5023.

Rasband, M. N. (2010). The axon initial segment and the maintenance of neuronal polarity. *Nat. Rev. Neurosci.* 11, 552–562. doi: 10.1038/nrn2852

Reillo, I., and Borrell, V. (2012). Germinal zones in the developing cerebral cortex of ferret: ontogeny, cell cycle kinetics, and diversity of progenitors. *Cereb. Cortex* 22, 2039–2054. doi: 10.1093/cercor/bhr284

Reillo, I., de Juan Romero, C., García-Cabezas, M. Á., and Borrell, V. (2011). A role for intermediate radial glia in the tangential expansion of the mammalian cerebral cortex. *Cereb. Cortex* 21, 1674–1694. doi: 10.1093/cercor/bhq238

Saffary, R., and Xie, Z. (2011). FMRP regulates the transition from radial glial cells to intermediate progenitor cells during neocortical development. *J. Neurosci.* 31, 1427–1439. doi: 10.1523/JNEUROSCI.4854-10.2011

Sauerland, C., Menzies, B. R., Glatzle, M., Seeger, J., Renfree, M. B., and Fietz, S. A. (2016). The basal radial glia occurs in marsupials and underlies the evolution of an expanded neocortex in therian mammals. *Cereb. Cortex* doi: 10.1093/cercor/bhw360 [Epub ahead of print].

Schenk, J., Wilsch-Bräuninger, M., Calegari, F., and Huttner, W. B. (2009). Myosin II is required for interkinetic nuclear migration of neural progenitors. *Proc. Natl. Acad. Sci. U S A* 106, 16487–16492. doi: 10.1073/pnas.0908928106

Sheen, V. L., Ganesh, V. S., Topcu, M., Sebire, G., Bodell, A., Hill, R. S., et al. (2004). Mutations in ARFGEF2 implicate vesicle trafficking in neural progenitor proliferation and migration in the human cerebral cortex. *Nat. Genet.* 36, 69–76. doi: 10.1038/ng1276

Shitamukai, A., Konno, D., and Matsuzaki, F. (2011). Oblique radial glial divisions in the developing mouse neocortex induce self-renewing progenitors outside the germinal zone that resemble primate outer subventricular zone progenitors. *J. Neurosci.* 31, 3683–3695. doi: 10.1523/JNEUROSCI.4773-10.2011

Shitamukai, A., and Matsuzaki, F. (2012). Control of asymmetric cell division of mammalian neural progenitors. *Dev. Growth Differ.* 54, 277–286. doi: 10.1111/j.1440-169x.2012.01345.x

Shu, T., Tseng, H. C., Sapir, T., Stern, P., Zhou, Y., Sanada, K., et al. (2006). Doublecortin-like kinase controls neurogenesis by regulating mitotic spindles and M phase progression. *Neuron* 49, 25–39. doi: 10.1016/j.neuron.2005.10.039

Siegenthaler, J. A., Ashique, A. M., Zarbalis, K., Patterson, K. P., Hecht, J. H., Kane, M. A., et al. (2009). Retinoic acid from the meninges regulates cortical neuron generation. *Cell* 139, 597–609. doi: 10.1016/j.cell.2009.10.004

Singh, K. K., Ge, X., Mao, Y., Drane, L., Meletis, K., Samuels, B. A., et al. (2010). Dixdc1 is a critical regulator of DISC1 and embryonic cortical development. *Neuron* 67, 33–48. doi: 10.1016/j.neuron.2010.06.002

Smart, I. H., Dehay, C., Giroud, P., Berland, M., and Kennedy, H. (2002). Unique morphological features of the proliferative zones and postmitotic compartments of the neural epithelium giving rise to striate and extrastriate cortex in the monkey. *Cereb. Cortex* 12, 37–53. doi: 10.1093/cercor/12.1.37

Stenzel, D., Wilsch-Bräuninger, M., Wong, F. K., Heuer, H., and Huttner, W. B. (2014). Integrin αvβ3 and thyroid hormones promote expansion of progenitors in embryonic neocortex. *Development* 141, 795–806. doi: 10.1242/dev.101907

Stocker, A. M., and Chenn, A. (2009). Focal reduction of αE-catenin causes premature differentiation and reduction of β-catenin signaling during cortical development. *Dev. Biol.* 328, 66–77. doi: 10.1016/j.ydbio.2009.01.010

Stocker, A. M., and Chenn, A. (2015). The role of adherens junctions in the developing neocortex. *Cell Adh. Migr.* 9, 167–174. doi: 10.1080/19336918.2015.1027478

Subramanian, L., Bershteyn, M., Paredes, M. F., and Kriegstein, A. R. (2017). Dynamic behaviour of human neuroepithelial cells in the developing forebrain. *Nat. Commun.* 8:14167. doi: 10.1038/ncomms14167

Sutor, B., and Hagerty, T. (2005). Involvement of gap junctions in the development of the neocortex. *Biochim. Biophys. Acta* 1719, 59–68. doi: 10.1016/j.bbamem.2005.09.005

Takeichi, M. (1977). Functional correlation between cell adhesive properties and some cell surface proteins. *J. Cell Biol.* 75, 464–474. doi: 10.1083/jcb.75.2.464

Tan, X., Liu, W. A., Zhang, X. J., Shi, W., Ren, S. Q., Li, Z., et al. (2016). Vascular influence on ventral telencephalic progenitors and neocortical interneuron production. *Dev. Cell* 36, 624–638. doi: 10.1016/j.devcel.2016.02.023

Taverna, E., Götz, M., and Huttner, W. B. (2014). The cell biology of neurogenesis: toward an understanding of the development and evolution of the neocortex. *Annu. Rev. Cell Dev. Biol.* 30, 465–502. doi: 10.1146/annurev-cellbio-101011-155801

Taverna, E., and Huttner, W. B. (2010). Neural progenitor nuclei IN Motion. *Neuron* 67, 906–914. doi: 10.1016/j.neuron.2010.08.027

Taverna, E., Mora-Bermúdez, F., Strzyz, P. J., Florio, M., Icha, J., Haffner, C., et al. (2016). Non-canonical features of the Golgi apparatus in bipolar epithelial neural stem cells. *Sci. Rep.* 6:21206. doi: 10.1038/srep21206

Tsai, J. W., Chen, Y., Kriegstein, A. R., and Vallee, R. B. (2005). LIS1 RNA interference blocks neural stem cell division, morphogenesis, and motility at multiple stages. *J. Cell Biol.* 170, 935–945. doi: 10.1083/jcb.200505166

Tsunekawa, Y., Britto, J. M., Takahashi, M., Polleux, F., Tan, S. S., and Osumi, N. (2012). Cyclin D2 in the basal process of neural progenitors is linked to non-equivalent cell fates. *EMBO J.* 31, 1879–1892. doi: 10.1038/emboj.2012.43

Tyler, W. A., and Haydar, T. F. (2013). Multiplex genetic fate mapping reveals a novel route of neocortical neurogenesis, which is altered in the Ts65Dn mouse model of Down syndrome. *J. Neurosci.* 33, 5106–5119. doi: 10.1523/JNEUROSCI.5380-12.2013

Vaccarino, F. M., Schwartz, M. L., Raballo, R., Nilsen, J., Rhee, J., Zhou, M., et al. (1999a). Changes in cerebral cortex size are governed by fibroblast growth factor during embryogenesis. *Nat. Neurosci.* 2, 246–253. doi: 10.1038/6350

Vaccarino, F. M., Schwartz, M. L., Raballo, R., Rhee, J., and Lyn-Cook, R. (1999b). Fibroblast growth factor signaling regulates growth and morphogenesis at multiple steps during brain development. *Curr. Top Dev. Biol.* 46, 179–200. doi: 10.1016/s0070-2153(08)60329-4

Wang, P. S., Chou, F. S., Ramachandran, S., Xia, S., Chen, H. Y., Guo, F., et al. (2016). Crucial roles of the Arp2/3 complex during mammalian corticogenesis. *Development* 143, 2741–2752. doi: 10.1242/dev.130542

Wang, X., Tsai, J. W., Lamonica, B., and Kriegstein, A. R. (2011). A new subtype of progenitor cell in the mouse embryonic neocortex. *Nat. Neurosci.* 14, 555–561. doi: 10.1038/nn.2807

Weitzdoerfer, R., Fountoulakis, M., and Lubec, G. (2002). Reduction of actin-related protein complex 2/3 in fetal Down syndrome brain. *Biochem. Biophys. Res. Commun.* 293, 836–841. doi: 10.1016/s0006-291x(02)00291-7

Wilsch-Bräuninger, M., Florio, M., and Huttner, W. B. (2016). Neocortex expansion in development and evolution—from cell biology to single genes. *Curr. Opin. Neurobiol.* 39, 122–132. doi: 10.1016/j.conb.2016.05.004

Wilsch-Bräuninger, M., Peters, J., Paridaen, J. T. M. L., and Huttner, W. B. (2012). Basolateral rather than apical primary cilia on neuroepithelial cells committed to delamination. *Development* 139, 95–105. doi: 10.1242/dev.069294

Xie, Z., Moy, L. Y., Sanada, K., Zhou, Y., Buchman, J. J., and Tsai, L. H. (2007). Cep120 and TACCs control interkinetic nuclear migration and the neural progenitor pool. *Neuron* 56, 79–93. doi: 10.1016/j.neuron.2007.08.026

Ye, F., Kang, E., Yu, C., Qian, X., Jacob, F., Yu, C., et al. (2017). DISC1 regulates neurogenesis via modulating kinetochore attachment of Ndel1/Nde1 during mitosis. *Neuron* doi: 10.1016/j.neuron.2017.10.010 [Epub ahead of print].

Yokota, Y., Eom, T. Y., Stanco, A., Kim, W. Y., Rao, S., Snider, W. D., et al. (2010). Cdc42 and Gsk3 modulate the dynamics of radial glial growth, inter-radial glial interactions and polarity in the developing cerebral cortex. *Development* 137, 4101–4110. doi: 10.1242/dev.048637

Conflict of Interest Statement: The authors declare that the research was conducted in the absence of any commercial or financial relationships that could be construed as a potential conflict of interest.

frontiers in Cellular Neuroscience

MINI REVIEW
published: 13 October 2017
doi: 10.3389/fncel.2017.00322

Seven in Absentia E3 Ubiquitin Ligases: Central Regulators of Neural Cell Fate and Neuronal Polarity

*Taren Ong[1,2] and David J. Solecki[2]**

[1] Cancer and Developmental Biology Track, Integrated Biomedical Sciences Graduate Program, University of Tennessee Health Science Center, Memphis, TN, United States, [2] Department of Developmental Neurobiology, St. Jude Children's Research Hospital, Memphis, TN, United States

During neural development, neural precursors transition from a proliferative state within their germinal niches to a migratory state as they relocate to their final laminar positions. Transitions across these states are coupled with dynamic alterations in cellular polarity. This key feature can be seen throughout the developing vertebrate brain, in which neural stem cells give rise to multipolar or unpolarized transit-amplifying progenitors. These transit-amplifying progenitors then expand to give rise to mature neuronal lineages that become polarized as they initiate radial migration to their final laminar positions. The conventional understanding of the cellular polarity regulatory program has revolved around signaling cascades and transcriptional networks. In this review, we discuss recent discoveries concerning the role of the Siah2 ubiquitin ligase in initiating neuronal polarity during cerebellar development. Given the unique features of Siah ubiquitin ligases, we highlight some of the key substrates that play important roles in cellular polarity and propose a function for the Siah ubiquitin proteasome pathway in mediating a post-translational regulatory network to control the onset of polarization.

Keywords: ubiquitin ligase, seven in absentia, neuronal polarity, cerebellar granule neuron, Pard complex

OPEN ACCESS

Edited by:
Froylan Calderon De Anda, University of Hamburg, Germany

Reviewed by:
Alfredo Cáceres, INEMEC-CONICET, Argentina
Yves Jossin, Catholic University of Louvain, Belgium

****Correspondence:***
David J. Solecki
david.solecki@stjude.org

Received: *22 May 2017*
Accepted: *26 September 2017*
Published: *13 October 2017*

Citation:
Ong T and Solecki DJ (2017) Seven in Absentia E3 Ubiquitin Ligases: Central Regulators of Neural Cell Fate and Neuronal Polarity. Front. Cell. Neurosci. 11:322. doi: 10.3389/fncel.2017.00322

INTRODUCTION

A salient feature of neurogenesis is the expansion of neural precursors within their germinal niches. This expansion is followed by cell cycle exit, cellular differentiation, and migration of the cells to their distant sites of function (Hatten, 1999). In the vertebrate brain, multipotent neural stem cells in the ventricular zone exhibit a bipolar morphology throughout neurogenesis. Progenitors that have acquired a neuronal fate sever their attachments from neural stem cells anchored in the ventricular zone as they move to their designated lamina (Rakic, 2003). During neurogenesis, some of these progenitors, such as intermediate progenitors in the cerebral cortex or granule neuron progenitors (GNPs) of the cerebellum, transition to a multipolar or unpolarized state before terminal differentiation (Singh and Solecki, 2015). In contrast, nonpolarized GNPs of the cerebellar cortex acquire polarity during differentiation, allowing them to undergo directed migration into the internal granular layer (IGL). During this process, the polarity complex must regulate the intercellular adhesions required for migration (Solecki et al., 2004; Famulski et al., 2010). Although cellular polarity transitions appear to occur dynamically throughout neurogenesis, our understanding of cell polarity regulation is limited to signaling cascades and transcriptional networks, which have slow reaction rates. Thus, the main challenge in understanding neurogenesis

and neuronal migration is to determine how the dynamic alterations in cellular polarity are regulated. Here, we review the evidence regarding the role of seven in absentia homolog (Siah) ubiquitin ligases in post-translational regulation of polarity and the mechanisms that regulate the interplay between cytoskeletal networks during neuronal migration.

SIAH/SINA

Ubiquitin ligases of the Siah family are composed of the RING catalytic domain, two zinc-finger domains, and a substrate-binding domain (House et al., 2006). The *Drosophila* seven in absentia (SINA) protein was first identified as being required for compound eye development (Carthew and Rubin, 1990). The compound eye consists of 800 identical ommatidia, each composed of clusters of eight photoreceptor neurons, designated R1–R8, surrounded by non-neuronal support cells, including cone cells (Carthew and Rubin, 1990). The photoreceptor lineages are not determined autonomously but through intracellular communication. The specification of each photoreceptor cell depends on the activation of the Ras–MAPK cascade by the *Drosophila* Egf receptor (DER) homolog, except that the R7 photoreceptor specification requires an additional burst of Ras–MAPK activity, which is triggered by another receptor tyrosine kinase, sevenless (sev) (Freeman, 1996). Sev is activated by its ligand bride of sevenless (BOSS), a transmembrane protein expressed by a neighboring R8 cell (Hart et al., 1993). Sev or BOSS loss-of-function (LOF) mutations cause the specific loss of the R7 photoreceptor in each ommatidium (Stark et al., 1976; Reinke and Zipursky, 1988). A recessive viable mutagenesis screen for genes affecting compound eye morphology demonstrated that SINA LOF phenocopies the BOSS or sev mutants. SINA was epistatically placed as the most downstream component of the Ras–MAPK inductive signal, as SINA LOF not only phenocopies loss of the inductive signal but also suppresses ectopic R7 induction driven by active mutants of sev, Ras, or the rolled MAPK (Fortini et al., 1992; Simon, 1994; **Figure 1**). SINA also regulates sensory organ precursor cell fate in a Ras-dependent manner by reducing Notch signaling (Carthew and Rubin, 1990). Subsequent studies have shown that SINA function is regulated by sev and the Ras–MAPK cascade to target for degradation of the *tramtrack* gene product, TTK88, which inhibits R7 photoreceptor specification (Li et al., 1997). SINA-induced TTK88 degradation requires Phyllopod, a Ras-activated adaptor protein that facilitates SINA binding to target proteins (Tang et al., 1997). Finally, suppressor and enhancer screens have revealed SINA regulatory proteins, such as UbcD1, which might be an E2 enzyme for SINA, and the musashi RNA-binding protein that regulates TTK88 translation, along with proteins that synergize with SINA, such as the Sin3a transcription co-repressor (Carthew et al., 1994; Hirota et al., 1999). Thus, *Drosophila* SINA is an adaptable modulator of cell fate that regulates post-translation programs of gene expression via the ubiquitin proteasome system.

In mice, Siah proteins are encoded by three functional genes, designated *Siah1a*, *Siah1b*, and *Siah2*, whereas humans have only two such genes, designated *SIAH1* and *SIAH2* (Della et al., 1993). *Siah1a* and *Siah1b* encode 282-amino acid proteins that are 98% identical, whereas *Siah2* encodes a 325-amino acid protein that is 85% identical to Siah1 but has a longer and highly divergent N-terminus (Della et al., 1993; Hu et al., 1997a). Siah proteins exist as dimers, wherein each monomer consists of an N-terminal RING domain, two zinc-finger motifs, and a C-terminal substrate-binding domain (Polekhina et al., 2002; House et al., 2006; **Figure 1A**). The RING domain and zinc-finger motifs are highly conserved between Sina and Siah (Hu et al., 1997a). Uniquely, the substrate-binding domain of Siah ligases forms a binding groove that specifically recognizes its substrates through a degron motif: Px[ARTE]xVxP (House et al., 2003, 2006). This sequence has remained mostly unchanged during evolution, being nearly identical in flies and vertebrates. Computational screening of the human, mouse, and fly proteomes with the Siah degron also reveals highly conserved targets. With this high degree of conservation of the Siah1 and Siah2 domain structure and degron targeting sequence, it is not surprising that these proteins have overlapping functions in terms of targeting proteins for ubiquitin proteasome degradation (Hu et al., 1997b); however, not only is Siah2 apparently more potent at targeting proteins for degradation, but a small panel of targets can be targeted for degradation only by a vertebrate Siah (Habelhah et al., 2002). Genetic studies demonstrate the functional diversity in *Siah* genes. *Siah1* knockout mice exhibit severe growth retardation, early lethality, and defective meiotic division during spermatogenesis (Dickins et al., 2002), whereas *Siah2* knockout mice exhibit a mild expansion of their myeloid progenitor cells and an altered hypoxia response (a detailed analysis of the brain structure and development has not been carried out in either mutant). The combined loss of *Siah1a* and *Siah2* leads to embryonic and neonatal lethality (Frew et al., 2003). However, this study only provided gross analysis of the brain and lacked any assessment of the cerebellum. Given that *ex vivo* silencing of Siah2 promotes cell cycle and germinal zone (GZ) exit (Famulski et al., 2010), we predict that these mice would exhibit a decrease in proliferation and accelerated differentiation of the GNPs. This will likely lead to reduced number of progenitors and a mild form of cerebellar hypoplasia.

In mammals, Siah ubiquitin ligases play a role in cellular homeostasis and stress response (**Figures 1C,D**). Most notably, in the hypoxic response pathway, Siah targets the prolyl hydroxylases Phd1 and Phd3 for degradation under hypoxic conditions, leading to the stabilization of the transcription factor hypoxia-inducible factor 1a (Hif1a) and the subsequent transcription of key hypoxia-response genes (Safran and Kaelin, 2003; Nakayama et al., 2004). Under normoxic conditions, prolyl hydroxylases target Hif1a for degradation (Bruick and McKnight, 2001; Epstein et al., 2001). Other substrates targeted by Siah are homeodomain-interacting protein kinase (HIPK2) in the DNA damage-response pathway (Calzado et al., 2009); AKAP121 in response to cellular ischemia and oxygen deprivation (Carlucci et al., 2008); GAPDH in hyperglycemia (Yego and Mohr, 2010); TRAF2 in the JNK/p38/NF-κB signaling pathway (Habelhah et al., 2002); TIN2 and Trf2 in cellular senescence (Fujita et al., 2010; Bhanot and Smith, 2012); and Sprouty, the negative

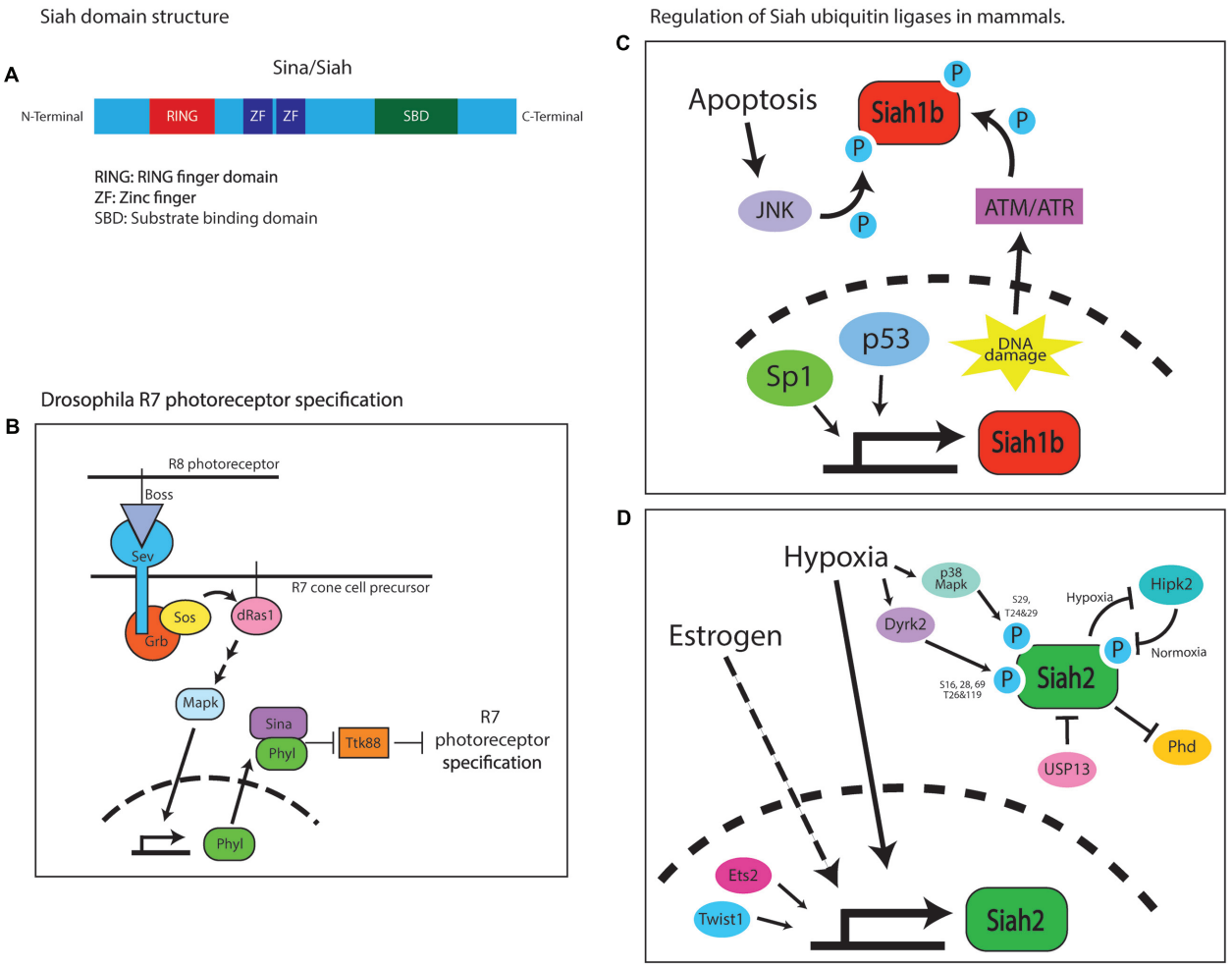

FIGURE 1 | Domain structure of Sina/Siah and its regulation in Drosophila and mammals. **(A)** Domain structure of Siah E3 ubiquitin ligase. **(B)** Schematic of the signaling pathway regulating the specification of the R7 photoreceptor. Sina is placed epistatically downstream of the drosophila Ras–MAPK cascade. Boss, bride of sevenless; Sev, sevenless; Grb, growth factor receptor bound protein; Sos, son of sevenless; Phyl, phyllopod; Ttk88, tramtrack88. **(C)** Schematic of the transcriptional and post-translational pathways involved in regulating Siah1b in mammals. In mice, Siah1b is regulated by p53 while human SIAH1 basal transcription is regulated by Sp1. Post-translationally, Siah1b is regulated through phosphorylation by JNK or ATM/ATM during events of cellular stress like apoptosis and DNA damage. **(D)** Schematic of the transcriptional and post-translational pathways involved in regulating Siah2 in mammals. Estrogen signaling and hypoxia upregulate Siah2 transcriptionally. Twist1 and Ets2 are transcription factors reported to activate transcription of Siah2. Post-transcriptionally, activity of Siah2 is regulated by phosphorylation by multiple kinases – Dryk2, p38, MAPK, and HIPK2, or via physical interaction with USP13. This figure is all original content.

regulator of the Ras–MAPK cascade (Nadeau et al., 2007). Siah ubiquitin ligases are also overexpressed in some cancers, including lung cancer (Ahmed et al., 2008), melanoma (Qi et al., 2008), prostate cancer (Qi et al., 2010), breast cancer (Wong et al., 2012), liver cancer (Malz et al., 2012), and pancreatic cancer (Schmidt et al., 2007).

Little is known about how Siah proteins are regulated transcriptionally. p53 regulates *Siah1b* in mice (Fiucci et al., 2004), and Sp1 regulates *SIAH1* basal promoter activity in humans (Maeda et al., 2002). Hypoxia and estrogen signaling have been shown to upregulate Siah2 mRNA (Frasor et al., 2005; Qi et al., 2008). The transcription factors E26 transformation-specific sequence 2, Ets2, and twist-related protein 1, Twist1, cooperate to activate Siah2 transcription in gastric epithelial cells (Das et al., 2016). More is known about how Siah proteins are regulated post-translationally; their abundance and activity are controlled by other interacting proteins or by their phosphorylation status. During hypoxia, Siah2 is phosphorylated by the p38 MAPK at serine 29 and threonines 24 and 29, or by Dyrk2 at serines 16, 28, and 69 and threonines 26 and 119, resulting in enhanced ubiquitination and degradation of the Siah2 substrate Phd3 (Khurana et al., 2006; Pérez et al., 2012). In normoxia, Siah2 is destabilized through phosphorylation at positions 26, 28, and 68 by the HIPK2, which is targeted for degradation by Siah2 during hypoxia (Calzado et al., 2009). A similar regulation pattern is seen with Siah1. For example, Siah1 is stabilized through phosphorylation at tyrosines 100 and 126 by a JNK-dependent pathway during apoptosis or at serine

19 by ATM/ATR in response to DNA damage (Xu et al., 2006; Winter et al., 2008). Besides phosphorylation, Siah2 activity can be modulated by the deubiquitinating enzyme USP13, which binds to and deubiquitinates Siah2, increasing its stability but diminishing its activity toward its substrates (Scortegagna et al., 2011). Hypoxia diminishes USP13 expression, resulting in a Siah2 with increased activity toward its substrates.

SIAH AND NEURONAL POLARITY

The results of recent studies have suggested a function for Siah2 in regulating a complex post-translational network that controls the onset of neuronal polarity during cerebellar granule neuron (CGN) differentiation (Famulski et al., 2010; Trivedi et al., 2017). The CGN is a powerful model with which to understand the linkage between differentiation and polarization in the developing nervous system. During the early stages of postnatal cerebellar development, GNPs proliferate and expand on the surface of the cerebellum. Upon differentiation, the CGNs must migrate radially to their final destinations deep within the cerebellum (Komuro et al., 2001; Leto et al., 2016). To exit the GZ, CGNs depend on the partitioning-defective (Pard) polarity signaling complex to mediate the cell-to-cell attachment and traction forces required for neurons to exit their GZ or migrate. The evolutionarily conserved Pard proteins are archetypal polarity-signaling molecules (Insolera et al., 2011; Nance and Zallen, 2011; McCaffrey and Macara, 2012): Pard3 and Pard6 adaptors form a complex with atypical PKC and CDC42 (Macara, 2004; Suzuki and Ohno, 2006; Goldstein and Macara, 2007) that is crucial for tight-junction formation (Nelson and Beitel, 2009), spindle orientation (Bultje et al., 2009; Sottocornola et al., 2010), cell migration, and axon formation (Barnes et al., 2008). Dissecting Pard protein function has advanced our mechanistic understanding of neuronal migration (Solecki et al., 2004, 2006, 2009; Trivedi et al., 2014; Singh et al., 2016): Both Pard3 and Pard6 are necessary and sufficient for CGN migration. Live-cell imaging revealed that Pard6 is enriched at the centrosome and that CGNs employ a two-stroke nucleokinesis cycle: the centrosome moves forward before somal translocation. Pard6 gain of function (GOF) or LOF disturbed coordinated movement showing that polarity signaling is essential for nucleokinesis (Solecki et al., 2004). Further studies revealed that actomyosin contractions in the CGN leading process generate the forces that propel migration and nucleokinesis. Disrupting Pard6 function halts nucleokinesis by reducing leading-process actomyosin dynamics, force generation, and appropriate leading process extension (Solecki et al., 2009). Moreover, Pard3 activity controls the directionality of CGN motility (Famulski et al., 2010). Polarity is classically defined as asymmetry in cellular architecture, intracellular organization (e.g., epithelial apical-basal polarity, neuronal axon-dendrite polarity) as well as cellular behaviors (e.g., directed migration or intracellular transport). Thus, by controlling events like leading process extension, asymmetric cytoskeletal organization (e.g., directed centrosome motility and actomyosin organization), and the directionality of movement the Pard complex shapes multiples aspects of CGN polarity during their transit to a final laminar position.

Our laboratory fortuitously discovered that Siah2 regulates polarity signaling in CGN GZ exit and adhesion by controlling Pard-complex activity (**Figure 2A**). Siah2 was the first E3 ubiquitin ligase found to interact with the Pard6 component of the Pard complex via a two-hybrid screen (Famulski et al., 2010). However, a computer-based screen revealed Pard3 to be the only member of the complex harboring a Siah degron sequence, Px[ATRE]xVxP. Siah2 overexpression leads to the ubiquitination and loss of Pard3, but not Pard6, in heterologous cells and primary CGNs, implying that Siah2 regulates polarity via Pard3 degradation. High Siah2 expression in the external germinal layer (EGL) led to the hypothesis that Siah2 regulated CGN GZ exit. *Siah2*^{GOF} blocks CGN migration to the IGL in *ex vivo* slices by restricting motility to the GZ niche, and co-expression of wild-type Pard3 or a degron mutant rescues IGL-directed migration when Siah is elevated. *Siah2* shRNA silencing or expression of a dominant-negative Siah2 spurs GZ exit after 24 h in culture. *In vitro*, *Siah2* overexpression maintained GNPs in a mesenchymal-like progenitor morphology and with a lack of polarized leading process extension while inhibition of Siah2 function produced the opposite phenotypes. Together, these results show that Siah activity inhibits GZ exit partly by antagonizing polarity through the degradation of Pard3. Whereas Pard6 regulates the cytoskeleton required for migration, the Siah2–Pard3 module controls CGN adhesion. JAM-C, a tight-junction molecule localized to the CGN leading process that interacts with Pard3, is also vital for GZ exit. Therefore, Siah2 activity inhibits JAM-C exocytosis and adhesion via Pard3. The mechanism of Siah2 downregulation is unknown, but it enables Pard3 accumulation and the subsequent recruitment of JAM-C to the membrane to initiate GZ exit.

Migrating polarized CGNs undergo a saltatory two-stroke nucleokinesis, in which dilation at the leading edge of the neuron is followed by the inflow of actomyosin complexes and cellular organelles and, finally, by nuclear translocation toward the dilation (Edmondson et al., 1988; Rivas and Hatten, 1995; Solecki et al., 2004, 2009; Tsai and Gleeson, 2005; Trivedi et al., 2014, 2017). The formation of a polarized leading process is fundamental to the polarization of developing CGNs and involves dynamic interplay between f-actin, microtubules, adhesion molecules, and force-generating molecular motors. Microtubule and cytoplasmic dynein plays a role in positioning cellular organelles and towing the nucleus during migration. Actomyosin complexes act within the leading process to mediate the traction forces that arise from the adhesion sites. Our limited understanding of polarized cytoskeletal interplay in migrating neurons, which is mostly investigated using low-resolution imaging, and a lack of candidate molecules to link cytoskeletal elements are key obstacles. Significant recent insights into these processes and how they are connected to neuronal differentiation were made by functionally analyzing the drebrin cytoskeletal adaptor (Trivedi et al., 2017). Drebrin links microtubule movements to the actomyosin cytoskeleton in growth cones and synapses (Geraldo et al., 2008; Geraldo and Gordon-Weeks, 2009; Merriam et al., 2013) but its function

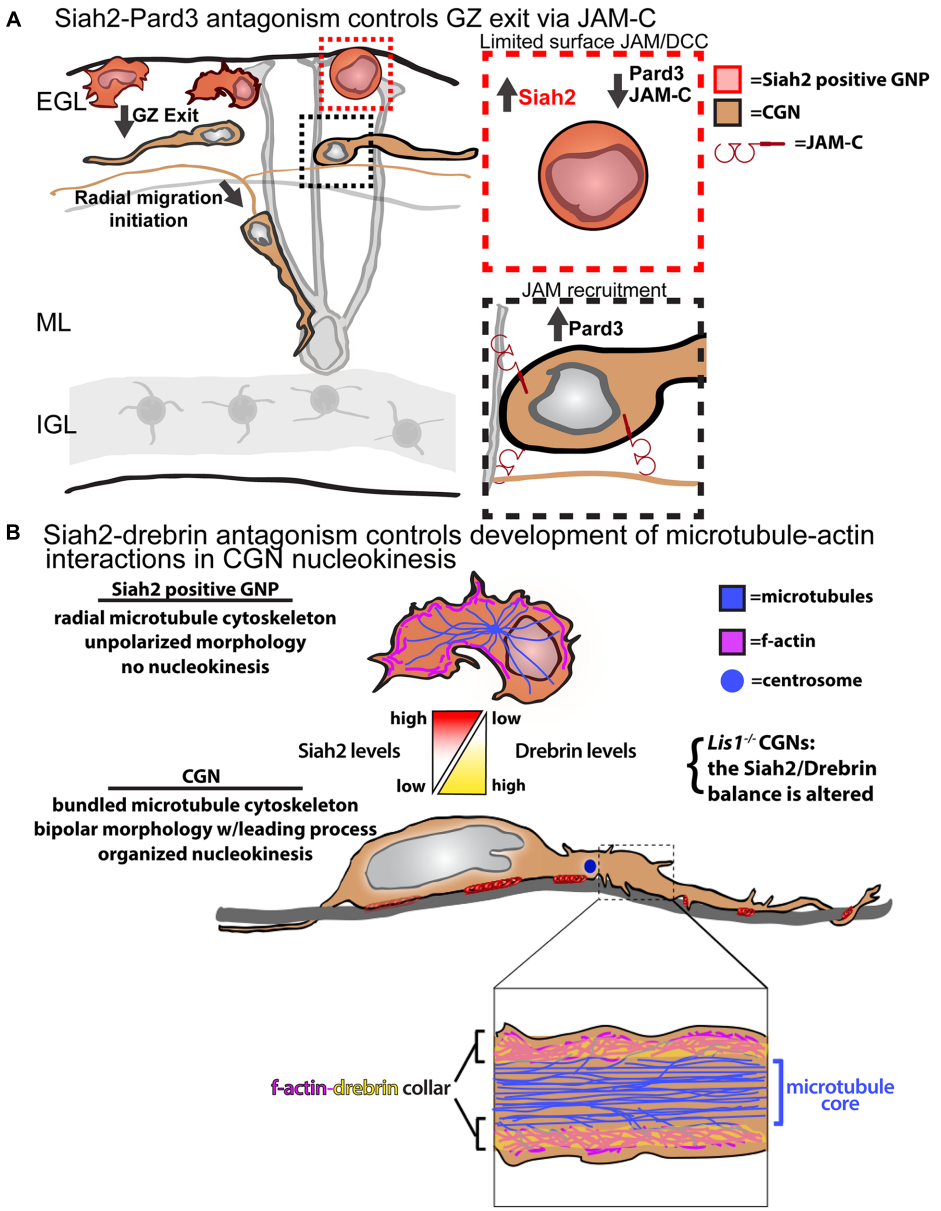

FIGURE 2 | Models for Siah2 antagonism of CGN GZ exit and cytoskeletal interactions. **(A)** Siah2 regulation of Pard3/JAM-C GZ adhesion events. **(B)** Siah2 regulation of microtubule–actin interactions via drebrin. Elements of the **A** panel were derived from Singh et al. (2016). Elements of the **B** panel were derived from Trivedi et al. (2017). Both panels do not require permission for reproduction.

in two-stroke motility remains unexplored. Not only is drebrin expression complementary to that of Siah2 in the P7 cerebellum, but *Siah2*^{silencing} led to enhanced drebrin expression in CGNs. Our biochemical studies showed that Siah2 expression reduced drebrin protein levels in a manner requiring Siah2 substrate binding and the VxP degron sequences of drebrin.

Live-cell imaging first indicated that drebrin might be involved in CGN cytoskeletal interplay, as the protein is cyclically transferred from the neuronal soma to the proximal leading process in migration. Lattice light-sheet microscopy, with its superior signal-to-noise ratio and spatial resolution, showed drebrin to be localized to two sub-plasma membrane f-actin-containing collars parallel to the long axis of the CGN leading process that were undetectable at lower resolution. Further examination of the relation of drebrin to plasma membrane, f-actin, and microtubules with super-resolution structured illumination imaging (with approximately 100-nm resolution) showed that the CGN proximal leading process possesses a central core of microtubules and that a layer of drebrin and f-actin intervenes between the plasma membrane and microtubules. These results were surprising, as previous migration models posited that microtubules directly interfaced

with the membrane in migrating neurons (Vallee et al., 2009). Functional live-cell imaging studies revealed the drebrin–actin cytoskeletal interface to be critical for CGN migration. Drebrin^{silencing} and dominant-negative inhibition of drebrin–microtubule interactions block the IGL-directed migration of CGNs in *ex vivo* slices without affecting migration speed, inhibit polarized leading-process extension, and randomize centrosome and nucleus movements in nucleokinesis. Finally, epistatic *ex vivo* and *in vitro* live imaging shows that Siah2-drebrin antagonism regulates GZ exit and nucleokinesis. These data imply that actin–microtubule interactions are critical in steering motility and that Siah2-drebrin antagonism is vital for regulating cytoskeletal interactions in developing CGNs (**Figure 2B**). Taken together, these results show that Siah2 regulates CGN migration through several aspects, including cellular adhesion and the cytoskeletal elements that propel migration.

A BROADER SIAH2 POLARITY NETWORK?

A major goal in developmental biology is to identify polarity-signaling components that will yield insights into the mechanisms controlling tissue morphogenesis. Given the key role of Siah2 in directly regulating cell polarity to control the movement of CGNs to their final laminae, we recently reviewed previous computational screens (Famulski et al., 2010; Trivedi et al., 2017) and noted other Siah2 targets relevant to GZ exit and migration. The same Siah degron screen that implicated Pard3 and drebrin as a Siah target was further analyzed by filtering degron-containing genes via validated CGN expression (via the RIKEN Cerebellar Transcriptome), and pathway analysis revealed common groups of proteins with Siah degrons. Interestingly, Numb, Aspp2 (apoptosis-stimulating of p53 protein 2), and Dab2 (Disabled 2) interact with Pard3 and are also substrates of Siah ubiquitin ligases, suggesting a broader role for Siah2 in polarity regulation. In this section, we will summarize what is known about Siah ligase interactions with these targets in non-neuronal cells and potential implications on the elusive cell biological functions associated with polarization in neurons.

Numb was revealed to be an interacting partner of Siah1 in a yeast two-hybrid screen (Susini et al., 2001). Interaction-mapping experiments and functional analyses confirmed this interaction and showed that endogenous Siah1 targets Numb for degradation in the LTR6 myeloid leukemia cell line. In the developing neocortex, radial glial cells (RGCs) are specialized multipotent progenitors that serve as migratory scaffolds for developing neurons. RGCs are polarized cells with a short apical process that contacts the ventricular surface via the apical end-foot and a long basal process that spans the entire thickness of the developing neuroepithelium (Rakic, 2003). The apical end-feet of RGCs form cadherin-based adherens junctions with each other, anchoring the cells to the ventricular surface (Kadowaki et al., 2007). These cadherin-based adhesions are regulated by Numb and Numb-like (Numbl), homologs of *Drosophila* Numb, an endocytic adaptor protein. In the developing cortex, Numb and Numbl accumulate at the apical end-feet of RGCs, where they co-localize with cadherins, conferring polarity on RGCs (Rašin et al., 2007). Conditional deletion of the *numb* and *numbl* genes affects the cadherin-based adherens junction and disrupts RGC polarity, leading to defects in cortical lamination defects and the generation of neuronal lineages. Given that both Numb and Pard3 have pro-adhesive activities Siah LOF enhancement of RGC junctions could be expected in the developing cerebral cortex of Siah mutant mice. Recently, the tumor suppressor Aspp2 was shown to regulate cell polarity by directly interacting with Pard3 (Sottocornola et al., 2010). This interaction is crucial to recruiting Pard3 to the apical surface of the developing neuroepithelium, the loss of which affects adherens junction formation. Consequently, the loss of Aspp2 affects cortical lamination and interkinetic nuclear migration and strongly perturbs CNS development. Aspp2 is required for tight-junction formation (Kim et al., 2014). Structure–function analysis revealed the presence of a Siah degron motif in Aspp2, the mutation of which abrogated its interaction with Siah2, preventing its proteasome-mediated degradation. Siah2 knockdown and Aspp2 overexpression accelerated tight-junction formation in NRK-52E kidney tubular epithelial cells. During neurogenesis, the maintenance of polarity is crucial to ensure proper cortical lamination, and the loss of polarity at the end of the neurogenic phase is equally important for RGCs to give rise to other non-neuronal cell types. In this context, Siah ubiquitin ligases may mediate the dissolution of adherens junctions by targeting Aspp2 or Numb for degradation, effectively downregulating polarity.

Siah regulation of polarity may extend beyond the adhesion turnover events described above to direct regulation of signaling events. Consistent with this, Pard3 interacts with Dab2, an endocytic adaptor that regulates the endocytosis of certain extracellular receptors and influences the trafficking of cell-signaling components (Traub, 2003). In a recent study, interaction between Pard3 and Dab2 was genetically required to regulate VEGFR endocytosis and turnover in endothelial cells within the angiogenic front in the developing retina (Nakayama et al., 2013). Both Pard3 and Dab2 contain Siah degrons, and Pard3 is a known substrate of Siah2, suggesting that Siah ligases play a role in endocytosis and perhaps in active turnover of Pard complex- and Dab2-linked surface receptors, such as VEGFR or disheveled. Taken together, novel Pard3 interactions in non-neuronal cells coupled with Siah2 regulation suggest a central function of the Pard complex and Siah2 may be related to adhesion and guidance receptor trafficking during neuronal polarization.

AUTHOR CONTRIBUTIONS

All authors listed have made a substantial, direct and intellectual contribution to the work, and approved it for publication.

FUNDING

The Solecki Laboratory is funded by ALSAC, by the March of Dimes (Grant No. 1-FY12-455) and by the National Institute

of Neurological Disorders and Stroke (NINDS) (Grant No. 1R01NS066936). The content is solely the responsibility of the authors and does not necessarily represent the official views of the NINDS or the National Institutes of Health.

ACKNOWLEDGMENT

The authors thank Keith A. Laycock, Ph.D., ELS, for editing the manuscript.

REFERENCES

Ahmed, A. U., Schmidt, R. L., Park, C. H., Reed, N. R., Hesse, S. E., Thomas, C. F., et al. (2008). Effect of disrupting seven-in-absentia homolog 2 function on lung cancer cell growth. *J. Natl. Cancer Inst.* 100, 1606–1629. doi: 10.1093/jnci/djn365

Barnes, A. P., Solecki, D., and Polleux, F. (2008). New insights into the molecular mechanisms specifying neuronal polarity in vivo. *Curr. Opin. Neurobiol.* 18, 44–52. doi: 10.1016/j.conb.2008.05.003

Bhanot, M., and Smith, S. (2012). TIN2 stability is regulated by the E3 ligase Siah2. *Mol. Cell. Biol.* 32, 376–384. doi: 10.1128/MCB.06227-11

Bruick, R. K., and McKnight, S. L. (2001). A conserved family of prolyl-4-hydroxylases that modify HIF. *Science* 294, 1337–1340. doi: 10.1126/science.1066373

Bultje, R. S., Castaneda-Castellanos, D. R., Jan, L. Y., Jan, Y.-N., Kriegstein, A. R., and Shi, S.-H. (2009). Mammalian Par3 regulates progenitor cell asymmetric division via notch signaling in the developing neocortex. *Neuron* 63, 189–202. doi: 10.1016/j.neuron.2009.07.004

Calzado, M. A., de la Vega, L., Möller, A., Bowtell, D. D. L., and Schmitz, M. L. (2009). An inducible autoregulatory loop between HIPK2 and Siah2 at the apex of the hypoxic response. *Nat. Cell Biol.* 11, 85–91. doi: 10.1038/ncb1816

Carlucci, A., Adornetto, A., Scorziello, A., Viggiano, D., Foca, M., Cuomo, O., et al. (2008). Proteolysis of AKAP121 regulates mitochondrial activity during cellular hypoxia and brain ischaemia. *EMBO J.* 27, 1073–1084. doi: 10.1038/emboj.2008.33

Carthew, R. W., Neufeld, T. P., and Rubin, G. M. (1994). Identification of genes that interact with the sina gene in *Drosophila* eye development. *Proc. Natl. Acad. Sci. U.S.A.* 91, 11689–11693. doi: 10.1073/pnas.91.24.11689

Carthew, R. W., and Rubin, G. M. (1990). *seven in absentia*, a gene required for specification of R7 cell fate in the Drosophila eye. *Cell* 63, 561–577. doi: 10.1016/0092-8674(90)90452-K

Das, L., Kokate, S. B., Rath, S., Rout, N., Singh, S. P., Crowe, S. E., et al. (2016) ETS2 and Twist1 promote invasiveness of *Helicobacter pylori*-infected gastric cancer cells by inducing Siah2. *Biochem. J.* 473, 1629–1640. doi: 10.1042/BCJ20160187

Della, N. G., Senior, P. V., and Bowtell, D. D. (1993). Isolation and characterisation of murine homologues of the *Drosophila* seven in absentia gene (sina). *Development* 117, 1333–1343.

Dickins, R. A., Frew, I. J., House, C. M., O'Bryan, M. K., Holloway, A. J., Haviv, I., et al. (2002). The ubiquitin ligase component Siah1a is required for completion of meiosis i in male mice. *Mol. Cell. Biol.* 22, 2294–2303. doi: 10.1128/MCB.22.7.2294-2303.2002

Edmondson, J. C., Liem, R. K., Kuster, J. E., and Hatten, M. E. (1988). Astrotactin: a novel neuronal cell surface antigen that mediates neuron-astroglial interactions in cerebellar microcultures. *J. Cell Biol.* 106, 505–517. doi: 10.1083/jcb.106.2.505

Epstein, A. C. R., Gleadle, J. M., McNeill, L. A., Hewitson, K. S., O'Rourke, J., Mole, D. R., et al. (2001). *C. elegans* EGL-9 and mammalian homologs define a family of dioxygenases that regulate HIF by prolyl hydroxylation. *Cell* 107, 43–54. doi: 10.1016/S0092-8674(01)00507-4

Famulski, J. K., Trivedi, N., Howell, D., Yang, Y., Tong, Y., Gilbertson, R., et al. (2010). Siah regulation of Pard3A controls neuronal cell adhesion during germinal zone exit. *Science* 330, 1834–1838. doi: 10.1126/science.1198480

Fiucci, G., Beaucourt, S., Duflaut, D., Lespagnol, A., Stumptner-Cuvelette, P., Géant, A., et al. (2004). Siah-1b is a direct transcriptional target of p53: identification of the functional p53 responsive element in the siah-1b promoter. *Proc. Natl. Acad. Sci. U.S.A.* 101, 3510–3515. doi: 10.1073/pnas.0400177101

Fortini, M. E., Simon, M. A., and Rubin, G. M. (1992). Signalling by the sevenless protein tyrosine kinase is mimicked by Rasl activation. *Nature* 355, 559–561. doi: 10.1038/355559a0

Frasor, J., Danes, J. M., Funk, C. C., and Katzenellenbogen, B. S. (2005). Estrogen down-regulation of the corepressor N-CoR: mechanism and implications for estrogen derepression of N-CoR-regulated genes. *Proc. Natl. Acad. Sci. U.S.A.* 102, 13153–13157. doi: 10.1073/pnas.0502782102

Freeman, M. (1996). Reiterative use of the EGF receptor triggers differentiation of all cell types in the *Drosophila* eye. *Cell* 87, 651–660. doi: 10.1016/S0092-8674(00)81385-9

Frew, I. J., Hammond, V. E., Dickins, R. A., Quinn, J. M. W., Walkley, C. R., Sims, N. A., et al. (2003). Generation and analysis of Siah2 mutant mice. *Mol. Cell. Biol.* 23, 9150–9161. doi: 10.1128/MCB.23.24.9150-9161.2003

Fujita, K., Horikawa, I., Mondal, A. M., Jenkins, L. M. M., Appella, E., Vojtesek, B., et al. (2010). Positive feedback between p53 and TRF2 during telomere-damage signalling and cellular senescence. *Nat. Cell Biol.* 12, 1205–1212. doi: 10.1038/ncb2123

Geraldo, S., and Gordon-Weeks, P. R. (2009). Cytoskeletal dynamics in growth-cone steering. *J. Cell Sci.* 122, 3595–3604. doi: 10.1242/jcs.042309

Geraldo, S., Khanzada, U. K., Parsons, M., Chilton, J. K., and Gordon-Weeks, P. R. (2008). Targeting of the F-actin-binding protein drebrin by the microtubule plus-tip protein EB3 is required for neuritogenesis. *Nat. Cell Biol.* 10, 1181–1189. doi: 10.1038/ncb1778

Goldstein, B., and Macara, I. G. (2007). The PAR proteins: fundamental players in animal cell polarization. *Dev. Cell* 13, 609–622. doi: 10.1016/j.devcel.2007.10.007

Habelhah, H., Frew, I. J., Laine, A., Janes, P. W., Relaix, F., Sassoon, D., et al. (2002). Stress-induced decrease in TRAF2 stability is mediated by Siah2. *EMBO J.* 21, 5756–5765. doi: 10.1093/emboj/cdf576

Hart, A. C., Harrison, S. D., Van Vactor, D. L., Rubin, G. M., and Zipursky, S. L. (1993). The interaction of bride of sevenless with sevenless is conserved between *Drosophila virilis* and *Drosophila melanogaster*. *Proc. Natl. Acad. Sci. U.S.A.* 90, 5047–5051. doi: 10.1073/pnas.90.11.5047

Hatten, M. E. (1999). Central nervous system neuronal migration. *Annu. Rev. Neurosci.* 22, 511–539. doi: 10.1146/annurev.neuro.22.1.511

Hirota, Y., Okabe, M., Imai, T., Kurusu, M., Yamamoto, A., Miyao, S., et al. (1999). Musashi and Seven in absentia downregulate Tramtrack through distinct mechanisms in *Drosophila* eye development. *Mech. Dev.* 87, 93–101. doi: 10.1016/S0925-4773(99)00143-4

House, C. M., Frew, I. J., Huang, H.-L., Wiche, G., Traficante, N., Nice, E., et al. (2003). A binding motif for Siah ubiquitin ligase. *Proc. Natl. Acad. Sci. U.S.A.* 100, 3101–3106. doi: 10.1073/pnas.0534783100

House, C. M., Hancock, N. C., Möller, A., Cromer, B. A., Fedorov, V., Bowtell, D. D. L., et al. (2006). Elucidation of the substrate binding site of Siah ubiquitin ligase. *Structure* 14, 695–701. doi: 10.1016/j.str.2005.12.013

Hu, G., Chung, Y.-L., Glover, T., Valentine, V., Look, A. T., and Fearon, E. R. (1997a). Characterization of human homologs of the *Drosophila* seven in absentia (sina) gene. *Genomics* 46, 103–111.

Hu, G., Zhang, S., Vidal, M., Baer, J. L., Xu, T., and Fearon, E. R. (1997b). Mammalian homologs of seven in absentia regulate DCC via the ubiquitin–proteasome pathway. *Genes Dev.* 11, 2701–2714.

Insolera, R., Chen, S., and Shi, S.-H. (2011). Par proteins and neuronal polarity. *Dev. Neurobiol.* 71, 483–494. doi: 10.1002/dneu.20867

Kadowaki, M., Nakamura, S., Machon, O., Krauss, S., Radice, G. L., and Takeichi, M. (2007). N-cadherin mediates cortical organization in the mouse brain. *Dev. Biol.* 304, 22–33. doi: 10.1016/j.ydbio.2006.12.014

Khurana, A., Nakayama, K., Williams, S., Davis, R. J., Mustelin, T., and Ronai, Z. (2006). Regulation of the Ring Finger E3 Ligase Siah2 by p38 MAPK. *J. Biol. Chem.* 281, 35316–35326. doi: 10.1074/jbc.M606568200

Kim, H., Claps, G., Möller, A., Bowtell, D., Lu, X., and Ronai, Z. A. (2014). Siah2 regulates tight junction integrity and cell polarity through control of ASPP2 stability. *Oncogene* 33, 2004–2010. doi: 10.1038/onc.2013.149

Komuro, H., Yacubova, E., Yacubova, E., and Rakic, P. (2001). Mode and tempo of tangential cell migration in the cerebellar external granular layer. *J. Neurosci.* 21, 527–540.

Leto, K., Arancillo, M., Becker, E. B. E., Buffo, A., Chiang, C., Ding, B., et al. (2016). Consensus paper: cerebellar development. *Cerebellum* 15, 789–828. doi: 10.1007/s12311-015-0724-2

Li, S., Li, Y., Carthew, R. W., and Lai, Z.-C. (1997). Photoreceptor cell differentiation requires regulated proteolysis of the transcriptional repressor Tramtrack. *Cell* 90, 469–478. doi: 10.1016/S0092-8674(00)80507-3

Macara, I. G. (2004). Par proteins: partners in polarization. *Curr. Biol.* 14, R160–R162. doi: 10.1016/j.cub.2004.01.048

Maeda, A., Yoshida, T., Kusuzaki, K., and Sakai, T. (2002). The characterization of the human Siah-1 promoter 1. *FEBS Lett.* 512, 223–226. doi: 10.1016/S0014-5793(02)02265-2

Malz, M., Aulmann, A., Samarin, J., Bissinger, M., Longerich, T., Schmitt, S., et al. (2012). Nuclear accumulation of seven in absentia homologue-2 supports motility and proliferation of liver cancer cells. *Int. J. Cancer* 131, 2016–2026. doi: 10.1002/ijc.27473

McCaffrey, L. M., and Macara, I. G. (2012). Signaling pathways in cell polarity. *Cold Spring Harb. Perspect. Biol.* 4:a009654. doi: 10.1101/cshperspect.a009654

Merriam, E. B., Millette, M., Lumbard, D. C., Saengsawang, W., Fothergill, T., Hu, X., et al. (2013). Synaptic regulation of microtubule dynamics in dendritic spines by calcium, F-actin, and drebrin. *J. Neurosci.* 33, 16471–16482. doi: 10.1523/JNEUROSCI.0661-13.2013

Nadeau, R. J., Toher, J. L., Yang, X., Kovalenko, D., and Friesel, R. (2007). Regulation of Sprouty2 stability by mammalian Seven-in-Absentia homolog 2. *J. Cell. Biochem.* 100, 151–160. doi: 10.1002/jcb.21040

Nakayama, K., Frew, I. J., Hagensen, M., Skals, M., Habelhah, H., Bhoumik, A., et al. (2004). Siah2 regulates stability of prolyl-hydroxylases, controls HIF1α abundance, and modulates physiological responses to hypoxia. *Cell* 117, 941–952. doi: 10.1016/j.cell.2004.06.001

Nakayama, M., Nakayama, A., van Lessen, M., Yamamoto, H., Hoffmann, S., Drexler, H. C. A., et al. (2013). Spatial regulation of VEGF receptor endocytosis in angiogenesis. *Nat. Cell Biol.* 15, 249–260. doi: 10.1038/ncb2679

Nance, J., and Zallen, J. A. (2011). Elaborating polarity: PAR proteins and the cytoskeleton. *Development* 138, 799–809. doi: 10.1242/dev.053538

Nelson, K. S., and Beitel, G. J. (2009). Cell junctions: lessons from a broken heart. *Curr. Biol.* 19, R122–R123. doi: 10.1016/j.cub.2008.12.002

Pérez, M., García-Limones, C., Zapico, I., Marina, A., Schmitz, M. L., Muñoz, E., et al. (2012). Mutual regulation between SIAH2 and DYRK2 controls hypoxic and genotoxic signaling pathways. *J. Mol. Cell Biol.* 4, 316–330. doi: 10.1093/jmcb/mjs047

Polekhina, G., House, C. M., Traficante, N., Mackay, J. P., Relaix, F., Sassoon, D. A., et al. (2002). Siah ubiquitin ligase is structurally related to TRAF and modulates TNF-α signaling. *Nat. Struct. Mol. Biol.* 9, 68–75. doi: 10.1038/nsb743

Qi, J., Nakayama, K., Cardiff, R. D., Borowsky, A. D., Kaul, K., Williams, R., et al. (2010). Siah2-dependent concerted activity of HIF and FoxA2 regulates formation of neuroendocrine phenotype and neuroendocrine prostate tumors. *Cancer Cell* 18, 23–38. doi: 10.1016/j.ccr.2010.05.024

Qi, J., Nakayama, K., Gaitonde, S., Goydos, J. S., Krajewski, S., Eroshkin, A., et al. (2008). The ubiquitin ligase Siah2 regulates tumorigenesis and metastasis by HIF-dependent and -independent pathways. *Proc. Natl. Acad. Sci. U.S.A.* 105, 16713–16718. doi: 10.1073/pnas.0804063105

Rakic, P. (2003). Developmental and evolutionary adaptations of cortical radial glia. *Cereb. Cortex* 13, 541–549. doi: 10.1093/cercor/13.6.541

Rašin, M.-R., Gazula, V.-R., Breunig, J. J., Kwan, K. Y., Johnson, M. B., Liu-Chen, S., et al. (2007). Numb and Numbl are required for maintenance of cadherin-based adhesion and polarity of neural progenitors. *Nat. Neurosci.* 10, 819–827. doi: 10.1038/nn1924

Reinke, R., and Zipursky, S. L. (1988). Cell-cell interaction in the drosophila retina: The bride of sevenless gene is required in photoreceptor cell R8 for R7 cell development. *Cell* 55, 321–330. doi: 10.1016/0092-8674(88)90055-4

Rivas, R. J., and Hatten, M. E. (1995). Motility and cytoskeletal organization of migrating cerebellar granule neurons. *J. Neurosci.* 15, 981–989.

Safran, M., and Kaelin, W. G. (2003). HIF hydroxylation and the mammalian oxygen-sensing pathway. *J. Clin. Invest.* 111, 779–783. doi: 10.1172/JCI200318181

Schmidt, R. L., Park, C. H., Ahmed, A. U., Gundelach, J. H., Reed, N. R., Cheng, S., et al. (2007). Inhibition of RAS-mediated transformation and tumorigenesis by targeting the downstream E3 ubiquitin ligase seven in absentia homologue. *Cancer Res.* 67, 11798–11810. doi: 10.1158/0008-5472.CAN-06-4471

Scortegagna, M., Subtil, T., Qi, J., Kim, H., Zhao, W., Gu, W., et al. (2011). USP13 enzyme regulates Siah2 ligase stability and activity via noncatalytic ubiquitin-binding domains. *J. Biol. Chem.* 286, 27333–27341. doi: 10.1074/jbc.M111.218214

Simon, M. A. (1994). Signal transduction during the development of the *Drosophila* R7 photoreceptor. *Dev. Biol.* 166, 431–442. doi: 10.1006/dbio.1994.1327

Singh, S., Howell, D., Trivedi, N., Kessler, K., Ong, T., Rosmaninho, P., et al. (2016). Zeb1 controls neuron differentiation and germinal zone exit by a mesenchymal-epithelial-like transition. *eLife* 5:e12717. doi: 10.7554/eLife.12717

Singh, S., and Solecki, D. J. (2015). Polarity transitions during neurogenesis and germinal zone exit in the developing central nervous system. *Front. Cell. Neurosci.* 9:62. doi: 10.3389/fncel.2015.00062

Solecki, D. J., Govek, E.-E., and Hatten, M. E. (2006). mPar6α controls neuronal migration. *J. Neurosci.* 26, 10624–10625. doi: 10.1523/JNEUROSCI.4060-06.2006

Solecki, D. J., Model, L., Gaetz, J., Kapoor, T. M., and Hatten, M. E. (2004). Par6α signaling controls glial-guided neuronal migration. *Nat. Neurosci.* 7, 1195–1203. doi: 10.1038/nn1332

Solecki, D. J., Trivedi, N., Govek, E.-E., Kerekes, R. A., Gleason, S. S., and Hatten, M. E. (2009). Myosin II motors and F-actin dynamics drive the coordinated movement of the centrosome and soma during CNS glial-guided neuronal migration. *Neuron* 63, 63–80. doi: 10.1016/j.neuron.2009.05.028

Sottocornola, R., Royer, C., Vives, V., Tordella, L., Zhong, S., Wang, Y., et al. (2010). ASPP2 binds Par-3 and controls the polarity and proliferation of neural progenitors during CNS development. *Dev. Cell* 19, 126–137. doi: 10.1016/j.devcel.2010.06.003

Stark, W. S., Walker, J. A., and Harris, W. A. (1976). Genetic dissection of the photoreceptor system in the compound eye of *Drosophila melanogaster*. *J. Physiol.* 256, 415–439. doi: 10.1113/jphysiol.1976.sp011331

Susini, L., Passer, B. J., Amzallag-Elbaz, N., Juven-Gershon, T., Prieur, S., Privat, N., et al. (2001). Siah-1 binds and regulates the function of Numb. *Proc. Natl. Acad. Sci. U.S.A.* 98, 15067–15072. doi: 10.1073/pnas.261571998

Suzuki, A., and Ohno, S. (2006). The PAR-aPKC system: lessons in polarity. *J. Cell Sci.* 119, 979–987. doi: 10.1242/jcs.02898

Tang, A. H., Neufeld, T. P., Kwan, E., and Rubin, G. M. (1997). PHYL acts to down-regulate TTK88, a transcriptional repressor of neuronal cell fates, by a SINA-dependent mechanism. *Cell* 90, 459–467. doi: 10.1016/S0092-8674(00)80506-1

Traub, L. M. (2003). Sorting it out. *J. Cell Biol.* 163, 203–208. doi: 10.1083/jcb.200309175

Trivedi, N., Ramahi, J. S., Karakaya, M., Howell, D., Kerekes, R. A., and Solecki, D. J. (2014). Leading-process actomyosin coordinates organelle positioning and adhesion receptor dynamics in radially migrating cerebellar granule neurons. *Neural Dev.* 9:26. doi: 10.1186/1749-8104-9-26

Trivedi, N., Stabley, D. R., Cain, B., Howell, D., Laumonnerie, C., Ramahi, J. S., et al. (2017). Drebrin-mediated microtubule–actomyosin coupling steers cerebellar granule neuron nucleokinesis and migration pathway selection. *Nat. Commun.* 8:14484. doi: 10.1038/ncomms14484

Tsai, L.-H., and Gleeson, J. G. (2005). Nucleokinesis in neuronal migration. *Neuron* 46, 383–388. doi: 10.1016/j.neuron.2005.04.013

Vallee, R. B., Seale, G. E., and Tsai, J.-W. (2009). Emerging roles for myosin II and cytoplasmic dynein in migrating neurons and growth cones. *Trends Cell Biol.* 19, 347–355. doi: 10.1016/j.tcb.2009.03.009

Winter, M., Sombroek, D., Dauth, I., Moehlenbrink, J., Scheuermann, K., Crone, J., et al. (2008). Control of HIPK2 stability by ubiquitin ligase Siah-1 and checkpoint kinases ATM and ATR. *Nat. Cell Biol.* 10, 812–824. doi: 10.1038/ncb1743

Wong, C. S. F., Sceneay, J., House, C. M., Halse, H. M., Liu, M. C. P., George, J., et al. (2012). Vascular normalization by loss of Siah2 results in increased

chemotherapeutic efficacy. *Cancer Res.* 72, 1694–1704. doi: 10.1158/0008-5472.CAN-11-3310

Xu, Z., Sproul, A., Wang, W., Kukekov, N., and Greene, L. A. (2006). Siah1 interacts with the scaffold protein POSH to promote JNK activation and apoptosis. *J. Biol. Chem.* 281, 303–312. doi: 10.1074/jbc.M509060200

Yego, E. C. K., and Mohr, S. (2010). Siah-1 protein is necessary for high glucose-induced glyceraldehyde-3-phosphate dehydrogenase nuclear accumulation and cell death in Müller cells. *J. Biol. Chem.* 285, 3181–3190. doi: 10.1074/jbc.M109.083907

Conflict of Interest Statement: The authors declare that the research was conducted in the absence of any commercial or financial relationships that could be construed as a potential conflict of interest.

frontiers in Cellular Neuroscience

MINI REVIEW
published: 16 June 2017
doi: 10.3389/fncel.2017.00163

Neuronal Polarity in the Embryonic Mammalian Cerebral Cortex

*Elif Kon, Alexia Cossard and Yves Jossin**

Mammalian Development and Cell Biology Unit, Institute of Neuroscience, Université catholique de Louvain, Brussels, Belgium

The cerebral cortex is composed of billions of neurons that can grossly be subdivided into two broad classes: inhibitory GABAergic interneurons and excitatory glutamatergic neurons. The majority of cortical neurons in mammals are the excitatory type and they are the main focus of this review article. Like many of the cells in multicellular organisms, fully differentiated neurons are both morphologically and functionally polarized. However, they go through several changes in polarity before reaching this final mature differentiated state. Neurons are derived from polarized neuronal progenitor/stem cells and their commitment to neuronal fate is decided by cellular and molecular asymmetry during their last division in the neurogenic zone. They migrate from their birthplace using so-called multipolar migration, during which they switch direction of movement several times, and repolarize for bipolar migration when the axon is specified. Therefore, neurons have to break their previous symmetry, change their morphology and adequately respond to polarizing signals during migration in order to reach the correct position in the cortex and start making connections. Finally, the dendritic tree is elaborated and the axon/dendrite morphological polarity is set. Here we will describe the function, establishment and maintenance of polarity during the different developmental steps starting from neural stem cell (NSC) division, neuronal migration and axon specification at embryonic developmental stages.

Keywords: neuron, polarity, neocortex, radial migration, multipolar migration, centrosome, reelin, ephrin

OPEN ACCESS

Edited by:
Froylan Calderon De Anda, University of Hamburg, Germany

Reviewed by:
Karun K. Singh, McMaster University, Canada
Simon Hippenmeyer, Institute of Science and Technology Austria, Austria

***Correspondence:**
Yves Jossin
yves.jossin@uclouvain.be

Received: *31 March 2017*
Accepted: *26 May 2017*
Published: *16 June 2017*

Citation:
Kon E, Cossard A and Jossin Y (2017) Neuronal Polarity in the Embryonic Mammalian Cerebral Cortex. Front. Cell. Neurosci. 11:163. doi: 10.3389/fncel.2017.00163

INTRODUCTION: DEVELOPMENT OF THE CEREBRAL CORTEX

The process of brain development is quite amazing. In just 9 months, the human embryonic brain, which starts with a few hundred cells, undergoes a period of explosive growth that results in the generation of close to 100 billion neural cells. The right kinds of neurons have to be made at the adequate time and at the correct location. Each of these neurons has to make connections with an appropriate set of target cells in order to form the neural circuits that underlie the correct functioning of the brain. This precise establishment of neural connections occurs not just in the brain proper but also in the spinal cord and in the peripheral nervous system. However, we will limit this review article to an important part of the brain called the neocortex that plays key roles in learning and memory, sensory and motor functions and the control of our emotions. Cortical neurons can be excitatory, meaning that they trigger an electrical impulse to their targets, or inhibitory. Excitatory neurons are born in the neocortical ventricular zone (VZ) and migrate radially towards the pia in order to form the cortical plate (CP; Anderson et al., 2002; Gorski et al., 2002; Lui et al., 2011). Cortical inhibitory neurons are called interneurons and make local connections. Their main function is to gate or inhibit the initiation

of an electrical impulse. Most of these cortical interneurons is born in the ganglionic eminences and migrates tangentially to reach the cortex (Hatten, 2002; Marin and Rubenstein, 2003; Hansen et al., 2013; Ma et al., 2013; Chu and Anderson, 2015). In the mammalian cortex, the majority of neurons are the excitatory type and we will mostly discuss this population of cells.

The cerebral cortex is the darker zone surrounding the white matter visible on coronal brain sections. This "gray matter" is composed of the cell bodies of different types of neurons that accumulate into six layers (Lui et al., 2011). Each layer comprises neurons that exhibit different morphologies, functions and properties. Excitatory neurons are either connected within the cortex in the same hemisphere or in a contralateral manner or connect to areas outside the cortex such as the spinal cord or the thalamus (Greig et al., 2013).

The formation of this layered structure relies on temporal ordering of stem cell self-renewal followed by well-regulated neurogenic divisions and finally the production of glia cells. Corticogenesis also depends on an extensive migration of immature neurons and their differentiation into fully functional neurons carrying an axon and multiple dendrites. These processes depend on correct polarization of the cells involved.

Polarity is a very important concept in cell biology. Cells are able to generate and maintain an asymmetrical and ordered distribution of structures along an axis resulting in asymmetric cell shape and/or cell functions. It involves a reorganization of cell-surface subdomains, the cell cytoskeleton, cellular organelles and proteins, and is usually triggered by external cues (Drubin and Nelson, 1996; Nelson, 2003). Polarity can be short-lived during dynamic processes or can be maintained for a protracted time such as the whole life of the cell. Virtually almost all cells in the body are polarized to some level and the establishment and maintenance of polarity is crucial during organogenesis.

Intrinsic mechanisms of neuronal polarity have been investigated for a long time using cultures of hippocampal and cortical neurons and focusing on the axon/dendrite axis (Dotti et al., 1988; Craig and Banker, 1994; Tahirovic and Bradke, 2009). However polarity regulation *in vivo* is quite different, mostly because it occurs in a more complex tridimensional environment and is under the influence of a concerted action of intrinsic and extrinsic signals. In addition, other polarizing events besides the axon/dendrite axis are necessary before reaching the final mature differentiation state. Neurons are first produced by neuronal progenitor/stem cells (under the influence of an apico-basal polarity) then migrate from their birthplace to their final destination (importance of a front-rear polarity) while the axon is specified and finally dendrites are formed (axon/dendrite polarity; **Figure 1**). Cortical neurons undergoing these polarizing events travel through different regions of the tissue and therefore migrate through different extracellular environments and polarizing signals. In addition, a functional relationship exists between the molecular mechanisms underlying polarized migration and the final axon/dendrite polarity. Indeed, the trailing process of migrating cortical excitatory neurons is the future axon that elongates at the same time as the cell migrates. Similarly the leading process transforms into apical dendrites after completion of migration (Rakic, 1972; Schwartz et al., 1991; Hatanaka and Murakami, 2002; Hatanaka and Yamauchi, 2013). Because polarity is involved in all these events, defects in its establishment or maintenance have a tremendous effect on the correct functioning of the brain and result in a broad spectrum of disorders such as microcephaly, lissencephaly, mental retardation, schizophrenia, autism and epilepsy (Francis et al., 2006; Liu, 2011; Manzini and Walsh, 2011; Folsom and Fatemi, 2013; Ishii et al., 2016).

In spite of the knowledge accumulated over the years, it is still unclear how polarizing signals coordinate the different steps that pave the journey of a cell from its birth to its final settlement and differentiation into a fully functional neuron. In this review article we will discuss apicobasal polarity during division, front-rear polarity during migration and axon/dendrite polarity during differentiation of cortical excitatory neurons at embryonic developmental stage *in vivo*. We will mostly describe what we know of these events in rodents as most *in vivo* studies of mammalian cerebral cortex development have been done in mice.

POLARITY IN EMBRYONIC NEURAL STEM CELLS AND THE REGULATION OF NEURONAL PRODUCTION

Excitatory neurons are produced by cortical neural stem cells (NSCs; **Figure 1**). Cortical NSCs contribute to most of the major cell types in the cortex: the different subtypes of excitatory neurons, astrocytes and oligodendrocytes (Campbell and Götz, 2002; Gorski et al., 2002; MuhChyi et al., 2013; Gallo and Deneen, 2014). NSCs line the ventricle in a region called VZ. Initially, they divide symmetrically in order to self-renew and amplify their number. This results in an expansion of the pool of NSCs and a lateral expansion of the tissue during embryonic day E9.5–E11.5 in mice (Takahashi et al., 1995).

Then, with the onset of neurogenesis, NSCs transform into another type of apical stem cells called radial glia cells (RGCs). RGCs continue to divide symmetrically, but asymmetric divisions are also observed. Asymmetric divisions create another RGC and a neuron (Miyata et al., 2004; Noctor et al., 2004). This starts the radial expansion of the tissue. With time, RGC division switches more often to the neurogenic asymmetric division. They also start producing intermediate progenitors or basal progenitors that migrate to the sub-VZ (sVZ) lying just above the VZ. Intermediate progenitors are restricted to one or two additional divisions, and all their progeny are neurons. This adds to the neuronal output from the RGCs (Haubensak et al., 2004; Sessa et al., 2008; Vasistha et al., 2015).

The sVZ that contains the intermediate progenitors is much larger in humans compared to mice and is divided into inner sVZ (ISVZ) and outer sVZ (OSVZ; LaMonica et al., 2012). An additional class of progenitor, called outer radial glia, has been described in the human OSVZ (Fietz et al., 2010). Outer radial glia are also present in ferret and mouse but at a much lower

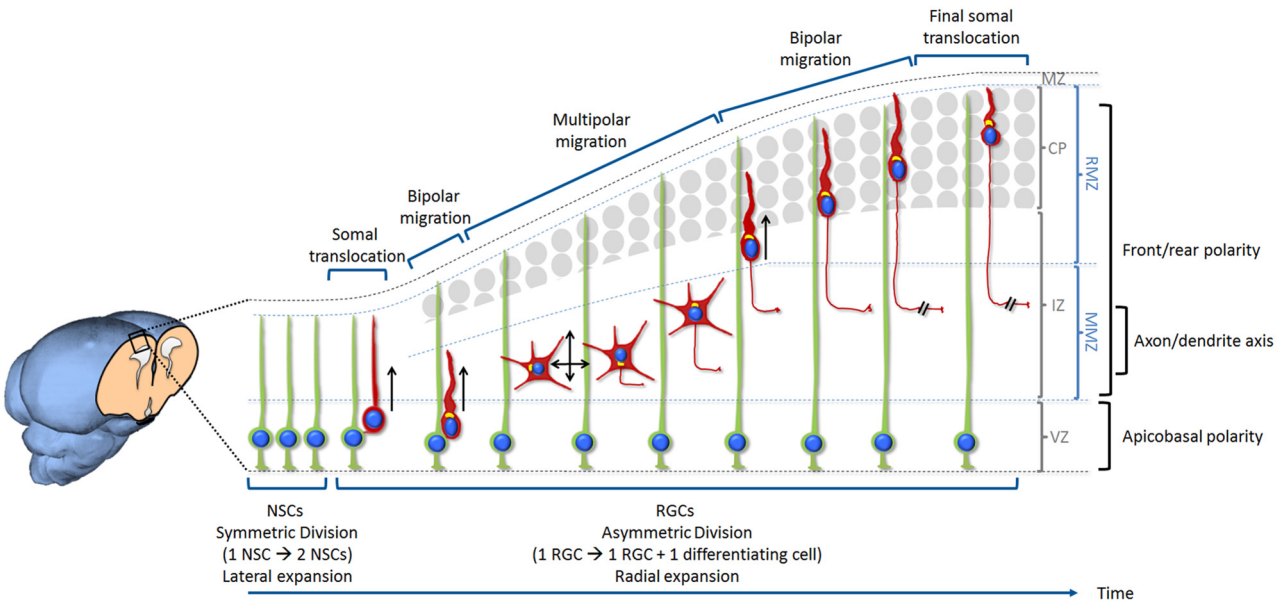

FIGURE 1 | Overview of neurogenesis, migration and differentiation of glutamatergic neurons in the developing mammalian cerebral cortex. Neural stem cells (NSCs) are located at the ventricular zone (VZ). Initially, NSCs divide symmetrically in order to self-renew and increase their number. This results in an expansion of the pool of NSCs and a lateral expansion of the tissue. With the onset of neurogenesis NSCs progressively switch into radial glia cells (RGCs) and start dividing asymmetrically in order to self-renew and produce neurons. This starts the radial expansion of the tissue. During the very early stage of cortical development, the cerebral wall is thin and neurons migrate for a very short distance. After division, new neurons detach from the apical surface while they still keep a basal process inherited from the division of the elongated mother cell. The basal process shortens while nucleus and organelles translocate within the elongated cytoplasm. This particular migration is called somal translocation. Later on, with the accumulation of neurons above the VZ, the thickness of the cerebral wall increases and the somal translocation mode of migration becomes less frequent. It is replaced by a multi-phase mode of migration: first a very short bipolar migration when neurons exit the VZ followed by a multipolar migration in the multipolar morphology zone (MMZ), comprising the sub-VZ (sVZ; not shown here) and the lower part of the intermediate zone (IZ). This is followed by a bipolar migration called locomotion taking place in the radial morphology zone (RMZ) which is made up of the upper part of the IZ and the cortical plate (CP). When neurons reach the top of the RMZ, they seem to proceed through a glia-independent final somal translocation during which the leading process remains attached to the marginal zone (MZ) and shortens as the cell soma moves upward. Like for many other cell types, the centrosome and Golgi apparatus (represented in yellow in the figure) are facing the direction of migration. During the multipolar migration, the position of the centrosome and Golgi apparatus play an instructive role in specifying the future axon. Then the centrosome and Golgi apparatus move away from the growing axon in order to play their role in specifying the orientation of neuronal migration. The events described in this figure are influenced by three types of polarization. Neurons are produced by RGCs (under the influence of an apico-basal polarity) then migrate from their birthplace to their final destination (importance of a front-rear polarity) while the axon is specified during the multipolar phase (axon/dendrite polarity). Bipolar migrating cells (using somal translocation or locomotion) are moving towards the top of the CP (shown by a black arrow). Multipolar migrating neurons switch direction of migration several times tangentially and radially (both apically and basally) but the net movement is still directed towards the CP (shown by two crossing black arrows).

number. They still possess the long radial fiber attached to the pial surface but do not exhibit a process attached to the VZ. The increased diversity and number of progenitor cells in the human cortex account in part for its expansion and gyration (Hansen et al., 2010; Dehay et al., 2015).

Temporal regulation of the ratio of asymmetric to symmetric divisions has been intensively studied in cortical NSCs and RGCs and is critical for balancing appropriate neuronal production with progenitor/stem cells maintenance. Polarized distribution of cellular components or proteins has been investigated as the source of asymmetry in daughter cell fate specification.

Apical Domain and Polarity Proteins

Cortical NSCs and RGCs exhibit an apicobasal polarity. Morphologically, they display a long pia-directed basal process that spans the entire cerebral wall and a short ventricle-directed apical process restricted to the VZ.

It was first suggested that asymmetric segregation of cellular components located at the apical domain between the two daughter cells during cytokinesis is important to regulate their fate. When only one of the daughter cell receives the apical domain, inheritance of this domain would lead to a self-renewing RGC while the other cell will begin migration and start differentiating into a neuron or intermediate progenitor (Kosodo et al., 2004; Marthiens and ffrench-Constant, 2009). In contrast, symmetrically dividing cortical NSCs would receive equal amounts of apical domain after division. However contradictory studies showed an equal distribution of the apical domain between the two daughter cells, even during asymmetric division, and demonstrated no correlation between cell fate of the two daughter cells and the ratio of their apical membrane size at cleavage (Konno et al., 2008; Noctor et al., 2008; Shitamukai et al., 2011). Because differentiating daughter cells inherit an apical domain, mechanisms important for the withdrawal of the apical process from the ventricular surface

must come into play before they delaminate. One suggested mechanism is the downregulation of Adherens Junction (AJs) proteins (Rousso et al., 2012; Itoh et al., 2013). Here the transcriptional repression of cadherins is regulated by proneural genes expressed in differentiating daughter cells. In the chick and mouse spinal cord, abscission of the apical end-foot has been proposed as an alternative mechanism (Das and Storey, 2014). In this model, abscission is dependent on actin-myosin contraction and results in loss of apical cell polarity.

Molecularly, apicobasal polarity is established and maintained in part by cadherin-based AJs (Chenn et al., 1998; Harris and Tepass, 2010). The apical and basolateral membranes are separated by the AJs while occludin-based tight junctions are lost during the transition from apical NSCs to RGCs (Aaku-Saraste et al., 1996). AJs asymmetrically distribute proteins at the apical/basal dimension in cortical NSCs and RGCs while anchoring together the apical end-feet of adjacent cells (Margolis and Borg, 2005). The polarity protein mPar3 is enriched at the lateral domain in the ventricular end-feet of RGCs during interphase but shows asymmetric segregation as the cell cycle progresses. The daughter cell that accumulates mPar3 will become the RGC while the other one will differentiate (Bultje et al., 2009). mPar3 is a known apical polarity protein forming a complex with mPar6 and aPKC and able to interact with Cdc42 (Joberty et al., 2000; Lin et al., 2000). Studies on mPar6 (Costa et al., 2008) and Cdc42 (Cappello et al., 2006) suggest that these apical complex proteins are essential for self-renewal of neural progenitors in the developing mammalian cortex. However, in contrast to its role in invertebrates, deletion of aPKCλ in mice midway through neurogenesis did not clearly affect cell fate decisions, maybe because of some redundancy with aPKCζ (Imai et al., 2006). Pals1 belongs to another apical polarity complex and its conditional removal causes premature withdrawal from the cell cycle (Kim et al., 2010).

Basolateral complex proteins are also essential for the maintenance of cell polarity. Disruption of basolateral proteins and AJs proteins affects the stemness, the balance between symmetric and asymmetric division and the overall cell polarity in RGCs (Shen et al., 2002; Klezovitch et al., 2004; Petersen et al., 2004; Kadowaki et al., 2007; Rasin et al., 2007; Gil-Sanz et al., 2014). In mutant mice deleted for Llgl1, apical NSCs display loss of cell polarity and fail to divide asymmetrically, to exit the cell cycle and to differentiate (Klezovitch et al., 2004). These mice exhibit severe brain disorganization and hemorrhagic hydrocephalus leading to neonatal death. On the other hand, mice with conditionally deleted Llgl1 using Nestin-Cre recombinase survive and show symptoms of epilepsy. Their brains display severe periventricular heterotopias caused by disruption of apical junctional complexes (Jossin et al., 2017). Mechanistically, the basolateral protein LLGL1 directly binds to and promotes internalization of N-cadherin while LLGL1 phosphorylation by the apical protein aPKC prevents this interaction. In this model, the local concentration of N-cadherin in AJs located at the basolateral-apical boundary will increase, while kept low at the lateral membrane domain via LLGL1-mediated internalization (Jossin et al., 2017). Numb is enriched in the apical end-feet of RGCs (Rasin et al., 2007). Loss of function of Numb and Numbl using *in utero* electroporation disrupts cadherin-based AJs and polarity of RGCs (Rasin et al., 2007). Conditional deletion of both Numb and Numbl in the brain results in different effects on proliferation depending on the Cre used for the deletion. If the excision occurs around E8.5 (nestin-Cre) before the onset of neurogenesis, NSCs are depleted (Petersen et al., 2002). If the deletion occurs around E10.5 (D6-Cre) after the onset of neurogenesis, proliferative RGCs are strongly reduced in number (Petersen et al., 2004). However, ablation at around E9.5 using the Emx-Cre driver results in hyperproliferation of RGCs and a defect in differentiation (Li et al., 2003). This discrepancy could be explained by the timing and type of cells targeted (NSCs vs. RGCs) or the severity of the observed disorganization of the proliferative zone causing non-cell-autonomous effects.

Overall these results show that polarity proteins play crucial roles in cell fate decision and the control of proliferation.

Basal Process

The basal end-foot of most NSCs and RGCs basal processes remains attached to the basal lamina throughout the cell cycle (Miyata et al., 2001; Noctor et al., 2001). Basal lamina, meninges, Cajal-Retzius cells and neurons constitute a niche that can signal to and influence NSCs and RGCs (Hartfuss et al., 2003; Seuntjens et al., 2009; Siegenthaler et al., 2009; Griveau et al., 2010). Moreover, the basal process may propagate signals from the end-foot to the cell body (Weissman et al., 2004; Rash et al., 2016). It is therefore not surprising that its inheritance has an influence on the maintenance of proliferative properties (Shitamukai et al., 2011). During the symmetric division of amplifying cortical NSCs, it can be split and equally divided among the two daughter cells (Kosodo et al., 2008), or it can be inherited by one cell while the other one re-extend its own basal process (Miyata et al., 2004). On the other hand, during the asymmetric division of RGCs, it is asymmetrically inherited by only one daughter cell that will self-renew whereas the other one differentiates into a neuron or an intermediate progenitor (Miyata et al., 2004; Shitamukai et al., 2011). Underscoring further its importance, it was shown that asymmetric distribution of Cyclin D2 mRNA at the basal end-foot ensures a RGC fate to the basally positioned daughter cell that inherits the basal process (Tsunekawa et al., 2012). More recently, Pilaz et al. (2016) showed that it is a site of active RNA movement and local translation.

All in all, it is possible that inheritance of both apical and basal processes is necessary to maintain a RGC phenotype.

Centrosome and Primary Cilium

In cortical NSCs and RGCs, the centrosome functions as the basal body of the primary cilium located at the apical domain. The primary cilium is a small appendage of the plasma membrane poking into the cerebrospinal fluid and is central to sensing extracellular signals and transducing signaling cascades. Primary

cilia are critical for normal brain development (Louvi and Grove, 2011). It seems that one of its functions is to determine the correct polarity of emerging RGCs. Indeed, disruption of the primary cilium activity that involves Arl13b results in a reversal of the apicobasal polarity of RGCs (Higginbotham et al., 2013). In these Arl13b mutant mice, cilia are present, but their function is impaired. RGC cell bodies are relocated from the VZ to near the pia surface, while glia end-feet-like structures are observed near the ventricle. The same group showed that conditionally deleting Arl13b later in development during the NSC to RGC transition period has less effect on the polarity and proliferation of RGCs, while deletion after the onset of neurogenesis does not affect RGC structure or division (Higginbotham et al., 2013). One of the signaling pathways conveyed by the primary cilium is Shh (Caspary et al., 2007; Rohatgi et al., 2007). Disruption of Gli3 function (a component of the Shh signaling cascade) after the onset of neurogenesis perturbs the regulation of RGCs proliferation without affecting apicobasal polarity (Wang et al., 2011; Wilson et al., 2012). All those results are suggesting that the primary cilium is important to determine polarity of NSCs and RGCs but is not necessary for its maintenance once it is set.

Molecular asymmetry is also observed at the level of the primary cilium and the associated centrosome during RGC division. A centrosome consists of a pair of centrioles (one mother and one daughter centriole) surrounded by an amorphous pericentriolar material. The two centrioles differ in structure and the older mother centriole supports ciliogenesis faster than the daughter centriole (Anderson and Stearns, 2009). During neurogenic asymmetric division, it was shown that the centrosome retaining the old mother centriole stays in the VZ and is preferentially inherited by RGCs, whereas the centrosome containing the new mother centriole is largely associated with differentiating cells (Wang et al., 2009). The primary cilium is dismantled during M phase and daughter cells have to re-establish it after mitosis completion. It was shown that the daughter cell receiving the older centriole re-form the primary cilium earlier than the other daughter and adopt a RGC fate (Paridaen et al., 2013). This asynchrony differentially exposes the daughter cells to primary cilium-transmitted signals and could explain the difference in fate.

In addition, the cell that inherits the younger centrosome forms a primary cilium located at the basolateral membrane instead of the apical membrane while still attached to the apical surface. The fate of this cell is to delaminate and become either a basal progenitor or a postmitotic neuron (Wilsch-Bräuninger et al., 2012). This asymmetrical inheritance of the primary cilium has consequences on the timing and quality of the signals it potentially receives such as proliferative cues present in the cerebrospinal fluid (Lehtinen et al., 2011).

In humans, diseases related to defects in primary cilia are associated with brain malformations and mental retardation (Rauch et al., 2008; Goetz and Anderson, 2010; Lee and Gleeson, 2011). Likewise, there are clear genetic links between centrosomal proteins and human brain diseases such as microcephaly (Woods et al., 2005; Kumar et al., 2009; Chavali et al., 2014). Notably, the multiple brain malformations observed in some microcephaly patients with specific mutations suggest that the centrosome and its associated proteins are involved in multiple aspects of brain development such as neurogenesis, polarity, migration or differentiation (Passemard et al., 2009; Nicholas et al., 2010; Yu et al., 2010).

POLARITY IN EARLY BORN NEURONS

During the very early stage of cortical development, the cerebral wall is thin and neurons migrate for a very short distance. After division, new neurons detach from the apical surface while they still keep a basal process inherited from the division of the elongated mother cell. The basal process shortens while nucleus and organelles translocate within the elongated cytoplasm (Nadarajah et al., 2001; Gupta et al., 2002). This particular migration is called somal translocation (**Figure 1**). The polarity is already set after cell division and seems to be inherited from the apicobasal polarity of the RGCs. This process is very similar to what occurs during retinal ganglion cell migration (Zolessi et al., 2006; Randlett et al., 2011).

In parallel with the somal translocation, the axon grows from the apical side of the translocating neuron. It is possible that, similarly to what was shown for Drosophila sensory neurons, molecular remnants such as the clustering of AJ components corresponding to the last mitotic cleavage might be important for axon specification (Pollarolo et al., 2011).

POLARITY IN MID TO LATE BORN NEURONS

Later on, with the accumulation of neurons above the VZ, the thickness of the cerebral wall increases and the somal translocation mode of migration becomes less frequent. It is replaced by a multi-phase mode of migration: a very short bipolar migration when neurons exit the VZ followed by an extended multipolar migration occurring in the multipolar morphology zone (MMZ), comprising the sVZ and the lower part of the intermediate zone (IZ). This is followed by a bipolar migration called locomotion taking place in the radial morphology zone (RMZ) which is made up of the upper part of the IZ and the cortical plate (CP; Shoukimas and Hinds, 1978; Nadarajah et al., 2001; Noctor et al., 2004; Jossin, 2011). When neurons reach the top of the RMZ, they seem to proceed through a glia-independent final somal translocation during which the leading process remains attached to the marginal zone (MZ) and shortens as the cell soma moves upward (Nadarajah et al., 2001; Sekine et al., 2011; **Figure 1**).

During the short bipolar migration at the VZ, cells are polarized towards the CP. Similarly to what occurs for early born cortical neurons and during retinal ganglion cell migration (Zolessi et al., 2006; Randlett et al., 2011), they might inherit polarity from the mother neuroepithelial cell. This is visible by the asymmetric distribution of N-cadherin at one pole of the daughter neuron after division (Gärtner et al., 2012). However the axon is not specified at that stage. When they reach the MMZ, they become multipolar. "Multipolar neurons" means that they lose their bipolar morphology and extend more than two neurites. Those neurites extend and retract frequently and

point to multiple directions. During this multipolar stage, they switch direction of migration several times tangentially and radially (both apically and basally) but the net movement is still directed towards the CP (Tabata and Nakajima, 2003; Bielas et al., 2004; Noctor et al., 2004; **Figure 1**). Nothing is known about the signals that triggers this bipolar to multipolar change of shape and polarity. One study however suggested the involvement of Connexin 43 (Liu et al., 2012). Another unanswered question is why they go through this multipolar stage. Multipolar migration might help neurons move across the IZ crowded with tangentially oriented axons but recent studies suggest a more functional role in tangentially dispersing cortical neurons (see below; Torii et al., 2009; Dimidschstein et al., 2013).

At the same time intermediate basal progenitors are produced and most of the late-born upper layer neurons come from these cells (Molyneaux et al., 2007; Sessa et al., 2008; Kowalczyk et al., 2009). Unlike RGCs, basal progenitors do not seem to possess an apicobasal polarity and therefore cannot provide a polarity cue to the multipolar neurons they give birth to.

Extracellular Signals for the Directionality of Multipolar Migration

While many regulatory pathways involved in the multipolar to bipolar migration transition have been investigated (briefly discussed in "Signals for Multipolar to Bipolar Transition" Section), only a few signaling pathways were proposed to regulate the directionality of multipolar neurons. Recently the extracellular protein Reelin has been shown to be involved in polarizing the movement of multipolar neurons towards the CP while they are migrating through the MMZ (Jossin, 2011; Jossin and Cooper, 2011; **Figure 2**). In the absence of Reelin (reeler mice), mid to late born neurons exhibit a broader and irregular distribution and fail to organize into layers (Boyle et al., 2011). In humans, mutations in the reelin pathway are associated with autosomal recessive lissencephaly and cerebellar hypoplasia, schizophrenia, autism and epilepsy (Hong et al., 2000; Chang et al., 2007; Folsom and Fatemi, 2013; Ishii et al., 2016). Reelin is secreted by Cajal-Retzius cells located in the MZ right above the CP (D'Arcangelo et al., 1995; Ogawa et al., 1995). Earlier studies showed that, while the full-length Reelin is mostly present near its secreting cells, only the processed protein and most importantly the active central processing fragment diffuse from the MZ into the deeper tissue such as the MMZ (Jossin et al., 2007). Interestingly, the MMZ is where the highest expression of receptors for Reelin is seen on migrating neurons (Uchida et al., 2009; Hirota et al., 2015). Later on, *in vivo* experiments and using time lapse videomicroscopy in organotypic and lattice cultures demonstrated that the inhibition of intracellular signaling induced by Reelin reduces the movement of multipolar neurons towards the CP and increases the tangential movements whereas the speed of migration is not affected (Jossin and Cooper, 2011). In parallel, fewer multipolar neurons point their Golgi apparatus (usually facing the direction of migration) towards the CP. Along this line, a function of Reelin in orienting the Golgi apparatus from the axon toward the future largest dendrite was shown *in vivo* and *in vitro* (Matsuki et al., 2010; Meseke et al., 2013).

The action of Reelin at the MMZ depends on the activation of Rap1 necessary to maintain a proper level of N-cadherin at the cell surface (Jossin and Cooper, 2011). After receiving this polarizing cue triggered by Reelin/Rap1/N-cadherin in the MMZ, cells downregulate the signal through degradation of Reelin receptors (Morimura et al., 2005; Uchida et al., 2009), N-cadherin (Kawauchi et al., 2010) and the intracellular adaptor protein Dab1 (Bock et al., 2004; Simó et al., 2010). This downregulation of the signal seems to be important for a correct organization of the cerebral cortex. For example, the ablation of Cullin 5 in migrating neurons results in an accumulation of active Dab1 protein and a cortical layering defect (Feng et al., 2007) while a stabilized mutant Dab1, which resists Cul5-dependent degradation, causes a similar phenotype (Simó et al., 2010).

It is worth noting that rescue experiments showed that activation of the Rap1/N-cadherin pathway only partially rescues the phenotype at the MMZ due to Reelin inhibition and that activation of Akt (which is activated by Reelin in neuronal culture; Beffert et al., 2002; Jossin and Goffinet, 2007) is also needed for a complete rescue (Jossin and Cooper, 2011).

Regulation of cell surface receptors like N-cadherin involves endocytosis, exocytosis, recycling and actin cytoskeleton. As such, molecules known to be involved in those functions such as RalA/B, Rac1 and Cdc42 are implicated in the Rap1-dependent polarization of multipolar neurons (Jossin and Cooper, 2011). Others like Rab5 and Rab11 were also involved in the regulation of N-cadherin in cortical neurons (Kawauchi et al., 2010).

A polarity model for Reelin was unexpected because the position where Reelin is produced does not seem to be important for its function in the embryonic cortex. Forcing the expression of Reelin at the VZ in a Reelin-deficient cortex is able to rescue an early aspect of the reeler phenotype (Magdaleno et al., 2002) and adding Reelin in the culture medium of reeler brain slices is able to rescue the organization of the CP (Jossin et al., 2004). Therefore, and as suggested before (Jossin, 2011), Reelin might rather act as a permissive signal allowing neurons to respond to another polarizing cue that still needs to be discovered.

Ephrin guidance factors and their Eph receptors also regulate the directionality of multipolar migration (Torii et al., 2009; Dimidschstein et al., 2013). Ephrins are cell-surface proteins that trigger a forward signal when binding to Eph family receptors present on other cells. In turn, Eph receptors can also trigger a signal to ephrins through a process of reverse signaling (Arvanitis and Davy, 2008). Eph receptors and ephrins are grouped into class A and class B based on their degree of sequence similarity and binding affinities, with ephrin-A binding to EphA receptors and ephrin-B binding to EphB receptors (Flanagan and Vanderhaeghen, 1998). It was first shown that the Ephrin-A/EphA forward signaling controls the lateral distribution of neurons by promoting a wider tangential migration during the multipolar stage (Torii et al., 2009). Later on it was demonstrated that ephrin-B1 reverse signaling may have an opposite effect and restricts the tangential migration of mutipolar neurons at the MMZ (Dimidschstein et al., 2013; **Figure 2**). This function however does not seem to be easily explained by pro-adhesive

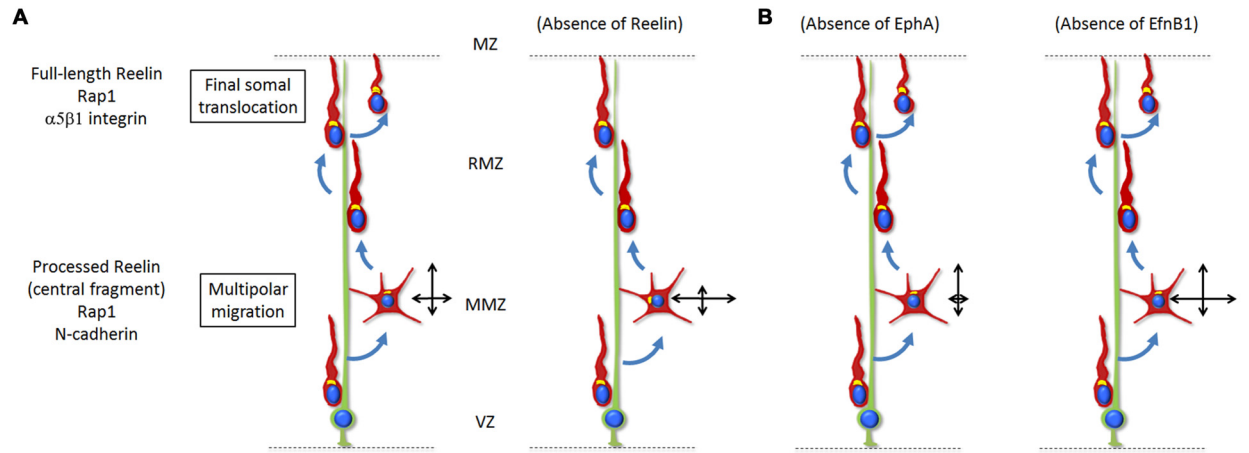

FIGURE 2 | (A) Reelin signaling, via Rap1 and N-Cadherin, regulates the orientation of multipolar neurons towards the top of the CP. Only the processed protein and most importantly the active central processing fragment diffuse from the MZ into the deeper tissue such as the MMZ. The absence of Reelin signaling results in disoriented migration (represented by the two crossing black arrows) with a reduced movement towards the CP and increased lateral movement in the tangential directions. During the last stages of radial migration, Reelin signaling controls the final somal translocation via inside-out activation of α5β1-Integrin signaling. The absence of Reelin signaling results in a defective final somal translocation. **(B)** Ephrin-A/EphA forward signaling controls the lateral distribution of neurons by promoting a wider tangential migration during the multipolar stage. Absence of the signal results in a decreased lateral movement. On the other hand, ephrin-B1 reverse signaling has an opposite effect and restricts the tangential migration of mutipolar neurons at the MMZ. Absence of the signal results in a wider lateral movement.

effects of Ephrin/Eph interactions (Dimidschstein et al., 2013). In this article, P-Rex1, a guanine-exchange factor for Rac3 was identified and shown to be required for the control of the lateral migration.

One intriguing question is whether Reelin and ephrins regulate the directionality of multipolar migration in a same pathway or in parallel. Indeed, an inhibition of the Reelin/NCad pathway does not only reduces the radial movement but also increases the lateral displacement of multipolar neurons (Jossin and Cooper, 2011) similarly to an inhibition of ephrin B. Unfortunately the final lateral dispersion was not investigated in this study. A genetic link between the Reelin signaling and ephrin Bs has been suggested (Sentürk et al., 2011). However another team could not confirm the genetic interaction between ephrin B and the canonical Reelin pathway in the radial positioning of cortical neurons (Pohlkamp et al., 2016). Further investigation is needed to definitively answer this question.

According to the concept of radial units, sister cells move from the VZ to the CP where they form functional units arranged as mini-columns (Rakic, 1988; Gao et al., 2013). Multipolar migration and the lateral dispersion that occurs during this critical stage may play an important physiological role since clonally related neurons establish preferential connectivity with each other and can share similar functional properties (Yu et al., 2009, 2012; Li et al., 2012). This seems to be relevant in terms of human health as inappropriate neuronal positioning and abnormal columnar organization have been reported in post-mortem analysis of cortical tissue from subjects with neuropsychiatric disorders and have been related to aging (Buxhoeveden and Casanova, 2002; Casanova and Tillquist, 2008; van Veluw et al., 2012).

Specification of the Axon at the IZ

In the past, most of the studies investigating axon/dendrite were carried out using dissociated cultures of rodent hippocampal and cortical neurons placed on a two-dimensional artificial substrate (Dotti et al., 1988; Craig and Banker, 1994; Tahirovic and Bradke, 2009). In this system neurons first extend several neurites during what is called stages 1 and 2. Then starts a phase of asymmetric growth (stage 3) during which one of the neurites differentiates into an axon. The main advantage of this system is to be in a well-controlled environment simpler than the *in vivo* situation.

Indeed, very few external signals are present in dissociated cell cultures and the neurons break symmetry randomly. This allowed the identification of several intracellular signaling pathways important for the polarization of the axon/dendrite axe *in vitro* including small GTPases, scaffolding proteins, microtubule-associated proteins, kinases and phosphatases (Arimura and Kaibuchi, 2007; Villarroel-Campos et al., 2016). *In vivo*, however, neurons are generated within a highly oriented three-dimensional tissue. Neuronal polarity is therefore most probably the result of a complex interaction between extracellular cues and intrinsic cell polarity pathways. Extracellular factors such as BDNF and IGF-1 exogenously applied to neuronal cultures have been suggested to initiate the specification of the axonal polarity (Sosa et al., 2006; Shelly et al., 2007). But axon formation was not affected in mice lacking those extracellular cues or their specific receptors (Klein et al., 1993; Jones et al., 1994; Kappeler et al., 2008). On the other hand, TGF-beta signaling has been shown to specify the axon *in vitro* and *in vivo* (Yi et al., 2010).

Several intracellular signaling proteins involved in axon/dendrite polarity *in vitro* have been confirmed *in vivo*:

in the double knockout mice for SAD-A and SAD-B kinases, axons were difficult to distinguish from dendrites and dendrites were abnormally oriented. Moreover, this polarity defect did not result from a growth deficiency (Kishi et al., 2005). Lkb1 is an upstream kinase for SAD-A and SAD-B and conditionally deleting Lkb1 resulted in a loss of axon formation (Asada et al., 2007; Barnes et al., 2007; Shelly et al., 2007). Cortical neuron-specific Par3 inhibition using *in utero* electroporation impaired axon/dendrite polarization *in vivo* (Funahashi et al., 2013). Genetic ablation of Cdc42 in the brain strongly suppressed axon formation *in vivo* and in culture, through modulation of actin dynamics (Garvalov et al., 2007). The implication of c-Jun amino-terminal kinase (JNK) enzymes in axon specification and elongation has been described *in vitro* (Oliva et al., 2006; Dajas-Bailador et al., 2008; Eminel et al., 2008; Sun et al., 2013). JNK is a family of three partially redundant isoforms and involved in apoptosis during early brain development (Kuan et al., 1999), rendering difficult the *in vivo* analysis of their contribution in axonal specification and elongation. Nevertheless, JNK1 mutant mice exhibit a defect in the maintenance of axonal integrity (Chang et al., 2003). Overall, these results confirm certain polarity genes as vital for axon/dendrite polarity establishment or maintenance *in vivo*.

At the IZ multipolar neurons migrate through horizontally oriented axons belonging to earlier-born neurons already installed in the CP. It has been suggested that a TAG1-dependent interaction between multipolar neurons and those axons helps the specification of an axon from multipolar cells (Namba et al., 2014). However, another study proposed that the interaction between radial glial fibers and the migrating neuron directs axon formation at the opposite side from the contact site (Xu et al., 2015). It is possible that both types of interactions are necessary.

In mid to late born neurons *in vivo*, axons are specified at the multipolar stage just before neurons resume a bipolar migration (de Anda et al., 2010; Hatanaka and Yamauchi, 2013; Sakakibara et al., 2014; **Figure 1**). It is therefore tempting to speculate that the specification of the axon is necessary for the polarization of migrating multipolar neurons towards the CP. However several studies suggest that this is not the case. Indeed, even though there is a defect in axonal growth in Rap1 conditional KO mice (Shah et al., 2016), an acute but partial inhibition of Rap1 affects the polarization of multipolar cells towards the CP without an apparent effect on axonal growth (Jossin and Cooper, 2011). Therefore the defect in the orientation of multipolar migration observed is independent of axonal growth. Similarly, Cdk5 is required for the multipolar to bipolar transition but these neurons still can form axons (Ohshima et al., 2007). Along the same line, the multipolar to bipolar transition is not affected by the lack of an axon: in the absence of LKB1 and SAD kinases or of TGF-beta signaling, migrating neurons failed to produce an axon even though they were able to become bipolar and extend a leading process (Barnes et al., 2007; Yi et al., 2010). Therefore it seems that polarization events necessary for: (1) the specification of an axon; (2) the directionality of multipolar neuronal migration; (3) the multipolar to bipolar transition; and (4) the directionality of bipolar neuronal migration all use at least some mechanisms that are distinct *in vivo*.

In humans, several disorders such as autism, schizophrenia, bipolar disorder, mental retardation and some forms of epilepsy are thought to have a perturbed cortical circuitry (Francis et al., 2006). Neuropathological observations in postmortem brain samples include subtle disturbances of cortical lamination and subcortical axonal morphology. Moreover, defects in proteins involved in the specification of axonal-dendrite axe of polarity lead to connectivity-related disorders (Maussion et al., 2008; Corbett et al., 2010; McFadden and Minshew, 2013; Nieto et al., 2013; Quach et al., 2015).

Centrosome

The position of the centrosome plays an important role in many polarization events. In neuronal culture *in vitro*, its localization specifies the future axon and therefore determines the axon-dendrite polarity (de Anda et al., 2005). *In vivo* the axon of cortical excitatory neurons is specified during the multipolar stage of migration (Shoukimas and Hinds, 1978; Hatanaka and Yamauchi, 2013). Then the axonal growth takes place in parallel with neuronal migration (Schwartz et al., 1991; Hatanaka and Murakami, 2002). A previous study suggested that centrosome and Golgi apparatus position plays an instructive role in specifying the location of axonal outgrowth (de Anda et al., 2010). Then they move away from the growing axon in order to play their role in instructing the orientation of neuronal migration (Shu et al., 2004; Tanaka et al., 2004; Tsai et al., 2007), suggesting that they are not necessary for axonal growth once it is specified *in vivo*. This is in agreement with a study showing that the centrosome is dispensable for axonal extension in hippocampal cell culture (Stiess et al., 2010).

It should be noted that the situation can be different in different models such as in the zebrafish retinal ganglion cells where the centrosome does not predict the site of axon emergence (Zolessi et al., 2006) or in the dsas-4 and dsas-6 mutant flies (with no centrioles) where the development of axons is quite normal (Basto et al., 2006). However, it is possible that these flies still possess the pericentriolar material or that the Golgi apparatus might compensate for the lack of centrioles as a site of microtubules nucleation (Efimov et al., 2007).

The centrosome is also important for orienting the migration of cortical neurons, especially during the locomotion of bipolar neurons along glia within the CP. Here the movement is saltatory (Nadarajah et al., 2001) with repetitions of a two-step cycle: the centrosome moves forward in the leading process then the nucleus follows (Tsai et al., 2007). The centrosome seems to regulate nuclear translocation. Microtubules surround the nucleus in a fork-like shape and extend to the centrosome (Xie et al., 2003) while SUN and Nesprin proteins connect the centrosome to the nucleus via microtubules during radial bipolar migration (Zhang et al., 2009). Lis1 and dynein, a microtubule minus-end-directed motor, are responsible for coupling nuclear translocation and centrosome movement (Tsai et al., 2007). Microtubules are oriented with their minus-end towards the centrosome and dynein is concentrated at a dilation in the leading process and near the nucleus. Therefore, Dynein may pull the centrosome forward toward the dilation and the nucleus toward the

centrosome (Tsai et al., 2007). In humans, abnormalities in centrosomal proteins such as lis1 cause lissencephalies and subcortical band heterotopia (Cardoso et al., 2000; Sicca et al., 2003).

Signals for Multipolar to Bipolar Transition

After making their way through the MMZ, multipolar neurons transform into bipolar neurons. They invade the RMZ and are polarized towards the pial surface. They exhibit a thick leading process and a thin axon growing at the rear (Noctor et al., 2001; Hatanaka and Murakami, 2002). This type of migration depends on radial glia fibers as substrate. An important step here is the transition from multipolar to bipolar migration. Many changes occur: the substrate for migration (from glial fiber-independent to glial fiber-dependent), the shape of the cell (multipolar to bipolar) and the speed of migration (from about 4 microns per hour to around 12 microns per hour when investigated in organotypic brain slice cultures). Several proteins including kinases, small GTPases, regulators of the cytoskeleton or membrane proteins have been discovered to be involved in this transition (Kawauchi et al., 2003; Nagano et al., 2004; LoTurco and Bai, 2006; Ohshima et al., 2007; Young-Pearse et al., 2007; Sapir et al., 2008; Sun et al., 2010; Nakamuta et al., 2011; Pacary et al., 2011; Westerlund et al., 2011; Lee et al., 2012; Falace et al., 2014; Inoue et al., 2014; Jacobshagen et al., 2014). Because of the diversity of molecules implicated, multiple mechanisms might explain the defect in the transition observed when they are inhibited. However it appears that a common feature is a direct or indirect regulation of the cytoskeleton. We will not discuss them here and would like to refer the readers to other recent reviews on the subject (Cooper, 2014; Ohtaka-Maruyama and Okado, 2015).

We have seen earlier that molecular pathways are involved in polarizing the movement of multipolar neurons towards the CP. Once they reach the top of the MMZ, they initiate their attachment to the radial glia fibers which might give them the signal to transform into bipolar cells but there is no hard proof for this and cells might become bipolar before they attach to the fibers. Since multipolar neurons switch direction of migration a few times while their net movement is oriented towards the CP, it is also possible that signals that trigger the multipolar to bipolar transition are actually reinforcing the polarity of the movement towards the CP already present in the multipolar cells.

Bipolar Migration

During bipolar migration, neurons exhibit a constant polarized migration towards the pial surface and migrate along radial glia fibers in order to reach the top of the CP (Noctor et al., 2001; Hatanaka and Murakami, 2002). Because the substrate of migration is the radial glia, it has been assumed that directionality was conferred by the fibers. It was shown that the interaction with radial fibers is mediated by Connexin 43 (Elias et al., 2007). Connexin 43 is expressed at the contact points between radial glia and migrating neurons. It interacts with the cytoskeleton enabling the stabilization of the leading process along the fibers. Interfering with Connexin 43 expression inhibits neuron migration into the RMZ (Elias et al., 2007).

Adhesion to the radial glia fibers is not the only factor regulating bipolar migration. Extracellular signals also come into play. At least one secreted cue is important to keep the directionality of the bipolar migration. Semaphorin-3A is a secreted factor expressed by the superficial layers of the CP that diffuses in a descending gradient across the cerebral wall. Semaphorin-3A receptors neuropilin-1 and several Plexins are expressed by migrating neurons (Polleux et al., 2000; Chen et al., 2008). Inhibition experiments and time lapse video microscopy showed that Sema3a and its receptors are important to keep bipolar neurons polarized towards the CP (Chen et al., 2008). Inhibited neurons showed a mis-oriented bipolar migration and exhibited a leading process pointing to the wrong direction. They accumulated within the different layers of the CP and at the border between the MMZ and RMZ. Modification of the location of Sema3A gradient in slice culture assays also affected the polarity of migration suggesting that it is acting as an attractive molecule rather than affecting the interaction with the radial fibers (Chen et al., 2008).

Other extracellular signaling proteins are important for a correct bipolar migration but might not do so by regulating the directionality of migration. Tgf-beta extracellular signaling is required for radial migration. Neurons inhibited for the receptor TgfbR2 are able to proceed through the multipolar to bipolar transition, and exhibit a correctly oriented leading process but are unable to migrate and remain stuck in the lower part of the CP (Yi et al., 2010).

As explained in "Extracellular Signals for the Directionality of Multipolar Migration" Section, once Reelin/NCad signaling has triggered polarization of multipolar neurons towards the CP, it is no longer required for the radial glia-dependent bipolar migration (Jossin and Cooper, 2011). But as soon as bipolar migrating neurons reach the top of the CP, they must proceed through a glia-independent terminal translocation during which neurons detach from the radial glia fiber and the leading process shortens as the soma moves upward (Nadarajah et al., 2001; Sekine et al., 2011). This time Reelin and Rap1 rather regulate integrin receptors while N-cadherin is not involved (Sekine et al., 2012). Reelin signaling in neurons reaching the top of the CP promotes neuronal adhesion to fibronectin through integrin α5β1. The activated integrin then allows final somal translocation (Sekine et al., 2012). Of note, earlier-born neurons also undergo glia-independent somal translocation but this does involved Reelin/Rap1/NCad (Gil-Sanz et al., 2013). For these early-born cells, somal translocation depends on the interaction between the leading process of migrating neurons and Cajal-Retzius cells. However, inhibition of this interaction did not affect cell polarization (localization of the Golgi apparatus ahead of the nucleus) and leading process extension (Gil-Sanz et al., 2013). The reeler phenotype in the cortex might therefore be a combination of the absence of Reelin's multiple functions at different stages of radial migration.

Finally, inhibition of the intracellular protein JNK inhibits bipolar migration but polarity of migration does not seem to be affected. JNK inhibition does not affect the multipolar

to bipolar transition. Neurons with inhibited JNK exhibit a leading process oriented in the correct direction but it is twisted and unable to lead the migration resulting in cells stalled at the bottom of the RMZ (Kawauchi et al., 2003).

CONCLUDING REMARK

Glutamatergic excitatory cortical neurons are born near the ventricle then travel long distances in order to reach their final destination within the cortex. Polarization events play critical roles during the embryonic development of the cortex. First, molecular and cellular polarity is essential for NSCs to self-renew and produce the adequate number of neurons at a correct timing. Then a precise coordination of extracellular and intrinsic polarity signals is necessary for the definition of the directionality of migration. Finally the axon/dendrite polarization occurs during the multipolar migration.

Advances in our understanding in polarization events have been made by using techniques to manipulate signaling pathways such as *in utero* electroporation and conditional gene knockout and by using live imaging techniques. However, an important challenge still facing the field is to discover how all these extracellular cues and intrinsic signals precisely regulate polarization events in a coordinated manner *in vivo*.

AUTHOR CONTRIBUTIONS

YJ wrote the manuscript. EK and AC substantially contributed to the manuscript through discussions.

ACKNOWLEDGMENTS

I gratefully thank J.A. Cooper and V. Vasioukhin, for helpful comments on the manuscript. YJ is a Fonds National de la Recherche Scientifique (FNRS) investigator. EK and AC are supported by Fonds pour la Formation à la Recherche dans l'Industrie et dans l'Agriculture (FRIA) fellowships. Research in the author's laboratory is supported by grants J.0129.15 and J.0179.16 from the FNRS.

REFERENCES

Aaku-Saraste, E., Hellwig, A., and Huttner, W. B. (1996). Loss of occludin and functional tight junctions, but not ZO-1, during neural tube closure—remodeling of the neuroepithelium prior to neurogenesis. *Dev. Biol.* 180, 664–679. doi: 10.1006/dbio.1996.0336

Anderson, S. A., Kaznowski, C. E., Horn, C., Rubenstein, J. L., and McConnell, S. K. (2002). Distinct origins of neocortical projection neurons and interneurons *in vivo*. *Cereb. Cortex* 12, 702–709. doi: 10.1093/cercor/12.7.702

Anderson, C. T., and Stearns, T. (2009). Centriole age underlies asynchronous primary cilium growth in mammalian cells. *Curr. Biol.* 19, 1498–1502. doi: 10.1016/j.cub.2009.07.034

Arimura, N., and Kaibuchi, K. (2007). Neuronal polarity: from extracellular signals to intracellular mechanisms. *Nat. Rev. Neurosci.* 8, 194–205. doi: 10.1038/nrn2056

Arvanitis, D., and Davy, A. (2008). Eph/ephrin signaling: networks. *Genes Dev.* 22, 416–429. doi: 10.1101/gad.1630408

Asada, N., Sanada, K., and Fukada, Y. (2007). LKB1 regulates neuronal migration and neuronal differentiation in the developing neocortex through centrosomal positioning. *J. Neurosci.* 27, 11769–11775. doi: 10.1523/JNEUROSCI.1938-07.2007

Barnes, A. P., Lilley, B. N., Pan, Y. A., Plummer, L. J., Powell, A. W., Raines, A. N., et al. (2007). LKB1 and SAD kinases define a pathway required for the polarization of cortical neurons. *Cell* 129, 549–563. doi: 10.1016/j.cell.2007.03.025

Basto, R., Lau, J., Vinogradova, T., Gardiol, A., Woods, C. G., Khodjakov, A., et al. (2006). Flies without centrioles. *Cell* 125, 1375–1386. doi: 10.1016/j.cell.2006.05.025

Beffert, U., Morfini, G., Bock, H. H., Reyna, H., Brady, S. T., and Herz, J. (2002). Reelin-mediated signaling locally regulates protein kinase B/Akt and glycogen synthase kinase 3β. *J. Biol. Chem.* 277, 49958–49964. doi: 10.1074/jbc.M209205200

Bielas, S., Higginbotham, H., Koizumi, H., Tanaka, T., and Gleeson, J. G. (2004). Cortical neuronal migration mutants suggest separate but intersecting pathways. *Annu. Rev. Cell Dev. Biol.* 20, 593–618. doi: 10.1146/annurev.cellbio.20.082503.103047

Bock, H. H., Jossin, Y., May, P., Bergner, O., and Herz, J. (2004). Apolipoprotein E receptors are required for reelin-induced proteasomal degradation of the neuronal adaptor protein disabled-1. *J. Biol. Chem.* 279, 33471–33479. doi: 10.1074/jbc.M401770200

Boyle, M. P., Bernard, A., Thompson, C. L., Ng, L., Boe, A., Mortrud, M., et al. (2011). Cell-type-specific consequences of Reelin deficiency in the mouse neocortex, hippocampus, and amygdala. *J. Comp. Neurol.* 519, 2061–2089. doi: 10.1002/cne.22655

Bultje, R. S., Castaneda-Castellanos, D. R., Jan, L. Y., Jan, Y. N., Kriegstein, A. R., and Shi, S. H. (2009). Mammalian Par3 regulates progenitor cell asymmetric division via notch signaling in the developing neocortex. *Neuron* 63, 189–202. doi: 10.1016/j.neuron.2009.07.004

Buxhoeveden, D. P., and Casanova, M. F. (2002). The minicolumn hypothesis in neuroscience. *Brain* 125, 935–951. doi: 10.1093/brain/awf110

Campbell, K., and Götz, M. (2002). Radial glia: multi-purpose cells for vertebrate brain development. *Trends Neurosci.* 25, 235–238. doi: 10.1016/s0166-2236(02)02156-2

Cappello, S., Attardo, A., Wu, X., Iwasato, T., Itohara, S., Wilsch-Bräuninger, M., et al. (2006). The Rho-GTPase cdc42 regulates neural progenitor fate at the apical surface. *Nat. Neurosci.* 9, 1099–1107. doi: 10.1038/nn1744

Cardoso, C., Leventer, R. J., Matsumoto, N., Kuc, J. A., Ramocki, M. B., Mewborn, S. K., et al. (2000). The location and type of mutation predict malformation severity in isolated lissencephaly caused by abnormalities within the LIS1 gene. *Hum. Mol. Genet.* 9, 3019–3028. doi: 10.1093/hmg/9.20.3019

Casanova, M. F., and Tillquist, C. R. (2008). Encephalization, emergent properties, and psychiatry: a minicolumnar perspective. *Neuroscientist* 14, 101–118. doi: 10.1177/1073858407309091

Caspary, T., Larkins, C. E., and Anderson, K. V. (2007). The graded response to Sonic Hedgehog depends on cilia architecture. *Dev. Cell* 12, 767–778. doi: 10.1016/j.devcel.2007.03.004

Chang, B. S., Duzcan, F., Kim, S., Cinbis, M., Aggarwal, A., Apse, K. A., et al. (2007). The role of RELN in lissencephaly and neuropsychiatric disease. *Am. J. Med. Genet. B Neuropsychiatr. Genet.* 144B, 58–63. doi: 10.1002/ajmg.b.30392

Chang, L., Jones, Y., Ellisman, M. H., Goldstein, L. S., and Karin, M. (2003). JNK1 is required for maintenance of neuronal microtubules and controls phosphorylation of microtubule-associated proteins. *Dev. Cell* 4, 521–533. doi: 10.1016/s1534-5807(03)00094-7

Chavali, P. L., Pütz, M., and Gergely, F. (2014). Small organelle, big responsibility: the role of centrosomes in development and disease. *Philos. Trans. R. Soc. Lond. B Biol. Sci.* 369:20130468. doi: 10.1098/rstb.2013.0468

Chen, G., Sima, J., Jin, M., Wang, K. Y., Xue, X. J., Zheng, W., et al. (2008). Semaphorin-3A guides radial migration of cortical neurons during development. *Nat. Neurosci.* 11, 36–44. doi: 10.1038/nn2018

Chenn, A., Zhang, Y. A., Chang, B. T., and McConnell, S. K. (1998). Intrinsic polarity of mammalian neuroepithelial cells. *Mol. Cell. Neurosci.* 11, 183–193. doi: 10.1006/mcne.1998.0680

Chu, J., and Anderson, S. A. (2015). Development of cortical interneurons. *Neuropsychopharmacology* 40, 16–23. doi: 10.1038/npp.2014.171

Cooper, J. A. (2014). Molecules and mechanisms that regulate multipolar migration in the intermediate zone. *Front. Cell. Neurosci.* 8:386. doi: 10.3389/fncel.2014.00386

Corbett, M. A., Bahlo, M., Jolly, L., Afawi, Z., Gardner, A. E., Oliver, K. L., et al. (2010). A focal epilepsy and intellectual disability syndrome is due to a mutation in TBC1D24. *Am. J. Hum. Genet.* 87, 371–375. doi: 10.1016/j.ajhg.2010.08.001

Costa, M. R., Wen, G., Lepier, A., Schroeder, T., and Götz, M. (2008). Par-complex proteins promote proliferative progenitor divisions in the developing mouse cerebral cortex. *Development* 135, 11–22. doi: 10.1242/dev.009951

Craig, A. M., and Banker, G. (1994). Neuronal polarity. *Annu. Rev. Neurosci.* 17, 267–310. doi: 10.1146/annurev.ne.17.030194.001411

Dajas-Bailador, F., Jones, E. V., and Whitmarsh, A. J. (2008). The JIP1 scaffold protein regulates axonal development in cortical neurons. *Curr. Biol.* 18, 221–226. doi: 10.1016/j.cub.2008.01.025

D'Arcangelo, G., Miao, G. G., Chen, S. C., Soares, H. D., Morgan, J. I., and Curran, T. (1995). A protein related to extracellular matrix proteins deleted in the mouse mutant reeler. *Nature* 374, 719–723. doi: 10.1038/374719a0

Das, R. M., and Storey, K. G. (2014). Apical abscission alters cell polarity and dismantles the primary cilium during neurogenesis. *Science* 343, 200–204. doi: 10.1126/science.1247521

de Anda, F. C., Meletis, K., Ge, X., Rei, D., and Tsai, L. H. (2010). Centrosome motility is essential for initial axon formation in the neocortex. *J. Neurosci.* 30, 10391–10406. doi: 10.1523/JNEUROSCI.0381-10.2010

de Anda, F. C., Pollarolo, G., Da Silva, J. S., Camoletto, P. G., Feiguin, F., and Dotti, C. G. (2005). Centrosome localization determines neuronal polarity. *Nature* 436, 704–708. doi: 10.1038/nature03811

Dehay, C., Kennedy, H., and Kosik, K. S. (2015). The outer subventricular zone and primate-specific cortical complexification. *Neuron* 85, 683–694. doi: 10.1016/j.neuron.2014.12.060

Dimidschstein, J., Passante, L., Dufour, A., van den Ameele, J., Tiberi, L., Hrechdakian, T., et al. (2013). Ephrin-B1 controls the columnar distribution of cortical pyramidal neurons by restricting their tangential migration. *Neuron* 79, 1123–1135. doi: 10.1016/j.neuron.2013.07.015

Dotti, C. G., Sullivan, C. A., and Banker, G. A. (1988). The establishment of polarity by hippocampal neurons in culture. *J. Neurosci.* 8, 1454–1468.

Drubin, D. G., and Nelson, W. J. (1996). Origins of cell polarity. *Cell* 84, 335–344. doi: 10.1016/s0092-8674(00)81278-7

Efimov, A., Kharitonov, A., Efimova, N., Loncarek, J., Miller, P. M., Andreyeva, N., et al. (2007). Asymmetric CLASP-dependent nucleation of noncentrosomal microtubules at the trans-Golgi network. *Dev. Cell* 12, 917–930. doi: 10.1016/j.devcel.2007.04.002

Elias, L. A., Wang, D. D., and Kriegstein, A. R. (2007). Gap junction adhesion is necessary for radial migration in the neocortex. *Nature* 448, 901–907. doi: 10.1038/nature06063

Eminel, S., Roemer, L., Waetzig, V., and Herdegen, T. (2008). c-Jun N-terminal kinases trigger both degeneration and neurite outgrowth in primary hippocampal and cortical neurons. *J. Neurochem.* 104, 957–969. doi: 10.1111/j.1471-4159.2007.05101.x

Falace, A., Buhler, E., Fadda, M., Watrin, F., Lippiello, P., Pallesi-Pocachard, E., et al. (2014). TBC1D24 regulates neuronal migration and maturation through modulation of the ARF6-dependent pathway. *Proc. Natl. Acad. Sci. U S A* 111, 2337–2342. doi: 10.1073/pnas.1316294111

Feng, L., Allen, N. S., Simo, S., and Cooper, J. A. (2007). Cullin 5 regulates Dab1 protein levels and neuron positioning during cortical development. *Genes Dev.* 21, 2717–2730. doi: 10.1101/gad.1604207

Fietz, S. A., Kelava, I., Vogt, J., Wilsch-Bräuninger, M., Stenzel, D., Fish, J. L., et al. (2010). OSVZ progenitors of human and ferret neocortex are epithelial-like and expand by integrin signaling. *Nat. Neurosci.* 13, 690–699. doi: 10.1038/nn.2553

Flanagan, J. G., and Vanderhaeghen, P. (1998). The ephrins and Eph receptors in neural development. *Annu. Rev. Neurosci.* 21, 309–345. doi: 10.1146/annurev.neuro.21.1.309

Folsom, T. D., and Fatemi, S. H. (2013). The involvement of Reelin in neurodevelopmental disorders. *Neuropharmacology* 68, 122–135. doi: 10.1016/j.neuropharm.2012.08.015

Francis, F., Meyer, G., Fallet-Bianco, C., Moreno, S., Kappeler, C., Socorro, A. C., et al. (2006). Human disorders of cortical development: from past to present. *Eur. J. Neurosci.* 23, 877–893. doi: 10.1111/j.1460-9568.2006.04649.x

Funahashi, Y., Namba, T., Fujisue, S., Itoh, N., Nakamuta, S., Kato, K., et al. (2013). ERK2-mediated phosphorylation of Par3 regulates neuronal polarization. *J. Neurosci.* 33, 13270–13285. doi: 10.1523/JNEUROSCI.4210-12.2013

Gallo, V., and Deneen, B. (2014). Glial development: the crossroads of regeneration and repair in the CNS. *Neuron* 83, 283–308. doi: 10.1016/j.neuron.2014.06.010

Gao, P., Sultan, K. T., Zhang, X. J., and Shi, S. H. (2013). Lineage-dependent circuit assembly in the neocortex. *Development* 140, 2645–2655. doi: 10.1242/dev.087668

Gärtner, A., Fornasiero, E. F., Munck, S., Vennekens, K., Seuntjens, E., Huttner, W. B., et al. (2012). N-cadherin specifies first asymmetry in developing neurons. *EMBO J.* 31, 1893–1903. doi: 10.1038/emboj.2012.41

Garvalov, B. K., Flynn, K. C., Neukirchen, D., Meyn, L., Teusch, N., Wu, X., et al. (2007). Cdc42 regulates cofilin during the establishment of neuronal polarity. *J. Neurosci.* 27, 13117–13129. doi: 10.1523/JNEUROSCI.3322-07.2007

Gil-Sanz, C., Franco, S. J., Martinez-Garay, I., Espinosa, A., Harkins-Perry, S., and Müller, U. (2013). Cajal-Retzius cells instruct neuronal migration by coincidence signaling between secreted and contact-dependent guidance cues. *Neuron* 79, 461–477. doi: 10.1016/j.neuron.2013.06.040

Gil-Sanz, C., Landeira, B., Ramos, C., Costa, M. R., and Müller, U. (2014). Proliferative defects and formation of a double cortex in mice lacking Mltt4 and Cdh2 in the dorsal telencephalon. *J. Neurosci.* 34, 10475–10487. doi: 10.1523/JNEUROSCI.1793-14.2014

Goetz, S. C., and Anderson, K. V. (2010). The primary cilium: a signalling centre during vertebrate development. *Nat. Rev. Genet.* 11, 331–344. doi: 10.1038/nrg2774

Gorski, J. A., Talley, T., Qiu, M., Puelles, L., Rubenstein, J. L., and Jones, K. R. (2002). Cortical excitatory neurons and glia, but not GABAergic neurons, are produced in the Emx1-expressing lineage. *J. Neurosci.* 22, 6309–6314.

Greig, L. C., Woodworth, M. B., Galazo, M. J., Padmanabhan, H., and Macklis, J. D. (2013). Molecular logic of neocortical projection neuron specification, development and diversity. *Nat. Rev. Neurosci.* 14, 755–769. doi: 10.1038/nrn3586

Griveau, A., Borello, U., Causeret, F., Tissir, F., Boggetto, N., Karaz, S., et al. (2010). A novel role for Dbx1-derived Cajal-Retzius cells in early regionalization of the cerebral cortical neuroepithelium. *PLoS Biol.* 8:e1000440. doi: 10.1371/journal.pbio.1000440

Gupta, A., Tsai, L. H., and Wynshaw-Boris, A. (2002). Life is a journey: a genetic look at neocortical development. *Nat. Rev. Genet.* 3, 342–355. doi: 10.1038/nrg799

Hansen, D. V., Lui, J. H., Flandin, P., Yoshikawa, K., Rubenstein, J. L., Alvarez-Buylla, A., et al. (2013). Non-epithelial stem cells and cortical interneuron production in the human ganglionic eminences. *Nat. Neurosci.* 16, 1576–1587. doi: 10.1038/nn.3541

Hansen, D. V., Lui, J. H., Parker, P. R., and Kriegstein, A. R. (2010). Neurogenic radial glia in the outer subventricular zone of human neocortex. *Nature* 464, 554–561. doi: 10.1038/nature08845

Harris, T. J., and Tepass, U. (2010). Adherens junctions: from molecules to morphogenesis. *Nat. Rev. Mol. Cell Biol.* 11, 502–514. doi: 10.1038/nrm2927

Hartfuss, E., Förster, E., Bock, H. H., Hack, M. A., Leprince, P., Luque, J. M., et al. (2003). Reelin signaling directly affects radial glia morphology and biochemical maturation. *Development* 130, 4597–4609. doi: 10.1242/dev.00654

Hatanaka, Y., and Murakami, F. (2002). *In vitro* analysis of the origin, migratory behavior and maturation of cortical pyramidal cells. *J. Comp. Neurol.* 454, 1–14. doi: 10.1002/cne.10421

Hatanaka, Y., and Yamauchi, K. (2013). Excitatory cortical neurons with multipolar shape establish neuronal polarity by forming a tangentially oriented axon in the intermediate zone. *Cereb. Cortex* 23, 105–113. doi: 10.1093/cercor/bhr383

Hatten, M. E. (2002). New directions in neuronal migration. *Science* 297, 1660–1663. doi: 10.1126/science.1074572

Haubensak, W., Attardo, A., Denk, W., and Huttner, W. B. (2004). Neurons arise in the basal neuroepithelium of the early mammalian telencephalon: a major site of neurogenesis. *Proc. Natl. Acad. Sci. U S A* 101, 3196–3201. doi: 10.1073/pnas.0308600100

Higginbotham, H., Guo, J., Yokota, Y., Umberger, N. L., Su, C. Y., Li, J., et al. (2013). Arl13b-regulated cilia activities are essential for polarized radial glial scaffold formation. *Nat. Neurosci.* 16, 1000–1007. doi: 10.1038/nn.3451

Hirota, Y., Kubo, K., Katayama, K., Honda, T., Fujino, T., Yamamoto, T. T., et al. (2015). Reelin receptors ApoER2 and VLDLR are expressed in distinct spatiotemporal patterns in developing mouse cerebral cortex. *J. Comp. Neurol.* 523, 463–478. doi: 10.1002/cne.23691

Hong, S. E., Shugart, Y. Y., Huang, D. T., Shahwan, S. A., Grant, P. E., Hourihane, J. O., et al. (2000). Autosomal recessive lissencephaly with cerebellar hypoplasia is associated with human RELN mutations. *Nat. Genet.* 26, 93–96. doi: 10.1038/79246

Imai, F., Hirai, S., Akimoto, K., Koyama, H., Miyata, T., Ogawa, M., et al. (2006). Inactivation of aPKClambda results in the loss of adherens junctions in neuroepithelial cells without affecting neurogenesis in mouse neocortex. *Development* 133, 1735–1744. doi: 10.1242/dev.02389

Inoue, M., Kuroda, T., Honda, A., Komabayashi-Suzuki, M., Komai, T., Shinkai, Y., et al. (2014). Prdm8 regulates the morphological transition at multipolar phase during neocortical development. *PLoS One* 9:e86356. doi: 10.1371/journal.pone.0086356

Ishii, K., Kubo, K. I., and Nakajima, K. (2016). Reelin and neuropsychiatric disorders. *Front. Cell. Neurosci.* 10:229. doi: 10.3389/fncel.2016.00229

Itoh, Y., Moriyama, Y., Hasegawa, T., Endo, T. A., Toyoda, T., and Gotoh, Y. (2013). Scratch regulates neuronal migration onset via an epithelial-mesenchymal transition-like mechanism. *Nat. Neurosci.* 16, 416–425. doi: 10.1038/nn.3336

Jacobshagen, M., Niquille, M., Chaumont-Dubel, S., Marin, P., and Dayer, A. (2014). The serotonin 6 receptor controls neuronal migration during corticogenesis via a ligand-independent Cdk5-dependent mechanism. *Development* 141, 3370–3377. doi: 10.1242/dev.108043

Joberty, G., Petersen, C., Gao, L., and Macara, I. G. (2000). The cell-polarity protein Par6 links Par3 and atypical protein kinase C to Cdc42. *Nat. Cell Biol.* 2, 531–539. doi: 10.1038/35019573

Jones, K. R., Fariñas, I., Backus, C., and Reichardt, L. F. (1994). Targeted disruption of the BDNF gene perturbs brain and sensory neuron development but not motor neuron development. *Cell* 76, 989–999. doi: 10.1016/0092-8674(94)90377-8

Jossin, Y. (2011). Polarization of migrating cortical neurons by Rap1 and N-cadherin: revisiting the model for the Reelin signaling pathway. *Small GTPases* 2, 322–328. doi: 10.4161/sgtp.18283

Jossin, Y., and Cooper, J. A. (2011). Reelin, Rap1 and N-cadherin orient the migration of multipolar neurons in the developing neocortex. *Nat. Neurosci.* 14, 697–703. doi: 10.1038/nn.2816

Jossin, Y., and Goffinet, A. M. (2007). Reelin signals through phosphatidylinositol 3-kinase and Akt to control cortical development and through mTor to regulate dendritic growth. *Mol. Cell. Biol.* 27, 7113–7124. doi: 10.1128/mcb.00928-07

Jossin, Y., Gui, L., and Goffinet, A. M. (2007). Processing of Reelin by embryonic neurons is important for function in tissue but not in dissociated cultured neurons. *J. Neurosci.* 27, 4243–4252. doi: 10.1523/JNEUROSCI.0023-07.2007

Jossin, Y., Ignatova, N., Hiesberger, T., Herz, J., Lambert de Rouvroit, C., and Goffinet, A. M. (2004). The central fragment of Reelin, generated by proteolytic processing *in vivo*, is critical to its function during cortical plate development. *J. Neurosci.* 24, 514–521. doi: 10.1523/JNEUROSCI.3408-03.2004

Jossin, Y., Lee, M., Klezovitch, O., Kon, E., Cossard, A., Lien, W., et al. (2017). Llgl1 connects cell polarity with cell-cell adhesion in embryonic neural stem cells. *Dev. Cell* 41, 481.e5–495.e5. doi: 10.1016/j.devcel.2017.05.002

Kadowaki, M., Nakamura, S., Machon, O., Krauss, S., Radice, G. L., and Takeichi, M. (2007). N-cadherin mediates cortical organization in the mouse brain. *Dev. Biol.* 304, 22–33. doi: 10.1016/j.ydbio.2006.12.014

Kappeler, L., De Magalhaes Filho, C., Dupont, J., Leneuve, P., Cervera, P., Perin, L., et al. (2008). Brain IGF-1 receptors control mammalian growth and lifespan through a neuroendocrine mechanism. *PLoS Biol.* 6:e254. doi: 10.1371/journal.pbio.0060254

Kawauchi, T., Chihama, K., Nabeshima, Y., and Hoshino, M. (2003). The *in vivo* roles of STEF/Tiam1, Rac1 and JNK in cortical neuronal migration. *EMBO J.* 22, 4190–4201. doi: 10.1093/emboj/cdg413

Kawauchi, T., Sekine, K., Shikanai, M., Chihama, K., Tomita, K., Kubo, K., et al. (2010). Rab GTPases-dependent endocytic pathways regulate neuronal migration and maturation through N-cadherin trafficking. *Neuron* 67, 588–602. doi: 10.1016/j.neuron.2010.07.007

Kim, S., Lehtinen, M. K., Sessa, A., Zappaterra, M. W., Cho, S. H., Gonzalez, D., et al. (2010). The apical complex couples cell fate and cell survival to cerebral cortical development. *Neuron* 66, 69–84. doi: 10.1016/j.neuron.2010.03.019

Kishi, M., Pan, Y. A., Crump, J. G., and Sanes, J. R. (2005). Mammalian SAD kinases are required for neuronal polarization. *Science* 307, 929–932. doi: 10.1126/science.1107403

Klein, R., Smeyne, R. J., Wurst, W., Long, L. K., Auerbach, B. A., Joyner, A. L., et al. (1993). Targeted disruption of the trkB neurotrophin receptor gene results in nervous system lesions and neonatal death. *Cell* 75, 113–122. doi: 10.1016/0092-8674(93)90683-h

Klezovitch, O., Fernandez, T. E., Tapscott, S. J., and Vasioukhin, V. (2004). Loss of cell polarity causes severe brain dysplasia in Lgl1 knockout mice. *Genes Dev.* 18, 559–571. doi: 10.1101/gad.1178004

Konno, D., Shioi, G., Shitamukai, A., Mori, A., Kiyonari, H., Miyata, T., et al. (2008). Neuroepithelial progenitors undergo LGN-dependent planar divisions to maintain self-renewability during mammalian neurogenesis. *Nat. Cell Biol.* 10, 93–101. doi: 10.1038/ncb1673

Kosodo, Y., Roper, K., Haubensak, W., Marzesco, A. M., Corbeil, D., and Huttner, W. B. (2004). Asymmetric distribution of the apical plasma membrane during neurogenic divisions of mammalian neuroepithelial cells. *EMBO J.* 23, 2314–2324. doi: 10.1038/sj.emboj.7600223

Kosodo, Y., Toida, K., Dubreuil, V., Alexandre, P., Schenk, J., Kiyokage, E., et al. (2008). Cytokinesis of neuroepithelial cells can divide their basal process before anaphase. *EMBO J.* 27, 3151–3163. doi: 10.1038/emboj.2008.227

Kowalczyk, T., Pontious, A., Englund, C., Daza, R. A., Bedogni, F., Hodge, R., et al. (2009). Intermediate neuronal progenitors (basal progenitors) produce pyramidal-projection neurons for all layers of cerebral cortex. *Cereb. Cortex* 19, 2439–2450. doi: 10.1093/cercor/bhn260

Kuan, C. Y., Yang, D. D., Samanta Roy, D. R., Davis, R. J., Rakic, P., and Flavell, R. A. (1999). The Jnk1 and Jnk2 protein kinases are required for regional specific apoptosis during early brain development. *Neuron* 22, 667–676. doi: 10.1016/s0896-6273(00)80727-8

Kumar, A., Girimaji, S. C., Duvvari, M. R., and Blanton, S. H. (2009). Mutations in STIL, encoding a pericentriolar and centrosomal protein, cause primary microcephaly. *Am. J. Hum. Genet.* 84, 286–290. doi: 10.1016/j.ajhg.2009.01.017

LaMonica, B. E., Lui, J. H., Wang, X., and Kriegstein, A. R. (2012). OSVZ progenitors in the human cortex: an updated perspective on neurodevelopmental disease. *Curr. Opin. Neurobiol.* 22, 747–753. doi: 10.1016/j.conb.2012.03.006

Lee, J. E., and Gleeson, J. G. (2011). A systems-biology approach to understanding the ciliopathy disorders. *Genome Med.* 3:59. doi: 10.1186/gm275

Lee, G. H., Kim, S. H., Homayouni, R., and D'Arcangelo, G. (2012). Dab2ip regulates neuronal migration and neurite outgrowth in the developing neocortex. *PLoS One* 7:e46592. doi: 10.1371/journal.pone.0046592

Lehtinen, M. K., Zappaterra, M. W., Chen, X., Yang, Y. J., Hill, A. D., Lun, M., et al. (2011). The cerebrospinal fluid provides a proliferative niche for neural progenitor cells. *Neuron* 69, 893–905. doi: 10.1016/j.neuron.2011.01.023

Li, Y., Lu, H., Cheng, P. L., Ge, S., Xu, H., Shi, S. H., et al. (2012). Clonally related visual cortical neurons show similar stimulus feature selectivity. *Nature* 486, 118–121. doi: 10.1038/nature11110

Li, H. S., Wang, D., Shen, Q., Schonemann, M. D., Gorski, J. A., Jones, K. R., et al. (2003). Inactivation of Numb and Numblike in embryonic dorsal forebrain impairs neurogenesis and disrupts cortical morphogenesis. *Neuron* 40, 1105–1118. doi: 10.1016/s0896-6273(03)00755-4

Lin, D., Edwards, A. S., Fawcett, J. P., Mbamalu, G., Scott, J. D., and Pawson, T. (2000). A mammalian PAR-3-PAR-6 complex implicated in Cdc42/Rac1 and aPKC signalling and cell polarity. *Nat. Cell Biol.* 2, 540–547. doi: 10.1038/35019582

Liu, J. S. (2011). Molecular genetics of neuronal migration disorders. *Curr. Neurol. Neurosci. Rep.* 11, 171–178. doi: 10.1007/s11910-010-0176-5

Liu, X., Sun, L., Torii, M., and Rakic, P. (2012). Connexin 43 controls the multipolar phase of neuronal migration to the cerebral cortex. *Proc. Natl. Acad. Sci. U S A* 109, 8280–8285. doi: 10.1073/pnas.1205880109

LoTurco, J. J., and Bai, J. (2006). The multipolar stage and disruptions in neuronal migration. *Trends Neurosci.* 29, 407–413. doi: 10.1016/j.tins.2006.05.006

Louvi, A., and Grove, E. A. (2011). Cilia in the CNS: the quiet organelle claims center stage. *Neuron* 69, 1046–1060. doi: 10.1016/j.neuron.2011.03.002

Lui, J. H., Hansen, D. V., and Kriegstein, A. R. (2011). Development and evolution of the human neocortex. *Cell* 146, 18–36. doi: 10.1016/j.cell.2011.06.030

Ma, T., Wang, C., Wang, L., Zhou, X., Tian, M., Zhang, Q., et al. (2013). Subcortical origins of human and monkey neocortical interneurons. *Nat. Neurosci.* 16, 1588–1597. doi: 10.1038/nn.3536

Magdaleno, S., Keshvara, L., and Curran, T. (2002). Rescue of ataxia and preplate splitting by ectopic expression of Reelin in reeler mice. *Neuron* 33, 573–586. doi: 10.1016/s0896-6273(02)00582-2

Manzini, M. C., and Walsh, C. A. (2011). What disorders of cortical development tell us about the cortex: one plus one does not always make two. *Curr. Opin. Genet. Dev.* 21, 333–339. doi: 10.1016/j.gde.2011.01.006

Margolis, B., and Borg, J. P. (2005). Apicobasal polarity complexes. *J. Cell Sci.* 118, 5157–5159. doi: 10.1242/jcs.02597

Marin, O., and Rubenstein, J. L. (2003). Cell migration in the forebrain. *Annu. Rev. Neurosci.* 26, 441–483. doi: 10.1146/annurev.neuro.26.041002.131058

Marthiens, V., and ffrench-Constant, C. (2009). Adherens junction domains are split by asymmetric division of embryonic neural stem cells. *EMBO Rep.* 10, 515–520. doi: 10.1038/embor.2009.36

Matsuki, T., Matthews, R. T., Cooper, J. A., van der Brug, M. P., Cookson, M. R., Hardy, J. A., et al. (2010). Reelin and stk25 have opposing roles in neuronal polarization and dendritic Golgi deployment. *Cell* 143, 826–836. doi: 10.1016/j.cell.2010.10.029

Maussion, G., Carayol, J., Lepagnol-Bestel, A. M., Tores, F., Loe-Mie, Y., Milbreta, U., et al. (2008). Convergent evidence identifying MAP/microtubule affinity-regulating kinase 1 (MARK1) as a susceptibility gene for autism. *Hum. Mol. Genet.* 17, 2541–2551. doi: 10.1093/hmg/ddn154

McFadden, K., and Minshew, N. J. (2013). Evidence for dysregulation of axonal growth and guidance in the etiology of ASD. *Front. Hum. Neurosci.* 7:671. doi: 10.3389/fnhum.2013.00671

Meseke, M., Cavus, E., and Förster, E. (2013). Reelin promotes microtubule dynamics in processes of developing neurons. *Histochem. Cell Biol.* 139, 283–297. doi: 10.1007/s00418-012-1025-1

Miyata, T., Kawaguchi, A., Okano, H., and Ogawa, M. (2001). Asymmetric inheritance of radial glial fibers by cortical neurons. *Neuron* 31, 727–741. doi: 10.1016/s0896-6273(01)00420-2

Miyata, T., Kawaguchi, A., Saito, K., Kawano, M., Muto, T., and Ogawa, M. (2004). Asymmetric production of surface-dividing and non-surface-dividing cortical progenitor cells. *Development* 131, 3133–3145. doi: 10.1242/dev.01173

Molyneaux, B. J., Arlotta, P., Menezes, J. R., and Macklis, J. D. (2007). Neuronal subtype specification in the cerebral cortex. *Nat. Rev. Neurosci.* 8, 427–437. doi: 10.1038/nrn2151

Morimura, T., Hattori, M., Ogawa, M., and Mikoshiba, K. (2005). Disabled1 regulates the intracellular trafficking of reelin receptors. *J. Biol. Chem.* 280, 16901–16908. doi: 10.1074/jbc.M409048200

MuhChyi, C., Juliandi, B., Matsuda, T., and Nakashima, K. (2013). Epigenetic regulation of neural stem cell fate during corticogenesis. *Int. J. Dev. Neurosci.* 31, 424–433. doi: 10.1016/j.ijdevneu.2013.02.006

Nadarajah, B., Brunstrom, J. E., Grutzendler, J., Wong, R. O., and Pearlman, A. L. (2001). Two modes of radial migration in early development of the cerebral cortex. *Nat. Neurosci.* 4, 143–150. doi: 10.1038/83967

Nagano, T., Morikubo, S., and Sato, M. (2004). Filamin A and FILIP (Filamin A-interacting protein) regulate cell polarity and motility in neocortical subventricular and intermediate zones during radial migration. *J. Neurosci.* 24, 9648–9657. doi: 10.1523/JNEUROSCI.2363-04.2004

Nakamuta, S., Funahashi, Y., Namba, T., Arimura, N., Picciotto, M. R., Tokumitsu, H., et al. (2011). Local application of neurotrophins specifies axons through inositol 1,4,5-trisphosphate, calcium, and Ca^{2+}/calmodulin-dependent protein kinases. *Sci. Signal.* 4:ra76. doi: 10.1126/scisignal.2002011

Namba, T., Kibe, Y., Funahashi, Y., Nakamuta, S., Takano, T., Ueno, T., et al. (2014). Pioneering axons regulate neuronal polarization in the developing cerebral cortex. *Neuron* 81, 814–829. doi: 10.1016/j.neuron.2013.12.015

Nelson, W. J. (2003). Adaptation of core mechanisms to generate cell polarity. *Nature* 422, 766–774. doi: 10.1038/nature01602

Nicholas, A. K., Khurshid, M., Désir, J., Carvalho, O. P., Cox, J. J., Thornton, G., et al. (2010). WDR62 is associated with the spindle pole and is mutated in human microcephaly. *Nat. Genet.* 42, 1010–1014. doi: 10.1038/ng.682

Nieto, R., Kukuljan, M., and Silva, H. (2013). BDNF and schizophrenia: from neurodevelopment to neuronal plasticity, learning, and memory. *Front. Psychiatry* 4:45. doi: 10.3389/fpsyt.2013.00045

Noctor, S. C., Flint, A. C., Weissman, T. A., Dammerman, R. S., and Kriegstein, A. R. (2001). Neurons derived from radial glial cells establish radial units in neocortex. *Nature* 409, 714–720. doi: 10.1038/35055553

Noctor, S. C., Martínez-Cerdeño, V., Ivic, L., and Kriegstein, A. R. (2004). Cortical neurons arise in symmetric and asymmetric division zones and migrate through specific phases. *Nat. Neurosci.* 7, 136–144. doi: 10.1038/nn1172

Noctor, S. C., Martínez-Cerdeno, V., and Kriegstein, A. R. (2008). Distinct behaviors of neural stem and progenitor cells underlie cortical neurogenesis. *J. Comp. Neurol.* 508, 28–44. doi: 10.1002/cne.21669

Ogawa, M., Miyata, T., Nakajima, K., Yagyu, K., Seike, M., Ikenaka, K., et al. (1995). The reeler gene-associated antigen on Cajal-Retzius neurons is a crucial molecule for laminar organization of cortical neurons. *Neuron* 14, 899–912. doi: 10.1016/0896-6273(95)90329-1

Ohshima, T., Hirasawa, M., Tabata, H., Mutoh, T., Adachi, T., Suzuki, H., et al. (2007). Cdk5 is required for multipolar-to-bipolar transition during radial neuronal migration and proper dendrite development of pyramidal neurons in the cerebral cortex. *Development* 134, 2273–2282. doi: 10.1242/dev.02854

Ohtaka-Maruyama, C., and Okado, H. (2015). Molecular pathways underlying projection neuron production and migration during cerebral cortical development. *Front. Neurosci.* 9:447. doi: 10.3389/fnins.2015.00447

Oliva, A. A. Jr., Atkins, C. M., Copenagle, L., and Banker, G. A. (2006). Activated c-Jun N-terminal kinase is required for axon formation. *J. Neurosci.* 26, 9462–9470. doi: 10.1523/JNEUROSCI.2625-06.2006

Pacary, E., Heng, J., Azzarelli, R., Riou, P., Castro, D., Lebel-Potter, M., et al. (2011). Proneural transcription factors regulate different steps of cortical neuron migration through Rnd-mediated inhibition of RhoA signaling. *Neuron* 69, 1069–1084. doi: 10.1016/j.neuron.2011.02.018

Paridaen, J. T., Wilsch-Brauninger, M., and Huttner, W. B. (2013). Asymmetric inheritance of centrosome-associated primary cilium membrane directs ciliogenesis after cell division. *Cell* 155, 333–344. doi: 10.1016/j.cell.2013.08.060

Passemard, S., Titomanlio, L., Elmaleh, M., Afenjar, A., Alessandri, J.-L., Andria, G., et al. (2009). Expanding the clinical and neuroradiologic phenotype of primary microcephaly due to *ASPM* mutations. *Neurology* 73, 962–969. doi: 10.1212/WNL.0b013e3181b8799a

Petersen, P. H., Zou, K., Hwang, J. K., Jan, Y. N., and Zhong, W. (2002). Progenitor cell maintenance requires numb and numblike during mouse neurogenesis. *Nature* 419, 929–934. doi: 10.1038/nature01124

Petersen, P. H., Zou, K., Krauss, S., and Zhong, W. (2004). Continuing role for mouse Numb and Numbl in maintaining progenitor cells during cortical neurogenesis. *Nat. Neurosci.* 7, 803–811. doi: 10.1038/nn1289

Pilaz, L. J., Lennox, A. L., Rouanet, J. P., and Silver, D. L. (2016). Dynamic mRNA transport and local translation in radial glial progenitors of the developing brain. *Curr. Biol.* 26, 3383–3392. doi: 10.1016/j.cub.2016.10.040

Pohlkamp, T., Xiao, L., Sultana, R., Bepari, A., Bock, H. H., Henkemeyer, M., et al. (2016). Ephrin Bs and canonical Reelin signalling. *Nature* 539, E4–E6. doi: 10.1038/nature20129

Pollarolo, G., Schulz, J. G., Munck, S., and Dotti, C. G. (2011). Cytokinesis remnants define first neuronal asymmetry *in vivo*. *Nat. Neurosci.* 14, 1525–1533. doi: 10.1038/nn.2976

Polleux, F., Morrow, T., and Ghosh, A. (2000). Semaphorin 3A is a chemoattractant for cortical apical dendrites. *Nature* 404, 567–573. doi: 10.1038/35007001

Quach, T. T., Honnorat, J., Kolattukudy, P. E., Khanna, R., and Duchemin, A. M. (2015). CRMPs: critical molecules for neurite morphogenesis and neuropsychiatric diseases. *Mol. Psychiatry* 20, 1037–1045. doi: 10.1038/mp.2015.77

Rakic, P. (1972). Mode of cell migration to the superficial layers of fetal monkey neocortex. *J. Comp. Neurol.* 145, 61–83. doi: 10.1002/cne.901450105

Rakic, P. (1988). Specification of cerebral cortical areas. *Science* 241, 170–176. doi: 10.1126/science.3291116

Randlett, O., Norden, C., and Harris, W. A. (2011). The vertebrate retina: a model for neuronal polarization *in vivo*. *Dev. Neurobiol.* 71, 567–583. doi: 10.1002/dneu.20841

Rash, B. G., Ackman, J. B., and Rakic, P. (2016). Bidirectional radial Ca^{2+} activity regulates neurogenesis and migration during early cortical column formation. *Sci. Adv.* 2:e1501733. doi: 10.1126/sciadv.1501733

Rasin, M. R., Gazula, V. R., Breunig, J. J., Kwan, K. Y., Johnson, M. B., Liu-Chen, S., et al. (2007). Numb and Numbl are required for maintenance of cadherin-based adhesion and polarity of neural progenitors. *Nat. Neurosci.* 10, 819–827. doi: 10.1038/nn1924

Rauch, A., Thiel, C. T., Schindler, D., Wick, U., Crow, Y. J., Ekici, A. B., et al. (2008). Mutations in the pericentrin (*PCNT*) gene cause primordial dwarfism. *Science* 319, 816–819. doi: 10.1126/science.1151174

Rohatgi, R., Milenkovic, L., and Scott, M. P. (2007). Patched1 regulates hedgehog signaling at the primary cilium. *Science* 317, 372–376. doi: 10.1126/science.1139740

Rousso, D. L., Pearson, C. A., Gaber, Z. B., Miquelajauregui, A., Li, S., Portera-Cailliau, C., et al. (2012). Foxp-mediated suppression of N-cadherin regulates neuroepithelial character and progenitor maintenance in the CNS. *Neuron* 74, 314–330. doi: 10.1016/j.neuron.2012.02.024

Sakakibara, A., Sato, T., Ando, R., Noguchi, N., Masaoka, M., and Miyata, T. (2014). Dynamics of centrosome translocation and microtubule organization in neocortical neurons during distinct modes of polarization. *Cereb. Cortex* 24, 1301–1310. doi: 10.1093/cercor/bhs411

Sapir, T., Sapoznik, S., Levy, T., Finkelshtein, D., Shmueli, A., Timm, T., et al. (2008). Accurate balance of the polarity kinase MARK2/Par-1 is required for proper cortical neuronal migration. *J. Neurosci.* 28, 5710–5720. doi: 10.1523/JNEUROSCI.0911-08.2008

Schwartz, M. L., Rakic, P., and Goldman-Rakic, P. S. (1991). Early phenotype expression of cortical neurons: evidence that a subclass of migrating neurons have callosal axons. *Proc. Natl. Acad. Sci. U S A* 88, 1354–1358. doi: 10.1073/pnas.88.4.1354

Sekine, K., Honda, T., Kawauchi, T., Kubo, K., and Nakajima, K. (2011). The outermost region of the developing cortical plate is crucial for both the switch of the radial migration mode and the Dab1-dependent "inside-out" lamination in the neocortex. *J. Neurosci.* 31, 9426–9439. doi: 10.1523/JNEUROSCI.0650-11.2011

Sekine, K., Kawauchi, T., Kubo, K., Honda, T., Herz, J., Hattori, M., et al. (2012). Reelin controls neuronal positioning by promoting cell-matrix adhesion via inside-out activation of integrin α5β1. *Neuron* 76, 353–369. doi: 10.1016/j.neuron.2012.07.020

Sentürk, A., Pfennig, S., Weiss, A., Burk, K., and Acker-Palmer, A. (2011). Ephrin Bs are essential components of the Reelin pathway to regulate neuronal migration. *Nature* 472, 356–360. doi: 10.1038/nature09874

Sessa, A., Mao, C. A., Hadjantonakis, A. K., Klein, W. H., and Broccoli, V. (2008). Tbr2 directs conversion of radial glia into basal precursors and guides neuronal amplification by indirect neurogenesis in the developing neocortex. *Neuron* 60, 56–69. doi: 10.1016/j.neuron.2008.09.028

Seuntjens, E., Nityanandam, A., Miquelajauregui, A., Debruyn, J., Stryjewska, A., Goebbels, S., et al. (2009). Sip1 regulates sequential fate decisions by feedback signaling from postmitotic neurons to progenitors. *Nat. Neurosci.* 12, 1373–1380. doi: 10.1038/nn.2409

Shah, B., Lutter, D., Tsytsyura, Y., Glyvuk, N., Sakakibara, A., Klingauf, J., et al. (2016). Rap1 GTPases are master regulators of neural cell polarity in the developing neocortex. *Cereb. Cortex* 27, 1253–1269. doi: 10.1093/cercor/bhv341

Shelly, M., Cancedda, L., Heilshorn, S., Sumbre, G., and Poo, M. M. (2007). LKB1/STRAD promotes axon initiation during neuronal polarization. *Cell* 129, 565–577. doi: 10.1016/j.cell.2007.04.012

Shen, Q., Zhong, W., Jan, Y. N., and Temple, S. (2002). Asymmetric Numb distribution is critical for asymmetric cell division of mouse cerebral cortical stem cells and neuroblasts. *Development* 129, 4843–4853.

Shitamukai, A., Konno, D., and Matsuzaki, F. (2011). Oblique radial glial divisions in the developing mouse neocortex induce self-renewing progenitors outside the germinal zone that resemble primate outer subventricular zone progenitors. *J. Neurosci.* 31, 3683–3695. doi: 10.1523/JNEUROSCI.4773-10.2011

Shoukimas, G. M., and Hinds, J. W. (1978). The development of the cerebral cortex in the embryonic mouse: an electron microscopic serial section analysis. *J. Comp. Neurol.* 179, 795–830. doi: 10.1002/cne.901790407

Shu, T., Ayala, R., Nguyen, M. D., Xie, Z., Gleeson, J. G., and Tsai, L. H. (2004). Ndel1 operates in a common pathway with LIS1 and cytoplasmic dynein to regulate cortical neuronal positioning. *Neuron* 44, 263–277. doi: 10.1016/j.neuron.2004.09.030

Sicca, F., Kelemen, A., Genton, P., Das, S., Mei, D., Moro, F., et al. (2003). Mosaic mutations of the LIS1 gene cause subcortical band heterotopia. *Neurology* 61, 1042–1046. doi: 10.1212/wnl.61.8.1042

Siegenthaler, J. A., Ashique, A. M., Zarbalis, K., Patterson, K. P., Hecht, J. H., Kane, M. A., et al. (2009). Retinoic acid from the meninges regulates cortical neuron generation. *Cell* 139, 597–609. doi: 10.1016/j.cell.2009.10.004

Simó, S., Jossin, Y., and Cooper, J. A. (2010). Cullin 5 regulates cortical layering by modulating the speed and duration of Dab1-dependent neuronal migration. *J. Neurosci.* 30, 5668–5676. doi: 10.1523/JNEUROSCI.0035-10.2010

Sosa, L., Dupraz, S., Laurino, L., Bollati, F., Bisbal, M., Cáceres, A., et al. (2006). IGF-1 receptor is essential for the establishment of hippocampal neuronal polarity. *Nat. Neurosci.* 9, 993–995. doi: 10.1038/nn1742

Stiess, M., Maghelli, N., Kapitein, L. C., Gomis-Rüth, S., Wilsch-Bräuninger, M., Hoogenraad, C. C., et al. (2010). Axon extension occurs independently of centrosomal microtubule nucleation. *Science* 327, 704–707. doi: 10.1126/science.1182179

Sun, Y., Fei, T., Yang, T., Zhang, F., Chen, Y. G., Li, H., et al. (2010). The suppression of CRMP2 expression by bone morphogenetic protein (BMP)-SMAD gradient signaling controls multiple stages of neuronal development. *J Biol Chem* 285, 39039–39050. doi: 10.1074/jbc.M110.168351

Sun, T., Yu, N., Zhai, L. K., Li, N., Zhang, C., Zhou, L., et al. (2013). c-Jun NH2-terminal kinase (JNK)-interacting protein-3 (JIP3) regulates neuronal axon elongation in a kinesin- and JNK-dependent manner. *J. Biol. Chem.* 288, 14531–14543. doi: 10.1074/jbc.M113.464453

Tabata, H., and Nakajima, K. (2003). Multipolar migration: the third mode of radial neuronal migration in the developing cerebral cortex. *J. Neurosci.* 23, 9996–10001.

Tahirovic, S., and Bradke, F. (2009). Neuronal polarity. *Cold Spring Harb. Perspect. Biol.* 1:a001644. doi: 10.1101/cshperspect.a001644

Takahashi, T., Nowakowski, R. S., and Caviness, V. S. Jr. (1995). The cell cycle of the pseudostratified ventricular epithelium of the embryonic murine cerebral wall. *J. Neurosci.* 15, 6046–6057.

Tanaka, T., Serneo, F. F., Higgins, C., Gambello, M. J., Wynshaw-Boris, A., and Gleeson, J. G. (2004). Lis1 and doublecortin function with dynein to mediate coupling of the nucleus to the centrosome in neuronal migration. *J. Cell Biol.* 165, 709–721. doi: 10.1083/jcb.200309025

Torii, M., Hashimoto-Torii, K., Levitt, P., and Rakic, P. (2009). Integration of neuronal clones in the radial cortical columns by EphA and ephrin-A signalling. *Nature* 461, 524–528. doi: 10.1038/nature08362

Tsai, J. W., Bremner, K. H., and Vallee, R. B. (2007). Dual subcellular roles for LIS1 and dynein in radial neuronal migration in live brain tissue. *Nat. Neurosci.* 10, 970–979. doi: 10.1038/nn1934

Tsunekawa, Y., Britto, J. M., Takahashi, M., Polleux, F., Tan, S. S., and Osumi, N. (2012). Cyclin D2 in the basal process of neural progenitors is linked to non-equivalent cell fates. *EMBO J.* 31, 1879–1892. doi: 10.1038/emboj.2012.43

Uchida, T., Baba, A., Pérez-Martinez, F. J., Hibi, T., Miyata, T., Luque, J. M., et al. (2009). Downregulation of functional Reelin receptors in projection neurons implies that primary Reelin action occurs at early/premigratory stages. *J. Neurosci.* 29, 10653–10662. doi: 10.1523/JNEUROSCI.0345-09.2009

van Veluw, S. J., Sawyer, E. K., Clover, L., Cousijn, H., De Jager, C., Esiri, M. M., et al. (2012). Prefrontal cortex cytoarchitecture in normal aging and Alzheimer's disease: a relationship with IQ. *Brain Struct. Funct.* 217, 797–808. doi: 10.1007/s00429-012-0381-x

Vasistha, N. A., García-Moreno, F., Arora, S., Cheung, A. F., Arnold, S. J., Robertson, E. J., et al. (2015). Cortical and clonal contribution of

Tbr2 expressing progenitors in the developing mouse brain. *Cereb. Cortex* 25, 3290–3302. doi: 10.1093/cercor/bhu125

Villarroel-Campos, D., Bronfman, F. C., and Gonzalez-Billault, C. (2016). Rab GTPase signaling in neurite outgrowth and axon specification. *Cytoskeleton* 73, 498–507. doi: 10.1002/cm.21303

Wang, H., Ge, G., Uchida, Y., Luu, B., and Ahn, S. (2011). Gli3 is required for maintenance and fate specification of cortical progenitors. *J. Neurosci.* 31, 6440–6448. doi: 10.1523/JNEUROSCI.4892-10.2011

Wang, X., Tsai, J. W., Imai, J. H., Lian, W. N., Vallee, R. B., and Shi, S. H. (2009). Asymmetric centrosome inheritance maintains neural progenitors in the neocortex. *Nature* 461, 947–955. doi: 10.1038/nature08435

Weissman, T. A., Riquelme, P. A., Ivic, L., Flint, A. C., and Kriegstein, A. R. (2004). Calcium waves propagate through radial glial cells and modulate proliferation in the developing neocortex. *Neuron* 43, 647–661. doi: 10.1016/j.neuron.2004.08.015

Westerlund, N., Zdrojewska, J., Padzik, A., Komulainen, E., Björkblom, B., Rannikko, E., et al. (2011). Phosphorylation of SCG10/stathmin-2 determines multipolar stage exit and neuronal migration rate. *Nat. Neurosci.* 14, 305–313. doi: 10.1038/nn.2755

Wilsch-Bräuninger, M., Peters, J., Paridaen, J. T. M. L., and Huttner, W. B. (2012). Basolateral rather than apical primary cilia on neuroepithelial cells committed to delamination. *Development* 139, 95–105. doi: 10.1242/dev.069294

Wilson, S. L., Wilson, J. P., Wang, C., Wang, B., and McConnell, S. K. (2012). Primary cilia and Gli3 activity regulate cerebral cortical size. *Dev. Neurobiol.* 72, 1196–1212. doi: 10.1002/dneu.20985

Woods, C. G., Bond, J., and Enard, W. (2005). Autosomal recessive primary microcephaly (MCPH): a review of clinical, molecular, and evolutionary findings. *Am. J. Hum. Genet.* 76, 717–728. doi: 10.1086/429930

Xie, Z., Sanada, K., Samuels, B. A., Shih, H., and Tsai, L. H. (2003). Serine 732 phosphorylation of FAK by Cdk5 is important for microtubule organization, nuclear movement and neuronal migration. *Cell* 114, 469–482. doi: 10.1016/s0092-8674(03)00605-6

Xu, C., Funahashi, Y., Watanabe, T., Takano, T., Nakamuta, S., Namba, T., et al. (2015). Radial glial cell-neuron interaction directs axon formation at the opposite side of the neuron from the contact site. *J. Neurosci.* 35, 14517–14532. doi: 10.1523/JNEUROSCI.1266-15.2015

Yi, J. J., Barnes, A. P., Hand, R., Polleux, F., and Ehlers, M. D. (2010). TGF-β signaling specifies axons during brain development. *Cell* 142, 144–157. doi: 10.1016/j.cell.2010.06.010

Young-Pearse, T. L., Bai, J., Chang, R., Zheng, J. B., LoTurco, J. J., and Selkoe, D. J. (2007). A critical function for β-amyloid precursor protein in neuronal migration revealed by in utero RNA interference. *J. Neurosci.* 27, 14459–14469. doi: 10.1523/JNEUROSCI.4701-07.2007

Yu, Y. C., Bultje, R. S., Wang, X., and Shi, S. H. (2009). Specific synapses develop preferentially among sister excitatory neurons in the neocortex. *Nature* 458, 501–504. doi: 10.1038/nature07722

Yu, Y. C., He, S., Chen, S., Fu, Y., Brown, K. N., Yao, X. H., et al. (2012). Preferential electrical coupling regulates neocortical lineage-dependent microcircuit assembly. *Nature* 486, 113–117. doi: 10.1038/nature10958

Yu, T. W., Mochida, G. H., Tischfield, D. J., Sgaier, S. K., Flores-Sarnat, L., Sergi, C. M., et al. (2010). Mutations in WDR62, encoding a centrosome-associated protein, cause microcephaly with simplified gyri and abnormal cortical architecture. *Nat. Genet.* 42, 1015–1020. doi: 10.1038/ng.683

Zhang, X., Lei, K., Yuan, X., Wu, X., Zhuang, Y., Xu, T., et al. (2009). SUN1/2 and Syne/Nesprin-1/2 complexes connect centrosome to the nucleus during neurogenesis and neuronal migration in mice. *Neuron* 64, 173–187. doi: 10.1016/j.neuron.2009.08.018

Zolessi, F. R., Poggi, L., Wilkinson, C. J., Chien, C. B., and Harris, W. A. (2006). Polarization and orientation of retinal ganglion cells *in vivo*. *Neural Dev.* 1:2. doi: 10.1186/1749-8104-1-2

Conflict of Interest Statement: The authors declare that the research was conducted in the absence of any commercial or financial relationships that could be construed as a potential conflict of interest.

frontiers in Cellular Neuroscience

REVIEW
published: 23 May 2017
doi: 10.3389/fncel.2017.00148

Reelin Signaling Inactivates Cofilin to Stabilize the Cytoskeleton of Migrating Cortical Neurons

Michael Frotscher[1], Shanting Zhao[2], Shaobo Wang[1] and Xuejun Chai[1]*

[1]Center for Molecular Neurobiology Hamburg (ZMNH), Institute for Structural Neurobiology, University Medical Center Hamburg-Eppendorf, Hamburg, Germany , [2]College of Veterinary Medicine, Northwest A&F University, Yangling, China

Neurons are highly polarized cells. They give rise to several dendrites but only one axon. In addition, many neurons show a preferred orientation. For example, pyramidal neurons of the cerebral cortex extend their apical dendrites toward the cortical surface while their axons run in opposite direction toward the white matter. This characteristic orientation reflects the migratory trajectory of a pyramidal cell during cortical development: the leading process (the future apical dendrite) extends toward the marginal zone (MZ) and the trailing process (the future axon) toward the intermediate zone (IZ) while the cells migrate radially to reach their destination in the cortical plate (CP). In this review article, we summarize the function of Reelin, an extracellular matrix protein synthesized by Cajal-Retzius cells in the MZ, in the development of the characteristic orientation of the leading processes running perpendicular to the cortical surface. Reelin promotes migration toward the cortical surface since late-generated cortical neurons in the *reeler* mutant are unable to reach upper cortical layers. Likewise, Reelin is important for the orientation and maintenance of the leading processes of migrating neurons since they are misoriented in the developing *reeler* cortex, as are the apical dendrites of pyramidal cells in the mature mutant. Reelin-induced phosphorylation of cofilin, an actin-associated protein, is crucial since pyramidal neurons transfected by *in utero* electroporation (IUE) with a non-phosphorylatable form of cofilin (*cofilin*^{S3A}) show severe migration defects reminiscent of those in the *reeler* mutant. Remarkably, migration of neurons in the cortex of *reeler* mice was partially rescued by transfecting them with *LIM kinase 1* (*LIMK1*), the kinase that induces phosphorylation of cofilin at serine3, or with a pseudo-phosphorylated cofilin mutant (*cofilin*^{S3E}). Together these results indicate that Reelin-induced phosphorylation of cofilin is an important component in the orientation and directed migration of cortical neurons and in their correct lamination.

Keywords: neuronal orientation, cortical pyramidal neuron, neuronal migration, leading process, trailing process, Reelin, cofilin, *in utero* electroporation

OPEN ACCESS

Edited by:
Annette Gaertner, Evotec (Germany), Germany

Reviewed by:
Eckart Förster, Ruhr University Bochum, Germany
Gonzalo Alvarez-Bolado, Heidelberg University, Germany

****Correspondence:***
Michael Frotscher
michael.frotscher@zmnh.uni-hamburg.de

Received: *10 February 2017*
Accepted: *05 May 2017*
Published: *23 May 2017*

Citation:
Frotscher M, Zhao S, Wang S and Chai X (2017) Reelin Signaling Inactivates Cofilin to Stabilize the Cytoskeleton of Migrating Cortical Neurons. Front. Cell. Neurosci. 11:148. doi: 10.3389/fncel.2017.00148

INTRODUCTION

The student of the mammalian cerebral cortex is impressed by two phenomena pointing to a well-ordered, non-random structural organization. First, there is the arrangement of cortical neurons in layers as seen in Nissl-stained sections or in sections immunostained using layer specific markers. Second, there is an almost uniform vertical orientation of the vast majority of cortical

neurons. This is nicely seen when cortical neurons are impregnated using the Golgi method which stains the cells with their axonal and dendritic processes (Golgi, 1873). The vertical orientation mainly comes about by the thick, long apical dendrites originating from the cell bodies and running toward the pial surface where they branch, forming apical tufts. From the opposite poles of the cell bodies the axons originate, which run toward the white matter. Thus, this vertical orientation of virtually all cortical pyramidal neurons nicely illustrates the characteristic bipolarity of nerve cells having one efferent process, the axon, and many dendrites being the receptive processes of the cell conveying incoming signals toward the cell body. In a cortical pyramidal cell the two processes, the apical dendrite and the axon, run in fact in opposite directions as noticed early on by investigators applying the Golgi method (e.g., Ramón y Cajal, 1911).

From a cell biological point of view numerous questions arise after this short description of cortical organization. Numerous researchers have dealt intensely with these questions during the last decades. In a landmark article, Berry and Rogers (1965) described for the first time that there is an "inside-out" lamination with early-generated neurons establishing the deep layers and late-generated neurons the superficial layers of the cerebral cortex. In a way, this finding came as a surprise because the late-generated neurons did not simply push away the early-generated ones, which would have resulted in an opposite layering. Late-generated neurons rather have to tackle the task of bypassing a densely packed layer of earlier generated cells. This also includes that late-generated neurons trespassing early-generated deep layer cells have to migrate for much longer distances to reach their destination. How is this achieved? How do late-generated neurons find their way to the surface of the cortex?

Developmental studies in various species and more recently real-time microscopy of migrating neurons in the cortex have contributed much to our understanding of the journey of late-generated neurons through the layers of their predecessors (Nadarajah et al., 2001; Nadarajah and Parnavelas, 2002). It has become clear that a migrating neuron moves in the direction of its thick leading process and that this is associated with a translocation of the nucleus in this direction. With the leading process becoming the main apical dendrite, the vertical orientation of pyramidal cells in the mature cortex represents a frozen picture of its development, particularly of the directionality of the migratory process. What are the signals that control this directionality? Radial glial cell processes span the distance between the ventricle and the cortical surface, serving as a guiding scaffold for migrating neurons (Rakic, 1972). What are the signals controlling their orientation? What are the signals that anchor the leading processes of pyramidal neurons to the pial surface and how is this particular vertical orientation of apical dendrites maintained throughout life?

Much has been learned in the past from mouse mutants. A perfect example is the *reeler* mutant described as early as in 1951 (Falconer, 1951). In this mutant, the normal inside-out lamination of the cerebral cortex is inverted and the majority of cortical pyramidal cells are misoriented, pointing to an important defect in molecular pathways but at the same time also to an interdependence of process orientation and cortical layer formation. With the discovery of Reelin, the molecule deficient in the *reeler* mutant, research in this area has exploded and our understanding of layer formation in the cortex and of the different players involved has significantly improved.

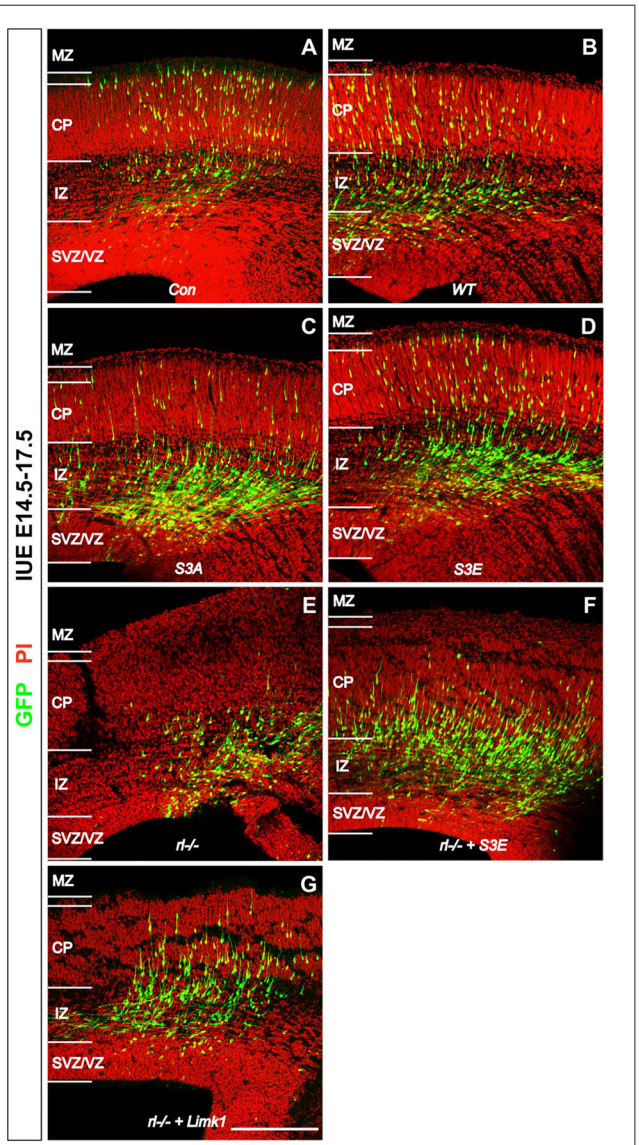

FIGURE 1 | Reelin-cofilin crosstalk during the migration of cortical neurons. (A,B) In wild-type cortices (*Con*) and in cortices transfected with wild-type cofilin (*cofilin*^{WT}), many GFP-positive cells have reached the cortical plate (CP) 3 days after *in utero* electroporation (IUE) on E 14.5. **(C,D)** In contrast, the majority of *cofilin*^{S3A}- and *cofilin*^{S3E}-transfected neurons have remained in the intermediate zone (IZ) and subventricular/ventricular zone (SVZ/VZ). **(E)** Similarly, very few cells have entered the CP in *reeler* slice cultures. **(F,G)** Slices from *reeler* embryos transfected with *cofilin*^{S3E} **(F)** or *LIM KINASE 1 (LIMK1)* **(G)** show partial rescue of the *reeler* phenotype with significantly more neurons invading the CP. MZ, marginal zone. Sections were counterstained with propidium iodide (PI). Scale bar: 100 μm (from Chai et al., 2016, reproduced with permission).

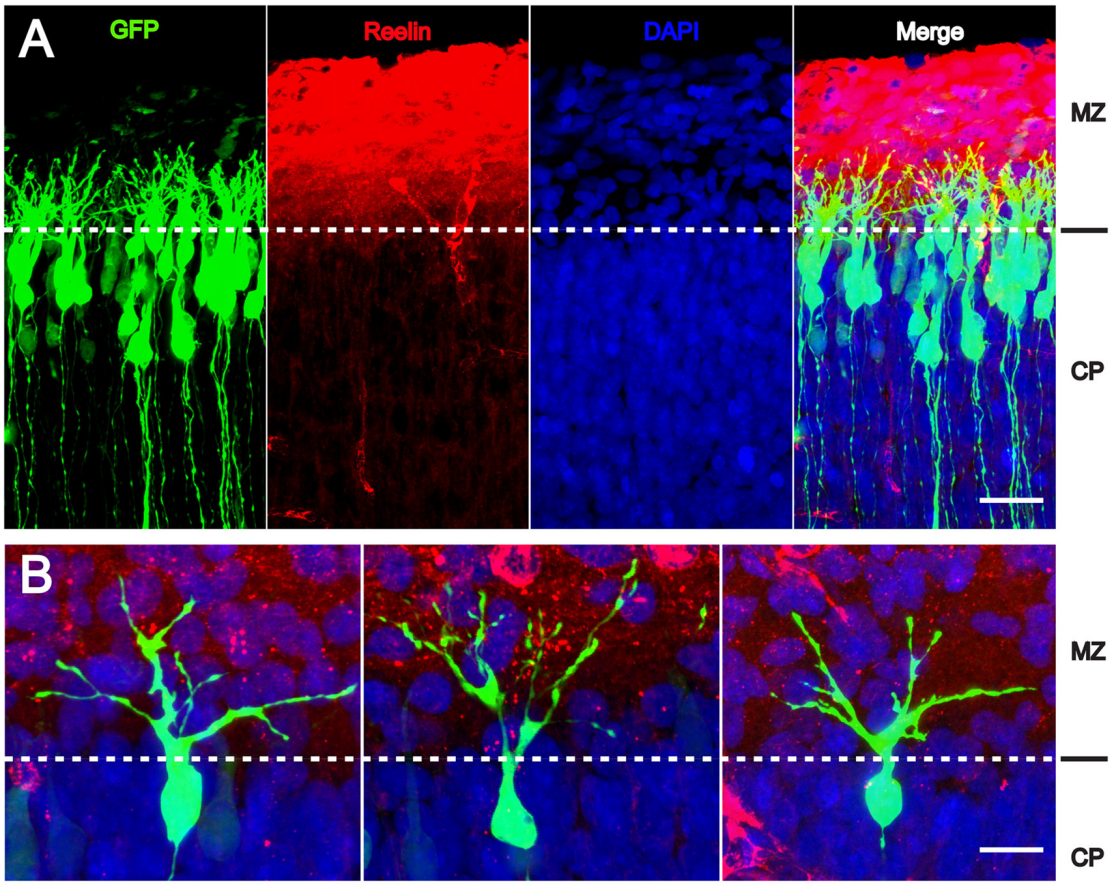

FIGURE 2 | Reelin-induced branching of the leading processes. (A,B) The leading processes of migrating neurons start to branch as soon as they reach the MZ containing Reelin. Transfection of wild-type embryos with *CAG-GFP* on E 14.5; fixation on E 17.5. CP, cortical plate. Scale bars: 40 μm **(A)**; 15 μm **(B)** (modified from Chai et al., 2015, with permission).

REELIN RECEPTORS AND THE REELIN SIGNALING CASCADE

The name Reelin is attributed to *reeler*, a natural mouse mutant described long before the Reelin gene was found (Falconer, 1951). As suggested by its name, the *reeler* mouse shows an impressive phenotype dominated by severe ataxia. Reelin is a large 400 kDa glycoprotein of the extracellular matrix which is synthesized and secreted by Cajal-Retzius cells (D'Arcangelo et al., 1995; Ogawa et al., 1995), an early class of cortical neurons that were described in detail in Golgi preparations by Santiago Rámon y Cajal and Gustaf Retzius at the turn of last century. Of note, Cajal-Retzius cells populate the marginal zone (MZ) of the developing cortex, future layer I. Thus, full-length Reelin and its fragments are highly concentrated at the top of the developing cortex, suggesting that this characteristic topographical distribution is important for the control of migratory processes underneath, i.e., for the migration of cortical neurons from the ventricle to the cortical surface. Is Reelin in the MZ an attractive molecule for newborn neurons generated near the ventricle? Nichols and Olson (2010) have shown that Reelin induces orientation and alignment of early-generated layer Vl neurons and preplate splitting. Moreover, a role for Reelin in the directed migration of cortical neurons is consistent with the observation that in *reeler* late-generated neurons are unable to migrate through deep, early-generated cell layers, likely because their attractive force is missing in the mutant (Zhao et al., 2004). However, in *reeler*, but not in wild type, layer I of the cortex, the former MZ, is densely populated, suggesting an opposite effect, a stop signal function for Reelin (Zhao and Frotscher, 2010). Could it be that full-length Reelin in the MZ has different functions than the various Reelin fragments, diffusing to deeper cortical layers? Reelin is composed of an N-terminal F-spondin-like domain, eight repeats, and a short and highly basic C-terminal region. Reelin is cleaved at two sites approximately located between repeats 2 and 3 and between repeats 6 and 7, resulting in a total of five different fragments (370 kDa, 270 kDa, 190 kDa, 180 kDa and 80 kDa) in addition to the full-length protein (Lambert de Rouvroit et al., 1999; Ignatova et al., 2004). Of note, inhibition of processing alters cortical lamination (unpublished observations).

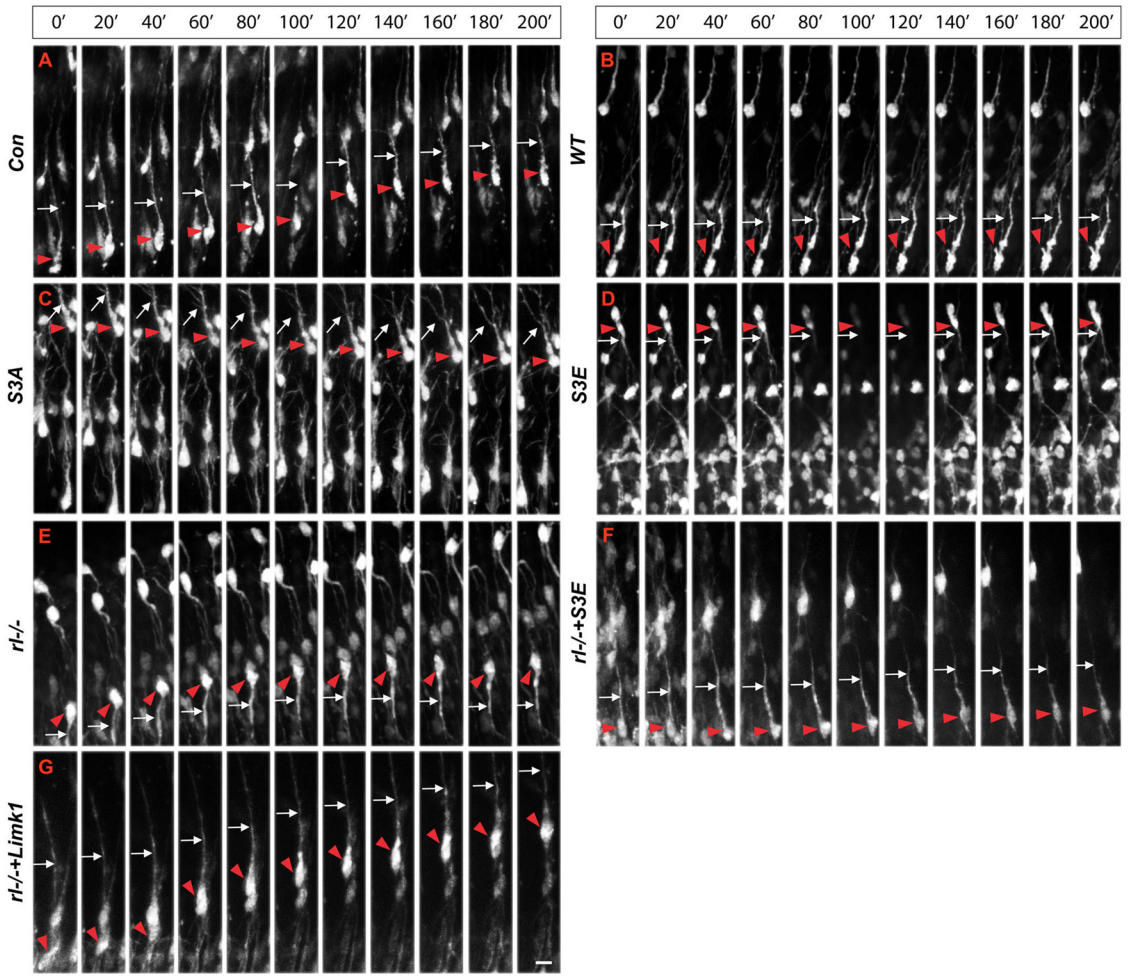

FIGURE 3 | Real-time microscopy of migrating neurons transfected with the different constructs. (A–G) Following in IUE on E 14.5, slice cultures were prepared on E 17.5 and single neurons were monitored over a period of 200 min. Red arrowheads mark the cell bodies and white arrows the leading processes of migrating neurons. The MZ is at the top of the figures, the VZ at the bottom. Note aberrant leading processes pointing toward the VZ in *reeler* neurons ($rl^{-/-}$) and neurons transfected with *cofilin*^{S3E}. Neurons in *reeler* slices transfected with *LIMK1* or *cofilin*^{S3E} show a normal leading process oriented toward the MZ. Scale bar: 15 μm (from Chai et al., 2016, reproduced with permission).

Or could it be that different Reelin receptors were involved? It came as a surprise that Reelin binds to lipoprotein receptors and that a double knockout mouse deficient in the two lipoprotein receptors, apolipoprotein E receptor 2 (ApoER2) and very low-density lipoprotein receptor (VLDLR), showed a *reeler* phenotype (D'Arcangelo et al., 1999; Hiesberger et al., 1999; Trommsdorff et al., 1999). Mutants deficient in only one of these receptors showed phenotypes that were milder and also different from each other (Hack et al., 2007). Thus, while in *ApoER2* knockout mice late-generated neurons were unable to bypass early-generated cells like in the *reeler* mutant, mutants deficient in *VLDLR* displayed another feature of the *reeler* phenotype, the characteristic invasion of the MZ (Hack et al., 2007). Indeed, the two receptor types were found differently distributed in the cortex with the VLDLR receptor being mainly located in upper cortical layers (Hirota et al., 2014), suggesting that this receptor would be responsible for the stop signal function of Reelin (Hack et al., 2007). Besides these two lipoprotein receptors, cadherin-related neuronal receptors (CNRs; Senzaki et al., 1999) and alpha3beta1 integrins (Dulabon et al., 2000) were described to function as Reelin receptors. Binding of Reelin to ApoER2 and VLDLR was found to induce the phosphorylation of disabled 1 (Dab1; Howell et al., 1999; Benhayon et al., 2003), an adaptor protein binding to the intracellular domains of the lipoprotein receptors. Mutants deficient in Dab1 showed a *reeler*-like phenotype (Sheldon et al., 1997). The Reelin signaling cascade involves in addition src family kinases which phosphorylate Dab1, phosphatidylinositol 3-kinase (PI3K), and glycogen synthase kinase 3 beta (GSK3B), the latter kinase being known to phosphorylate Tau (Hiesberger et al., 1999). Hyperphosphorylation of

Tau is a hallmark of Alzheimer's disease, suggesting an involvement of the Reelin signaling cascade in the pathology of this disorder but further work is needed to obtain a clearer picture.

REELIN ACTS UPSTREAM OF COFILIN TO FACILITATE MIGRATION

We previously found that Reelin induces phosphorylation (activation) of LIM kinase 1 (LIMK1), a kinase that in turn induces phosphorylation of cofilin (Chai et al., 2009). Cofilin is an actin-depolymerizing protein that is inactivated by its phosphorylation at serine3 (Arber et al., 1998; Yang et al., 1998). Since Reelin induces the phosphorylation of cofilin, one is tempted to conclude that Reelin counteracts cytoskeletal reorganization and in turn stabilizes the actin cytoskeleton in neuronal processes. In the present review article we will not discuss other molecules of the Reelin signaling cascade in detail but will focus on Reelin's role in the stabilization of the actin cytoskeleton as an important prerequisite for the stability of the leading process which is needed for nuclear translocation during migratory activity. The reader is referred to several other review articles dealing in more detail with the various aspects of Reelin function (Rakic and Caviness, 1995; Curran and D'Arcangelo, 1998; Frotscher, 1998, 2010; Jossin et al., 2003; Tissir and Goffinet, 2003; Förster et al., 2006a,b; Cooper, 2008, 2013; Zhao and Frotscher, 2010; Chai and Frotscher, 2016).

Some time ago Bellenchi et al. (2007) reported that conditional cofilin mutants showed migration defects reminiscent of the reeler phenotype. Chai et al. (2009) then demonstrated that the amounts of phosphorylated cofilin are significantly reduced in *reeler* and that application of recombinant Reelin to *reeler* tissue significantly increased the phosphorylation of cofilin, suggesting that Reelin-induced cofilin phosporylation is important for the normal lamination of the cerebral cortex. This hypothesis was recently confirmed by *in utero* electroporation (IUE) experiments (Chai et al., 2016). Transfection of newly born cortical neurons with a non-phosphorylatable form of cofilin (*cofilin*^{S3A}) revealed a significant migration defect of the transfected cells, which remained near their site of origin in the subventricular zone (SVZ)—very much reminiscent of the *reeler* phenotype. Neurons transfected with a pseudophosphorylated form (*cofilin*^{S3E}) also showed a migration defect. Remarkably, transfection of *reeler* embryos with *LIMK1* seemingly forced the phosphorylation of cofilin in these animals and resulted in a partial rescue of the migration defect in *reeler*, as did transfection with pseudophosphorylated *cofilin*^{S3E}. These results on GFP-expressing neurons were obtained by IUE on embryonic day (E) 14.5, sacrificing the embryos on E17.5 and counterstaining sections of the cortex for propidium iodide (PI; **Figure 1**). Remarkably, neurons transfected with the cofilin mutants, similarly to GFP transfected *reeler* neurons, often showed leading processes oriented toward the ventricle. Collectively, these results suggest that Reelin-induced stabilization of the leading process, likely by the phosphorylation of cofilin, is an essential step in the proper orientation and migration directionality of late-generated cortical neurons.

REELIN ACTS ON BOTH NEURONS AND RADIAL GLIAL CELLS

During early stages of corticogenesis, newborn neurons find their way through the yet thin cortical wall. They only have to migrate from the ventricular zone (VZ)/SVZ to the deep cortical layers. As already pointed out, late-generated cortical neurons destined to superficial layers have to migrate for longer distances. This holds particularly true since the cortical plate (CP) and the intermediate zone (IZ) have become thicker at later developmental stages due to the continuous arrival of numerous neurons and the development of their dendritic and axonal processes. In order to traverse these larger distances successfully, late-generated neurons migrate along radial glial fibers, which span out between the ventricle and the pial surface, serving as a guiding scaffold for migrating cells (Rakic, 1972). Is Reelin involved in the correct orientation and targeting of radial glial fibers?

In a previous study, we were able to show that glial fibrillary acidic protein (GFAP)-positive processes of radial glial cells studied in a stripe choice assay with Reelin-containing stripes next to control stripes, started to branch as soon as they reached the Reelin stripes (Förster et al., 2002), suggesting that Reelin induces the branching of radial glial processes. Remarkably, when studying GFP-labeled radial glial fibers *in vivo*, they were found to branch as soon as they reached the Reelin-containing MZ (Chai et al., 2015). Next, we studied radial glial fibers in *reeler* mutant tissue and found that the number of branches arising from the main radial process was significantly reduced in *reeler* when compared to wild-type radial glial fibers (Chai et al., 2015). We concluded that Reelin induces the branching of radial glial fibers arriving at the MZ, thereby anchoring them to the cortical surface and allowing for the detachment of migrating neurons, which then finalize the migratory process by terminal translocation of the nucleus in the absence of a guiding radial fiber. Remarkably, branching of processes is associated with increased reorganization of the cytoskeleton, and future studies need to find out how Reelin in the MZ induces both branching and stabilization of the actin cytoskeleton by cofilin phosphorylation.

Since radial glial cells are precursors of neurons, we hypothesized that also the leading processes of neurons would start to branch upon arrival at the MZ. Indeed, the leading processes gave rise to branches precisely upon arrival at the Reelin-containing MZ (**Figure 2**). In the mature animal these branches in layer I represent the apical tuft of cortical pyramidal cells. When studying branching of the leading processes by real-time microscopy, we noticed that migration by nuclear translocation was terminated as soon as the large nucleus arrived at the thin branches of the main shaft of the leading process, suggesting that mechanical obstruction might play a role in the migratory arrest of late-generated neurons (Chai et al., 2015; O'Dell et al., 2015). As a result, the MZ containing the thin

branches of the leading processes is almost free of cell bodies. Accordingly, the stop signal function of Reelin would be two-fold: first, Reelin induces branching of the leading processes that cannot be entered by the translocating nucleus. Second, binding of Reelin to VLDLR receptors terminates migratory activity in wild-type neurons, but not in *reeler* neurons and in neurons deficient in VLDLR. Accordingly, many neurons in *VLDLR* knockout mice show "overmigration" into the MZ (Hack et al., 2007). In *reeler* mutants, Reelin-induced branching of radial glial fibers and of the leading processes of neurons is absent and neurons are not anchored to the MZ by these branches of the leading process. As a consequence, the leading processes do not remain attached to the cortical surface and point to various directions, often toward the VZ. We accordingly observed many neurons in *reeler* that did not migrate toward the cortical surface but in opposite direction toward the VZ. Similar observations were occasionally made in neurons transfected by IUE with the non-phosphorylatable form of cofilin (*cofilin*^{S3A}) and more often in embryos transfected with *cofilin*^{S3E}. These findings in particular underscore the significant role of Reelin-induced cofilin phosphorylation for the orientation of the leading process and directed migration of cortical neurons. Indeed, we have previously shown that the phosphorylated form of cofilin is much enriched in and near the MZ (Chai et al., 2009). It is remarkable to note in this context that transfection of *reeler* embryos with pseudophosphorylated *cofilin*^{S3E} or *LIMK1* partially rescued orientation of the leading processes and the migration defect in *reeler*. In order to study the migratory behavior of the living cells in some detail, IUE with the various constructs was performed on E 14.5 and slice cultures of neocortex were prepared 3 days later, when many neurons destined to superficial layers were migrating (**Figure 3**). Together, these findings indicate that Reelin plays an important role in the proper orientation and stabilization of the leading process, allowing for directed migration towards the cortical surface. Moreover, proper orientation of the leading process and its attachment to the MZ provides the tension required for nuclear translocation and the successful bypassing of early generated deep-layer neurons.

We were impressed to find such significant migration defects when transfecting wild-type embryos with *cofilin*^{S3A} and *cofilin*^{S3E} and to observe partial rescue of the *reeler* phenotype following transfection with *LIMK1*—although many other molecular players such as molecules of the tubulin cytoskeleton (e.g., Meseke et al., 2013; Förster, 2014), proneural transcription factors such as Rnd proteins (Pacary et al., 2011), and CLASP2 (Dillon et al., 2017) are also known to control the cytoskeleton of neuronal cells and extension and orientation of the leading process, migration by nuclear translocation associated with a myosin II-dependent flow of actin filaments (He et al., 2010), and eventually layer formation in the cerebral cortex.

AUTHOR CONTRIBUTIONS

MF developed the concept of this review article and wrote the manuscript. SZ, SW and XC performed the majority of the experiments reviewed in this article and contributed to manuscript writing and editing.

ACKNOWLEDGMENTS

The authors wish to thank the members of the Zhao lab and Frotscher lab for many stimulating discussions. The studies summarized in this review article were supported by grants from the Deutsche Forschungsgemeinschaft (FR 620/12-2, FR 620/13-1 and FR 620/14-1 to MF) and the National Natural Science Foundation of China (No. 31572477 to SZ). MF is Research Professor for Neuroscience of the Hertie Foundation.

REFERENCES

Arber, S., Barbayannis, F. A., Hanser, H., Schneider, C., Stanyon, C. A., Bernard, O., et al. (1998). Regulation of actin dynamics through phosphorylation of cofilin by LIM-kinase. *Nature* 393, 805–809. doi: 10.1038/31729

Bellenchi, G. C., Gurniak, C. B., Perlas, E., Middei, S., Ammassari-Teule, M., and Witke, W. (2007). N-cofilin is associated with neuronal migration disorders and cell cycle control in the cerebral cortex. *Genes Dev.* 21, 2347–2357. doi: 10.1101/gad.434307

Benhayon, D., Magdaleno, S., and Curran, T. (2003). Binding of purified Reelin to ApoER2 and VLDLR mediates tyrosine phosphorylation of disabled-1. *Mol. Brain Res.* 112, 33–45. doi: 10.1016/s0169-328x(03)00032-9

Berry, M., and Rogers, A. W. (1965). The migration of neuroblasts in the developing cerebral cortex. *J. Anat.* 991, 691–709.

Chai, X., and Frotscher, M. (2016). How does Reelin signaling regulate the neuronal cytoskeleton during migration? *Neurogenesis* 3:e1242455. doi: 10.1080/23262133.2016.1242455

Chai, X., Förster, E., Zhao, S., Bock, H. H., and Frotscher, M. (2009). Reelin stabilizes the actin cytoskeleton of neuronal processes by inducing *n*-cofilin phosphorylation at serine3. *J. Neurosci.* 29, 288–299. doi: 10.1523/JNEUROSCI.2934-08.2009

Chai, X., Fan, L., Shao, H., Lu, X., Zhang, W., Li, J., et al. (2015). Reelin induces branching of neurons and radial glial cells during corticogenesis. *Cereb. Cortex* 25, 3640–3653. doi: 10.1093/cercor/bhu216

Chai, X., Zhao, S., Fan, L., Zhang, W., Lu, X., Shao, H., et al. (2016). Reelin and cofilin cooperate during the migration of cortical neurons: a quantitative morphological analysis. *Development* 143, 1029–1040. doi: 10.1242/dev.134163

Cooper, J. A. (2008). A mechanism for inside-out lamination in the neocortex. *Trends Neurosci.* 31, 113–119. doi: 10.1016/j.tins.2007.12.003

Cooper, J. A. (2013). Cell biology in neuroscience: mechanisms of cell migration in the nervous system. *J. Cell Biol.* 202, 725–734. doi: 10.1083/jcb.201305021

Curran, T., and D'Arcangelo, G. (1998). Role of reelin in the control of brain development. *Brain Res. Rev.* 26, 285–294. doi: 10.1016/s0165-0173(97)00035-0

D'Arcangelo, G., Miao, G. G., Chen, S. C., Soares, H. D., Morgan, J. I., and Curran, T. (1995). A protein related to extracellular matrix proteins deleted in the mouse mutant reeler. *Nature* 374, 719–723. doi: 10.1038/374719a0

D'Arcangelo, G., Homayouni, R., Keshvara, L., Rice, D. S., Sheldon, M., and Curran, T. (1999). Reelin is a ligand for lipoprotein receptors. *Neuron* 24, 471–479. doi: 10.1016/s0896-6273(00)80860-0

Dillon, G. M., Tyler, W. A., Omuro, K. C., Kambouris, J., Tyminski, C., Henry, S., et al. (2017). CLASP2 links Reelin to the cytoskeleton during neocortical development. *Neuron* 93, 1344.e5–1358.e5. doi: 10.1016/j.neuron.2017.02.039

Dulabon, L., Olson, E. C., Taglienti, M. G., Eisenhuth, S., McGrath, B., Walsh, C. A., et al. (2000). Reelin binds alpha3beta1 integrin and inhibits neuronal migration. *Neuron* 27, 33–44. doi: 10.1016/s0896-6273(00)00007-6

Falconer, D. S. (1951). Two new mutants, "trembler" and "reeler", with neurological actions in the house mouse (*Mus musculus* L.). *J. Genet.* 50, 192–201.

Förster, E. (2014). Reelin, neuronal polarity and process orientation of cortical neurons. *Neuroscience* 269, 102–111. doi: 10.1016/j.neuroscience.2014.03.004

Förster, E., Tielsch, A., Saum, B., Weiss, K. H., Johanssen, C., Graus-Porta, D., et al. (2002). Reelin, disabled 1 and beta1 integrins are required for the formation of the radial glial scaffold in the hippocampus. *Proc. Natl. Acad. Sci. U S A* 99, 13178–13183. doi: 10.1073/pnas.202035899

Förster, E., Zhao, S., and Frotscher, M. (2006a). Laminating the hippocampus. *Nat. Rev. Neurosci.* 7, 259–267. doi: 10.1038/nrn1882

Förster, E., Jossin, Y., Zhao, S., Chai, X., Frotscher, M., and Goffinet, A. M. (2006b). Recent progress in understanding the role of Reelin in radial neuronal migration, with specific emphasis on the dentate gyrus. *Eur. J. Neurosci.* 23, 901–909. doi: 10.1111/j.1460-9568.2006.04612.x

Frotscher, M. (1998). Cajal-Retzius cells, Reelin, and the formation of layers. *Curr. Opin. Neurobiol.* 8, 570–575. doi: 10.1016/s0959-4388(98)80082-2

Frotscher, M. (2010). Role for Reelin in stabilizing cortical architecture. *Trends Neurosci.* 33, 407–414. doi: 10.1016/j.tins.2010.06.001

Golgi, C. (1873). Sulla struttura della sostanza grigia della cervello. *Gazz. Med. Ital. Lombardia* 6, 244–246.

Hack, I., Hellwig, S., Junghans, D., Brunne, B., Bock, H. H., Zhao, S., et al. (2007). Divergent roles of ApoER2 and Vldlr in the migration of cortical neurons. *Development* 134, 3883–3891. doi: 10.1242/dev.005447

He, M., Zhang, Z. H., Guan, C. B., Xia, D., and Yuan, X. B. (2010). Leading tip drives soma translocation via forward F-actin flow during neuronal migration. *J. Neurosci.* 30, 10885–10898. doi: 10.1523/JNEUROSCI.0240-10.2010

Hiesberger, T., Trommsdorff, M., Howell, B. W., Goffinet, A., Mumby, M. C., Cooper, J. A., et al. (1999). Direct binding of Reelin to VLDL receptor and ApoE receptor 2 induces tyrosine phosphorylation of disabled-1 and modulates tau phosphorylation. *Neuron* 24, 481–489. doi: 10.1016/s0896-6273(00)80861-2

Hirota, Y., Kubo, K. I., Katayama, K. I., Honda, T., Fujino, T., Yamamoto, T. T., et al. (2014). Reelin receptors ApoER2 and VLDLR are expressed in distinct spatio-temporal patterns in developing mouse cerebral cortex. *J. Comp. Neurol.* 523, 463–478. doi: 10.1002/cne.23691

Howell, B. W., Herrick, T. M., and Cooper, J. A. (1999). Reelin-induced tyrosine phosphorylation of disabled 1 during neuronal positioning. *Genes Dev.* 13, 643–648. doi: 10.1101/gad.13.6.643

Ignatova, N., Sindic, C. J., and Goffinet, A. M. (2004). Characterization of the various forms of the Reelin protein in the cerebrospinal fluid of normal subjects and in neurological diseases. *Neurobiol. Dis.* 15, 326–330. doi: 10.1016/j.nbd.2003.11.008

Jossin, Y., Bar, I., Ignatova, N., Tissir, F., De Rouvroit, C. L., and Goffinet, A. M. (2003). The reelin signaling pathway: some recent developments. *Cereb. Cortex* 13, 627–633. doi: 10.1093/cercor/13.6.627

Lambert de Rouvroit, C., de Bergeyck, V., Cortvrindt, C., Bar, I., Eeckhout, Y., and Goffinet, A. M. (1999). Reelin, the extracellular matrix protein deficient in reeler mutant mice, is processed by a metalloproteinase. *Exp. Neurol.* 156, 214–217. doi: 10.1006/exnr.1998.7007

Meseke, M., Cavus, E., and Förster, E. (2013). Reelin promotes microtubule dynamics in processes of developing neurons. *Histochem. Cell Biol.* 139, 283–297. doi: 10.1007/s00418-012-1025-1

Nadarajah, B., and Parnavelas, J. G. (2002). Modes of neuronal migration in the developing cerebral cortex. *Nat. Rev. Neurosci.* 3, 423–432. doi: 10.1038/nrn845

Nadarajah, B., Brunstrom, J. E., Grutzendler, J., Wong, R. O., and Pearlman, A. L. (2001). Two modes of radial migration in early development of the cerebral cortex. *Nat. Neurosci.* 4, 143–150. doi: 10.1038/83967

Nichols, A. J., and Olson, E. C. (2010). Reelin promotes neuronal orientation and dendritogenesis during preplate splitting. *Cereb. Cortex* 20, 2213–2223. doi: 10.1093/cercor/bhp303

O'Dell, R. S., Cameron, D. A., Zipfel, W. R., and Olson, E. C. (2015). Reelin prevents apical neurite retraction during terminal translocation and dendrite initiation. *J. Neurosci.* 35, 10659–10674. doi: 10.1523/JNEUROSCI.1629-15.2015

Ogawa, M., Miyata, T., Nakajima, K., Yagyu, K., Seike, M., Ikenaka, K., et al. (1995). The reeler gene-associated antigen on Cajal-Retzius neurons is a crucial molecule for laminar organization of cortical neurons. *Neuron* 14, 899–912. doi: 10.1016/0896-6273(95)90329-1

Pacary, E., Heng, J., Azzarelli, R., Riou, P., Castro, D., Lebel-Potter, M., et al. (2011). Proneural transcription factors regulate different steps of cortical neuron migration through Rnd-mediated inhibition of RhoA signaling. *Neuron* 69, 1069–1084. doi: 10.1016/j.neuron.2011.02.018

Rakic, P. (1972). Mode of cell migration to the superficial layers of fetal monkey neocortex. *J. Comp. Neurol.* 145, 61–83. doi: 10.1002/cne.901450105

Rakic, P., and Caviness, V. S. (1995). Cortical development: view from neurological mutants two decades later. *Neuron* 14, 1101–1104. doi: 10.1016/0896-6273(95)90258-9

Ramón y Cajal, S. R. (1911). *Histologie du système nerveux de l'homme et des vertébrés*. Paris: Maloine.

Senzaki, K., Ogawa, M., and Yagi, T. (1999). Proteins of the CNR family are multiple receptors for Reelin. *Cell* 99, 635–647. doi: 10.1016/s0092-8674(00)81552-4

Sheldon, M., Rice, D. S., D'Arcangelo, G., Yoneshima, H., Nakajima, K., Mikoshiba, K., et al. (1997). Scrambler and yotari disrupt the disabled gene and produce a reeler-like phenotype in mice. *Nature* 389, 730–733. doi: 10.1038/39601

Tissir, F., and Goffinet, A. M. (2003). Reelin and brain development. *Nat. Rev. Neurosci.* 4, 496–505. doi: 10.1038/nrn1113

Trommsdorff, M., Gotthardt, M., Hiesberger, T., Shelton, J., Stockinger, W., Nimpf, J., et al. (1999). Reeler/disabled-like disruption of neuronal migration in knockout mice lacking the VLDL receptor and ApoE receptor 2. *Cell* 97, 689–701. doi: 10.1016/s0092-8674(00)80782-5

Yang, N., Higuchi, O., Ohashi, K., Nagata, K., Wada, A., Kangawa, K., et al. (1998). Cofilin phosphorylation by LIM-kinase 1 and its role in rac-mediated actin reorganization. *Nature* 393, 809–812. doi: 10.1038/31735

Zhao, S., and Frotscher, M. (2010). Go or stop? Divergent roles of Reelin in radial neuronal migration. *Neuroscientist* 16, 421–434. doi: 10.1177/1073858410367521

Zhao, S., Chai, X., Förster, E., and Frotscher, M. (2004). Reelin is a positional signal for the lamination of dentate granule cells. *Development* 131, 5117–5125. doi: 10.1242/dev.01387

Conflict of Interest Statement: The authors declare that the research was conducted in the absence of any commercial or financial relationships that could be construed as a potential conflict of interest.

frontiers in Cellular Neuroscience

ORIGINAL RESEARCH
published: 16 June 2017
doi: 10.3389/fncel.2017.00169

Serping1/C1 Inhibitor Affects Cortical Development in a Cell Autonomous and Non-cell Autonomous Manner

Anna Gorelik[1], *Tamar Sapir*[1], *Trent M. Woodruff*[2] *and Orly Reiner*[1]*

[1] *Department of Molecular Genetics, Weizmann Institute of Science, Rehovot, Israel,* [2] *School of Biomedical Sciences, The University of Queensland, St Lucia, QLD, Australia*

Current knowledge regarding regulation of radial neuronal migration is mainly focused on intracellular molecules. Our unbiased screen aimed at identification of non-cell autonomous mechanisms involved in this process detected differential expression of *Serping1* or C1 inhibitor, which is known to inhibit the initiation of the complement cascade. The complement cascade is composed of three pathways; the classical, lectin, and the alternative pathway; the first two are inhibited by C1 inhibitor, and all three converge at the level of C3. Knockdown or knockout of *Serping1* affected neuronal stem cell proliferation and impaired neuronal migration in mice. Knockdown of *Serping1* by *in utero* electroporation resulted in a migration delay of the electroporated cells as well as their neighboring cells demonstrating a non-cell autonomous effect. Cellular polarity was also affected. Most importantly, expression of protein components mimicking cleaved C3 rescued the knockdown of *Serping1*, indicating complement pathway functionality. Furthermore, we propose that this activity is mediated mainly via the complement peptide C5a receptors. Whereas addition of a selective C3a receptor agonist was minimally effective, the addition of a dual C3aR/C5a receptor agonist significantly rescued *Serping1* knockdown-mediated neuronal migration defects. Our findings suggest that modulating *Serping1* levels in the developing brain may affect the complement pathway in a complex way. Collectively, our findings demonstrate an unorthodox activity for the complement pathway during brain development.

Keywords: Serping1, C1 inhibitor, innate immune complement pathway, neuronal migration, neuronal stem cell proliferation

OPEN ACCESS

Edited by:
Annette Gaertner,
Evotec (Germany), Germany

Reviewed by:
Alice Davy,
Université Toulouse III Paul Sabatier, France
Ali Shariati,
Stanford University, United States

***Correspondence:**
Orly Reiner
orly.reiner@weizmann.ac.il

Received: *28 February 2017*
Accepted: *01 June 2017*
Published: *16 June 2017*

Citation:
Gorelik A, Sapir T, Woodruff TM and Reiner O (2017) Serping1/C1 Inhibitor Affects Cortical Development in a Cell Autonomous and Non-cell Autonomous Manner. Front. Cell. Neurosci. 11:169. doi: 10.3389/fncel.2017.00169

INTRODUCTION

Deciphering what is the function of molecules expressed in the developing brain is a daunting task. Therefore, several years ago we embarked on an unbiased functional screen aimed at detecting molecules, which may affect neuronal migration in a non-cell autonomous way (Greenman et al., 2015). One of the differentially expressed genes detected in this screen was *Serping1* (Serpin peptidase inhibitor, clade G, member 1) encoding for the C1 inhibitor protein. C1 inhibitor is a member of the serpin family of protease inhibitors (reviewed by Davis et al., 2008). Similar to other serpin family protease inhibitors, the mechanism of inhibition requires a physical contact between the inhibitor and a specific protease, followed by a conformational change and formation of a covalent bond between the inhibitor and the serine residue which is part of the protease active site. C1 inhibitor has a key role in the complement pathway where it inhibits initiation proteases

in either the classical pathway (C1r and C1s) or the lectin pathway (MASP1 and MASP2) (Presanis et al., 2003; Parej et al., 2013). C1 inhibitor has additional important substrates that include contact system proteases (factor XII, plasma kallikrein), an intrinsic coagulation protease (factor XI) and the fibrinolytic proteases (plasmin, tissue plasminogen activator). However, based on our recent studies demonstrating the expression and function of the complement system in brain development (Coulthard et al., 2017; Gorelik et al., 2017), the current study on the role of *Serping1* in the developing brain has been focused on its relationship within the complement pathway. In addition to protease inhibition, C1 inhibitor can physically bind and functionally affect the interaction between complement factor C3b and complement factor B and thus to interfere also with the alternative pathway (Jiang et al., 2001). Additional functional interactions include different extracellular matrix components, endothelial cells and leukocytes, gram negative endotoxin, and several infectious agents (reviewed by Davis et al., 2008).

C1 inhibitor has been associated with several diseases. Addition of C1 inhibitor has been shown to be neuroprotective in case of ischemic injury (De Simoni et al., 2004; Storini et al., 2005; Gesuete et al., 2009; Heydenreich et al., 2012). However, it is likely that the neuroprotection is not mediated solely via the activity of C1 inhibitor on the complement pathway. Expression of multiple components of the complement pathway, including C1 inhibitor has also been demonstrated in Alzheimer's disease, which may reflect ongoing inflammation in the brains of the patients (Walker et al., 1995; Veerhuis et al., 1998; Yasojima et al., 1999). It has been suggested that reduced levels of C1 inhibitor may be a biomarker for Alzheimer's disease (Akuffo et al., 2008; Cutler et al., 2008; Chiam et al., 2015; Muenchhoff et al., 2015; Morgan et al., 2017).

Deficiency of C1 inhibitor is a rare autosomal dominant disease known as Hereditary angioedema (HAE) with an estimated prevalence of 1:50,000, where about 25% of the patients exhibit *de novo* mutations (Bowen et al., 2010). Patients with HAE may experience recurrent edema of the skin and submucosal tissue associated with pain syndromes, nausea, vomiting, diarrhea, and life-threatening airway swellings. Risk of dying from airway obstruction if left untreated is significant. Additional symptoms may present as well and the manifestations and severity of HAE are highly variable. In this disease, the low levels of active C1 inhibitor in the plasma leads to unregulated activation of the complement and contact cascades and the development of angioedema with its associated complications. Complement system activation results in decreased levels of C4 and C2, while contact system activation results in cleavage of high molecular weight kininogen. Studies conducted in a mouse model for this disease revealed that both homozygous and heterozygous mice exhibit increased vascular permeability in comparison with wild-type littermates (Han, 2002). They have further shown that this phenotype is mediated through the bradykinin type 2 receptor.

In contrast to its roles in innate immunity, very little is known about the expression and functional activity of *Serping1* in the developing brain. A study examining single cell RNA expression in the E14 developing mouse brain revealed that *Serping1* is expressed in subventricular zone (SVZ) basal progenitors (Kawaguchi et al., 2008). In this study, we therefore set out to investigate the role of this interesting molecule in the developing cortex and how its function there relates to the complement pathway.

RESULTS

Serping1 Is Expressed in the Developing Brain

Serping1 was detected in developing mouse brains (E14.5-E17.5) in an unbiased screen aimed at identifying molecules which may affect neuronal migration in a non-cell autonomous way (Greenman et al., 2015). The screen was designed to highlight changes between genes expressed in stalled cells that acquire either a bipolar (following *Dclk* shRNA treatment) or a multipolar appearance (following *Dclk* shRNA treatment). The results of the screen showed that the levels of *Serping1* were 2.10-fold higher in *Dclk* shRNA vs. *Dcx* shRNA. The differences at the mRNA level were verified by realtime qPCR (59.6 $\pm$ 1.5% in *Dcx* shRNA compared to *Dclk* shRNA, $n = 6$, *Student's t-test*, $p = 0.0047$, Supplementary Figure 1A) and were also recapitulated at the protein level, with an elevation of 159.6 $\pm$ 8.82% in SERPING1 protein in *Dclk* shRNA-treated brains vs. *Dcx* shRNA-treated brains ($n = 5$, *Student's t-test,* $p = 0.041$, Supplementary Figure 1A). Following these results we next examined *Serping1* mRNA expression in the developing cortex using real-time qPCR (Supplementary Figure 1B). When the expression was normalized to that observed on E13.5, similar levels were noted on E14.5, followed by an observed decreased expression on E16.5 and E18.5. RNA *in situ* hybridization data from E14.5 brain section taken from (http://www.genepaint.org) demonstrated that *Serping1* mRNA is expressed in the developing cortex, where the highest expression levels are seen in the SVZ as previously reported (Kawaguchi et al., 2008). However, in addition *Serping1* mRNA was expressed in the ventricular zone, and lower levels of expression could also be observed in the cortical plate (Supplementary Figure 1C). The timing and pattern of *Serping1* expression suggested that this gene may participate in neuronal stem cell proliferation.

Serping1 Affects Neuronal Stem Cell Proliferation

To investigate the role of *Serping1* in regulation of neuronal stem cell proliferation during mouse embryonic brain development two models were used. In the first, we knocked-down gene expression using *in utero* electroporation of an shRNA expressing plasmid, and in the second we generated knockout embryos using CRISPR/Cas9 gene editing technology (Ran et al., 2013; Wang et al., 2013) (Supplementary Figures 2A,B). *Serping1* shRNA effectively reduced the levels of *Serping1* mRNA by 37.5 $\pm$ 8.9% in comparison to control (qPCR, $n = 9$, *Student's t-test* $p = 0.00012$), as well as SERPING1 protein in the developing brain (52.7 $\pm$ 5.6% compared to control, $n = 4$, $p = 0.0064$). Neuronal stem cell proliferation was tested by application of a short IdU pulse, which is incorporated during S phase following by immunostaining

of embryonic brain sections using the respective antibodies. Embryos were *in utero* electroporated at E13 and analyzed at E14. The analysis was targeted at the IdU/GFP positive cells, which were likely to receive the respective shRNA plasmids. There was a statistically significant difference between the IdU/GFP double positive cells, where the introduction of *Serping1* shRNA reduced the number of cells in S-phase (*Student's t-test* 21 ± 2.2% vs. 14.5 ± 1.4, $n = 5$, $p = 0.037$, **Figures 1A,B**). In addition,

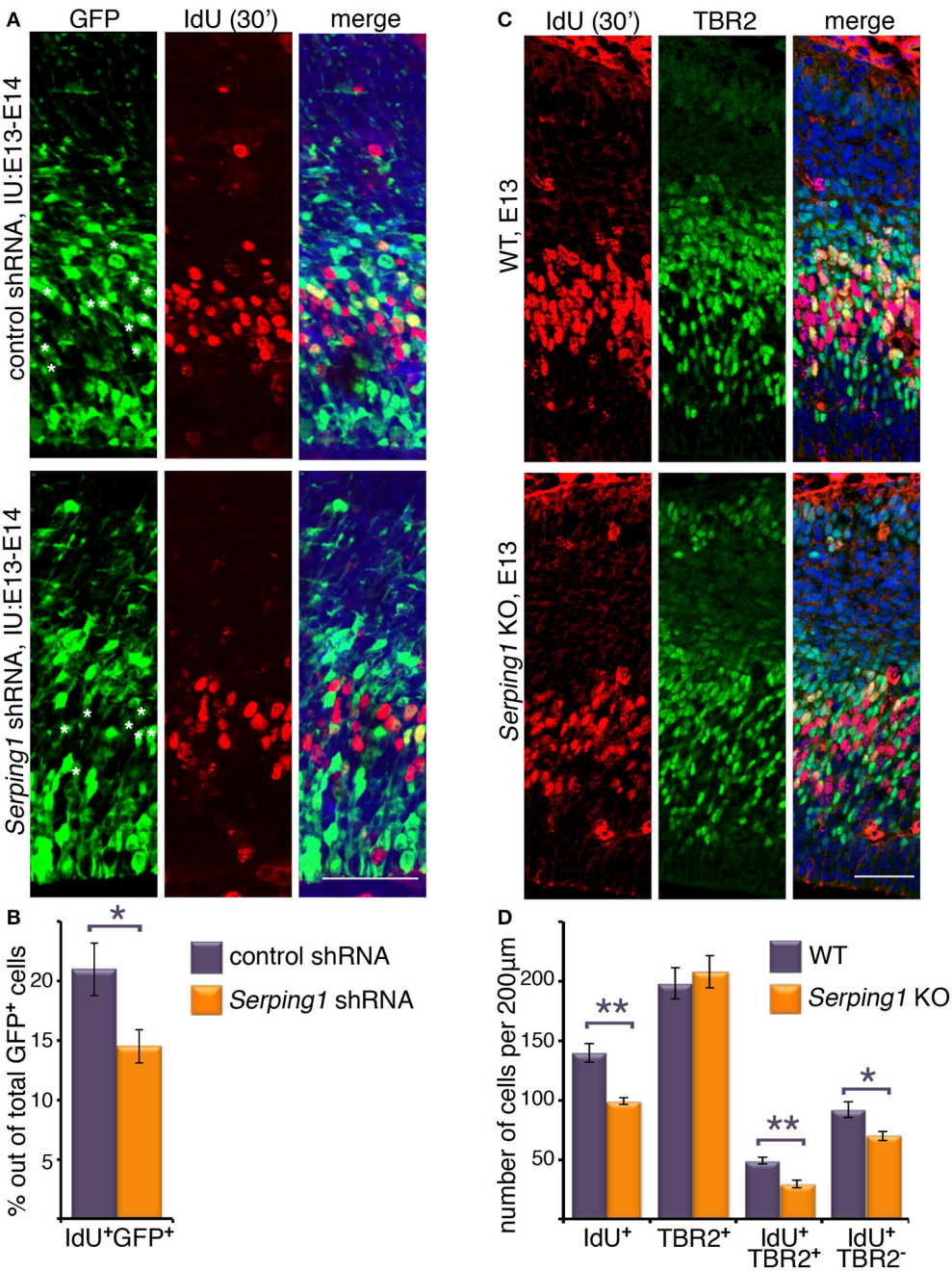

FIGURE 1 | *Serping1* affects neuronal stem cell proliferation. **(A,B)** Embryonic brains were *in utero* electroporated with control shRNA or *Serping1* shRNA at E13 and at E14 were treated with IdU for 30 min. The brains were cryosectioned and immunostained with anti-IdU antibodies. GFP labeled the electroporated cells. IMARIS software was used to count the total GFP-positive cells and the double GFP- and IdU-positive cells within slices of the same size (230 µm in length). Double-positive cells are marked with white asterisks in the GFP panel. The relative proportion of double-positive cells to the total number of GFP-positive cells was calculated (**B**, *Student t*-test, $n = 5$, $^{*}p < 0.05$). **(C,D)** Brains of E13 *Serping1* KO and littermate WT were treated with IdU for 30 min. The brains were cryosectioned and immunostained with anti-IdU and anti-TBR2 antibodies. The number of IdU-positive, TBR2-positive, double positive, IdU-positive TBR2-negative cells was counted **(D)** in identical areas of the cortices (200 µm in length). *Welch's t*-test, $n = 6$, $^{*}p < 0.05$, $^{**}p < 0.01$. The scale bars are 50 µm.

embryos in which *Serping1* was knocked out were generated. Brain sections were immunostained for IdU and also for TBR2, a basal progenitors marker, using the respective antibodies (**Figure 1C**). Similar to the trend observed in case of *Serping1* knockdown, a significant reduction in the number of IdU positive cells was noted (*Student's t-test, Welch-corrected* 140 ± 8 vs. 99 ± 2.7, $n = 6$, $p = 0.0028$, control and *Serping1* KO, respectively, **Figures 1C,D**). Whereas, the total number of TBR2 positive cells did not differ between the wild-type and the knockout, there was a clear difference in the number of IdU/TBR2 positive cells, where less cells were double labeled in the KO (*Student's t-test,* 49 ± 3.13 vs. 29 ± 2.9, $n = 5,6$, respectively, $p = 0.0012$, **Figures 1C,D**), thus suggesting that in the *Serping1* KO there is a reduction of intermediate progenitors at E14. In addition, the number of IdU positive/TBR2 negative cells was also decreased in the *Serping1* KO (*Student's t-test,* 92.2 ± 6.8, $n = 5$ vs. 69.83 ± 3.85, $n = 6$, $p = 0.0154$, **Figures 1C,D**). To check whether the observed differences resulted from alterations in S phase duration, double labeling using two thymidine analogs was performed. Embryos were *in utero* electroporated at E13 with either control shRNA or *Serping1* shRNA. On E14 the cells were labeled with EdU for the duration of 2.5 h and then with IdU for 0.5 h (Supplementary Figure 3). No significant differences in the proportion of EdU/GFP double positive cells (14.1 ± 0.5% in *Serping1* shRNA vs. 16.5 ± 1.6% in control, $n = 7$, Sidak's multiple comparison test) or IdU/EdU/GFP triple positive cells (7.8 ± 0.8 vs. 10.6 ± 0.6%, $n = 7$) thus suggesting that the cell cycle length was not affected. The proportion of IdU/GFP double positive cells was reduced in *Serping1* shRNA consistent with previous experiments (17.4 ± 1.2% vs. 23.5 ± 0.9, $n = 7$). In addition significantly more GFP only positive cells were noted in case of *Serping1* shRNA treatment, suggesting that these cells were not actively in S-phase during the tested period (76.3 ± 1.1 vs. 70.6 ± 1.5%, $n = 7$). Collectively, our results suggest that knockdown or knockout of *Serping1* results in a reduction in the number of cycling cells of both ventricular zone (radial) and intermediate (basal) progenitors during cortical development.

Serping1 Affects Radial Migration in a Cell Autonomous and Non-cell Autonomous Way

The possible role of *Serping1* in regulation of radial migration was investigated by knockdown of the gene using *in utero* electroporation of *Serping1* shRNA and by studying knockout embryos generated by CRISPR/Cas9 gene editing. *Serping1* shRNA significantly impaired radial neuronal migration (compare control in **Figure 2A** to **Figure 2B**), and this phenotype was partially rescued following the addition of *Serping1* shRNA-resistant form (*Serping1*^{res}) (**Figure 2C**). The position of the GFP positive cells was quantified in five bins across the width of the cortex. A two-way ANOVA demonstrated that the number of cells in the different bins differed between the control and *Serping1* shRNA in four out of five bins (**Figure 2D**). Addition of *Serping1*^{res} restored the level of SERPING1 protein to control levels (data not shown) and significantly improved the position of the cells in three out of four bins (**Figure 2D**). Neuronal migration impairment was also detected in *Serping1* knockout embryos in comparison with wild type litter-mates (**Figures 2E,F** quantified in **Figure 2G**). Neurons were birth-dated with a uridine analog at E14.5 and their relative position in the cortex was scored at E18. The distribution of neurons along the width of the cortex significantly differed in three out of five bins (**Figure 2G**). Next, the identity of the stalled cells at E18 was examined (**Figures 2H–L**). Although most of the *Serping1* shRNA treated cells have not reached the cortical plate (compare the GFP+ cells in **Figure 2I** vs. **Figure 2H**), the majority express the superficial layer marker CUX1 and not the deep layer marker TBR1 (**Figures 2J–L**). In the postnatal brain (at P8), *Serping1* shRNA treated cells did reach the cortical plate, nevertheless, even in low magnifications, it is possible to observe that their morphology differs from that observed in the control (**Figures 2M,N**).

Next, the possibility that *Serping1* may affect neuronal migration in a non-cell autonomous way in addition to the cell autonomous effect observed above was examined (**Figure 3**). The experimental design included labeling and monitoring two distinct populations in the developing embryonic brain by consecutive electroporation. The first population was treated with shRNA (at day E13) and labeled with GFP. The position of the first population reflected cell autonomous effects. The second cell population was electroporated with a red fluorescent protein only a day later (E14) and thus its behavior is presumed to reflect non-cell autonomous effects emanating from the first (green) population. We concluded that the effect of *Serping1* knockdown was both cell autonomous and non-cell autonomous; it affected the genetically modified cells as well as the neighboring cells. Although in the control, later born cells (red) successfully migrated through the layer of previously born cells (green) treated with control shRNA (**Figures 3A–C**, quantification in **Figures 3A',B'**), the migration of the red cell population through the green cell layer, which was treated with *Serping1* shRNA, was markedly impaired (**Figures 3D–F**,**D,E'**, compare **Figure 3B** and **Figure 3B'** to **Figure 3E** and **Figure 3E'**, the correlation of the relative position of the red cells in B and E is -0.03). When the order was reversed, the later born *Serping1* knockdown cells did not impair the motility of earlier born control green (**Figures 3G–I**,**G', H'** the correlation of the relative position of the red cells in B and green cells in G is 0.92) or red positive cells (**Figures 3J–L**,**J',K'**, the correlation of the relative position of the red cells in **Figure 3B** and red cells in **Figure 3J** is 0.76). The observed non-cell autonomous effect was not due to residual, stable *Serping1* shRNA in the cortex. *Serping1* shRNA and GFP plasmids were injected into the cortex at E13 but not electroporated, a day later, a red fluorescent plasmid was injected and electroporated. No GFP positive cells were noticed at E18 and no neuronal migration impairment was noted (**Figures 3M–O**,**M',N'**). A non-cell autonomous effect was also observed using a different approach. The cells neighboring *in utero* E13 electroporated cells were labeled at E14 by a uridine analog, and their position in the cortex was analyzed at E18. The relative distribution of the IdU labeled cells in the *in utero* electroporated side of the

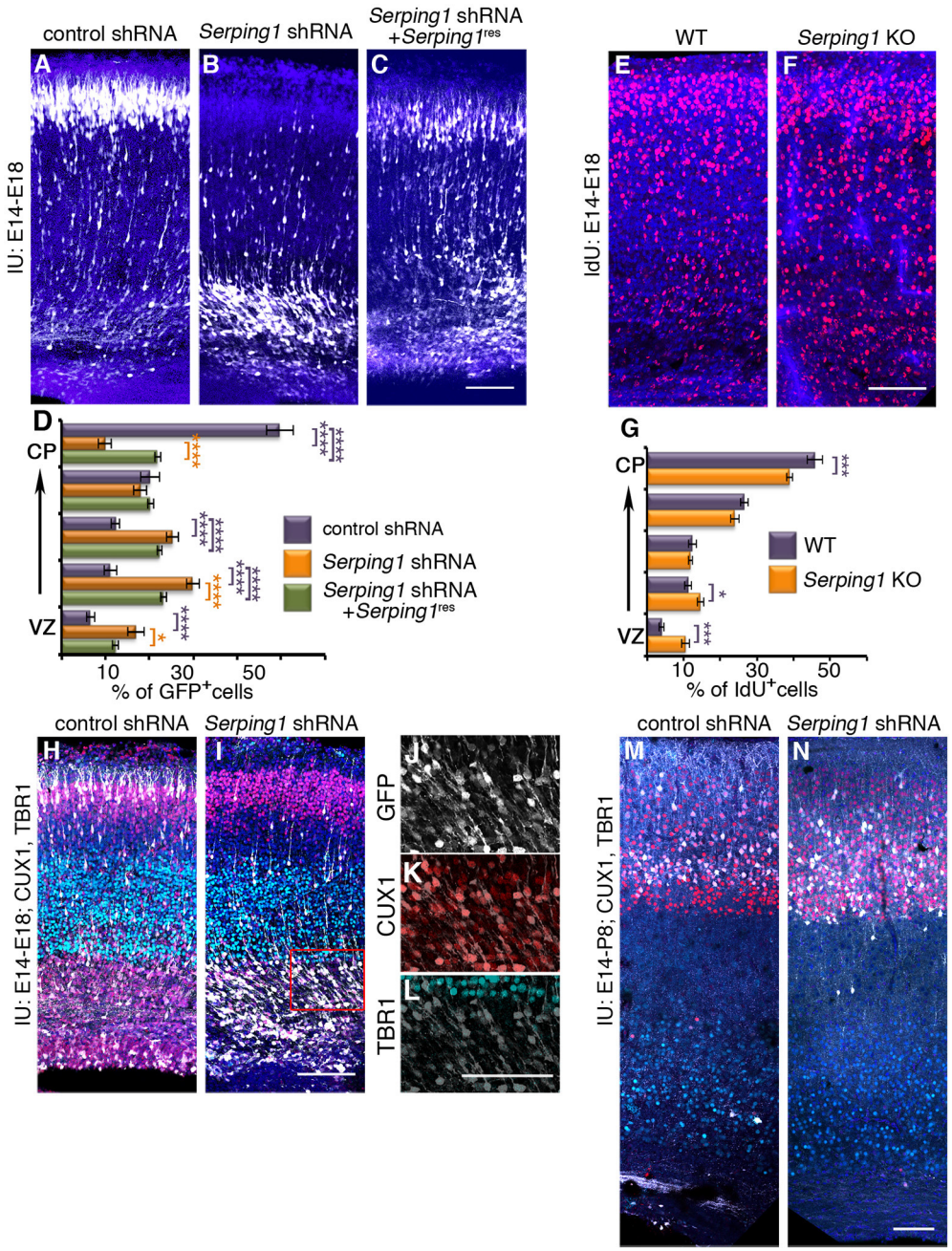

FIGURE 2 | *Serping1* affects neuronal migration. **(A–D)** *Serping1* knockdown affects neuronal migration. Brains were electroporated *in utero* (E14-E18) with control shRNA **(A)**, *Serping1* shRNA alone **(B)** or in combination with *Serping1* resistant to the shRNA **(C)**. **(D)** The position of GFP+ neurons across the width of the cortex was analyzed and is shown in 5 bins (from the VZ to the CP). The statistical significance of comparison to control is shown in violet. The statistical significance of comparison to *Serping1* shRNA is shown in orange. Two-way ANOVA, $n = 11$, $^{*}p < 0.05$, $^{****}p < 0.0001$. **(E–G)** *Serping1* KO affects neuronal migration. *Serping1* KO embryos **(F)** and littermate controls **(E)** were labeled with IdU on E13 and the position of IdU-positive neurons was analyzed on E18 and is shown **(G)** in 5 bins (from the VZ to the CP). Two-way ANOVA, $n = 12$, $^{*}p < 0.05$, $^{***}p < 0.001$. **(H–L)** The identity of electroporated cells. Slices of control shRNA and *Serping1* shRNA were immunostained with anti-CUX1 (red) and anti-TBR1 (light green) antibodies. *Serping1* shRNA arrested cells are shown in higher magnification **(J–L)**. **(M–N)** Postnatal positioning and the identity of control and *Serping1* knockdown cells. Brains electroporated *in utero* on E14 with control shRNA **(M)** or *Serping1* shRNA **(N)** were immunostained at postnatal day 8 (P8) with anti-CUX1 (red) or anti-TBR1 (light-green) antibodies. The scale bars are 100 μm.

brain differed significantly from the relative distribution of IdU labeled cells on the non-*in utero* electroporated side of the brain (Supplementary Figure 4A–B', three out of five bins showed significant differences Supplementary Figure 4C). Taken together, our data suggest that SERPING1 participates in regulation of radial neuronal migration in

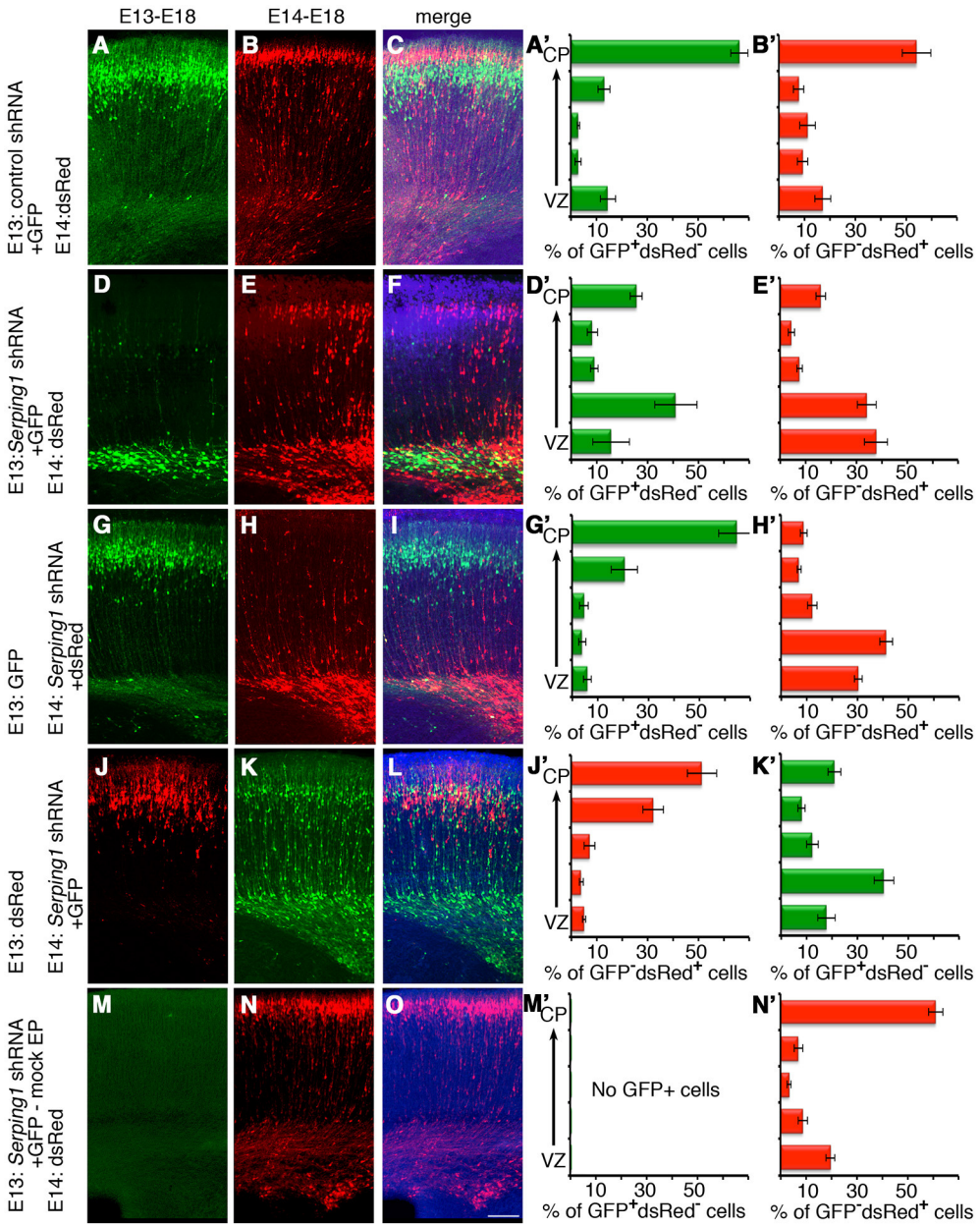

FIGURE 3 | Non-cell autonomous effects of *Serping1* shRNA. **(A–F)** *Serping1* shRNA exhibits non-cell autonomous effects. Brains were *in utero* electroporated with control shRNA **(A–C)** or *Serping1* shRNA **(D–F)** together with GFP on E13, followed by electroporation with dsRed on E14. The analysis was performed on E18. GFP-positive neurons **(A,D)**, dsRed-positive neurons **(B,E)**, and merged images **(C,F)** are shown. The position of GFP-positive dsRed-negative **(A',D')** and dsRed-positive GFP-negative **(B',E')** cells was analyzed. The distribution of the dsRed-positive GFP-negative cells **(E,E')** demonstrates non-cell autonomous effect of *Serping1* shRNA (compare to **B,B'**). $n = 6$. **(G–O)** Controls of non-cell autonomous experiment. **(G–L)** The population of the neurons can be easily segregated as demonstrated by the inverse order of electroporation. Brains were electroporated with GFP on E13 and with *Serping1* shRNA with dsRed on E14 **(G–I)**, or vice versa brains were electroporated with dsRed on E13 and with *Serping1* shRNA with GFP on E14 **(J–L)**. Cells treated with shRNA demonstrated impaired migration **(H',K')**. In both conditions cells without shRNA had no defect in migration (**G,G'**,**J,J'**). **(M–O)** Control experiment demonstrates that there is no left-over of the plasmids in between electroporations. *Serping1* shRNA together with GFP were injected but not electroporated into the ventricle on E13. dsRed was electroporated on E14. On E18 there are no GFP-positive cells **(M,M')**. The migration of dsRed-positive cells was not affected **(N,N')**. The scale bar is 100 μm.

a cell autonomous as well as in a non-cell autonomous fashion.

Closer inspection of the stalled cells revealed that they exhibit long processes (**Figures 4A,B**). In addition, it appeared that wild-type cells that were in close vicinity to the *Serping1* shRNA treated cells also exhibited very long processes (**Figure 4C**). The length of the leading edge of individual cells was quantified and the leading-edge length of either *Serping1* shRNA treated cells or of their red neighbors significantly differed from the values of the controls (**Figure 4D**). Therefore, western

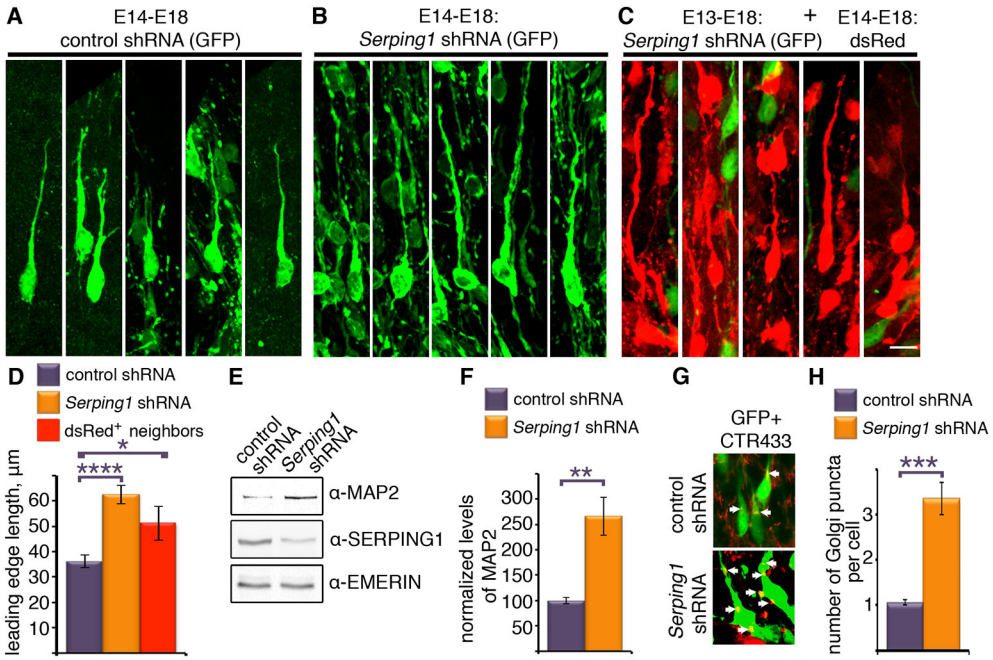

FIGURE 4 | *Serping1* influences neuronal morphology in a cell-autonomous and non-cell autonomous way. **(A–D)**. Brains were *in utero* electroporated with control shRNA **(A)** or *Serping1* shRNA **(B)** together with GFP (E14-E18). Representatives of individual cells from the IZ are shown **(C)**. Brains were *in utero* electroporated with *Serping1* shRNA on E13 and with dsRed on E14. DsRed positive cells arrested in IZ (E18) are shown. The length of the leading edge was measured on high-magnification 3D reconstruction images with ImageJ software. The lengths of the leading edges were compared between the conditions **(D)**. One-way ANOVA, Turkey HSD, $n = 16$, $^{*}p < 0.05$, $^{****}p < 0.0001$. The scale bar is 10 µm. **(E,F)** Brains were *in utero* electroporated with control shRNA or *Serping1* shRNA together with GFP (E14-E17). The electroporated areas were dissected under fluorescent binocular. The dissected areas were lysed and western blotted using anti-MAP2, anti-SERPING1 and anti-EMERIN antibodies. The levels of MAP2 were normalized to EMERIN. Levels of MAP2 relative to control (in %) are presented **(F)**. $n = 3$, *Student t*-test, $^{**}p < 0.01$ **(G–H)**. Golgi analysis in *Serping1* knockdown compared to control. Control shRNA or *Serping1* shRNA electroporated brain sections (E14-E18) were immunostained with Golgi marker antibodies (CTR433). Immunostaining of the Golgi are presented together with GFP. White arrows show position of Golgi. The scale bar is 10 µm. Quantification of the number of Golgi clusters per cell ($n = 20$, *Student t*-test) are shown **(H)** $^{***}p < 0.001$.

blot analyses were conducted using several antibodies. Most strikingly, the levels of MAP2 increased more than 2.5-fold in *Serping1* shRNA brain lysates (**Figures 4E,F**). No differences were noted for phospho-DCX and phospho-ERK antibodies. MAP2 (microtubule-associated protein 2) is a prominent microtubule associated protein expressed in the developing brain (Dinsmore and Solomon, 1991). The increased levels of MAP2 are consistent with the observed morphological changes. Although the elongated *Serping1* shRNA treated cells appeared to be bipolar, immunostaining with a Golgi marker that appears as a packed cluster at the basal side of nucleus in the migrating bipolar control cells, revealed that the cells have not completed polarization. On average more than three Golgi clusters were noted in the treated cells instead of one observed in control cells (**Figures 4G,H**).

Serping1 Is Part of the Complement Pathway

Finally, we evaluated whether the developmental effects of *Serping1*, were due to its role within the complement pathway. *Serping1*, or C1 inhibitor, participates in the three activation arms of the complement system. It covalently binds and inhibits the activity of the C1r and C1s serine proteases that are involved in initiation of the classical pathway (hence the origin of the name C1 inhibitor). However, it also covalently binds and inhibits the activity of the closely related MASP1 and MASP2 proteases, which initiate the lectin pathway. It can also physically bind and functionally affect the interaction between complement factor C3b and complement factor B, and thus to interfere also with the alternative pathway(see schematic presentation in **Figure 5**). Therefore, *Serping1* or C1 inhibitor inhibits all the activation arms of complement. Complement activation will lead to an increase in the levels of cleaved C3, which can be detected by anti-C3b antibodies. Brain lysates from *Serping1* shRNA treated and control treated were therefore analyzed by western blot using anti-C3b antibodies (**Figure 6A**). Contrary to our expectations, a small yet significant reduction in the levels of C3b were noted (**Figure 6B**). It was postulated that pathway activation may result in rescue of neuronal migration impairment and we next queried the effect of C3 mimicry cleavage products (scheme in **Figure 6C**) and either the single C3a receptor (C3aR), or the dual C3aR/C5a receptor (C5aR) agonists in combination with *Serping1* shRNA. As previously observed, *Serping1* shRNA impairs neuronal migration (**Figures 6D,D'**). When the C3a mimicry product was expressed *in utero* together with *Serping1* shRNA no effect was observed (**Figures 6E-E'**).

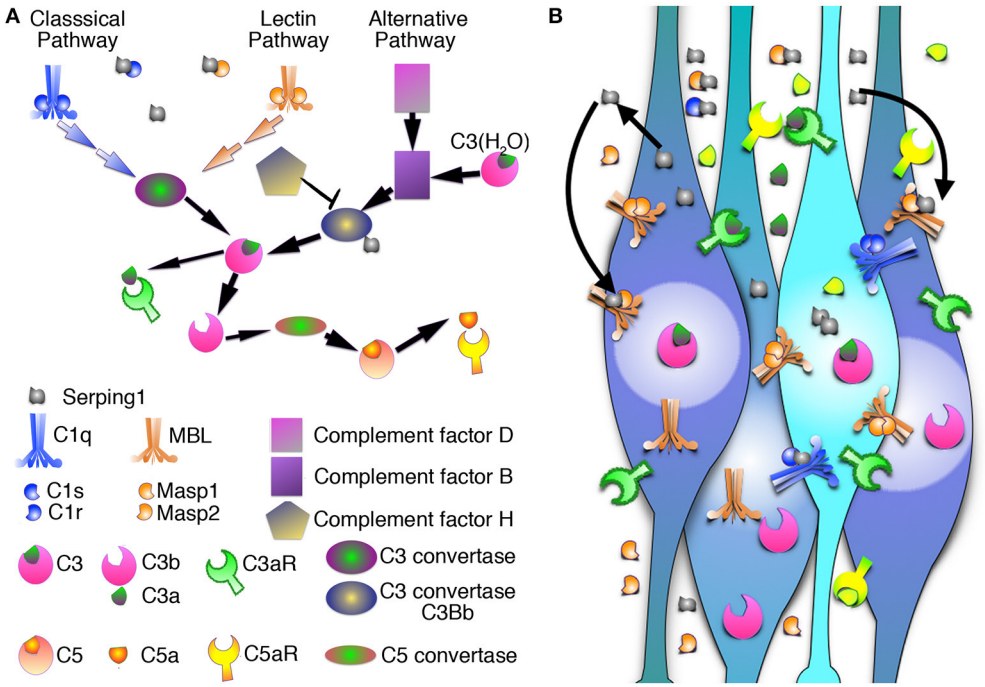

FIGURE 5 | Schematic representation of the complement pathway. **(A)** Three parallel arms of the complement pathway: the classical pathway, the lectin pathway, and the alternative pathway converge on the level of the C3 that is cleaved by C3 convertase (C4bC2a in the classical and lectin pathway, or C3-H2OBb in the alternative pathway) into C3a anaphylotoxin and C3b. C3aR binds C3a. C3b is recruited to form C5 convertase, which processes inactive C5 into C5a anaphylotoxin and C5b. C5aR binds C5a. All three pathways are regulated by Serping1 or C1 inhibitor. **(B)** Schematic representation of Serping1 cell-autonomous and non-cell autonomous roles in migrating neurons. Serping1 is expressed and secreted by neurons and inhibits complement pathway by direct interaction with C1s, C1r, Masp1, and Masp2. Serping1 functions in the extracellular matrix and influences both the neuron it was secreted from and neighboring neurons.

The effect of the addition of the downstream C3aR agonist corroborated this finding, which minimally affected the proper position of migrating neurons (**Figures 6F,F'**). Addition of the C3 mimicry cleavage products C3b alpha or less effectively C3b beta, significantly improved neuronal migration (**Figures 6G–H'**), suggesting that activation of C3 cleavage is required for proper neuronal migration. Furthermore, the addition of the dual C3aR/C5aR agonist completely restored neuronal positioning to control levels (**Figures 6I–I'**), supporting that downstream complement activation at the level of C5a is required for proper migration of pyramidal neurons to the cortical plate.

DISCUSSION

The Role of *Serping1* in the Developing Cortex

Collectively our findings suggest that *Serping1* (C1 inhibitor) is important for cortical development at several stages. At early stages of cortical development *Serping1* is important for the proliferation of neuronal stem cells. A decrease was noted in the number of cells in S phase that include both radial glia and intermediate progenitors. The effect may be transient since the total number of TBR2 positive basal progenitors, cells was not affected. *Serping1* has been reported to be expressed in the SVZ basal progenitors (Kawaguchi et al., 2008), yet our study is the first demonstrating a direct role for this gene product in neuronal stem cell proliferation. Our previous studies showed that knockdown or knockout of other components of the complement pathway affects neuronal stem cell proliferation in different ways. Knockout of C3 increased the number of mitotic intermediate progenitors (phospho-Histone positive), whereas knockdown of *Masp1* did not affect the number of progenitors in S phase (IdU positive) and knockdown of *Masp2* resulted in a statistically significant increase in the number labeled progenitors (IdU positive) (Gorelik et al., 2017). These highly variable outcomes may suggest that within neuronal stem cell progenitors there is not a linear relationship between changes in the components of the complement pathway and neuronal stem cell proliferation. Alternatively, it is possible that the spatiotemporal expression pattern in different subsets of neuronal progenitors dictates the outcome of pathway modulation. Following exit from the cell cycle, cortical neurons migrate along the processes of the radial glia to reach the cortical plate. Knockdown or knockout of *Serping1* impairs radial migration. The delay in reaching the cortical plate did not affect cell identity, and the stalled cells express CUX1 similar to the control cells. Migration delay is transient and in the postnatal brain, the cells eventually reach the cortical plate. Interestingly, *Serping1* knockdown affected not only the manipulated cells but also their neighbors; thus it is working both in a cell autonomous and a non-cell autonomous

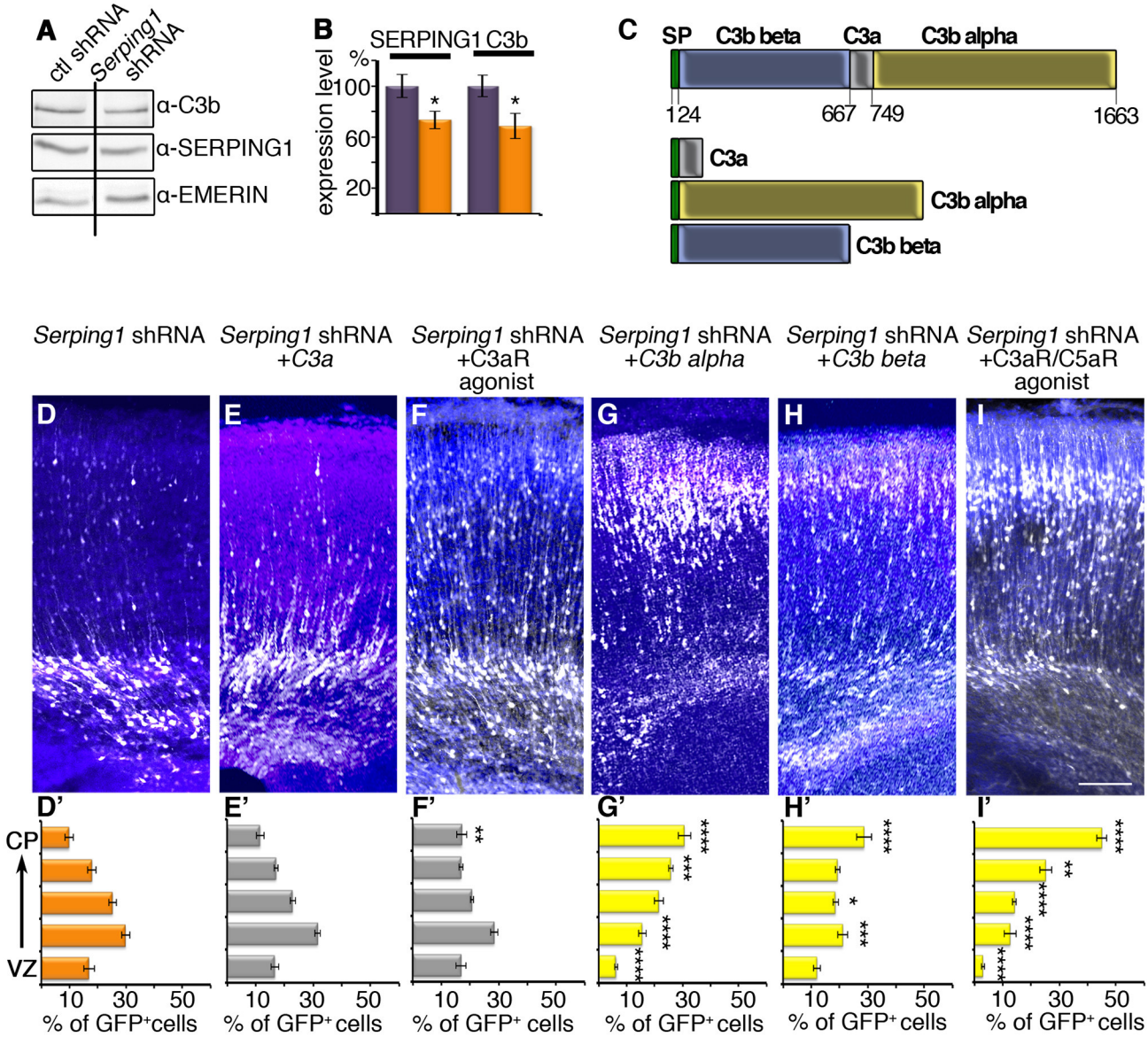

FIGURE 6 | *Serping1* in the complement pathway. **(A,B)** Levels of activated C3 (C3b) are slightly reduced in the *Serping1* shRNA compared to control. Areas from the brains electroporated *in utero* on E14 with control or *Serping1* shRNA were dissected on E17 and subjected to western blot analysis with anti-C3b antibodies, anti-SERPING1 and anti-EMERIN antibodies. The levels of SERPING1 and C3b were normalized to EMERIN and quantified ($n = 9$). *$p < 0.05$. **(C)** Schematic representation of C3. The proteolytic cleavage of C3 on aa 667 and aa 749 results in C3a peptide and C3b, composed of two subunits: C3b beta and C3b alpha. Three fragments mimicking the cleavage products of C3, all with an N-terminal signal peptide (SP, green). **(D–I)** Rescue of *Serping1* shRNA migration phenotype with C3 fragments and peptides, agonists of Complement receptors. Brains were electroporated (E14-E18) with *Serping1* shRNA alone **(D)** or together with either *C3a* **(E)**, C3aR agonist **(F)**, *C3b alpha* **(G)**, *C3b beta* **(H)**, or dual C3aR/C5aR agonist **(I)**. The scale bar is 100 μm. The distribution of neurons along the cortex in 5 bins is shown **(D'–I')**. All conditions were compared to *Serping1* shRNA. Two-way ANOVA, $n = 11$, *$p < 0.05$, **$p < 0.01$, ***$p < 0.001$, ****$p < 0.0001$.

way. The cell autonomous and non-cell autonomous effect was noticed not only on the position of the cells in the developing cerebral cortex, but was also seen in the cellular morphology of the neighboring cells. *Serping1* knockdown cells exhibited long leading processes, which were also observed in near neighbors. These extended processes may be due to elevated levels of the microtubule-associated protein MAP2, which was detected by western blot analysis of brain lysates. The non-cell autonomous effects may be of particular interest when considering the possibilities of somatic mutations in the developing brain. The notion that somatic mutations play an important role in human disease has been widely accepted in case of cancer, in which even genetic mutations usually require a second somatic hit to initiate the development of tumors (Hanahan and Weinberg, 2000). Furthermore, conceptual progress in the last decade allows us to assimilate that participation in disease progression

is not restricted to the very cells that are mutated, but also to the adjacent "healthy" tissue which changes its properties as a consequence of the presence of the mutated cells (review Hanahan and Weinberg, 2011). Emerging evidence suggest that somatic mutations may also participate in brain diseases (review Gleeson et al., 2000). Perhaps one of best-known examples is *DCX,* an X-linked gene (des Portes et al., 1998; Gleeson et al., 1998), in which mutations result in lissencephaly in males and a "doublecortex" phenotype in females due to random X-inactivation. On the other hand, somatic mutations in the same gene in males result in the "doublecortex" phenotype (Gleeson et al., 2000). *Serping1* non-cell autonomous effects then adds on to another gene characterized from the same screen *Atx*, which also exhibited non-cell autonomous effects (Greenman et al., 2015).

The Role of Serping1 in Migrating Neurons in Relation to the Complement Pathway

Our unbiased screen for molecules, which participate in non-cell autonomous regulation of neuronal migration revealed Serping1 as a molecule, which is differentially expressed and allowed us to uncover an unexpected role of the innate immune complement pathway in the regulation of neuronal migration (Gorelik et al., 2017). There may be several possible reasons as for why this pathway has been recruited to function in a non-cell autonomous fashion in the developing brain. The pathway consists of a cascade of proteases, coupled with many inherent regulatory steps. Many of the pathway components are secreted or bound to the cell surface, ideal for cell-cell communication (reviews Walport, 2001; Fujita, 2002; Rutkowski et al., 2010; Stephan et al., 2012). As opposed to cell destruction induced by the complement pathway in response to pathogens (Fujita, 2002), this pathway has a vital role in migrating neurons. Based on our data, we suggest that activation of the pathway may result in reshaping of cells, possibly via partial opsonization, or tagging of multipolar neurites, enabling the polarity transition of neurons toward successful migration along radial glia. Our experimental results also indicate that the developing brain uses components of the complement in a non-orthodox way, as knockdown of Serping1 did not trigger activation of the pathway. However, the C3a peptide, or a C3a receptor agonist did not rescue neuronal positioning following Serping1 shRNA mediated knockdown. These results are different from those obtained following knockdown of *Masp2, C3,* or in *C3* KO mice, where either the single or the dual agonists rescued migration (Gorelik et al., 2017). C3a has been demonstrated to act as a chemo-attractant during collective cell migration of neural crest cells (Carmona-Fontaine et al., 2011) and enteric neural crest cells (Broders-Bondon et al., 2016). In case of in *Serping1* shRNA treatments, fragments mimicking C3 cleavage (C3b beta and alpha) rescued the migration impairment neurons. Moreover, our data indicate that signaling is likely to be also transmitted through the complement C5a receptors, which when activated, completely rescued neuronal migration deficits observed in the case of *Serping1* knockdown. It should be noted that this study could not distinguish between a role for C5a receptor 1 or C5a receptor 2 (C5L2). However, it has been previously demonstrated that perturbations in C5a receptor 1 signaling during rodent brain development can result in select neuronal defects (Benard et al., 2008; Denny et al., 2013; Coulthard et al., 2017), possibly indicating a predominant role for this receptor subtype in embryonic development (Hawksworth et al., 2014). Regardless, our study adds to the evidence for widespread roles for complement fragments C3a and C5a in development (Hawksworth et al., 2016).

The complement system is indeed a complex pathway with three "linear" arms that converge but also interconnect at several point. We therefore cannot be confident about the exact regulatory mechanism and possible positive and negative feedback loops in which *Serping1* relates to the pathway in the context of progenitor proliferation and neuronal migration. In many respects, this process exhibits analogies to the previously described role of the complement pathway in successful elimination of excess numbers of synapses, which is developmentally regulated (Stevens et al., 2007; Schafer et al., 2012). Other components of the immune system, such as the major histocompatibility complex (MHC) and many others, have been shown to play a role in the developing brain (reviews Boulanger and Shatz, 2004; Boulanger, 2009). Furthermore, the uniqueness and unexpected results following Serping1 knockdown may be due to additional activities of this potent molecule beside the complement system (Davis et al., 2008), which should be investigated in the future.

METHODS AND MATERIALS

Plasmids and Primers

The following shRNA constructs were cloned into pSuper vector (Brummelkamp et al., 2002): *Dcx* shRNA1 (5′- GCTCAAGTG ACCACCAAGGCTAT) (Bai et al., 2003); *Dclk* shRNA1 (5′- GGT TCGATTCTAC AGAAAT) (Koizumi et al., 2006). The following shRNA was purchased from OpenBiosystems (ThermoScientific) in pLKO.1 vector: *Serping1* shRNA (5′- CCTGACGATGCCTCA TATAA). The control shRNA plasmid used is pLKO.1-TRC control (Addgene) containing non-hairpin 18 bp sequence (5′- CCGCAGGTATGCAACGCG).

A plasmid containing the complete coding sequences of *Serping1* (BC002026.1) was purchased from OpenBiosystems (ThermoScientific) and subcloned into pCAGGS plasmid. This plasmid was used as a basis for creating shRNA resistant plasmids. 4 mismatches with the shRNA sequence were inserted in the original sequences by PCR using the following primer: 5′- AAGCTCGAGCTGTCCAAATTCCTG CCCACTTACCTACCA TGCCACACATAAAGT (*Serping1*).

A plasmid containing the complete coding sequences of *C3* (BC043338.1) was purchased from OpenBiosystems (ThermoScientific). C3a was subcloned from the C3 plasmid with following primers: 5′- ATATGGCTAGCTCAGTACAGT TGATGGAAA and 5′- ATAGCGGCCGCTCACCTGGCCAGG CCCAGCACG. C3b beta was subcloned from the C3 plasmid with following primers: 5′- ATATGGCTAGCATCCCCATGT ATTCCATCATT and 5′- ATAGCGGCCGCTCAGGCTGCT GGCTTGGTGCACTC. *C3b alpha* was subcloned from the *C3*

plasmid with following primers: 5′- ATATGGCTAGCATCC CCATGTATTCCATCATT and 5′- ATAGCGG CCGCTCAGT TGGGACAACCATAAAC. The C3 fragments were subcloned into the pCAGGS plasmid that contained C3 signal peptide (5′- ATGGGGGACCAGCTTCAGGGTCCCAGCTACTAGTGC TACTGCTGCTGTTGGCCAGCTCCCCATTAGCTCTGGGG).

For Real-Time PCR of *Serping1* the following primers were used: 5′- GCCCAATTCGATGACCATAC and 5′- AAGTTG GTGCTTTGGGAACA; 5′- GCCCAATTCGATGACCATAC and 5'-AGTGGGGTTGAGAGCCTTTT; 5′ –TTCCCTGAA AGAGATGACTCCTGGA and 5′- CGTTGGCTACTTTAC CCATGGTGTC; 5′- TGGAGTCCCCCAGAGCCTACA and 5′- GAGGAGGCTGGCAATGCTGA. *29rps* primers were used as a reference: 5′- GTATTTGCGGATCAGACCGT and 5′- CTG AAGGCAAGATGGGTCA.

For PCR of *Serping1* cDNA the following primers were used: 5′- AGAGAGCTTCCCTGAAAGAGATG and 5'- TGA GGAGGCTGGCAATGCTGA.

Antibodies

Rabbit anti SERPING1/C1INH (Santa Cruz, H-300, 1:250), rabbit anti EMERIN (Santa Cruz, FL-254, 1:1,000), mouse anti-MAP2 (Sigma-Aldrich, HM-2, 1:500), rat anti C3b antibodies (Hycult Biotech, 1:500, HM1065) were used for western blotting.

The following antibodies were used for immunostainings: chicken anti TBR2 (Millipore, 1:100, AB15894), rabbit anti CUX1 (anti CDP, Santa Cruz, 1:100, SC-13024), chicken anti TBR1 (Millipore, 1:100, AB2261), mouse anti IdU-B44 (BD Biosciences, 1:200, 347580), chicken anti GFP (Abcam, 1:1000). Mouse CTR433 antibodies (1:50, Jasmin et al., 1989), a Golgi marker, was kindly provided by Dr. Michel Bornens (Institute Curie, Paris, France).

Complement Agonist Peptides

The selective C3aR agonist, WWGKKYRASKLGLAR ("super-agonist" Wu et al., 2013), and a C5aR agonist, YSFKPMPLaR ("EP54" Woodruff et al., 2001) were synthesized as previously described (Woodruff et al., 2001; Wu et al., 2013). It should be noted that the C5aR agonist also activates C3aR (Scully et al., 2010) and thus is described herein as a dual C3aR/C5aR agonist. The agonists (1 μg/mg) were injected to the ventricles of the embryos together with the indicated plasmids.

Animals

Animal protocols were approved by the Weizmann Institute IACUC and were carried out in accordance with their approved guidelines. ICR mice were purchased from Harlan laboratories. Male and female embryos were used in the study.

CRISPR/Cas9 Knockout Generation

Cas9 plasmid and plasmids encoding guide RNAs were purchased from the University of Utah Mutation Generation lab. The following oligonucleotides were used for construction of gRNA vectors:

1. Serping1: 5′ ACACCGGCTACACTGGTTGTTGGCCG and 5′ AAAACGGCCAACAACCAGTGTAGCCG (location 2:24847967-24847990: + strand);

In vitro transcribed Cas9 RNA(100 ng/ul), and sg RNA(50 ng/ul), were injected into one cell fertilized embryos isolated from superovulated CB6F1 hybrid mice mated with CB6F1 males Harlan Biotech Israel Ltd. (Rehovot, Israel). Injected embryos were transferred into the oviducts of pseudopregnant ICR females as previously described (Wang et al., 2013). For migration analysis the pregnant mice were subjected to IdU injection at E14.5 and sacrificed at E18. Genomic DNA from the treated embryos was analyzed for mutations in the mutated genes using High Resolution Melt (HRM) analysis and confirmed by Sanger sequencing. For the proliferation analysis the mice from established mouse line were used. The genotype verification was performed with the following primers: 5′- TTCCCTGAAAGA GATGACTCCTGGA and 5′- CGTTGGCTACTTTACCCATGG TGTC.

IdU Injection

The thymidine analog iododeoxyuridine (IdU) was injected intraperitoneally (0.01 ml of 5 mg/ml IdU solution per gram body weight) into pregnant mice at the indicated time points.

EdU Labeling and Click Chemistry

For labeling cells in S phase, pregnant mice (E14) were injected with (50 mg/gr body weight) 5-ethynyl-2′-deoxyuridine (EdU) solution and were scarified 30 min post-injection. The brains were removed and fixed in 2.5% PFA-PBS overnight, washed and cryoporotected by immersion in 30% sucrose-PBS solution. The cryosections (10 μm) were pretreated in boiling sodium citrate buffer (10 mM, pH 6) for 30 min. The click reaction was performed with Cy3 azide (2.5 μM) in the PBS-based buffer containing 100 mM Tris-HCl, 1 mM $CuSO_4$, and 100 mM ascorbic acid. This reaction was followed by a click reaction with a non-fluorescent molecule (Phenylthiomethyl-Azide 20 mM, SIGMA). After treatment with 10 mM ascorbic acid and 4 mM $CuSO_4$, followed by incubation with 20 mM EDTA, the relevant immunostainings were performed.

In utero Electroporation

Plasmids were transfected by *in utero* electroporation using previously described methods (Saito and Nakatsuji, 2001; Tabata and Nakajima, 2001). Prior to surgery the animals were injected with buprenorphine (2 mg/Kg BW, subcutaneously). Pregnant ICR mice at E14.5 days post-gestation (E14), were anesthetized by injection of ketamine 10%/xylazine 20 mg/ml (1/10 mixture, 0.01 μl per g of body weight, intraperitoneally), alternatively Isofluran anesthesia was used. The uterine horns were exposed, and plasmid mixed with Fast Green (2 μg/μl, Sigma) were microinjected through the uterus into the lateral ventricles of embryos by pulled glass capillaries (Sutter Instrument, Novato, CA). The concentration of plasmids was 0.5 μg/μl for pCAGGS-GFP, 2 μg/μl for shRNA construct and 1–1.5 μg for overexpression plasmids. Electroporation was accomplished by discharging five 41 mV 50 ms long pulses with 950 ms intervals, generated by a NepaGene electroporator. The pulses were delivered using 10 mm diameter platinum plated tweezers electrodes (Protech international Inc., San Antonio, TX) placed at either side or the head of each through the uterus. Animals

were sacrificed 4 days after electroporation at E18.5 (E18). Embryos with well-distinctive positive GFP signal in cortex visible through fluorescent binocular were intracardially perfused using 4% paraformaldehyde–phosphate buffered saline (PFA-PBS). Embryos with dotted, double hit or hit outside the cortex were not included in the study. Brains were post-fixed overnight and sectioned (60 μm; vibrotome, Leica). For examination of long-term effects of the treatments *in utero* electroporation was performed at E14, the mice delivered and the pups of postnatal day 8 (P8) were used for the experiments. For proliferation experiments embryos were *in utero* electroporated on E13.5 (E13) with 7 mm electrodes (39 mV pulses). IdU was injected in 24 h after electroporation for 30 min. Post-fixed brains were cryopreserved in sucrose and cryosections (10 μm) were used for proliferation analysis. For double electroporation the first *in utero* electroporation was performed at E13.5 with 7 mm electrodes (39 mV pulses). The second electroporation was performed 24 h later as described above.

Immunocytochemistry

Floating vibratome sections (60 μm) were permeabilized using 0.1% Triton X-100 and blocked in blocking solution (PBS, 0.1% Triton X-100, 10% HS; 10% FBS) for 60 min. Antibodies were incubated in blocking solution over night at 4°C. After washing, appropriate secondary antibodies (Jackson ImmunoResearch) were diluted in blocking solution, and incubated for 2 h at room temperature. Slices were mounted onto glass slides using Aqua Polymount (Polysciences). For IdU immunostainings (E18) the brain slices were pretreated with HCl (30') followed by neutralization with borate buffer. For IdU immunostainings (E13 and E14) the cryosections (10 μm) were used. Antigen retrieval procedure was performed by boiling slides in sodium citrate buffer (10 mM, pH 6) for 30 min.

Microscopy, Quantification, and Statistical Analyses

Images were taken using confocal microscopy (LSM780, LSM800 Zeiss), equipped with Axio Observer Z1 microscope, and imaged with either Plan-apochromat 20x/0.8, or Plan-apochromat 40x/1.2, or Plan-apochromat 63x/1.4 oil objectives. The scaling data are 0.624X0.624 μm per pixel for 20X magnification, 0.312X0.312 μm per pixel for 40X magnification, and 0.198X0.198X0.51 μm per voxol for 60X magnification. The images were processed by ZEN software and/or Imaris software.

Cell count, positioning and colocalization analyses were performed using Imaris software (Bitplane Inc., Zurich, Switzerland, Imaris core module). At least three brains were analyzed for each treatment. Four representative slices from each brain were chosen for analysis. The size of the area of interest was determined and preserved per each experiment. For each slice the area of interest was positioned so that the center of the electroporated area is in the center of the area of interest. For the cell count and positioning the relevant channel of an area of interest was analyzed with "Spots" module of Imaris, every spot labeling approximate center of the cell body. The "y" position of all the dots was analyzed by Microsoft Excel Histogram tool. The data were presented in percentages out of total analyzed cells per bin. For **Figure 1B** an average of 135.6 ± 8.3 (control shRNA) and 129 ± 15.4 (Serping1 shRNA) GFP-positive cells were analyzed per each slice. For **Figure 2D** an average of 490.8 ± 44.1 (control shRNA), 704 ± 51.8 (Serping1 shRNA), and 662.1 ± 52.8 (Serping1 shRNA +Serping1res) GFP-positive cells were analyzed per slice. For **Figure 2G** an average of 249.5 ± 12.4 (WT) and 259.5 ± 13.6 (Serping1 KO) IdU-positive cells were analyzed per slice. For **Figure 3** an average of 175.6 ± 14.3 (**Figure 3A'**), 180 ± 12.5 (**Figure 3B'**), 267.6 ± 37 (**Figure 3D'**), 182 ± 17.2 (**Figure 3E'**), 174.6 ± 19.5 (**Figure 3G'**), 137.1 ± 11.5 (**Figure 3H'**), 111.7 ± 9.3 (**Figure 3J'**), 166 ± 13.3 (**Figure 3K'**), 112 ± 21 (**Figure 3N'**) GFP- or dsRed-positive cells were analyzed per slice. For Supplementary Figure 4C an average of 275.1 ± 24.5 (electroporated side) and 226.7 ± 30.9 (non-electroporated side) cells were analyzed per slice. Statistical analysis was performed by Student's or Welch's *t*-tests or one-way or two-way analysis of variance (ANOVA) followed by Bonferroni multiple comparison analysis, using PRISM 7 for Mac (GraphPad software). Error bars represent standard error. For the measurement of leading edge length high resolution z-stack images were collected of the relevant slices. The analysis was performed with the ImageJ program.

Real-Time qRT-PCR

For confirmation of shRNA efficiency neurospheres from E13.5 were grown in Neurobasal medium (Gibco) supplemented with B27, glutamax, gentamicine, EGF (20 ng/ml), bFGF (20 ng/ml), and heparin for 2 days. The cells were transfected by NEPA21 electroporator (Nepagene) according to manufacturer's instructions. The cells were grown for additional 48 h and collected for RNA isolation (TRI reagent, Sigma). After Dnase treatment (Sigma), first-strand cDNA synthesis was done using M-MLV RT (Promega). Relative levels of Serping1 expression were normalized to the 29rps gene. Real-time PCR with SYBR FAST ABI qPCR kit (Kapa Biosystems) was performed using StepOnePlus Real-Time PCR System (Applied Biosystems). E13, E14, E16, E18 cortices ($n = 6$ for each time point) were dissected in cold PBS and fast-freeze in liquid nitrogen. RNA preparation and Real-time RT-PCR were performed as described above.

Western Blot

Brains were *in utero* electroporated with control shRNA or Serping1 shRNA together with GFP (E14-E17). The electroporated areas were dissected under fluorescent binocular. The dissected areas were homogenized in lysis buffer (50 mM Tris-HCl pH7.5; 150 mM NaCl; 1 mM EDTA; 1 mM EGTA; 1% Triton X-100) supplemented with protease inhibitor cocktail (Sigma). Fifty microgram of total protein was mixed with SDS sample buffer, separated by SDS-PAGE and subjected to western blot analysis with the indicated antibodies.

AUTHOR CONTRIBUTIONS

AG and TS planned, conducted experiments, analyzed data, and wrote the manuscript. TW contributed receptor agonists,

planned experiments, and wrote the manuscript. OR planned experiments, analyzed the data, and wrote the manuscript.

FUNDING

The research has been supported by the Israel Science Foundation (grant no. 347/15), the Legacy Heritage Biomedical Program of the Israel Science Foundation (grant no. 322/13), Weizmann-FAPESP supported by a research grant from the Dr. Beth Rom-Rymer Stem Cell Research Fund, Nella and Leon Benoziyo Center for Neurological Diseases, Yeda-Sela Center for Basic Research, Jeanne and Joseph Nissim Foundation for Life Sciences Research, Wohl Biology Endowment Fund, Fritz Thyssen Stiftung, Lulu P. and David J. Levidow Fund for Alzheimers Diseases and Neuroscience Research the Helen and Martin Kimmel Stem Cell Research Institute, the Kekst Family Institute for Medical Genetics, the David and Fela Shapell Family Center for Genetic Disorders Research. TW is supported by a National Health and Medical Research Council Career Development Fellowship (APP1105420).

ACKNOWLEDGMENTS

We are grateful for the help of Rebecca Haffner-Krausz, Golda Damari, Alina Maizenberg, Sima Peretz, Ofira Higfa, Yehuda Melamed, Osnat Amram, Oz Yirmiyahu, and Sergey Viukov from the Weizmann Institute of Science, Allison R. Bialas and Beth Stevens from the Children's Hospital, Harvard Medical School, Boston and Timothy Dahlem, Utah University. OR is the incumbent of the Bernstein-Mason Chair of Neurochemistry.

SUPPLEMENTARY MATERIAL

The Supplementary Material for this article can be found online at: http://journal.frontiersin.org/article/10.3389/fncel.2017.00169/full#supplementary-material

REFERENCES

Akuffo, E. L., Davis, J. B., Fox, S. M., Gloger, I. S., Hosford, D., Kinsey, E. E., et al. (2008). The discovery and early validation of novel plasma biomarkers in mild-to-moderate Alzheimer's disease patients responding to treatment with rosiglitazone. *Biomarkers* 13, 618–636. doi: 10.1080/13547500802445199

Bai, J., Ramos, R. L., Ackman, J. B., Thomas, A. M., Lee, R. V., and LoTurco, J. J. (2003). RNAi reveals doublecortin is required for radial migration in rat neocortex. *Nat. Neurosci.* 6, 1277–1283. doi: 10.1038/nn1153

Benard, M., Raoult, E., Vaudry, D., Leprince, J., Falluel-Morel, A., Gonzalez, B. J., et al. (2008). Role of complement anaphylatoxin receptors (C3aR, C5aR) in the development of the rat cerebellum. *Mol. Immunol.* 45, 3767–3774. doi: 10.1016/j.molimm.2008.05.027

Boulanger, L. M. (2009). Immune proteins in brain development and synaptic plasticity. *Neuron* 64, 93–109. doi: 10.1016/j.neuron.2009.09.001

Boulanger, L. M., and Shatz, C. J. (2004). Immune signalling in neural development, synaptic plasticity and disease. *Nat. Rev. Neurosci.* 5, 521–531. doi: 10.1038/nrn1428

Bowen, T., Cicardi, M., Farkas, H., Bork, K., Longhurst, H. J., Zuraw, B., et al. (2010). 2010 International consensus algorithm for the diagnosis, therapy and management of hereditary angioedema. *Allergy Asthma Clin. Immunol.* 6:24. doi: 10.1186/1710-1492-6-24

Broders-Bondon, F., Paul-Gilloteaux, P., Gazquez, E., Heysch, J., Piel, M., Mayor, R., et al. (2016). Control of the collective migration of enteric neural crest cells by the Complement anaphylatoxin C3a and N-cadherin. *Dev. Biol.* 414, 85–99. doi: 10.1016/j.ydbio.2016.03.022

Brummelkamp, T. R., Bernards, R., and Agami, R. (2002). A system for stable expression of short interfering RNAs in mammalian cells. *Science* 296, 550–553. doi: 10.1126/science.1068999

Carmona-Fontaine, C., Theveneau, E., Tzekou, A., Tada, M., Woods, M., Page, K. M., et al. (2011). Complement fragment C3a controls mutual cell attraction during collective cell migration. *Dev. Cell* 21, 1026–1037. doi: 10.1016/j.devcel.2011.10.012

Chiam, J. T., Dobson, R. J., Kiddle, S. J., and Sattlecker, M. (2015). Are blood-based protein biomarkers for Alzheimer's disease also involved in other brain disorders? A systematic review. *J. Alzheimer's Dis.* 43, 303–314. doi: 10.3233/JAD-140816

Coulthard, L. G., Hawksworth, O. A., Li, R., Balachandran, A., Lee, J. D., Sepehrband, F., et al. (2017). Complement C5aR1 signaling promotes polarization and proliferation of embryonic neural progenitor cells through PKCζ. *J. Neurosci.* 37, 5395–5407. doi: 10.1523/JNEUROSCI.0525-17.2017

Cutler, P., Akuffo, E. L., Bodnar, W. M., Briggs, D. M., Davis, J. B., Debouck, C. M., et al. (2008). Proteomic identification and early validation of complement 1 inhibitor and pigment epithelium-derived factor: Two novel biomarkers of Alzheimer's disease in human plasma. *Proteomics Clin. Appl.* 2, 467–477. doi: 10.1002/prca.200780101

Davis, A. E., Mejia, P., and Lu, F. (2008). Biological activities of C1 inhibitor. *Mol. Immunol.* 45, 4057–4063. doi: 10.1016/j.molimm.2008.06.028

De Simoni, M. G., Rossi, E., Storini, C., Pizzimenti, S., Echart, C., and Bergamaschini, L. (2004). The powerful neuroprotective action of C1-inhibitor on brain ischemia-reperfusion injury does not require C1q. *Am. J. Pathol.* 164, 1857–1863. doi: 10.1016/s0002-9440(10)63744-3

Denny, K. J., Coulthard, L. G., Jeanes, A., Lisgo, S., Simmons, D. G., Callaway, L. K., et al. (2013). C5a receptor signaling prevents folate deficiency-induced neural tube defects in mice. *J. Immunol.* 190, 3493–3499. doi: 10.4049/jimmunol.1203072

des Portes, V., Pinard, J. M., Billuart, P., Vinet, M. C., Koulakoff, A., Carrie, A., et al. (1998). A novel CNS gene required for neuronal migration and involved in X-linked subcortical laminar hetrotropia and lissencephaly syndrome. *Cell* 92, 51–61. doi: 10.1016/S0092-8674(00)80898-3

Dinsmore, J. H., and Solomon, F. (1991). Inhibition of MAP2 expression affects both morphological and cell division phenotypes of neuronal differentiation. *Cell* 64, 817–826. doi: 10.1016/0092-8674(91)90510-6

Fujita, T. (2002). Evolution of the lectin-complement pathway and its role in innate immunity. *Nat. Rev. Immunol.* 2, 346–353. doi: 10.1038/nri800

Gesuete, R., Storini, C., Fantin, A., Stravalaci, M., Zanier, E. R., Orsini, F., et al. (2009). Recombinant C1 inhibitor in brain ischemic injury. *Ann. Neurol.* 66, 332–342. doi: 10.1002/ana.21740

Gleeson, J. G., Allen, K. M., Fox, J. W., Lamperti, E. D., Berkovic, S., Scheffer, I., et al. (1998). *Doublecortin*, a brain-specific gene mutated in human X-linked lissencephaly and double cortex syndrome, encodes a putative signaling protein. *Cell* 92, 63–72. doi: 10.1016/s0092-8674(00)80899-5

Gleeson, J. G., Minnerath, S., Kuzniecky, R. I., Dobyns, W. B., Young, I. D., Ross, M., et al. (2000). Somatic and germline mosaic mutations in the doublecortin gene are associated with variable phenotypes. *Am. J. Hum. Genet.* 67, 574–581. doi: 10.1086/303043

Gorelik, A., Sapir, T., Haffner-Krausz, R., Olender, T., Woodruff, T. M., and Reiner, O. (2017). Developmental activities of the complement pathway in migrating neurons. *Nat. Commun.* 8:15096. doi: 10.1038/ncomms15096

Greenman, R., Gorelik, A., Sapir, T., Baumgart, J., Zamor, V., Segal-Salto, M., et al. (2015). Non-cell autonomous and non-catalytic activities of ATX in the developing brain. *Front. Neurosci.* 9:53. doi: 10.3389/fnins.2015.00053

Han, E. D. (2002). Increased vascular permeability in C1 inhibitor-deficient mice mediated by the bradykinin type 2 receptor. *J. Clin. Investig.* 109, 1057–1063. doi: 10.1172/jci200214211

Hanahan, D., and Weinberg, R. A. (2000). The hallmarks of cancer. *Cell* 100, 57–70. doi: 10.1016/S0092-8674(00)81683-9

Hanahan, D., and Weinberg, R. A. (2011). Hallmarks of cancer: the next generation. *Cell* 144, 646–674. doi: 10.1016/j.cell.2011.02.013

Hawksworth, O. A., Coulthard, L. G., and Woodruff, T. M. (2016). Complement in the fundamental processes of the cell. *Mol. Immunol.* 84, 17–25. doi: 10.1016/j.molimm.2016.11.010

Hawksworth, O. A., Coulthard, L. G., Taylor, S. M., Wolvetang, E. J., and Woodruff, T. M. (2014). Brief report: complement C5a promotes human embryonic stem cell pluripotency in the absence of FGF2. *Stem Cells* 32, 3278–3284. doi: 10.1002/stem.1801

Heydenreich, N., Nolte, M. W., Gob, E., Langhauser, F., Hofmeister, M., Kraft, P., et al. (2012). C1-inhibitor protects from brain ischemia-reperfusion injury by combined antiinflammatory and antithrombotic mechanisms. *Stroke* 43, 2457–2467. doi: 10.1161/strokeaha.112.660340

Jasmin, B. J., Cartaud, J., Bornens, M., and Changeux, J. P. (1989). Golgi apparatus in chick skeletal muscle: changes in its distribution during end plate development and after denervation. *Proc. Natl. Acad. Sci. U.S.A.* 86, 7218–7222.

Jiang, H., Wagner, E., Zhang, H., and Frank, M. M. (2001). Complement 1 inhibitor is a regulator of the alternative complement pathway. *J. Exp. Med.* 194, 1609–1616. doi: 10.1084/jem.194.11.1609

Kawaguchi, A., Ikawa, T., Kasukawa, T., Ueda, H. R., Kurimoto, K., Saitou, M. (2008). Single-cell gene profiling defines differential progenitor subclasses in mammalian neurogenesis. *Development* 135, 3113–3124. doi: 10.1242/dev.022616

Koizumi, H., Tanaka, T., and Gleeson, J. G. (2006). Doublecortin-like kinase functions with doublecortin to mediate fiber tract decussation and neuronal migration. *Neuron* 49, 55–66. doi: 10.1016/j.neuron.2005.10.040

Morgan, A. R., Touchard, S., O'Hagan, C., Sims, R., Majounie, E., Escott-Price, V., et al. (2017). The correlation between inflammatory biomarkers and polygenic risk score in alzheimer's disease. *J. Alzheimer's Dis.* 56, 25–36. doi: 10.3233/JAD-160889

Muenchhoff, J., Poljak, A., Song, F., Raftery, M., Brodaty, H., Duncan, M., et al. (2015). Plasma protein profiling of mild cognitive impairment and Alzheimer's disease across two independent cohorts. *J. Alzheimer's Dis.* 43, 1355–1373. doi: 10.3233/JAD-141266

Parej, K., Dobo, J., Zavodszky, P., and Gal, P. (2013). The control of the complement lectin pathway activation revisited: both C1-inhibitor and antithrombin are likely physiological inhibitors, while alpha2-macroglobulin is not. *Mol. Immunol.* 54, 415–422. doi: 10.1016/j.molimm.2013.01.009

Presanis, J. S., Hajela, K., Ambrus, G., Gál, P., and Sim, R. B. (2003). Differential substrate and inhibitor profiles for human MASP-1 and MASP-2. *Mol. Immunol.* 40, 921–929. doi: 10.1016/j.molimm.2003.10.013

Ran, F. A., Hsu, P. D., Wright, J., Agarwala, V., Scott, D. A., and Zhang, F. (2013). Genome engineering using the CRISPR-Cas9 system. *Nat. Protoc.* 8, 2281–2308. doi: 10.1038/nprot.2013.143

Rutkowski, M. J., Sughrue, M. E., Kane, A. J., Mills, S. A., Fang, S., and Parsa, A. T. (2010). Complement and the central nervous system: emerging roles in development, protection and regeneration. *Immunol. Cell Biol.* 88, 781–786. doi: 10.1038/icb.2010.48

Saito, T., and Nakatsuji, N. (2001). Efficient gene transfer into the embryonic mouse brain using *in vivo* electroporation. *Dev. Biol.* 240, 237–246. doi: 10.1006/dbio.2001.0439

Schafer, D. P., Lehrman, E. K., Kautzman, A. G., Koyama, R., Mardinly, A. R., Yamasaki, R., et al. (2012). Microglia sculpt postnatal neural circuits in an activity and complement-dependent manner. *Neuron* 74, 691–705. doi: 10.1016/j.neuron.2012.03.026

Scully, C. C., Blakeney, J. S., Singh, R., Hoang, H. N., Abbenante, G., Reid, R. C., et al. (2010). Selective hexapeptide agonists and antagonists for human complement C3a receptor. *J. Med. Chem.* 53, 4938–4948. doi: 10.1021/jm1003705

Stephan, A. H., Barres, B. A., and Stevens, B. (2012). The complement system: an unexpected role in synaptic pruning during development and disease. *Annu. Rev. Neurosci.* 35, 369–389. doi: 10.1146/annurev-neuro-061010-113810

Stevens, B., Allen, N. J., Vazquez, L. E., Howell, G. R., Christopherson, K. S., Nouri, N., et al. (2007). The classical complement cascade mediates CNS synapse elimination. *Cell* 131, 1164–1178. doi: 10.1016/j.cell.2007.10.036

Storini, C., Rossi, E., Marrella, V., Distaso, M., Veerhuis, R., Vergani, C., De Simoni, M. G., et al. (2005). C1-inhibitor protects against brain ischemia-reperfusion injury via inhibition of cell recruitment and inflammation. *Neurobiol. Dis.* 19, 10–17. doi: 10.1016/j.nbd.2004.11.001

Tabata, H., and Nakajima, K. (2001). Efficient *in utero* gene transfer system to the developing mouse brain using electroporation: visualization of neuronal migration in the developing cortex. *Neuroscience* 103, 865–872. doi: 10.1016/s0306-4522(01)00016-1

Veerhuis, R., Janssen, I., Hoozemans, J. J., De Groot, C. J., Hack, C. E., and Eikelenboom, P. (1998). Complement C1-inhibitor expression in Alzheimer's disease. *Acta Neuropathol.* 96, 287–296. doi: 10.1007/s004010050896

Walker, D. G., Yasuhara, O., Patston, P. A., McGeer, E. G., and McGeer, P. L. (1995). Complement C1 inhibitor is produced by brain tissue and is cleaved in Alzheimer disease. *Brain Res.* 675, 75–82. doi: 10.1016/0006-8993(95)00041-N

Walport, M. J. (2001). Complement. First of two parts. *N. Engl. J. Med.* 344, 1058–1066. doi: 10.1056/NEJM200104053441406

Wang, H., Yang, H., Shivalila, C. S., Dawlaty, M. M., Cheng, A. W., Zhang, F., et al. (2013). One-step generation of mice carrying mutations in multiple genes by CRISPR/Cas-mediated genome engineering. *Cell* 153, 910–918. doi: 10.1016/j.cell.2013.04.025

Woodruff, T. M., Strachan, A. J., Sanderson, S. D., Monk, P. N., Wong, A. K., Fairlie, D. P., et al. (2001). Species dependence for binding of small molecule agonist and antagonists to the C5a receptor on polymorphonuclear leukocytes. *Inflammation* 25, 171–177. doi: 10.1023/A:1011036414353

Wu, M. C., Brennan, F. H., Lynch, J. P., Mantovani, S., Phipps, S., Wetsel, R. A., et al. (2013). The receptor for complement component C3a mediates protection from intestinal ischemia-reperfusion injuries by inhibiting neutrophil mobilization. *Proc. Natl. Acad. Sci. U.S.A.* 110, 9439–9444. doi: 10.1073/pnas.1218815110

Yasojima, K., McGeer, E. G., and McGeer, P. L. (1999). Complement regulators C1 inhibitor and CD59 do not significantly inhibit complement activation in Alzheimer disease. *Brain Res.* 833, 297–301. doi: 10.1016/S0006-8993(99)01514-0

Conflict of Interest Statement: The authors declare that the research was conducted in the absence of any commercial or financial relationships that could be construed as a potential conflict of interest.

frontiers in Cellular Neuroscience

ORIGINAL RESEARCH
published: 01 May 2017
doi: 10.3389/fncel.2017.00122

Loss of Elp3 Impairs the Acetylation and Distribution of Connexin-43 in the Developing Cerebral Cortex

Sophie Laguesse[1,2†], Pierre Close[2,3], Laura Van Hees[1,2], Alain Chariot[2,3,4], Brigitte Malgrange[1,2] and Laurent Nguyen[1,2*]*

[1]GIGA-Neurosciences, University of Liège, Liège, Belgium, [2]Interdisciplinary Cluster for Applied Genoproteomics (GIGA-R), University of Liège, Liège, Belgium, [3]GIGA-Molecular Biology of Diseases, University of Liège, Liège, Belgium, [4]Walloon Excellence in Lifesciences and Biotechnology (WELBIO), Wallonia, Belgium

The Elongator complex is required for proper development of the cerebral cortex. Interfering with its activity *in vivo* delays the migration of postmitotic projection neurons, at least through a defective α-tubulin acetylation. However, this complex is already expressed by cortical progenitors where it may regulate the early steps of migration by targeting additional proteins. Here we report that connexin-43 (Cx43), which is strongly expressed by cortical progenitors and whose depletion impairs projection neuron migration, requires Elongator expression for its proper acetylation. Indeed, we show that Cx43 acetylation is reduced in the cortex of Elp3cKO embryos, as well as in a neuroblastoma cell line depleted of Elp1 expression, suggesting that Cx43 acetylation requires Elongator in different cellular contexts. Moreover, we show that histones deacetylase 6 (HDAC6) is a deacetylase of Cx43. Finally, we report that acetylation of Cx43 regulates its membrane distribution in apical progenitors of the cerebral cortex.

Keywords: acetylation, cerebral cortex, connexin-43, elongator, HDAC6

OPEN ACCESS

Edited by:
Annette Gaertner, KU Leuven, Belgium

Reviewed by:
Rafael Linden, Federal University of Rio de Janeiro, Brazil
Kerry Lee Tucker, University of New England, USA

***Correspondence:**
Sophie Laguesse
sophie.laguesse@hotmail.com
Laurent Nguyen
lnguyen@ulg.ac.be

†Present address:
Sophie Laguesse, Department of Neurology, University of California San Francisco, CA, USA.

Received: *10 January 2017*
Accepted: *12 April 2017*
Published: *01 May 2017*

Citation:
Laguesse S, Close P, Van Hees L, Chariot A, Malgrange B and Nguyen L (2017) Loss of Elp3 Impairs the Acetylation and Distribution of Connexin-43 in the Developing Cerebral Cortex. Front. Cell. Neurosci. 11:122. doi: 10.3389/fncel.2017.00122

INTRODUCTION

The neocortex is a highly organized structure made of six distinct neuronal layers, which differ in terms of connectivity and gene expression profile (Molyneaux et al., 2007). The establishment of the laminated cortical structure implies a coordinated generation, migration and differentiation of neurons during embryonic development (Noctor et al., 2001). Excitatory projection neurons arise from progenitor cells located in the ventricular (VZ) and subventricular zones (SVZ) of the dorsal telencephalon (Götz and Huttner, 2005). Newborn neurons migrate radially along radial glial fibers to the cortical plate (CP) and settle into neuronal laminae. Neuronal migration is a dynamic and highly regulated process including distinct phases associated with specific morphologies (Ohtaka-Maruyama and Okado, 2015). Numerous molecular pathways controlling neuronal migration have been identified, including cytoskeletal regulators such as doublecortin, filamin A, and Lis1 (Kriegstein and Noctor, 2004; Liu, 2011; Moon and Wynshaw-Boris, 2013). We previously reported that Elongator is a critical player in the control of cortical neuron migration (Creppe et al., 2009; Tielens et al., 2016). Elongator is a macromolecular complex composed by two copies of six individual subunits (Glatt et al., 2012), with Elp3 being the enzymatic core that contains an acetyltransferase (HAT) domain (Winkler et al., 2002). Several functions have been attributed to Elongator (Nguyen et al., 2010; Glatt and Müller, 2013). Besides its central role as a tRNA-modifying protein (Ladang et al., 2015; Laguesse et al., 2015; Delaunay et al., 2016), Elp3 has been shown to

regulate the acetylation of three proteins: histone H3 in the nucleus (Winkler et al., 2002), bruchpilot at the drosophila neuromuscular junction (Miskiewicz et al., 2011) and α-tubulin in migrating post-mitotic projection neurons (Creppe et al., 2009). We previously showed that reducing Elongator activity in post-mitotic neurons correlates with reduced α-tubulin acetylation and impaired migration to the CP (Creppe et al., 2009). However, as Elongator subunits are also found in the VZ/SVZ of the developing cortex (Creppe et al., 2009; Laguesse et al., 2015), we hypothesized that other targets of Elongator (direct or indirect) play a role in the regulation of early steps of migration, contributing to the overall migration impairment observed after depletion of Elongator.

The GAP junction protein connexins (Cx) are highly expressed in neural progenitor cells during cortical development where they regulate different aspects of neurogenesis (Sutor and Hagerty, 2005; Elias and Kriegstein, 2008; Orellana et al., 2013). Among them, connexin-43 (Cx43) is highly expressed by neurons and neuronal progenitors during development (Rouach et al., 2002). Cx43 controls the differentiation and the interkinetic nuclear migration of neuronal progenitors (Liu et al., 2010; Santiago et al., 2010; Rinaldi et al., 2014), the tangential to radial migratory switch of migrating interneurons invading the cortical wall (Elias et al., 2010), and the radial migration of projection neurons (Elias et al., 2007; Elias and Kriegstein, 2008; Cina et al., 2009; Liu et al., 2012; Qi et al., 2016). During radial migration, Cx43 is expressed at the contact point between migrating neurons and radial glial fibers, and targeting Cx43 impairs neuronal migration (Elias et al., 2007; Cina et al., 2009). Cx43 is regulated by numerous post-translational modifications (Solan and Lampe, 2009; Johnstone et al., 2012) including lysine acetylation, which controls its subcellular localization in mouse cardiomyocytes (Colussi et al., 2011).

Here, we showed that Cx43 interacts with both Elp1 and Elp3 in the developing mouse cortex as well as in different cell lines, and that proper acetylation of Cx43 requires Elongator activity, a post-translational modification removed by histones deacetylase 6 (HDAC6). We thus investigated the possible function of Cx43 acetylation and demonstrated that this post-translational modification regulates Cx43 cellular localization in Hela cells and in the developing cortex.

MATERIALS AND METHODS

Animals

Time-pregnant NMRI (Janvier Labs, Saint Berthevin, France), FoxG1$^{cre/WT}$ and Elp3$^{loxp/loxp}$ mice backcrossed in 129/SvJ genetic background were housed under standard conditions. This study was carried out in accordance with the recommendations of the guidelines of the Belgian Ministry of Agriculture in agreement with European Community Council Directive for the care and use of laboratory animals of 22 September 2010 (2010/63/EU) and approved by the local ethics committee. The generation of the conditional Elp3 knock-out mouse required breeding of Elp3$^{loxp/loxp}$ mice with FoxG1$^{cre/WT}$ mice (Hébert and McConnell, 2000), as previously described (Laguesse et al., 2015). The following primers were used for genotyping FoxG1 and Cre recombinase: 5′-GCC GCC CCC CGA CGC CTG GGT GAT-3′, 5′-TGG TGG TGG TGA TGA TGA TGG TGA TGC TGG-3′ and 5′-ATA ATC GCG AAC ATC TTC AGG TTC TGC GGG-3′.

RNA Extractions and qRT-PCR

Total RNA was extracted from cortices of E14.5 embryos. RNA extraction was performed using the All prep DNA/RNA/protein kit (Qiagen, Hilden, Germany). All RNA samples were treated with DNAse I (Roche, Basel, Switzerland). Synthesis of cDNA was performed on total RNA, which was reverse-transcribed with SuperScript III reverse transcriptase (ThermoFisher Scientific, Waltham, MA, USA) according to the manufacturer's instructions. Resulting cDNA was used for quantitative PCR, using Faststart Universal SYBR Green Master (Roche). Thermal cycling was performed on an Applied Biosystem 7900HT Fast Real-Time PCR detection system (Applied Biosystems, Foster city, CA, USA). The quantity of each mRNA transcript was measured and expressed relative to Glyceraldehyde-3-Phosphate deshydrogenase (*GAPDH*). The following primers were designed with Primer3 software: *GJA1* forward 5′-GGA CTG CTT TCT CTC ACG TC-3′ and *GJA1* reverse 5′-GAG CGA GAG ACA CCA AGG AC-3′; *GAPDH* forward 5′-GCA CAG TCA AGG CCG AGA AT-3′ and *GAPDH* reverse 5′-GCC TTC TCC ATG GTG GTG AA-3′.

Cell Cultures, Stable Line Establishment and Transfections

Human Glioblastoma (U87) and Adenocarcinoma (Hela) cells were cultured in DMEM medium supplemented with Bovine fetal serum (FBS) 10%. Mouse Neuroblastoma cells (N2A) were cultured in DMEM supplemented with FBS 10% and glutamine 2 mM. Human embryonic kidney HEK-293 lentiX cells (Clontech, Moutain View, CA, USA) and HEK-293 cells were cultivated in DMEM supplemented with FBS 10%, glutamine 1%. To generate HEK-293 stably expressing ELP3-FLAG proteins, cells were transfected with pIRES-Elp3-puro construct and selected in 1 μg/ml puromycin (Sigma Aldrich, St Louis, MO, USA). Cells were maintained in selecting media for 3 weeks and surviving cells were used for experiment after transgene expression confirmation. Cell transfections were performed using lipofectamine 2000 according to manufacturer's protocol (ThermoFisher Scientific). Cells were lysed or fixed 48 h after transfection. Trichostatin A (TSA; 5 mM in DMSO, Sigma-Aldrich) was added to the medium at a final concentration of 1 μM for 4 h before cell fixation or lysis.

Plasmids Constructs and Preparation

ORFs encoding human Elp3 were cloned into pIRESpuro (Clontech) with a FLAG tag at the C terminus. Flag-HDAC6 in pcDNA3 has been described previously (Viatour et al., 2003). All constructs were sequence verified. Cx43 was subcloned from the clone image MC205621 (Origene, Rockville, MD, USA) by high fidelity PCR using NheI-Cx43 forward primer and

EcoRV-reverse primer and inserted into the pCAGGS-IRES-GFP vector. To obtain Cx43-4KR, directed mutagenesis was performed on the pCAGGS-Cx43-IRES-GFP (Agilent, Santa Clara, CA, USA), replacing K9R, K162R, K234R and K264R. Plasmids DNA were prepared using a Plasmid Endofree Maxi Kit (Qiagen).

Lentivirus Production and Infection

Lentivirus production and lentiviral infections were performed as previously described (Creppe et al., 2009). Briefly, HEK-293 lentiX cells were transfected with the lentiviral packaging vectors VSVG and R8.91 and the pLL3.7 shELP1 or pLL3.7 shSCR using Fugene6 (Promega, Madison, WI, USA) in Opti-MEM medium. Twenty-four hours after transfection, medium was changed to DMEM-FBS 10%. Seventy-two hours after transfection, supernatant containing the viral particles was collected and passed through 0.22 μm filter. The supernatant was then used to infect N2A cells two times consecutively for 6 h with Polybrene® (Sigma-Aldrich) added at 5 μg/mL. Efficacy of infection was determined by GFP expression.

Immunohistochemistry

Embryonic brains (E14.5) were dissected in 0.1 M phosphate-buffered saline pH7.4 (PBS) and were fixed at 4°C in 4% paraformaldehyde (PFA) for 1 h. Fixed samples were cryoprotected overnight in 20% sucrose in PBS at 4°C, embedded in OCT Compound (VWR International, Leuven, Belgium) and sectioned (12 μm) onto slides (SuperFrost Plus, VWR International) using a cryostat. Cells were fixed at RT in 4% PFA for 15 min and rinsed three times with PBS. Frozen cryosections and fixed cells were washed three times in PBS-Triton 0.1% (PBST) and blocked for 1 h at room temperature in PBST containing 10% donkey serum (Jackson Immunoresearch Laboratories, West Grove, PA, USA). Sections were incubated overnight at 4°C with the following primary antibodies: anti-Elp3 (1:1000, gift from J. Svejstrup, Cancer Research UK London Research Institute, South Mimms, UK), anti-Cx43 (1:500, rabbit, Abcam, Cambridge, UK), anti-Cx43 IF1 (1:500, mouse, Max Planck institute, Munchen, Germany, Sosinsky et al., 2007), anti-GFP (1:500, goat, Abcam). After washing, sections were incubated for 1 h at room temperature with either anti-mouse, anti-rabbit, or anti-goat secondary antibodies coupled to Rhodamine-redX or FITC (Jackson Immunoresearch Laboratories). Nuclei were counterstained with Hoechst 33342 (1:1000, ThermoFisher Scientific), washed in PBST and coverslipped using Aqua Polymount (Polysciences Inc, Washington, DC, USA). The slides were stored in the dark at 4°C. For images analyses, sections were analyzed by confocal microscopy using A1Ti confocal microscope (Nikon) and ImageJ software. Images of cortical slices were acquired with a 40× objective with a *z*-interval of 1 μm (*z*-stack = 5 images) or with a 60× objective with a *z*-interval of 1 μm (*z*-stack = 5 images). The quantifications of intracellular and membrane fluorescent signal intensities in Hela cells were conducted using ImageJ software.

Immunoprecipitation and Western Blot Analysis

Dissected E14.5 embryonic cortices were incubated in lysis buffer (50 mM Tris-HCl pH 7.4, 450 mM NaCl, 1% triton, 10 mM NaF, 1 mM Na_3VO_4 and proteases inhibitors, Roche). Cells were lysed in another lysis buffer (50 mM Tris-HCl pH 7.4, 150 mM NaCl, 1% triton, 10 mM NaF, 1 mM Na_3VO_4 and proteases inhibitors, Roche). Proteins were extracted by centrifugation (10,000 *g*) for 10 min at 4°C, and quantified using BCA method (Pierce). Immunoprecipitation (IP) was carried out using the following antibodies at 1/250: anti-HA (rabbit, Santa Cruz Technology SCT, Santa Cruz, CA, USA), anti-HA (mouse, SCT), anti-Flag (mouse, Sigma-Aldrich), anti-ELP1 (Close et al., 2006), anti-ELP3 (gift from J. Svejstrup, Cancer Research UK London Research Institute, South Mimms, UK), anti-Cx43 (rabbit, Abcam), followed by 1 h incubation with protein A/G plus agarose beads. Anti-HA IP was carried out as control. Beads were washed out six times with the lysis buffer. Protein samples were then mixed with loading buffer and incubated at 95°C for 5 min, then separated by SDS-PAGE and transferred to 0.45 μm PVDF membranes (Millipore, Billerica, MA, USA). Membranes were blocked 1 h in a solution containing non-fat milk, then incubated O/N at 4°C with the following antibodies anti-ELP1 (Close et al., 2006), anti-Cx43 (Abcam), anti-pan-acetylated lysine (Cell signaling technology, Danvers, MA, USA). HRP-conjugated antibodies were applied for 1 h at RT (conjugated anti-mouse, anti-rabbit, GE Healthcare, Waukesha, WI, USA). Membranes were developed with the ECL chemiluminescent reagent (Thermo scientific, Rockford, IL, USA) using Hyperfilm ECL (GE Healthcare). ImageJ was used for optical density quantification.

Statistical Analyses

Statistics for dual comparisons were generated using unpaired two-tailed Student's *t*-tests. Statistical analyses were performed using graphPad Prism 5.0 Software (GraphPad software Inc., San Diego, CA, USA). Values are presented as mean ± SEM $^{*}p < 0.05$, $^{**}p < 0.01$, $^{***}p < 0.001$ for all statistics.

RESULTS

Elongator Interacts with Connexin 43 in the Developing Cortex

Cx43 is expressed in neurons and progenitors of the developing cortex of the rat brain, with high levels of expression in the VZ/SVZ and reduced levels in the CP (Elias et al., 2007; Qi et al., 2016). We analyzed the expression of Cx43 in E14.5 embryonic mouse brain and observed a punctate staining throughout the cortical wall, with a stronger labeling of the VZ cells (**Figures 1A–H**). The different subunits of Elongator are expressed in migrating projection neurons, but are also found in the VZ/SVZ progenitor cells (Creppe et al., 2009; Laguesse et al., 2015). We thus immunolabeled embryonic cortices to detect Cx43 and Elp3, and we observed a strong co-expression of both proteins in cortical progenitor cells that are lining the ventricle (**Figures 1B,F–H**). Co-IP experiments on

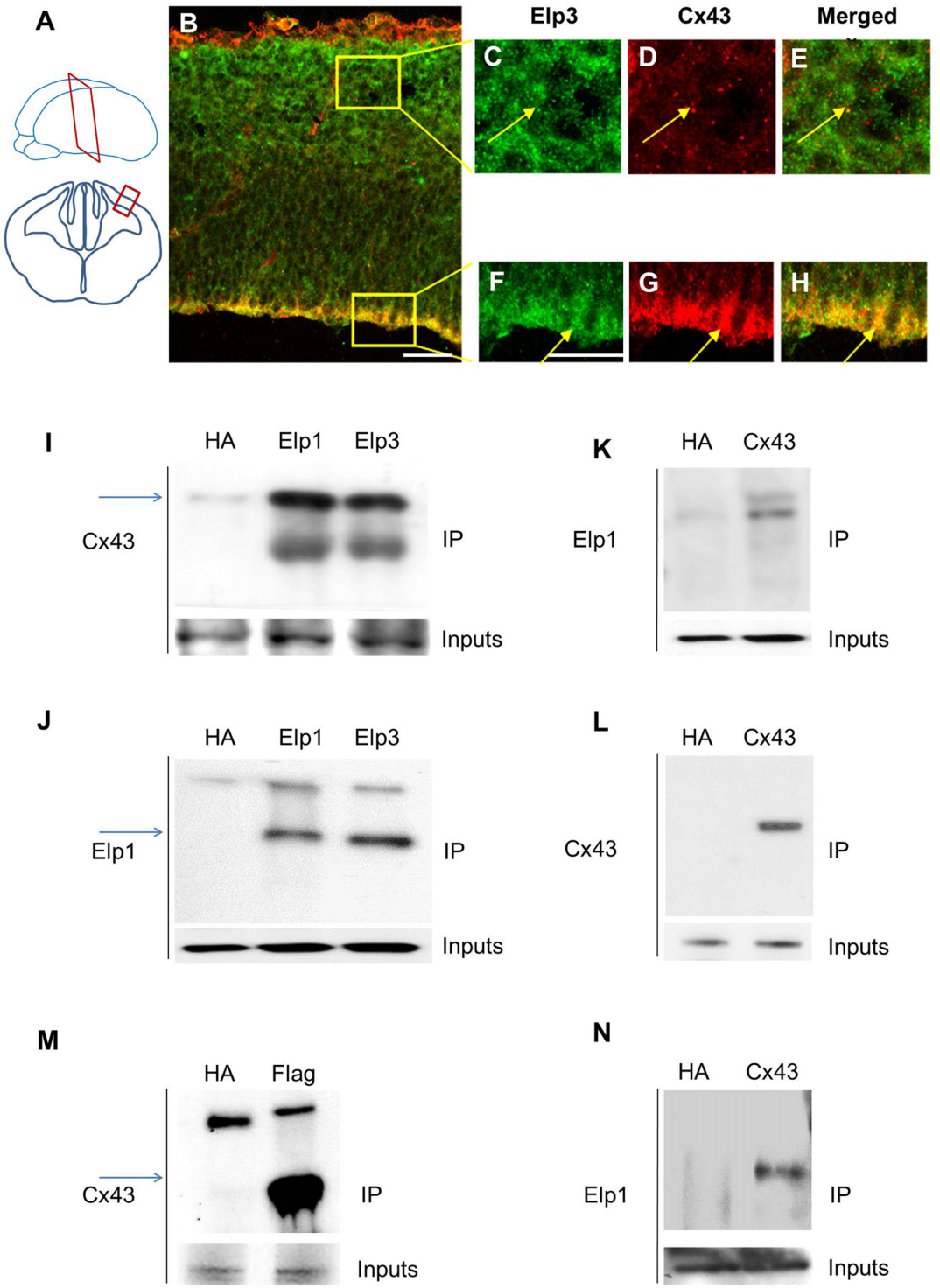

FIGURE 1 | Elongator interacts with connexin 43 (Cx43) in the developing cortex. (A) Scheme illustrating the location of the coronal section (12 μm) of E14.5 wild-type (WT) cortex. **(B–H)** Immunodetection of Cx43 (red) and Elp3 (green) in E14.5 WT cortex showing co-expression of both Elp3 and Cx43 in cortical plate (CP) neurons **(C–E)** and in the ventricular (VZ)/subventricular zones (SVZ) neuronal progenitors **(F–H)**. **(I–L)** Immunoprecipitates from E14.5 mouse embryos cortices were subjected to anti-ELP1 or anti-Cx43 western blot analysis; corresponding western blots were performed on crude cell extracts (inputs). **(M)** Immunoprecipitates from HEK293 cell line stably expressing flag-ELP3 were subjected to anti-Cx43 western blot analysis and showed an interaction between Cx43 and ELP3. Corresponding western blots were performed on crude cell extracts (inputs). **(N)** Forty-eight hours after transfection of Cx43 in N2A cells, immunoprecipitates from N2A cells homogenate were subjected to anti-ELP1 western blot and showed an interaction between Cx43 and ELP1. Bar scale, 50 μm.

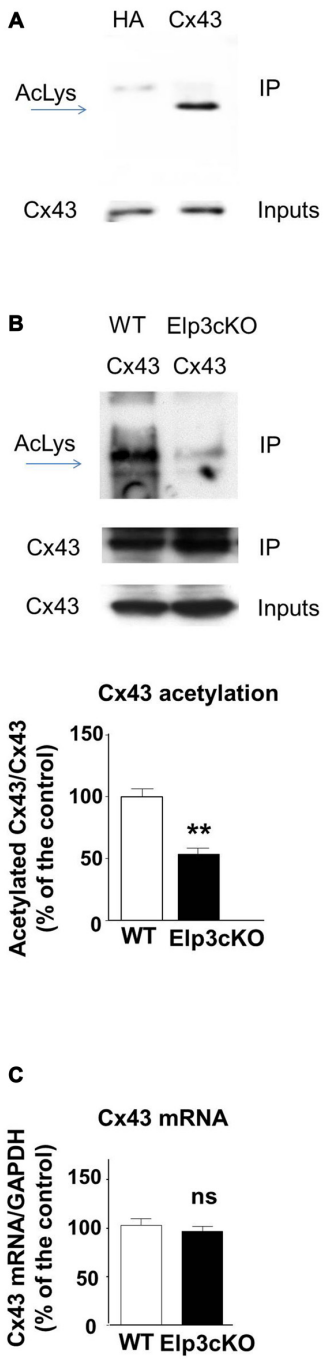

FIGURE 2 | Cx43 is acetylated in the developing cortex.
(A,B) Immunoprecipitates from E14.5 WT **(A)** or Elp3cKO **(B)** mouse embryos cortices were subjected to anti- pan acetyl lysine western blot analysis. Corresponding western blots were performed on crude cell extracts (inputs). Data are presented as the average ratio of acetylated Cx43 to Cx43 ± SEM, and are expressed as percentage of WT controls. Significance was determined using two-tailed unpaired *t*-test $t_{(4)} = 5.11$, $p = 0.007$. $n = 3$. **(C)** *Cx43* mRNA levels were determined by qRT-PCR in E14.5 WT and Elp3cKO cortex. Data are presented as the average ratio of *Cx43* to glyceraldehyde-3-Phosphate deshydrogenase (*GAPDH*) ± SEM, and expressed as percentage of WT control. Significance was determined using two-tailed unpaired *t*-test $t_{(4)} = 0.668$, $p = 0.54$. $n = 4$. $^{**}p < 0.01$.

microdissected tissue from the cerebral cortex of E14.5 embryos demonstrated an *in vivo* interaction between Cx43 and both Elp1 and Elp3 (**Figures 1I–L**). We also generated a HEK293 cell line stably expressing flag-Elp3, and we detected a comparable interaction between flag-ELP3 and Cx43 *in vitro* (**Figure 1M**). This interaction was further confirmed in a neuroblastoma cell line (**Figure 1N**).

Connexin 43 is Acetylated in the Developing Cortex

In the developing mouse heart, Cx43 assembles into GAP junctions expressed at the intercalated discs that physically delimitate cardiomyocytes, and Cx43 acetylation has been shown to control such localization (Colussi et al., 2011). To determine whether Cx43 is acetylated in the developing mouse cortex, we performed western blot to detect acetylated lysine(s) in Cx43 immunoprecipitate from E14.5 mouse cortical extracts (**Figure 2A**). The acetylation level of Cx43 but not its expression (**Figure 2B** (inputs), **Figure 2C**) was reduced in the cortex of E14.5 Elp3cKO embryos (breeding of Elp3loxlox mice with FoxG1: Cre mice (Hébert and McConnell, 2000), as previously described (Laguesse et al., 2015)), as compared to WT embryos (**Figure 2B**). Altogether, these results show that Elongator is required for the proper acetylation of Cx43 in the mouse developing cerebral cortex.

Elongator and HDAC6 Regulate Connexin 43 Acetylation

The transfer or removal of acetyl groups on lysine residues is mediated by two classes of enzymes: the lysine acetyltransferases (KATs) and lysine deacetylases (KDACs), also known as HDACs (Menzies et al., 2016; Simon et al., 2016). HDACs are grouped into four classes, depending on sequence homology. Classes I, II and IV are Zinc-dependent HDACs, whereas class III consists of NAD^+-dependent sirtuins (SIRT1 and 2). HDACs play important roles in the regulation of transcription, but they also act on a large set of non-histones proteins, like transcription factors, translation-associated proteins, proteins involved in cytoskeleton regulation or cell signaling, to regulate several functions (Yao and Yang, 2011; Roche and Bertrand, 2016). In order to identify the enzyme responsible for Cx43 deacetylation, we treated cultured U87 cells with TSA, a potent inhibitor of class I, II and IV HDACs but not class III sirtuins (Codd et al., 2009), or DMSO as control. As shown in **Figure 3A**, TSA treatment of U87 cells significantly increased Cx43 acetylation levels, suggesting that the Cx43 deacetylase is a member of HDAC family. HDAC6 is found in the cytoplasm and promotes the deacetylation of multiple targets including α-tubulin, cortactin and HSP90 (Kovacs et al., 2005; Zhang et al., 2007; Li et al., 2011). We thus tested the ability of HDAC6 to promote Cx43 deacetylation. As shown in **Figure 3B**, HDAC6 overexpression reduced the acetylation of Cx43 in N2A cells, suggesting that HDAC6 is a deacetylase that targets Cx43. We next deciphered whether Elongator also promotes Cx43 acetylation in N2A cell line. For this purpose, we infected

N2A cells with a lentivirus delivering shRNA against ELP1, because it has previously been reported to destabilize the Elongator complex (Petrakis et al., 2004; Close et al., 2006; Creppe et al., 2009). As shown in **Figure 4A**, ELP1 depletion in N2A cells resulted in decreased Cx43 acetylation level. We further showed that inhibition of HDACs activity was not sufficient to counteract the impact of the depletion of ELP1 on Cx43 acetylation (**Figure 4B**). Altogether, these results suggest that Elongator is necessary for proper acetylation of Cx43, a post-translational modification removed at least in part by HDAC6.

Acetylation of Cx43 Regulates its Membrane Localization *In Vitro*

It has been previously shown that acetylated Cx43 delocalizes from the membrane and is mainly found in the cytoplasm and in the nucleus (Colussi et al., 2011). We thus analyzed the cellular localization of Cx43 in Hela cells before and after TSA treatment. We overexpressed Cx43 and showed that in basal conditions, Cx43 formed connexons at the contact points between cells (**Figure 5A**). However, TSA treatment delocalized Cx43 from the membrane to a more cytoplasmic position (**Figures 5B,E**), in line with previous results (Colussi et al., 2011). As Cx43 contains many lysine residues, we used the posttranslational modification database PHOSIDA to identify potentially acetylable lysines (Gnad et al., 2011). We identified four lysines (K) predicted to be acetylated with more than 90% confidence: K9, K162, K234 and K264. In order to generate a non-acetylable form of Cx43, we replaced the four corresponding lysines by arginine residues (R), as previously described (Li et al., 2002; Qiang et al., 2010; Colussi et al., 2011; Jiménez-Canino et al., 2016). Cx43-4KR was also found in connexons connecting Hela cells (**Figures 5C,E**), but unlike Cx43-WT, TSA treatment did not trigger its delocalization from the membrane, and Cx43-4KR was still found at the contact points between cells after TSA treatment (**Figures 5D,E**). This suggests that the cellular localization of Cx43 is regulated through acetylation, which triggers Cx43 delocalization from the membrane.

Increased Cx43 Membrane Localization in the VZ Progenitor Cells of Elp3cKO

As Cx43 acetylation regulates its subcellular localization and is reduced in Elp3cKO embryonic cortices, we assessed the impact of the loss of Elp3 on Cx43 localization. We labeled Cx43 in E14.5 WT and Elp3cKO cortex with a specific antibody, which detects Cx43 only when present at the membrane (IF1 antibody; Sosinsky et al., 2007) and analyzed its distribution in the cortical wall. In WT cortex, we observed membrane Cx43 labeling throughout the cortical wall with some accumulation detected in the VZ/SVZ, as compared to the IZ and CP (**Figures 6A–F**). In the Elp3cKO cortex, we observed a reduced Cx43 labeling in the IZ/CP compared to the WT littermate (**Figures 6G,H**), which is likely the consequence of the reduced neuron population observed upon loss of Elp3 in cortical progenitors (Laguesse et al., 2015). However, as shown in **Figures 6I–L**, our results showed a stronger labeling of Cx43 in the VZ progenitor cells of Elp3cKO embryos compared to the WT cortex, without change of total Cx43 protein and mRNA expression (**Figures 2B,C**). This suggests that the reduced acetylation of Cx43 occurring upon loss of Elongator activity promotes its membrane localization.

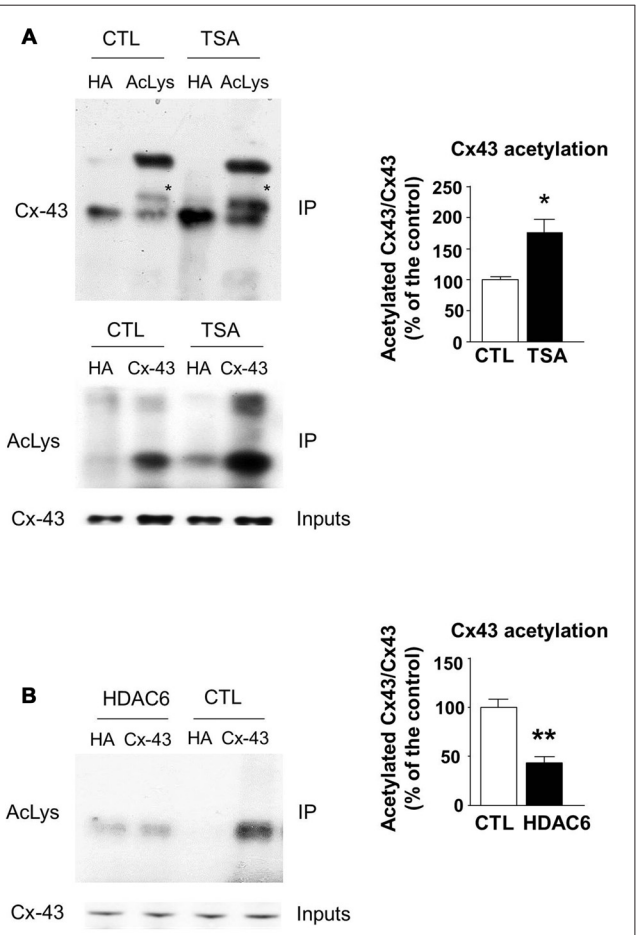

FIGURE 3 | Histones deacetylase 6 (HDAC6) regulates Cx43 acetylation levels. (A) U87 cells were treated with trichostatine A (TSA) or DMSO as control (CTL) for 4 h. Immunoprecipitation (IP) were carried out using anti-pan acetyl lysine antibodies or anti-HA as control, followed by western blot analysis using specific anti-Cx43 antibody (upper panel); or Cx43 IP was carried out and followed by western blot using anti-pan acetyl lysine antibody (lower panel). Corresponding western blot were performed on crude cell extracts (inputs). Data are presented as the average ratio of acetylated Cx43 to Cx43 ± SEM, and are expressed as percentage of control. Significance was determined using two-tailed unpaired *t*-test $t_{(4)} = 3.29$, $p = 0.03$. $n = 3$. Stars indicate the band corresponding to Cx43. **(B)** N2A cells were transfected with Cx43 and HDAC6 or the empty plasmid as control (CTL) and were lysed 48 h later. IPs were carried out using anti-Cx43 or anti-HA antibodies and followed by western blot analysis using a pan acetyl lysine antibody. Data are presented as the average ratio of acetylated Cx43 to Cx43 ± SEM, and are expressed as percentage of control. Significance was determined using two-tailed unpaired *t*-test $t_{(4)} = 5.12$, $p = 0.007$. $n = 3$. $^{*}p < 0.05$; $^{**}p < 0.01$.

DISCUSSION

Here we present evidences showing that Cx43 is acetylated and interacts with Elongator in the developing cortex as well

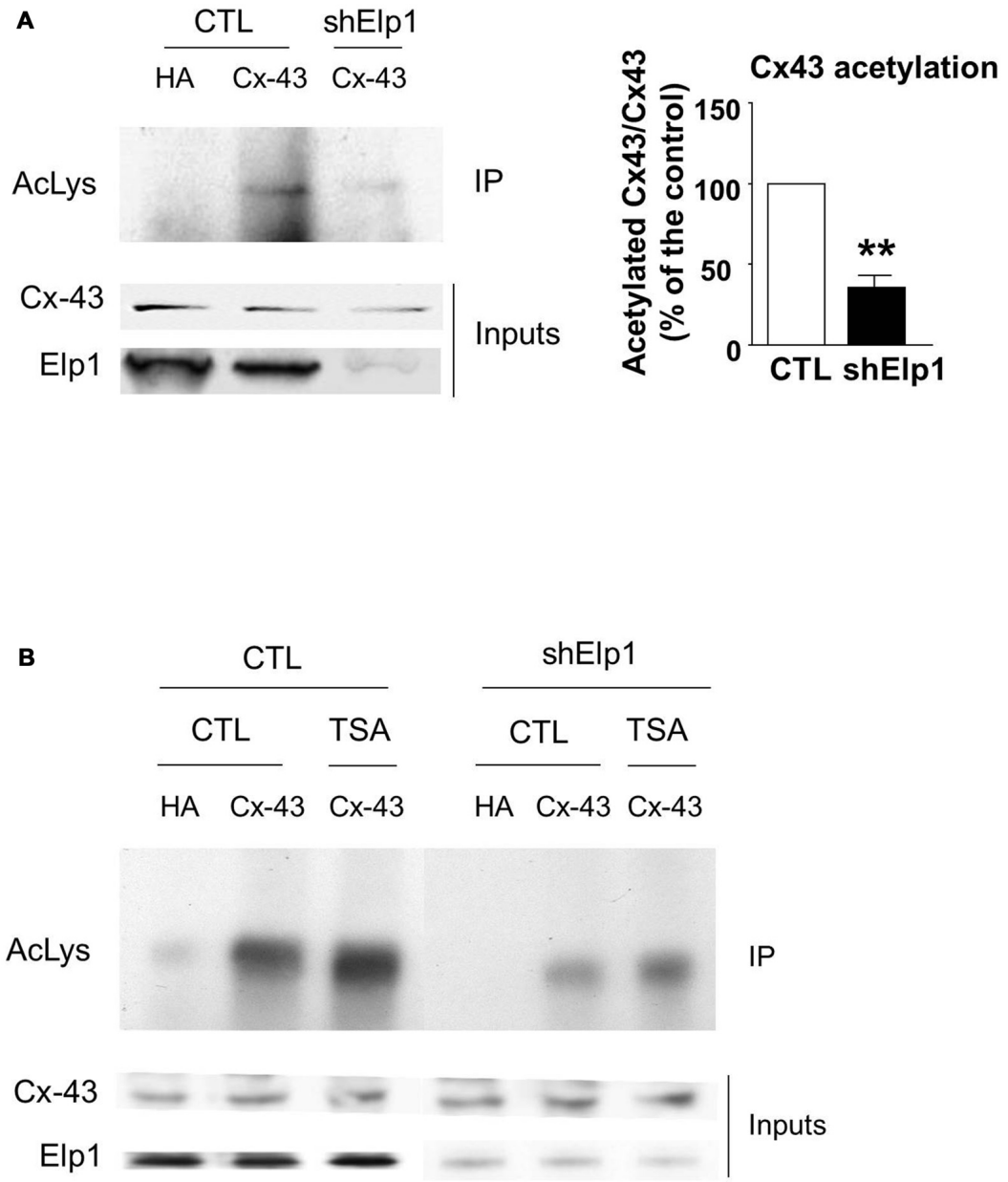

FIGURE 4 | Elongator depletion results in reduced Cx43 acetylation levels. (A,B) N2A cells were transfected with Cx43 and were infected 24 h later with Ltv-shElp1 or Ltv-SCR as control (CTL). Seventy-two hours after lentiviral infection, cells were treated with TSA or DMSO for 4 h **(B)** and IP of Cx43 was carried out, followed by western blot using an anti-pan acetyl lysine antibody. Corresponding western blots were performed on crude cell extracts (inputs). Data are presented as the average ratio of acetylated Cx43 to Cx43 ± SEM, and are expressed as percentage of control. Significance was determined using two-tailed unpaired *t*-test $t_{(3)} = 6.77$, $p = 0.007$. $n = 3$. $^{**}p < 0.01$.

as in several cell lines. We further show that depletion of Elongator *in vivo* impairs the acetylation of Cx43, suggesting that Elp3 promotes Cx43 acetylation in the developing cerebral cortex. We also identified HDAC6 as a deacetylase of Cx43. Finally, our data suggest that the acetylation of Cx43 regulates its localization in cortical progenitors.

We previously reported that Elongator controls the radial migration of projection neurons partly through α-tubulin acetylation (Creppe et al., 2009). However, Elongator is also functionally expressed in cortical progenitor cells, where loss of its activity results in impaired tRNA modification and protein translation, triggering the unfolded protein response that ultimately leads to defects in neurogenesis (Laguesse et al., 2015). Given that Elongator functions in neuronal migration and is expressed in cortical progenitors, we reasoned that Elongator could triggers the early steps of neuronal migration

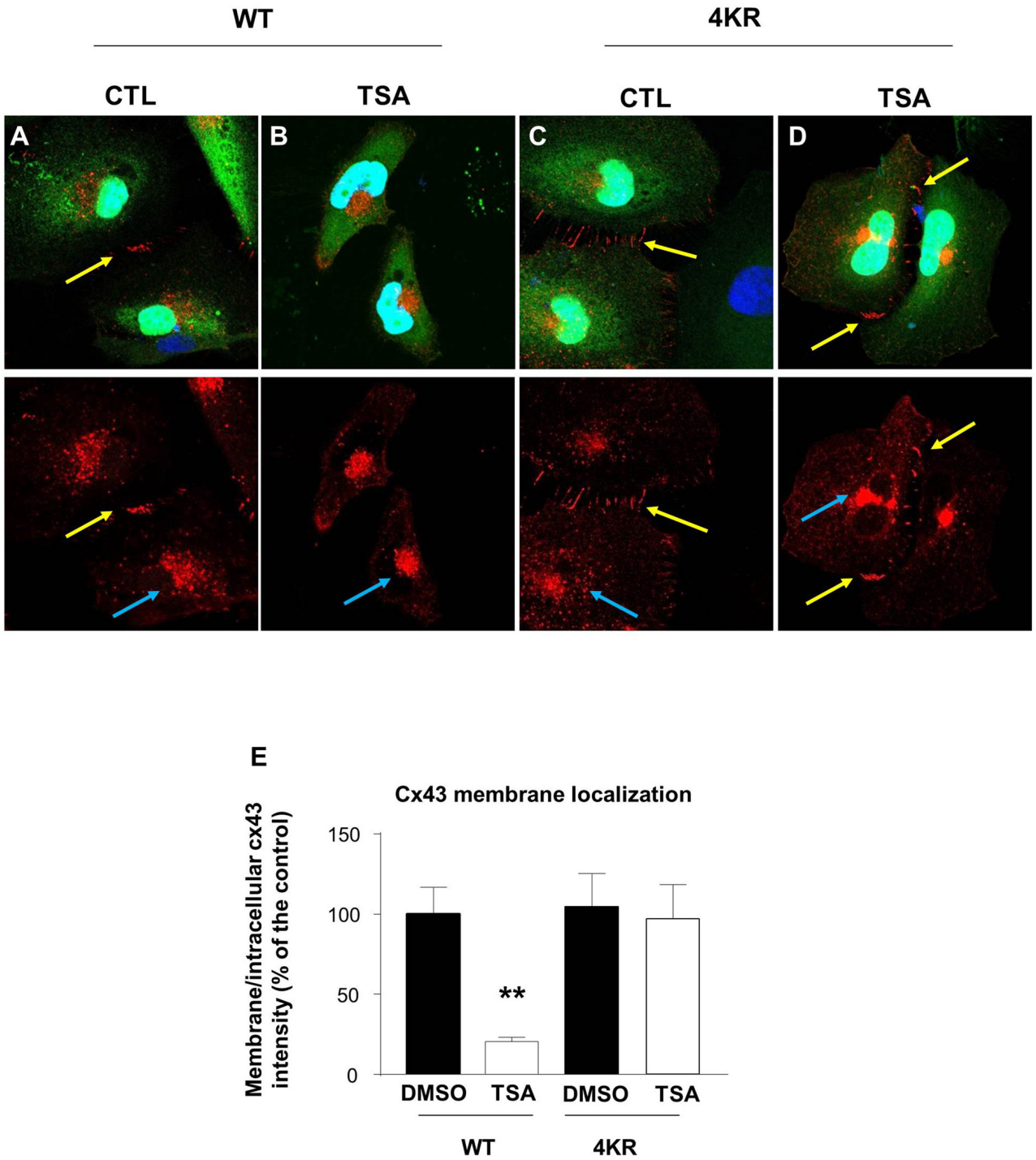

FIGURE 5 | Acetylation regulates Cx43 localization. (A–D) Hela cells were transfected with Cx43-WT-GFP **(A,B)** or Cx43-4KR-GFP **(C,D)** and were treated with TSA or DMSO as control (CTL) for 4 h. Immunodetection of Cx43 (red, cx43 rabbit, Abcam) in transfected Hela cells (green, GFP) and DAPI (blue) showed the different cellular localization of Cx43-WT and Cx43-4KR upon TSA treatment. Yellow arrows indicate connexons between two adjacent cells; blue arrows indicate intracellular Cx43 labeling. **(E)** Cx43 membrane localization was determined by measuring the ratio of membrane and intracellular immunofluorescence intensity. $^{**}p < 0.01$.

in the projection neuron progenitors. Cx43 is mainly expressed in the VZ/SVZ of the developing cortex and its loss has been reported to delay radial migration of projection neurons (Elias and Kriegstein, 2008; Cina et al., 2009), a phenotype

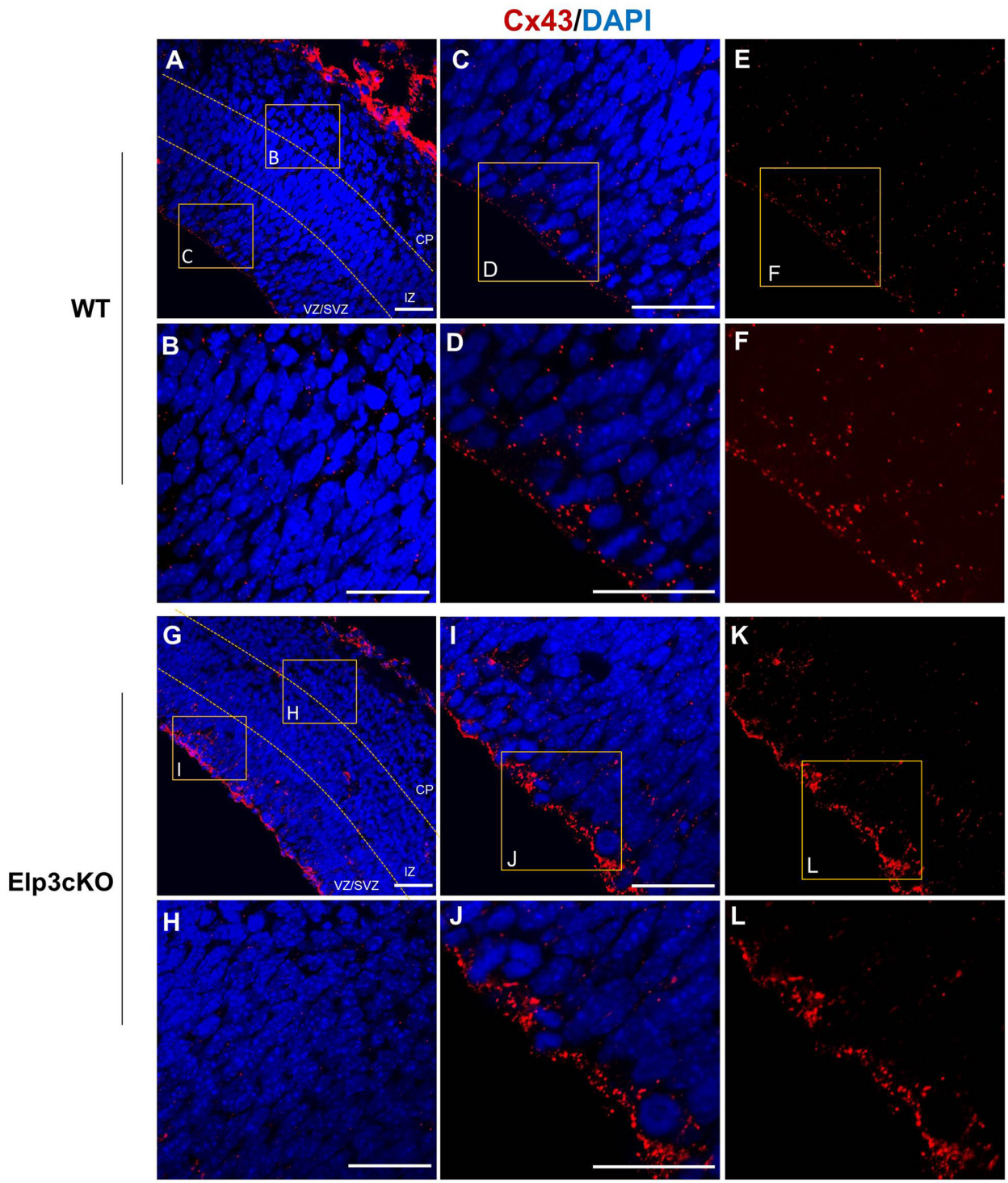

FIGURE 6 | Cx43 membrane localization is enhanced in Elp3cKO cortical progenitors. (A–L) Immunodetection of membrane Cx43 (red, Cx43 IF1 antibody) and DAPI (blue) in the cortical wall of WT **(A–F)** and Elp3cKO **(G–L)** E14.5 embryos show increased membrane distribution of Cx43 in the VZ progenitor cells of Elp3cKO embryos compared to WT embryos. Bar scale, 50 μm.

similar to the one observed upon knockdown of Elongator subunits (Creppe et al., 2009). We found that Cx43 interacts with both Elp1 and Elp3 in the developing cortex, as well as in several cell lines. We also showed the existence of a co-expression

of Cx43 and Elongator throughout the cortical wall, which is stronger in neuronal progenitors lining the lateral ventricle. This suggests a potential regulation of Cx43 by Elongator in the VZ/SVZ of the developing cortex.

Cx43 is regulated by several post-translational modifications, including phosphorylation (Solan and Lampe, 2009; Alstrom et al., 2015), ubiquitination (Ribeiro-Rodrigues et al., 2015; Leithe, 2016), nitrosylation (Johnstone et al., 2012; Lohman et al., 2016) and acetylation (Colussi et al., 2011; Meraviglia et al., 2015). These modifications regulate a great variety of biological processes, including degradation, changes in binding partners or subcellular localization. We showed that Cx43 is acetylated in the developing cortex, and that its acetylation is reduced in the cortex of Elp3cKO embryos. Our results suggest a new role for Elp3 in the regulation of Cx43 acetylation *in vivo*, which is further supported by results obtained in cell lines. Thus, along with α-tubulin in migrating projection neurons (Creppe et al., 2009) and bruchpilot at the pre-synaptic density of the *Drosophila* neuromuscular junctions whose acetylation is necessary for proper structure of the synapse (Miskiewicz et al., 2011), we suggest that Cx43 is another putative target of Elp3 in VZ/SVZ progenitors of the developing cortex. However, whether Cx43 acetylation is directly regulated by the acetyltransferase activity of Elp3, or indirectly via the upregulated unfolded protein response observed in cortical progenitors of Elp3cKO embryos (Laguesse et al., 2015) is still an open question.

Interestingly, Cx43 acetylation in cardiomyocytes requires the activity of the histone acetyltransferase p300/CBP-associated factor (PCAF), which is a member of the Gcn5-related N-acetyltransferase (GNAT) HAT family that also comprises Elp3 (Sterner and Berger, 2000). Similar to Elp3, PCAF has been shown to acetylate non-histones proteins such as β-catenin (Ge et al., 2009), Akt1 (Zhang et al., 2015), Stat3 (Cai et al., 2014) and lin28 (Wang et al., 2014). It would be interesting to test whether PCAF is also involved in the regulation of Cx43 acetylation in the developing cortex. On the other hand, we showed that Cx43 acetylation is increased upon TSA treatment, suggesting that Cx43 deacetylation depends on HDACs, and we further identified HDAC6 as one deacetylase of Cx43. HDAC6 has a cytoplasmic localization and has been shown to acetylate α-tubulin, as well as other cytoplasmic targets such as HSP90, Cortactin or β-catenin (Li et al., 2011; Yao and Yang, 2011). Interestingly, Colussi et al. (2011) showed a constitutive association of HDAC3, -4 and -5 with Cx43 in cardiomyocytes, and a co-localization at the membrane but also in cytoplasmic and nuclear compartments. These HDACs are known to dynamically shuttle between the nucleus and the cytoplasm in a signal-dependent manner (Li and Yang, 2016). It would thus be of interest to test whether these HDACs could also regulate Cx43 acetylation in the developing cortex.

Phosphorylation and acetylation of Cx43 have been shown to regulate its cellular localization (Sosinsky et al., 2007; Colussi et al., 2011; Qi et al., 2016). Indeed, in migrating neurons, Cx43 phosphorylation at Ser^{279} and Ser^{282} has been found to block its membrane expression and to promote proteasome-dependent degradation (Qi et al., 2016). In cardiomyocytes, Cx43 acetylation leads to its delocalization from the membrane toward intracellular compartment (Colussi et al., 2011). In line with the latter result, we showed in Hela cells that Cx43-WT was present at the membrane under normal conditions, but delocalized from the membrane following TSA treatment. The non-acetylable Cx43-4KR was also found at the membrane in normal conditions, but TSA treatment did not modify its cellular localization, strengthening the idea that Cx43 acetylation regulates its subcellular localization. Our data also showed an excessive membrane localization of Cx43 in the VZ progenitor cells upon loss of Elp3, suggesting that Elp3-dependent acetylation regulates Cx43 cellular localization in neuronal progenitor cells during cortex development.

Cx43 is a GAP junction subunit expressed in many cell types and tissues (Oyamada et al., 2005). Six Cx43 monomers associate to form hexameric hemichannels, also called connexons, which can combine with connexons on adjacent cells to form GAP junctions allowing the exchange of small molecules and ions (Laird, 2006). Besides the communication properties of GAP junctions, it has been reported that connexons can transport ATP and assist in calcium signaling (Goodenough and Paul, 2003) and also promote adhesion in migrating projection neurons (Lin et al., 2002; Elias et al., 2007, 2010; Cotrina et al., 2008; Elias and Kriegstein, 2008). Specifically, it has been shown that Cx43 is necessary for radial migration of projection neurons as well as for the tangential to radial migratory switch in migrating interneurons, and that this function of Cx43 is mediated by adhesion properties of GAP junctions/connexon rather than their channel function (Elias et al., 2007, 2010; Kameritsch et al., 2012). It would thus be interesting to test whether Cx43 acetylation controls the adhesion properties of connexons between cortical progenitor cells or between migrating neurons and radial glia, and determine if replacing the endogenous Cx43 with Cx43-4KR would lead to adhesion and/or migration defects.

AUTHOR CONTRIBUTIONS

SL and LN designed the experiment. SL performed the experiment and SL and PC analyzed the data. PC generated the flag-Elp3 cell line. SL and LN wrote the manuscript. BM, AC and PC edited the manuscript. LVH participated in the revisions. All authors discussed the results and implications and commented on the manuscript.

ACKNOWLEDGMENTS

LN and PC, are Research Associates from Fonds De La Recherche Scientifique (F.R.S)-F.N.R.S. and BM and AC are Directors from F.R.S-F.N.R.S. This work was supported by the F.R.S.-F.N.R.S., the Fonds Léon Fredericq, the Fondation Médicale Reine Elisabeth, the Fondation Simone et Pierre Clerdent, the Belgian Science Policy (IAP-VII network P7/20; to LN), ARC (ARC11/16-01 to LN and AC), the ERANET Neuron (STEM-MCD to LN); AC is funded by the WELBIO Program of the Walloon Region.

REFERENCES

Alstrom, J. S., Stroemlund, L. W., Nielsen, M. S., and MacAulay, N. (2015). Protein kinase C-dependent regulation of connexin43 gap junctions and hemichannels. *Biochem. Soc. Trans.* 43, 519–523. doi: 10.1042/BST20150040

Cai, K., Wan, Y., Wang, Z., Wang, Y., Zhao, X., and Bao, X. (2014). C5a promotes the proliferation of human nasopharyngeal carcinoma cells through PCAF-mediated STAT3 acetylation. *Oncol. Rep.* 32, 2260–2266. doi: 10.3892/or.2014.3420

Cina, C., Maass, K., Theis, M., Willecke, K., Bechberger, J. F., and Naus, C. C. (2009). Involvement of the cytoplasmic C-terminal domain of connexin43 in neuronal migration. *J. Neurosci.* 29, 2009–2021. doi: 10.1523/JNEUROSCI.5025-08.2009

Close, P., Hawkes, N., Cornez, I., Creppe, C., Lambert, C. A., Rogister, B., et al. (2006). Transcription impairment and cell migration defects in elongator-depleted cells: implication for familial dysautonomia. *Mol. Cell* 22, 521–531. doi: 10.1016/j.molcel.2006.04.017

Codd, R., Braich, N., Liu, J., Soe, C. Z., and Pakchung, A. A. (2009). Zn(II)-dependent histone deacetylase inhibitors: suberoylanilide hydroxamic acid and trichostatin A. *Int. J. Biochem. Cell Biol.* 41, 736–739. doi: 10.1016/j.biocel.2008.05.026

Colussi, C., Rosati, J., Straino, S., Spallotta, F., Berni, R., Stilli, D., et al. (2011). Nepsilon-lysine acetylation determines dissociation from GAP junctions and lateralization of connexin 43 in normal and dystrophic heart. *Proc. Natl. Acad. Sci. U S A* 108, 2795–2800. doi: 10.1073/pnas.1013124108

Cotrina, M. L., Lin, J. H., and Nedergaard, M. (2008). Adhesive properties of connexin hemichannels. *Glia* 56, 1791–1798. doi: 10.1002/glia.20728

Creppe, C., Malinouskaya, L., Volvert, M. L., Gillard, M., Close, P., Malaise, O., et al. (2009). Elongator controls the migration and differentiation of cortical neurons through acetylation of alpha-tubulin. *Cell* 136, 551–564. doi: 10.1016/j.cell.2008.11.043

Delaunay, S., Rapino, F., Tharun, L., Zhou, Z., Heukamp, L., Termathe, M., et al. (2016). Elp3 links tRNA modification to IRES-dependent translation of LEF1 to sustain metastasis in breast cancer. *J. Exp. Med.* 213, 2503–2523. doi: 10.1084/jem.20160397

Elias, L. A., and Kriegstein, A. R. (2008). Gap junctions: multifaceted regulators of embryonic cortical development. *Trends Neurosci.* 31, 243–250. doi: 10.1016/j.tins.2008.02.007

Elias, L. A., Turmaine, M., Parnavelas, J. G., and Kriegstein, A. R. (2010). Connexin 43 mediates the tangential to radial migratory switch in ventrally derived cortical interneurons. *J. Neurosci.* 30, 7072–7077. doi: 10.1523/JNEUROSCI.5728-09.2010

Elias, L. A., Wang, D. D., and Kriegstein, A. R. (2007). Gap junction adhesion is necessary for radial migration in the neocortex. *Nature* 448, 901–907. doi: 10.1038/nature06063

Ge, X., Jin, Q., Zhang, F., Yan, T., and Zhai, Q. (2009). PCAF acetylates β-catenin and improves its stability. *Mol. Biol. Cell* 20, 419–427. doi: 10.1091/mbc.e08-08-0792

Glatt, S., and Müller, C. W. (2013). Structural insights into Elongator function. *Curr. Opin. Struct. Biol.* 23, 235–242. doi: 10.1016/j.sbi.2013.02.009

Glatt, S., Séraphin, B., and Müller, C. W. (2012). Elongator: transcriptional or translational regulator? *Transcription* 3, 273–276. doi: 10.4161/trns.21525

Gnad, F., Gunawardena, J., and Mann, M. (2011). PHOSIDA 2011: the posttranslational modification database. *Nucleic Acids Res.* 39, D253–D260. doi: 10.1093/nar/gkq1159

Goodenough, D. A., and Paul, D. L. (2003). Beyond the gap: functions of unpaired connexon channels. *Nat. Rev. Mol. Cell Biol.* 4, 285–294. doi: 10.1038/nrm1072

Götz, M., and Huttner, W. B. (2005). The cell biology of neurogenesis. *Nat. Rev. Mol. Cell Biol.* 6, 777–788. doi: 10.1038/nrm1739

Hébert, J. M., and McConnell, S. K. (2000). Targeting of cre to the *Foxg1 (BF-1)* locus mediates *loxP* recombination in the telencephalon and other developing head structures. *Dev. Biol.* 222, 296–306. doi: 10.1006/dbio.2000.9732

Jiménez-Canino, R., Lorenzo-Díaz, F., Jaisser, F., Farman, N., Giraldez, T., and Alvarez de la Rosa, D. (2016). Histone deacetylase 6-controlled Hsp90 acetylation significantly alters mineralocorticoid receptor subcellular dynamics but not its transcriptional activity. *Endocrinology* 157, 2515–2532. doi: 10.1210/en.2015-2055

Johnstone, S. R., Billaud, M., Lohman, A. W., Taddeo, E. P., and Isakson, B. E. (2012). Posttranslational modifications in connexins and pannexins. *J. Membr. Biol.* 245, 319–332. doi: 10.1007/s00232-012-9453-3

Kameritsch, P., Pogoda, K., and Pohl, U. (2012). Channel-independent influence of connexin 43 on cell migration. *Biochim. Biophys. Acta* 1818, 1993–2001. doi: 10.1016/j.bbamem.2011.11.016

Kovacs, J. J., Murphy, P. J., Gaillard, S., Zhao, X., Wu, J. T., Nicchitta, C. V., et al. (2005). HDAC6 regulates Hsp90 acetylation and chaperone-dependent activation of glucocorticoid receptor. *Mol. Cell* 18, 601–607. doi: 10.1016/j.molcel.2005.04.021

Kriegstein, A. R., and Noctor, S. C. (2004). Patterns of neuronal migration in the embryonic cortex. *Trends Neurosci.* 27, 392–399. doi: 10.1016/j.tins.2004.05.001

Ladang, A., Rapino, F., Heukamp, L. C., Tharun, L., Shostak, K., Hermand, D., et al. (2015). Elp3 drives Wnt-dependent tumor initiation and regeneration in the intestine. *J. Exp. Med.* 212, 2057–2075. doi: 10.1084/jem.20142288

Laguesse, S., Creppe, C., Nedialkova, D. D., Prévot, P. P., Borgs, L., Huysseune, S., et al. (2015). A dynamic unfolded protein response contributes to the control of cortical neurogenesis. *Dev. Cell* 35, 553–567. doi: 10.1016/j.devcel.2015.11.005

Laird, D. W. (2006). Life cycle of connexins in health and disease. *Biochem. J.* 394, 527–543. doi: 10.1042/bj20051922

Leithe, E. (2016). Regulation of connexins by the ubiquitin system: implications for intercellular communication and cancer. *Biochim. Biophys. Acta* 1865, 133–146. doi: 10.1016/j.bbcan.2016.02.001

Li, G., Jiang, H., Chang, M., Xie, H., and Hu, L. (2011). HDAC6 alpha-tubulin deacetylase: a potential therapeutic target in neurodegenerative diseases. *J. Neurol. Sci.* 304, 1–8. doi: 10.1016/j.jns.2011.02.017

Li, M., Luo, J., Brooks, C. L., and Gu, W. (2002). Acetylation of p53 inhibits its ubiquitination by Mdm2. *J. Biol. Chem.* 277, 50607–50611. doi: 10.1074/jbc.c200578200

Li, L., and Yang, X. J. (2016). Molecular and functional characterization of histone deacetylase 4 (HDAC4). *Methods Mol. Biol.* 1436, 31–45. doi: 10.1007/978-1-4939-3667-0_4

Lin, J. H., Takano, T., Cotrina, M. L., Arcuino, G., Kang, J., Liu, S., et al. (2002). Connexin 43 enhances the adhesivity and mediates the invasion of malignant glioma cells. *J. Neurosci.* 22, 4302–4311.

Liu, J. S. (2011). Molecular genetics of neuronal migration disorders. *Curr. Neurol. Neurosci. Rep.* 11, 171–178. doi: 10.1007/s11910-010-0176-5

Liu, X., Hashimoto-Torii, K., Torii, M., Ding, C., and Rakic, P. (2010). Gap junctions/hemichannels modulate interkinetic nuclear migration in the forebrain precursors. *J. Neurosci.* 30, 4197–4209. doi: 10.1523/JNEUROSCI.4187-09.2010

Liu, X., Sun, L., Torii, M., and Rakic, P. (2012). Connexin 43 controls the multipolar phase of neuronal migration to the cerebral cortex. *Proc. Natl. Acad. Sci. U S A* 109, 8280–8285. doi: 10.1073/pnas.1205880109

Lohman, A. W., Straub, A. C., and Johnstone, S. R. (2016). Identification of connexin43 phosphorylation and S-nitrosylation in cultured primary vascular cells. *Methods Mol. Biol.* 1437, 97–111. doi: 10.1007/978-1-4939-3664-9_7

Menzies, K. J., Zhang, H., Katsyuba, E., and Auwerx, J. (2016). Protein acetylation in metabolism - metabolites and cofactors. *Nat. Rev. Endocrinol.* 12, 43–60. doi: 10.1038/nrendo.2015.181

Meraviglia, V., Azzimato, V., Colussi, C., Florio, M. C., Binda, A., Panariti, A., et al. (2015). Acetylation mediates Cx43 reduction caused by electrical stimulation. *J. Mol. Cell. Cardiol.* 87, 54–64. doi: 10.1016/j.yjmcc.2015.08.001

Miskiewicz, K., Jose, L. E., Bento-Abreu, A., Fislage, M., Taes, I., Kasprowicz, J., et al. (2011). ELP3 controls active zone morphology by acetylating the ELKS family member Bruchpilot. *Neuron* 72, 776–788. doi: 10.1016/j.neuron.2011.10.010

Molyneaux, B. J., Arlotta, P., Menezes, J. R., and Macklis, J. D. (2007). Neuronal subtype specification in the cerebral cortex. *Nat. Rev. Neurosci.* 8, 427–437. doi: 10.1038/nrn2151

Moon, H. M., and Wynshaw-Boris, A. (2013). Cytoskeleton in action: lissencephaly, a neuronal migration disorder. *Wiley Interdiscip. Rev. Dev. Biol.* 2, 229–245. doi: 10.1002/wdev.67

Nguyen, L., Humbert, S., Saudou, F., and Chariot, A. (2010). Elongator—an emerging role in neurological disorders. *Trends Mol. Med.* 16, 1–6. doi: 10.1016/j.molmed.2009.11.002

Noctor, S. C., Flint, A. C., Weissman, T. A., Dammerman, R. S., and Kriegstein, A. R. (2001). Neurons derived from radial glial cells establish radial units in neocortex. *Nature* 409, 714–720. doi: 10.1038/35055553

Ohtaka-Maruyama, C., and Okado, H. (2015). Molecular pathways underlying projection neuron production and migration during cerebral cortical development. *Front. Neurosci.* 9:447. doi: 10.3389/fnins.2015.00447

Orellana, J. A., Martinez, A. D., and Retamal, M. A. (2013). Gap junction channels and hemichannels in the CNS: regulation by signaling molecules. *Neuropharmacology* 75, 567–582. doi: 10.1016/j.neuropharm.2013.02.020

Oyamada, M., Oyamada, Y., and Takamatsu, T. (2005). Regulation of connexin expression. *Biochim. Biophys. Acta* 1719, 6–23. doi: 10.1016/j.bbamem.2005.11.002

Petrakis, T. G., Wittschieben, B. O., and Svejstrup, J. Ø. (2004). Molecular architecture, structure-function relationship, and importance of the Elp3 subunit for the RNA binding of holo-elongator. *J. Biol. Chem.* 279, 32087–32092. doi: 10.1074/jbc.M403361200

Qi, G. J., Chen, Q., Chen, L. J., Shu, Y., Bu, L. L., Shao, X. Y., et al. (2016). Phosphorylation of connexin 43 by Cdk5 modulates neuronal migration during embryonic brain development. *Mol. Neurobiol.* 53, 2969–2982. doi: 10.1007/s12035-015-9190-6

Qiang, L., Banks, A. S., and Accili, D. (2010). Uncoupling of acetylation from phosphorylation regulates FoxO1 function independent of its subcellular localization. *J. Biol. Chem.* 285, 27396–27401. doi: 10.1074/jbc.M110.140228

Ribeiro-Rodrigues, T. M., Catarino, S., Pinho, M. J., Pereira, P., and Girao, H. (2015). Connexin 43 ubiquitination determines the fate of gap junctions: restrict to survive. *Biochem. Soc. Trans.* 43, 471–475. doi: 10.1042/BST20150036

Rinaldi, F., Hartfield, E. M., Crompton, L. A., Badger, J. L., Glover, C. P., Kelly, C. M., et al. (2014). Cross-regulation of Connexin43 and beta-catenin influences differentiation of human neural progenitor cells. *Cell Death Dis.* 5:e1017. doi: 10.1038/cddis.2013.546

Roche, J., and Bertrand, P. (2016). Inside HDACs with more selective HDAC inhibitors. *Eur. J. Med. Chem.* 121, 451–483. doi: 10.1016/j.ejmech.2016.05.047

Rouach, N., Avignone, E., Meme, W., Koulakoff, A., Venance, L., Blomstrand, F., et al. (2002). Gap junctions and connexin expression in the normal and pathological central nervous system. *Biol. Cell* 94, 457–475. doi: 10.1016/s0248-4900(02)00016-3

Santiago, M. F., Alcami, P., Striedinger, K. M., Spray, D. C., and Scemes, E. (2010). The carboxyl-terminal domain of connexin43 is a negative modulator of neuronal differentiation. *J. Biol. Chem.* 285, 11836–11845. doi: 10.1074/jbc.M109.058750

Simon, R. P., Robaa, D., Alhalabi, Z., Sippl, W., and Jung, M. (2016). KATching-Up on small molecule modulators of lysine acetyltransferases. *J. Med. Chem.* 59, 1249–1270. doi: 10.1021/acs.jmedchem.5b01502

Solan, J. L., and Lampe, P. D. (2009). Connexin43 phosphorylation: structural changes and biological effects. *Biochem. J.* 419, 261–272. doi: 10.1042/BJ20082319

Sosinsky, G. E., Solan, J. L., Gaietta, G. M., Ngan, L., Lee, G. J., Mackey, M. R., et al. (2007). The C-terminus of connexin43 adopts different conformations in the Golgi and gap junction as detected with structure-specific antibodies. *Biochem. J.* 408, 375–385. doi: 10.1042/bj20070550

Sterner, D. E., and Berger, S. L. (2000). Acetylation of histones and transcription-related factors. *Microbiol. Mol. Biol. Rev.* 64, 435–459. doi: 10.1128/mmbr.64.2.435-459.2000

Sutor, B., and Hagerty, T. (2005). Involvement of gap junctions in the development of the neocortex. *Biochim. Biophys. Acta* 1719, 59–68. doi: 10.1016/j.bbamem.2005.09.005

Tielens, S., Huysseune, S., Godin, J. D., Chariot, A., Malgrange, B., and Nguyen, L. (2016). Elongator controls cortical interneuron migration by regulating actomyosin dynamics. *Cell Res.* 26, 1131–1148. doi: 10.1038/cr.2016.112

Viatour, P., Legrand-Poels, S., van Lint, C., Warnier, M., Merville, M. P., Gielen, J., et al. (2003). Cytoplasmic IkappaBalpha increases NF-kappaB-independent transcription through binding to histone deacetylase (HDAC) 1 and HDAC3. *J. Biol. Chem.* 278, 46541–46548. doi: 10.1074/jbc.M306381200

Wang, L. X., Wang, J., Qu, T. T., Zhang, Y., and Shen, Y. F. (2014). Reversible acetylation of Lin28 mediated by PCAF and SIRT1. *Biochim. Biophys. Acta* 1843, 1188–1195. doi: 10.1016/j.bbamcr.2014.03.001

Winkler, G. S., Kristjuhan, A., Erdjument-Bromage, H., Tempst, P., and Svejstrup, J. Q. (2002). Elongator is a histone H3 and H4 acetyltransferase important for normal histone acetylation levels *in vivo*. *Proc. Natl. Acad. Sci. U S A* 99, 3517–3522. doi: 10.1073/pnas.022042899

Yao, Y. L., and Yang, W. M. (2011). Beyond histone and deacetylase: an overview of cytoplasmic histone deacetylases and their nonhistone substrates. *J. Biomed. Biotechnol.* 2011:146493. doi: 10.1155/2011/146493

Zhang, S., Sun, G., Wang, Z., Wan, Y., Guo, J., and Shi, L. (2015). PCAF-mediated Akt1 acetylation enhances the proliferation of human glioblastoma cells. *Tumour Biol.* 36, 1455–1462. doi: 10.1007/s13277-014-2522-8

Zhang, X., Yuan, Z., Zhang, Y., Yong, S., Salas-Burgos, A., Koomen, J., et al. (2007). HDAC6 modulates cell motility by altering the acetylation level of cortactin. *Mol. Cell* 27, 197–213. doi: 10.1016/j.molcel.2007.05.033

Conflict of Interest Statement: The authors declare that the research was conducted in the absence of any commercial or financial relationships that could be construed as a potential conflict of interest.

frontiers in Cellular Neuroscience

ORIGINAL RESEARCH
published: 20 April 2017
doi: 10.3389/fncel.2017.00107

The Kinesin Adaptor Calsyntenin-1 Organizes Microtubule Polarity and Regulates Dynamics during Sensory Axon Arbor Development

Tristan J. Lee[1,2,3], *Jacob W. Lee*[1,2], *Elizabeth M. Haynes*[1,2,4], *Kevin W. Eliceiri*[4] *and Mary C. Halloran*[1,2,3]*

[1] Department of Zoology, University of Wisconsin-Madison, Madison, WI, USA, [2] Department of Neuroscience, University of Wisconsin-Madison, Madison, WI, USA, [3] Neuroscience Training Program, University of Wisconsin-Madison, Madison, WI, USA, [4] Laboratory for Optical and Computational Instrumentation, University of Wisconsin-Madison, Madison, WI, USA

Axon growth and branching, and development of neuronal polarity are critically dependent on proper organization and dynamics of the microtubule (MT) cytoskeleton. MTs must organize with correct polarity for delivery of diverse cargos to appropriate subcellular locations, yet the molecular mechanisms regulating MT polarity remain poorly understood. Moreover, how an actively branching axon reorganizes MTs to direct their plus ends distally at branch points is unknown. We used high-speed, *in vivo* imaging of polymerizing MT plus ends to characterize MT dynamics in developing sensory axon arbors in zebrafish embryos. We find that axonal MTs are highly dynamic throughout development, and that the peripheral and central axons of sensory neurons show differences in MT behaviors. Furthermore, we show that Calsyntenin-1 (Clstn-1), a kinesin adaptor required for sensory axon branching, also regulates MT polarity in developing axon arbors. In wild type neurons the vast majority of MTs are directed in the correct plus-end-distal orientation from early stages of development. Loss of Clstn-1 causes an increase in MTs polymerizing in the retrograde direction. These misoriented MTs most often are found near growth cones and branch points, suggesting Clstn-1 is particularly important for organizing MT polarity at these locations. Together, our results suggest that Clstn-1, in addition to regulating kinesin-mediated cargo transport, also organizes the underlying MT highway during axon arbor development.

Keywords: calsyntenin, EB3, axon branching, microtubule polarity, zebrafish

OPEN ACCESS

Edited by:
Froylan Calderon De Anda, University of Hamburg, Germany

Reviewed by:
Esther Stoeckli, University of Zurich, Switzerland
David Solecki, St. Jude Children's Research Hospital, USA

***Correspondence:**
Mary C. Halloran
mchalloran@wisc.edu

Received: *24 January 2017*
Accepted: *29 March 2017*
Published: *20 April 2017*

Citation:
Lee TJ, Lee JW, Haynes EM, Eliceiri KW and Halloran MC (2017) The Kinesin Adaptor Calsyntenin-1 Organizes Microtubule Polarity and Regulates Dynamics during Sensory Axon Arbor Development. Front. Cell. Neurosci. 11:107. doi: 10.3389/fncel.2017.00107

INTRODUCTION

Development of polarized neuronal morphology requires tight control of MT dynamics and orientation. MTs are important both for the motile processes that underlie neurite growth, and to provide tracks for directed axonal transport of molecular cargo. MTs must organize with correct polarity for delivery of cargos to specific cell locations via the direction-specific motors dynein and kinesins. In axons, MTs are organized with plus ends directed distally while dendrites have either mixed MT polarity in vertebrate neurons or mostly minus-end-distal MTs in invertebrates (reviewed in Baas and Lin, 2011). Although MT polarity is critical for neuronal development and function, the mechanisms that organize MTs remain poorly understood. The process of axon

branching involves increased MT dynamics (Yu et al., 1994; Dent et al., 1999; Gallo, 2011; Ketschek et al., 2015) and requires local MT severing (Yu et al., 2008; Qiang et al., 2010). New MT plus ends generated by severing, depolymerization, or nucleation, must be correctly organized with plus-ends-distal at branch points, yet how this is accomplished in an actively branching axon is unknown.

Increasing evidence shows that motor molecules have key roles in organizing MT polarity. The mitotic kinesins, Kinesin-6, and -12, which slide MTs along one another, contribute to MT polarity in mammalian neurons and regulate the transport of minus-end-distal MTs into dendrites (Yu et al., 2000; Lin et al., 2012). Kinesin-1 also can mediate MT sliding by crosslinking antiparallel MTs, a process that can drive initial neurite outgrowth in *Drosophila* neurons (Lu et al., 2013; del Castillo et al., 2015), and that contributes to MT polarity in *C. elegans* dendrites by transporting plus-end-distal MTs out of the dendrite (Yan et al., 2013). Kinesin-2, a motor that can associate with MT plus ends, functions to orient plus ends at dendritic branch points in *Drosophila* neurons (Mattie et al., 2010). The minus end directed motor protein dynein transports short MTs anterogradely along the actin network of axons in mammalian neurons (Ahmad et al., 1998; Baas and Mozgova, 2012). In *Drosophila,* dynein is required for correct MT polarity in axons, and acts by removing aberrant minus-end-distal MTs from the axons (Zheng et al., 2008; del Castillo et al., 2015). In addition to motor proteins, other MT binding proteins also have been shown to be important for organization of MT polarity, including *C. elegans* CRMP/UNC-33 (Maniar et al., 2011), vertebrate TRIM46 (van Beuningen et al., 2015), and the MT nucleator gamma-tubulin (Nguyen et al., 2014). Although several molecular players have been identified, our understanding of their mechanisms of action is incomplete, and whether additional regulators have roles in orchestrating MT polarity is not known.

Our data show that the kinesin adaptor Clstn-1 functions to organize MT polarity during axon development. Calsyntenins are cadherin superfamily transmembrane proteins expressed in the nervous system (Vogt et al., 2001; Hintsch et al., 2002). Several studies have demonstrated functions for calsyntenins in diverse processes including learning (Ikeda et al., 2008; Hoerndli et al., 2009), memory (Preuschhof et al., 2010) and synapse formation (Pettem et al., 2013; Um et al., 2014). Calsyntenins have also been implicated in Alzheimer's disease (Araki et al., 2003; Ringman et al., 2012; Vagnoni et al., 2012; Uchida et al., 2013). These studies indicate important roles for calsyntenins in neural function, although their mechanisms of action are still not well understood. Most known functions of Clstn-1 involve its ability to bind kinesin light chain (KLC) and link cargo to kinesin-1 motors. For example, Clstn-1 regulates trafficking and processing of amyloid precursor protein (Konecna et al., 2006; Araki et al., 2007; Steuble et al., 2012; Vagnoni et al., 2012) and mediates synapse maturation by trafficking NMDA receptors to synapses (Ster et al., 2014). We showed previously that Clstn-1 is required for sensory axon branching during development and that it functions in part by regulating endosomal transport from the cell body to developing axons and branch points (Ponomareva et al., 2014). In addition, Clstn-1 recently was shown to regulate localization of axon guidance receptors to growth cone membranes (Alther et al., 2016). Interestingly, Clstn-1 has been shown to activate kinesin-1 motor activity (Kawano et al., 2012). Its binding to KLC relieves KLC autoinhibition (Yip et al., 2016), which in turn allows KLC to bind kinesin heavy chain (KHC) and relieve KHC autoinhibition (Wong and Rice, 2010), thereby activating the motor. Thus, Clstn-1 can potentially influence axonal transport both by mediating cargo binding to motors and by affecting kinesin motor activity.

Multiple studies have used live imaging approaches with plus end binding proteins to visualize MT orientation and dynamics in developing neuronal axons in culture (e.g., Stepanova et al., 2003, 2010; Marx et al., 2013; Li et al., 2014). Live imaging in *Drosophila* neurons showed that MTs display mixed polarity at the initial stage of axon formation from the cell body, but then reorganize to become predominantly plus-end-distal as axons extend (del Castillo et al., 2015). Similarly, in cultured rat hippocampal neurons, immature neurites have mixed MT polarity and plus-end-distal polarity is established once the axon is specified (Kollins et al., 2009; Yau et al., 2016). Because the extracellular environment strongly influences intracellular signaling and cytoskeletal dynamics, a current challenge is to understand how MT behaviors are regulated as neurons develop *in vivo* under the influence of their natural cellular environment. This has been difficult because of technical challenges imaging such rapid processes in 3D neurons *in vivo*. However, recent studies have accomplished live *in vivo* imaging of MTs in invertebrate preparations (e.g., Zheng et al., 2008; Maniar et al., 2011; Yan et al., 2013; Nguyen et al., 2014) and in mouse brain (Kleele et al., 2014; Yau et al., 2016), although they have not characterized MT behaviors in axons that are actively developing *in vivo*.

Here we use zebrafish sensory neurons as a vertebrate model to investigate MT dynamics and development of MT polarity *in vivo*. Vertebrate sensory neurons extend separate axons to the central nervous system and to the periphery. The central and peripheral axons grow along distinct pathways through very different extracellular environments, and are guided by different molecular signals and substrates (Liu and Halloran, 2005; Andersen et al., 2011). The peripheral axons branch extensively, while central axons do not. Thus, sensory neurons provide an excellent model to study MT behavior in branching vs. non-branching axons and in separate axon compartments of one neuron. We used high-speed, high resolution swept field confocal microscopy and EB3-GFP to image MT dynamics as axons develop in their natural 3D environment. Interestingly, we find differences in MT dynamics in central vs. peripheral axons, potentially reflecting different molecular signals acting in the two axon types. Moreover, we find that Clstn-1 is required for proper MT polarity specifically in peripheral axons. Peripheral axons in Clstn-1 mutant embryos showed an increased percentage and frequency of retrograde EB3-GFP comets. These aberrant retrograde comets originate predominantly near growth cones and branch points, suggesting Clstn-1 may function specifically at these locations to organize MT polarity.

MATERIALS AND METHODS

Animals

Zebrafish (*Danio rerio*) were maintained on a 14/10 h light/dark cycle. Embryos were maintained at 28.5°C and staged as described previously (Kimmel et al., 1995). Wild type AB strain or Clstn-1$^{uw7-/-}$ mutant (Ponomareva et al., 2014) embryos of either sex were used for experiments. Clstn-1$^{-/-}$ mutants were identified by DNA sequencing as previously described (Ponomareva et al., 2014). All animals in these studies were handled in accordance with the National Institutes of Health Guide for the care and use of laboratory animals, and the University of Wisconsin Institutional Animal Care and Use Committee (IACUC). These studies were approved by the University of Wisconsin IACUC.

DNA Constructs, Morpholinos (MOs), and Injection

DNA expression constructs were made using the Multisite Gateway Cloning System (Invitrogen) into Tol2 vectors (Kwan et al., 2007). The human EB3 gene fused to eGFP (Stepanova et al., 2003) was cloned behind a *cis*-regulatory element of the *neurogenin1* gene (*-3.1ngn1*) (Blader et al., 2003) to drive expression in RB neurons. To mosaically label RB neurons, 5 pg of *-3.1ngn1:EB3-GFP* and 12 pg of *-3.1ngn1:TagRFP-CAAX* DNA (Andersen et al., 2011) were coinjected into one-cell stage embryos. For MO knockdown, the Clstn-1 splice blocking MO (Ponomareva et al., 2014) was injected at 750 μM in 1 nl volumes into one-celled stage embryos.

In situ Hybridization

Zebrafish Clstn-1 cDNA was obtained from Open Biosystems in a pME18S-FL3 vector. A T7 promoter site was added to the Clstn-1 cDNA via PCR with the following primers: forward 5′-GGATGTTGCCTTTACTTCTA-3′, and reverse 5′-TAA TACGACTCACTATAGGGAGACGACCTGCAGCTCGAG CACA-3′.

A digoxigenin-labeled riboprobe for Clstn-1 mRNA was synthesized using *in vitro* transcription with T7 RNA polymerase (Roche) and then hydrolyzed to 200–500 base pair sized fragments by alkaline hydrolysis (Cox et al., 1984). Whole-mount *in situ* hybridization was performed as described previously (Ponomareva et al., 2014).

Quantitative Real-Time PCR

Total RNA was isolated from clutches of 50 embryos at 24 h post fertilization (hpf) by flash freezing in liquid nitrogen and extraction with TRIzol (Invitrogen). One microgram total RNA per sample was used for reverse transcription with a 50/50 mix of oligo (dT) and random hexamer primers (SuperScript III First Strand Synthesis System; Invitrogen). Reverse transcriptase negative controls were also performed for each sample. For quantitative real time PCR (qPCR), 50 ng cDNA was used as template in a 20 μl reaction with the Clstn-1 primers forward: 5′-ACTGTCAACCCAATGGAGACTTAC-3′ and reverse 5′-CATCCTCGCTTTCCTCCTCTTC-3′, or the Ef1α primers forward 5′-CTTCTCAGGCTGACTGTGC-3′ and reverse 5′-CCGCTAGCATTACCCTCC-3′. qPCR was performed on a StepOnePlus system using PowerUp SYBR Green Master Mix (both Applied Biosystems) per manufacturer's instructions. Three technical replicates per sample/target were run on each of two plates, totaling six averaged for each biological replicate. The reaction was performed with a pre-incubation for 2 min at 50°C then 2 min at 95°C, followed by 40 amplification cycles (95°C for 15 s, 58°C for 15 s, and 72°C for 60 s). Cycling was followed by melt curve analysis to check for spurious amplification. A separate standard curve experiment demonstrated that both primer sets had efficiencies of ∼100%. qPCR results were analyzed using StepOnePlus™ Software v2.2.2 (Applied Biosystems) generating cycle threshold (Ct) values. Clstn-1 expression was normalized to Ef1α expression (ΔCt). Fold change was calculated by $2^{(\Delta\Delta Ct)}$. Statistics were calculated using Prism 7 (GraphPad Software). The difference in *clstn-1* expression was analyzed with an unpaired Student's *t*-test and errors are reported as SEM.

In vivo Time-Lapse Imaging

For live imaging, embryos were anesthetized in 0.02% tricaine and mounted in 1% low melting agarose in 10 mM HEPES E3 medium as previously described (Andersen et al., 2011). Live high speed imaging of EB3-GFP comets was performed with an Opterra Swept-Field confocal microscope (Bruker Nano Surfaces FM) equipped with a Nikon CFI Plan Apo VC 60x (NA 1.40) or 100x oil-immersion objective (NA 1.40). Embryos were imaged at stages between 18 and 26 hpf, while peripheral axons are initiating and arborizing. Z-stacks of 5–50 1-μm optical sections were captured at 2–9 s time intervals, for total durations between 3 and 20 min.

Quantification and Data Analysis

EB3-GFP movies were built in Volocity software (PerkinElmer) and stabilized in FIJI (Schindelin et al., 2012) using the image stabilizer plugin if necessary. Comets were defined as discrete GFP accumulations that lasted at least 3 frames (at least 6 s). EB3 comet speed and directionality were determined from kymographs made in FIJI (Schindelin et al., 2012) using the multiple kymograph plugin (developed by J. Rietdorf and A. Seitz, European Molecular Biology Laboratory, 2004). For comparisons of comets in proximal and distal axon segments the terminal branches of peripheral axons were defined as distal and non-terminal branches were proximal. For central axons, proximal was defined as the region within 50 μm of the cell body, and distal was defined as within 50 μm of the growth cone, for axons longer than 100 μm.

We measured the average velocity of each comet run and then averaged all the comet velocities within an axon segment. Statistical analysis of comet velocity was performed using either the student's *t*-test or one-way ANOVA, with Dunnett's post-test as appropriate. For all comet distance comparisons, we first tested whether the axon segment lengths in each experimental group were not different from one another by *t*-test or one-way ANOVA with Brown-Forsythe post-test, to ensure the comet distance comparisons were valid. The distance between a retrograde EB3 comet's origin and the distal growth cone or branch point was

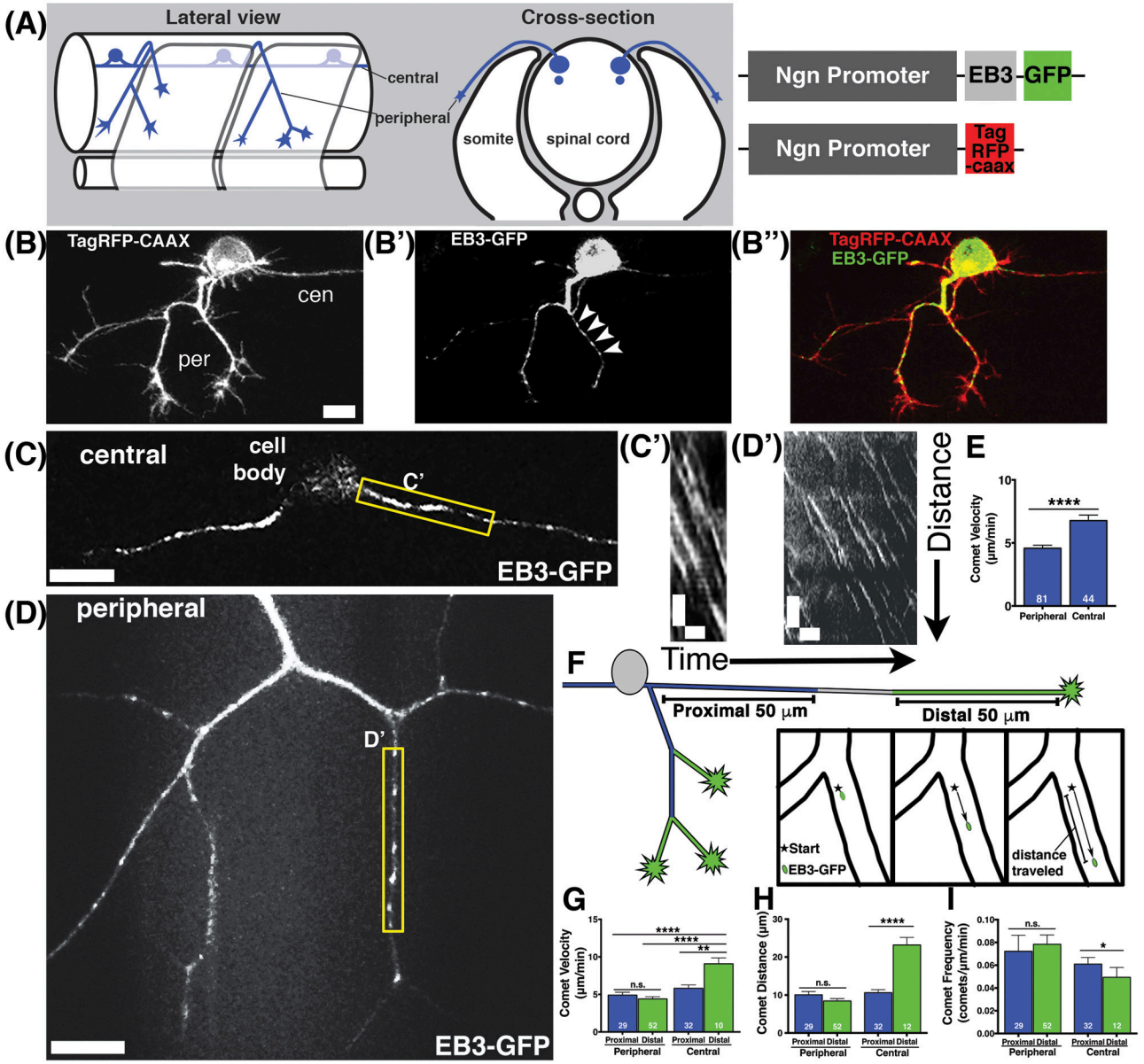

FIGURE 1 | Characterization of microtubule dynamics in sensory neurons. (A) Schematic of RB neurons and DNA constructs with RB promoter (Ngn) driving expression of EB3-GFP or TagRFP-CAAX to label the plasma membrane. **(B)** RB neurons labeled with TagRFP-CAAX to visualize the peripheral (per) and central (cen) axons. **(B')** EB3-GFP labels polymerizing MT plus ends. Representative comets are marked with arrowheads. **(B")** Overlay of membrane label (red) and EB3-GFP (green). Scale bars are 10 μm in this and all subsequent neuron images. **(C,D)** RB neurons expressing EB3-GFP in central axons **(C)** or peripheral axons **(D)**. **(C',D')** Representative kymographs were made from regions outlined with yellow box in central axons **(C')** or peripheral axons **(D')**. All kymographs are oriented with distance on the y axis (μm) and time on the x axis (minutes) with the proximal origin at the top left and the first time point on the left. Scale bars are 5 μm (y) and 1 min (x) for these and all other kymographs. **(E)** EB3 comets have greater velocity in central axons than peripheral axons (mean peripheral velocity = 4.578 μm/min, $n = 81$ axon segments; mean central velocity = 6.769 μm/min, n = 44 axon segments; $^{****}p < 0.0001$ student's *t*-test). **(F)** Schematic showing proximal (blue) and distal (green) regions of central and peripheral axons, with inset box showing how comet distance was measured. **(G)** EB3 comets in the distal regions of central axons are significantly faster than those in proximal regions (mean distal central velocity = 9.32 μm/min, $n = 12$ axon segments; mean proximal central velocity = 5.81 μm/min, $n = 32$ axon segments, $^{**}p = 0.0002$ student's *t*-test; mean proximal peripheral velocity = 4.90 μm/min, $n = 29$ axon segments, $^{****}p < 0.0001$ student's *t*-test; mean distal peripheral velocity = 4.40 μm/min, $n = 52$ axon segments, $^{****}p < 0.0001$ student's *t*-test). **(H)** Central axon comets travel further in distal regions than proximal ones (mean proximal central distance = 10.63 μm, $n = 32$ axon segments; mean distal central distance = 23.20 μm, $n = 12$ axon segments; $^{****}p < 0.0001$ student's *t*-test). **(I)** Comet frequency is significantly lower in distal central axon segments than proximal segments (mean proximal central frequency = 0.061 comets/μm/min, $n = 32$ axon segments, mean distal central frequency = 0.040 comets/μm/min, $n = 12$ axon segments; $^{*}p = 0.045$ student's *t*-test).

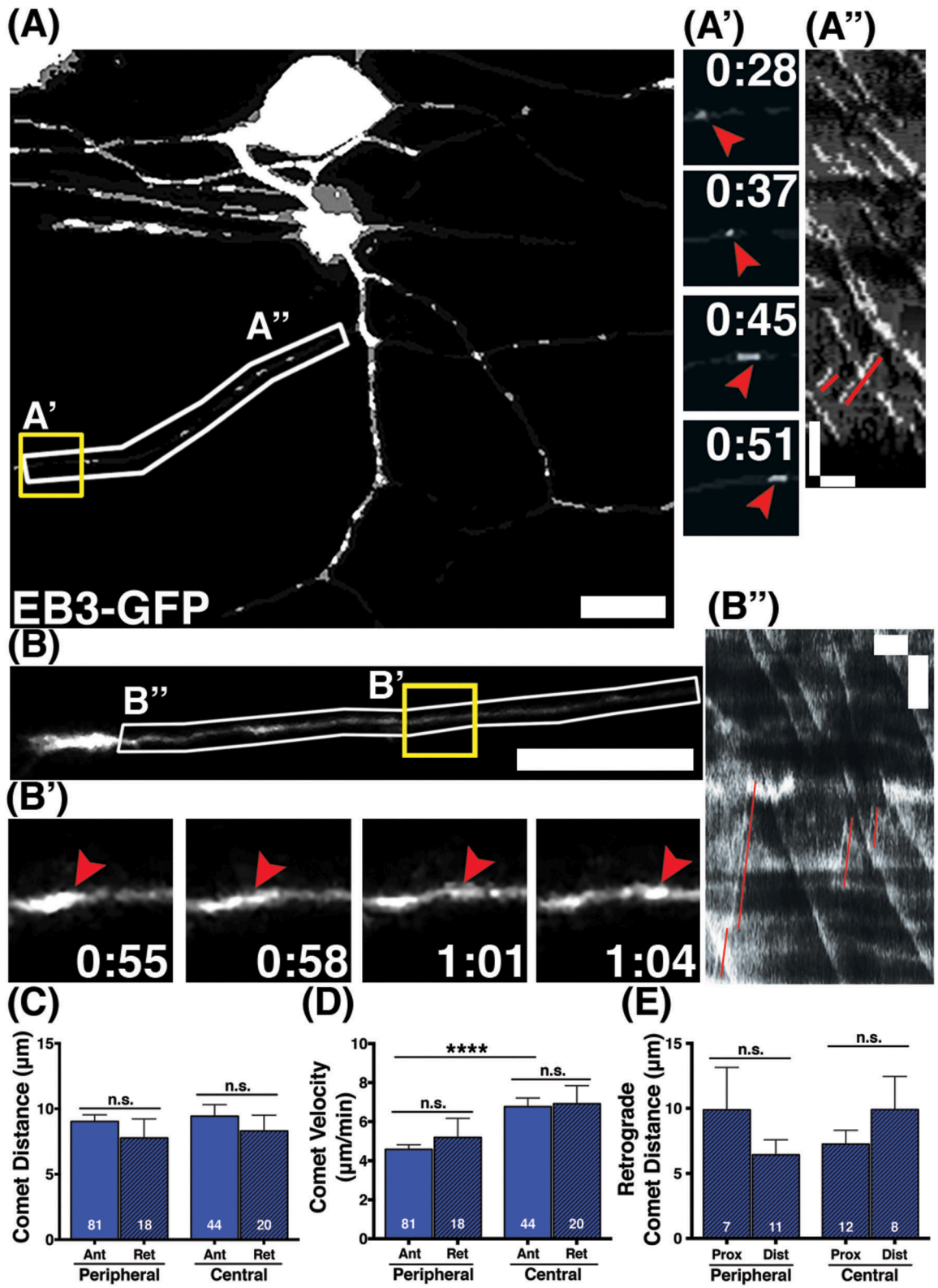

FIGURE 2 | Behavior of retrograde comets in wild type axons. (A,B) Wild type neurons expressing EB3-GFP. Small subsets of comets travel retrogradely in peripheral **(A)** and central **(B)** axons. Scale bars are 10 µm. **(A',B')** Time-lapse sequences of representative retrograde comets in yellow boxes. Time is shown in

(Continued)

FIGURE 2 | Continued
min:sec. **(A",B")** Kymographs of regions outlined by white boxes in **(A**,**B)**. Retrograde comets can be visualized as positively sloped lines (red) in the kymographs. Scale bars are 5 μm (y) and 1 min (x). **(C)** The distance retrograde comets travel does not significantly differ from anterograde comets in peripheral or central axons, (mean peripheral anterograde distance = 9.03 μm, $n = 81$ axon segments, mean peripheral retrograde distance = 7.77 μm, $n =$ axon segments, $p = 0.33$ student's *t*-test; mean central anterograde distance = 9.43 μm, $n = 44$ axon segments, mean central retrograde distance = 8.31 μm, $n = 20$ axon segments, $p = 0.47$ student's *t*-test). **(D)** Retrograde comet velocities do not differ from anterograde comets. Anterograde comet velocity data is the same as in **Figure 1**, shown here again for comparison, $^{****}p < 0.0001$, student's *t*-test (mean peripheral retrograde velocity = 5.19 μm/min, $n = 18$ axon segments; mean central retrograde velocity = 6.91 μm/min, $n = 20$ axon segments). **(E)** Retrograde comets traveled similar distances in proximal and distal axon regions (mean peripheral proximal distance = 9.89 μm, $n = 7$ axon segments, mean peripheral distal distance = 6.42 μm, $n = 11$ axon segments, $p = 0.26$ student's *t*-test; mean central proximal distance = 7.24 μm, $n = 12$ axon segments, mean central distal distance = 9.90 μm, $n = 8$ axon segments, $p = 0.29$ student's *t*-test).

measured in terminal and proximal axon segments respectively. Statistical analysis of comet distance was performed using either the student's *t*-test or one-way ANOVA, with Dunnett's post-test as appropriate.

In the filopodia movies the first 3 min were analyzed for filopodia stability and collapse. Filopodial protrusions along axon shafts were included in the analysis, but growth cone filopodia were not included. Filopodia were defined as narrow protrusions from the axon shaft that were at least 1 μm long. All statistical analyses were performed using Prism 7 (GraphPad Software). Errors are reported as SEM.

RESULTS

Characterization of MT Dynamics during Sensory Axon Development *In vivo*

To investigate the behavior of MTs during axon development and branching *in vivo*, we used zebrafish spinal sensory Rohon-Beard (RB) neurons as a model system. Each RB neuron extends ascending and descending central axons within the spinal cord that fasciculate with one another and are largely unbranched, and one peripheral axon that exits the spinal cord, grows to the skin, and branches extensively (**Figure 1A**). We imaged MT polymerization dynamics using the MT plus-tip binding protein EB3 fused to GFP. EB3-GFP binds the plus ends of actively polymerizing MTs, which appear as moving GFP puncta, or "comets" (Stepanova et al., 2003). We mosaically labeled RB neurons by injecting DNA encoding EB3-GFP driven by regulatory elements from the neurogenin-1 gene (*-3.1ngn1*) (Blader et al., 2003), together with DNA encoding membrane targeted TagRFP (*-3.1ngn1:TagRFP-CAAX*) to visualize neuron morphology (**Figures 1A,B,B',B"**). We used swept-field confocal microscopy, in which a linear pinhole array or slit is held stationary, and the light column is swept over the sample with mirrors, thereby increasing the speed of image acquisition (Castellano Munoz et al., 2012). The swept-field confocal allows imaging of rapid MT polymerization events in 3D. We captured z-stacks at 2–5 s intervals and imaged for periods ranging from 5 to 20 min. We imaged embryos at stages from 18 to 26 hpf, when RB axon arbors are actively developing and branching.

We found that MTs were highly dynamic and actively polymerizing in developing axons (**Figures 1C,D**, Movie S1). Comet frequencies were greater in peripheral axons than in central axons suggesting peripheral axons have more actively polymerizing MTs (mean peripheral axon frequency = 0.077 comets/μm/min, n = 81 axon segments; mean central axon frequency = 0.055 comets/μm/min, $n = 44$ axon segments; $^{*}p = 0.044$ student's *t*-test). We quantified EB3 comet velocity by generating kymographs (**Figures 1C',D'**) and found that comets were significantly faster in central axons than in peripheral axons (**Figure 1E**). Moreover, analysis of EB3-GFP comets with respect to position in the axons (proximal vs. distal to the cell body) revealed that the fastest comets were in the distal regions of central axons. In central axons, distal segments were defined as within 50 μm of the growth cone, and proximal as within 50 μm of the cell body. Most central axons were longer than 100 μm at the time of imaging, so these segments were not adjacent to one another. In peripheral axons, distal segments were defined as the terminal axon branch segments ending in a growth cone, and all others segments were defined as proximal (**Figure 1F**). In peripheral axons, comet velocities were not significantly different between proximal and distal segments. In contrast, comets in distal central axons moved significantly faster than those in proximal central axons or in peripheral axons (**Figure 1G**). Comets in distal central axons also traveled longer distances (**Figure 1H**) than those in proximal regions and were less frequent (**Figure 1I**). The lower comet frequency together with longer distance suggest that MTs are more inclined to continue polymerizing for longer stretches without undergoing catastrophe in distal central axons. At this developmental stage, central axons extend at rapid rates and are fasciculating with other central axons (Andersen et al., 2011). While the regions of central axons close to the cell body are not as tightly fasciculated with other axons, the more distal segments where we see faster MT polymerization have extensive fasciculation, suggesting fasciculation may influence MT stability. These wild type analyses reveal distinctive MT behaviors in different axon compartments and suggest that fasciculating axons and actively branching, non-fasciculating axons growing in different extracellular environments experience signals that influence MT dynamics differently.

Developing axons must organize their MTs with plus ends directed distally from the cell body. We analyzed the direction of EB3-GFP comets to determine MT polarity during axon growth and branching stages. The majority of EB3-GFP comets moved in the anterograde direction in both central and peripheral axons (94 and 96% respectively), indicating that most polymerizing MTs were organized with plus ends distal during axon growth. However, both central and peripheral axons had a small proportion of retrograde comets (6%

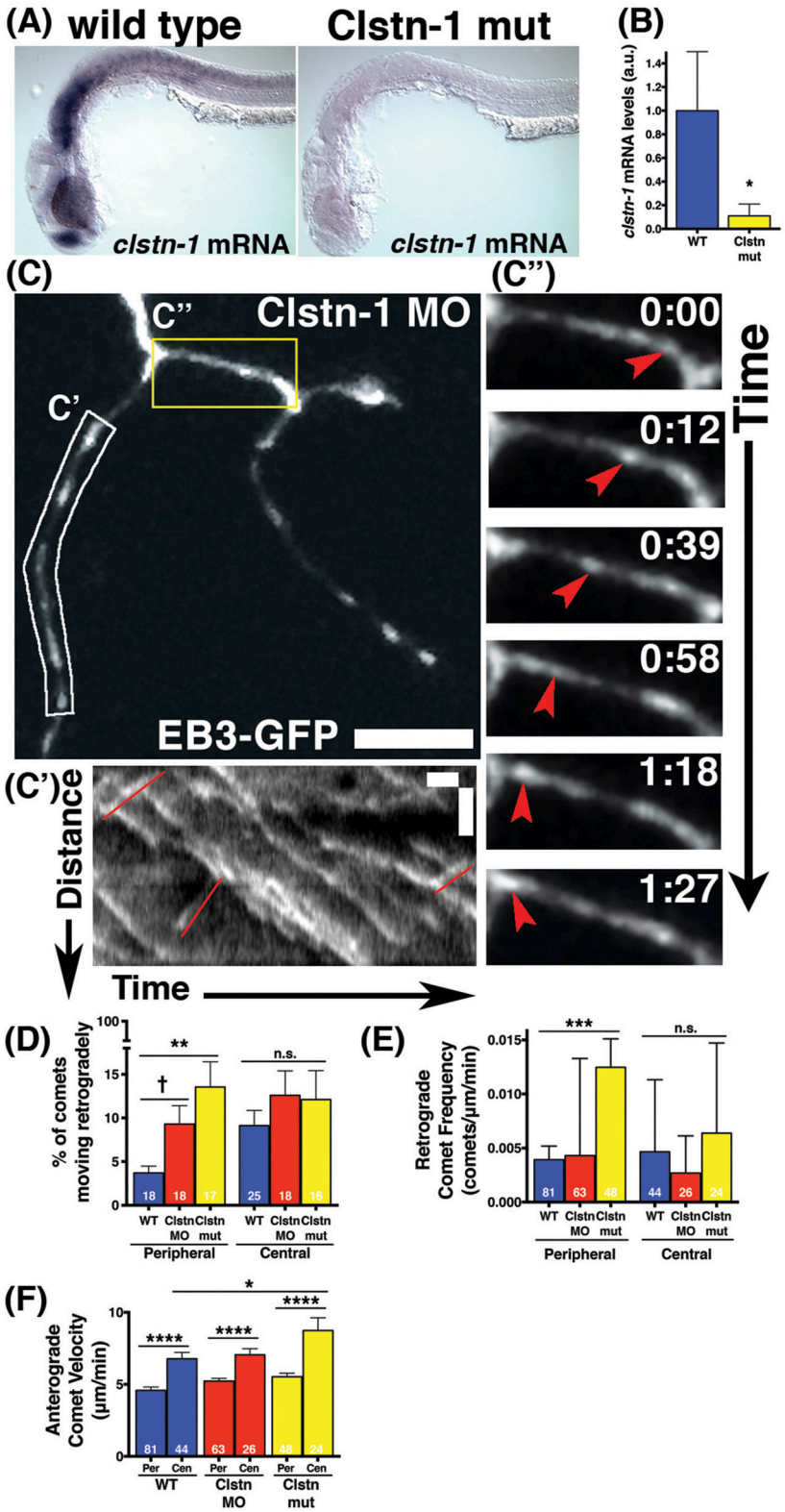

FIGURE 3 | Clstn-1 loss-of-function (lof) disrupts MT polarity in sensory neuron peripheral axons. (A) *In situ* hybridization showing *clstn-1* mRNA expression in 24 hpf wild type or Clstn-1$^{-/-}$ embryos. **(B)** qPCR results showing *clstn-1* mRNA expression levels normalized to an EF1α positive control (wild type mRNA = −4.681, $n = 3$ biological replicates of 50 embryos; Clstn-1$^{-/-}$ mRNA = −7.616, $n = 2$ biological replicates of 50 embryos; $^*p = 0.014$ student's *t*-test). **(C)** RB

(Continued)

FIGURE 3 | Continued
neuron labeled with EB3-GFP in Clstn-1 MO injected embryo. Retrograde comets appear frequently in Clstn-1 lof peripheral axons. Scale bar is 10 μm. **(C')** Kymograph of the white boxed region in C shows several retrograde comets highlighted in red. Scale bars are 5 μm (y) and 1 min (x). **(C")** Time-lapse sequences of the yellow boxed area show a retrograde comet traveling between two branch points (red arrowheads). Time is shown in min:sec. **(D)** Clstn-1 lof embryos have a higher percentage of retrograde comets than wild type (WT). (WT peripheral = 3.69%, $n = 18$ neurons; Clstn-1 MO peripheral = 9.29%, $n = 18$ neurons, † significant via student's *t*-test comparison to wild type, $p = 0.012$, but not with Dunnett's post-test after one-way ANOVA $p = 0.086$; Clstn-1$^{-/-}$ peripheral = 13.55%, $n = 17$ neurons, ***$p = 0.0009$ student's *t*-test, **$p = 0.0017$ Dunnett's post-test; $p = 0.0034$ one-way ANOVA). In central axons, there is no significant difference in percentage of retrograde comets between wild type and Cltn-1 lof. (WT central = 9.11%, $n = 25$ neurons; Clstn-1 MO central = 12.60%, $n = 18$ neurons, $p = 0.27$ student's *t*-test, $p = 0.49$ Dunnett's post-test; Clstn-1$^{-/-}$ central = 12.10%, $n = 16$ neurons, $p = 0.39$ student's *t*-test, $p = 0.61$ Dunnett's post-test; one-way ANOVA $p = 0.54$). **(E)** Clstn-1$^{-/-}$ neurons have a higher frequency of retrograde comets in peripheral axons than wild type (mean WT peripheral frequency = 0.0039 comets/μm/min, $n = 81$ axon segments; mean Clstn-1 MO peripheral frequency = 0.0043 comets/μm/min, $n = 63$ axon segments, $p = 0.90$ Dunnett's post-test; mean Clstn-1$^{-/-}$ peripheral frequency = 0.012 comets/μm/min, $n = 47$ axon segments, ***$p = 0.0007$ Dunnett's post-test; one-way ANOVA ***$p = 0.0006$). **(F)** In Clstn-1 lof neurons anterograde comets in central axons travel faster than those in peripheral axons, similar to wild type, (mean Clstn-1 MO peripheral velocity = 5.23 μm/min, $n = 63$ axon segments, mean Clstn-1 MO central velocity = 7.05 μm/min, $n = 26$ axon segments, ****$p < 0.0001$ student's *t*-test; mean Clstn-1$^{-/-}$ peripheral velocity = 5.53 μm/min, $n = 48$ axon segments, mean Clstn-1$^{-/-}$ central velocity = 8.74 μm/min, $n = 24$ axon segments, ****$p < 0.0001$ student's *t*-test, wild type velocity data repeated from **Figure 1** show here again for comparison). Clstn-1$^{-/-}$ anterograde comets in central axons travel faster than their wild type counterparts (WT vs. Clstn-1$^{-/-}$ mean central velocity *$p = 0.031$ Dunnett's post-test, WT vs. Clstn-1 MO mean central velocity: $p = 0.91$ Dunnett's post-test, *$p = 0.048$ one-way ANOVA).

of comets in central axons and 4% in peripheral axons; **Figures 2A,A',A",B,B',B"**). Overall, retrograde comets traveled at equivalent speeds and distances as anterograde comets, in both central and peripheral axons (**Figures 2C–E**), indicating that if a MT forms in the incorrect orientation its capacity for polymerization is similar to correctly oriented MTs. We asked whether retrograde comets were more frequent at particular stages of development. RB central axons initiate outgrowth first, followed by peripheral axons a couple hours later (Andersen et al., 2011). We compared neurons that had not yet formed a peripheral axon vs. those that had a primary peripheral axon branch, secondary, tertiary or quaternary peripheral branches. Retrograde comets in central and peripheral axons were found at all stages of development. We also analyzed retrograde comet behavior in proximal vs. distal axon regions to ask if there are location-based differences in behavior. In both peripheral and central axons, we saw no significant difference in retrograde comet rates or distance along the proximal-distal axis. Overall, these results indicate that occasional mispolarized MTs exist during axon development, although neurons likely have high fidelity mechanisms to prevent these MTs throughout development.

Clstn-1 Regulates MT Polarity

We previously showed that the kinesin adaptor Clstn-1 is specifically required for RB peripheral axon formation and branching, and that it functions in part by regulating endosomal trafficking from the cell body to axons and branch points (Ponomareva et al., 2014). To determine whether Clstn-1 influences MT dynamics, we imaged EB3-GFP in Clstn-1 loss of function (lof) embryos (**Figure 3**). We used both a Clstn-1 mutant, Clstn-1^{uw7}, and a Clstn-1 splice blocking morpholino that we showed previously to be effective and to produce the same peripheral axon branching phenotype as the mutant (Ponomareva et al., 2014). The Clstn-1^{uw7} allele was generated with TALENs and has a single base deletion resulting in a frame shift and premature stop in exon 2 (Ponomareva et al., 2014). We found that some Clstn-1$^{uw7-/-}$ homozygous mutant animals were adult viable and we raised a homozygous line to generate embryos for these EB3-GFP imaging experiments. To ask whether *clstn-1* mRNA undergoes nonsense-mediated degradation in the mutants, we analyzed mRNA expression with *in situ* hybridization and quantitative real-time PCR (qPCR). *In situ* hybridization showed a strong reduction in *clstn-1* mRNA in the Clstn-1$^{-/-}$ mutants compared to wild type (**Figure 3A**). This finding was substantiated by the qPCR analysis, which showed that the mutant embryos have *clstn-1* mRNA levels at 11.6% that of wild type levels (**Figure 3B**). Thus, the mutants are likely to be either null or strong hypomorphs, although we cannot rule out the possibility that some truncated Clstn-1 protein is present.

EB3-GFP imaging in Clstn-1 lof embryos showed an effect on MT polarity. The percentage of EB3-GFP comets traveling retrogradely in peripheral RB axons was significantly increased in Clstn-1 lof neurons (**Figures 3C,C',C",D**, Movie S2). We also measured the retrograde comet frequency (number of retrograde comets per micron per minute) and found a significant increase in peripheral axons of Clstn-1$^{-/-}$ neurons (**Figure 3E**). In contrast, there was not a significant difference in percentage or frequency of retrograde comets in central axons (**Figures 3D,E**), suggesting that Clstn-1 functions specifically in peripheral axons. Overall, these results suggest that central and peripheral axons employ different mechanisms to regulate MT polarity, and that Clstn-1 is part of the mechanism that prevents MT misorientation in peripheral axons. This finding also is consistent with our previous work showing that Clstn-1 is required specifically for peripheral axon outgrowth and branching, but not for central axon growth (Ponomareva et al., 2014).

In addition to influencing MT polarity, Clstn-1 also appears to affect polymerization rates of correctly oriented MTs in central axons. In Clstn-1 lof embryos, anterograde EB3-GFP comets were faster in central axons than in peripheral axons (**Figure 3F**), similar to wild type embryos. However, the effect was more pronounced in Clstn-1$^{-/-}$ neurons, where the central axon comet rates were significantly faster than those in wild type central axons (**Figure 3F**). This finding could suggest that normal Clstn-1 activity slows MT polymerization rates in central axons. However, this result may also reflect a more indirect effect due to the reduced peripheral axon branching in Clstn-1

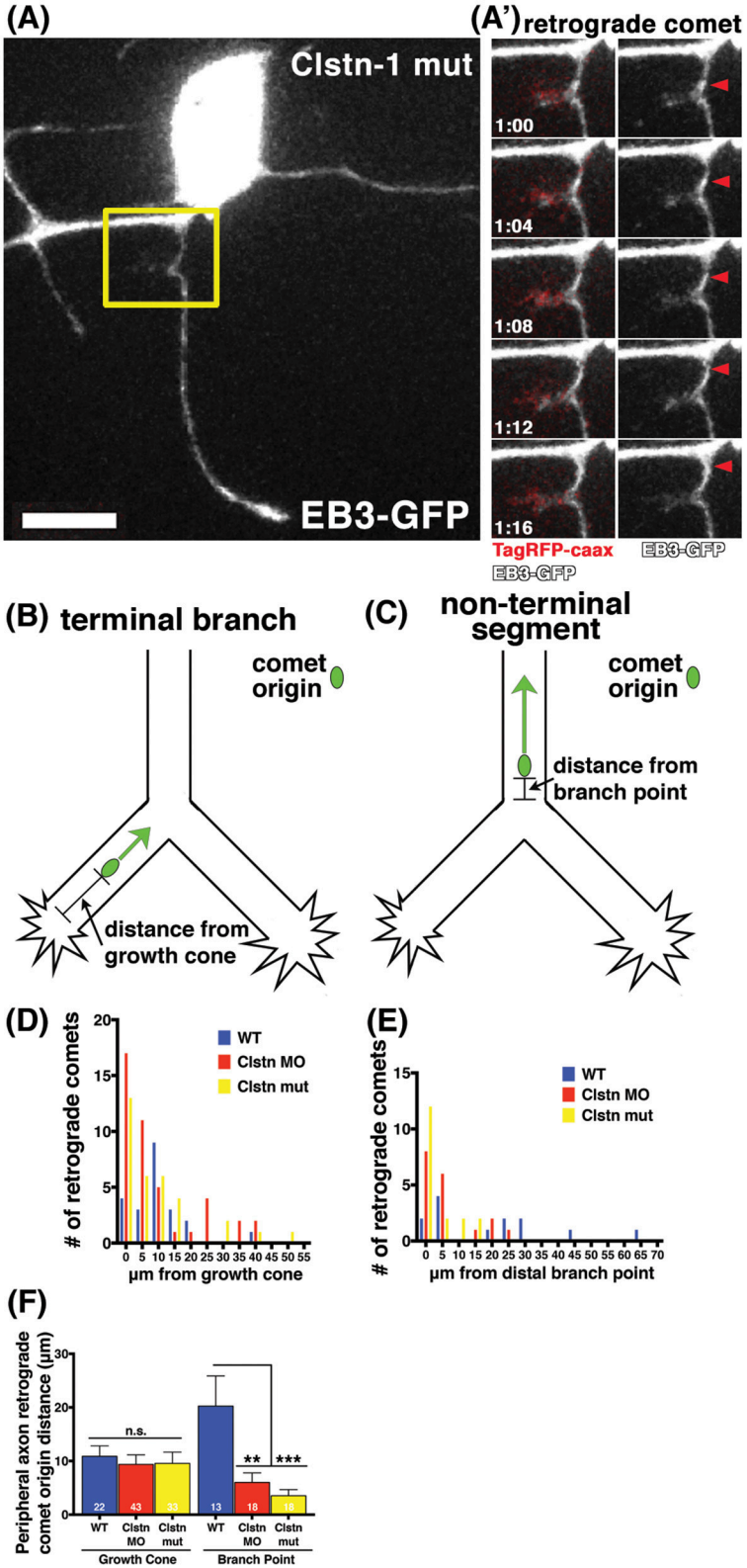

FIGURE 4 | EB3 comets originate near branch points and growth cones in sensory neuron peripheral axons. (A) RB neuron labeled with EB3-GFP and TagRFP-caax in a Clstn-1 mutant embryo. **(A')** Yellow box outlines area shown in time-lapse sequence, which shows a retrograde comet originating from a newly

(Continued)

FIGURE 4 | Continued
forming branch. Scale bar is 10 μm. Time is shown in min:sec. **(B)** In terminal peripheral axon branches the distance between the origin of retrograde EB3-GFP comets and the growth cone was measured. **(C)** In non-terminal peripheral axon segments the distance between the origin of retrograde EB3-GFP comets and the distal branch point was measured. **(D)** Histogram showing the number of retrograde comets originating at indicated distance from the growth cone. **(E)** Histogram showing the number of retrograde comets originating at indicated distance from branch point. **(F)** Retrograde comets of Clstn-1 lof originate closer to branch points than wild type (WT mean distance to branch point = 20.26 μm, $n = 13$ comets; Clstn-1 MO mean distance to branch point = 6.02 μm, $n = 18$ comets, Dunnett's post-test $^{**}p = 0.0030$ Dunnett's post-test; Clstn-1$^{-/-}$ near BP distance = 3.55 μm, $n = 18$ comets, $^{***}p = 0.0005$ Dunnett's post-test; $^{***}p = 0.0006$ one-way ANOVA).

lof (Ponomareva et al., 2014). It is possible that the process of generating peripheral axon branches diverts resources such as free tubulin from the central axon, slowing MT polymerization in wild type central axons. The less branched Clstn-1 lof peripheral arbors may not exert such an effect on central axons.

Clstn-1 Organizes MT Polarity near Branch Points and Growth Cones

Little is known about the mechanisms by which MT polarity is maintained at branch points while axons are actively branching, a process that involves MT severing and increased dynamics (Gallo, 2011). MTs are highly dynamic in growth cones (Tanaka and Kirschner, 1991; Tanaka et al., 1995; Buck and Zheng, 2002) and others have reported increased incidence of retrograde comets in distal axon segments near growth cones (Stepanova et al., 2003; Ma et al., 2004). RB peripheral axons branch both by growth cone bifurcation and by interstitial branching, and we previously showed that Clstn-1 is required for both types of branching (Ponomareva et al., 2014). To ask whether Clstn-1 functions to organize MT polarity during these processes, we analyzed the relationship between retrograde EB3-GFP comets and branch points or growth cones. We found that retrograde comets often originated near growth cones or branch points in Clstn-1 lof neurons (**Figures 4A,A"**, Movie S3). We measured distances between retrograde comet origins and the growth cone in terminal branches of the arbor (**Figure 4B**), or between retrograde comet origins and the nearest distal branch point in more proximal, non-terminal axon segments (**Figure 4C**). In terminal branches, most of the retrograde comets originated within 10 μm of the growth cone in Clstn-1 lof (**Figure 4D**; 76.7% in Clstn-1 MO, 69.7% in Clstn-1 mutant, and 50% in wild type). The mean distance between comet and growth cone did not differ between wild type and Clstn-1 lof (**Figure 4F**). In non-terminal axon segments, most retrograde comets originate near branch points in Clstn-1 lof embryos (77.78% within 10 μm in Clstn-1 mutants, 83.3% in Clstn-1 MO), while they are more evenly distributed in wild type neurons (46.2% within 10 μm) (**Figure 4E**). Moreover, the mean distance between retrograde comet origin and branch points in non-terminal axon segments is significantly shorter in Clstn-1 lof (**Figure 4F**). Together these results show that the increased retrograde comets in Clstn-1 lof occur predominantly near growth cones and branch points and suggest that Clstn-1 plays a role suppressing retrograde comet formation at these locations.

Clstn-1 Stabilizes Nascent Branches

We previously reported that Clstn-1 loss reduces the number of filopodial protrusions and interstitial branches in peripheral sensory axons (Ponomareva et al., 2014). MT invasion into filopodia is required for their stabilization and conversion into an axon branch (Gallo, 2011). We asked if Clstn-1 affects MT invasion or stabilization in nascent branches. We quantified the collapse frequency of filopodia (potential nascent branches) along peripheral axon shafts and found that Clstn-1 lof significantly increases the number of filopodia that collapse compared to wild type neurons (**Figure 5D**). We then analyzed the behavior of EB3 comets in peripheral axon filopodia to determine how Clstn-1 might affect MT dynamics in these structures. We observed stable filopodia invaded by EB3 comets in both wild type (**Figure 5A**) and Clstn-1 lof. We also saw many filopodia that were not invaded by EB3 comets during the imaging period, in both wild type and Clstn-1 lof, many of which collapsed (**Figure 5B**). In some cases, we saw stable filopodia with stationary EB3-GFP accumulations at their tips (**Figures 5C,C1–C3**), similar to what others have observed in cultured neurons (Stepanova et al., 2003; Marx et al., 2013), which may indicate the opposing forces of anterograde MT polymerization and retrograde flow of actin (Marx et al., 2013). We measured the frequency of EB3-GFP comet invasion into filopodia, and found no significant difference in EB3 invasions between wild type and Clstn-1 lof (**Figure 5E**), nor in the percentage of filopodia being invaded by EB3-GFP (WT = 22.28%, $n = 14$ neurons, Clstn-1 MO = 23.13%, $n = 8$ neurons, Clstn-1$^{-/-}$ = 10.42%, $n = 8$ neurons, $p = 0.55$ one-way ANOVA). However, of the filopodia not invaded by EB3-GFP, a significantly larger percentage collapsed during a 3 min period in Clstn-1 lof compared to wild type (**Figure 5F**). These results suggest that Clstn-1 is important for filopodial stabilization, but does not act by promoting increased invasion of polymerizing MTs. However, it is possible that Clstn-1 regulates filopodial invasion by short MTs that are not actively polymerizing and would not be labeled by EB3-GFP.

DISCUSSION

Our experiments using high speed swept field confocal microscopy have provided the first imaging of MT dynamics while axons are actively branching and developing their arborization pattern *in vivo*. We were able to characterize MT dynamics in two types of axons from one neuron as they develop in separate environments and undergo different tasks: straight growth along a CNS fascicle vs. branching in the periphery. We show that the kinesin adaptor Clstn-1 regulates MT polarity, a novel function for a kinesin adaptor that is not known or predicted to directly bind MTs. Moreover, our results suggest Clstn-1 is particularly important for organizing

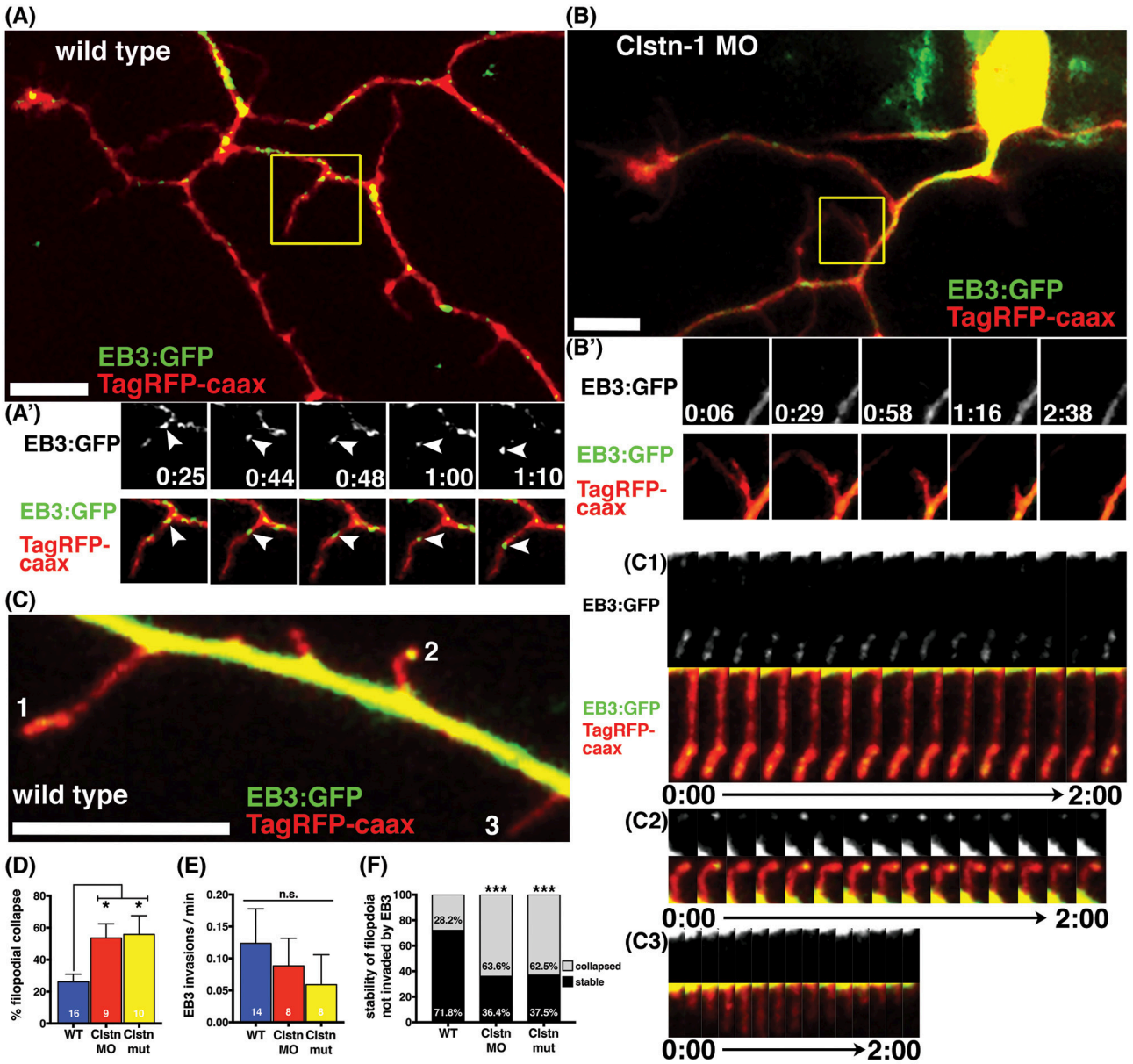

FIGURE 5 | Clstn-1 is required for stability of filopodia along peripheral axon shafts. (A) Neuron in wild type embryo labeled with TagRFP-caax and EB3-GFP. Stable filopodia structures are often invaded by MTs as seen in the time-lapse sequence in **(A')**. Time is in min:sec. Scale bar is 10 μm in this and all other neuron images. **(B)** Neuron in Clstn-1 MO embryo showing collapse of a filopidum in time-lapse sequence in **(B')**. Filopodia in Clstn-1 lof more frequently collapse, as shown in Clstn-1 MO neuron. Collapsing filopodia usually do not have invading EB3 comets as shown in this montage. **(C)** Segment of peripheral axon labeled with TagRFP-caax and EB3-GFP. EB3-GFP signal brightness is increased to show fainter signal in filopodia. Filopodia labeled 1, 2, and 3 are shown in time-lapse in **(C1–C3)**. Time-lapse sequences showing stable filopodia containing static EB3-GFP accumulations at their distal tips over several minutes in **(C1,C2)**, while collapsing filopodia have no EB3 accumulations, as seen in C3. **(D)** A greater percentage of filopodia collapse in Clstn-1 lof than in wild type (WT collapse = 26.11% in $n = 16$ neurons, Clstn-1 MO collapse = 53.62% in $n = 9$ neurons, $^{*}p = 0.039$ Dunnett's post-test, Clstn-$1^{-/-}$ collapse = 55.83% in $n = 10$ neurons, $^{*}p = 0.020$ Dunnett's post-test, $^{*}p = 0.0145$ one-way ANOVA). **(E)** There is no significant difference in the rate of EB3-GFP invasions into filopodia between wild type and Clstn-1 lof (mean WT rate = 0.124 comets/min, $n = 14$ neurons; mean Clstn-1 MO rate = 0.0885 comets/min, $n = 8$ neurons; mean Clstn-$1^{-/-}$ rate = 0.0724 comets/min, $n = 8$ neurons; $p = 0.068$ one-way ANOVA). **(F)** Percentages of filopodia not invaded by MTs that collapse or remain stable during a 3-min period. (WT = 28.2%, $n = 71$ filopodia; Clstn-1 MO = 63.6%, $n = 33$ filopodia, $^{**}p = 0.0003$ chi-squared test; Clstn-$1^{-/-}$ = 52.5%, $n = 40$ filopodia, $^{***}p = 0.0002$ chi-squared test).

MT polarity at branch points, and that branching axons have unique mechanisms to organize MTs.

MTs show increased dynamics and unbundling during axon branch formation (Yu et al., 1994; Dent et al., 1999; Gallo, 2011; Ketschek et al., 2015), and MT severing is required for interstitial axon branching (Yu et al., 2008; Qiang et al., 2010). Neurons must keep MTs correctly oriented with plus ends distal during this dynamic process. Our results show that the

increased number of misoriented MTs in Clstn-1 lof neurons often originate near branch points. Moreover, we only saw a significant increase in retrograde EB3-GFP comets in the branched peripheral axons and not in the unbranched central axons, which supports the idea that during axon branching, there are different or additional mechanisms to organize MTs not present in unbranched axons. Branch point specific mechanisms to organize MT polarity have also been described in dendrites. In *Drosophila* dendrites, Centrosomin associates with Golgi outposts at branch points and tips to promote retrograde MT nucleation and polymerization (Yalgin et al., 2015). PSD-95 influences MT organization at dendritic branch points through its interaction with EB3 (Sweet et al., 2011). Interestingly, both Centrosomin and PSD-95 regulate dendrite branch formation, suggesting disruption of proper MT organization near branch points can disrupt branch formation. We previously showed that RB neurons in Clstn-1 lof embryos have fewer peripheral axons and those that form have fewer branches (Ponomareva et al., 2014). It is possible that the increased number of misoriented MTs in Clstn-1 lof directly leads to branch failure. The fact that our EB3-GFP analysis in peripheral axons was done in the population of neurons that were able to form a peripheral axon, i.e., those less affected by Clstn-1 loss, suggests we are under-reporting the effects of Clstn-1 lof on MTs and underscores the importance of Clstn-1 for proper MT organization.

In addition to their different capacity for branching, the peripheral and central RB axons also have other differences in behavior, pathways, and extracellular environment. The central axons fasciculate with one another while the peripheral axons mutually repel each other on contact (Liu and Halloran, 2005; Sagasti et al., 2005). We also showed previously that central and peripheral axons respond differently to guidance cues and have different molecular requirements for growth (Liu and Halloran, 2005). For example, the central axons require the adhesion protein TAG-1 for growth and fasciculation, while peripheral axons do not. Our results showing that MTs polymerize faster and for longer distances without catastrophe in distal central axons, where axons have extensive cell-cell interactions in the fascicle, could potentially reflect a stabilizing effect of fasciculation on MTs. In addition, distal central axons presumably are less likely to be directly populated with MTs polymerizing from the centrosome compared with the regions closer to the cell body. The more stable MTs in distal regions may reflect additional mechanisms to maintain MT stability in regions far from the centrosome.

The mechanisms by which axons prevent or remove misoriented, minus-end-out MTs are not well understood. One possibility is that misoriented MTs are selectively depolymerized or destabilized. Our finding that retrograde comets extend for similar distances as anterograde comets argues against such a mechanism. Another possibility is that dynein transports misoriented MTs out of the axon. Dynein is required for MT polarity in *Drosophila* axons (Zheng et al., 2008; del Castillo et al., 2015) and is proposed to act by tethering to cortical actin and walking toward the minus end of misoriented MTs, thereby sliding them back to the cell body (del Castillo et al., 2015). Clstn-1 could potentially influence this process via its effects on the kinesin-1 motor. KHC can crosslink MTs via a second MT-binding domain in its C-terminal region (Jolly et al., 2010; Lu et al., 2013; Yan et al., 2013). Clstn-1 activation of KLC (Yip et al., 2016) allows KLC to bind KHC, which inhibits its C-terminal MT binding, freeing the C-terminal to bind cargo (Wong and Rice, 2010). Thus, Clstn-1 could function indirectly to modulate MT crosslinking, which in turn could influence dynein's ability to slide MTs. Finally, it is also possible that Clstn-1 influences MT polarity more indirectly, for example by mediating transport of other proteins that regulate MTs. Future experiments will be necessary to uncover precise mechanisms of Clstn-1 activity.

AUTHOR CONTRIBUTIONS

TL and MH designed the study, analyzed data, and co-wrote the manuscript. TL, JL, and EH carried out the experiments. KE developed and provided imaging and analytical tools. All authors read and approved the manuscript.

FUNDING

This work was supported by National Institute of Health grants R01NS042228, R56NS086934 and R01NS086934 to MH, R44MH065724 to KE, and T32GM007507 to TL.

ACKNOWLEDGMENTS

The authors would like to acknowledge Julie Last for her assistance with swept field confocal imaging. We thank Olga Ponomareva for helpful discussions, and Kelsey Baubie, Elizabeth Roehl, William Davis, Kassandra Ford, Kevin Grunewald, Matthew Goelz, Christina Lindop, Maia Gumnit, and Matthew Scott for fish care and/or technical assistance.

SUPPLEMENTARY MATERIAL

The Supplementary Material for this article can be found online at: http://journal.frontiersin.org/article/10.3389/fncel.2017.00107/full#supplementary-material

REFERENCES

Ahmad, F. J., Echeverri, C. J., Vallee, R. B., and Baas, P. W. (1998). Cytoplasmic dynein and dynactin are required for the transport of microtubules into the axon. *J. Cell Biol.* 140, 391–401. doi: 10.1083/jcb.140.2.391

Alther, T. A., Domanitskaya, E., and Stoeckli, E. T. (2016). Calsyntenin 1 mediated trafficking of axon guidance receptors regulates the switch in axonal responsiveness at a choice point. *Development* 143, 994–1004. doi: 10.1242/dev.127449

Andersen, E. F., Asuri, N. S., and Halloran, M. C. (2011). *In vivo* imaging of cell behaviors and F-actin reveals LIM-HD transcription factor regulation of peripheral versus central sensory axon development. *Neural Dev.* 6:27. doi: 10.1186/1749-8104-6-27

Araki, Y., Tomita, S., Yamaguchi, H., Miyagi, N., Sumioka, A., Kirino, Y., et al. (2003). Novel cadherin related membrane proteins, Alcadeins, enhance the

X11 like protein mediated stabilization of amyloid beta protein precursor metabolism. *J. Biol. Chem.* 278, 49448–49458. doi: 10.1074/jbc.M306024200

Araki, Y., Kawano, T., Taru, H., Saito, Y., Wada, S., Miyamoto, K., et al. (2007). The novel cargo Alcadein induces vesicle association of kinesin 1 motor components and activates axonal transport. *EMBO J.* 26, 1475–1486. doi: 10.1038/sj.emboj.7601609

Baas, P. W., and Lin, S. (2011). Hooks and comets: the story of microtubule polarity orientation in the neuron. *Dev. Neurobiol.* 71, 403–418. doi: 10.1002/dneu.20818

Baas, P. W., and Mozgova, O. I. (2012). A novel role for retrograde transport of microtubules in the axon. *Cytoskeleton* 69, 416–425. doi: 10.1002/cm.21013

Blader, P., Plessy, C., and Strahle, U. (2003). Multiple regulatory elements with spatially and temporally distinct activities control neurogenin1 expression in primary neurons of the zebrafish embryo. *Mech. Dev.* 120, 211–218. doi: 10.1016/S0925-4773(02)00413-6

Buck, K. B., and Zheng, J. Q. (2002). Growth cone turning induced by direct local modification of microtubule dynamics. *J. Neurosci.* 22, 9358–9367.

Castellano Munoz, M., Peng, A. W., Salles, F. T., and Ricci, A. J. (2012). Swept field laser confocal microscopy for enhanced spatial and temporal resolution in live cell imaging. *Microsc. Microanal.* 18, 753–760. doi: 10.1017/S1431927612000542

Cox, K. H., DeLeon, D. V., Angerer, L. M., and Angerer, R. C. (1984). Detection of mrnas in sea urchin embryos by *in situ* hybridization using asymmetric RNA probes. *Dev. Biol.* 101, 485–502. doi: 10.1016/0012-1606(84)90162-3

del Castillo, U., Winding, M., Lu, W., and Gelfand, V. I. (2015). Interplay between kinesin 1 and cortical dynein during axonal outgrowth and microtubule organization in Drosophila neurons. *Elife* 4:e10140.

Dent, E. W., Callaway, J. L., Szebenyi, G., Baas, P. W., and Kalil, K. (1999). Reorganization and movement of microtubules in axonal growth cones and developing interstitial branches. *J. Neurosci.* 19, 8894–8908.

Gallo, G. (2011). The cytoskeletal and signaling mechanisms of axon collateral branching. *Dev. Neurobiol.* 71, 201–220. doi: 10.1002/dneu.20852

Hintsch, G., Zurlinden, A., Meskenaite, V., Steuble, M., Fink Widmer, K., Kinter, J., et al. (2002). The calsyntenins a family of postsynaptic membrane proteins with distinct neuronal expression patterns. *Mol. Cell. Neurosci.* 21, 393–409. doi: 10.1006/mcne.2002.1181

Hoerndli, F. J., Walser, M., Frohli Hoier, E., de Quervain, D., Papassotiropoulos, A., and Hajnal, A. (2009). A conserved function of C. elegans CASY 1 calsyntenin in associative learning. *PLoS ONE*4:e4880. doi: 10.1371/journal.pone.0004880

Ikeda, D. D., Duan, Y., Matsuki, M., Kunitomo, H., Hutter, H., Hedgecock, E. M., et al. (2008). CASY 1, an ortholog of calsyntenins/alcadeins, is essential for learning in Caenorhabditis elegans. *Proc. Natl. Acad. Sci. U.S.A.* 105, 5260–5265. doi: 10.1073/pnas.0711894105

Jolly, A. L., Kim, H., Srinivasan, D., Lakonishok, M., Larson, A. G., and Gelfand, V. I. (2010). Kinesin 1 heavy chain mediates microtubule sliding to drive changes in cell shape. *Proc. Natl. Acad. Sci. U.S.A.* 107, 12151–12156. doi: 10.1073/pnas.1004736107

Kawano, T., Araseki, M., Araki, Y., Kinjo, M., Yamamoto, T., and Suzuki, T. (2012). A small peptide sequence is sufficient for initiating kinesin 1 activation through part of TPR region of KLC1. *Traffic* 13, 834–848. doi: 10.1111/j.1600-0854.2012.01350.x

Ketschek, A., Jones, S., Spillane, M., Korobova, F., Svitkina, T., and Gallo, G. (2015). Nerve growth factor promotes reorganization of the axonal microtubule array at sites of axon collateral branching. *Dev. Neurobiol.* 75, 1441–1461. doi: 10.1002/dneu.22294

Kimmel, C. B., Ballard, W. W., Kimmel, S. R., Ullmann, B., and Schilling, T. F. (1995). Stages of embryonic development of the zebrafish. *Dev. Dyn.* 203, 253–310. doi: 10.1002/aja.1002030302

Kleele, T., Marinkovic, P., Williams, P. R., Stern, S., Weigand, E. E., Engerer, P., et al. (2014). An assay to image neuronal microtubule dynamics in mice. *Nat. Commun.* 5:4827. doi: 10.1038/ncomms5827

Kollins, K. M., Bell, R. L., Butts, M., and Withers, G. S. (2009). Dendrites differ from axons in patterns of microtubule stability and polymerization during development. *Neural Dev.* 4:26. doi: 10.1186/1749-8104-4-26

Konecna, A., Frischknecht, R., Kinter, J., Ludwig, A., Steuble, M., Meskenaite, V., et al. (2006). Calsyntenin 1 docks vesicular cargo to kinesin 1. *Mol. Biol. Cell* 17, 3651–3663. doi: 10.1091/mbc.E06-02-0112

Kwan, K. M., Fujimoto, E., Grabher, C., Mangum, B. D., Hardy, M. E., Campbell, D. S., et al. (2007). The Tol2kit: a multisite gateway based construction kit for Tol2 transposon transgenesis constructs. *Dev. Dyn.* 236, 3088–3099. doi: 10.1002/dvdy.21343

Li, L., Fothergill, T., Hutchins, B. I., Dent, E. W., and Kalil, K. (2014). Wnt5a evokes cortical axon outgrowth and repulsive guidance by tau mediated reorganization of dynamic microtubules. *Dev. Neurobiol.* 74, 797–817. doi: 10.1002/dneu.22102

Lin, S., Liu, M., Mozgova, O. I., Yu, W. Q., and Baas, P. W. (2012). Mitotic motors coregulate microtubule patterns in axons and dendrites. *J. Neurosci.* 32, 14033–14049. doi: 10.1523/JNEUROSCI.3070-12.2012

Liu, Y., and Halloran, M. C. (2005). Central and peripheral axon branches from one neuron are guided differentially by Semaphorin3D and transient axonal glycoprotein 1. *J. Neurosci.* 25, 10556–10563. doi: 10.1523/JNEUROSCI.2710-05.2005

Lu, W., Fox, P., Lakonishok, M., Davidson, M. W., and Gelfand, V. I. (2013). Initial neurite outgrowth in Drosophila neurons is driven by kinesin powered microtubule sliding. *Curr. Biol.* 23, 1018–1023. doi: 10.1016/j.cub.2013.04.050

Ma, Y., Shakiryanova, D., Vardya, I., and Popov, S. V. (2004). Quantitative analysis of microtubule transport in growing nerve processes. *Curr. Biol.* 14, 725–730. doi: 10.1016/j.cub.2004.03.061

Maniar, T. A., Kaplan, M., Wang, G. J., Shen, K., Wei, L., Shaw, J. E., et al. (2011). UNC 33 (CRMP) and ankyrin organize microtubules and localize kinesin to polarize axon dendrite sorting. *Nat. Neurosci.* 15, 48–56. doi: 10.1038/nn.2970

Marx, A., Godinez, W. J., Tsimashchuk, V., Bankhead, P., Rohr, K., and Engel, U. (2013). Xenopus cytoplasmic linker associated protein 1 (XCLASP1) promotes axon elongation and advance of pioneer microtubules. *Mol. Biol. Cell* 24, 1544–1558. doi: 10.1091/mbc.E12-08-0573

Mattie, F. J., Stackpole, M. M., Stone, M. C., Clippard, J. R., Rudnick, D. A., Qiu, Y., et al. (2010). Directed microtubule growth, +TIPs, and kinesin 2 are required for uniform microtubule polarity in dendrites. *Curr. Biol.* 20, 2169–2177. doi: 10.1016/j.cub.2010.11.050

Nguyen, M. M., McCracken, C. J., Milner, E. S., Goetschius, D. J., Weiner, A. T., Long, M. K., et al. (2014). Gamma tubulin controls neuronal microtubule polarity independently of Golgi outposts. *Mol. Biol. Cell* 25, 2039–2050. doi: 10.1091/mbc.E13-09-0515

Pettem, K. L., Yokomaku, D., Luo, L., Linhoff, M. W., Prasad, T., Connor, S. A., et al. (2013). The specific alpha neurexin interactor calsyntenin 3 promotes excitatory and inhibitory synapse development. *Neuron* 80, 113–128. doi: 10.1016/j.neuron.2013.07.016

Ponomareva, O. Y., Holmen, I. C., Sperry, A. J., Eliceiri, K. W., and Halloran, M. C. (2014). Calsyntenin 1 regulates axon branching and endosomal trafficking during sensory neuron development *in vivo*. *J. Neurosci.* 34, 9235–9248. doi: 10.1523/JNEUROSCI.0561-14.2014

Preuschhof, C., Heekeren, H. R., Li, S. C., Sander, T., Lindenberger, U., and Backman, L. (2010). KIBRA and CLSTN2 polymorphisms exert interactive effects on human episodic memory. *Neuropsychologia* 48, 402–408. doi: 10.1016/j.neuropsychologia.2009.09.031

Qiang, L., Yu, W., Liu, M., Solowska, J. M., and Baas, P. W. (2010). Basic fibroblast growth factor elicits formation of interstitial axonal branches via enhanced severing of microtubules. *Mol. Biol. Cell* 21, 334–344. doi: 10.1091/mbc.E09-09-0834

Ringman, J. M., Schulman, H., Becker, C., Jones, T., Bai, Y., Immermann, F., et al. (2012). Proteomic changes in cerebrospinal fluid of presymptomatic and affected persons carrying familial Alzheimer disease mutations. *Arch. Neurol.* 69, 96–104. doi: 10.1001/archneurol.2011.642

Sagasti, A., Guido, M. R., Raible, D. W., and Schier, A. F. (2005). Repulsive interactions shape the morphologies and functional arrangement of zebrafish peripheral sensory arbors. *Curr. Biol.* 15, 804–814. doi: 10.1016/j.cub.2005.03.048

Schindelin, J., Arganda Carreras, I., Frise, E., Kaynig, V., Longair, M., Pietzsch, T., et al. (2012). Fiji: an open source platform for biological image analysis. *Nat. Methods* 9, 676–682. doi: 10.1038/nmeth.2019

Stepanova, T., Slemmer, J., Hoogenraad, C. C., Lansbergen, G., Dortland, B., De Zeeuw, C. I., et al. (2003). Visualization of microtubule growth in cultured neurons via the use of EB3 GFP, (end binding protein 3 green fluorescent protein). *J. Neurosci.* 23, 2655–2664.

Stepanova, T., Smal, I., van Haren, J., Akinci, U., Liu, Z., Miedema, M., et al. (2010). History dependent catastrophes regulate axonal microtubule behavior. *Curr. Biol.* 20, 1023–1028. doi: 10.1016/j.cub.2010.04.024

Ster, J., Steuble, M., Orlando, C., Diep, T. M., Akhmedov, A., Raineteau, O., et al. (2014). Calsyntenin 1 regulates targeting of dendritic NMDA receptors and dendritic spine maturation in CA1 hippocampal pyramidal cells during postnatal development. *J. Neurosci.* 34, 8716–8727. doi: 10.1523/JNEUROSCI.0144-14.2014

Steuble, M., Diep, T. M., Schatzle, P., Ludwig, A., Tagaya, M., Kunz, B., et al. (2012). Calsyntenin 1 shelters APP from proteolytic processing during anterograde axonal transport. *Biol. Open* 1, 761–774. doi: 10.1242/bio.20121578

Sweet, E. S., Previtera, M. L., Fernandez, J. R., Charych, E. I., Tseng, C. Y., Kwon, M., et al. (2011). PSD 95 Alters Microtubule Dynamics via an Association With EB3. *J. Neurosci.* 31, 1038–1047. doi: 10.1523/JNEUROSCI.1205-10.2011

Tanaka, E., Ho, T., and Kirschner, M. W. (1995). The role of microtubule dynamics in growth cone motility and axonal growth. *J. Cell Biol.* 128, 139–155. doi: 10.1083/jcb.128.1.139

Tanaka, E. M., and Kirschner, M. W. (1991). Microtubule behavior in the growth cones of living neurons during axon elongation. *J. Cell Biol.* 115, 345–363. doi: 10.1083/jcb.115.2.345

Uchida, Y., Gomi, F., Murayama, S., and Takahashi, H. (2013). Calsyntenin 3 C terminal fragment accumulates in dystrophic neurites surrounding abeta plaques in tg2576 mouse and Alzheimer disease brains: its neurotoxic role in mediating dystrophic neurite formation. *Am. J. Pathol.* 182, 1718–1726. doi: 10.1016/j.ajpath.2013.01.014

Um, J. W., Pramanik, G., Ko, J. S., Song, M. Y., Lee, D., Kim, H., et al. (2014). Calsyntenins function as synaptogenic adhesion molecules in concert with neurexins. *Cell Rep.* 6, 1096–1109. doi: 10.1016/j.celrep.2014.02.010

Vagnoni, A., Perkinton, M. S., Gray, E. H., Francis, P. T., Noble, W., and Miller, C. C. (2012). Calsyntenin 1 mediates axonal transport of the amyloid precursor protein and regulates Abeta production. *Hum. Mol. Genet.* 21, 2845–2854. doi: 10.1093/hmg/dds109

van Beuningen, S. F. B., Will, L., Harterink, M., Chazeau, A., van Battum, E. Y., Frias, C. P., et al. (2015). TRIM46 controls neuronal polarity and axon specification by driving the formation of parallel microtubule arrays. *Neuron* 88, 1208–1226. doi: 10.1016/j.neuron.2015.11.012

Vogt, L., Schrimpf, S. P., Meskenaite, V., Frischknecht, R., Kinter, J., Leone, D. P., et al. (2001). Calsyntenin 1, a proteolytically processed postsynaptic membrane protein with a cytoplasmic calcium binding domain. *Mol. Cell. Neurosci.* 17, 151–166. doi: 10.1006/mcne.2000.0937

Wong, Y. L., and Rice, S. E. (2010). Kinesin's light chains inhibit the head and microtubule binding activity of its tail. *Proc. Natl. Acad. Sci. U.S.A.* 107, 11781–11786. doi: 10.1073/pnas.1005854107

Yalgin, C., Ebrahimi, S., Delandre, C., Yoong, L. F., Akimoto, S., Tran, H., et al. (2015). Centrosomin represses dendrite branching by orienting microtubule nucleation. *Nat. Neurosci.* 18, 1437–1445. doi: 10.1038/nn.4099

Yan, J., Chao, D. L., Toba, S., Koyasako, K., Yasunaga, T., Hirotsune, S., et al. (2013). Kinesin 1 regulates dendrite microtubule polarity in *Caenorhabditis elegans*. *Elife* 2:e00133. doi: 10.7554/eLife.00133

Yau, K. W., Schatzle, P., Tortosa, E., Pages, S., Holtmaat, A., Kapitein, L. C., et al. (2016). Dendrites *in vitro* and *in vivo* contain microtubules of opposite polarity and axon formation correlates with uniform plus end out microtubule orientation. *J. Neurosci.* 36, 1071–1085. doi: 10.1523/JNEUROSCI.2430-15.2016

Yip, Y. Y., Pernigo, S., Sanger, A., Xu, M., Parsons, M., Steiner, R. A., et al. (2016). The light chains of kinesin 1 are autoinhibited. *Proc. Natl. Acad. Sci. U.S.A.* 113, 2418–2423. doi: 10.1073/pnas.1520817113

Yu, W., Qiang, L., Solowska, J. M., Karabay, A., Korulu, S., and Baas, P. W. (2008). The microtubule severing proteins spastin and katanin participate differently in the formation of axonal branches. *Mol. Biol. Cell* 19, 1485–1498. doi: 10.1091/mbc.E07-09-0878

Yu, W. Q., Ahmad, F. J., and Baas, P. W. (1994). Microtubule Fragmentation and Partitioning in the Axon during Collateral Branch Formation. *J. Neurosci.* 14, 5872–5884.

Yu, W., Cook, C., Sauter, C., Kuriyama, R., Kaplan, P. L., and Baas, P. W. (2000). Depletion of a microtubule associated motor protein induces the loss of dendritic identity. *J. Neurosci.* 20, 5782–5791.

Zheng, Y., Wildonger, J., Ye, B., Zhang, Y., Kita, A., Younger, S. H., et al. (2008). Dynein is required for polarized dendritic transport and uniform microtubule orientation in axons. *Nat. Cell Biol.* 10, 1172–1180. doi: 10.1038/ncb1777

Conflict of Interest Statement: The authors declare that the research was conducted in the absence of any commercial or financial relationships that could be construed as a potential conflict of interest.

frontiers in Cellular Neuroscience

ORIGINAL RESEARCH
published: 28 August 2017
doi: 10.3389/fncel.2017.00260

Myosin-V Induces Cargo Immobilization and Clustering at the Axon Initial Segment

*Anne F. J. Janssen†, Roderick P. Tas†, Petra van Bergeijk, Rosalie Oost, Casper C. Hoogenraad and Lukas C. Kapitein **

Cell Biology, Department of Biology, Faculty of Science, Utrecht University, Utrecht, Netherlands

The selective transport of different cargoes into axons and dendrites underlies the polarized organization of the neuron. Although it has become clear that the combined activity of different motors determines the destination and selectivity of transport, little is known about the mechanistic details of motor cooperation. For example, the exact role of myosin-V in opposing microtubule-based axon entries has remained unclear. Here we use two orthogonal chemically-induced heterodimerization systems to independently recruit different motors to cargoes. We find that recruiting myosin-V to kinesin-propelled cargoes at approximately equal numbers is sufficient to stall motility. Kinesin-driven cargoes entering the axon were arrested in the axon initial segment (AIS) upon myosin-V recruitment and accumulated in distinct actin-rich hotspots. Importantly, unlike proposed previously, myosin-V did not return these cargoes to the cell body, suggesting that additional mechanism are required to establish cargo retrieval from the AIS.

Keywords: polarized transport, motor proteins, myosin-V, kinesin, axon initial segment, motor cooperation

OPEN ACCESS

Edited by:
Froylan Calderon De Anda, University of Hamburg, Germany

Reviewed by:
Alfredo Cáceres, INEMEC-CONICET, Argentina
Matthew N. Rasband, Baylor College of Medicine, United States
Matthew s Grubb, King's College London, United Kingdom

***Correspondence:**
Lukas C. Kapitein
l.kapitein@uu.nl

† These authors have contributed equally to this work.

Received: *26 January 2017*
Accepted: *11 August 2017*
Published: *28 August 2017*

Citation:
Janssen AFJ, Tas RP, van Bergeijk P, Oost R, Hoogenraad CC and Kapitein LC (2017) Myosin-V Induces Cargo Immobilization and Clustering at the Axon Initial Segment. Front. Cell. Neurosci. 11:260. doi: 10.3389/fncel.2017.00260

INTRODUCTION

The selective transport of different cargoes into axons and dendrites underlies the polarized organization of the neuron. Recent work has revealed that different motor proteins have a different selectivity for axons and dendrites. For example, some kinesins selectively target axons, while others target both axons and dendrites (Huang and Banker, 2012; Lipka et al., 2016). In addition, myosin-V has been implicated in selective targeting to dendrites (Lewis et al., 2009). Expression of a dominant negative form of myosin-Va caused the non-specific localization of cargo otherwise enriched in the somatodendritic compartment. Furthermore, coupling a protein to a myosin-Va binding domain was sufficient to cause its somatodendritic localization. More recent work has reported that vesicles with dendritic cargoes often enter the axon, but stop and reverse in the axon initial segment (AIS) in a process that depends on myosin-Va and an intact actin cytoskeleton (Al-Bassam et al., 2012). Nevertheless, the exact contribution of actin and myosin-V to axonal exclusion has remained controversial, given that actin disruption also distorted the sorting of cargoes into the proper carriers (Petersen et al., 2014). In addition, whether recruitment or activation of myosin-V is sufficient to cause the reversal of dendritic cargo has remained unclear.

Although, it has become clear that the combined activity of different motors determines transport destination and selectivity, little is known about the mechanistic details of motor cooperation. For example, it is not known whether acute activation or recruitment of myosin-V is sufficient to oppose kinesin-based axon entries. More generally, how the outcome of multiple motors depends on the relative amounts of motor proteins recruited to cellular cargoes has

remained unexplored. Elegant *in vitro* assays have used DNA origami to assemble well-defined combinations of different motor proteins (Derr et al., 2012), but similar control has not yet been achieved inside cells. Previously, acute recruitment of different motor proteins using chemically-induced heterodimerization has been used to probe combinatorial motor activity in non-neuronal cells (Kapitein et al., 2010b, 2013). These experiments revealed that, in non-neuronal COS7 cells, recruitment of myosin-V is sufficient to attenuate kinesin-propelled cargo (Kapitein et al., 2013). However, in these assays, the motors could not be recruited independently, which would enable sequential recruitment of different motors.

Here we introduce a new assay that allows the independent recruitment of different motor proteins. We find that recruiting myosin-V to kinesin-propelled cargoes at approximately equal numbers is sufficient to stall motility. Kinesin-driven cargoes entering the axon were arrested in the AIS upon myosin-V recruitment and accumulated in distinct actin-rich hotspots. Importantly, unlike proposed previously, myosin-V did not return these cargoes to the cell body, suggesting that additional mechanism are required to establish cargo retrieval from the AIS.

RESULTS

To establish an assay for the independent recruitment of different motors, the FKBP-rapalog-FRB heterodimerization system was combined with a recently introduced chemically-induced heterodimerization system in which the cell-permeable, AM-modified plant hormone gibberellin triggers the interaction between a GID1 and a GAI domain (Miyamoto et al., 2012). We chose this dimerization system over light-induced systems, because, similar to the FKBP-rapalog-FRB system, the induced complex formation has been reported to be essentially irreversible. As a result, the available sites on the cargoes will be quickly saturated as long as the number of GAI-labeled motors in the cell is higher than the total number of GID1-sites on the cargoes, irrespective of the exact concentrations. Therefore, if both heterodimerization systems are combined in one peroxisome-targeting construct, PEX3-mRFP-FKBP-linker-GID1, the FRB and GAI domains will be recruited with roughly equal probabilities.

To test the independent recruitment of different motors, COS7 cells were transfected with PEX3-mRFP-FKBP-linker-GID1, Kif17-GFP-GAI, and MyoVb-iRFP-FRB (**Figures 1A,B**). Upon addition of gibberellin, Kif17-GFP-GAI was recruited to PEX3-mRFP-FKBP-linker-GID1 and peroxisomes were rapidly redistributed to the cell periphery (**Figure 1C**, middle column). Similar to previous observations, peroxisomes in the cell periphery remained mobile even after reaching the periphery of the cell (Kapitein et al., 2013). In addition, contrary to FKBP-based heterodimerization, we noted that a subset of peroxisomes was already mobile at the periphery before addition of gibberellin, indicating some degree of background heterodimerization. To still ensure independent recruitment of different motors, gibberelin-based motor recruitment was always performed prior to rapalog-based recruitment.

Twenty five minutes after addition of gibberellin to recruit kinesin, rapalog was added to recruit myosin-V (**Figure 1A**), resulting in an arrest of the kinesin-driven motility and the accumulation of peroxisomes near the cell cortex (**Figure 1C**, right column, **Figure 1D**; **Supplemental Video 1**). These effects were quantified using two previously introduced metrics (van Bergeijk et al., 2015). First, we calculated for all frames the radius required to include 90% of the fluorescence intensity of the peroxisomes ($R_{90\%}$), which revealed that peroxisomes moved rapidly to the periphery upon recruitment of kinesin, but did not move much further upon recruitment of myosin-V (**Figures 1E,F**). Second, we used image correlation analysis to measure the overall frame-to-frame similarity during the experiment. In the absence of transport, two subsequent images are largely identical and the correlation index will be close to 1, whereas a value of 0 indicates that all organelles have moved to previously unoccupied positions. The correlation index decreased upon kinesin recruitment, reflecting the increased peroxisome mobility, whereas it increased after recruitment of myosin, indicating that peroxisome became less motile (**Figures 1E,F**). This decrease in motility was not observed without recruitment of myosin although cargo reached the cell periphery. This is reflected in the correlation index which remains low without myosin recruitment. Thus, different heterodimerization systems can be combined to independently recruit different motor proteins, and the recruitment of myosin-V to kinesin motors at roughly equal numbers is sufficient to arrest kinesin-driven motility.

We next switched to neurons to examine how activation of myosin-V alters the kinesin-driven transport of peroxisomes into the axon. We used the kinesin-1 KIF5B, because this motor has been reported to efficiently target cargoes selectively into the axon (Song et al., 2009; Kapitein et al., 2010a; Petersen et al., 2014; **Supplemental Figures 1A–C**). Indeed, the addition of gibberellin to dissociated hippocampal neurons expressing PEX3-mRFP-FKBP-linker-GID1, Kif5-GFP-GAI, and MyoVb-iRFP-FRB induced a burst of peroxisome motility into the axon ($n = 16$ cells, **Figures 2A–D**). Remarkably, the subsequent addition of rapalog to recruit myosin-V resulted in the appearance of several spots in the proximal axon where axon-entering peroxisomes would cluster together, whereas further down the axon ($>35\,\mu m$) such clusters did not emerge ($n = 15$ cells, cells with ≥ 2 induced clusters and $>75\,\mu m$ axon length imaged were included, **Figures 2A–D**; **Supplemental Video 2**). Quantification revealed that the percentage of cells that had more than two proximal axonal accumulations increased from 6.25 to 75% during the first 40 min after addition of rapalog (**Figure 2D**). Thus, the acute, close-to-equimolar recruitment of myosin-V to kinesin-1 driven, axon-entering cargoes clusters these cargoes in the proximal axon.

Previous work has suggested that myosin-V can drive retrograde axonal transport, thereby returning to the cell body cargoes that have erroneously entered the axon (Watanabe et al., 2012). In contrast, we observed that myosin-V induced the appearance of cargo clusters that were largely immobile. To analyze the motility of the myosin-V induced peroxisome clusters in more detail and test for retrograde motility, we

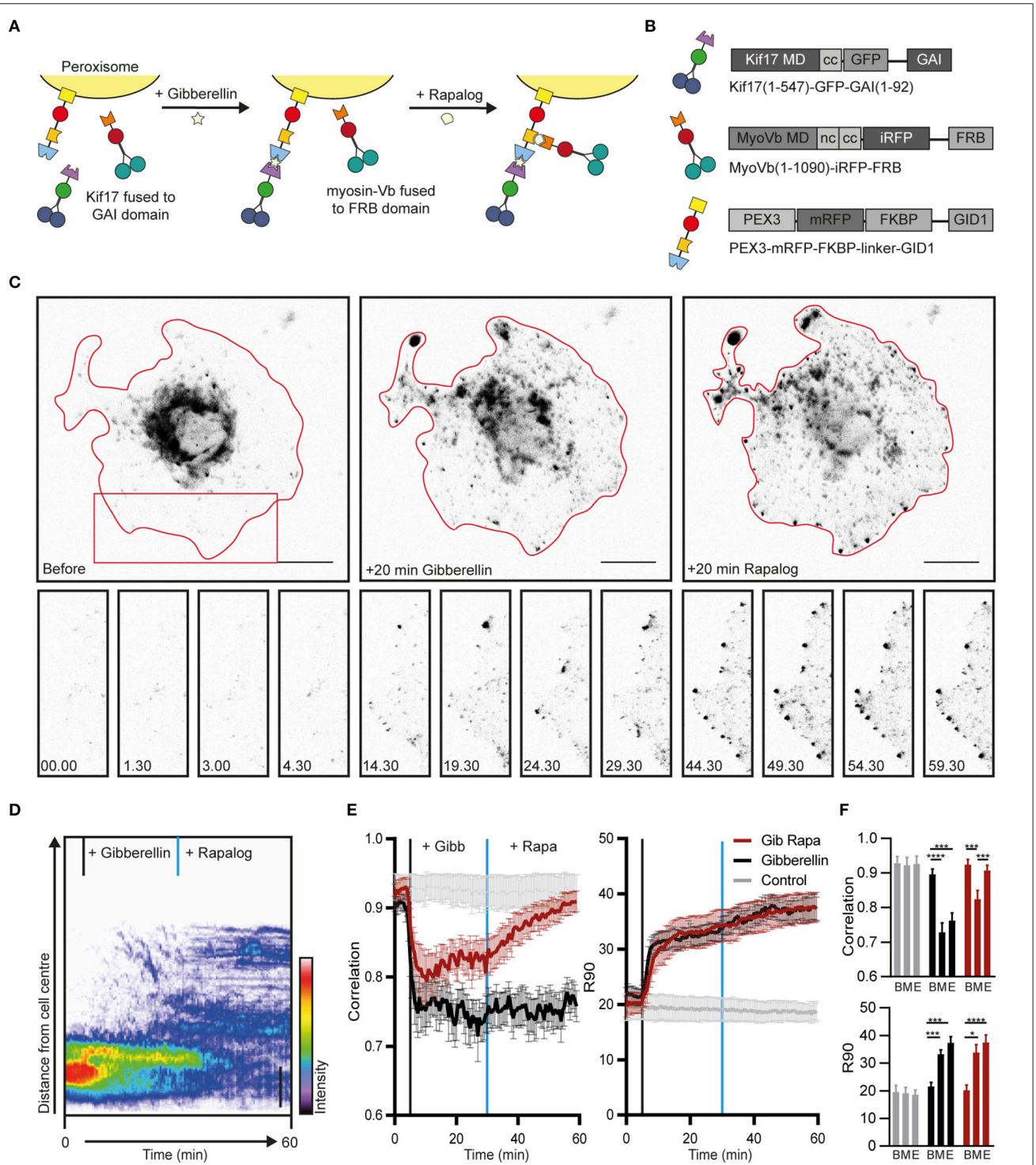

FIGURE 1 | Sequential recruitment of kinesin and myosin-V in COS7 cells. **(A)** Assay: Sequential recruitment of kinesin and myosin-V by addition of gibberellin and rapalog, respectively. **(B)** Overview of constructs. MD, motor domain; CC, coiled coil; NC, neck coil; GAI, gibberellin insensitive; GID1, Gibberellin insensitive dwarf1. **(C)** Peroxisome distribution before recruitment of motors and after sequential recruitment of kinesin and myosin-V. Red curves indicate cell outline. Panels show individual frames of a cut out. Scale bar, 20 μm. **(D)** Radial kymograph indicating the redistribution of fluorescent peroxisomes relative to the cell axis. Vertical lines indicate addition of gibberellin (black) and rapalog (blue). Scale bar, 10 μm. **(E)** Displacement (expressed in $R_{90\%}$) and correlation (frame-to-frame similarity from 0 to 1) vs. time for cells without added ligands (control, gray), cells with addition of gibberelin only (Gibberelin, black), and cells with addition of gibberellin and rapalog (Gib + rapa, red). $N = 12$, 16, and 14 cells for control, gibbellin, and gib+rapa groups, respectively. Data was obtained from 2 experiments, mean ± s.e.m. Vertical lines indicate time of addition of gibberellin (black) and rapalog (blue), if added. **(F)** Averages of ten frames of each cell at $t = 0$–4.5 min (before, B), $t = 25$–29.5 min (middle, M), and $t = 55$–59.5 min (end, E). $^{*}P < 0.05$, $^{***}P < 0.001$, $^{****}P < 0.0001$, Friedman test, Dunn's *post-hoc* test.

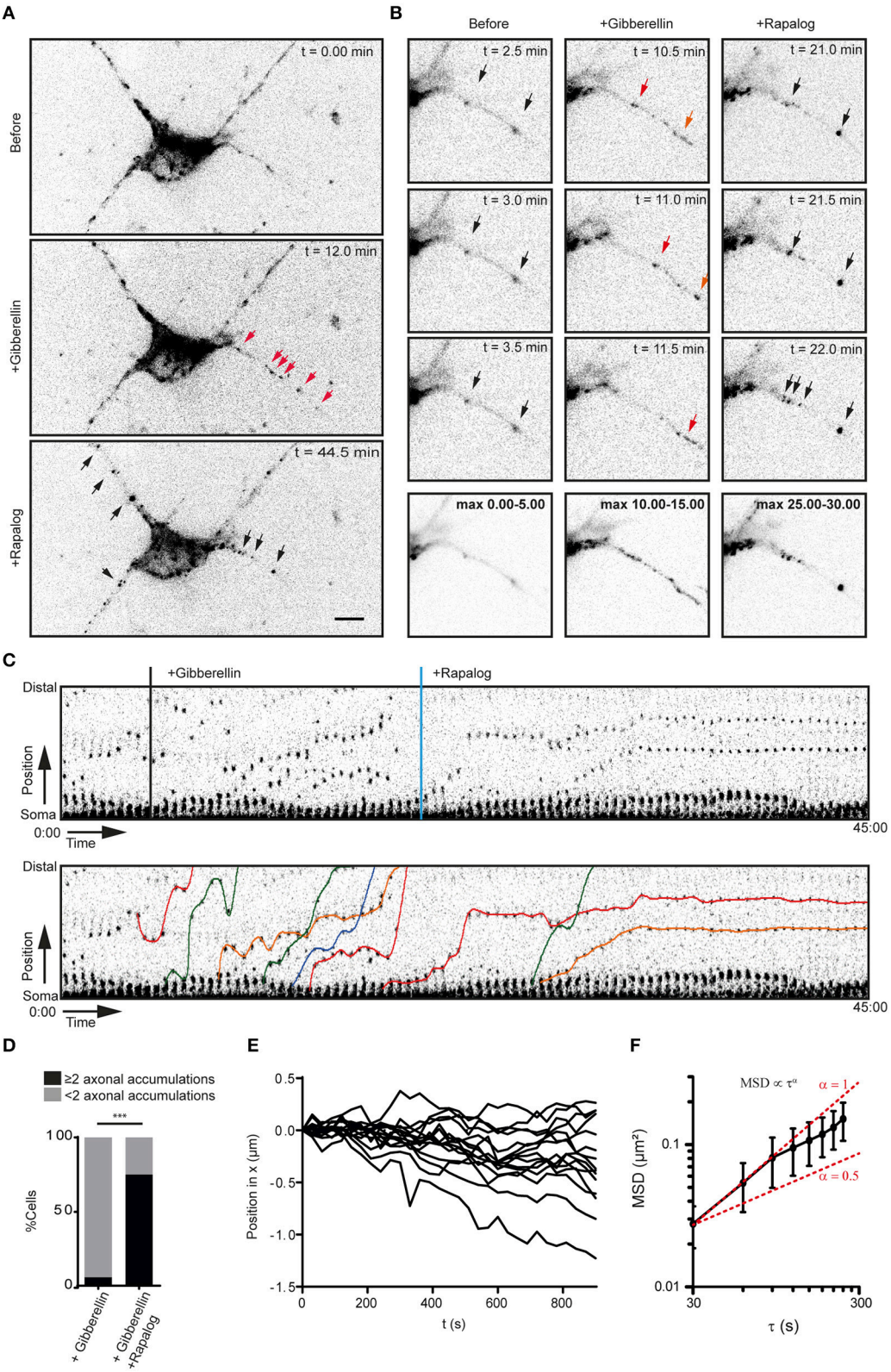

FIGURE 2 | Myosin-V anchors kinesin-1 propelled peroxisomes in the proximal axon and somatodendritic compartment. **(A)** Dissociated hippocampal neuron showing the distribution of PEX3-mRFP-FKBP-linker-GID1 before (top), after the recruitment of Kif5-GFP-GAI through addition of gibberellin (middle) and after the

(Continued)

FIGURE 2 | Continued
addition of rapalog to recruit MyoVb-iRFP-FRB (bottom). Red arrows indicate motile peroxisomes, black arrows indicate non-motile peroxisome accumulations. Scale bar, 10 μm. **(B)** Zoom of the proximal axon of neuron in **(A)** before (left), plus gibberellin (middle), and plus rapalog (right). Bottom row shows a maximum projection of a 5 min interval before (left) or after the addition of dimerizers (middle, right). **(C)** Sequential frames of the proximal axon of a dissociated hippocampal neuron treated and imaged as in **(A)**. Manually annotated tracks are displayed superimposed on the bottom panel. **(D)** Number of stalled peroxisome accumulations in the axon before and after anchoring with MyoVb. In all cases, recruitment of kinesin upon addition of gibberellin induced a burst of perxosisomes into the axon. $n = 16$ and $n = 24$ for control and +Rapalog, respectively $^{***}p < 0.001$ Fisher Exact test. **(E)** Relative displacements of myosin-V anchored clusters 10 min after the addition of rapalog. Negative and positive displacement indicates retrograde and anterograde movement, respectively. **(F)** Mean square displacement analysis of myosin-V anchored peroxisome clusters tracked for at least 25 intervals of 30 s mean ± *sd* ($n = 26$). Red lines show example curves with slopes $\alpha = 1$ and $\alpha = 0.5$ (i.e., log(MSD) α log τ, representative of purely diffusive or confined motility, respectively.

traced individual peroxisome clusters (**Figure 2E**) and averaged their mean-squared displacements (MSD) for different time intervals (**Figure 2F**). The power dependence α of the MSD with increasing time intervals τ, MSDα τ^{α}, is the anomalous diffusion exponent (Saxton and Jacobson, 1997) and indicates whether motility is completely random ($\alpha \approx 1$, diffusive), directed ($1 < \alpha \leq 2$, superdiffusive), or confined ($0 < \alpha < 1$, subdiffusive). Our analysis revealed that the clusters were confined and that the average displacement over >13 min was <500 nm [i.e., $(0.25\,\mu m^2)^{1/2}$, **Figure 2F**]. Thus, myosin-V does not drive retrograde transport, but anchors cargo at specific locations in the proximal axon.

To explore how myosin-V affects the motility of cargoes that autonomously travel into the axon, we next turned to Rab3-positive vesicles. When myosin-Vb was recruited to Rab3 vesicles using the FKBP-rapalog-FRB system (**Figure 3A**), we observed the emergence of immobile clusters of Rab3-positive vesicles in the first part of the axon, whereas the motility of vesicles in the distal axon did not appear affected, based on inspection of the kymographs (**Figures 3B,C**; **Supplemental Video 3**). In addition, motility arrest and clustering was observed in the somatodendritic compartment (data not shown). Rab3 vesicle clustering was not observed upon treatment with rapalog or gibberellin in the absence of MyoVb-iRFP-FRB expression or without addition of rapalog in the presence of the motor (**Supplemental Figures 2A,B**). To test whether clustering was selective for the AIS, we repeated the experiment, followed by staining for the AIS marker Ankyrin-G (**Figures 3D,E**). Quantitative analysis of the Rab3 cluster relative to the staining of Ankyrin-G revealed that 92 ± 17% of clusters were found in AIS (average ± *sd*, $n = 9$ cells; **Figure 3F**). MSD analysis revealed an anomalous diffusion exponent of ∼1 for time scales <360 s (**Figure 3G**). At longer times, the MSD leveled off, suggesting that Rab3 cluster motility was confined to 700–800 nm [i.e., $(0.6\,\mu m^2)^{1/2}$]. It is important to note that the selective clustering in the AIS could be a trivial consequence of the very low levels of myosin-V in the remainder of the axon (**Figure 3H**). Nevertheless, these results demonstrate that myosin-V induces cargo clustering, rather than retrograde transport.

Recent work has suggested a role for specialized actin structures in the AIS in myosin-V based cargo retrieval (Watanabe et al., 2012). To examine the relation between myosin-V induced cargo clustering and the actin cytoskeleton, we next performed superresolution microscopy to image actin and Rab3 in MyoVb-GFP-FRB and FKBP-tdTomato-Rab3c expressing neurons (**Figures 4A,B**). To visualize actin, we purified GFP-tagged Lifeact, a small probe that transiently interacts with polymerized actin and can be used to achieve the repetitive low density labeling required for single molecule localization microscopy (Kiuchi et al., 2015). To visualize Rab3, we used DNA-PAINT, in which a secondary antibody is labeled with an oligonucleotide that can transiently hybridize with a fluorescently labeled complementary strand, which also ensures repetitive low density labeling (Jungmann et al., 2014). After optimization of the extraction and fixation protocols, this enables us to perform two-color nanoscopy of the actin network and rab3 vesicles.

In control cells that were not treated with rapalog, we observed both regularly spaced actin stripes, as described previously (Xu et al., 2013), long actin fibers and distinct actin patches with concentrated staining (**Figure 4A**). No apparent colocalization between actin and Rab3 was observed in these cells. In cells treated with rapalog, a clear colocalization between Rab3 accumulations and actin-rich regions was observed (**Figure 4B**). The diameter of Rab3 structures that were colocalized with actin patches was about two times greater compared to Rab3 structures outside these patches or in cells without rapalog treatment (**Figure 4C**). This suggests that multiple vesicles have coalesced on these patches, consistent with our live imaging data of cluster formation (**Figures 3B,C**). Furthermore, Rab3 clusters were only observed in the proximal and not the distal axon (**Figures 4D,E**). These data demonstrate that actin patches are the site of myosin-mediated anchoring.

DISCUSSION

We have developed an assay for the sequential recruitment of motor proteins to specific cargoes. Using this assay, we were able to show that recruiting myosin-V to kinesin-1-driven cargo is sufficient for myosin to attenuate kinesin-driven motility of peroxisomes in COS7 cells. Future work will be directed toward exploring the myosin-kinesin ratio at which stalling still occurs. In addition, the outcome of other motor combinations could also be explored, for example kinesins and dyneins or combinations of different kinesin motors.

We were able to show a similar anchoring behavior in neurons where peroxisomes coupled to kinesin entered the axon, but were subsequently anchored at the AIS by myosin-V recruitment. Similar results were obtained upon recruitment of myosin-V to Rab3-positive vesicles. No reversals of myosin-V anchored peroxisomes back into the cell soma were observed. These

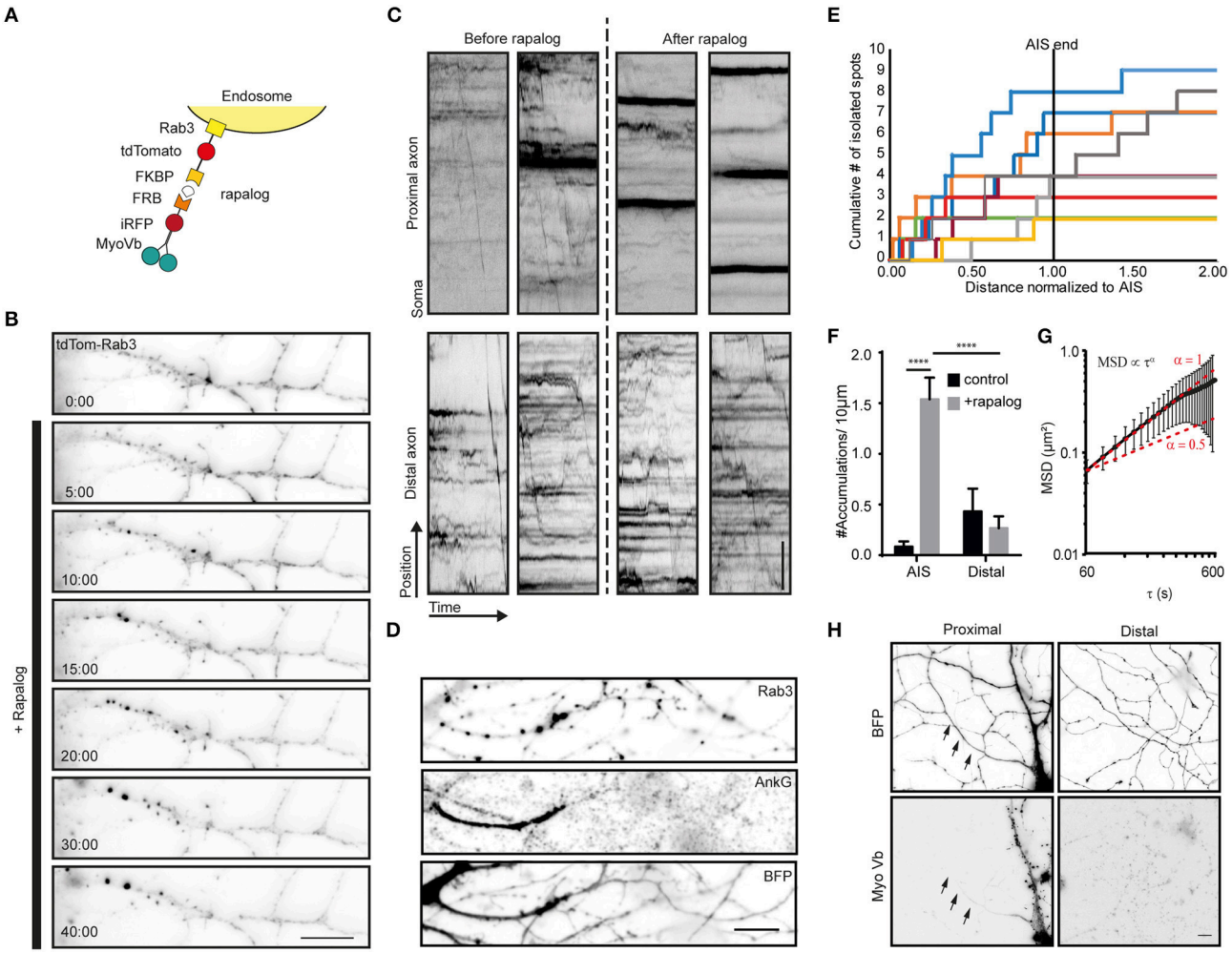

FIGURE 3 | Myosin-V anchors Rab3 vesicles in the proximal axon of hippocampal neurons. **(A)** Assay: Recruitment of myosin-V to Rab3 vesicles by addition of rapalog. **(B)** Rab3 positive vesicle distribution in the proximal axon. Upon coupling of myosin-Vb to vesicles by addition of rapalog, Rab3 vesicles start accumulating in big puncta. Scale bar, 10 µm. **(C)** Kymographs of Rab3 vesicles in the proximal and distal axon. Short timelapses were acquired with 500 ms intervals before and after addition of rapalog. For imaging of distal axons after rapalog treatment, cells were chosen 1 h after rapalog addition that showed clear Rab3 anchoring in their proximal axon. Scale bar, 5 µm. **(D)** Rab3 distribution after myosin-Vb recruitment, together with a staining for Ankyrin-G to indicate the AIS. BFP was used as a fill to show the overall morphology. Scale bar, 10 µm. **(E)** Plot of the cumulative number of Rab3 accumulations found in the axon normalized to the AIS determined for cells after rapalog addition to recruit myosin-Vb. **(F)** Number of accumulations found in the AIS and the distal axon as determined using Ankyrin-G staining. The number of accumulation were determined in fixed cells with and without addition of rapalog Mean ± *sd* ($n = 9$ for both conditions), 2-way ANOVA reveals $F_{interaction} = 26.27$, $p = 0.0001$. *Post-hoc* multiple comparison testing: $^{****}p < 0.0001$. **(G)** Mean square displacement analysis of myosin-V anchored peroxisome clusters tracked for at least 25 intervals of 20 s. Mean ± *sd* ($n = 18$). **(H)** Distribution of the MyoVb(1-1090)-EGFP-FRB construct. The axon is indicated by arrows. Scale bar, 10 µm.

results support a model in which myosin-V stalls the motility of dendritic vesicles that erroneously entered the axon, but also demonstrate that recruitment of myosin-V is not sufficient to bring these cargoes back into the soma to facilitate delivery to their proper destination. These finding are consistent with earlier work demonstrating that the coupling of a myosin-Va binding domain of Melanophilin to vesicles with no specific localization increases their halting frequency in the AIS but not the frequency of reversals (Al-Bassam et al., 2012).

Myosin-V-induced anchoring was also observed in the dendrites and soma, suggesting that this anchoring does not depend on specific feature of the AIS, but will occur whenever cargoes with active myosin-V enter actin-rich regions. Indeed, actin hotspots in the distal axon were also described by others (Ganguly et al., 2015). We do not exclude that recruitment of other proteins could also affect the transport of cargoes, for example due to steric effects. However, myosin-5 is recruited to kinesin that is already attached to an organelle and therefore the increase in size is not as dramatic compared to recruiting myosin-5 to a free kinesin. More importantly, myosin-5 recruitment stalls transport on actin patches, which suggests that this effect is at least specific to an actin-binding protein. Although, myosin-V

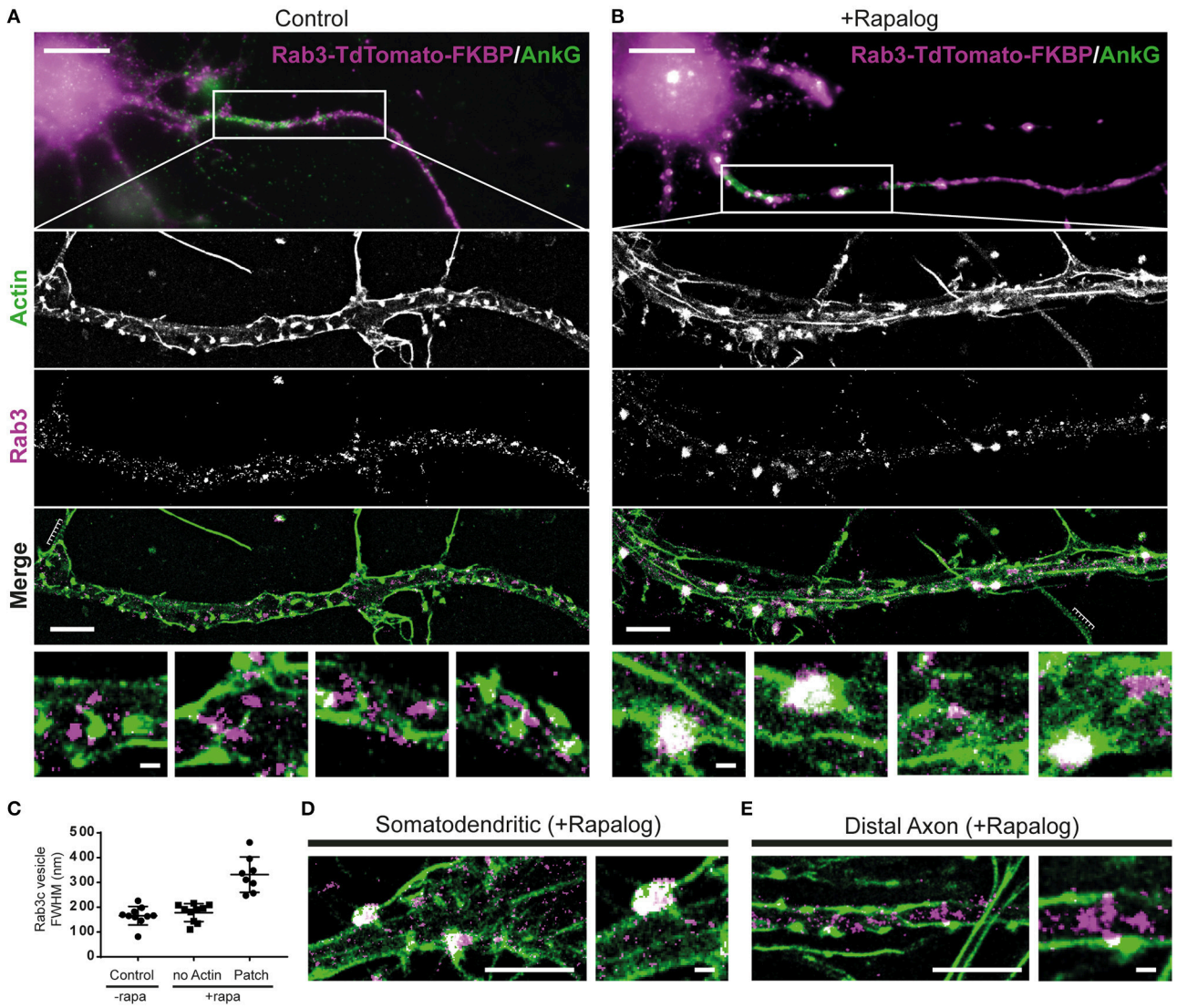

FIGURE 4 | Myosin-V-anchored Rab-3 vesicles accumulate on actin patches in the proximal axon. **(A,B)** Single molecule localization microscopy of sequentially imaged lifeAct-GFP protein-PAINT and DNA-PAINT to visualize actin and Rab3, respectively. DIV10 neurons overexpressing MyosinVb-HA-FRB and Rab3-tdTomato-FKBP, post-stained for TdTomato and AnkyrinG. Axons were identified by AnkyrinG staining. Super-resolution images are shown for the regions indicated in the widefield images (top panel). Control **(A)** and MyosinVb coupled Rab3 vesicles **(B)** are imaged together with actin (middle 3 panels). Scale bar: top panel 10 μm, middle panels 2 μm, zooms 0.2 μm. **(C)** Quantification of the FWHM of Rab3 structures in control and rapalog-treated cells. Myosin-coupled Rab3 vesicles were separated based on their colocalization with actin patches. Mean ± *sd* are depicted ($n = 8$–10 for 2 cells per condition). **(D)** Super-resolution image and zoom of Rab3 cluster colocalization with actin in the somatodendritic compartment. Scale bar: left panel 2 μm, right panel 0.2 μm. **(E)** Super resolution image and zoom of Rab3 vesicles and actin in the distal axon. Scale bar: left panel 2 μm, right panel 0.2 μm.

based anchoring is not restricted to the axon, the actin in the AIS still establishes an important vesicle filter, because it enables the halting of cargo that is not supposed to enter the axon. This suggests that the cargo recruitment and/or activation state of myosin-V determines whether the cargo is allowed to pass the AIS. Upon anchoring, the subsequent recruitment of dynein could return the cargo to the cell body. This is consistent with recent work on the dynein regulator NDEL, which was shown to localize to the AIS via an interaction with the scaffolding protein Ankyrin-G and facilite cargo reversal (Kuijpers et al., 2016).

EXPERIMENTAL PROCEDURES

DNA Constructs and Protein Purification

DNA constructs used in this study were cloned in pGW1-CMV and pβactin-16-pl vectors. The pβactin-PEX3-mRFP-FKBP-linker-GID1 construct was made by PCR amplification of the GID1 domain with addition of a linker (SAGGSAGGSAGG), then ligated into the SpeI and NotI sites of the pβactin-PEX3-mRFP vector described previously (Kapitein et al., 2010b), followed by PCR amplification of FKBP(1x) and insertion into

the EcoRI and SalI sites of the construct. The FKBP encoding fragments were described previously (Kapitein et al., 2010b).

pβactin-MyoVb-(amino acid 1-1090)-GFP-FRB was described before (Kapitein et al., 2013). MyoVb-(1-1090)-iRFP-FRB (myosin-Vb) was generated by replacing the GFP by iRFP using the EcoRI and SpeI sites. Kif17md-GFP-GAI was generated by insertion of Kif17MD (aa 1-547 of human KIF17) in AscI and SalI sites, GFP in SalI and SpeI sites, and GAI(1-92) in SpeI and NotI sites of pβactin. FKBP-tdTomato-Rab3c was generated by insertion of PCR-amplified tdTomato in SalI and SpeI site, Mouse Rab3c in SpeI and NotI sites and FKBP(1x) in BamHI and SalI sites of the pβactin-16-pl vector.

To visualize actin using single molecule localization microscopy lifeAct-GFP was purified and used as a transient binding probe (Kiuchi et al., 2015). In brief, lifeAct- GS linker -GFP was cloned into a PET28a vector with a C-terminal 6x His sequence and transformed into BL21DE3 bacteria. Bacteria were grown until OD0.6 and induced with 1 mM IPTG overnight at 17°C. Cells were then pelleted and resuspended in resuspension buffer [20 mM HNa2PO4, 300 mM NaCl, 0.5% glycerol, 7% glucose, EDTA-free protease inhibitor (Roche Diagnostics GmbH), 1 mM dithiothreitol (DTT), pH 7.4]. Cells were lysed by sonication and the soluble and insoluble fraction were separated by centrifugation. Ni-NTA (Roche) beads were washed with resuspension buffer and incubated with the soluble supernatant for 1.5 h at 4°C. After incubation, the beads with bound proteins were washed 5 times with wash buffer (10 mM HNa2PO4, 300 mM NaCl, 30 mM imidazole, 1 mM DTT, pH 7.4). Finally lifeAct-GFP was eluted in Elution Buffer (10 mM HNa2PO4, 300 mM NaCl, 300 mM imidazole, 1 mM DTT, pH 7.4) and snap-frozen at −80°C with 10% glycerol.

Cell Cultures and Transfection

COS-7 cells were cultured in DMEM/Ham's F10 (1:1) medium containing 10% FCS and penicillin/streptomycin. Cells were plated on 18-mm diameter coverslips 2–4 days before transfection. Cells were transfected with Fugene6 transfection reagent (Roche) according to the manufacturer's protocol and imaged 1 day after transfection.

Primary hippocampal cultures were prepared from embryonic day 18 (E18) rat brains (Kapitein et al., 2010c). Cells were plated on coverslips coated with poly-L-lysine (30 $\mu g\ ml^{-1}$) and laminin (2 $\mu g\ ml^{-1}$). Hippocampal cultures were grown in Neurobasal medium (NB) supplemented with B27 (Invitrogen), 0.5 mM glutamine, 12.5 μM glutamate, and penicillin plus streptomycin. Transfections of hippocampal neurons were performed 48 h before imaging with lipofectamine 2000 (Invitrogen). DNA (1.8 μg per well) was mixed with 3.3 μl lipofectamine 2000 in 200 ml NB, incubated for 30 min, and added to the neurons in NB supplemented with 0.5 mM glutamine at 37°C in 5% CO_2. After 60–90 min neurons were washed with NB and transferred to the original medium at 37°C in 5% CO_2 for 2 days. Transport assays in neurons were imaged at day-*in-vitro* 12–16.

Live-Cell Imaging

Time-lapse live-cell imaging of peroxisomes in hippocampal neurons was performed on a Nikon Eclipse TE2000E (Nikon) equipped with an incubation chamber (Tokai Hit; INUG2-ZILCS-H2) mounted on a motorized stage (Prior; Kapitein et al., 2013). Coverslips (18 mm) were mounted in metal rings covered with conditioned medium. Cells were imaged every 30 s for 60 min using a 40× objective [Plan Fluor, numerical aperture (NA) 1.3, Nikon] and a Coolsnap HQ2 CCD camera (Photometrics).

Peroxisomes in COS7 and neurons were images using a 40x objective (Plan Fluor, numerical aperture (NA) 1.3, Nikon) in Ringer's solution (10 mM HEPES, 155 mM NaCl, 5 mM KCl, 1 mM $CaCl_2$, 1 mM $MgCl_2$, 2 mM NaH_2PO_4, and 10 mM glucose, pH 7.4) or conditioned culture medium, respectively. Rab3 vesicles in neurons were imaged in conditioned medium using a 100× objective (Apo TIRF, 1.49 NA, Nikon). A mercury lamp (Osram) and filter wheel containing ET-GFP (49002), ET-dsRed (49005), ET-mCherry (49008), and ET-GFPmCherry (59022) emission filters (all Chroma) were used for excitation. Rab3 in neurons were imaged on a CoolSNAP MYO CCD camera (Photometrics) and peroxisomes in neurons and COS7 cells with a Coolsnap HQ camera (Photometrics, Tucson, AZ). During imaging, all cells were maintained at 37°C, as well as 5% CO_2 when using conditioned medium.

Cell-permeable gibberellin (GA3IAM, a gift from Dr. T. Inoue; Miyamoto et al., 2012) and Rapalog (AP21967 from Ariad Pharmaceuticals) were added during image acquisition to reach a final concentration of 150–300 and 100 nM, respectively at the indicated time points. In hippocampal neurons, the axon was identified based on morphology and Rab3 vesicle enrichment. The proximal axon was defined as the first part of the axon before branching, whereas distal axon refers to axonal segments after at least 2 branch points.

To identify the axon in live cell imaging experiments (**Supplemental Figure 1**), neurons were stained for extracellular Neurofascin before imaging. Coverslips were placed in cultured medium containing anti-neurofascin (Neuromab, mouse, 1/200) for 10 min. Coverslips where then washed 5 times by briefly dipping them in neurobasal. Subsequently, coverslips were incubated with anti-mouse AlexaFluor405 (Life Technologies, anti-mouse, 1/100) for 10 min. After 5 additional washes cells were place back into their cultured medium before imaging.

Cell Fixation and Single Molecule Localization Imaging

Cells transfected with Rab3-TdTomato-FKBP, MyosinVb-HA-FRB, and a BFP fill (**Figures 3D–H**) were fixed with 4% PFA in PBS for 10 min at 37°C. Subsequently, cells were washed 2 times with PBS, permeabilized with 0.25% triton in PBS for 10 min and washed again 3 times with PBS. After washing, cells were blocked for 45 min in blocking solution (2% w/v BSA, 0.2% w/v gelatin, 10 mM glycine, 50 mM NH4Cl in PBS, pH 7.4) and incubated overnight with anti-Ankyrin-G (1/200, mouse, Life technologies). Cells were further incubated with anti-mouse Alexa647 (1/400, Life technologies) and mounted for imaging in mowiol.

To determine the localization of the Rab3 accumulation (**Figure 3**) samples were imaged on a Nikon eclipse TI upright microscope with a 40x objective (UPLFLN, NA 1.3). Myosin-Vb localization was imaged on an Olympus BX53

upright microscope with a 60x objective (oil, UPLSAPO, NA1.35).

For simultaneous super-resolution imaging of Rab3 and actin (**Figure 4**) cells overexpressing Rab3-TdTomato-FKBP and MyosinVb-HA-FRB (either treated with rapalog or not), were pre-extracted 1 min with 0.35% glutaraldehyde and 0.25% triton-x in cytoskeleton buffer (Xu et al., 2013). Cells were then further fixed with 4% PFA. Subsequently, samples were washed 3x with PBS followed by 10 min permeabilization in PBS + 0.25% triton-x. After 3 more 5 min washes in PBS, samples were blocked in 3% BSA for 45 min followed by overnight 4°C staining with anti-AnkG (1/200, mouse, Life technologies) and anti-RFP (1/500, rabbit, Rockland) in blocking buffer. After incubation cells were washed 3 times 10 min in PBS and incubated with secondary anti-mouse AlexaFluor488 (1/400, Life Technologies) and anti-rabbit-D2 from the Ultivue-2 super resolution 2-plex kit (1/100, Ultivue) for 1.5 h at room temperature in blocking buffer. After 3 additional washes samples were mounted in a Ludin chamber in Imaging Buffer (Ultivue). Single-molecule microscopy was performed on a Nikon Ti-E microscope equipped with a 100x Apo TIRF oil immersion objective (NA. 1.49) and Perfect Focus System 3. Excitation was achieved via a custom illumination pathway with a Lighthub-6 (Omicron) containing a 638 nm laser (BrixX 500 mW multimode, Omicron), a 488 nm laser (Luxx 200 mW, Omicron), and a 405 nm laser (Luxx 60 mW, Omicron). Emission light was separated from excitation light with a quad-band polychroic mirror (ZT405/488/561/640 rpc, Chroma), a quad-band emission filter (ZET405/488/561/640 m, Chroma), and an additional single-band emission filter (ET525/50 m for green emission and ET655lp for far-red emission, Chroma). Fluorescence was detected using a sCMOS camera (Hamamatsu Flash 4.0v2). Samples were positioned in the *x*- and y-direction with an M-687 PILine stage (PI).

For super-resolution imaging, first cells expressing Rab3-TdTomato were selected and AnkyrinG was imaged to identify the axon. LifeAct-GFP and Imager strand I2-650 (Ultivue) were diluted so that single molecule binding events could be observed for both channels. Subsequently, the relatively weak AnkyrinG AlexaFluor488 staining was completely bleached and LifeAct based protein-PAINT (Kiuchi et al., 2015) was performed by observing single binding and unbinding effects. Subsequently, DNA-PAINT was performed similarly for Rab3 structures stained with rabbit-D2 and Imager strand I-2. For both channels between 8,000 and 15,000 frames were acquired with a 100 ms exposure time to reconstruct super resolved images of both actin and Rab3. Images were then reconstructed using our ImageJ plugin called DoM (Detection of Molecules, https://github.com/ekatrukha/DoM_Utrecht) which has previously been described in detail (Yau et al., 2014; Chazeau et al., 2016).

Image Processing and Analysis

Images of live cells were processed and analyzed using MetaMorph (Molecular Devices), LabVIEW (National Instruments) software and ImageJ (NIH). Drift correction was applied using the StackReg plugin for ImageJ (Thevenaz et al., 1998) for time series during which multiple positions were recorded using a motorized stage.

To generate the radial kymograph, pixels that were above the set threshold were inserted into a histogram representing the intensity vs. the distance from the center of the cell. This was done for each video frame using the camera pixel size as bin size (Kapitein et al., 2010b).

For analysis of redistribution dynamics in COS7 cells, cells were masked to exclude contributions from neighboring cells to the analysis. A threshold was set for all images of a time-lapse recording at ∼6–12 times the standard deviation of the background above the background to yield binary images. These thresholds were set manually such that individual peroxisomes were suprathreshold (by an experimenter who was not blind to experimental group). The same thresholds were set for analysis of the $R_{90\%}$ and calculations of the correlation index. To quantify peroxisome redistribution upon recruitment of motor proteins in COS7 cells, the radius required to include 90% of the total intensity of the cell, $R_{90\%}(t)$, was calculated for each frame as described previously (Kapitein et al., 2010b). To quantify changes in the dynamics of peroxisomes upon recruitment of (additional) motor proteins, we calculated the time-dependent frame-to-frame correlation index$c_\tau(t)$ as described before (van Bergeijk et al., 2015). A value of 1 for $c_\tau(t)$ indicates that particles are completely anchored and thus their position is unchanged after a time τ, whereas a value of 0 means that all particles moved to locations that were previously unoccupied. For statistical analysis on R90% and correlation index, average values of 10 frames at t = 0–4.5, 25–29.5, and 55–59.5 min were used. Friedman test was performed with Dunn's *post-hoc* test.

To quantify the movement of the peroxisome or Rab3 accumulations formed after recruiting Myosin-V in the proximal axon (**Figures 2E**, **3G**), their positions were analyzed between 10 and 25 min after the addition of rapalog with 30 s interval acquisition. The spots were tracked using the trackmate plugin for ImageJ. For every time point the x-position relative to the initial position was plotted. For these trajectories, mean square displacement analysis was performed using the MSDanalyzer (Tarantino et al., 2014) class for MATLAB, including tracks that were at least 25 time points long (n = 26 for **Figure 2E** and n = 18 for **Figure 3G**).

To analyze Rab3 clustering (**Figures 3E,F**), the number of bright isolated spots as shown in **Figure 3D** were compared between the proximal axon (colocalizing with the AIS marker Ankyrin-G, which marked a segment with visibly identifiable boundaries) and more distal segments (further than the second branch), both in the presence and absence of rapalog. For the quantification of the Rab3 accumulations relative to the AIS, the AIS length was measured manually based on the bright Ankyrin-G staining that defines the AIS. Subsequently, the location of the rab3 accumulation was divided by the measured length of the AIS.

AUTHOR CONTRIBUTIONS

LK conceived research. PvB, RO, and AJ designed, created, and tested constructs. AJ and RT performed experiments and analyzed data. CH provided conceptual input and provided neuron cultures. AJ, RT, and LK wrote the paper with input from all other authors. LK supervised research.

ACKNOWLEDGMENTS

We are grateful to Dr. T. Inoue for the gift of AM-modified gibberellin. This work was supported by the Netherlands Organization for Scientific Research (NWO) (NWO-ALW-VICI to CH, NWO-ALW-VIDI to LK), the Dutch Technology Foundation STW, which is part of the NWO (to CH and LK), and the European Research Council (ERC Starting Grant to LK, ERC Consolidator Grant to CH).

SUPPLEMENTARY MATERIAL

The Supplementary Material for this article can be found online at: http://journal.frontiersin.org/article/10.3389/fncel.2017.00260/full#supplementary-material

Supplemental Figure 1 | Corresponds to **Figure 2**. **(A)** GFP fill (left) and live neurofascin staining (middle) of a cell expressing GFP, Pex3-mRFP-FKBP, and Kif5-GFP-FRB. **(B)** Partial maximum projections of the peroxisome-redistribution experiment performed on the cell in **(A)**, before (left) and after rapalog addition (right). Red arrows indicate the axon identified by neurofascin. **(C)** Percentage of cells with peroxisome targeting into the axon or both axon and dendrite, after recruitment of kif5-GFP-FRB. In all cases the axon was identified by the live neurofascin staining as in **(A,B)**. $n = 21$.

Supplemental Figure 2 | Corresponds to **Figure 3**. **(A)** Rab3 positive vesicle distribution in the proximal axon of a neuron that co-expressed myosin-Vb, but was not treated with ligands (left panels), or did not express myosin Vb and was treated with Gibberellin (middle panels) or rapalog (right panels). In these control conditions Rab3 vesicles do not accumulate in big puncta as seen by selective recruitment of myosinVb. Scale bar, 10 μm. **(B)** Kymographs of Rab3 vesicles in the proximal axon of cells co-expressing myosin-Vb with and without addition of rapalog, or cells without myosinVb and treated with Gibberellin or Rapalog. Timelapse images were acquired with 20 s intervals. Arrows indicate Rab3 accumulations appearing after rapalog addition. Scale bar, 5 μm.

Supplemental Video 1 | Sequential recruitment of kinesin and myosin-V in a COS7 cell. This video corresponds to **Figure 1**. Anchoring of kinesin propelled cargo by Myosin-V in a COS7 cell. Total time: 60 min. Acquired with 30 s between frames. 600x sped up.

Supplemental Video 2 | Myosin-V anchors kinesin-1 propelled peroxisomes in the proximal axon. This video corresponds to **Figure 2**. Anchoring of kinesin propelled cargo by Myosin-V in a hippocampal neuron. Total time: 60 min. Acquired with 30 s between frames. 600x sped up.

Supplemental Video 3 | Myosin-V anchors Rab3 vesicles in the AIS of hippocampal neurons. This video corresponds to **Figure 3**. Anchoring and clustering of Rab3 vesicles in the proximal axon of hippocampal neurons. Total time: 40 min. Acquired with 10 s between frames. 200x sped up.

REFERENCES

Al-Bassam, S., Xu, M., Wandless, T. J., and Arnold, D. B. (2012). Differential trafficking of transport vesicles contributes to the localization of dendritic proteins. *Cell Rep.* 2, 89–100. doi: 10.1016/j.celrep.2012.05.018

Chazeau, A., Katrukha, E. A., Hoogenraad, C. C., and Kapitein, L. C. (2016). Studying neuronal microtubule organization and microtubule-associated proteins using single molecule localization microscopy. *Methods Cell Biol.* 131, 127–149. doi: 10.1016/bs.mcb.2015.06.017

Derr, N. D., Goodman, B. S., Jungmann, R., Leschziner, A. E., Shih, W. M., and Reck-Peterson, S. L. (2012). Tug-of-war in motor protein ensembles revealed with a programmable DNA origami scaffold. *Science* 338, 662–665. doi: 10.1126/science.1226734

Ganguly, A., Tang, Y., Wang, L., Ladt, K., Loi, J., Dargent, B., et al. (2015). A dynamic formin-dependent deep F-actin network in axons. *J. Cell Biol.* 210, 401–417. doi: 10.1083/jcb.201506110

Huang, C., and Banker, G. (2012). The translocation selectivity of the kinesins that mediate neuronal organelle transport. *Traffic* 13, 549–564. doi: 10.1111/j.1600-0854.2011.01325.x

Jungmann, R., Avendano, M. S., Woehrstein, J. B., Dai, M., Shih, W. M., and Yin, P. (2014). Multiplexed 3D cellular super-resolution imaging with DNA-PAINT and Exchange-PAINT. *Nat. Methods* 11, 313–318. doi: 10.1038/nmeth.2835

Kapitein, L. C., Schlager, M. A., Kuijpers, M., Wulf, P. S., Van Spronsen, M., MacKintosh, F. C., et al. (2010a). Mixed microtubules steer dynein-driven cargo transport into dendrites. *Curr. Biol.* 20, 290–299. doi: 10.1016/j.cub.2009.12.052

Kapitein, L. C., Schlager, M. A., van der Zwan, W. A., Wulf, P. S., Keijzer, N., Hoogenraad, C. C., et al. (2010b). Probing intracellular motor protein activity using an inducible cargo trafficking assay. *Biophys. J.* 99, 2143–2152. doi: 10.1016/j.bpj.2010.07.055

Kapitein, L. C., Van Bergeijk, P., Lipka, J., Keijzer, N., Wulf, P. S., Katrukha, E. A., et al. (2013). Myosin-V opposes microtubule-based cargo transport and drives directional motility on cortical actin. *Curr. Biol.* 23, 828–834. doi: 10.1016/j.cub.2013.03.068

Kapitein, L. C., Yau, K. W., and Hoogenraad, C. C. (2010c). Microtubule dynamics in dendritic spines. *Methods Cell Biol.* 97, 111–132. doi: 10.1016/S0091-679X(10)97007-6

Kiuchi, T., Higuchi, M., Takamura, A., Maruoka, M., and Watanabe, N. (2015). Multitarget super-resolution microscopy with high-density labeling by exchangeable probes. *Nat. Methods* 12, 743–746. doi: 10.1038/nmeth.3466

Kuijpers, M., Van De Willige, D., Freal, A., Chazeau, A., Franker, M., Hofenk, J., et al. (2016). Dynein regulator NDEL1 controls polarized cargo transport at the axon initial segment. *Neuron* 89, 461–471. doi: 10.1016/j.neuron.2016.01.022

Lewis, T. L., Mao, T., Svoboda, K., and Arnold, D. B. (2009). Myosin-dependent targeting of transmembrane proteins to neuronal dendrites. *Nat. Neurosci.* 12, 568–576. doi: 10.1038/nn.2318

Lipka, J., Kapitein, L. C., Jaworski, J., and Hoogenraad, C. C. (2016). Microtubule-binding protein doublecortin-like kinase 1 (DCLK1) guides kinesin-3-mediated cargo transport to dendrites. *EMBO J.* 35, 302–318. doi: 10.15252/embj.201592929

Miyamoto, T., Derose, R., Suarez, A., Ueno, T., Chen, M., Sun, T., et al. (2012). Rapid and orthogonal logic gating with a gibberellin-induced dimerization system. *Nat. Chem. Biol.* 8, 465–470. doi: 10.1038/nchembio.922

Petersen, J. D., Kaech, S., and Banker, G. (2014). Selective microtubule-based transport of dendritic membrane proteins arises in concert with axon specification. *J. Neurosci.* 34, 4135–4147. doi: 10.1523/JNEUROSCI.3779-13.2014

Saxton, M. J., and Jacobson, K. (1997). Single-particle tracking: applications to membrane dynamics. *Annu. Rev. Biophys. Biomol. Struct.* 26, 373–399. doi: 10.1146/annurev.biophys.26.1.373

Song, A., Wang, D., Chen, G., Li, Y., Luo, J., Duan, S., et al. (2009). A selective filter for cytoplasmic transport at the axon initial segment. *Cell* 136, 1148–1160. doi: 10.1016/j.cell.2009.01.016

Tarantino, N., Tinevez, J. Y., Crowell, E. F., Boisson, B., Henriques, R., Mhlanga, M., et al. (2014). TNF and IL-1 exhibit distinct ubiquitin requirements for inducing NEMO-IKK supramolecular structures. *J. Cell Biol.* 204, 231–245. doi: 10.1083/jcb.201307172

Thevenaz, P., Ruttimann, U. E., and Unser, M. (1998). A pyramid approach to subpixel registration based on intensity. *IEEE Trans. Image Process.* 7, 27–41. doi: 10.1109/83.650848

van Bergeijk, P., Adrian, M., Hoogenraad, C. C., and Kapitein, L. C. (2015). Optogenetic control of organelle transport and positioning. *Nature* 518, 111–114. doi: 10.1038/nature 14128

Watanabe, K., Al-Bassam, S., Miyazaki, Y., Wandless, T. J., Webster, P., and Arnold, D. B. (2012). Networks of polarized actin filaments in the axon initial segment provide a mechanism for sorting axonal and dendritic proteins. *Cell Rep.* 2, 1546–1553. doi: 10.1016/j.celrep.2012. 11.015

Xu, K., Zhong, G., and Zhuang, X. (2013). Actin, spectrin, and associated proteins form a periodic cytoskeletal structure in axons. *Science* 339, 452–456. doi: 10.1126/science.1232251

Yau, K. W., Van Beuningen, S. F., Cunha-Ferreira, I., Cloin, B. M., Van Battum, E. Y., Will, L., et al. (2014). Microtubule minus-end binding protein CAMSAP2 controls axon specification and dendrite development. *Neuron* 82, 1058–1073. doi: 10.1016/j.neuron.2014.04.019

Conflict of Interest Statement: The authors declare that the research was conducted in the absence of any commercial or financial relationships that could be construed as a potential conflict of interest.

frontiers in Cellular Neuroscience

ORIGINAL RESEARCH
published: 10 April 2017
doi: 10.3389/fncel.2017.00096

MicroRNA-182 Regulates Neurite Outgrowth Involving the PTEN/AKT Pathway

*Wu M. Wang†, Gang Lu†, Xian W. Su, Hao Lyu and Wai S. Poon**

Division of Neurosurgery, Department of Surgery, Prince of Wales Hospital, The Chinese University of Hong Kong, Hong Kong, China

MicroRNAs are implicated in neuronal development and maturation. Neuronal maturation, including axon outgrowth and dendrite tree formation, is regulated by complex mechanisms and related to several neurodevelopmental disorders. We demonstrated that one neuron-enriched microRNA, microRNA-182 (miR-182), played a significant role in regulating neuronal axon outgrowth and dendrite tree formation. Overexpression of miR-182 promoted axon outgrowth and complexity of the dendrite tree while also increasing the expression of neurofilament-M and neurofilament-L, which provide structural support for neurite outgrowth. However, a reduction of miR-182 inhibited neurite outgrowth. Furthermore, we showed that miR-182 activated the AKT pathway by increasing AKT phosphorylation on S473 and T308 and inhibiting PTEN activity by increasing phosphorylation on S380. Inhibition of AKT activity with the PI3-K inhibitor LY294002 could downregulate AKT and PTEN phosphorylation and suppress axon outgrowth. In addition, we showed that *BCAT2* might be the target of miR-182 that takes part in the regulation of neuronal maturation; blockage of endogenous BCAT2 promotes axon outgrowth and AKT activity. These observations indicate that miR-182 regulates axon outgrowth and dendrite maturation involving activation of the PTEN/AKT pathway.

Keywords: microRNA-182, axon outgrowth, dendrite, AKT, BCAT2

OPEN ACCESS

Edited by:
Froylan Calderon De Anda, University of Hamburg, Germany

Reviewed by:
Karun K. Singh, McMaster University, Canada
Jenny Lucy Fiedler, Universidad de Chile, Chile

****Correspondence:***
Wai S. Poon
wpoon@cuhk.edu.hk

† These authors have contributed equally to this work.

Received: *28 December 2016*
Accepted: *20 March 2017*
Published: *10 April 2017*

Citation:
Wang WM, Lu G, Su XW, Lyu H and Poon WS (2017) MicroRNA-182 Regulates Neurite Outgrowth Involving the PTEN/AKT Pathway. Front. Cell. Neurosci. 11:96. doi: 10.3389/fncel.2017.00096

INTRODUCTION

During brain development, neurons are generated in the ventricular zone and subventricular zone (SVZ) (Dehay and Kennedy, 2007). Neuronal maturation passes through five stages morphologically, including filopodia, immature neurites, axon outgrowth, mature neurites, and premature dendritic spines. After being dissociated from the embryonic brain, neurons form several filopodia; several hours later, the neurons generate numbers of immature neurites; one of these immature neurites extends rapidly and develops to axon, and other neurites become immature dendrites. When axons and dendrites are mature, the neurons form synaptic contacts which enable to transmit electrical signal (Arimura and Kaibuchi, 2007). During the neuronal maturation, large numbers of microRNAs contribute to these processes (Kosik, 2006).

MicroRNAs are a class of conserved non-coding RNAs containing about 22 nucleotides that modulate gene expression by targeting messenger RNA (mRNA), which leads to reduced translational efficiency, thereby influencing many biological processes. MicroRNAs are well-known to take part in many cellular processes, and have been found with distinct expression patterns in neural cells (Kosik, 2006). For example, miR-137 is specifically expressed in neurons compared

with neural stem cells (NSCs) and astrocytes (Smrt et al., 2010). MicroRNAs also have different expression pattern in axon and dendrites. MiR-9 is expressed in axons of primary cortical neurons (Dajas-Bailador et al., 2012); miR-138, which functions to control dendrite development, is highly enriched in brain and localized within dendrites (Siegel et al., 2009).

Furthermore, microRNAs have also been demonstrated to take part in the regulation of neurite outgrowth and spine morphogenesis. Overexpression of miR-34a significantly decreases the number of neurite branches (Agostini et al., 2011), and miR-9 negatively regulates axon branching by targeting microtubule stability-related genes (Dajas-Bailador et al., 2012). MiR-134, a brain-specific microRNA, negatively modulates the size of dendritic spine of rat hippocampal neurons (Schratt et al., 2006). The miR-182/183/96 cluster is specifically expressed in sensory neurons and is involved in maintaining cone photoreceptor outer segments (Xu et al., 2007; Busskamp et al., 2014). MiR-182 has been recently found to prevent retinal degeneration (Lumayag et al., 2013). Quantitative real-time PCR and *in situ* hybridization reveal that the miR-182/183/96 cluster is highly expressed in dorsal root ganglion neurons, and the expression is decreased in injured neurons compared with controls (Aldrich et al., 2009). So far, there are no direct evidence for miR-182 regulating neurite growth in neurons of the central nervous system, but recent literatures identify that miR-182 is an important modulator of memory formation and regulates dendrite branching out of trigeminal sensory neurons (Griggs et al., 2013; Wang et al., 2016; Woldemichael et al., 2016).

MicroRNAs are involved in crucial biological processes by modulating signal transduction pathway (Inui et al., 2010). The PTEN/AKT pathway regulated by microRNAs plays important roles in neuronal maturation. MiR-9 and miR-124 regulate dendritic branching via AKT/GSK3β pathway (Xue et al., 2016); PTEN/miR-29a pathway modulates neurite outgrowth (Zou et al., 2015). In neuronal regeneration, PTEN/AKT pathway regulated by microRNA *bantam* enhances the regeneration of sensory neuron axons and dendrites (Song et al., 2012). Co-deletion of *PTEN* and *SOCS3* induces regrowth of retinal axons (Bei et al., 2016); both *PTEN* and *SOCS3* deletion greatly increases the intrinsic regenerative ability of injured retinal ganglion cells (RGCs), resulting in robust long-distance axon regeneration in optic nerve injury model (Sun et al., 2011).

In the cellular signal pathway, some essential genes are identified as downstream or upstream signals of PTEN/AKT. In the brain, branched-chain aminotransferase (BCAT) is a critical enzyme in the catabolism of the essential branched chain amino acids (BCAAs) leucine, valine, and isoleucine. In this catabolism, glutamate as a product of the BCAA catabolism is the major excitatory neurotransmitter and precursor of γ-aminobutyric acid (GABA). There are two BCAT isoforms, mitochondrial BCATm and cytosolic BCATc which are expressed in cultured astrocytes and neurons (Bixel et al., 2001; Castellano et al., 2007; Cole et al., 2012). BCAT2 is a kind of BCATm, which are ubiquitously presented in all tissues in the mitochondria of cells (Hull et al., 2012). It is a newly identified target of miR-182 that negatively regulates AKT activity, and BCAT2 depletion results in a significant increase in cardiomyocyte size and phosphorylation of AKT (S473) (Li et al., 2016). In our study, we investigated the functions of miR-182 in axon outgrowth and dendrite branching out of cortical neurons, and demonstrated that BCAT2/PTEN/AKT pathway might participate in the regulation of neuron maturation.

MATERIALS AND METHODS

Ethics Statement

All of our experiments were performed in accordance with the recommendations of the Animal Experimentation Ethics Committee of The Chinese University of Hong Kong. The protocol was approved by the Animal Experimentation Ethics Committee of The Chinese University of Hong Kong (Ref. No. 16-060-MIS).

Collection of Primary NSCs

Mouse NSCs were obtained from the SVZ of an adult mouse brain (Walker and Kempermann, 2014). Briefly, the lateral wall of lateral ventricle was dissected and dissociated into single cells by 0.05% trypsin-EDTA, and the cells were seeded into Petri dishes with KnockOut TM D-MEM/F-12 medium containing StemPro Neural Supplement (2%), bFGF (20 ng/ml), EGF (20 ng/ml), GlutaMAX-I Supplement (2 mM), heparin (6 units/ml) and ascorbic acid (200 μM). The SVZ-derived neurospheres were incubated for 6–7 days and replaced with fresh medium every 3 days. For neuron differentiation, NSCs were plated into dishes coated with poly-D-lysine (Sigma) and laminin (Invitrogen) in a 1:1 mix of Neurobasal Medium and DMEM/F12 supplemented with N2 (Gibco), B27 (Gibco), 10 ng/ml BDNF (Peprotech), and 200 mM ascorbic acid (Sigma). Half of the medium was replaced every other day. After 2 weeks of culture, the ratio of the mixture of Neurobasal Medium and DMEM/F12 was changed to 3:1; the N2 supplement was reduced to 0.5%, and the BDNF was increased to 20 ng/ml (Thier et al., 2012).

Cortical Neuron Culture

Primary cortical neuron cultures were prepared from embryonic day 18.5 (E18.5) mouse brain. Chamber slides (Nunc) were coated with 100 μg/ml poly-L-lysine (Sigma) and 5 μg/ml laminin (Invitrogen) at 37°C in an incubator for 3 h to overnight, then washed twice with distilled water, and air dried 20 min. Cortices were digested with 1× trypsin-EDTA for 15 min at 37°C, and then the reaction was stopped with trypsin inhibitor for 3 min at room temperature. After washing with dissection buffer containing 1× HBSS without Ca^{2+} and Mg^{2+} (Invitrogen), 10 mM HEPES buffer (Invitrogen), 0.5% glucose and 100 units/ml antibiotics (penicillin and streptomycin) (Invitrogen), the tissues were triturated by gently pipetting in plating medium containing MEM without glutamine (Life Technologies), 10% FBS (Gibco), 1 mM L-glutamine (Invitrogen), 10 mM Hepes (Invitrogen), and 50 units/ml antibiotics (penicillin and streptomycin) (Invitrogen) until fully dissociated. Cells were diluted to an appropriate concentration and plated in chamber slides (Nunc) pre-coated with poly-L-lysine (Sigma) and laminin (Invitrogen). Three hours

later, cells were grown in culture medium containing neurobasal medium (Invitrogen), 2% B27 supplement (Invitrogen), 0.5 mM L-glutamine (Invitrogen), and 50 units/ml antibiotics (penicillin and streptomycin) (Invitrogen) (Kaech and Banker, 2006).

Western Blot

Proteins were extracted with RIPA buffer containing protease inhibitor cocktail, and the concentration of which was measured with a BCA kit. Proteins (10–20 μg) were loaded into 8–10% SDS-polyacrylamide gel. Following SDS-PAGE, proteins were transferred to nitroate cellulose membrane, blocked with 5% non-fat milk, incubated overnight with primary antibodies at 4°C, and washed three times with TBST for 10 min. After the proteins had been incubated with secondary antibodies for 2 h at room temperature, signals were detected by enhanced chemiluminescent (Thermo Fisher Scientific). The following primary antibodies were used: rabbit anti-PTEN (1:1000; Cell Signaling Technology #9188), rabbit anti-p$^{(Ser380)}$ PTEN (1:1000; Cell Signaling Technology #9551), rabbit anti-AKT (1:1000; Cell Signaling Technology #4691), rabbit anti-p$^{(Ser473)}$-AKT (1:1000; Cell Signaling Technology #4060), rabbit anti-p$^{(Thr308)}$-AKT (1:1000; Cell Signaling Technology #13038), phospho-p44/42 MAPK (Erk1/2)$^{(Thr202/Tyr204)}$ (1:1000; Cell Signaling Technology #9106), p44/42 MAPK (Erk1/2) (1:1000; Cell Signaling Technology #9102), mouse anti-β-actin (1:2000; ImmunoWay #YM3028), rabbit anti-Neurofilament-L (NF-L; 1:1000; Cell Signaling Technology #2837), mouse anti-Neurofilament-M (NF-M; 1:1000; Cell Signaling Technology #2838) and rabbit anti-BCAT2 (1:500; Abcam #ab95976). The secondary antibodies used were: anti-mouse HRP-linked antibody (1:2000; Cell Signal Technologies #7076) and anti-rabbit HRP-linked antibody (1:2000; Cell Signal Technologies #7074).

Morphological Analysis

Cortical neurons were transfected with 60 nM scramble mimics as control, 60 nM miR-182-5p mimics, 60 nM negative control inhibitor mimics, 60 nM miR-182 inhibitor mimics, 60 nM negative control siRNA, 60 nM BCAT2 siRNA-1 mimics (TechDragon #siRNA no. 1330304) and 60 nM BCAT2 siRNA-2 mimics (TechDragon #siRNA no. 1330305) plus *GFP*-encoding plasmid at 1 day *in vitro* (DIV) by using Lipofectamine 3000 reagent (Invitrogen), incubated with lipofectamine 3000 and MicroRNA agomir or antagomir at 37°C, 5% CO_2 for 24 h, washed once with 1× PBS and replaced with fresh medium. 36 h later, analyzed for axon outgrowth; also transfected at 5 DIV, and 48 h later, analyzed for dendrite development. The *GFP*-encoding plasmid is promoted by the CAG promoter, and the plasmid was a generous gift from Professor Zhao Hui (School of Biomedical Sciences, The Chinese University of Hong Kong).

Lengths of axons and dendrites were quantified by NIH Image J. The statistical analysis of total dendritic branch tip number (TDBTN), average dendrite branching length (ADBL), and total dendrite branching length (TDBL) were done with GraphPad Prism 6. The projection images were traced with NIH Image J, and dendritic complexity was analyzed with Image J by using the Sholl analysis plugin (Anirvan Ghosh Lab). A series of concentric circles at 15 and 25 μm intervals were drawn around the soma, and crossings of dendrites with each circle were counted automatically. Images for axon and dendrite analysis were taken by using 20× objectives under Zeiss microscope with a CCD camera.

RNA Extraction, RT-PCR, and Real-Time PCR

The total RNAs from mouse brain tissues were isolated with TRIzol (Ambion). For gene expression, 1 μg of total RNAs were used to do reverse transcription with High-Capacity cDNA Reverse Transcription Kits (Applied Biosystems). For microRNA detection, 100 ng of total RNAs were reverse transcribed by using M-MuLV Reverse Transcriptase (New England Biolabs) and a RT primer for adding an anchored poly (T) tag to the miRNA sequence (Alvarez and Nourbakhsh, 2014). Then, the following PCR could be performed with a universal primer and a microRNA-specific primer. The PCR products were detected with SYBR Green dye, and SYBR assays were performed on an Applied Biosystems 7500 Real-Time PCR system. Relative expression was calculated by delta threshold cycles (Ct), using normalization to GAPDH for gene expression detection and to U6 for microRNA detection. The expression measures were recorded from triplicate samples, each of which was analyzed by triplicate qPCR assay. In our results, the average Cts of GAPDH, BCAT2, U6, and miR-182 are 23.64967, 25.017, 17.004, and 21.24467. The primer information for Real-Time PCR was described in **Table 1**.

Immunostaining

Neural stem cells were cultured for 2 days in StemPro NSCs culture medium (Gibco). The NSCs and differentiated neurons were collected, washed three times with PBS, fixed in 4% PFA for 20 min at room temperature, and permeabilised with 0.3% Triton X-100 for 10 min. After blocked with 5% BSA for 10 min, cells were incubated with primary antibodies overnight at 4°C, and signals were detected by a fluorescence microscope. Cell nuclei were visualized with DAPI. Primary antibodies included: rabbit anti-Nestin (Santa Cruz Biotechnology #sc-20978) and rabbit anti-β III tubulin (Abcam #ab18207); secondary antibodies included a donkey anti-rabbit IgG secondary antibody (Life Technologies #A16036).

Construction of Vectors

3′ UTR-containing fragments of *BCAT2* were amplified by PCR using Platinum Pfx DNA Polymerase and inserted into the SacI and XbaI sites of pmir-GLO (Promega). The primer information was described in **Table 1**.

Luciferase Reporter Assay

HEK-293T cells were plated in 96-well plates at 2.5 × 10^4 cells per well and co-transfected with 60 nM scramble mimics or 60 nM miR-182 mimics plus 0.5 ng/μl plasmids of pmir-GLO-mBCAT2-3′ UTR using Lipofectamine 3000 (Life Technologies), and each group is triplicate. 293T cells were cultured for 2 days after transfection and lysed with Dual-Glo Luciferase reagent. Luciferase activity was detected with the Dual-Glo Luciferase Assay System (Promega) according to the manufacturer's

TABLE 1 | Primer list.

mu-miR-138-5p Forward	AGCTGGTGTTGTGAATCAG
mmu-miR-138-5p Reverse	CAGTTTTTTTTTTTTTTCGGCCT
mmu-miR-219a-5p Forward	CAGTGATTGTCCAAACGCA
mmu-miR-219a-5p Reverse	GGTCCAGTTTTTTTTTTTTTTTAGAATTG
mmu-miR-338-3p Forward	GCAGTCCAGCATCAGTGA
mmu-miR-338-3p Reverse	GTCCAGTTTTTTTTTTTTTTCAACA
mmu-miR-21-5p Forward	GCAGTAGCTTATCAGACTGATG
mmu-miR-21-5p Reverse	GGTCCAGTTTTTTTTTTTTTTCAAC
mmu-miR-219b-5p Forward	CAGAGATGTCCAGCCACA
mmu-miR-219b-5p Reverse	GTCCAGTTTTTTTTTTTTTTCGAG
mmu-miR-32-5p Forward	CGCAGTATTGCACATTACTAAG
mmu-miR-32-5p Reverse	TCCAGTTTTTTTTTTTTTTGCAAC
mmu-miR-20a-5p Forward	GCAGTAAAGTGCTTATAGTGCAG
mmu-miR-20a-5p Reverse	GTCCAGTTTTTTTTTTTTTTCTACCT
mmu-miR-542-3p Forward	CGCAGTGTGACAGATTG
mmu-miR-542-3p Reverse	GGTCCAGTTTTTTTTTTTTTTCAG
mmu-miR-32-5p Forward	CGCAGTATTGCACATTACTAAG
mmu-miR-32-5p Reverse	TCCAGTTTTTTTTTTTTTTGCAAC
mmu-miR-17-3p Forward	TGCAGTGAAGGCACTTG
mmu-miR-17-3p Reverse	GGTCCAGTTTTTTTTTTTTTTCTACA
mmu-miR-17-3p Forward	TGCAGTGAAGGCACTTG
mmu-miR-17-3p Reverse	GGTCCAGTTTTTTTTTTTTTTCTACA
mmu-miR-342-5p Forward	AGAGGGGTGCTATCTGTG
mmu-miR-342-5p Reverse	TCCAGTTTTTTTTTTTTTTCAATCAC
mmu-miR-193a-3p Forward	CAGAACTGGCCTACAAAGTC
mmu-miR-193a-3p Reverse	CCAGTTTTTTTTTTTTTTACTGGGA
mmu-miR-130a-3p Forward	CAGCAGTGCAATGTTAAAAGG
mmu-miR-130a-3p Reverse	GGTCCAGTTTTTTTTTTTTTTTATGC
mmu-miR-181d-5p Forward	AGAACATTCATTGTTGTCGGT
mmu-miR-181d-5p Reverse	GTCCAGTTTTTTTTTTTTTTTACCCA
mmu-miR-340-3p Forward	GCAGTCCGTCTCAGTTAC
mmu-miR-340-3p Reverse	GGTCCAGTTTTTTTTTTTTTTTGCT
m*Meis2* Forward	GTTTTCTTGACTGGGCTTTCCC
m*Meis2* Reverse	GGTCTCCGTACATGGAAGCG
m*Adam23* Forward	CCTAGCGCCACCAATCTCAT
m*Adam23* Reverse	AAGGTGGCATTCCTCCAGTG
m*Zdhhc8* Forward	GATTTCCTCCACTGCCGCT
m*Zdhhc8* Reverse	AGCTCTTGTCAACCATGGGC
m*Sema5a* Forward	CATCTGGGCTGGTGTGTGAC
m*Sema5a* Reverse	TCTGGGAACGTGTCTTCTGC
m*Cttn* Forward	GTGGGCCATGAGTACCAGTC
m*Cttn* Reverse	TTGCCACCGAAGCCACTAGA
m*Adcy6* Forward	TGACTGGCTGGAGGGATACA
m*Adcy6* Reverse	CCCCAAGCTGTTTTCCGTTC
m*Ntng1* Forward	CTCCGGATATTACCTGTGGA
m*Ntng1* Reverse	CTAGGATCATTTGGTCTGGA
m*Frs2* Forward	ATGCCCAGACGTAATGGTGA
m*Frs2* Reverse	TCAGAAGACCATGTGAGCACT
m*Rapgef5* Forward	GCCATTGGAGTCTGGCAGCT
m*Rapgef5* Reverse	CACAGATGCCAGCTCTTGCA
m*Rgs17* Forward	GAGAGCATCCAGGTCCTAGA
m*Rgs17* Reverse	CTCGTATATCATCCTGGCCT
m*Pdzd8* Forward	CACACCCTGCCCAGTTACAA
m*Pdzd8* Reverse	CCACTGCTCAGCTCAAGTGT
m*Rcor1* Forward	GCTCGCTGGACAACGGAAGA
m*Rcor1* Reverse	CAGGTCCATTGGTCTCGTCT
m*Pax8* Forward	GTTTGAGCGGCAGCATTACC
m*Pax8* Reverse	TCCTGCTTTATGGCGAAGGG
m*Bcl11a* Forward	CATCTTCCCTGCGCCATCTTT
m*Bcl11a* Reverse	GAATGGCTTCAAGAGGTTCGG
m*Bcat2* Forward	GAAGACGGAGTACTGGAGCTG
m*Bcat2* Reverse	TGGCTCCGTACTGAATAGCC
m*Bcact2* 3′ UTR to pmirGLO Forward	CGAGCTCAGAGACTCAAGAGAAG TGCAATAGG
m*Bcact2* 3′ UTR to pmirGLO Reverse	TGCTCTAGATTCTTGTTCTTTGG CATTTTATTTC

protocol, and the results were determined by normalizing to the Renilla luciferase activities of three independent experiments.

Cell Proliferation Assay

We used PI (Sigma) /Hoechst (Life Technologies #H1399) and Trypan Blue to detect cell apoptosis, and used a kit (Promega, G3580) to detect cell proliferation ability. For the cell proliferation assay kit, cortical neurons were plated in 4×10^4 cells per well in 96-well plate, and transfected with microRNAs at 1 DIV. Pipet 20 μl of one solution reagent into each well of 96-well plate containing 100 μl of culture medium. Incubate the plate at 37°C for 1–4 h, and then record the absorbance at 490 nm.

Ingenuity Pathway Analysis (IPA)

Datasets represented a gene list were submitted to the Ingenuity Pathway Analysis Tool (IPA tool; Ingenuity H Systems, Redwood City, CA, USA[1]) for core analysis.

Statistical Analysis

The results presented are the average of at least three experiments with standard errors of the mean. Statistical analyses were performed with an unpaired, two-tailed Student's *t*-test and one-way ANOVA, and the data remain normally distributed. One-way ANOVA with *post hoc* test was performed for multiple comparisons. A p-value of <0.05 was considered to indicate statistical significance. Statistical analyses were performed using GraphPad Prism 6.

RESULTS

MiR-182 is Enriched in Neurons

To identify microRNAs that may regulate neuronal development, NSCs were dissociated from the SVZ zone of adult mouse brain and differentiated into neurons (Gage, 2000). We stained the NSCs with primary antibody of anti-Nestin (**Figure 1A**) and stained the neurons differentiated from NSCs with β III tubulin (**Figure 1B**). Recent evidence shows that numbers of microRNAs are specifically expressed in neurons and promote axon extension (Jovicic et al., 2013; Hancock et al., 2014). In

[1]http://www.ingenuity.com

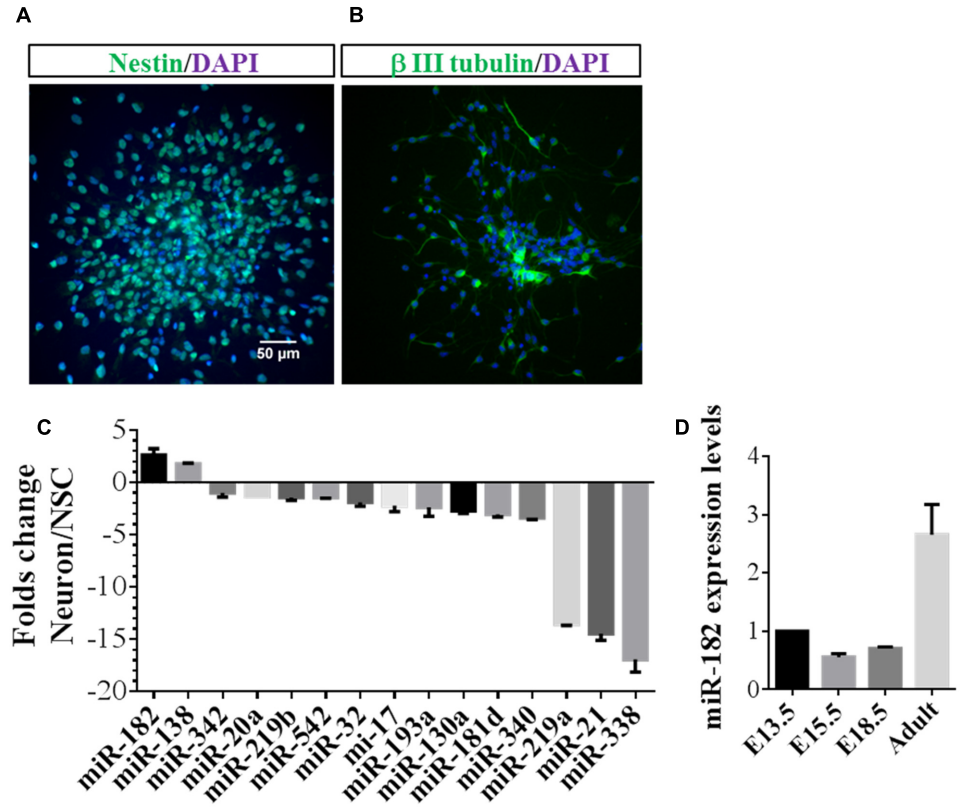

FIGURE 1 | MiR-182 is highly expressed in neurons compared with neural stem cells. (A) Undifferentiated neural stem cells which were dissociated from adult mouse brain expressed Nestin. **(B)** Neurons differentiated from neural stem cells expressed β III tubulin. **(C)** Identification of specific miRNAs in neurons compared with neural stem cells. The relative ratios comparing differentiated to undifferentiated NSCs are shown. MiR-182 and miR-138 showed specific high expression in neurons compared with undifferentiated neural stem cells. **(D)** MiR-182 expression during mouse brain development at embryonic days 13.5, 15.5, 18.5, and adult mouse.

a companion paper, we designed primers and quantitatively identified microRNAs that were enriched in neurons relative to NSCs. Several microRNAs, particularly miR-182 and miR-138, showed enrichment in neurons but not in NSCs, whereas other microRNAs, such as miR-338, miR-21, and miR-219a were enriched in NSCs but not in neurons (**Figure 1C**). These results were consistent with previous results revealing that miR-182 is enriched in neurons compared with astrocytes (Smrt et al., 2010), and miRNAs specifically enriched in neurons were identified by microRNA array (Jovicic et al., 2013).

MiR-182 is known to be highly expressed in sensory cell types (Li et al., 2010) and involved in plasticity and memory (Griggs et al., 2013). We reasoned that if miR-182 were critical for neurodevelopment and function, it should be expressed in neurons of mouse brain. Hence, we detected miR-182 expression levels during different stages of mouse brain development and found that they increased significantly from E13.5 to adult (**Figure 1D**). We hypothesized whether miR-182 has functions in the later stage of neurite growth, and found that the expression of miR-182 was increased from 2 days after birth to adult (**Supplementary Figure S1A**). *In vitro* results showed that miR-182 expression levels were upregulated from 1 to 7 DIV in primary cultured neurons (**Supplementary Figure S1B**). Together, these data and other published literatures suggest that miR-182 plays functional roles in neurons.

MiR-182 Promotes Axon Outgrowth in Cortical Neurons

MicroRNAs were found to play important roles in promoting neuronal differentiation and maturation. Here, we tried to investigate the function of miRNAs in neuronal maturation. As miR-182 is enriched in neurons, we reasoned that miR-182 might regulate neuron development during brain development. We co-transfected with miR-182, miR-138, and miR-31 each plus *GFP*-encoding plasmid into primary cultured cortical neurons at 1 DIV to investigate whether microRNAs overexpression in neurons could affect axon outgrowth. At 36 h after transfection, individual cortical neurons expressing GFP were imaged using fluorescence microscopy. The morphology of axons and soma, which was manually traced and measured by Image J software, showed that miR-182 promoted axon outgrowth by increasing axon length (**Figures 2A,B**). The statistical results are described in **Figure 2C**. In contrast, miR-138 showed no difference in axon outgrowth (data not shown). The overexpression of miR-182 was confirmed by

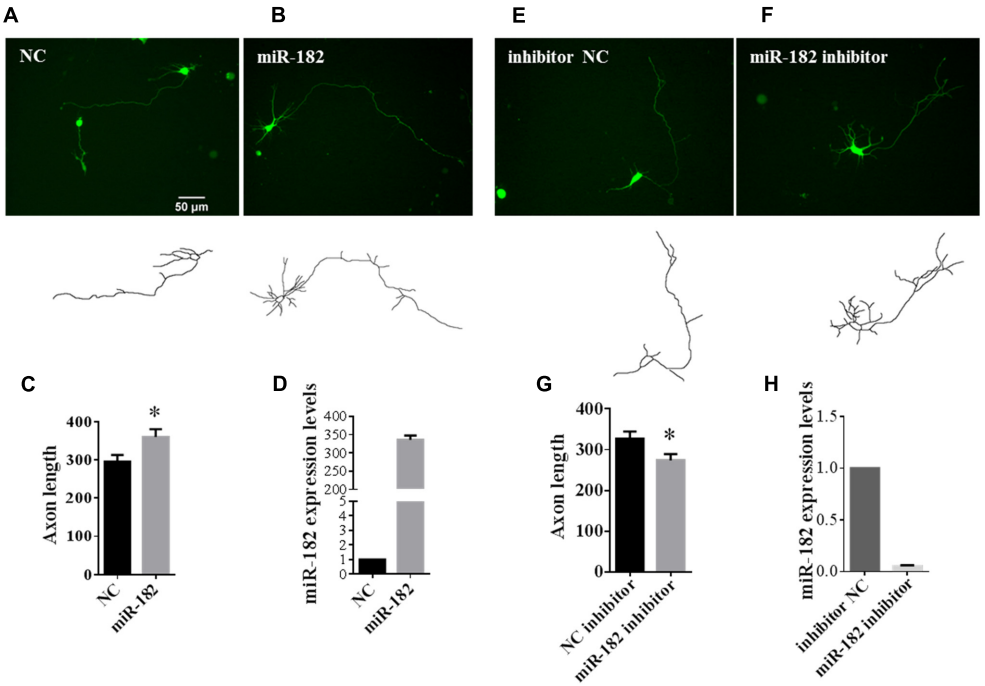

FIGURE 2 | MiR-182 promotes axon outgrowth. (A,B) A schematic diagram showing scramble microRNA and miR-182 mimics plus *GFP*-encoding plasmid that were transfected into cortical neurons at 1 DIV and imaged at 3 DIV. **(C)** Quantification of axon length. Data were presented as mean ± SEM. $*p < 0.05$ by Student's *t*-test, $N = 3$ independent experiments; at least 35 neurons were analyzed in each experiment. **(D)** The expression levels of miR-182 were measured by qRT-PCR. **(E,F)** Blocking of endogenous miR-182 reduced axon length compared with controls. **(G)** Quantification of axon length. Data were presented as mean ± SEM. $*p < 0.05$ by Student's *t*-test, $N = 3$ independent experiments; at least 35 neurons were analyzed in each experiment. **(H)** Expression levels of miR-182 as measured by qRT-PCR.

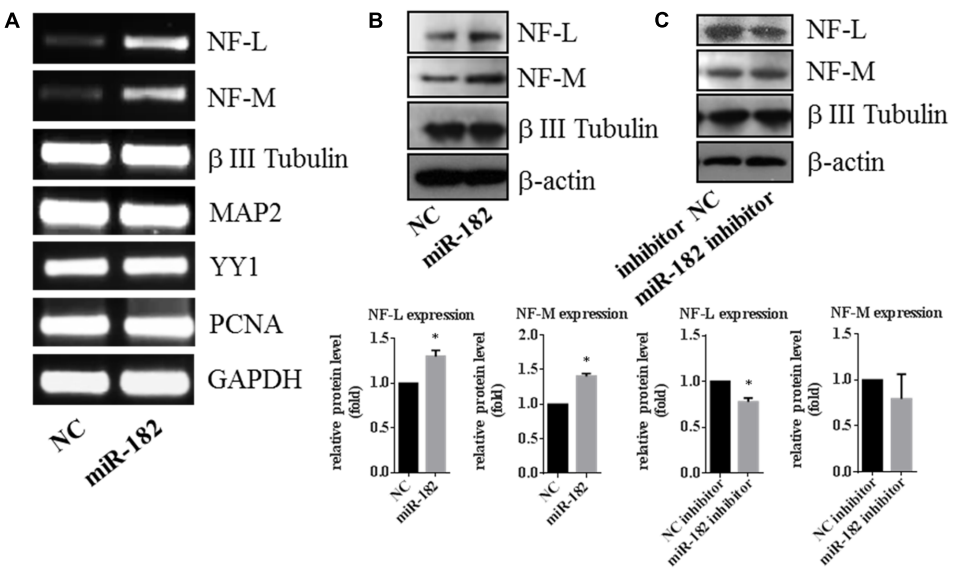

FIGURE 3 | Expression of neurofilament is regulated by miR-182. (A) Expressions of neurofilament-M and -L were upregulated by miR-182 in the RT-PCR results, whereas the reference genes (MAP2 and β III Tubulin) showed no differences. **(B)** MiR-182 promoted neurofilament-M and -L expression by western blot ($*p < 0.05$). **(C)** Blocking of the endogenous miR-182 inhibited the expression of neurofilament-L in protein level, and had no effects on neurofilament-M ($*p < 0.05$).

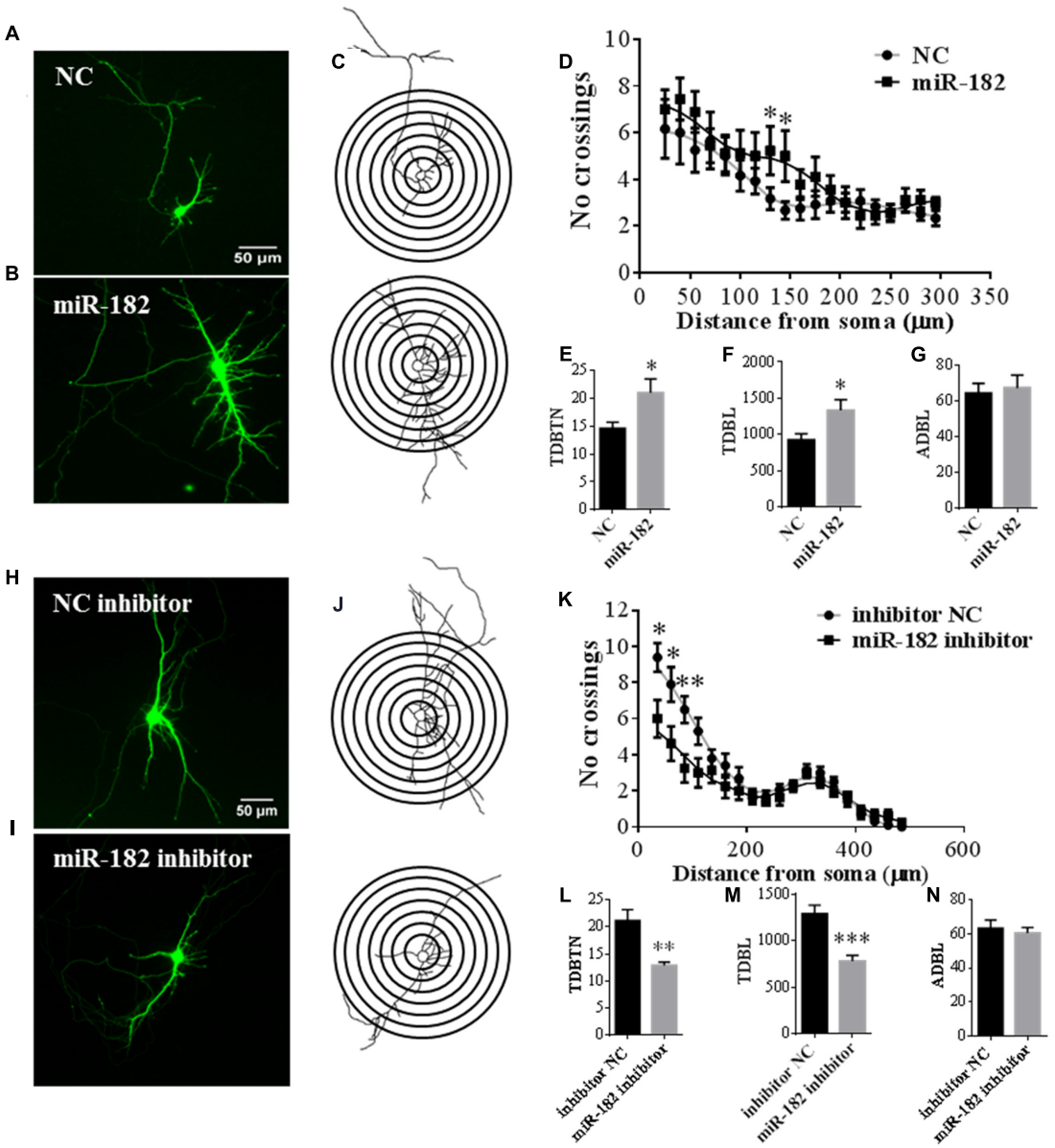

FIGURE 4 | MiR-182 promotes dendrite branching out. (A,B) Cortical neurons were transfected with scramble mimics and miR-182 mimics (60 nM) at 5 DIV. After 48 h, neurons were harvested and images were recorded. A representative image is shown each for neurons transfected with scramble microRNA mimics and miR-182 mimics. **(C)** Representative picture of the Sholl analysis. **(D)** Quantitative results of the number of dendrite process intersections by Sholl analysis. MiR-182 increased dendritic branching at the distance of 130 and 145 μm from the soma. One-way ANOVA, Tukey's post-test (*$p < 0.05$); 35 neurons were analyzed in each condition. **(E–G)** Quantification of total dendritic branch tip number (TDBTN), average dendritic branch length (ADBL) and total dendritic branch length (TDBL) in cortical neurons at 7 DIV (*$p < 0.05$). **(H,I)** Cortical neurons at 5 DIV were transfected with mimics of inhibitor negative control and miR-182 inhibitor (60 nM) plus *GFP*-encoding plasmid. Blockage of endogenous miR-182 decreased dendrite complexity, as determined by Sholl analysis. **(J)** Representative images of neurons subjected to Sholl analysis. **(K)** Quantification of dendrite complexity by Sholl analysis showed that blockage of endogenous miR-182 decreased dendrite branching at the distances of 35, 60, and 85 μm from the soma (*$p < 0.05$, **$p < 0.01$). **(L–N)** Quantification of total dendritic branch tip number (TDBTN), average dendritic branch length (ADBL) and total dendritic branch length (TDBL) for dendrites (**$p < 0.01$, ***$p < 0.001$).

qRT-PCR (**Figure 2D**). To verify the function of miR182 in regulating axon outgrowth, we blocked the endogenous miR-182 by transfecting with antisense oligonucleotides (**Figures 2E,F**). The results showed that miR-182 inhibitor could suppress axon outgrowth compared with the control group (**Figure 2G**), and miR-182 expression was detected by quantitative real-time PCR (**Figure 2H**).

As a neuron marker, neurofilaments (NFs), which consist of three subunits termed neurofilament-L (NF-L), neurofilament-M (NF-M) and neurofilament-H, are thought to provide structural

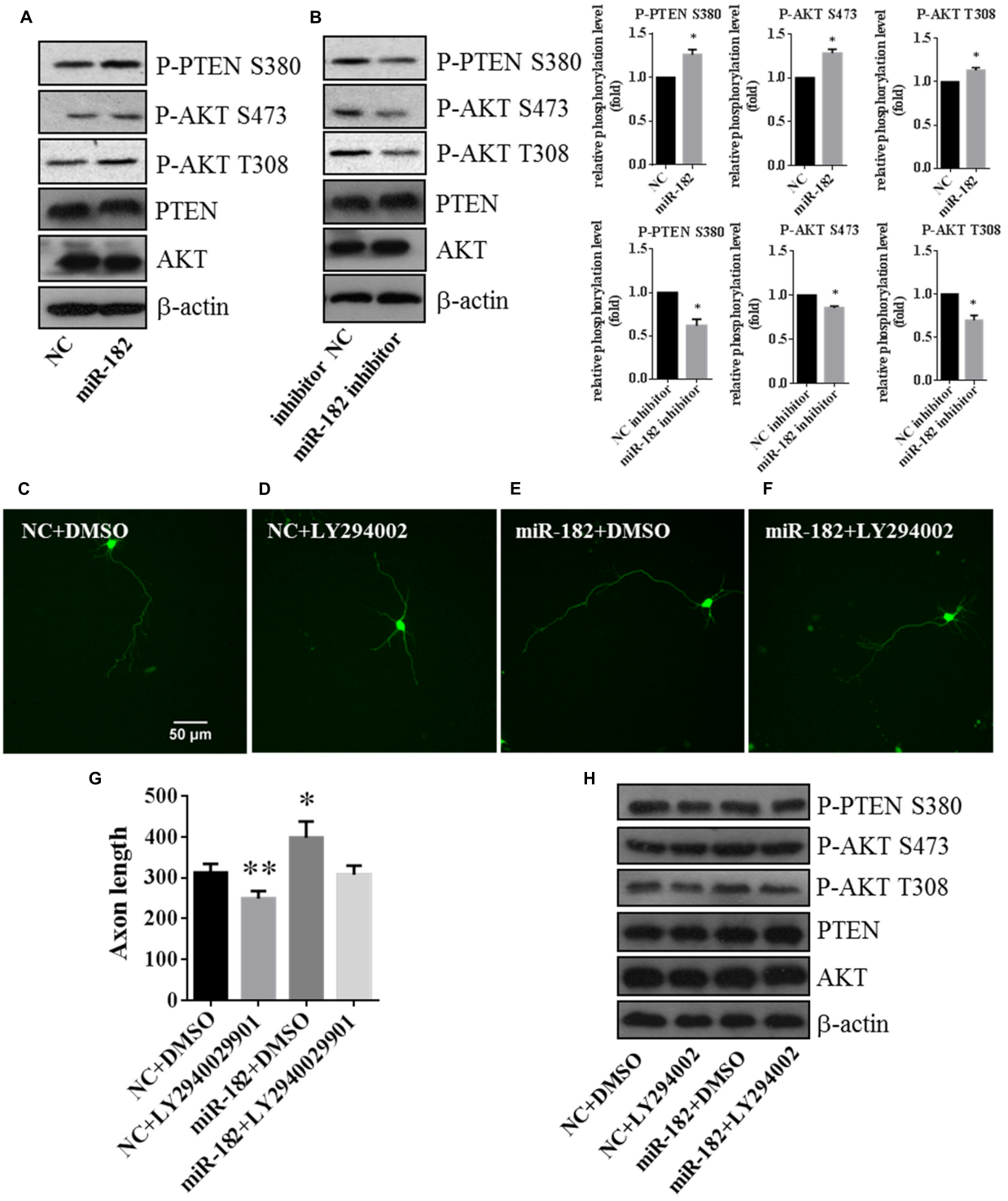

FIGURE 5 | PTEN/AKT pathway is involved in regulating axon outgrowth. (A) Cellular fractions overexpressing miR-182 were analyzed by western blot using antibodies against P-AKT S473, P-AKT T308, AKT, PTEN, and P-PTEN S380. β-actin was used as the loading control, and the data represented the results of at least three different experiments. **(B)** Phosphorylation of AKT and PTEN was analyzed when miR-182 was downregulated. **(C–F)** Representative cortical neurons transfected with microRNA scramble plus DMSO, microRNA scramble plus LY294002, miR-182 plus DMSO and miR-182 plus LY294002. **(G)** Quantification of axon length (*$p < 0.05$, **$p < 0.01$). **(H)** Primary cultured cortical neurons were transfected with scramble microRNA plus DMSO, microRNA scramble plus LY294002, miR-182 plus DMSO and miR-182 plus LY294002, and analyzed by western blot using antibodies against P-AKT S473, P-AKT T308, AKT, PTEN, and P-PTEN S380.

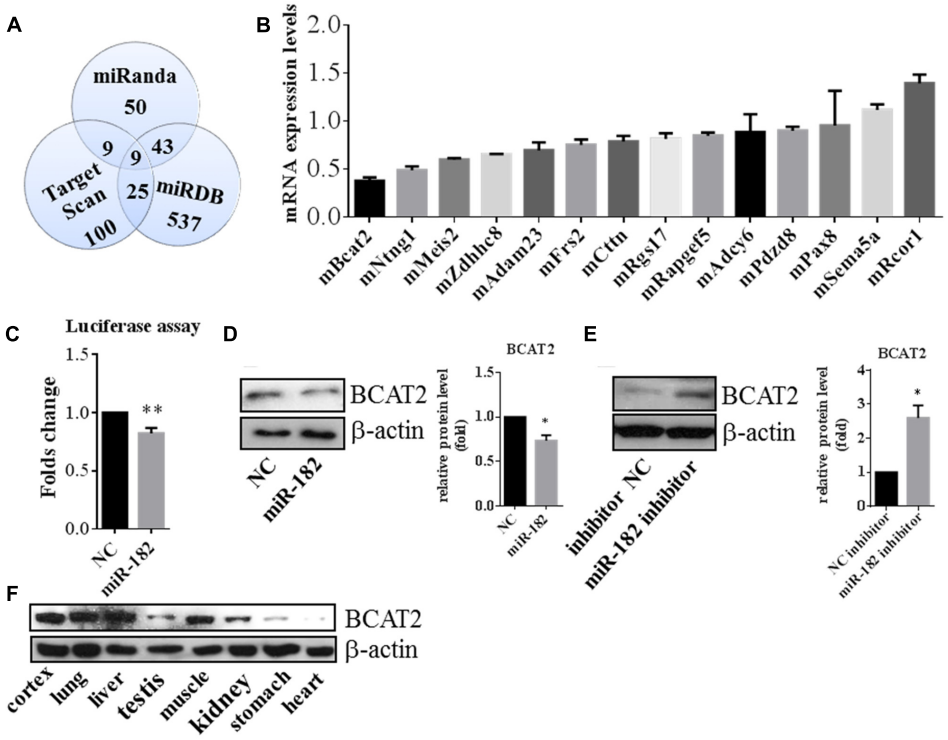

FIGURE 6 | BCAT2 is a translational target of miR-182. (A) Predicting targets of miR-182-5p by comparing the performance of three databases, including Miranda, Target Scan, and miRDB. **(B)** Quantitative real-time PCR indicated that BCAT2 expression was significantly decreased in cortical neurons by miR-182 mimics. **(C)** HEK-293T cells were transfected with miR-182 mimics and scramble mimics each plus luciferase-*BCAT2*-3′ UTR reporter vector. MiR-182 reduced the luciferase intensity compared with the control (**$p < 0.01$). **(D)** MiR-182 reduced the expression of BCAT2 in protein levels in primary cultured neurons (*$p < 0.05$). **(E)** Blockage of endogenous miR-182 increased the expression of BCAT2 by western blot in primary cultured neurons (*$p < 0.05$). **(F)** Expression pattern of BCAT2 in different tissue of mouse embryo by western blot.

support for mature axons (Nixon and Shea, 1992; Lee and Shea, 2014). We found that the expression of NF-L and NF-M was regulated by miR-182. Overexpression of miR-182 increased the expression of NF-L and NF-M in mRNA levels by RT-PCR, but β III tubulin and MAP2 as reference genes were not influenced by miR-182 (**Figure 3A**); in protein levels by western blot (**Figure 3B**). Western blot results showed that inhibition of miR-182 decreased the protein level of NF-L, but it had no influence on the protein levels of NF-M by western blot (**Figure 3C**). It indicated that miR-182 promoted axon outgrowth by regulating NF-L.

We tested the cell viability by PI/Hoechst staining and Trypan blue staining after transfection with microRNAs (**Supplementary Figure S2A**), and detected the cell dynamic viability after transfection for 3 days by cell proliferation assay (**Supplementary Figure S2B**). **Supplementary Figure S2C** showed the transfection efficiency of scramble mimics which conjugated with FAM fluorescence dye.

MiR-182 Regulates Dendrite Branching Out

Dendrites have important functional implications in synapse formation and electroneurographic signal-passing in mature neurons (Jan and Jan, 2010). As miR-182 is known to be enriched in neurons, we further studied the functions of miR-182 on dendrite development and neuron maturation. To evaluate its influence on the complexity of dendrite tree, primary cortical neurons were co-transfected with *GFP*-encoding plasmid containing miR-182 mimics and scramble mimics at 5 DIV. Ectopic expression of miR-182 significantly increased the dendrite complexity (**Figures 4A,B**). We performed Sholl analysis to analyze the dendrite morphology by measuring the number of dendrites that intersected concentric circles at different distances from the soma (Sholl, 1953) (**Figure 4C**). The results showed that miR-182 significantly increased the complexity of the dendrite tree at a distance between 130 and 145 μm from the soma (**Figure 4D**). TDBTN and TDBL were significantly increased, but ADBL remained unchanged (**Figures 4E–G**).

In contrast, the inhibition of miR-182 expression resulted in a significant reduction of total dendritic length and branch numbers (**Figures 4H,I**); and the number of intersections was significantly reduced between the distance of 35–85 μm from the soma (**Figures 4J,K**); TDBTN and TDBL were significantly reduced (**Figures 4L,M**), but ADBL was not changed (**Figure 4N**). Together, these data suggested that miR-182 overexpression caused changes in dendrite branching and

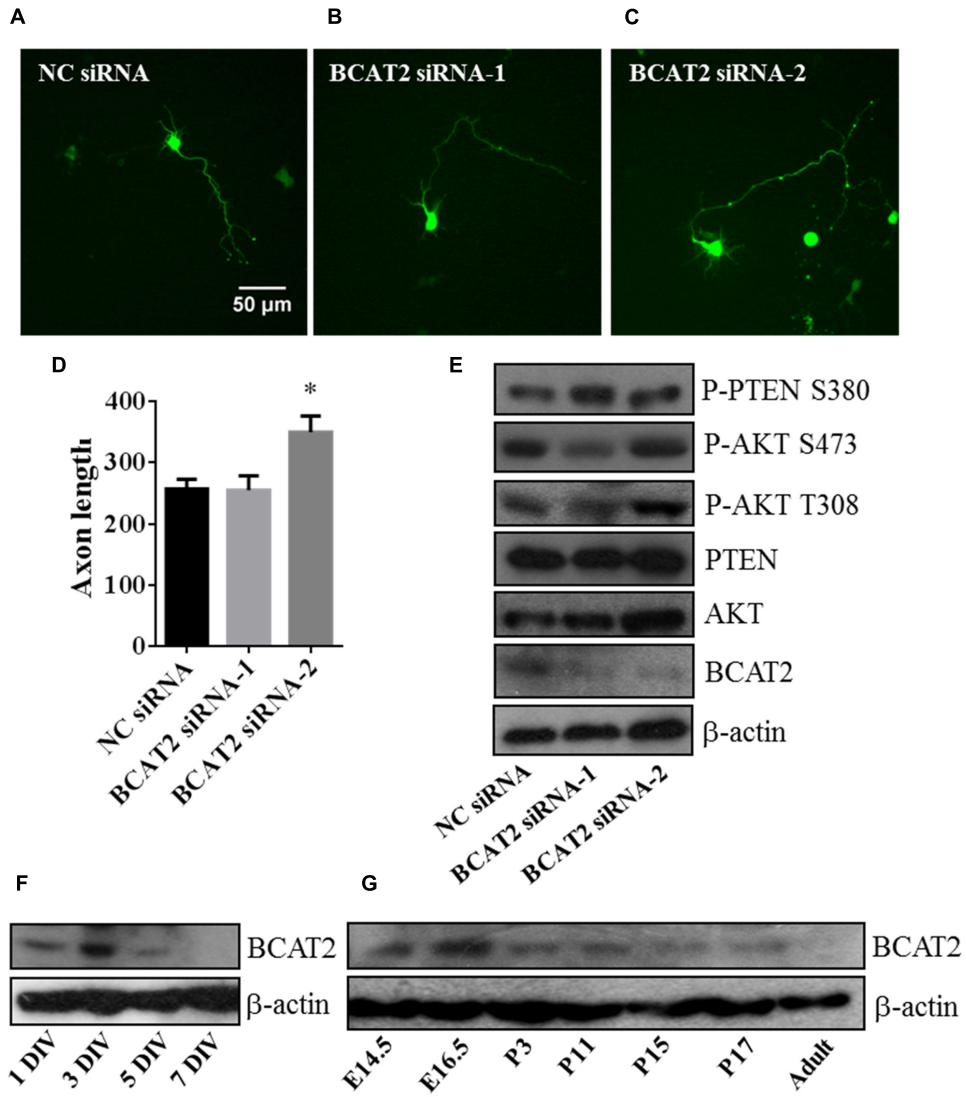

FIGURE 7 | Blockage of endogenous BCAT2 promotes axon outgrowth and increases AKT activity. (A–C) Cortical neurons were transfected with negative control siRNA, BCAT2 siRNA-1, and BCAT2 siRNA-2 each plus *GFP*-encoding plasmid at 1 DIV. **(D)** Quantification of axon length and BCAT2 siRNA-2 increased axon length (*$p < 0.05$). **(E)** BCAT2 siRNA-2 increased the phosphorylation of AKT S473, T308, and PTEN S380 in primary cultured neurons. **(F)** BCAT2 expressions in cultured neurons at 1, 3, 5, and 7 DIV. **(G)** BCAT2 expressions in mouse brain cortex from embryonic 14.5 to adult.

neuronal maturation; thus, it might play important roles during mouse brain development.

PTEN/AKT Pathway is Involved in Regulating Dendrite Branching Out

We investigated the mechanism of miR-182 in the regulation of neuronal development, and detected the activity of the PI3K/AKT, RAF/ERK, and JNK pathways. MicroRNAs regulate dendrite branching out via AKT pathway, which is known to play roles in the regulation of dendritic morphogenesis and to increase the complexity of the dendritic tree (Kumar et al., 2005; Xue et al., 2016). We found that overexpression of miR-182 increased the activity of AKT in T308 and S473 and blockage of the endogenous miR-182 inhibited AKT activity (**Figures 5A,B**), but there are no effects on Erk activity by miR-182 (**Supplementary Figure S3**). PTEN is an inhibitor of PI3K which promotes AKT activity, and the phosphorylation of PTEN S380 negatively regulates PTEN activity by preventing its recruitment into a protein complex (Vazquez et al., 2001). In our results, overexpression of miR-182 inhibited the activity of PTEN by increasing its phosphorylation (**Figure 5A**), and the phosphorylation of PTEN was decreased when the endogenous miR-182 was blocked (**Figure 5B**). Activation of the PI3K/AKT pathway increases dendritic complexity in neurons (Kumar et al., 2005), consistent with our findings of the induction of axon outgrowth and dendritic branching by miR-182.

Meanwhile, to investigate whether endogenous AKT activities are necessary for axon outgrowth, we inhibited the PI3K/AKT

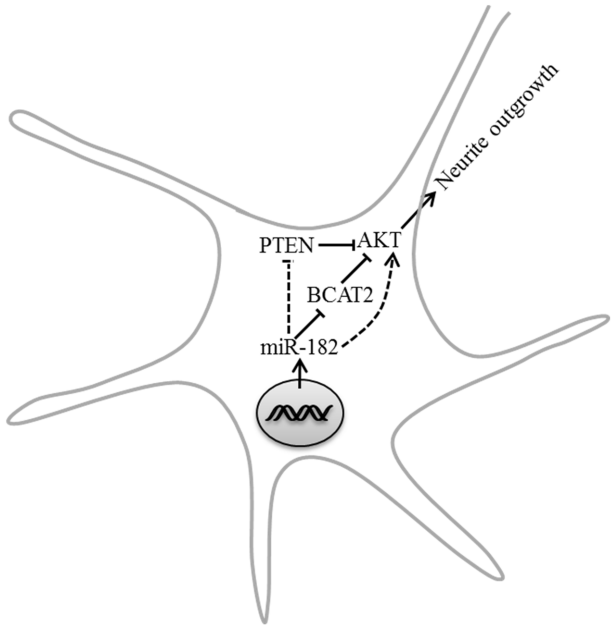

FIGURE 8 | Model depicting the roles of miR-182 in regulating neurite outgrowth. MiR-182 was involved in the inhibition of BCAT2 and resulted in increasing AKT activity, which might lead to neurite outgrowth.

pathway by adding PI3K inhibitor LY294002 plus transfection with scramble mimics and miR-182 mimics. We found that the AKT activity (S473 and T308) and the phosphorylation of PTEN (S380) decreased compared with the non-drug group (**Figure 5H**). The statistic of axon length was consistent with the western blot result that LY294002 could rescue the influence on AKT activity regulated by miR-182 (**Figures 5C–G**). These data verified that miR-182 promoted neuronal maturation by activating the AKT pathway.

Taken together, these results showed that miR-182 inhibited the activity of PTEN and promoted the phosphorylation of AKT, indicating that miR-182 regulated axon outgrowth and dendrite branching out involving the PTEN/AKT pathway.

BCAT2 is a Translational Target of miR-182

To explore the mechanism of miR-182 in regulation of neurite outgrowth, we attempted to identify the target gene of miR-182. First, we predicted the miR-182 target genes using three public databases, including miRanda, Target Scan, and miRDB; and identified nine candidate targets to be common (**Figure 6A**). We compared the expression of 14 target candidates of miR-182 by quantitative real-time PCR in primary cultured cortical neurons, which were transfected with scramble mimics and miR-182 mimics at 1 DIV and lysed at 3 DIV. We found that *BCAT2* expression was significantly downregulated by miR-182 (**Figure 6B**). *BCAT2* is known to be a target of miR-182 in PIGF mice and mouse embryonic fibroblasts (Li et al., 2016). Furthermore, a 3′ UTR-containing fragment of mouse *BCAT2* was amplified and cloned into the luciferase reporter plasmid to detect the luciferase activity. The luciferase activity was significantly downregulated by miR-182 (**Figure 6C**), consistent with the results of a previous report (Li et al., 2016). Meanwhile, protein levels of BCAT2 were significantly decreased in cortical neurons overexpressing miR-182 (**Figure 6D**), but the expression of BCAT2 increased when blocking the endogenous miR-182 by the inhibitor (**Figure 6E**). Meanwhile, we detected the BCAT2 protein expression in different tissues of the E15.5 mouse; found that BCAT2 was highly expressed in cortex, lung, and liver (**Figure 6F**).

To verify the function of BCAT2, we transfected with two siRNA mimics into primary cultured neurons for downregulating the endogenous BCAT2, and deficiency of BCAT2 by siRNA-2 promoted axon outgrowth (**Figures 7A–D**). In western blot results, BCAT2 siRNA-2 increased the activity of AKT and decreased the activity of PTEN (**Figure 7E**). Meanwhile, we investigated the expression profile of BCAT2 in cultured neurons and brain tissue after birth, and found that the expression tendency was decreased (**Figures 7F,G**); it was consistent with the expression profile of miR-182 (**Supplementary Figure S1**). In cardiomyocytes, *BCAT2* deletion promotes AKT activity by increasing the phosphorylation of Ser-473 (Li et al., 2016). MiR-182 may regulate neurite outgrowth by targeting *BCAT2* and further increasing AKT activity and promoting neuronal maturation.

DISCUSSION

Literatures described that microRNAs play vital roles in neuronal development and are essential for the development of central nervous system (Wayman et al., 2008). MiR-182 is highly expressed in the retina (Xu et al., 2007) and identified as the most abundant among axonal miRNAs of RGCs. Loss of miR-182 causes RGC axon targeting defects *in vivo* (Bellon et al., 2017). In a companion paper, we compared the expression levels of several microRNAs between NSCs and neurons, and found that miR-182 was enriched in neurons. Overexpression of miR-182 promoted axon outgrowth and dendrite branching out in mouse cortical neurons; it implicated that miR-182 played a role in neuronal maturation in the early stage of neuronal development. The conclusion of a study described that miR-182 could regulate trigeminal sensory neurons by promoting dendrite branching (Wang et al., 2016), and it was consistent with our results.

The small GTPases of Rho subfamily are critical regulators of axon outgrowth and dendrite elaboration. Cdc42 (cell division cycle 42), Rac1 (Ras-related C3 botulinum toxin substrate 1), and RhoA (Ras homologous member A) are three well-studied Rho GTPases. Cdc42 and Rac1 are positive regulators of axon growth and dendrite development, but RhoA is a negative regulator (Luo, 2000; Suo et al., 2012). Recently, a study showed that miR-182 is involved in structural plasticity and memory formation by regulating the expression of cortactin and Rac1 (Griggs et al., 2013). In the mentioned literature, miR-182 is low expressed in lateral amygdala, and the inner mechanism of miR-182 regulation of amygdala-dependent memory formation was still unclear.

There is a possibility that miR-182 plays distinct role in different areas of brain, like cerebral cortex and lateral amygdala.

In our results, miR-182 increased the expression of NF-L and NF-M in mRNA and protein levels. It indicates that miR-182 regulates neurites outgrowth through indirect effects in NF-L and NF-M. MiR-182 may bind to other target which is the repressor of neurofilaments, and eliminate the effects of inhibition for the neurofilaments expression. Because miR-182 has many other potential targets predicted by the software, whether miR-182 regulates neurite outgrowth through neurofilaments on other targets needs to be investigated in the future.

MiR-182 inhibits apoptosis and promotes survival in medulloblastoma cells by regulating the PI3K/AKT/mTOR signaling axis (Weeraratne et al., 2012). In our work, miR-182 promoted neuronal maturation by increasing AKT phosphorylation and inhibiting PTEN activity. The PTEN/AKT pathway is critical for dendritic morphogenesis (Kumar et al., 2005) and involved in neuron survival controlled by microRNAs (Wong et al., 2013; Han et al., 2014). BCAT2 is expressed in brain tissue (Hull et al., 2012; Zampieri et al., 2013), but no evidence was offered for the function of BCAT in neurite growth before. In this paper, we presented the first report to introduce BCAT's effects in neurite outgrowth, and discovered that *BCAT2* could be considered as a target of miR-182 for regulating neurite outgrowth. Blockage of the endogenous BCAT2 by siRNA promoted axon outgrowth through PTEN/AKT pathway. The results are partly consistent with a previous report that *BCAT2* is a target of miR-182, and BCAT2 deficiency promotes AKT activation by increasing the phosphorylation of Ser473 in cardiomyocytes (Li et al., 2016). BCAT2 catalyzes the first step in the mitochondrial catabolism of BCAAs, and BCAAs provide nitrogen for the synthesis of glutamate, an excitatory neurotransmitter; BCAAs appear to increase the phosphorylation of AKT S473 by activating mTORC2 (Tato et al., 2011; Li et al., 2016). BCAAs catalyzed by BCAT2 may be the direct regulator of AKT and PTEN, but we have no evidence.

Inhibition of BCAT may be useful for the treatment of behavioral and neurodegenerative disorders (Hu et al., 2006). As the expression of BCAT2 was decreased after birth (**Figure 7G**), BCAT2 expression pattern may be different in neuron injury. We chose several published target genes of miR-182 and PTEN/AKT pathway to do Ingenuity Pathway Analysis (IPA) and found it was more related to cell morphology and nervous system development (**Supplementary Figures S4A,B**). MiR-182 plays important roles in the synaptic connectivity of photoreceptors and retinal regeneration (Lumayag et al., 2013), and a literature described that miR-182 plays a role in regulating CLOCK expression after hypoxia-ischemia brain injury (Ding et al., 2015). It is worthy of further investigation for the function of miR-182 and BCAT2 in neuron regeneration.

CONCLUSION

Our results first show that one of neuron-enriched microRNAs, miR-182, has an important modulatory role in neuron development. Both overexpression and inhibition of miR-182 have significant but opposite effects in axon outgrowth and dendrite branching out, and PTEN/AKT pathway is involved in the regulation of neurite outgrowth by miR-182. We also find that BCAT2 is a target of miR-182; deficiency of BCAT2 increases the activity of AKT and promotes neurite growth (**Figure 8**).

AUTHOR CONTRIBUTIONS

Conceived and designed the experiments: WW, GL, and WP. Performed the experiments and analyzed the data: WW, GL, XS, HL, and WP. Wrote the paper: WW, GL, and WP. All authors contributed to the revision of the article and approved the final version of the manuscript.

FUNDING

This work was supported by National Natural Science Foundation of China (81271393) and Research Grants Council of Hong Kong (Ref No. 472913).

SUPPLEMENTARY MATERIAL

The Supplementary Material for this article can be found online at: http://journal.frontiersin.org/article/10.3389/fncel.2017.00096/full#supplementary-material

FIGURE S1 | Expression profile of miR-182 in brain cortex after birth and cultured neurons. (A) Expression profile of miR-182 in brain cortex from postnatal 2 to adult. **(B)** MiR-182 expression profile in cultured neurons at 1, 3, 5, and 7 DIV.

FIGURE S2 | Cell viability test. (A) PI/Hoechst and Trypan blue staining for cultured neurons transfected with microRNA scramble, miR-182 mimics, inhibitor negative control mimics, and miR-182 inhibitor mimics. **(B)** Cell proliferation assay for cultured neurons transfected with microRNA scramble, miR-182 mimics, inhibitor negative control mimics, and miR-182 inhibitor mimics from day 1 to day 3 after transfection. **(C)** MicroRNA transfection efficiency test in neurons and FAM fluorescence dye is conjugated to microRNA.

FIGURE S3 | MiR-182 had no effect on Erk pathway. Detecting phosphorylation of Erk1/2 by western blot, and had no effects by miR-182.

FIGURE S4 | Ingenuity Pathway Analysis (IPA) for miR-182 and PTEN/AKT pathway. (A) The network relationship among targets genes of miR-182 and PTEN/AKT. **(B)** The influence on different physiological medicine by miR-182 and PTEN/AKT pathway in IPA.

REFERENCES

Agostini, M., Tucci, P., Steinert, J. R., Shalom-Feuerstein, R., Rouleau, M., Aberdam, D., et al. (2011). microRNA-34a regulates neurite outgrowth, spinal morphology, and function. *Proc. Natl. Acad. Sci. U.S.A.* 108, 21099–21104. doi: 10.1073/pnas.1112063108

Aldrich, B. T., Frakes, E. P., Kasuya, J., Hammond, D. L., and Kitamoto, T. (2009). CHANGES in expression of sensory organ-specific microRNAs in rat dorsal

root ganglia in association with mechanical hypersensitivity induced by spinal nerve ligation. *Neuroscience* 164, 711–723. doi: 10.1016/j.neuroscience.2009.08.033

Alvarez, M. L., and Nourbakhsh, M. (2014). *RNA Mapping: Methods and Protocols*. New York, NY: Springer Science Business Media.

Arimura, N., and Kaibuchi, K. (2007). Neuronal polarity: from extracellular signals to intracellular mechanisms. *Nat. Rev. Neurosci.* 8, 194–205. doi: 10.1038/nrn2056

Bei, F., Lee, H. H., Liu, X., Gunner, G., Jin, H., Ma, L., et al. (2016). Restoration of visual function by enhancing conduction in regenerated axons. *Cell* 164, 219–232. doi: 10.1016/j.cell.2015.11.036

Bellon, A., Iyer, A., Bridi, S., Lee, F. C., Ovando-Vazquez, C., Corradi, E., et al. (2017). miR-182 regulates Slit2-mediated axon guidance by modulating the local translation of a specific mRNA. *Cell Rep.* 18, 1171–1186. doi: 10.1016/j.celrep.2016.12.093

Bixel, M., Shimomura, Y., Hutson, S., and Hamprecht, B. (2001). Distribution of key enzymes of branched-chain amino acid metabolism in glial and neuronal cells in culture. *J. Histochem. Cytochem.* 49, 407–418. doi: 10.1177/002215540104900314

Busskamp, V., Krol, J., Nelidova, D., Daum, J., Szikra, T., Tsuda, B., et al. (2014). miRNAs 182 and 183 are necessary to maintain adult cone photoreceptor outer segments and visual function. *Neuron* 83, 586–600. doi: 10.1016/j.neuron.2014.06.020

Castellano, S., Casarosa, S., Sweatt, A. J., Hutson, S. M., and Bozzi, Y. (2007). Expression of cytosolic branched chain aminotransferase (BCATc) mRNA in the developing mouse brain. *Gene Expr. Patterns* 7, 485–490. doi: 10.1016/j.modgep.2006.10.010

Cole, J. T., Sweatt, A. J., and Hutson, S. M. (2012). Expression of mitochondrial branched-chain aminotransferase and alpha-keto-acid dehydrogenase in rat brain: implications for neurotransmitter metabolism. *Front. Neuroanat.* 6:18. doi: 10.3389/fnana.2012.00018

Dajas-Bailador, F., Bonev, B., Garcez, P., Stanley, P., Guillemot, F., and Papalopulu, N. (2012). microRNA-9 regulates axon extension and branching by targeting Map1b in mouse cortical neurons. *Nat. Neurosci.* doi: 10.1038/nn.3082 [Epub ahead of print].

Dehay, C., and Kennedy, H. (2007). Cell-cycle control and cortical development. *Nat. Rev. Neurosci.* 8, 438–450. doi: 10.1038/nrn2097

Ding, X., Sun, B., Huang, J., Xu, L. X., Pan, J., Fang, C., et al. (2015). The role of miR-182 in regulating pineal CLOCK expression after hypoxia-ischemia brain injury in neonatal rats. *Neurosci. Lett.* 591, 75–80. doi: 10.1016/j.neulet.2015.02.026

Gage, F. H. (2000). Mammalian neural stem cells. *Science* 287, 1433–1438.

Griggs, E. M., Young, E. J., Rumbaugh, G., and Miller, C. A. (2013). MicroRNA-182 regulates amygdala-dependent memory formation. *J. Neurosci.* 33, 1734–1740. doi: 10.1523/JNEUROSCI.2873-12.2013

Han, Z., Chen, F., Ge, X., Tan, J., Lei, P., and Zhang, J. (2014). miR-21 alleviated apoptosis of cortical neurons through promoting PTEN-Akt signaling pathway in vitro after experimental traumatic brain injury. *Brain Res.* 1582, 12–20. doi: 10.1016/j.brainres.2014.07.045

Hancock, M. L., Preitner, N., Quan, J., and Flanagan, J. G. (2014). MicroRNA-132 is enriched in developing axons, locally regulates rasa1 mRNA, and promotes axon extension. *J. Neurosci.* 34, 66–78. doi: 10.1523/Jneurosci.3371-13.2014

Hu, L. Y., Boxer, P. A., Kesten, S. R., Lei, H. J., Wustrow, D. J., Moreland, D. W., et al. (2006). The design and synthesis of human branched-chain amino acid aminotransferase inhibitors for treatment of neurodegenerative diseases. *Bioorg. Med. Chem. Lett.* 16, 2337–2340. doi: 10.1016/j.bmcl.2005.07.058

Hull, J., Hindy, M. E., Kehoe, P. G., Chalmers, K., Love, S., and Conway, M. E. (2012). Distribution of the branched chain aminotransferase proteins in the human brain and their role in glutamate regulation. *J. Neurochem.* 123, 997–1009. doi: 10.1111/jnc.12044

Inui, M., Martello, G., and Piccolo, S. (2010). MicroRNA control of signal transduction. *Nat. Rev. Mol. Cell Biol.* 11, 252–263. doi: 10.1038/nrm2868

Jan, Y. N., and Jan, L. Y. (2010). Branching out: mechanisms of dendritic arborization. *Nat. Rev. Neurosci.* 11, 316–328. doi: 10.1038/nrn2836

Jovicic, A., Roshan, R., Moisoi, N., Pradervand, S., Moser, R., Pillai, B., et al. (2013). Comprehensive expression analyses of neural cell-type-specific miRNAs identify new determinants of the specification and maintenance of neuronal phenotypes. *J. Neurosci.* 33, 5127–5137. doi: 10.1523/JNEUROSCI.0600-12.2013

Kaech, S., and Banker, G. (2006). Culturing hippocampal neurons. *Nat. Protoc.* 1, 2406–2415. doi: 10.1038/nprot.2006.356

Kosik, K. S. (2006). The neuronal microRNA system. *Nat. Rev. Neurosci.* 7, 911–920. doi: 10.1038/nrn2037

Kumar, V., Zhang, M. X., Swank, M. W., Kunz, J., and Wu, G. Y. (2005). Regulation of dendritic morphogenesis by Ras-PI3K-Akt mTOR and Ras-MAPK signaling pathways. *J. Neurosci.* 25, 11288–11299. doi: 10.1523/Jneurosci.2284-05-2005

Lee, S., and Shea, T. B. (2014). The high molecular weight neurofilament subunit plays an essential role in axonal outgrowth and stabilization. *Biol. Open* 3, 974–981. doi: 10.1242/bio.20149779

Li, H., Kloosterman, W., and Fekete, D. M. (2010). MicroRNA-183 family members regulate sensorineural fates in the inner ear. *J. Neurosci.* 30, 3254–3263. doi: 10.1523/JNEUROSCI.4948-09.2010

Li, N., Hwangbo, C., Jaba, I. M., Zhang, J., Papangeli, I., Han, J., et al. (2016). miR-182 modulates myocardial hypertrophic response induced by angiogenesis in heart. *Sci. Rep.* 6:21228. doi: 10.1038/srep21228

Lumayag, S., Haldin, C. E., Corbett, N. J., Wahlin, K. J., Cowan, C., Turturro, S., et al. (2013). Inactivation of the microRNA-183/96/182 cluster results in syndromic retinal degeneration. *Proc. Natl. Acad. Sci. U.S.A.* 110, E507–E516. doi: 10.1073/pnas.1212655110

Luo, L. (2000). Rho GTPases in neuronal morphogenesis. *Nat. Rev. Neurosci.* 1, 173–180. doi: 10.1038/35044547

Nixon, R. A., and Shea, T. B. (1992). Dynamics of neuronal intermediate filaments: a developmental perspective. *Cell Motil. Cytoskeleton* 22, 81–91. doi: 10.1002/cm.970220202

Schratt, G. M., Tuebing, F., Nigh, E. A., Kane, C. G., Sabatini, M. E., Kiebler, M., et al. (2006). A brain-specific microRNA regulates dendritic spine development. *Nature* 439, 283–289. doi: 10.1038/nature04367

Sholl, D. A. (1953). Dendritic organization in the neurons of the visual and motor cortices of the cat. *J. Anat.* 87, 387–406.

Siegel, G., Obernosterer, G., Fiore, R., Oehmen, M., Bicker, S., Christensen, M., et al. (2009). A functional screen implicates microRNA-138-dependent regulation of the depalmitoylation enzyme APT1 in dendritic spine morphogenesis. *Nat. Cell Biol.* 11, 705–716. doi: 10.1038/ncb1876

Smrt, R. D., Szulwach, K. E., Pfeiffer, R. L., Li, X., Guo, W., Pathania, M., et al. (2010). MicroRNA miR-137 regulates neuronal maturation by targeting ubiquitin ligase mind bomb-1. *Stem Cells* 28, 1060–1070. doi: 10.1002/stem.431

Song, Y., Ori-McKenney, K. M., Zheng, Y., Han, C., Jan, L. Y., and Jan, Y. N. (2012). Regeneration of *Drosophila* sensory neuron axons and dendrites is regulated by the Akt pathway involving Pten and microRNA bantam. *Genes Dev.* 26, 1612–1625. doi: 10.1101/gad.193243.112

Sun, F., Park, K. K., Belin, S., Wang, D., Lu, T., Chen, G., et al. (2011). Sustained axon regeneration induced by co-deletion of PTEN and SOCS3. *Nature* 480, 372–375. doi: 10.1038/nature10594

Suo, L., Lu, H., Ying, G., Capecchi, M. R., and Wu, Q. (2012). Protocadherin clusters and cell adhesion kinase regulate dendrite complexity through Rho GTPase. *J. Mol. Cell Biol.* 4, 362–376. doi: 10.1093/jmcb/mjs034

Tato, I., Bartrons, R., Ventura, F., and Rosa, J. L. (2011). Amino acids activate mammalian target of rapamycin complex 2 (mTORC2) via PI3K/Akt signaling. *J. Biol. Chem.* 286, 6128–6142. doi: 10.1074/jbc.M110.166991

Thier, M., Worsdorfer, P., Lakes, Y. B., Gorris, R., Herms, S., Opitz, T., et al. (2012). Direct conversion of fibroblasts into stably expandable neural stem cells. *Cell Stem Cell* 10, 473–479. doi: 10.1016/j.stem.2012.03.003

Vazquez, F., Grossman, S. R., Takahashi, Y., Rokas, M. V., Nakamura, N., and Sellers, W. R. (2001). Phosphorylation of the PTEN tail acts as an inhibitory switch by preventing its recruitment into a protein complex. *J. Biol. Chem.* 276, 48627–48630. doi: 10.1067/jbc.C100556200

Walker, T. L., and Kempermann, G. (2014). One mouse, two cultures: isolation and culture of adult neural stem cells from the two neurogenic zones of individual mice (issue 93, art e51225, 2014). *J. Vis. Exp.* 2014:e51225. doi: 10.3791/51225

Wang, Y., Zhao, X., Wu, X., Dai, Y., Chen, P., and Xie, L. (2016). microRNA-182 mediates Sirt1-induced diabetic corneal nerve regeneration. *Diabetes Metab. Res. Rev.* 65, 2020–2031. doi: 10.2337/db15-1283

Wayman, G. A., Davare, M., Ando, H., Fortin, D., Varlamova, O., Cheng, H. Y., et al. (2008). An activity-regulated microRNA controls dendritic plasticity by down-regulating p250GAP. *Proc. Natl. Acad. Sci. U.S.A.* 105, 9093–9098. doi: 10.1073/pnas.0803072105

Weeraratne, S. D., Amani, V., Teider, N., Pierre-Francois, J., Winter, D., Kye, M. J., et al. (2012). Pleiotropic effects of miR-183∼96∼182 converge to regulate cell survival, proliferation and migration in medulloblastoma. *Acta Neuropathol.* 123, 539–552. doi: 10.1007/s00401-012-0969-965

Woldemichael, B. T., Jawaid, A., Kremer, E. A., Gaur, N., Krol, J., Marchais, A., et al. (2016). The microRNA cluster miR-183/96/182 contributes to long-term memory in a protein phosphatase 1-dependent manner. *Nat. Commun.* 7:12594. doi: 10.1038/ncomms12594

Wong, H. K., Veremeyko, T., Patel, N., Lemere, C. A., Walsh, D. M., Esau, C., et al. (2013). De-repression of FOXO3a death axis by microRNA-132 and -212 causes neuronal apoptosis in Alzheimer's disease. *Hum. Mol. Genet.* 22, 3077–3092. doi: 10.1093/hmg/ddt164

Xu, S., Witmer, P. D., Lumayag, S., Kovacs, B., and Valle, D. (2007). MicroRNA (miRNA) transcriptome of mouse retina and identification of a sensory organ-specific miRNA cluster. *J. Biol. Chem.* 282, 25053–25066. doi: 10.1074/jbc.M700501200

Xue, Q., Yu, C., Wang, Y., Liu, L., Zhang, K., Fang, C., et al. (2016). miR-9 and miR-124 synergistically affect regulation of dendritic branching via the AKT/GSK3beta pathway by targeting Rap2a. *Sci. Rep.* 6:26781. doi: 10.1038/srep26781

Zampieri, T. T., Pedroso, J. A., Furigo, I. C., Tirapegui, J., and Donato, J. Jr. (2013). Oral leucine supplementation is sensed by the brain but neither reduces food intake nor induces an anorectic pattern of gene expression in the hypothalamus. *PLoS ONE* 8:e84094. doi: 10.1371/journal.pone.0084094

Zou, H., Ding, Y., Wang, K., Xiong, E., Peng, W., Du, F., et al. (2015). MicroRNA-29A/PTEN pathway modulates neurite outgrowth in PC12 cells. *Neuroscience* 291, 289–300. doi: 10.1016/j.neuroscience.2015.01.055

Conflict of Interest Statement: The authors declare that the research was conducted in the absence of any commercial or financial relationships that could be construed as a potential conflict of interest.

frontiers in Cellular Neuroscience

ORIGINAL RESEARCH
published: 29 March 2017
doi: 10.3389/fncel.2017.00086

Geometrical Determinants of Neuronal Actin Waves

Caterina Tomba[1,2], Céline Braïni[1,3], Ghislain Bugnicourt[1], Floriane Cohen[3], Benjamin M. Friedrich[4], Nir S. Gov[5] and Catherine Villard[1,3]**

[1] Université Grenoble Alpes, Centre National de la Recherche Scientifique (CNRS), Institut Néel, Grenoble, France, [2] Université Grenoble Alpes, Centre National de la Recherche Scientifique (CNRS), Laboratoire des Technologies de la Microélectronique, CEA-LETI, Grenoble, France, [3] Laboratoire PhysicoChimie Curie, Institut Curie, Pierre-Gilles de Gennes Institute for Microfluidics, CNRS, PSL Research University, Paris, France, [4] Biological Algorithms Group, Center for Advancing Electronics Dresden, Technische Universität Dresden, Dresden, Germany, [5] Department of Chemical Physics, Weizmann Institute of Science, Rehovot, Israel

Hippocampal neurons produce in their early stages of growth propagative, actin-rich dynamical structures called actin waves. The directional motion of actin waves from the soma to the tip of neuronal extensions has been associated with net forward growth, and ultimately with the specification of neurites into axon and dendrites. Here, geometrical cues are used to control actin wave dynamics by constraining neurons on adhesive stripes of various widths. A key observable, the average time between the production of consecutive actin waves, or mean inter-wave interval (IWI), was identified. It scales with the neurite width, and more precisely with the width of the proximal segment close to the soma. In addition, the IWI is independent of the total number of neurites. These two results suggest a mechanistic model of actin wave production, by which the material conveyed by actin waves is assembled in the soma until it reaches the threshold leading to the initiation and propagation of a new actin wave. Based on these observations, we formulate a predictive theoretical description of actin wave-driven neuronal growth and polarization, which consistently accounts for different sets of experiments.

Keywords: axon, polarization, actin wave, micropatterns, modeling

OPEN ACCESS

Edited by:
Froylan Calderon De Anda, University of Hamburg, Germany

Reviewed by:
Olivier Thoumine, Centre National de la Recherche Scientifique, France
Yu-Feng Wang, Harbin Medical University, China

****Correspondence:***
Catherine Villard
catherine.villard@curie.fr
Nir S. Gov
nir.gov@weizmann.il

Received: *03 January 2017*
Accepted: *13 March 2017*
Published: *29 March 2017*

Citation:
Tomba C, Braïni C, Bugnicourt G, Cohen F, Friedrich BM, Gov NS and Villard C (2017) Geometrical Determinants of Neuronal Actin Waves. Front. Cell. Neurosci. 11:86. doi: 10.3389/fncel.2017.00086

INTRODUCTION

Growing neuronal branches (neurites) regularly exhibit propagative actin-based membrane deformations, or actin waves, which travel from the cellular body (soma) to the neurite tip. Actin waves are physiological events generic for a large set of mammalian neurons, e.g., of hippocampal or cortical origin. They have been observed both in dissociated neurons in culture and within brain slices (Katsuno et al., 2015; Flynn et al., 2009). The role of these directional structures in neuronal growth and polarization was already underlined in the first descriptions of this phenomenon in the literature, about two decades ago (Ruthel and Banker, 1998). Actin waves are associated with outbursts of neurite growth following the possible reactivation of the growth cone, and thereby contribute to the fast elongation of the nascent axon. Interestingly, these outbursts result from two successive events occurring at the tip: the tip first retracts as soon as the actin wave leaves the soma, and then grows forward when this actin wave merges with the growth cone. This suggests that actin waves, as already proposed in the seminal work of Ruthel and Banker (Ruthel and Banker, 1999), might create tension and exert pulling forces along neurites, which are important players implied in neurite growth and axonal specification (Lamoureux et al., 2002; Franze and Guck, 2010). As compared to non-neuronal actin waves [e.g., actin ruffles

(Goicoechea et al., 2006), circular waves (Bernitt et al., 2015) and planar waves (Sun et al., 2015)], neuronal actin waves have remained poorly studied for many years, and the wave generation mechanism still remains elusive. Several in-depth studies published in recent years have however provided new insights into the role and characteristics of these propagative structures. First, actin waves seem to propagate using directional actin treadmilling that generates mechanical force (Katsuno et al., 2015). Actin polymerization and depolymerization is accompanied by the presence of several actin-associated proteins, such as Arp3, cofilin, or shootin within the actin wave (Flynn et al., 2009; Toriyama et al., 2006; Tilve et al., 2015). Interestingly, the wave of actin polymerization directs microtubule-based transport by triggering an upstream wave of microtubule polymerization mediated by a transient widening of the neurite shaft (Winans et al., 2016). This picture is in agreement with the presence of microtubule-associated proteins like doublecortin within actin waves (Tint et al., 2009). Finally, it should be noted that fin-like propagative structures similar to neuronal actin waves have been observed in 3T3 cells grown on nanofibers, conferring to these non-neuronal cells neurite-like protrusions (Guetta-Terrier et al., 2015).

In a previous study, we have shown that the control of the neurite width using micropatterns of adhesion yielded a fine tuning of both the length of neurites and the localization of axonal specification (Tomba et al., 2014). To consider the role of actin waves in neuronal growth, in the present work we have used predetermined neuronal morphologies to get new insight into the geometrical determinants of the actin wave dynamics, including temporal periodicity and induced neurite growth. This allowed us to develop a predictive model of neurite length and axonal polarization using the neurite width-dependent characteristics of actin waves. We further confronted this model to various sets of neuronal morphologies and found overall good agreement between both.

METHODS

Neuron Culture, Labeling, and Imaging

Embryonic day E18 mice hippocampi of Oncins France 1 or C57BL/6J mouse (Charles River) were dissected. We used both strains depending on the availability of animals at the time of culture (we did not encounter any statistically significant differences in actin wave dynamics between the two strains, as repeatedly checked on different patterns before merging the data). These hippocampi were then dissociated in MEM medium supplemented with 10% horse serum, 1% L-Glutamine, 1% Sodium pyruvate, and 0.05% Peni-streptomycine (Invitrogen). Neurons were plated on Poly-L-Lysine (Sigma, P2636) coated coverslips and kept first (for 3 h) in the dissociation medium and then in the maintenance medium of Neurobasal supplemented with 2% B27, 1% L-Glutamine, and 0.05% Peni-streptomycine (Invitrogen). Neurons were fixed in 4% paraformaldehyde and immunostained with standard techniques, after a permeabilization step of 30 min in PBS supplemented with 2% BSA and 0.25% Triton. The following antibodies and respective secondary antibodies were used in the indicated dilutions: for microtubules, rat anti-tubulin antibody (clone YL1/2, 1:500) and Alexa488 coupled (Invitrogen, 1:250), for axons, Tau (clone Tau-1, Millipore, 1:500), and CY3 coupled (Invitrogen, 1:250), for DNA, Hoechst (Invitrogen, 1:1000).

Isolated fixed neurons were analyzed with an upright Olympus BX51 microscope using a x20 dry objective (LMPLFL20x from Olympus, NA 0.4) and a F-View camera. Images of living neurons were acquired using three different inverted microscopes equipped with x20 dry, phase contrast objectives (NA 0.4): Olympus IX71 (Hamamatsu ORCA-ER camera), Zeiss Axiovert 200M (AxioCam camera), and Leica microscope DMi8 (Hamamatsu ORCA Flash 4.0 V2 camera). All were equipped with a heated work plate, a humidifier, a CO_2 delivery system and a motorized stage to allow multi-position and multi-condition acquisitions. Images were acquired every 2–4 min. Only propagative growth cone-like structures were counted as actin waves (see Fig. S1).

The study was carried out in accordance with European Community guidelines on the care and use of laboratory animals: 86/609/EEC. The research purpose and the protocol are described in the Ethical Annex of ERCadg project CellO, which was approved and is regularly reviewed by the ERCEA. Institut Curie animal facility has received license #C75-05-18, 24/04/2012, reporting to Comité d'Ethique en matiére d'expérimentation animale Paris Centre et Sud (National registration number: #59).

Statistical Tests

Data were analyzed using Prism 7.0 (GraphPad Software, Inc.). Two-tailed unpaired non parametric Mann-Whitney U test were used for comparing IWI distributions (**Figures 1**, **2**) and net tip elongation (**Figure 3C**). Chi-square tests were used for analyzing the slopes of the linear regression fits of the graphs of **Figure 4**. Distributions in **Figures 1**, **2**, **4** are defined by their mean and standard deviation (*SD*) values.

Patterning

Poly-L-lysine patterns were transferred on silanized substrates (18×18 mm^2 coverslips from VWR, ref. 631–1331). After an oxygen plasma cleaning step (50W) of 2 min in duration, silanization was performed in a liquid phase using the 3Methacryloxypropyltrimethoxysilane (Bind-Silane, Sigma). Then, patterns were defined using UV classical photolithography steps, including Shipley S1805 photoresist spinning (4,000 rpm, 0.5 μm thickness, 115°C annealing step for 1 min), insulation through a mask, development (Microposit concentrate 1:1, Shipley), Poly-L-lysine deposition (1 mg/ml over night), and lift-off using an ultra-sound ethanol bath.

RESULTS

Geometrical Cues Determine Properties of Actin Waves

Diverse neuronal morphologies were produced from the design of various micropatterns of adhesion, in order to challenge the production of actin waves in situations involving e.g., different neurite widths, or different neurite number. More precisely, in a first set of experiments, we studied neurons with 2 neurites,

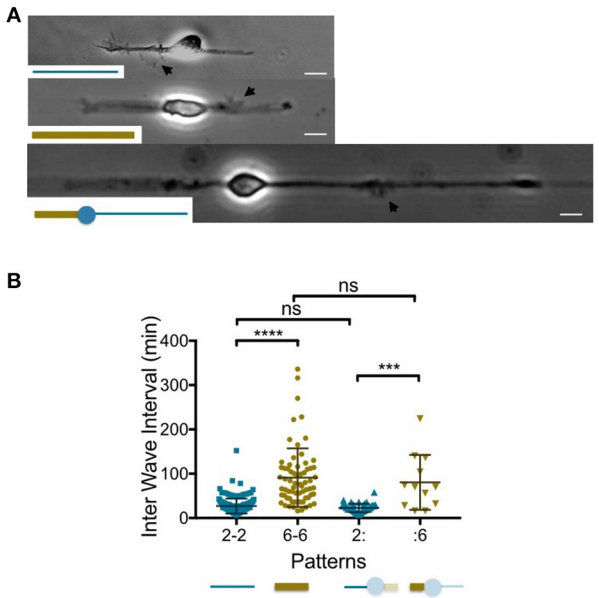

FIGURE 1 | Temporal patterns of waves according to the neurite width. **(A).** Images of 1 day *in vitro* neurons grown on 2 μm (top) and 6 μm (middle) wide adhesive stripes and a combination of both (bottom). Black arrows point to actin waves. Adhesive patterns are represented in the insets. Scale bars:10 μm. **(B)** Distribution of the time intervals between two successive actin waves computed at the neurite level (Inter Wave Intervals: IWI) for the three different neuron geometries shown in **(A)**. The corresponding patterns are represented below the graph using the same color code as the one chosen to plot the IWI distributions (blue and gold for the 2 μm and 6 μm wide stripes, respectively). The neurites of interest for the 2:6 pattern appear opaquely. Mean values and *SD*: 27.1 ± 16.8 min (2-2, $n = 173$, 4 cells), 91.1 ± 65.9 min (6-6, $n = 68$, 6 cells), 22.7 ± 9.5 min (2: $n = 45$, 4 cells), 80.5 ± 61.8 min (:6, $n = 12$, 4 cells). ns: $p > 0.5$, ***$p < 0.004$, ****$p < 0.0001$.

on patterns in which each neurite was constrained to grow on either a 2 or 6 μm wide stripe, or on stripes with a varying width, from 2 to 6 μm and from 6 to 2 μm, respectively. In another set of experiments, we constrained neurons to grow on patterns inducing different numbers of neurites. Time-lapse experiments using phase contrast imaging were used to identify propagative actin waves (Fig. S1 and supplementary movie; See also the Materials and Methods Section).

The Neurite Width Controls the Production Rate of Actin Waves

Following previous results showing that neurite elongation was slowed down when neurites were allowed to spread on 6 μm, as compared to 2 μm wide stripes (Tomba et al., 2014), we studied the temporal rate of actin wave production in similar geometries of adhesion. Linear adhesive patterns with widths of 2 or 6 μm, respectively, were produced, leading to 2-branched neurons displaying diametrically opposed neurites spreading on 2 or 6 μm wide stripes (these designs are referenced later on by the nomenclature 2-2 or 6-6, respectively). We selected young stage 2 neurons (Dotti et al., 1988), i.e., neurons of rather symmetric neurite length taken at 1–2 days *in vitro* (1-2 DIV) displaying a ratio between the longest and the shortest neurite lower than 1.5, except for transient and reversible neurite asymmetry due to soma displacement (see supplementary movie). Such an early stage of development is considered as the most relevant time window to assess the role of actin waves (Winans et al., 2016). We also designed a pattern combining diametrically opposed 2 and 6 μm wide stripes. A central disk of adhesion of 15 μm diameter was introduced in this asymmetric pattern to set the location of the soma and therefore the width of both neurites. In our nomenclature, this pattern is labeled "2:6," with the mark ":" standing for the 15 μm disk. **Figure 1A** displays images of neurons grown on the three types of patterns, 2-2, 6-6, and 2:6, all exhibiting a single actin wave. It should be noted that, in the 2:6 patterns, we could not obtain well-formed 6 μm wide stumps before the 2 μm wide branch gets rather long, as illustrated by the cell shown in **Figure 1A**. This point is highlighted in Fig.S2A displaying the average neurite lengths for all conditions at 2 DIV and showing that 2:6 patterns inherently produce the most asymmetric neurons in length.

To evaluate the rate of actin wave initiation in these three geometrical configurations (i.e., 2-2, 6-6, and 2:6 patterns), we computed a quantitative characteristic, the Inter Wave Interval (IWI), corresponding to the time interval between the initiation of two consecutive actin waves within a given neurite. In the case of stripes with uniform width, data from both neurites of each of the analyzed cells were merged. For an overview of the way actin waves distribute temporally between the two branches, see Fig. S3 displaying the directional correlations between two subsequent actin waves.

The graph of **Figure 1B** summarizes our results. Strikingly, the mean interval between consecutive actin wave production events seems to scale with the pattern width. Actin waves are indeed about three times less frequent on wide neurites that elongate on 6 μm wide stripes, as compared to neurite growing on 2 μm wide stripes. This finding is further strengthened by the results obtained on the 2:6 patterns. We observed no significant differences between the IWI's distributions from the 2 μm wide branch of the 2:6 pattern and the distribution of IWIs obtained on 2 μm wide stripes (2-2 pattern). The same observation was made for the 6 μm wide branches. In other words, each branch of the 2:6 pattern behaved independently of the other: this suggests that actin waves are initiated according to a temporal pattern defined locally at the neurite level.

Actin waves travel distally along neurites but usually emerge near the soma. We therefore wondered if the width of the proximal segment alone was responsible for the observed distributions of IWIs. To answer this question, we designed variants of the previous patterns combining 2 and 6 μm wide stripes *along* a single branch (see Tomba et al., 2014). For instance, a 2 μm wide stump was inserted at the basis of a 6 μm wide stripe, yielding a geometry labeled as "−26" (see **Figure 2A** for an example of a neuron grown on a 2:26 pattern, according to the terminology defined above). The reverse situation, i.e., a 6 μm wide stump inserted at the basis of a 2 μm wide stripe was also used (and referenced as "−62"). Finally, to ensure that actin waves were initiated on stripes of uniform width near the soma, the lengths of the 2 or 6 μm wide proximal stumps were taken to be at least two times longer than the

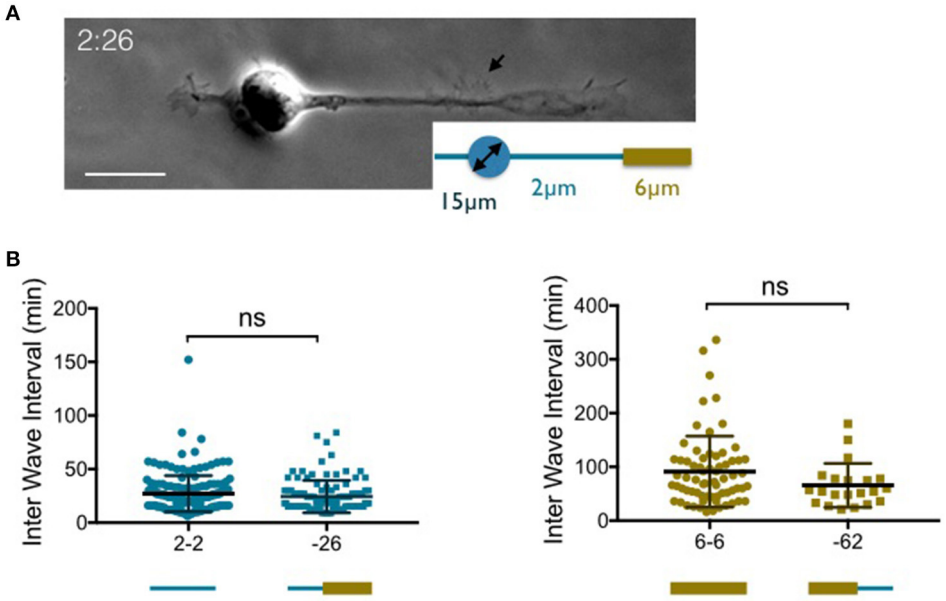

FIGURE 2 | Temporal patterns of waves according to the width of the neurite base. (A) Images of a neuron grown on 2:26 adhesive pattern (see the inset) made of a 15 μm disk to anchor the soma and a 2 μm wide stripe that enlarges up to 6 μm on the right neurite 40 μm away from the edge of the soma. Scale bar: 15 μm. **(B)** Distribution of the time intervals between two successive actin waves along a given neurite (inter wave intervals: IWI) in different configurations where the width of the neurite base is either 2 μm (left) or 6 μm (right). Mean values and *SD*: 27.1 ± 16.8 min (2-2, $n = 173$, 4 cells) 24.3 ± 15.1min (−26, $n = 105$, 4 cells), 91.1 ± 65.9 min (6-6, $n = 68$, 6 cells) and 65.7 ± 40.8 min (−62, $n = 21$, 6 cells). ns: $p = 0.21$ (2-2 vs. −26) and $p > 0.99$ (6-6 vs. −62).

typical longitudinal actin wave dimension, i.e., about 10 μm (**Figure 1A**).

The graphs of **Figure 2B** show that there is no significant difference between the rate of actin wave production along neurites elongating on 2-2 and −26 stripes. The same observation was made between 6-6 and −62 geometries. This indicates that the geometrical control of the periodicity of actin waves is localized within the region of emergence of these structures near the soma.

The Net Growth Triggered by the Arrival of an Actin Wave at the Neurite Tip Depends on the Neurite Width

It was reported in the seminal papers of Ruthel and Banker (Ruthel and Banker, 1999) that actin waves were triggering a retraction of the neurite tip while moving forward, then its extension. The combination of both phenomena resulted in a net forward growth of the tip. A similar observation was recently reported by Winans et al. (2016) who stated that, at 1 DIV, 90% of actin waves yield neurite outgrowth when reaching the tip, suggesting the central role of actin waves in the early stages of neuronal growth. Here, we computed the distributions of the net displacement of the neurite tip associated to actin waves produced on 2 and 6 μm wide stripes, respectively (only actin waves that could be followed up to the tip where taken into account). In all the experiments selected, the onset of actin waves and their position during their propagation were measured (**Figures 3A,B**). The progressive retrograde motion of the tip seemed well correlated with the time span of these propagative structures. Defining the duration of the extension phase was less straightforward. We noted however that similar time constants seemed to be involved in the retraction and extension processes, as illustrated by the rather symmetric shapes of the corresponding peaks in the curves representing the tip position versus time (**Figure 3B**). We thus decided to compute the tip extension during a time span equal to the duration of its retraction, as expressed by the identical widths of the red and blue rectangles in the inset of **Figure 3B**. Other criteria could have been chosen, e.g., to wait for a stabilization of the position of the tip consecutive to the burst of growth triggered by the actin wave, but then our observation would have depended strongly on the time elapsed between two successive actin waves on the same neurite. The relatively short duration chosen to compute the neurite extension phase might consistently lead to an underestimation of the total neurite elongation. However, our procedure should provide a precise proxy for neurite elongation that allows a comparison between different adhesive patterns.

Using the above procedure, we found that the increment of growth per actin wave λ_w was larger for 6 μm wide than for 2 μm wide stripes, i.e., $\lambda_6 = 1.46$ μm ($n = 57$, 5 cells) and $\lambda_2 = 0.61$ μm ($n = 201$, 5 cells), respectively, as illustrated in **Figure 3C**. Note that previous work reported larger values of net growth in the range of 2–4.5 μm per wave, using a longer time window at the expense of a less clearly defined criterion (Ruthel and Banker, 1999). But even in the presence of a proportional measurement bias, as described just above, the ratio between these numbers should correctly quantify the ratio of growth induced by the waves on each of these stripes.

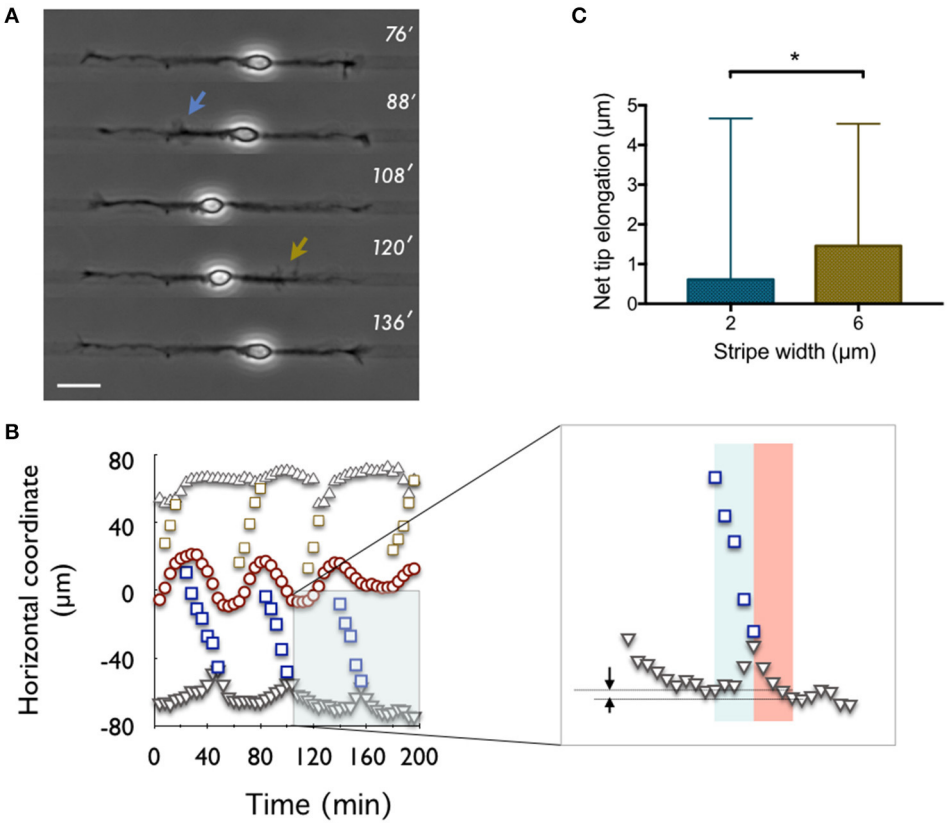

FIGURE 3 | Net tip elongation per actin wave. (A) Time-lapse recording (indicated in minutes: 0′ is 24 h after plating) of a neuron developing on a 6 μm wide stripe (pattern 6-6). The adhesive pattern is revealed by phase contrast imaging as a dark stripe on a lighter gray non-adhesive background. Scale bar: 20 μm. **(B)** Coordinates of waves (open symbols), neurite tips (solid gray symbols), and soma center (red symbols) as a function of time for the neuron shown in **(A)**. The origin of the spatial coordinates is set to the initial soma position. Inset: zoomed region of the main graph. Arrows express the net tip growth that results from the sum of the initial tip retraction and the subsequent growth spurt computed within the blue and red windows, respectively. **(C)** Distribution of the net tip elongation per actin wave on 2 μm (blue) and 6 μm (gold) wide stripes, i.e., the 2-2 and 6-6 patterns, respectively. Mean values: 0.61 μm (2-2, $n = 201$, 5 cells) and 1.46 μm (6-6, $n = 57$, 5 cells). $^*p = 0.0355$.

The Production Rate of Actin Waves by the Cell is Independent of the Number of Neurites

The above experiments suggest a local control of actin wave production, at the neurite basis. In order to test this observation in a different context, we explored a configuration in which the neurite width is set at a fixed value (2 μm), and the number of neurites varies. We therefore designed adhesive geometries with a central disk (diameter 15 μm) and 2 μm thin lines symmetrically distributed around this disk in order to produce neurons with 2, 3, or 4 branches (see **Figure 4A** for the sketches of the adhesive patterns and images of typical cells).

The distribution of IWI computed in two different ways, i.e., at the neurite and cell levels, similarly to **Figure 1**, **2**, respectively), is reported in **Figure 4B** for each geometry. Interestingly, the mean values of IWI at the neurite level increases nearly proportionally with the number of branches, whereas the global rate of production of actin waves computed at the cell level does not vary significantly with the number of branches. Note that this invariance of the mean IWI computed at the scale of the entire neuron versus the number of branches is associated with a conservation of the total neurite length at 2 DIV (Fig. S2B).

Modeling Neuron Growth and Axonal Polarization Using the Geometrical Determinants of Actin Waves

In a previous work, we had studied the influence of patterns geometry on neurite length at 3DIV, and on the localization of axonal specification [see Tomba et al. (2014), and the supplementary material of this work]. Basically, we used in (Tomba et al., 2014) 4 different types of 2 branch patterns built from 2 and 6 μm wide adhesive stripes. As an example, a pattern defined by a 6 μm wide stripe on one side of a 15 μm-diameter disk, and a diametrically opposed 2 μm wide stump that will further be allowed to enlarge to up to 6 μm after a length l will be defined as a 6:26 pattern. Similarly, we produced 6:62, 2:26, and 2:62 patterned neurons with l=20, 40, 60, and 100 μm except for the 2:62 pattern (where l = 10 and 30 μm). The results could be interpreted by a phenomenological model, in

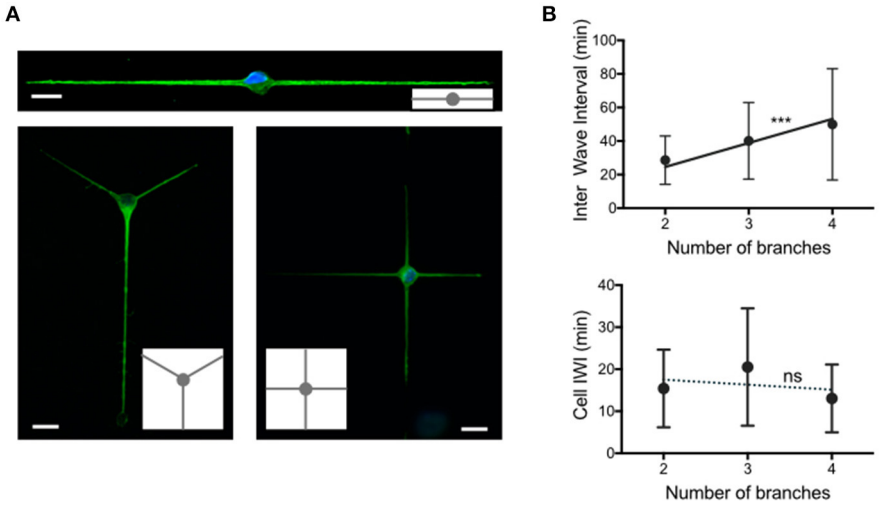

FIGURE 4 | Temporal patterns of waves according to the number of neurites. (A) Images of 2 days *in vitro* neurons extending 2, 3, and 4 neurites grown on adhesive patterns made of 2 μm wide stripes and a central 15 μm diameter disk. Green: YL1/2, microtubules. Blue: Hoechst, nuclei. Adhesive patterns are represented in gray in the insets. Scale bars: 15 μm. **(B)** Distribution of the time intervals between two successive actin waves (Inter Wave Interval, IWI), computed at the neurite level (top) and at the cell (soma) level (bottom) for the three different configurations shown in **(A)** The solid line in the top graph of slope 14.3 min/branch constitutes the fit of our data following the hypothesis that actin waves are produced at a constant rate in the soma and distributed randomly along neurites (***$p = 0.0005$). Top graph mean values and *SD*: 28.6 ± 14.4 min (2 branches, $n = 155$, 5 cells), 40.1 ± 22.8 min (3 branches, $n = 113$, 2 cells) and 49.9 ± 33.2 (4 branches, $n = 179$, 3 cells). Bottom graph mean values and *SD*: 15.4 ± 9.2 min (2 branches, $n = 166$, 5 cells), 20.5 ± 14.0 min (3 branches, $n = 115$, 2 cells) and 13.0 ± 8.1 (4 branches, $n = 188$, 3 cells). The linear regression analysis of the data as a function of the stripe width is represented as a dashed line in the bottom graph (ns: $p = 0.9$).

which the tip was assumed to grow at a speed defined by the local stripe width at the tip's location, and by the polarization state of the neurite (dendrite or axon). All the experiments were accounted for by a single set of parameters of the model—i.e., the critical length that sets the axonal fate, the width of the critical length distribution and the width and polarization dependent growth rates. This model, however, did not provide insight in the mechanisms responsible for these behaviors.

Actin-Wave Based Model of Neurite Growth and Polarization

In the present work, we used our findings about the geometrical determinants of actin waves obtained from simple patterns to build a new mechanistic model of neuronal growth and polarization, assuming that these growth and polarization and mainly driven by actin waves. This model was then compared with the experimental data previously obtained at 3 DIV on the more complex sets of patterns described above.

More specifically, we modeled the elongation of the neurites along the adhesive stripes from the following assertions, motivated by the accumulated experimental observations:

(a) Growth velocity is affected by the rate of actin-wave initiation, which in turn is determined by the proximal width (close to the soma) of the adhesive stripe on which the undifferentiated neurite is growing. This velocity is obtained from the product of the width-dependent actin wave mean initiation rate (**Figure 1**) by the length increment of the tip induced per actin wave (**Figure 3D**).

(b) Neurites have a certain probability to turn into axons, which signals for the whole cell to polarize. In the model, this polarization event will occur when the neurite length exceeds a critical length, the distribution of which is assumed as Gaussian. This neurite will then differentiate into an axon, while all other neurites will then become dendrites. This part of the model, motivated by previous studies in this field (Seetapun and Odde, 2010; Yamamoto et al., 2012), is unchanged from (Tomba et al., 2014).

(c) The growth velocity of the differentiated neurites will follow the change in the mean rate of actin wave initiation induced by the event of axonal determination, i.e., increase in the axon and decrease in the dendrites.

These assertions are mathematically expressed as described below.

The average growth velocity v of the neurite tip in condition of controlled neuronal geometries is ruled by the following set of equations:

$$v_w = \alpha \lambda_w \omega_w \tag{1}$$

where ω_w is the production rate of actin waves on an initial stripe segment of width w, λ_w the growth increment per actin wave and α a free parameter expressing the proportional measurement bias discussed in section 2.2.

In addition, this velocity v_w will change by a concentration/dilution factor θ, if the growing tip has moved past a stripe width change, to account for the conservation of the material conveyed by actin waves, i.e.,

$$\mathbf{v_w} = \alpha \lambda_\mathbf{w} \omega_\mathbf{w} \theta \tag{2}$$

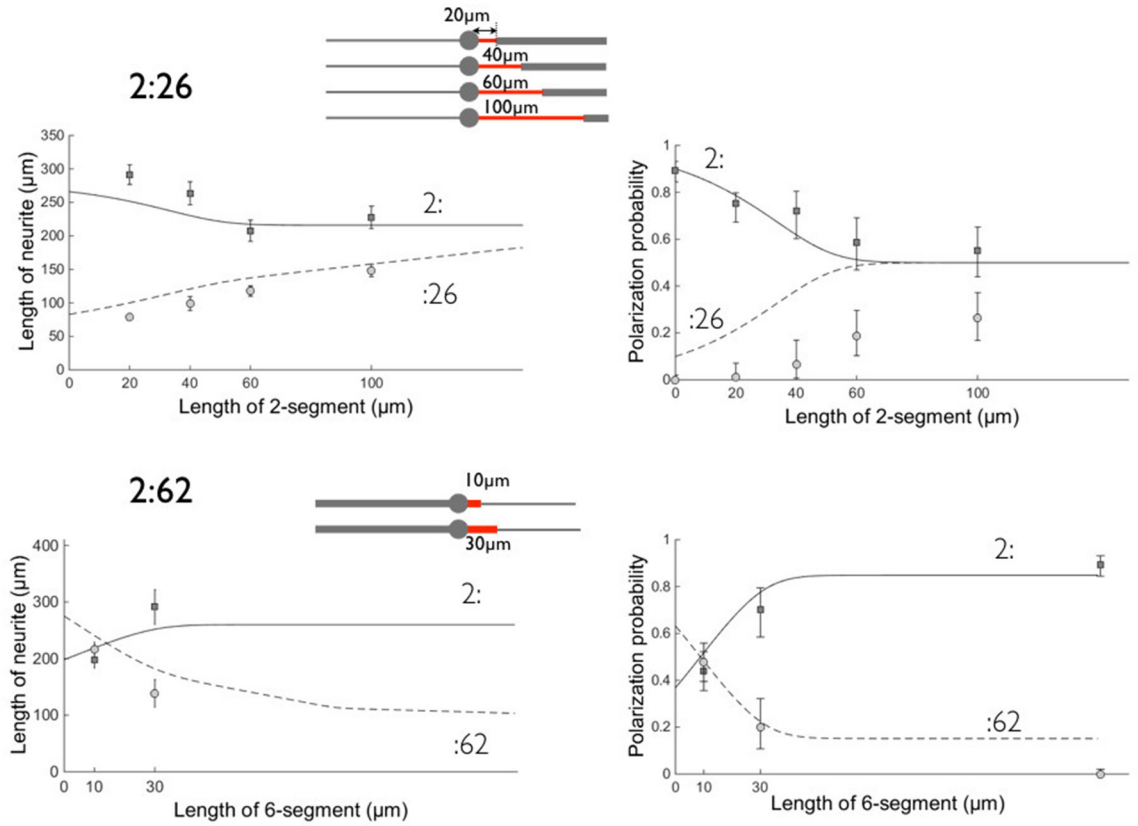

FIGURE 5 | Comparison between experimental data and the model on patterns 2:26 and 2:62. Left: neurite lengths, **right:** polarization probabilities. All results were obtained at 3 days *in vitro*. Symbols denote the experimental data and lines the result of the model calculation: Circles (dashed line) correspond to the :26 and :62 branches and squares (solid line) to the :2 opposite branch. Errors bars represent the standard error of the mean (length data) or 95% confidence interval (polarization data). The parameters used in this calculation are: $T = 72$ h, $v_2 = \alpha\ \lambda_2\omega_2 \approx 3\ \mu$m/hr, $v_6 = \alpha\ \lambda_6\omega_6 \approx 1.8\ \mu$m/h ($\alpha = 2.2$), $\beta = 1.4$, $\gamma = 0.6$, $\theta = 2$. As previously (see Tomba et al., 2014), we took $L_{pol} = 50\ \mu$m, $\sigma_{pol} = 20\ \mu$m, and we inserted polarization data obtained on 2:6 patterns (we located them arbitrarily at a coordinate l = 150 µm for 2:62 data). The schemes of the patterns are shown for each set of geometries with the proximal stump of variable length in red.

$\theta > 1$ (resp. $\theta < 1$) when the actin wave passes from a wide (resp. thin) region to a thinner (resp. wider) region, so that the material delivered to the leading edge at the tip is concentrated (resp. diluted) and therefore gives a larger (resp. smaller) net growth.

Following polarization, the equations displayed below will rule the growth of axons and of future dendrites:

$$\begin{aligned} v_{w\ (axon)} &= \beta v_{w\ (neurite)}, \\ v_{w\ (dend.)} &= \gamma v_{w\ (neurite)} \end{aligned} \tag{3}$$

Experimentally, β and γ express the change in actin wave initiation mean rate following the event of axonal determination in our present model, as addressed in the following section.

Experiments Specifying the Parameters of the Model

First, we model L_{pol} by a Gaussian distribution with mean $L_{pol} = 50\ \mu$m and standard deviation $\sigma_{pol} = 20\ \mu$m, as already considered in the work of Tomba et al. (2014). This choice matches with the observed length of the initial axonal segment, a structure implied in action potential generation.

The set of parameters associated with actin waves are the following: $\alpha, \omega_w, \lambda_w, \theta, \beta, \gamma$ with $w = 2$ or 6 µm. We have already experimentally determined ω_w and λ_w for both values of w (see **Figures 1**, **3**, respectively).

To determine β and γ, we seek the rates of production of actin waves in the nascent axon and in the future dendrite, as compared to the rate obtained in undifferentiated, symmetric neurons (cf. the data shown in **Figure 1**). We selected 1 DIV neurons with already well-developed symmetric neurites and followed them up to 2 DIV (see Fig. S4A). Interestingly, we observed no obvious change in the periodicity of actin waves at the soma level when neurons evolve from a symmetric to an asymmetric morphology evoking a transition to a polarized state (see Fig. S4B). This observation suggests a constraint on β and γ, such that $\frac{\gamma+\beta}{2} = 1$.

To go further, we then considered another set of patterned neurons on stripes characterized by asymmetric lengths (with one neurite at least 50% longer that the other) and already long neurites ($> 50\ \mu$m), so that one neurite should have differentiated into an axon. We measured the IWI of each branch and found a mean value of $\frac{\beta}{\gamma} = r \approx 2.2 \pm 0.57$, meaning that

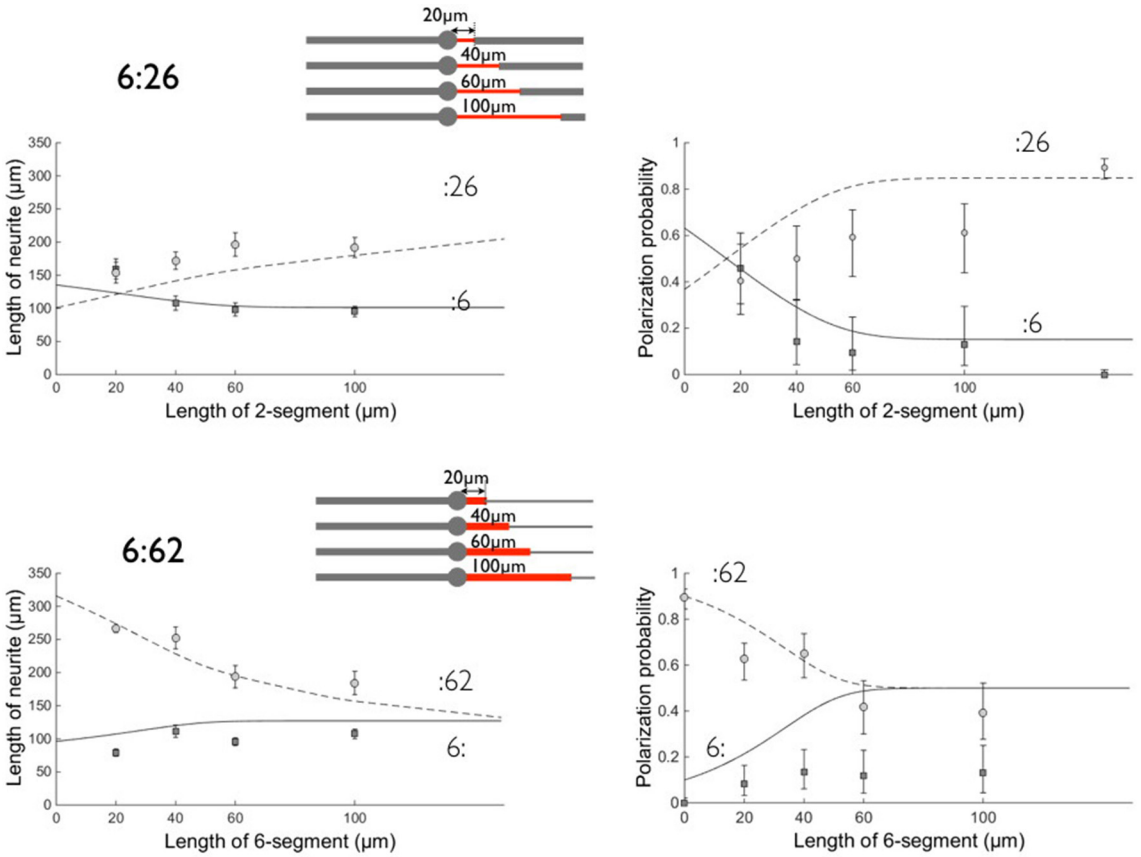

FIGURE 6 | Comparison between experimental data and the model on patterns 6:26 and 6:62. Left: neurite lengths, right: polarization probabilities. All results were obtained after 3 days of growth. Symbols denote the experimental data and lines the result of the model calculation (see **Figure 5**). Circles (dashed line) correspond to the :26 and :62 branches and squares (solid line) to the :6 opposite branch. Errors bars represent the standard error of the mean (length data) or 95% confidence interval (polarization data). Same values of fit parameters as in **Figure 5**. Polarization data obtained on 2:6 patterns are, as in **Figure 5**, located arbitrarily at a coordinate l = 150 µm in the 6:26 graph. The schemes of the patterns are shown for each set of geometries with the proximal stump of variable length in red.

axons convey roughly twice as many actin waves as dendrites (Fig. S5).

Combined with the relation $\gamma + \beta = 2$, this yields: $\gamma = \frac{2}{1+r} \approx 0.6$, $\beta = r\gamma \approx 1.4$.

Finally, we expect the dilution factor θ to be at most equal to the ratio $\frac{w_i}{w_f}$ of the widths before/after the transition region, as the material is delivered and spread over the leading edge that spans the stripe width. In our model, θ will remain a free fitted parameter. Similarly, the value of the parameter α that tunes the absolute value of neurite growth is also an adjustable parameter of the model.

Results of the Model

The data of Tomba et al. (2014) were used to challenge our new model. We used the above numbers deduced from the experiments of the present work. In addition, we let θ (i.e., the dilution/concentration factor of the wave material when the neurite width changes) and α (i.e., the width-independent coefficient regarding the amplitude of the tip net growth induced by an actin wave) as the only two free parameters. The comparison between the model and the experimental data is shown in **Figures 5**, **6**. Note that axons were identified through Tau-1 immunolabelling (see Fig. S6 for a few examples of stained neurons).

DISCUSSION

As previously, the model gives higher polarization probabilities than experiments, in particular when the Tau-1 labeling should be observed on 6 µm wide stripes. Following (Tomba et al., 2014), we associated this discrepancy with a possible impaired establishment of the Tau-1 gradient under this condition of unusual neurite spreading.

We found reasonable fits using $\theta = 2$ for the concentration factor when the waves move from 6 to 2 µm wide stripes (and $1/\theta$ for the dilution factor in the symmetric case). Although lower than expected from the ratio $\frac{w_i}{w_f} = 3$, this value lies in the range $1 < \theta < 3$, expressing the existence of an effective concentration/dilution effect according to our model. We also found $\alpha \sim 2.2$, i.e., a bare growth

velocity along the 2 μm stripe of 3 μm/h. This value $\alpha > 1$ supports the view that we probably have underestimated the values of λ_w by choosing an arbitrary time window over which to compare the net forward growth per waves on 2 and 6 μm wide stripes. This value of α might also reflect the fact that lengths were computed at 3 DIV in order to retrieve polarization data, i.e., at a stage in which actin waves might have a lower contribution to neuronal growth (Winans et al., 2016).

Notwithstanding the above question, however, we emphasize that with only two free parameters, our model consistently accounts for different sets of experiments using a variety of patterns. In addition, it successfully captures a qualitative feature of the experiments that was not covered by the previous model of Tomba et al. (2014), i.e., the crossing of the curves associated with the length and polarization probabilities of the two branches of the 2:62 and 6:26 patterns versus the length l of the proximal stump. For example we found that, for a 20 μm long 6 μm wide stump of the 2:62 patterns, the :62 branch was experimentally the longest one (i.e., longer than the :2 branch). From our present model, this situation arises from the association of three phenomena that boost the growth velocity of the −62 branch from the very beginning: (i) the 6 μm wide short segment delivers an actin wave with a high quantity of material, i.e. 2.4 times higher than delivered on the 2 μm wide branch; (ii) this material is further concentrated into the remaining 2 μm wide portion of the neurite, boosting its growth by a factor $\theta = 2$ and making it win the competition for polarization by reaching the critical length before the other (2 μm) branch; (iii) following its differentiation into an axon, the :62 branch undergoes an even faster growth. This advantage in favor of the :62 branch is lost for longer 6 μm wide portions, since the growth velocity is then dominated by the $\lambda_2\omega_2$ term during a time window long enough to allow the 2 μm wide branch to undergo axonal polarization. For the same reasons, the competition between the 6: and the :26 branches is biased in favor of the 6: branch, when the 2 μm wide stump is short: this is a consequence of the dominant role of the dilution effect at the :26 transition, combined with the lower amount of materials transported by actin waves in this configuration. Note that our model takes into account the effect of the proximal segment even if its length l goes to zero. The longitudinal extension of actin waves should impose a cut-off of the order of 10 μm (i.e., the longitudinal extension of an actin wave) below which our assumptions and model are no longer valid.

In addition, the same values of the modeling parameters (except for θ which was not needed anymore) were used to model the results obtained at 2 DIV on the 2-3-4 patterns built from 2 μm wide stripes (see also Fig. S2A for results regarding neurite length associated to 2-3-4 branches patterns). In these calculations, we assumed that the initiation rate per neurite is diminished by the factor 1/(number of branches), to account for the conservation of actin-wave initiating material at the soma. Fig. S7 shows a very reasonable fit of our experimental data, which constitutes an additional support for our description of the role of actin waves in neuronal growth.

Lastly, although the model presented in this work is based on the consequences of the initiation and propagation of actin waves and does not deal with the microscopic mechanisms behind these phenomena, we made a few observations that may feed a future mechanistic model of actin waves. In **Figures 3A,B** we observed, as did previous authors (Ruthel and Banker, 1999; Winans et al., 2016), that actin waves were pulling on the neurite tip. Due to the limited surface of adhesion provided to the soma by adhesive stripes, we also observed a nucleokinesis phenomenon associated with the propagation of actin waves. Actin waves seem therefore to behave like propagative contractile nodes exerting tension between the soma and the tip. This observation, and the contribution of actin waves in neurite elongation emphasized in the present work, echoes existing literature about the role of mechanical forces and neurite tension in neuronal growth (Zheng et al., 1991; Chada et al., 1997; Lamoureux et al., 2002). This suggests that, besides the supply of membrane and other materials provided by actin waves (Ruthel and Banker, 1999; Flynn et al., 2009; Toriyama et al., 2006), these structures also contribute to the generation of mechanical forces inside neurites. Indeed, we observed that poly-lysine functionalized polystyrene beads attached to the neurite membrane were systematically transported in retrograde fashion to the soma (data not shown). Such an observation was already reported in DRG neurons, and attributed to plasma membrane flow due to differential membrane tension between the growth cone and the soma (Dai and Sheetz, 1995). How this retrograde flow would be connected to the anterograde transport provided by actin waves and would contribute to build membrane tension is an exciting question that we hope will motivate further studies.

CONCLUSION

In this work, we provide a quantitative characterization of the generation of actin waves in different neuronal morphologies, efficiently modulated by the use of micropatterns of adhesion. We found that the rate of production of actin waves was independent on the number of neurites, suggesting that the material conveyed by actin waves is produced at the soma level. In addition, our finding that the rate of production of actin waves scales with the proximal neurite width might suggest that this material is stochastically distributed at the neurite base until it reaches the threshold required to build a propagative actin wave. Therefore, micropatterns of adhesion proved to be very fruitful to dissect and reveal the properties of actin waves in controlled conditions. In addition, they provided a valuable tool to test, on a large set of various neuronal morphologies, a model built using simple assumptions about the geometrical determinants of actin waves

We hope that these novel results regarding actin waves will contribute to their understanding and orient future molecular and biomechanical studies of these propagative structures.

AUTHOR CONTRIBUTIONS

CT and CV designed the experiments and analyzed the data. CT, CB, and FC did neuron cultures and time-lapse

experiments. GB contributed to the exploratory phase of experiments leading to this work. NG did the modeling and BF contributed to it. BF, NG, CT, and CV wrote the paper.

FUNDING

This work was supported in part by the European Research Council Advanced Grant No. 321107 "CellO," ANR Investissement d'Avenir, and the IPGG Labex and Equipex. N.S.G. is the incumbent of the Lee and William Abramowitz Professorial Chair of Biophysics.

ACKNOWLEDGMENTS

We thank Isabelle Grandjean and Manon Chartier from the Animal Facility of the Curie Institute for their support for mice. This work was performed in part in the Technological platform of Institute Pierre-Gilles de Gennes (UMS 3750) and in other part in the NanoFab facility of Institut Néel.

SUPPLEMENTARY MATERIAL

The Supplementary Material for this article can be found online at: http://journal.frontiersin.org/article/10.3389/fncel.2017.00086/full#supplementary-material

REFERENCES

Bernitt, E., Koh, C. G., Gov, N., and Döbereiner, H. G. (2015). Dynamics of actin waves on patterned substrates: a quantitative analysis of circular dorsal ruffles. *PLoS ONE* 10:e0115857. doi: 10.1371/journal.pone.0115857

Chada, S., Lamoureux, P., Buxbaum, R. E., and Heidemann, S. R. (1997). Cytomechanics of neurite outgrowth from chick brain neurons. *J. Cell Sci.* 110, 1179–1186.

Dai, J., and Sheetz, M. P. (1995). Axon membrane flows from the growth cone to the cell body. *Cell* 83, 693–701. doi: 10.1016/0092-8674(95)90182-5

Dotti, C. G., Sullivan, C. A., and Banker, G. A. (1988). The establishment of polarity by hippocampal neurons in culture. *J. Neurosci.* 8, 1454–1468.

Flynn, K. C., Pak, C. W., Shaw, A. E., Bradke, F., and Bamburg, J. R. (2009). Growth cone-like waves transport actin and promote axonogenesis and neurite branching. *Dev. Neurobiol.* 69, 761–779. doi: 10.1002/dneu.20734

Franze, K., and Guck, J. (2010). The biophysics of neuronal growth. *Rep. Prog. Phys.* 73:094601. doi: 10.1088/0034-4885/73/9/094601

Goicoechea, S., Arneman, D., Disanza, A., Garcia-Mata, R., Scita, G., and Otey, C. A. (2006). Palladin binds to Eps8 and enhances the formation of dorsal ruffles and podosomes in vascular smooth muscle cells. *J. Cell Sci.* 119, 3316–3324. doi: 10.1242/jcs.03076

Guetta-Terrier, C., Monzo, P., Zhu, J., Long, H., Venkatraman, L., Zhou, Y., et al. (2015). Protrusive waves guide 3D cell migration along nanofibers. *J. Cell Biol.* 211, 683–701. doi: 10.1083/jcb.201501106

Katsuno, H., Toriyama, M., Hosokawa, Y., Mizuno, K., Ikeda, K., Sakumura, Y., et al. (2015). Actin migration driven by directional assembly and disassembly of membrane-anchored actin filaments. *Cell Rep.* 12, 648–660. doi: 10.1016/j.celrep.2015.06.048

Lamoureux, P., Ruthel, G., Buxbaum, R. E., and Heidemann, S. R. (2002). Mechanical tension can specify axonal fate in hippocampal neurons. *J. Cell Biol.* 159, 499–508. doi: 10.1083/jcb.200207174

Ruthel, G., and Banker, G. (1998). Actin-dependent anterograde movement of growth-cone-like structures along growing hippocampal axons: a novel form of axonal transport? *Cell Motil. Cytoskeleton* 40, 160–173. doi: 10.1002/(SICI)1097-0169(1998)40:2<160::AID-CM5>3.0.CO;2-J

Ruthel, G., and Banker, G. (1999). Role of moving growth cone-like "wave" structures in the outgrowth of cultured hippocampal axons and dendrites. *J. Neurobiol.* 39, 97–106. doi: 10.1002/(SICI)1097-4695(199904)39:1<97::AID-NEU8>3.0.CO;2-Z

Seetapun, D., and Odde, D. J. (2010). Cell-length-dependent microtubule accumulation during polarization. *Curr. Biol.* 20, 979–988. doi: 10.1016/j.cub.2010.04.040

Sun, X., Driscoll, M. K., Guven, C., Das, S., Parent, C. A., Fourkas, J. T., et al. (2015). Asymmetric nanotopography biases cytoskeletal dynamics and promotes unidirectional cell guidance. *Proc. Natl. Acad. Sci. U.S.A.* 112, 12557–12562. doi: 10.1073/pnas.1502970112

Tilve, S., Difato, F., and Chieregatti, E. (2015). Cofilin 1 activation prevents the defects in axon elongation and guidance induced by extracellular alpha-synuclein. *Sci. Rep.* 5:16524. doi: 10.1038/srep16524

Tint, I., Jean, D., Baas, P. W., and Black, M. M. (2009). Doublecortin associates with microtubules preferentially in regions of the axon displaying actin-rich protrusive structures. *J. Neurosci.* 29, 10995–11010. doi: 10.1523/JNEUROSCI.3399-09.2009

Tomba, C., Braïni, C., Wu, B., Gov, N. S., and Villard, C. (2014). Tuning the adhesive geometry of neurons: length and polarity control. *Soft Matter* 10, 2381–2387. doi: 10.1039/c3sm52342j

Toriyama, M., Shimada, T., Kim, K. B., Mitsuba, M., Nomura, E., Katsuta, K., et al. (2006). Shootin1: a protein involved in the organization of an asymmetric signal for neuronal polarization. *J. Cell Biol.* 175, 47–157. doi: 10.1083/jcb.200604160

Winans, A. M., Collins, S. R., and Meyer, T. (2016). Waves of actin and microtubule polymerization drive microtubule-based transport and neurite growth before single axon formation. *Elife* 5:e12387. doi: 10.7554/elife.12387

Yamamoto, H., Demura, T., Morita, M., Banker, G. A., Tanii, T., and Nakamura, S. (2012). Differential neurite outgrowth is required for axon specification by cultured hippocampal neurons. *J. Neurochem.* 123, 904–910. doi: 10.1111/jnc.12001

Zheng, J., Lamoureux, P., Santiago, V., Dennerll, T., Buxbaum, R. E., and Heidemann, S. R. (1991). Tensile regulation of axonal elongation and initiation. *J. Neurosci.* 11, 1117–1125.

Conflict of Interest Statement: The authors declare that the research was conducted in the absence of any commercial or financial relationships that could be construed as a potential conflict of interest.

frontiers in Cellular Neuroscience

MINI REVIEW
published: 18 May 2017
doi: 10.3389/fncel.2017.00147

Dendritic Actin Cytoskeleton: Structure, Functions, and Regulations

*Anja Konietzny, Julia Bär and Marina Mikhaylova**

DFG Emmy Noether Group 'Neuronal Protein Transport,' Center for Molecular Neurobiology (ZMNH), University Medical Center Hamburg-Eppendorf, Hamburg, Germany

Actin is a versatile and ubiquitous cytoskeletal protein that plays a major role in both the establishment and the maintenance of neuronal polarity. For a long time, the most prominent roles that were attributed to actin in neurons were the movement of growth cones, polarized cargo sorting at the axon initial segment, and the dynamic plasticity of dendritic spines, since those compartments contain large accumulations of actin filaments (F-actin) that can be readily visualized using electron- and fluorescence microscopy. With the development of super-resolution microscopy in the past few years, previously unknown structures of the actin cytoskeleton have been uncovered: a periodic lattice consisting of actin and spectrin seems to pervade not only the whole axon, but also dendrites and even the necks of dendritic spines. Apart from that striking feature, patches of F-actin and deep actin filament bundles have been described along the lengths of neurites. So far, research has been focused on the specific roles of actin in the axon, while it is becoming more and more apparent that in the dendrite, actin is not only confined to dendritic spines, but serves many additional and important functions. In this review, we focus on recent developments regarding the role of actin in dendrite morphology, the regulation of actin dynamics by internal and external factors, and the role of F-actin in dendritic protein trafficking.

Keywords: dendrites, actin, cytoskeleton, protein trafficking, Arp2/3-complex, formin, cofilin

OPEN ACCESS

Edited by:
Annette Gaertner, Evotec, Germany

Reviewed by:
Pirta Elina Hotulainen, Minerva Foundation Institute for Medical Research, Finland
Elisa D'Este, Max Planck Institute, Germany

****Correspondence:***
Marina Mikhaylova, marina.mikhaylova@zmnh.uni-hamburg.de

Received: *28 February 2017*
Accepted: *05 May 2017*
Published: *18 May 2017*

Citation:
Konietzny A, Bär J and Mikhaylova M (2017) Dendritic Actin Cytoskeleton: Structure, Functions, and Regulations. Front. Cell. Neurosci. 11:147. doi: 10.3389/fncel.2017.00147

INTRODUCTION

The unique ability of neurons to compute and allocate information relies on their polarized morphology, which comprises several functionally distinct compartments. Dendrites are long, highly branched extensions from the cell body that can reach hundreds of microns, forming a widespread and complex arbor. They integrate information from typically thousands of synaptic inputs, which is then further transmitted via the cell body to the neuron's single axon (Magee, 2000; Gulledge et al., 2005). Dendrites can be morphologically and functionally sub-compartmentalized, particularly in pyramidal neurons (Shah et al., 2010; Yuan et al., 2015). One of the critical aspects in establishment and maintenance of the dendritic structure is the well-controlled turnover of cytoskeletal elements (Tsaneva-Atanasova et al., 2009). F-actin and microtubules (MTs) are the main mediators of neuronal polarity. Their organization is spatially and temporally controlled by numerous actin binding proteins (ABPs) and microtubule associated proteins, which extensively interact and feed back to each other (Georges et al., 2008; Coles and Bradke, 2015). The process of neuronal polarization is largely driven by an intrinsic program (Horton et al., 2006), however,

this program is subject to modification by diverse environmental stimuli, including synaptic activity, that can rapidly feed back to the cytoskeleton. In light of novel discoveries related to the role and organization of neuronal F-actin, in this review we will focus on the mechanisms and molecular players that fine-tune the actin cytoskeleton, thereby controlling dendrite morphology and function.

ORGANIZATION OF F-ACTIN IN DENDRITES

Actin filaments can be arranged in linear or in branched conformations, and together with stable MT arrays and neurofilaments they form the cytoskeleton in dendrites (Yuan et al., 2012; Sainath and Gallo, 2014). Perhaps the most striking F-actin-based structures in dendrites are so-called spines, small membranous protrusions that harbor synapses. F-actin arrangement within spines is very dynamic and is subject to constant activity-dependent remodeling (Okamoto et al., 2004). Apart from that, additional F-actin based structures within the shafts of dendrites have been discovered more recently: actin patches, longitudinal fibers, and rings (**Figures 1A,B**). **Actin patches** are areas of a few microns enriched in branched F-actin (Willig et al., 2014), and were suggested to serve as outgrowth points for filopodia (Korobova and Svitkina, 2010). **Longitudinal actin fibers** are long bundles of F-actin that traverse along the lengths of dendrites (D'Este et al., 2015; Bär et al., 2016). Their properties and functions are so far unexplored. **Actin rings**, originally described in axons (Xu et al., 2013), are periodic cortical actin structures that are also present in dendrites and in necks of dendritic spines (D'Este et al., 2015; Bär et al., 2016; He et al., 2016). According to the current model, this periodic lattice consists of several short and stable actin filaments, capped by α-adducin, and crosslinked by α/β-spectrin tetramers that define the spacing between the rings (Xu et al., 2013; Qu et al., 2016). These structures are thought to support neurite shape, help in organization of proteins along the plasma membrane (Xu et al., 2013), stabilize the underlying MT cytoskeleton (Qu et al., 2016) and could influence spine neck elasticity during transport of organelles (Bär et al., 2016).

REGULATION OF DENDRITIC ACTIN CYTOSKELETON

Controlling F-Actin Turnover: Actin Nucleation Factors, Severing and Capping Proteins

Like in any other cell, many functions of actin in neurons relate to its ability to polymerize and depolymerize in response to cellular signaling. Although not specifically studied in dendrites, numerous ABPs are known that cooperate in controlling the structure and stability of F-actin networks and their ability to shape cellular membranes. A summary can be found in **Table 1**, whereas in the text below we will focus on the mechanisms that may be particularly relevant in the regulation of dendritic F-actin.

As the rate-limiting step in actin polymerization, nucleation is a crucial point in regulating F-actin dynamics. Several actin nucleators, including the Arp2/3-complex, WASP-homology-2 (WH2) domain proteins and formin-homology (FH) proteins, facilitate this process. The **Arp2/3-complex** is the only known regulator for actin branching. It requires an existing actin filament, from which it nucleates a new filament branch (Smith et al., 2013). The Arp2/3-complex is activated by membrane-associated interactors, such as neuronal Wiskott–Aldrich Syndrome protein (N-WASP) or WASP-family verprolin-homologous protein (WAVE) (Korobova and Svitkina, 2010). Arp2/3-complex-dependent polymerization of branched actin networks generates widespread pushing forces against the plasma membrane, accounting for its prominent role in the maturation and enlargement of dendritic spines (Bosch et al., 2014; Spence et al., 2016). Another mechanism of activation involves the F-actin binding protein **cortactin**, which can bind and activate the Arp2/3-complex both directly and indirectly via N-WASP (Kowalski et al., 2005; Korobova and Svitkina, 2008). The Arp2/3-complex and cortactin are enriched in both axonal and dendritic growth cones of young hippocampal neurons (Strasser et al., 2004) and in dendritic spines of mature neurons (Hering and Sheng, 2003). While overexpression of Arp2/3-complex subunits or N-WASP affect both dendrite and axon development, a deficiency of those proteins induces excessive growth and branching exclusively of the axon (Strasser et al., 2004; Pinyol et al., 2007). Dendritic phenotypes seen at the later stages of development are mostly related to attenuated filopodia and spine formation (Spence et al., 2016). The precise molecular mechanisms behind such differential effects have yet to be elucidated (Sainath and Gallo, 2014). Still, it hints at a functional redundancy with other actin nucleators specific to dendrite development. Here, elaboration critically depends on the WH2-domain nucleator **Cobl** (Ahuja et al., 2007), which acts as a positive regulator of neurite outgrowth and branching in rat primary hippocampal neurons (Hou et al., 2015).

Formins are actin nucleators downstream of Rho-GTPases (Matusek et al., 2008; Kühn and Geyer, 2014). They nucleate unbranched actin filaments and are mainly associated with the outgrowth of filopodia (Hotulainen et al., 2009). Additionally, they play a role in coordinating MT functions, since they have a distinct MT bundling activity (Bartolini et al., 2008). Formins are involved in proper axon development (Matusek et al., 2008), and in the formation of a deep actin network within the axon, where actin filaments are nucleated from the surface of stationary endosomes in so-called "F-actin hotspots" (Ganguly et al., 2015). Whether the same mechanism is behind the formation of F-actin patches and longitudinal F-actin bundles that have been observed in dendrites (D'Este et al., 2015; Sidenstein et al., 2016) is unknown. Interestingly, another WH2-domain nucleator, **Spire** (Spir-1/2), directly interacts with the formins Fmn-1/2 (Pechlivanis et al., 2009). It was shown that in several non-neuronal cell types, those two proteins are recruited to recycling endosomes and cooperate in the nucleation of F-actin from the vesicle's surface (Schuh, 2011; Pylypenko et al., 2016). Whether

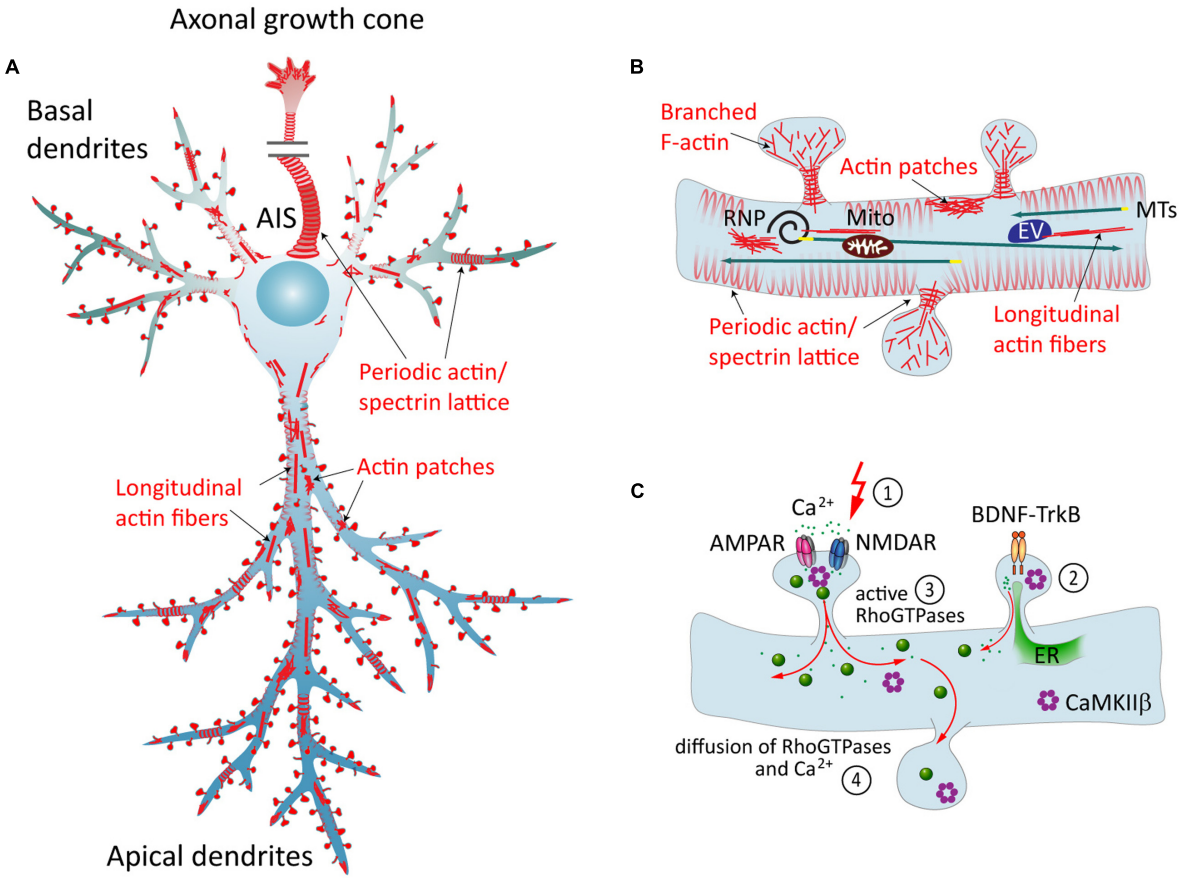

FIGURE 1 | The neuronal actin cytoskeleton and its regulation by external factors. (A) Overview of different actin structures present in pyramidal neurons: local F-actin enrichments called actin patches, longitudinal actin fibers, and a cortical periodic actin/spectrin lattice termed "actin rings" can be found throughout axon and in dendrites. **(B)** Dendritic spines contain branched F-actin in the head, and straight bundles as well as a periodic actin lattice in the neck. Directed transport of cargo from the soma to the dendrite is carried out via MTs, and can then be subjected to activity-dependent positioning at the base of activated spines in an F-actin and myosin-dependent manner. EV = endosomal vesicle, RNP = ribonucleoprotein, Mito = mitochondrium. **(C)** Dynamics of the dendritic actin cytoskeleton are influenced by external cues. Those include the transduction of external signals to the actin cytoskeleton via cell-surface receptors that couple to Rho-GEFs or ABPs, and Ca^{2+} signaling. The latter involves Ca^{2+} influx through glutamate receptors following synaptic stimulation (1), and Ca^{2+} release from internal stores, triggered for instance by BDNF-TrkB-signaling (2). Both pathways include the activation of Rho-GTPases (3), which act as "molecular switches" that govern a multitude of cellular functions. Diffusible factors, like Ca^{2+}, Rho-GTPases, CaMKIIβ and other downstream effectors, can spread the signal from their activation site to the dendrite and to other spines (4). ER = endoplasmatic reticulum.

this mechanism is active in neurons has not been investigated so far. However, since the expression patterns of Spire1 and Fmn-2 markedly overlap in the mouse brain (Schumacher et al., 2004), the existence of such a mechanism in neurons seems plausible.

F-actin turnover is greatly accelerated by filament severing proteins, like the closely related **ADF** and **cofilin-1** (Sarmiere and Bamburg, 2004). They increase the number of uncapped ends that may undergo polymerization and regulate the G/F-actin pool (Andrianantoandro and Pollard, 2006). Binding of ADF/cofilin to F-actin additionally induces a conformational change, which can affect binding of other ABPs (Ngo et al., 2016). The activity of ADF/cofilin is tightly regulated via several mechanisms, including phosphorylation (CaMKII, LIMK) and dephosphorylation (calcineurin, slingshot). For a detailed review on ADF/cofilin, see (Kanellos and Frame, 2016). Of note, cofilin-1 activity is instrumental for the dynamic plasticity of dendritic spines (Noguchi et al., 2016), and it is possible that activated cofilin-1 could spread out from a single activated spine to drive re-organization of F-actin in associated dendritic compartments.

Extracellular Factors Controlling Actin Dynamics in Dendrites

There is a vast number of studies addressing the role of **cell adhesion molecules** (CAMs) and extracellular guidance cues in neuronal cell migration, axon pathfinding, axon-dendrite contact formation and dendritic spine plasticity (Togashi et al., 2009), whereas their role in dendritogenesis has been somewhat overlooked. Those cell surface receptors associate directly with ABPs, thereby translating environmental cues into local changes in actin dynamics (Leshchyns'ka and Sytnyk, 2016).

Neural CAM1 (**NCAM1**) has been extensively studied for its role in neuronal development (Li et al., 2013; Leshchyns'ka and

TABLE 1 | Actin binding proteins in neurons and their cross-talk with MTs.

Protein group	Function in neurons	Binding partners	Reference
Actin monomer (G-actin) binding			
β-Thymosin	G-actin "buffer," blocks all known assembly reactions but with a high on/off rate		Yarmola and Bubb, 2004
Profilin	Actin nucleotide exchange factor; maintains G/F-actin ratio together with capping proteins	ROCK, Formin, VASP, WAVE, WASP, Drebrin	Witke et al., 1998; Da Silva et al., 2003
CAP	*Cyclase associated protein*; actin nucleotide exchange factor; sequesters G-actin and severs F-actin; role in growth cone and dendrite development	Profilin, Abp1, Abl, Ras, Cofilin	Ono, 2013; Kumar et al., 2016
Nucleators			
Arp2/3-complex	F-actin branching in lamellipodia growth cones, and spine heads	WASP, WAVE, Cortactin	Korobova and Svitkina, 2008; Hotulainen et al., 2009
Formins	Filament nucleation in filopodia, growth cones and along axon; synergize with other actin nucleators	Rho, Rac, Cdc42, Spire, APC	Matusek et al., 2008; Ganguly et al., 2015
Cobl	Role in dendrite branching and growth cones	CaM, Syndapin-1	Ahuja et al., 2007
Spire	Dendrite arborization in *Drosophila* sensory neurons; cooperates with formin-1/2; Myosin V recruitment	Formin-1/2, Myosin Vb	Ferreira et al., 2014; Pylypenko et al., 2016
Elongation-promoting factors			
Ena/VASP	Accelerate elongation and prevent capping; role in filopodia formation and neurite elaboration	WAVE, Profilin	Dent et al., 2007; Kwiatkowski et al., 2007; Chen et al., 2014
Barbed end capping			
CapZ	Maintains G/F actin ratio together with profilin; role in neurite elaboration		Davis et al., 2009
Adducin	Promotes F-actin bundling and spectrin binding; component of actin rings	Spectrin	Leite et al., 2016
Pointed end capping			
Tropomodulins	Stabilize F-actin and decelerate actin dynamics; associated with growth cones	Tropomyosins	Cox et al., 2003; Schevzov et al., 2012
Crosslinkers/Bundling			
Fimbrin	Axiogenesis	Spectrin	Oprea et al., 2008
Spectrin	Couples F-actin cytoskeleton to plasma membrane; component of actin rings	Adducin, Fimbrin, α-Actinin	Bennett and Baines, 2001; Xu et al., 2013
α-Actinin	Calcium sensitive; role in dendrite elaboration and branching		Hodges et al., 2014
Severing			
ADF/cofilin	Bind and sever F-actin, enhance depolymerization; role in spines and LTP; bind G-actin and enhance nucleation	CaMKII, LIMK, Calcineurin, Slingshot, CAP	Meyer and Feldman, 2002; Andrianantoandro and Pollard, 2006
Gelsolin	Severs F-actin, directly activated by Ca^{2+}; role in growth cone and spines	Ca^{2+}	Furukawa et al., 1997; Star et al., 2002
Stabilizing			
Cortactin	Stabilization of F-actin; activation of Arp2/3; in filopodia and growth cones	Arp2/3, WASP	Kowalski et al., 2005; Korobova and Svitkina, 2008
Abp1	Associates with newly formed, dynamic F-actin; concentrated at subcortical post-synaptic scaffold	Arp2/3, WASP, Cobl	Kessels et al., 2000; Pinyol et al., 2007
Drebrin	Stabilizes actin, competitively inhibits binding of tropomyosins, myosins, fascin and other ABPs; recruits MT into growth cones and dendritic spines	EB3	Geraldo et al., 2008; Merriam et al., 2013
Tropomyosin	Bind along actin filaments; role in dendrite elaboration; effect depends on interaction with other ABPs		Schevzov et al., 2005; Tojkander et al., 2011; Curthoys et al., 2014
Actin-MT crosslinkers			
MAP1/2	Ability to crosslink microtubules with F-actin; formation and stabilization of neurites		Roger et al., 2004; Szebenyi et al., 2005

(Continued)

TABLE 1 | Continued

Protein group	Function in neurons	Binding partners	Reference
MACF1	*MT-actin crosslinking factor 1,* also known as *ACF7, Shortstop,* and *kakapo;* Role in dendrite branching		Sun et al., 2001; Applewhite et al., 2010
EB3	MT plus-end tracking protein (+TIP); can simultaneously link to actin via drebrin; role during neuritogenesis	Drebrin	Geraldo et al., 2008
APC	*Adenomatous polyposis coli protein*; possesses actin nucleation activity and might crosslink to MT via the +TIP IQGAP	IQGAP, mDia	Watanabe et al., 2004; Okada et al., 2010
Formins	Simultaneous actin- and MT-binding activity; might also crosslink actin and MT via APC:IQGAP	APC	Bartolini et al., 2008; Breitsprecher et al., 2012
CTTNBP2	*Cortactin-binding protein 2,* neuron-specific, possible interactor between cortactin and microtubules	Cortactin	Shih et al., 2014
CLIP170	*EB3-associated +TIP*; might link MT to actin via IQGAP	IQGAP	Swiech et al., 2011
P140Cap	*EB3-associated +TIP*; might link MT to actin via cortactin	Cortactin	Jaworski et al., 2009
Abl	*Ableson-family of non-receptor tyrosine kinases*; bind both actin and MT; activate WAVE complex	WAVE, Ena/VASP	Moresco, 2005; Colicelli, 2010
Motor proteins			
Myosin II; with light chains RLC and ELC	Network contraction; F-actin shearing; remodeling of actin network in growth cones and in spines undergoing LTP	MLCK, ROCK, MLCP	Medeiros et al., 2006; Rex et al., 2010; Koskinen et al., 2014

Sytnyk, 2016). It was shown recently that the isoform NCAM180 is highly enriched at dendritic growth cones in rat primary hippocampal neurons during dendritogenesis (Frese et al., 2017). Knockdown of NCAM1 led to reduced dendrite lengths, most likely due to absence of NCAM1-mediated actin stabilization, since many different ABPs were found to be associated with its intracellular domain (Pollerberg et al., 2013; Frese et al., 2017). These results suggest a novel role of NCAM180 in dendritic arborization. Of note, other NCAM family proteins have also been reported to be involved in dendritic branching and morphology in *C. elegans* (Dong et al., 2013).

Integrins are another type of surface receptors in direct contact with the actin cytoskeleton. They interact with components of the extracellular matrix (ECM) and affect actin dynamics through associated **Abl-family tyrosine kinases**, of which **Arg** is particularly abundant in the nervous system and localizes to dendritic spines (Lin et al., 2013). Arg controls both dendritic spine and dendrite arbor stability through distinct pathways: it promotes binding of cortactin to F-actin to stabilize spines (MacGrath and Koleske, 2012), and attenuates Rho activity to stabilize dendrite arbors (Moresco, 2005; Lin et al., 2013).

An important feature of mature neurons is dendrite compartmentalization, for example the distinction between apical and basal dendrites, or between proximal and distal regions of apical dendrites. Those compartments are characterized by the expression of specific sets of ion channels (Ginger et al., 2013). Little is known about the mechanisms behind this distinction, however, several studies demonstrated that the large secreted matrix glycoprotein **Reelin** influences positioning of the Golgi apparatus toward the future apical dendrite (Leemhuis and Bock, 2011; Meseke et al., 2013), and that it is required for establishing and maintaining the molecular identity of the distal dendritic compartment of pyramidal neurons (Kupferman et al., 2014). Reelin signals through lipoprotein-receptors, activating both the GSK3β- and PI3K-Rho-GTPase-pathways, which influence the MT and actin cytoskeleton, respectively (González-Billault et al., 2005; Leemhuis and Bock, 2011). Additionally, Reelin-signaling was found to inactivate ADF/cofilin via LIMK, thereby stabilizing F-actin (Chai et al., 2009, 2016).

Role of Synaptic Activity in Shaping the Dendritic Actin Cytoskeleton

Apart from direct contact with the ECM and neighboring cells, another important factor for dendrite survival and stabilization is synaptic input (Niell et al., 2004). Increased calcium influx via glutamate receptors and L-type Ca^{2+}-channels at excitatory synapses stabilizes dendritic branches (Lohmann et al., 2002). In addition, neurotrophic signaling via brain-derived neurotrophic factor (BDNF) modulates calcium signaling. Activation of the TrkB receptor by BDNF triggers multiple downstream pathways, which promote synaptic potentiation but also dendrite growth and stabilization (Horch and Katz, 2002; Wang et al., 2015). The downstream signaling is mediated by the activation of Rac1-GTPase and MAP-kinases, which influence both the actin and microtubule cytoskeleton, and of PLC-γ and PI3-kinase, which trigger the release of calcium from the endoplasmic reticulum (ER) (*reviewed in* Huang and Reichardt, 2003).

Although most of the Ca^{2+}-dependent effects have been described in spines, Ca^{2+} diffuses from activated spines and thus can activate dendritic targets (**Figure 1C**). Cytoplasmic Ca^{2+}-signaling is largely transduced via the ubiquitous Ca^{2+}-sensor calmodulin (CaM), which rapidly activates CaM-kinases and calcineurin (Ca^{2+}/CaM-dependent phosphatase). **CaMKII**, at the center of many signaling cascades, regulates formation, growth, and branching of dendrites locally via **Rho-GTPases,** which modulate cytoskeleton turnover, and globally via activation of transcription factors (*reviewed in* Redmond and Ghosh, 2005). Apart from this, CaMKIIβ possesses an F-actin binding

ability, enabling the dodecameric holoenzyme to cross-link and stabilize actin networks (Lin and Redmond, 2008; Na et al., 2016). Activated CaMKII is then released from F-actin, which constitutes one of the many ways to link Ca^{2+}-signaling to the regulation of the actin cytoskeleton. Several other ABPs are known to be directly influenced by CaM/Ca^{2+}, including spectrins and actinin, ADF/cofilin and gelsolin (Oertner and Matus, 2005) and Cobl (Hou et al., 2015). However, there may still be additional, so far unidentified calcium sensors that directly couple Ca^{2+}-signaling to actin dynamics.

Numerous ABPs are further indirectly activated downstream of CaM/Ca^{2+} and CaMKII via Rho-GTPases (Boekhoorn and Hoogenraad, 2013). Three well-studied Rho-GTPases that drive cytoskeleton-mediated dendrite morphogenesis are **RhoA, Rac1** and **Cdc42** (Negishi and Katoh, 2002). It was shown that during potentiation of synaptic spines, Rho-GTPases get activated and can then diffuse along the membrane into the dendrite and neighboring spines (Murakoshi et al., 2011). While this kind of "spillover" has been suggested to play a role in clustering of activated synaptic inputs (*discussed in* van Bommel and Mikhaylova, 2016), continued signaling within the dendritic shaft might as well be involved in activity-dependent stabilization of the whole dendrite (**Figure 1C**).

Rho-GTPases activate a myriad of both intertwining and antagonistic pathways that signal to the actin and microtubule cytoskeleton, their effectors including kinases, formins, MAPs, WASP-family proteins and other ABPs. For a detailed review on Rho-GTPases and their role in organizing the actin cytoskeleton, see (Sit and Manser, 2011).

F-ACTIN IN TRANSPORTING AND LOCALIZATION OF CARGO WITHIN DENDRITES

Maintenance of the polarized dendrite morphology does not only depend on the cytoskeletal scaffold, but also on the constant supply of membrane components and dendrite-specific cargo (Hanus and Ehlers, 2016). Long-range intra-dendritic cargo transport is typically carried out via MTs and associated motors. However, actin and actin-dependent motors (myosins) have been shown to mediate the transport and/or anchoring of certain cargos, which include mRNA, translational machinery and mitochondria (Ligon and Steward, 2000; *reviewed in* Martin and Ephrussi, 2010).

For transport, **mRNA** is packaged into ribonucleoprotein particles (RNPs) containing specific targeting factors, and is delivered from the soma to the dendrite via MTs. Some RNPs are targeted to spines in an activity-dependent manner, which requires the presence of F-actin (Huang et al., 2007; Yoon et al., 2016). Likewise, myosin Va (MyoVa) was shown to facilitate the accumulation of RNPs in spines (Yoshimura et al., 2006). As a general model, activity-dependent targeting of cargo to activated synapses has been proposed to involve myosins located at the spine neck, which take up cargo that has been unloaded from passing MT-motors in a Ca^{2+}-dependent manner (Hanus et al., 2014). Similarly, it has been shown that dendritic mitochondria show activity-induced movement toward dendritic spines in dissociated neurons. This process likely involves Arp2/3-complex-mediated actin polymerization via mitochondria-associated WAVE1 (Sung et al., 2008). It has been speculated that this mechanism might ensure the local energy supply at sites of activity. However, in dendrites within intact tissues, mitochondria are mainly immobile and localize stably to synapses and branch points (Faits et al., 2016), so the *in vivo* role of this observation is uncertain. In this context, the possibility that actin rings could serve as cargo-docking sites has been brought up, which would allow precise control of mitochondria localization (Gallo, 2013). Supporting this, the speed of axonal mitochondria transport decreased in an α-adducin knockout background, which affects the integrity of actin rings (Leite et al., 2016), and in axons of *Drosophila* neurons, knockdown of MyoV and MyoVI impacts mitochondria transport (Pathak et al., 2010).

Within the actin-rich environment of dendritic spines, myosin motors are known to play an important role in the transport of vesicular cargo (Osterweil et al., 2005; Wang et al., 2008). In cerebellar Purkinje neurons, MyoVa acts as a processive organelle transporter that moves the ER into dendritic spines, which is required for long-term synaptic depression (Wagner et al., 2011). Whether this motor is also involved in the more dynamic spine-localization of ER in other types of neurons, just like the role of myosins in transport and anchoring of dendritic organelles in general, still remains to be explored.

CONCLUDING REMARKS

Our current knowledge of the organization, polarity, and dynamics of actin along dendritic shafts is very incomplete, although the recent development of super-resolution microscopy has provided us with additional tools to study the architecture of the actin cytoskeleton in greater detail. So far, it has led to the discovery of a periodic actin lattice along the lengths of neurites, as well as actin patches and deep actin filaments, whose function and properties are still unexplored. Particularly because of the high degree of conservation among species, it would be interesting to learn more about the mechanisms and nucleation factors involved in formation and regulation of these structures.

Synaptic input and cell contacts play a critical role in the stabilization of dendrites. All of those inputs converge to finally modulate cytoskeleton dynamics, with the main effectors being MTs and F-actin. Thanks to extensive research efforts, a myriad of intertwining pathways and molecular cascades that signal to the cytoskeleton have been described. However, how a given input might lead to an observed output in such a complicated multi-factor system is often hard to reconstruct in detail. Therefore, our understanding of how those different pathways are coordinated and integrated within the cell would greatly benefit from a concerted *in silico* modeling approach. A special interest lies on the question how and to what extent the wealth of described signaling factors that modulate F-actin dynamics within dendritic spines can extend their signaling into dendritic shafts, as a

diffusional activity has for example been described for Rho-GTPases and cofilin.

A lot of research regarding mechanisms shaping neuronal actin networks, including their modulation by intrinsic and extrinsic signaling, has been focused on the axon, and here it is important to test whether the identified mechanisms and pathways of F-actin remodeling are applicable to dendrites as well. For example, it will be important to investigate whether dendritic F-actin patches, which at first glance appear to share a similar structure with axonal F-actin "hotspots," actually originate from stationary endosomes as well, or whether they constitute their own unique features. For now, we conclude that in analogy to the axon, the dendritic actin cytoskeleton might play a two-fold role: stable, cortical actin rings provide mechanical support, while dynamic, underlying filaments sustain physiological processes related to dendritic and synaptic plasticity.

AUTHOR CONTRIBUTIONS

AK, JB, and MM wrote the manuscript and all authors commented on the final version.

FUNDING

This work was supported by grants from the Deutsche Forschungsgemeinschaft (DFG Emmy-Noether Programm (Ml 1923/1-1) and FOR2419 (MI 1923/2-1).

REFERENCES

Ahuja, R., Pinyol, R., Reichenbach, N., Custer, L., Klingensmith, J., Kessels, M. M., et al. (2007). Cordon-bleu is an actin nucleation factor and controls neuronal morphology. *Cell* 131, 337–350. doi: 10.1016/j.cell.2007.08.030

Andrianantoandro, E., and Pollard, T. D. (2006). Mechanism of actin filament turnover by severing and nucleation at different concentrations of ADF/Cofilin. *Mol. Cell* 24, 13–23. doi: 10.1016/j.molcel.2006.08.006

Applewhite, D. A., Grode, K. D., Keller, D., Zadeh, A., Slep, K. C., and Rogers, S. L. (2010). The spectraplakin short stop is an actin–microtubule cross-linker that contributes to organization of the microtubule network. *Mol. Biol. Cell* 21, 1714–1724. doi: 10.1091/mbc.E10-01-0011

Bär, J., Kobler, O., van Bommel, B., and Mikhaylova, M. (2016). Periodic F-actin structures shape the neck of dendritic spines. *Sci. Rep.* 6:37136. doi: 10.1038/srep37136

Bartolini, F., Moseley, J. B., Schmoranzer, J., Cassimeris, L., Goode, B. L., and Gundersen, G. G. (2008). The formin mDia2 stabilizes microtubules independently of its actin nucleation activity. *J. Cell Biol.* 181, 523–536. doi: 10.1083/jcb.200709029

Bennett, V., and Baines, A. J. (2001). Spectrin and ankyrin-based pathways: metazoan inventions for integrating cells into tissues. *Physiol. Rev.* 81, 1353–1392.

Boekhoorn, K., and Hoogenraad, C. C. (2013). Regulation of AMPA-type glutamate receptor trafficking. *Cell. Migr. Form. Neuronal Connect.* 2, 811–822.

Bosch, M., Castro, J., Saneyoshi, T., Matsuno, H., Sur, M., and Hayashi, Y. (2014). Structural and molecular remodeling of dendritic spine substructures during long-term potentiation. *Neuron* 82, 444–459. doi: 10.1016/j.neuron.2014.03.021

Breitsprecher, D., Jaiswal, R., Bombardier, J. P., Gould, C. J., Gelles, J., and Goode, B. L. (2012). Rocket launcher mechanism of collaborative actin assembly defined by single-molecule imaging. *Science* 336, 1164–1168. doi: 10.1126/science.1218062

Chai, X., Fo, E., Zhao, S., Bock, H. H., and Frotscher, M. (2009). Reelin stabilizes the actin cytoskeleton of neuronal processes by inducing n-cofilin phosphorylation at serine3. *J. Neurosci.* 29, 288–299. doi: 10.1523/JNEUROSCI.2934-08.2009

Chai, X., Zhao, S., Fan, L., Zhang, W., Lu, X., Shao, H., et al. (2016). Reelin and cofilin cooperate during the migration of cortical neurons: a quantitative morphological analysis. *Development* 1, 1029–1040. doi: 10.1242/dev.134163

Chen, X. J., Squarr, A. J., Stephan, R., Chen, B., Higgins, T. E., Barry, D. J., et al. (2014). Ena/VASP proteins cooperate with the WAVE complex to regulate the actin cytoskeleton. *Dev. Cell* 30, 569–584. doi: 10.1016/j.devcel.2014.08.001

Coles, C. H., and Bradke, F. (2015). Coordinating neuronal actin-microtubule dynamics. *Curr. Biol.* 25, R677–R691. doi: 10.1016/j.cub.2015.06.020

Colicelli, J. (2010). ABL tyrosine kinases: evolution of function, regulation, and specificity. *Sci. Signal.* 3:re6. doi: 10.1126/scisignal.3139re6

Cox, P. R., Fowler, V., Xu, B., Sweatt, J. D., Paylor, R., and Zoghbi, H. Y. (2003). Mice lacking tropomodulin-2 show enhanced long-term potentiation, hyperactivity, and deficits in learning and memory. *Mol. Cell. Neurosci.* 23, 1–12.

Curthoys, N. M., Freittag, H., Connor, A., Desouza, M., Brettle, M., Poljak, A., et al. (2014). Tropomyosins induce neuritogenesis and determine neurite branching patterns in B35 neuroblastoma cells. *Mol. Cell. Neurosci.* 58, 11–21. doi: 10.1016/j.mcn.2013.10.011

Da Silva, J. S., Medina, M., Zuliani, C., Di Nardo, A., Witke, W., and Dotti, C. G. (2003). RhoA/ROCK regulation of neuritogenesis via profilin IIa-mediated control of actin stability. *J. Cell Biol.* 162, 1267–1279. doi: 10.1083/jcb.200304021

Davis, D. A., Wilson, M. H., Giraud, J., Xie, Z., Tseng, H. C., England, C., et al. (2009). Capzb2 interacts with β-tubulin to regulate growth cone morphology and neurite outgrowth. *PLoS Biol.* 7:e1000208. doi: 10.1371/journal.pbio.1000208

Dent, E. W., Kwiatkowski, A. V., Mebane, L. M., Philippar, U., Barzik, M., Rubinson, D. A., et al. (2007). Filopodia are required for cortical neurite initiation. *Nat. Cell Biol.* 9, 1347–1359. doi: 10.1038/ncb1654

D'Este, E., Kamin, D., Göttfert, F., El-Hady, A., and Hell, S. (2015). STED nanoscopy reveals the ubiquity of subcortical cytoskeleton periodicity in living neurons. *Cell Rep.* 10, 1246–1251. doi: 10.1016/j.celrep.2015.02.007

Dong, X., Liu, O. W., Howell, A. S., and Shen, K. (2013). An extracellular adhesion molecule complex patterns dendritic branching and morphogenesis. *Cell* 155, 296–307. doi: 10.1016/j.cell.2013.08.059

Faits, M. C., Zhang, C., Soto, F., and Kerschensteiner, D. (2016). Dendritic mitochondria reach stable positions during circuit development. *Elife* 5:e11583.. doi: 10.7554/eLife.11583

Ferreira, T. A., Ou, Y., Li, S., Giniger, E., and van Meyel, D. J. (2014). Dendrite architecture organized by transcriptional control of the F-actin nucleator Spire. *Development* 141, 650–660. doi: 10.1242/dev.099655

Frese, C. K., Mikhaylova, M., Stucchi, R., Gautier, V., Liu, Q., Mohammed, S., et al. (2017). Quantitative map of proteome dynamics during neuronal differentiation. *Cell Rep.* 18, 1527–1542. doi: 10.1016/j.celrep.2017.01.025

Furukawa, K., Fu, W., Li, Y., Witke, W., Kwiatkowski, D. J., and Mattson, M. P. (1997). The actin-severing protein gelsolin modulates calcium channel and NMDA receptor activities and vulnerability to excitotoxicity in hippocampal neurons. *J. Neurosci.* 17, 8178–8186.

Gallo, G. (2013). More than one ring to bind them all: recent insights into the structure of the axon. *Dev. Neurobiol.* 73, 799–805. doi: 10.1002/dneu.22100

Ganguly, A., Tang, Y., Wang, L., Ladt, K., Loi, J., Dargent, B., et al. (2015). A dynamic formin-dependent deep F-actin network in axons. *J. Cell Biol.* 210, 401–417. doi: 10.1083/jcb.201506110

Georges, P. C., Hadzimichalis, N. M., Sweet, E. S., and Firestein, B. L. (2008). The yin-yang of dendrite morphology: unity of actin and microtubules. *Mol. Neurobiol.* 38, 270–284. doi: 10.1007/s12035-008-8046-8

Geraldo, S., Khanzada, U. K., Parsons, M., Chilton, J. K., and Gordon-Weeks, P. R. (2008). Targeting of the F-actin-binding protein drebrin by the microtubule plus-tip protein EB3 is required for neuritogenesis. *Nat. Cell Biol.* 10, 1181–1189. doi: 10.1038/ncb1778

Ginger, M., Broser, P., and Frick, A. (2013). Three-dimensional tracking and analysis of ion channel signals across dendritic arbors. *Front. Neural Circuits* 7:61. doi: 10.3389/fncir.2013.00061

González-Billault, C., Del Río, J. A., Ureña, J. M., Jiménez-Mateos, E. M., Barallobre, M. J., Pascual, M., et al. (2005). A role of MAP1B in reelin-dependent neuronal migration. *Cereb. Cortex* 15, 1134–1145. doi: 10.1093/cercor/bhh213

Gulledge, A. T., Kampa, B. M., and Stuart, G. J. (2005). Synaptic integration in dendritic trees. *J. Neurobiol.* 64, 75–90. doi: 10.1002/neu.20144

Hanus, C., and Ehlers, M. D. (2016). Specialization of biosynthetic membrane trafficking for neuronal form and function. *Curr. Opin. Neurobiol.* 39, 8–16. doi: 10.1016/j.conb.2016.03.004

Hanus, C., Kochen, L., Tom Dieck, S., Racine, V., Sibarita, J. B., Schuman, E. M., et al. (2014). Synaptic control of secretory trafficking in dendrites. *Cell Rep.* 7, 1771–1778. doi: 10.1016/j.celrep.2014.05.028

He, J., Zhou, R., Wu, Z., Carrasco, M. A., Kurshan, P. T., Farley, J. E., et al. (2016). Prevalent presence of periodic actin-spectrin-based membrane skeleton in a broad range of neuronal cell types and animal species. *Proc. Natl. Acad. Sci. U.S.A.* 113, 6029–6034. doi: 10.1073/pnas.1605707113

Hering, H., and Sheng, M. (2003). Activity-dependent redistribution and essential role of cortactin in dendritic spine morphogenesis. *J. Neurosci.* 23, 11759–11769.

Hodges, J. L., Vilchez, S. M., Asmussen, H., Whitmore, L. A., and Horwitz, A. R. (2014). α-Actinin-2 mediates spine morphology and assembly of the post-synaptic density in hippocampal neurons. *PLoS ONE* 9:e101770. doi: 10.1371/journal.pone.0101770

Horch, H. W., and Katz, L. C. (2002). BDNF release from single cells elicits local dendritic growth in nearby neurons. *Nat. Neurosci.* 5, 1177–1184. doi: 10.1038/nn927

Horton, A. C., Yi, J. J., and Ehlers, M. D. (2006). Cell type-specific dendritic polarity in the absence of spatially organized external cues. *Brain Cell Biol.* 35, 29–38. doi: 10.1007/s11068-006-9003-y

Hotulainen, P., Llano, O., Smirnov, S., Tanhuanpää, K., Faix, J., Rivera, C., et al. (2009). Defining mechanisms of actin polymerization and depolymerization during Dendritic spine morphogenesis. *J. Cell Biol.* 185, 323–339. doi: 10.1083/jcb.200809046

Hou, W., Izadi, M., Nemitz, S., Haag, N., Kessels, M. M., and Qualmann, B. (2015). The actin nucleator cobl is controlled by calcium and calmodulin. *PLoS Biol.* 13:e1002233. doi: 10.1371/journal.pbio.1002233

Huang, E. J., and Reichardt, L. F. (2003). Trk receptors: roles in neuronal signal transduction. *Annu. Rev. Biochem.* 72, 609–642. doi: 10.1146/annurev.arplant.53.091401.143329

Huang, F., Chotiner, J. K., and Steward, O. (2007). Actin polymerization and ERK phosphorylation are required for Arc/Arg3.1 mRNA targeting to activated synaptic sites on dendrites. *J. Neurosci.* 27, 9054–9067. doi: 10.1523/JNEUROSCI.2410-07.2007

Jaworski, J., Kapitein, L. C., Gouveia, S. M., Dortland, B. R., Wulf, P. S., Grigoriev, I., et al. (2009). Dynamic microtubules regulate dendritic spine morphology and synaptic plasticity. *Neuron* 61, 85–100. doi: 10.1016/j.neuron.2008.11.013

Kanellos, G., and Frame, M. C. (2016). Cellular functions of the ADF/cofilin family at a glance. *J. Cell Sci.* 129, 3211–3218. doi: 10.1242/jcs.187849

Kessels, M. M., Engqvist-Goldstein, Å. E. Y., and Drubin, D. G. (2000). Association of mouse actin-binding protein 1 (mAbp1/SH3P7), an Src kinase target, with dynamic regions of the cortical actin cytoskeleton in response to Rac1 activation. *Mol. Biol. Cell* 11, 393–412. doi: 10.1091/mbc.11.1.393

Korobova, F., and Svitkina, T. (2008). Arp2/3 complex is important for filopodia formation, growth cone motility, and neuritogenesis in neuronal cells. *Mol. Biol. Cell* 19, 1516–1574. doi: 10.1091/mbc.E07-09-0964

Korobova, F., and Svitkina, T. (2010). Molecular architecture of synaptic actin cytoskeleton in hippocampal neurons reveals a mechanism of dendritic spine morphogenesis. *Mol. Biol. Cell* 21, 165–176. doi: 10.1091/mbc.E09

Koskinen, M., Bertling, E., Hotulainen, R., Tanhuanpää, K., and Hotulainen, P. (2014). Myosin IIb controls actin dynamics underlying the dendritic spine maturation. *Mol. Cell. Neurosci.* 61, 56–64. doi: 10.1016/j.mcn.2014.05.008

Kowalski, J. R., Egile, C., Gil, S., Snapper, S. B., Li, R., and Thomas, S. M. (2005). Cortactin regulates cell migration through activation of N-WASP. *J. Cell Sci.* 118, 79–87. doi: 10.1242/jcs.01586

Kühn, S., and Geyer, M. (2014). Formins as effector proteins of Rho GTPases. *Small GTPases* 5:e29513. doi: 10.4161/sgtp.29513

Kumar, A., Paeger, L., Kosmas, K., Kloppenburg, P., Noegel, A. A., and Peche, V. S. (2016). Neuronal actin dynamics. Spine density and neuronal dendritic complexity are regulated by CAP2. *Front. Cell. Neurosci.* 10:180. doi: 10.3389/fncel.2016.00180

Kupferman, J. V., Basu, J., Russo, M. J., Guevarra, J., Cheung, S. K., and Siegelbaum, S. A. (2014). Reelin signaling specifies the molecular identity of the pyramidal neuron distal dendritic compartment. *Cell* 158, 1335–1347. doi: 10.1016/j.cell.2014.07.035

Kwiatkowski, A. V., Rubinson, D. A., Dent, E. W., van Veen, J. E., Leslie, J. D., Zhang, J., et al. (2007). Ena/VASP is required for neuritogenesis in the developing cortex. *Neuron* 56, 441–455. doi: 10.1016/j.neuron.2007.09.008

Leemhuis, J., and Bock, H. H. (2011). Reelin modulates cytoskeletal organization by regulating Rho GTPases. *Commun. Integr. Biol.* 4, 254–257. doi: 10.4161/cib.4.3.14890

Leite, S. C., Sampaio, P., Sousa, V. F., Nogueira-Rodrigues, J., Pinto-Costa, R., Peters, L. L., et al. (2016). The actin-binding protein α-adducin is required for maintaining axon diameter. *Cell Rep.* 15, 490–498. doi: 10.1016/j.celrep.2016.03.047

Leshchyns'ka, I., and Sytnyk, V. (2016). Reciprocal interactions between cell adhesion molecules of the immunoglobulin superfamily and the cytoskeleton in neurons. *Front. Cell Dev. Biol.* 4:9. doi: 10.3389/fcell.2016.00009

Li, S., Leshchyns'ka, I., Chernyshova, Y., Schachner, M., and Sytnyk, V. (2013). The neural cell adhesion molecule (NCAM) associates with and signals through p21-activated kinase 1 (Pak1). *J. Neurosci.* 33, 790–803. doi: 10.1523/JNEUROSCI.1238-12.2013

Ligon, L. A., and Steward, O. (2000). Role of microtubules and actin filaments in the movement of mitochondria in the axons and dendrites of cultured hippocampal neurons. *J. Comp. Neurol.* 427, 351–361.

Lin, Y.-C., and Redmond, L. (2008). CaMKIIbeta binding to stable F-actin in vivo regulates F-actin filament stability. *Proc. Natl. Acad. Sci. U.S.A.* 105, 15791–15796. doi: 10.1073/pnas.0804399105

Lin, Y.-C., Yeckel, M. F., and Koleske, A. J. (2013). Abl2/Arg controls dendritic spine and dendrite arbor stability via distinct cytoskeletal control pathways. *J. Neurosci.* 33, 1846–1857. doi: 10.1523/JNEUROSCI.4284-12.2013

Lohmann, C., Myhr, K. L., and Wong, R. O. L. (2002). Transmitter-evoked local calcium release stabilizes developing dendrites. *Nature* 418, 177–181. doi: 10.1038/nature00850

MacGrath, S. M., and Koleske, A. J. (2012). Arg/Abl2 modulates the affinity and stoichiometry of binding of cortactin to F-Actin. *Biochemistry* 51, 6644–6653. doi: 10.1021/bi300722t

Magee, J. C. (2000). Dendritic integration of excitatory synaptic input. *Nat. Rev. Neurosci.* 1, 181–190. doi: 10.1038/35044552

Martin, K. C., and Ephrussi, A. (2010). mRNA localization: gene expression in the spatial dimension. *Cell* 136, 719–730. doi: 10.1016/j.cell.2009.01.044.mRNA

Matusek, T., Gombos, R., Szécsényi, A., Sánchez-Soriano, N., Czibula, A., Pataki, C., et al. (2008). Formin proteins of the DAAM subfamily play a role during axon growth. *J. Neurosci.* 28, 13310–13319. doi: 10.1523/JNEUROSCI.2727-08.2008

Medeiros, N. A., Burnette, D. T., and Forscher, P. (2006). Myosin II functions in actin-bundle turnover in neuronal growth cones. *Nat. Cell Biol.* 8, 215–226. doi: 10.1038/ncb1367

Merriam, E. B., Millette, M., Lumbard, D. C., Saengsawang, W., Fothergill, T., Hu, X., et al. (2013). Synaptic regulation of microtubule dynamics in dendritic spines by calcium. F-actin, and drebrin. *J. Neurosci.* 33, 16471–16482. doi: 10.1523/JNEUROSCI.0661-13.2013

Meseke, M., Rosenberger, G., and Förster, E. (2013). Reelin and the Cdc42/Rac1 guanine nucleotide exchange factor αPIX/Arhgef6 promote dendritic Golgi translocation in hippocampal neurons. *Eur. J. Neurosci.* 37, 1404–1412. doi: 10.1111/ejn.12153

Meyer, G., and Feldman, E. L. (2002). Signaling mechanisms that regulate actin-based motility processes in the nervous system. *J. Neurochem.* 83, 490–503. doi: 10.1046/j.1471-4159.2002.01185.x

Moresco, E. M. Y. (2005). Integrin-mediated dendrite branch maintenance requires abelson (Abl) family kinases. *J. Neurosci.* 25, 6105–6118. doi: 10.1523/JNEUROSCI.1432-05.2005

Murakoshi, H., Wang, H., and Yasuda, R. (2011). Local, persistent activation of Rho GTPases during plasticity of single dendritic spines. *Nature* 472, 100–104. doi: 10.1038/nature09823

Na, Y., Park, S., Lee, C., Sockanathan, S., Huganir, R. L., Worley, P. F., et al. (2016). Real-time imaging reveals properties of glutamate-induced Arc/Arg 3.1 translation in neuronal dendrites. *Neuron* 91, 561–573. doi: 10.1016/j.neuron.2016.06.017

Negishi, M., and Katoh, H. (2002). Rho family GTPases as key regulators for neuronal network formation. *J. Biochem.* 132, 157–166.

Ngo, K. X., Umeki, N., Kijima, S. T., Kodera, N., Ueno, H., Furutani-Umezu, N., et al. (2016). Allosteric regulation by cooperative conformational changes of actin filaments drives mutually exclusive binding with cofilin and myosin. *Sci. Rep.* 6:35449. doi: 10.1038/srep35449

Niell, C. M., Meyer, M. P., and Smith, S. J. (2004). In vivo imaging of synapse formation on a growing dendritic arbor. *Nat. Neurosci.* 7, 254–260. doi: 10.1038/nn1191

Noguchi, J., Hayama, T., Watanabe, S., Ucar, H., Yagishita, S., Takahashi, N., et al. (2016). State-dependent diffusion of actin-depolymerizing factor/cofilin underlies the enlargement and shrinkage of dendritic spines. *Sci. Rep.* 6:32897. doi: 10.1038/srep32897

Oertner, T. G., and Matus, A. (2005). Calcium regulation of actin dynamics in dendritic spines. *Cell Calcium* 37, 477–482. doi: 10.1016/j.ceca.2005.01.016

Okada, K., Bartolini, F., Deaconescu, A. M., Moseley, J. B., Dogic, Z., Grigorieff, N., et al. (2010). Adenomatous polyposis coli protein nucleates actin assembly and synergizes with the formin mDia1. *J. Cell Biol.* 189, 1087–1096. doi: 10.1083/jcb.201001016

Okamoto, K.-I., Nagai, T., Miyawaki, A., and Hayashi, Y. (2004). Rapid and persistent modulation of actin dynamics regulates postsynaptic reorganization underlying bidirectional plasticity. *Nat. Neurosci.* 7, 1104–1112. doi: 10.1038/nn1311

Ono, S. (2013). The role of cyclase-associated protein in regulating actin filament dynamics - more than a monomer-sequestration factor. *J. Cell Sci.* 126, 3249–3258. doi: 10.1242/jcs.128231

Oprea, G. E., Kröber, S., McWhorter, M. L., Rossoll, W., Müller, S., Krawczak, M., et al. (2008). Plastin 3 is a protective modifier of autosomal recessive spinal muscular atrophy. *Science* 320, 524–527. doi: 10.1126/science.1155085

Osterweil, E., Wells, D. G., and Mooseker, M. S. (2005). A role for myosin VI in postsynaptic structure and glutamate receptor endocytosis. *J. Cell Biol.* 168, 329–338. doi: 10.1083/jcb.200410091

Pathak, D., Sepp, K. J., and Hollenbeck, P. J. (2010). Evidence that myosin activity opposes microtubule-based axonal transport of mitochondria. *J. Neurosci.* 30, 8984–8992. doi: 10.1523/JNEUROSCI.1621-10.2010

Pechlivanis, M., Samol, A., and Kerkhoff, E. (2009). Identification of a short spir interaction sequence at the C-terminal end of formin subgroup proteins. *J. Biol. Chem.* 284, 25324–25333. doi: 10.1074/jbc.M109.030320

Pinyol, R., Haeckel, A., Ritter, A., Qualmann, B., and Kessels, M. M. (2007). Regulation of N-WASP and the Arp2/3 complex by Abp1 controls neuronal morphology. *PLoS ONE* 2:e400. doi: 10.1371/journal.pone.0000400

Pollerberg, G. E., Thelen, K., Theiss, M. O., and Hochlehnert, B. C. (2013). The role of cell adhesion molecules for navigating axons: density matters. *Mech. Dev.* 130, 359–372. doi: 10.1016/j.mod.2012.11.002

Pylypenko, O., Welz, T., Tittel, J., Kollmar, M., Chardon, F., Malherbe, G., et al. (2016). Coordinated recruitment of Spir actin nucleators and myosin V motors to Rab11 vesicle membranes. *Elife* 5:e17523. doi: 10.7554/eLife.17523

Qu, Y., Hahn, I., Webb, S., and Prokop, A. (2016). Periodic actin structures in neuronal axons are required to maintain microtubules. *Mol. Biol. Cell* 28, 296–308. doi: 10.1101/049379

Redmond, L., and Ghosh, A. (2005). Regulation of dendritic development by calcium signaling. *Cell Calcium* 37, 411–416. doi: 10.1016/j.ceca.2005.01.009

Rex, C., Gavin, C. F., Rubio, M. D., Kramar, E. A., Chen, L. Y., Jia, Y., et al. (2010). Myosin IIB regulates actin dynamics during synaptic plasticity and memory formation. *Neuron* 67, 603–617. doi: 10.1016/j.neuron.2010.07.016

Roger, B., Al-Bassam, J., Dehmelt, L., Milligan, R. A., and Halpain, S. (2004). MAP2c, but not tau, binds and bundles F-actin via its microtubule binding domain. *Curr. Biol.* 14, 363–371. doi: 10.1016/j.cub.2004.01.058

Sainath, R., and Gallo, G. (2014). Cytoskeletal and signaling mechanisms of neurite formation. *Cell Tissue Res.* 359, 267–278. doi: 10.1007/s00441-014-1955-0

Sarmiere, P. D., and Bamburg, J. R. (2004). Regulation of the neuronal actin cytoskeleton by ADF/cofilin. *J. Neurobiol.* 58, 103–117. doi: 10.1002/neu.10267

Schevzov, G., Bryce, N. S., Almonte-Baldonado, R., Joya, J., Lin, J. J.-C., Hardeman, E., et al. (2005). Specific features of neuronal size and shape are regulated by tropomyosin isoforms. *Mol. Biol. Cell* 16, 3425–3437. doi: 10.1091/mbc.E04

Schevzov, G., Curthoys, N. M., Gunning, P. W., and Fath, T. (2012). Functional diversity of actin cytoskeleton in neurons and its regulation by tropomyosin. *Int. Rev. Cell Mol. Biol.* 298, 33–94. doi: 10.1016/B978-0-12-394309-5.00002-X

Schuh, M. (2011). An actin-dependent mechanism for long-range vesicle transport. *Nat. Cell Biol.* 13, 1431–1436. doi: 10.1038/ncb2353

Schumacher, N., Borawski, J. M., Leberfinger, C. B., Gessler, M., and Kerkhoff, E. (2004). Overlapping expression pattern of the actin organizers Spir-1 and formin-2 in the developing mouse nervous system and the adult brain. *Gene Expr. Patterns* 4, 249–255. doi: 10.1016/j.modgep.2003.11.006

Shah, M. M., Hammond, R. S., and Hoffman, D. (2010). Dendritic ion channel trafficking and plasticity. *Trends Neurosci.* 33, 307–316. doi: 10.1016/j.tins.2010.03.002.Dendritic

Shih, P., Lee, S., Chen, Y., and Hsueh, Y. (2014). Cortactin binding protein 2 increases microtubule stability and regulates dendritic arborization. *J. Cell Sci.* 127(Pt 16), 3521–3534. doi: 10.1242/jcs.149476

Sidenstein, S. C., D'Este, E., Böhm, M. J., Danzl, J. G., Belov, V. N., and Hell, S. W. (2016). Multicolour multilevel STED nanoscopy of actin/spectrin organization at synapses. *Sci. Rep.* 6:26725. doi: 10.1038/srep26725

Sit, S.-T., and Manser, E. (2011). Rho GTPases and their role in organizing the actin cytoskeleton. *J. Cell Sci.* 124, 679–683. doi: 10.1242/jcs.064964

Smith, B. A., Daugherty-Clarke, K., Goode, B. L., and Gelles, J. (2013). Pathway of actin filament branch formation by Arp2/3 complex revealed by single-molecule imaging. *Proc. Natl. Acad. Sci. U.S.A.* 110, 1285–1290. doi: 10.1073/pnas.1211164110

Spence, E. F., Kanak, D. J., Carlson, B. R., and Soderling, S. H. (2016). The Arp2/3 complex is essential for distinct stages of spine synapse maturation, including synapse unsilencing. *J. Neurosci.* 36, 9696–9709. doi: 10.1523/JNEUROSCI.0876-16.2016

Star, E. N., Kwiatkowski, D. J., and Murthy, V. N. (2002). Rapid turnover of actin in dendritic spines and its regulation by activity. *Nat. Neurosci.* 5, 239–246.

Strasser, G. A., Rahim, N. A., Vanderwaal, K. E., Gertler, F. B., and Lanier, L. M. (2004). Arp2/3 is a negative regulator of growth cone translocation. *Neuron* 43, 81–94. doi: 10.1016/j.neuron.2004.05.015

Sun, D., Leung, C. L., and Liem, R. K. (2001). Characterization of the microtubule binding domain of microtubule actin crosslinking factor (MACF): identification of a novel group of microtubule associated proteins. *J. Cell Sci.* 114, 161–172.

Sung, J. Y., Engmann, O., Teylan, M. A., Nairn, A. C., Greengard, P., and Kim, Y. (2008). WAVE1 controls neuronal activity-induced mitochondrial distribution in dendritic spines. *Proc. Natl. Acad. Sci. U.S.A.* 105, 3112–3116. doi: 10.1073/pnas.0712180105

Swiech, L., Blazejczyk, M., Urbanska, M., Pietruszka, P., Dortland, B. R., Malik, A. R., et al. (2011). CLIP-170 and IQGAP1 cooperatively regulate dendrite morphology. *J. Neurosci.* 31, 4555–4568. doi: 10.1523/JNEUROSCI.6582-10.2011

Szebenyi, G., Bollati, F., Bisbal, M., Sheridan, S., Faas, L., Wray, R., et al. (2005). Activity-driven dendritic remodeling requires microtubule-associated protein 1A. *Curr. Biol.* 15, 1820–1826. doi: 10.1016/j.cub.2005.08.069

Togashi, H., Sakisaka, T., and Takai, Y. (2009). Cell adhesion molecules in the central nervous system. *Cell Adh. Migr.* 3, 29–35.

Tojkander, S., Gateva, G., Schevzov, G., Hotulainen, P., Naumanen, P., Martin, C., et al. (2011). A molecular pathway for myosin II recruitment to stress fibers. *Curr. Biol.* 21, 539–550. doi: 10.1016/j.cub.2011.03.007

Tsaneva-Atanasova, K., Burgo, A., Galli, T., and Holcman, D. (2009). Quantifying neurite growth mediated by interactions among secretory vesicles, microtubules, and actin networks. *Biophys. J.* 96, 840–857. doi: 10.1016/j.bpj.2008.10.036

van Bommel, B., and Mikhaylova, M. (2016). Talking to the neighbours: the molecular and physiological mechanisms of clustered synaptic plasticity. *Neurosci. Biobehav. Rev.* 71, 352–361. doi: 10.1016/j.neubiorev.2016.09.016

Wagner, W., Brenowitz, S. D., and Hammer, J. A. I. (2011). Myosin-Va transports the endoplasmic reticulum into the dendritic spines of purkinje neurons. *Nat. Cell Biol.* 1, 40–48. doi: 10.1038/ncb2132

Wang, L., Chang, X., She, L., Xu, D., Huang, W., and Poo, M.-M. (2015). Autocrine action of BDNF on dendrite development of adult-born hippocampal neurons. *J. Neurosci.* 6, 8384–8393. doi: 10.1523/JNEUROSCI.4682-14.2015

Wang, Z., Edwards, J. G., Riley, N., Provance, D. W., Karcher, R., Li, X., et al. (2008). Myosin Vb mobilizes recycling endosomes and AMPA receptors for postsynaptic plasticity. *Cell* 135, 535–548. doi: 10.1016/j.cell.2008.09.057

Watanabe, T., Wang, S., Noritake, J., Sato, K., Fukata, M., Takefuji, M., et al. (2004). Interaction with IQGAP1 links APC to Rac1. Cdc42, and actin filaments during cell polarization and migration. *Dev. Cell* 7, 871–883. doi: 10.1016/j.devcel.2004.10.017

Willig, K. I., Steffens, H., Gregor, C., Herholt, A., Rossner, M. J., and Hell, S. W. (2014). Nanoscopy of filamentous actin in cortical dendrites of a living mouse. *Biophys. J.* 106, L01–L03. doi: 10.1016/j.bpj.2013.11.1119

Witke, W., Podtelejnikov, A. V., Di Nardo, A., Sutherland, J. D., Christine, B., Gurniak, et al. (1998). In mouse brain profilin I and profilin II associate with regulators of the endocytic pathway and actin assembly. *EMBO J.* 17, 967–976. doi: 10.1093/emboj/17.4.967

Xu, K., Zhong, G., and Zhuang, X. (2013). Actin, spectrin, and associated proteins form a periodic cytoskeletal structure in axons. *Science* 339, 452–456. doi: 10.1126/science.1232251

Yarmola, E. G., and Bubb, M. R. (2004). Effects of profilin and thymosin β4 on the critical concentration of actin demonstrated in vitro and in cell extracts with a novel direct assay. *J. Biol. Chem.* 279, 33519–33527. doi: 10.1074/jbc.M404392200

Yoon, Y. J., Wu, B., Buxbaum, A. R., Das, S., Tsai, A., English, B. P., et al. (2016). Glutamate-induced RNA localization and translation in neurons. *Proc. Natl. Acad. Sci. U.S.A.* 113, E6877–E6886. doi: 10.1073/pnas.1614267113

Yoshimura, A., Fujii, R., Watanabe, Y., Okabe, S., Fukui, K., and Takumi, T. (2006). Myosin-Va facilitates the accumulation of mRNA/protein complex in dendritic spines. *Curr. Biol.* 16, 2345–2351. doi: 10.1016/j.cub.2006.10.024

Yuan, A., Rao, M. V., Veeranna, and Nixon, R. A. (2012). Neurofilaments at a glance. *J. Cell Sci.* 125, 3257–3263. doi: 10.1242/jcs.104729

Yuan, Y., Seong, E., Singh, D., and Arikkath, J. (2015). Differential regulation of apical-basolateral dendrite outgrowth by activity in hippocampal neurons. *Front. Cell. Neurosci.* 9:314. doi: 10.3389/fncel.2015.00314

Conflict of Interest Statement: The authors declare that the research was conducted in the absence of any commercial or financial relationships that could be construed as a potential conflict of interest.

frontiers in Cellular Neuroscience

REVIEW
published: 24 April 2017
doi: 10.3389/fncel.2017.00115

The Segregated Expression of Voltage-Gated Potassium and Sodium Channels in Neuronal Membranes: Functional Implications and Regulatory Mechanisms

Maël Duménieu[1†], Marie Oulé[1†], Michael R. Kreutz[1,2] and Jeffrey Lopez-Rojas[1]*

[1]*Research Group Neuroplasticity, Leibniz Institute for Neurobiology, Magdeburg, Germany,* [2]*Leibniz Group "Dendritic Organelles and Synaptic Function", University Medical Center Hamburg-Eppendorf, Center for Molecular Neurobiology (ZMNH), Hamburg, Germany*

Neurons are highly polarized cells with apparent functional and morphological differences between dendrites and axon. A critical determinant for the molecular and functional identity of axonal and dendritic segments is the restricted expression of voltage-gated ion channels (VGCs). Several studies show an uneven distribution of ion channels and their differential regulation within dendrites and axons, which is a prerequisite for an appropriate integration of synaptic inputs and the generation of adequate action potential (AP) firing patterns. This review article will focus on the signaling pathways leading to segmented expression of voltage-gated potassium and sodium ion channels at the neuronal plasma membrane and the regulatory mechanisms ensuring segregated functions. We will also discuss the relevance of proper ion channel targeting for neuronal physiology and how alterations in polarized distribution contribute to neuronal pathology.

Keywords: voltage-gated sodium channels, voltage-gated potassium channels, polarized trafficking, compartmentalization, voltage-gated ion channels, axon initial segment, dendrites, node of Ranvier

OPEN ACCESS

Edited by:
Annette Gaertner, KU Leuven, Belgium

Reviewed by:
Juan S. Bonifacino, National Institute of Child Health and Human Development (NIH), USA
Pietro Fazzari, Consejo Superior de Investigaciones Científicas (CSIC), Spain

***Correspondence:**
Jeffrey Lopez-Rojas
jeffrey.lopez@lin-magdeburg.de

[†]These authors have contributed equally to this work.

Received: *09 February 2017*
Accepted: *05 April 2017*
Published: *24 April 2017*

Citation:
Duménieu M, Oulé M, Kreutz MR and Lopez-Rojas J (2017) The Segregated Expression of Voltage-Gated Potassium and Sodium Channels in Neuronal Membranes: Functional Implications and Regulatory Mechanisms. Front. Cell. Neurosci. 11:115. doi: 10.3389/fncel.2017.00115

INTRODUCTION

The neuronal cytoarchitecture defines two main cellular compartments: dendrites that receive, integrate and propagate synaptic input (Häusser et al., 2000; Magee and Johnston, 2005; Stuart and Spruston, 2015) and the axon that eventually converts these processed inputs into variable patterns of action potential (AP), with fast and robust transmission to distant postsynaptic targets. Whereas some ion channels can be found all along the neuronal plasma membrane (Lim et al., 2000; Trimmer and Rhodes, 2004; Kirizs et al., 2014), others exhibit a more restricted expression pattern to either the axon or the somatodendritic region (Kerti et al., 2012). The functional properties of each cellular compartment and membraneous subcompartment critically depend on the type of voltage-gated ion channels (VGCs) inserted in the corresponding membrane (Lai and Jan, 2006; Beck and Yaari, 2008; Remy et al., 2010).

This review article summarizes current knowledge regarding potassium and sodium channels trafficking and surface expression and highlights the remaining questions regarding the mechanisms by which segregation of these ion channels at the plasma membrane is achieved.

We focus on specific potassium and sodium VGCs: Kv1, Kv4.2 and Kv2.1 and Nav1.2, Nav1.6, respectively. These channels are critical in controlling neuronal intrinsic excitability and are among the best investigated VGCs (Vacher et al., 2008; Catterall, 2012; Vacher and Trimmer, 2012; Trimmer, 2015; **Table 1**). Principles underlying their polarized distribution and function in neurons are better understood and might be paradigmatic to understand the mechanisms controlling the subcellular distribution and function of other ion channels present in axons and dendrites.

SEGREGATED DISTRIBUTION OF VGCs IN DENDRITES

Kv4.2 and Nav1.6 Channels in Dendrites

The structural properties of dendrites, i.e., thickness and number of branches among others, define in part how they conduct and integrate synaptic signals (Segev and Rall, 1998; Stuart and Spruston, 2015). In addition, the expression pattern of different classes of VGCs is a key feature that determines the electrical properties of dendrites (Lai and Jan, 2006; Trimmer, 2015). Potassium channels are the most diverse family of ion channels and are present throughout the brain (Lai and Jan, 2006; Luján, 2010; Trimmer, 2015). These channels are composed of several pore-forming α subunits that interact with auxiliary subunits such as K^+ channel Interacting Proteins (KChIPs), DPPX, Kvβ and AMIGO. The association of the α subunits with the auxiliary subunits changes the electrophysiological and biophysical properties of the channels (An et al., 2000; Bähring et al., 2001; Shibata et al., 2003; Peltola et al., 2011) and can also affect their expression level and distribution pattern (An et al., 2000; Shibata et al., 2003). At the functional level, potassium channels in dendrites are key regulators of dendritic excitability as they strongly filter and shape electrical signals traveling between synapses and the soma and all the way back from soma to synapses (Watanabe et al., 2002; Takigawa and Alzheimer, 2003; van Welie et al., 2004; Misonou et al., 2005b; Chen and Johnston, 2006; Kim and Hoffman, 2008).

Regarding sodium channels, to date nine Nav channels α subunit isoforms have been identified (Nav1.1–1.9), each channel being composed of one α subunit with four domains that form the pore of the channel. Nav channels also interact with auxiliary β subunits (β_{1-4}) that regulate their trafficking or biophysical properties (Patino and Isom, 2010; O'Malley and Isom, 2015). Whereas the expression pattern and physiological function of Nav channels are relatively clear in the axon (see the corresponding section for more details) their localization in the somatodendritic compartment is not well investigated. Nonetheless, upon synchronous stimulation dendritic Nav channels can generate local dendritic spikes in pyramidal cells (Golding and Spruston, 1998; Spruston, 2008; Sun et al., 2014; Kim et al., 2015), a regenerative mechanism that has been shown to facilitate synaptic plasticity in CA1 (Kim et al., 2015) and CA2 (Sun et al., 2014) pyramidal neurons.

The Proximodistal Dendritic Gradient of Kv4.2 and Nav1.6 Channels Influence Distance-Dependent Dendritic Integration of Synaptic Signals

Upon membrane depolarization, the opening of the voltage-gated Kv4.2 channel generates the A-type current (Chen et al., 2006), dampening dendritic electrical signals (Hoffman et al., 1997). The importance of this channel in dendritic integration is further illustrated by the key role of its downregulation in the induction and expression of LTP in CA1 pyramidal cells (Frick et al., 2004; Chen et al., 2006), as well as its role in memory formation (Lugo et al., 2012; Truchet et al., 2012; Vernon et al., 2016). Kv4.2 is found on somatic and dendritic membranes, as well as in spines of CA1 pyramidal cells (Jerng et al., 2004; Rhodes et al., 2004; Kerti et al., 2012; **Figure 1**). Although immunogold staining have shown slight differences in the density of Kv4.2 labeling between proximal and distal dendrites of CA1 pyramidal cells (Kerti et al., 2012), the actual A-type current is much larger at the very distal dendrites compared to the proximal ones (Hoffman et al., 1997). The discrepancy between the Kv4.2 expression pattern and dendritic A-type current amplitude suggests different regulation of the channel depending on its location along the proximodistal dendritic axis.

TABLE 1 | Summary of localization, accessory subunits and physiological functions of voltage-gated potassium and sodium channels.

Ion channels	Localization	Accessory proteins	Physiological functions
Kv1.1, Kv1.2	Distal AIS and juxtaparanode	Kvβ2 subunit	Regulation of AP threshold. Membrane repolarization. Spatially restrict propagation of excitation.
Kv1.4	Distal AIS, juxtaparanode and presynaptic sites	Kvβ2 subunit	Mediates a fast hyperpolarizing current. Associates with AIS- and nodal-Kv1.1/Kv1.2 heteromers, influencing their surface expression.
Kv2.1	Proximal dendrites, soma and AIS	AMIGO	Single channels: regulate high frequency firing. Clustered channels: non-conducting, but contribute to the excitation-gene transcription coupling.
Kv4.2	Spines, dendrites and soma	DPP6/DPPX and KChIPs	Dampens the propagation of depolarizing signals.
Nav1.2	AIS and nodes of Ranvier$_{(immature\ axon)}$ Proximal AIS$_{(mature\ axon)}$	β_{1-4} subunit	AP generation $_{(immature\ axon)}$ AP back-propagation$_{(mature\ axon)}$
Nav1.6	Dendrites, soma, distal AIS and nodes of Ranvier	β_{1-4} subunit	Generation of dendritic spikes. High efficiency axonal AP generation.

For clarity, the table refers mainly to CA1 pyramidal cells.

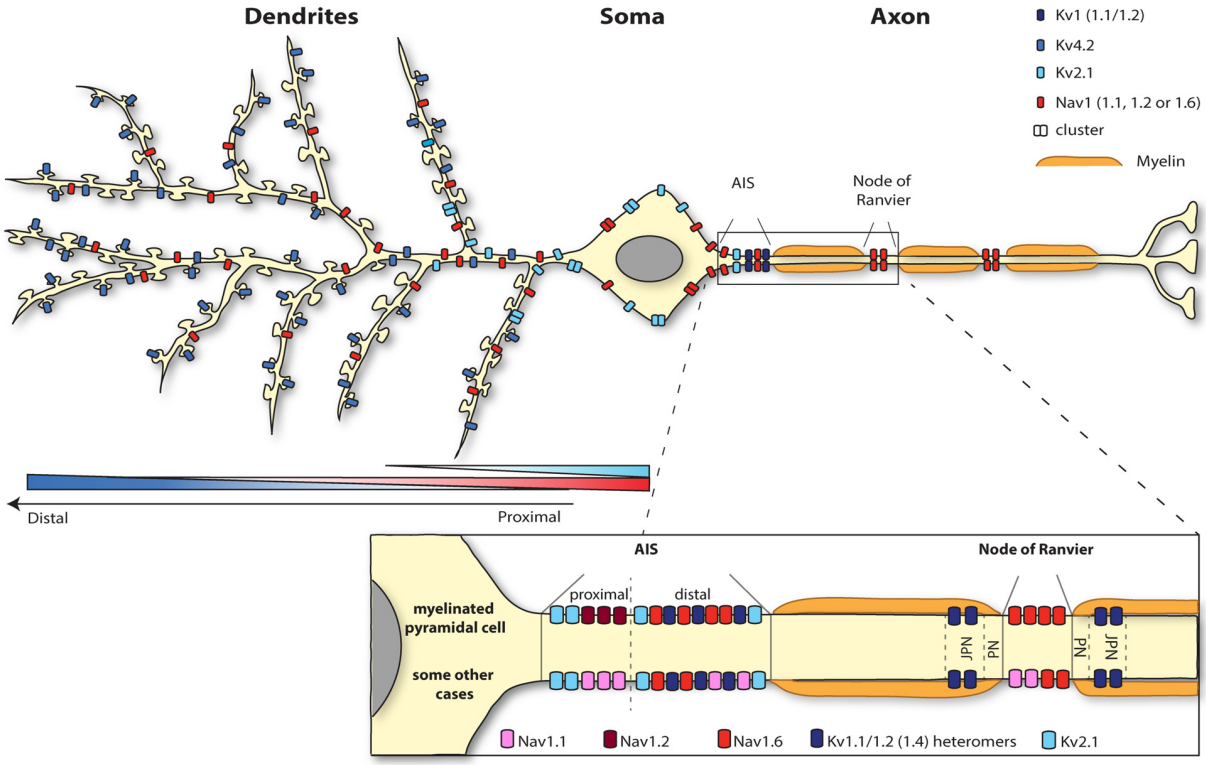

FIGURE 1 | Segregation of the neuronal surface expression of potassium and sodium channels. Kv4.2 channels are expressed all along the dendrites and spines of pyramidal cells according to an increasing proximodistal gradient. Kv2.1 channel expression is restricted to the soma and the very proximal dendrites. Sodium channels are highly concentrated at the level of the axon initial segment (AIS; Nav1.1, 1.2 and 1.6) and nodes of Ranvier (1.2 and 1.6). Whereas myelinated pyramidal cells express Nav1.2 and Nav1.6 at the level of the AIS, Nav1.1 as well as Nav 1.2 and 1.6 are present at the AIS region of retinal bipolar cells, retinal ganglion cells, parvalbumine-positive interneurons (neocortex and hippocampus), Purkinje cells and spinal cord motoneurons for instance. Nav1.6 is also expressed in the somatodendritic compartment (but not spines) of CA1 pyramidal cells following a decreasing proximodistal gradient.

Concurrently, upon membrane depolarization the opening of sodium channels further depolarizes the membrane contributing to an enhanced excitability. From all sodium channels, Nav1.6 is the main subtype identified in the dendritic membrane of CA1 pyramidal cells, suggesting that this channel is responsible for the generation of the dendritic sodium spikes in this cell type. Nav1.6 is expressed throughout the neuron, from the nodes of Ranvier to dendrites (Caldwell et al., 2000; Krzemien et al., 2000; **Figure 1**). Since the intensity of labeling is much weaker on dendrites (around 40 times less) than in the axon (Lorincz and Nusser, 2010), Nav1.6 was not always detected in immunolabeling studies (Lorincz and Nusser, 2008; Hu et al., 2009). A recent study using electron microscopy has revealed that Nav1.6 channel is indeed present in the somatodendritic compartment, but excluded from spine synapses, of CA1 pyramidal cells with a decreasing proximodistal gradient of expression (Lorincz and Nusser, 2010; **Figure 1**).

Thus, Kv4.2 and Nav1.6 channels exhibit opposing proximodistal expression patterns and the prominent expression of Kv4.2 together with the weak expression of Nav1.6 in distal dendrites reduces the likelihood of distal synaptic signals to reach the soma. In contrast, the large density of Nav1.6 channels and the reduced expression of Kv4.2 channel in proximal dendrites make the transmission of synaptic stimuli impinging on this area much more reliable. Intuitively, dampening the transmission of distal signals over proximal ones seems not to be meaningful for dendritic integration. The physiological relevance for dendritic integration of setting such ion channel gradients still remain to be fully understood. Nevertheless, downregulation of Kv4.2 channel is crucial for local dendritic plasticity of CA1 pyramidal cells, and specifically for the modulation of dendritic sodium spikes, potentially mediated by Nav1.6 channel (Losonczy and Magee, 2006; Losonczy et al., 2008; Weber et al., 2016). Hence, concomitant regulation of the surface expression or activity of both channels appears to be a major process for shaping dendritic integration.

Molecular Mechanisms Setting Dendritic Proximodistal Expression Gradients

Segregated targeting of ion channels to the somatodendritic compartment

Two main classes of auxiliary subunits are known to interact with the Kv4.2 channel: the KChIP (Shibata et al., 2003; Rhodes et al., 2004) which most likely interact with the intracellular

N-terminus of the channel (for review Jerng et al., 2004) and the Dipeptidyl Peptidase-like Protein (DPP) subunit (Nadal et al., 2003; Kim et al., 2008) whose interaction is proposed to be mediated by the transmembrane domain of the DPP protein and the voltage sensor domain of the potassium channel (Ren et al., 2005; Zagha et al., 2005). Kv4.2 co-localizes with KChIP2 in apical and basal dendrites of hippocampal and cortical pyramidal cells (Rhodes et al., 2004) and KChIP1-3 associate with the Kv4.2 channel to promote its surface expression by facilitating the release of the channel from the endoplasmic reticulum (ER; Shibata et al., 2003). This mechanism might involve the masking of the cytoplasmic ER retention signal located in the N-terminal domain of the α subunit, raising the idea that the N-terminus of the channel is necessary for both binding to KChIPs and ER retention (Shibata et al., 2003; **Figure 2A**). Interestingly, due to the unique presence of a K-channel inactivation suppressor (KIS) domain on the KChIP4a (Holmqvist et al., 2002), this auxiliary subunit does not promote the trafficking of Kv4.2 channel outside of the ER (Shibata et al., 2003). But the coassembly of KChIP4a with Kv4.2 and other KChIP subunits allows the complex to be expressed at the surface level (Shibata et al., 2003). Indeed in COS7 cells phosphorylation of a specific serine residue (S552) of the Kv4.2 channel by PKA leads to an increased surface expression of the channel in complex with KChIP4a (Lin et al., 2011). Thus, it seems that surface expression of Kv4.2 channel can be finely tuned depending on the stoichiometry of the coassembly of Kv4.2 channel with KChIP subunits, as well as the phosphorylation status of the channel. The DPPX auxiliary subunit, also called DPP6, a member of the DPP protein family, is expressed in the same population of neurons than Kv4.2 channel and its expression is also restricted to the somatodendritic compartment. In CHO cells, the coexpression of Kv4.2 channel with DPPX targets the channel at the cell surface, whereas Kv4.2 channel expressed alone is sequestered in the perinuclear ER (Nadal et al., 2003). DPPX presents homology with the CD26 protein (Nadal et al., 2003), known for its role in cell adhesion and interaction with the extracellular matrix (ECM; Hildebrandt et al., 2000). The DPPX homologous extracellular cysteine-rich domain is thought to be important for the extracellular regulation of the trafficking of Kv4.2 channel in complex with DPPX (Nadal et al., 2003). Even though Kv4.2 auxiliary subunits are critical for the targeting of the channel to the somatodendritic compartment, how these proteins influence the segregated expression of the channel still remains elusive.

Microtubule-based dendritic transport of Kv4.2 is supported by the kinesin Kif17 in cortical cells cultures, most likely through interaction with the C-terminus (but not the Kv4.2 dileucine motif; Chu et al., 2006), whereas association of Kv4.2 with myosin Va, an actin-based motor, restricts the expression of the channel to the somatodendritic region (Lewis et al., 2009; **Figure 2A**). Comparison of the trafficking mechanism of Kv4.2 and Kv2.1 channels have shown that channels are sorted at the Golgi apparatus into different vesicle pools, each pool being transported in a compartment-specific manner (Jensen et al., 2014). Jensen et al. (2014) have demonstrated in hippocampal primary neurons that mutation of the C-terminal domain of the channels (Kv4.2LL/AV and Kv2.1S586A) causes their mislocalization, with expression of the Kv4.2 channel at the somatodendritic compartment as well as in the axon, and expression of the Kv2.1 all along the dendritic plasma membrane. Interestingly, Jensen et al. (2014) also reported that disruption of actin polymerization using latrunculin A alters the motility of Kv2.1-contaning, but not Kv4.2-containing vesicles. However blocking actin polymerization with cytochalasin D led to a diffuse targeting of the Kv4.2 channel in a study by Lewis et al. (2009). These discrepant observations raise questions regarding the role of actin in the transport of Kv4.2-containing vesicles. Nevertheless, one hypothesis could be that actin-based transport is used for short distance transport to the proximal dendrites or from dendritic shaft to the spine, whereas Kv4.2 channels expressed distally are trafficked based on long distance microtubule-based transport (**Figure 2A**).

Rivera et al. (2003) identified a dileucine-containing motif in the C-terminus of Kv4.2 as sufficient and necessary for the dendritic expression of the channel (**Figure 2B**). Interestingly, elimination of the dileucine-containing motif causes the targeting of the channel predominantly at cell body, and to a lesser extent at the proximal part of both dendrites and axon, thereby suggesting cell body "default-targeting" of the channel (Rivera et al., 2003).

Several members of the Kv family have been shown to interact with proteins located at the postsynaptic density, most notably the membrane-associated guanylate kinases (MAGUKs; Gardoni et al., 2007; Lin et al., 2011; Fourie et al., 2014). In CA1 pyramidal cells, the Kv4.2 channel also associates with the A-kinase-anchoring protein (AKAP) complex, providing local coupling with kinase and phosphatase signaling. AKAP79/150, a member of the AKAP family, interacts with Kv4.2 channel through its MAGUK-binding site, but this interaction does not require the interaction of Kv4.2 channels with the MAGUK PDZ domains (Lin et al., 2011). Whereas association of PKA with AKAP79/150 decreases the surface expression of the Kv4.2 channel, the binding of calcineurin with the AKAP complex potentiates its surface expression (Lin et al., 2011). In parallel, Kv4.2 channel also interacts with other synaptic proteins, such as SAP97, through the C-terminus of the channel and the PDZ domain of the SAP97 protein (Gardoni et al., 2007). Findings from this study indicate that CaMKII-dependent Ser39 and Ser232 phosphorylation of the SAP97 protein increases the expression of the Kv4.2 channel at dendritic spines (Gardoni et al., 2007), suggesting that CaMKII-dependent SAP97 phosphorylation is important for synaptic trafficking of Kv4.2 channel (**Figure 2B**).

The Kv4.2 channel contains various residues that can be phosphorylated by diverse kinases such as PKA, PKC, CaMKII and ERK (Adams et al., 2000; Anderson et al., 2000; Varga et al., 2004; Schrader et al., 2009). While CaMKII-mediated phosphorylation of Ser438 and/or Ser459 enhances the surface expression of Kv4.2 channel (Varga et al., 2004), PKA-mediated phosphorylation of the Ser552 decreases the surface expression of the channel (Hammond et al., 2008). A study suggests that phosphorylation could be used as well as a discrete tag

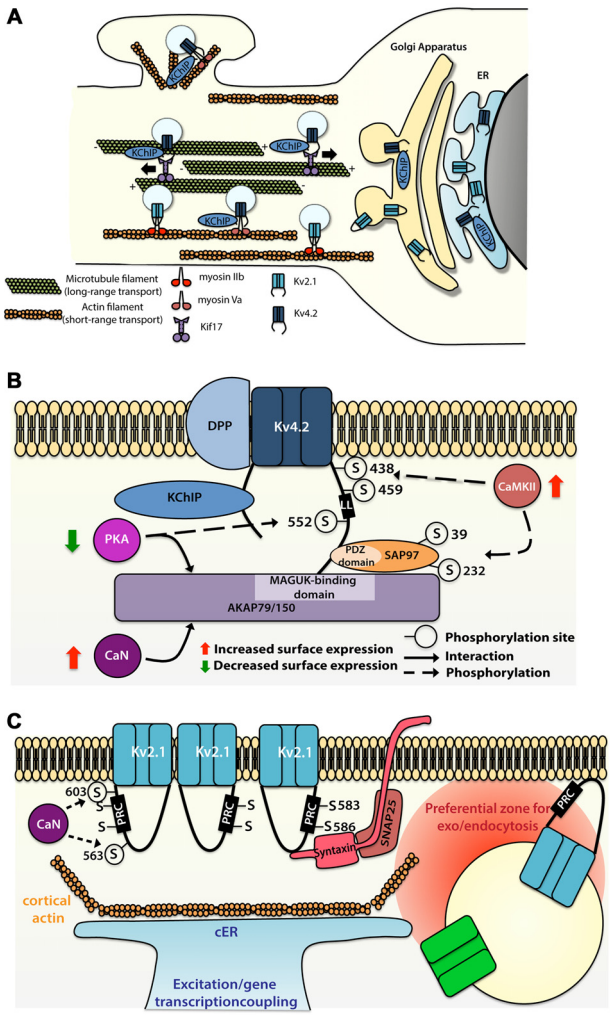

FIGURE 2 | Molecular mechanisms allowing segregated expression of the dendritic Kv4.2 and Kv2.1 channels. (A) Sorting and trafficking of Kv4.2 and Kv2.1 channels. Association of Kv4.2 channel with auxiliary protein K^+ channel Interacting Protein (KChIP) targets the channel to the cell surface. Kif17 ensures microtubule-based transport whereas myosin Va is used for actin-based transport of Kv4.2 channel on proximal dendrites and spines. Myosin IIb transports Kv2.1 to the somatodendritic compartment. **(B)** Intrinsic motifs, posttranslational regulations and binding partners regulating Kv4.2 surface expression. **(C)** Intrinsic motifs, posttranslational regulations and binding partners regulating Kv2.1 cluster formation and function.

for targeting. Indeed, the Kv4.2 channel exhibits different phosphorylated sites (ERK sites, N-terminal PKA sites or C-terminal PKA sites) depending on their localization along the dendritic tree of different cell types (Varga et al., 2000).

Contrary to the axonal compartment, in dendrites the expression pattern, trafficking and insertion mechanisms of Nav channels remain largely elusive. Combination of fluorescence techniques with high-density single-particle tracking has revealed that Nav1.6 channels are organized as small clusters (~230 nm) formed of 2–20 Nav1.6 channels at the surface of the soma (Akin et al., 2015; **Figure 1**). Strikingly, the removal of the ankyrin-G (AnkG)-binding motif of the Nav1.6 channel, crucial for its localization at the axon initial segment (AIS) region (Gasser et al., 2012), does not alter the formation of the nanoclusters observed at the surface of the soma (Akin et al., 2016). Cluster formation was also actin-independent and did not occur at the vicinity of the Kv2.1-mediated membrane trafficking hubs that are observed at the surface of the neuronal membrane (Akin et al., 2016). The AnkG-independent surface expression of the Nav1.6 channel in the soma of CA1 pyramidal cells suggest that compartment-specific binding partners could direct the expression of Nav1.6 channel to either the somatodendritic region or the axonal one.

It should be noted that Nav1.1 has been as well identified in the somatodendritic compartment of CA1 pyramidal cells (Westenbroek et al., 1989; Gong et al., 1999; for review, see Trimmer and Rhodes, 2004; Vacher et al., 2008). However, a more recent study from Lorincz and Nusser (2010) did not find Nav1.1 subunit expression in CA1 pyramidal cells, but only on axonal processes and AIS of GABAergic interneurons.

Establishment of dendritic proximodistal gradient and activity-dependent regulation of ion channels surface expression

In addition to its role in the surface targeting of the Kv4.2 channel, the auxiliary subunit DPP6/DPPX is thought to be important for the establishment of the proximodistal gradient of expression of Kv4.2. Knock-out of this auxiliary subunit leads to a reduced A-type current in the distal dendrites (Sun et al., 2011). However, the molecular mechanism through which DPP6 contributes to set such a gradient is unknown.

In cultured hippocampal neurons Kv4.2 channels can be removed from spines, where they are supposed to be enriched (Kim et al., 2005), through clathrin-mediated internalization triggered by NMDAR activation and increase in calcium-influx into the cell (Kim et al., 2007). Using a FRAP assay on CA1 pyramidal cells, Nestor and Hoffman (2012) have demonstrated that Kv4.2 mobility is positively regulated by AMPAR-dependent induction of PKA-mediated phosphorylation of Ser552 targeting the channel for clathrin-mediated internalization only at the distal dendrites (**Figure 2B**). Dynamic regulation of Kv4.2 channel surface expression fits with previous studies showing that activity-induced downregulation of the channel facilitates dendritic integration (Losonczy and Magee, 2006; Weber et al., 2016), helping synaptic signals to overcome the proximodistal gradient of Kv4.2.

The Somatodendritic Voltage-Gated Kv2.1 Channel forms Segregated Membrane Clusters that Participate to Novel Ion Channels Insertion and Retrieval

The Kv2.1 channel, a potassium channel that mediates the majority of the delayed-rectifier K^+ currents (Murakoshi and Trimmer, 1999), regulates membrane excitability during high frequency firing (Du et al., 2000; Misonou et al., 2005b). It is abundantly expressed throughout the brain and is particularly prominent in the hippocampus (Murakoshi and Trimmer, 1999; Antonucci et al., 2001). Several immunohistochemical studies

have shown that Kv2.1 is expressed at similar levels in the AIS, soma and very proximal part of the dendrites (Lim et al., 2000; Trimmer and Rhodes, 2004; Kirizs et al., 2014; **Figure 1**). Kv2.1-containing vesicles traffic on actin filaments through an association with myosin IIb (Jensen et al., 2014; **Figure 2A**). Interestingly, it has been observed that mutation of S586 of the Kv2.1, which is important for its expression at the somatodendritic membrane, does not alter surface expression at the AIS (Jensen et al., 2014), suggesting somatodendritic and axonal compartment-specific mechanisms, at least partially independent from each other, allowing the sorting of the channel to one of those regions.

Compared to other Kv channels, the Kv2.1 channel has the peculiarity to associate in large clusters (1–2 μm) at the membrane surface (Trimmer, 1991; Scannevin et al., 1996; O'Connell et al., 2006; Tamkun et al., 2007), whereas other channels show a more diffuse localization (Tamkun et al., 2007; **Figure 2C**). Given its pivotal role in the regulation of high frequency firing and its ubiquitous brain expression, cellular and molecular mechanisms regulating the expression and targeting of Kv2.1 channel have been extensively studied. A Proximal Restriction and Clustering signal (PRC signal) has been suggested to mediate the surface expression pattern of the Kv2.1 channel (Lim et al., 2000; **Figure 2C**). This uncommon signal in the cytoplasmic domain, which is rich in serine and threonine residues (7/26 positions), does not contain tyrosine or di-leucine motifs required for endosomal sorting and is supposed to exclusively ensure the clustering of the Kv2.1 channel at the surface membrane. The precise mechanism by which the PRC signal targets and sets the clustering of the Kv2.1 channel is not yet known. In addition it was shown that the interaction between both N-and C-termini of the Kv2.1 channel is necessary for efficient targeting of the channel at the membrane surface and this interaction is mediated by regions in the N- and C-termini that are normally involved in the interaction with auxiliary subunits in other classes of potassium channels (Mohapatra et al., 2008).

Surprisingly, Tamkun et al. (2007) showed that Kv2.1 channels have comparable lateral mobility at the plasma membrane irrespective of whether those channels were part or not of the clusters. This observation suggests that no static anchoring with classical scaffolding proteins occurs arguing in favor of a corral-forming fence restraining the diffusion of the channel. In some cases, Kv2.1 channels outside the clusters could readily diffuse within the cluster where they could be trapped and confined for up to an hour (Tamkun et al., 2007). The authors proposed a model in which Kv2.1 channels interact through their C-termini with accessory proteins located beneath the membrane, potentially in a phosphorylated-dependent manner, defining a cluster located within cortical actin wells.

While non-clustered Kv2.1 channel are responsible for the high-threshold delayed-rectifier current, clustered Kv2.1 channels are non-conducting but are instead able to sense membrane potential linking membrane potential changes to intracellular signaling cascades (O'Connell et al., 2010; Fox et al., 2013b). An interesting aspect of the Kv2.1 channel localization is its close association with subsurface cisternae (Fox et al., 2013a, 2015)—intracellular ER-derived membranes—that buffer and store intracellular calcium necessary for propagation of signaling cascades important for the regulation of neuronal trafficking (**Figure 2C**). Subsurface cisternae are called cortical endoplasmic reticulum (cER) and are suggested to form a hub that supports the trafficking of plasma membrane proteins (Fox et al., 2013a). In HEK cells Kv2.1 channel initiates the formation of this plasma membrane-ER junction (Fox et al., 2015) thanks to its remodeling, while Kv2.1 declustering upon glutamate stimulation led to retraction of cER away from plasma membrane, suggesting that the association of Kv2.1 channel with subsurface cisternae could couple electrical membranous events with intracellular calcium homeostasis. Moreover, preventing channel clustering by mutating two serine residues (S583 and S586), located within the C-terminal PRC sequence of Kv2.1 channel, also blocks cER remodeling (**Figure 2C**). Deutsch et al. (2012) demonstrated that Kv2.1-contaning vesicles actually tether and deliver cargo at the vicinity of the channel clusters in both HEK cells and cultured hippocampal neurons. Furthermore, quantum dot analysis showed that delivery and recycling of Kv2.1 channel occurs in a perimeter of 0.5 μm away from the cluster fence. Strikingly, they observed that Kv2.1 channel clusters are also used as a trafficking platform for insertion and retrieval of the non-clustering Kv1.4 channels (Deutsch et al., 2012) and later Cav1.2 channel has also been shown to be located in close proximity of Kv2.1 channel (Fox et al., 2015). Altogether these observations led to the speculation that these clusters are preferential locations for the exo- and endocytosis of different ion channels (**Figure 2C**), an important process that could participate to the segregation of ion channels membrane expression. The potential role of Kv2.1 channel in non-conducting phenomena is also supported by other observations. Some studies have focused on the role of Kv2.1 channel in vesicle-plasma membrane fusion (Feinshreiber et al., 2009, 2010). Of interest, Kv2.1 channel can interact with syntaxin and SNAP-25 (**Figure 2C**), two SNARE family proteins, which are known for their prominent role in vesicle fusion (Ramakrishnan et al., 2012; Südhof, 2013; Vardjan et al., 2013), supporting the idea that Kv2.1 platforms promote the insertion and recycling of other membrane proteins. Along these lines, the lack of proper Kv2.1 channel cluster formation might lead to alteration of local plasma membrane identity and the associated downstream signaling cascade. Thus, disruption of Kv2.1 channel clustering might induce mislocalization of other proteins and thereby dysfunction of dendritic signaling.

COMPARTMENTALIZED DISTRIBUTION OF VGCs IN AXONS

Nav Channels

Distribution and Function of Axonal Nav Ion Channels

Although Nav1.1 is mostly somatodendritic in principal cells, it is the dominant isoform in AIS of various GABAergic interneurons (Ogiwara et al., 2007; Lorincz and Nusser, 2008; Catterall et al., 2010; Tian et al., 2014) and is localized at

the AIS and nodes of retinal cells (Van Wart et al., 2007; Puthussery et al., 2013) and motor neurons (Duflocq et al., 2008, 2011). In these cell types, Nav1.1 channel localization in the AIS region was mainly restricted to a narrow proximal domain in contact with the soma (Van Wart et al., 2007; Duflocq et al., 2008, 2011; Lorincz and Nusser, 2008), suggesting that this channel might regulate voltage propagation between the AIS and the somatodendritic compartment. The exact function of Nav1 channels expressed at the AIS and nodes of Ranvier in these cell types is still unclear but its dysfunction leads to variable disorders ranging from epilepsy (Wimmer et al., 2010) to autism and paralysis (Arancibia-Carcamo and Attwell, 2014). Nav1.3 is mostly absent in mature neurons but is present in the axon of dorsal root ganglion (DRGs) neurons where its expression is upregulated following injury and has been implicated in pain disorders (Lindia et al., 2005; Cummins et al., 2007). Expression of Nav1.4 has been so far only shown in skeletal muscles. Nav1.5 is mostly found in the heart, even though it has been reported to be punctually expressed in the brain (Wu et al., 2002) but not much is known about its neuronal function. Nav1.7, Nav1.8 and Nav1.9 are differentially expressed in various subtypes of DRGs sensory neurons, possibly underlying their respective functions (Vacher et al., 2008). They have been less studied than central nervous system (CNS) neurons isoforms but their role in pain signaling make them target of further research (Cummins et al., 2007; Bao, 2015).

Nav 1.2 and Nav1.6 are the most prominent isoforms expressed in axons of neuronal principal cells. Outside of the AIS and nodes of Ranvier, Nav1.2 seems rather uniformly localized along unmyelinated fascicles of both myelinated and unmyelinated axons in mature neurons (Caldwell et al., 2000; Boiko et al., 2001, 2003; Van Wart et al., 2007). In neuronal development it is also transiently expressed at the AIS and in nodes of Ranvier. In mature neurons it is replaced by Nav1.6 (Boiko et al., 2001, 2003; Ratcliffe et al., 2001; Rios et al., 2003). In mature cortical pyramidal neurons, Nav1.2 is maintained at the proximal AIS, segregated from Nav1.6 and it has been suggested to control back-propagation of APs to the soma (Dulla and Huguenard, 2009; Hu et al., 2009). The function of Nav1.2 in non-myelinated axon is unclear but it could in principle allow active propagation of spikes, supporting micro-saltatory or saltatory-like conduction of APs (Johnston et al., 1996; Caldwell et al., 2000; Zeng and Tang, 2009; Neishabouri and Faisal, 2014; Freeman et al., 2016; but see Black et al., 2002).

Nav1.6 channels are the main component of AIS and nodes of Ranvier in most CNS neurons (Boiko et al., 2001, 2003; Ratcliffe et al., 2001; Rios et al., 2003) and they have been shown to be the main controllers of spike generation (Hu et al., 2009). This is due to their hyperpolarized voltage-dependance, kinetic properties and increased persistent current as compared to Nav1.2, making it a more excitable isoform (Burbidge et al., 2002; Rush et al., 2005; Kole and Stuart, 2008; Hu et al., 2009). Nav1.6 shows similar functional properties as Nav1.2 when their respective α subunits are expressed in TsA-201 cells (Chen et al., 2008), suggesting that regulation of Nav1.6, possibly by β subunits, is required for their specific function. Nav1.6 is expressed in a gradually increasing concentration along the AIS and is predominantly enriched in the distal AIS (Inda et al., 2006; Kole et al., 2007; Van Wart et al., 2007; Lorincz and Nusser, 2008; Hu et al., 2009), which might be important to isolate the axon from the somatic capacitance and enhance sharpness of APs generation (Brette, 2013). It is tempting to speculate that similar to their role at the AIS, Nav1.6 control APs regeneration at nodes of Ranvier although this has not yet been directly demonstrated (Arancibia-Carcamo and Attwell, 2014).

Targeting Nav Channels to the Axon

Nav channels are clustered at the level of the AIS and nodes of Ranvier by tethering to AnkG (Bréchet et al., 2008; Brachet et al., 2010) which is linked to the cytoskeleton by direct interaction with the actin-binding protein β IV spectrin (Ratcliffe et al., 2001; **Figures 3A,B**). An AnkG binding domain has been first identified in the II-III cytoplasmic loop of the C-terminal region of the Nav1.2 α subunit (Garrido et al., 2003; Fache et al., 2004). This binding domain is conserved among Nav isoforms (Lemaillet et al., 2003) and has been shown to be sufficient to target Nav1.6 to AIS and nodes (Gasser et al., 2012). In addition, the Nav1.2 II-III linker contains an endocytosis signal that promotes clearance of Nav1.2 from the somatodendritic domains (Garrido et al., 2003; Fache et al., 2004; **Figure 3A**) but such signal has not yet been identified for Nav1.6 subunits (Garrido et al., 2001; Lai and Jan, 2006; Akin et al., 2015; Liu et al., 2015). This difference might be explained by the fact that Nav1.6 is expressed later in development and relies on more specific targeting mechanisms than Nav1.2.

How Nav channels get transported into the axon was unclear until a recent study suggests that AnkG and Nav1.2 associate early during biosynthesis and that AnkG acts as a cargo adaptor to mediate KiF5B/kinesin-1 based axonal transport of Nav1.2 in 7 DIV hippocampal neurons (Barry et al., 2014; **Figure 3A**). It was not directly assessed in this study if Nav1.6 is transported following the same AnkG-KiF5B interaction but published data support this idea. Nav1.6 is targeted to the AIS thanks to the conserved AnkG-binding domain of Navs (Gasser et al., 2012). In addition, Nav1.6 AIS targeting depends on vesicular trafficking (Akin et al., 2015). Finally axonal transport of Nav1.8 in DRGs neurons of the peripheral nervous system is also dependent on KiF5B (Su et al., 2013). The role of AnkG as a cargo adaptator and the contribution of this KiF5B-based vesicular transport to the maintenance of Nav in mature neurons was not directly assessed, but this appears likely since KiF5B maintains an axonal transport activity in mature neurons (Xu et al., 2010; Barry et al., 2014) and because AnkG is necessary for the maintenance of the AIS and Nav density (Hedstrom et al., 2008). Altogether, these studies suggest that early Nav-AnkG association in the ER and further cargo transport mediated by axonal-specific motors is an important determinant of Nav polarized expression (**Figure 3A**).

How the Nav-AnkG complexes get disattached from KiF5B and inserted in the plasma membrane at specific locations remains unknown (Jones and Svitkina, 2016). The interaction of Navs with AnkG is promoted by phosphorylation of their

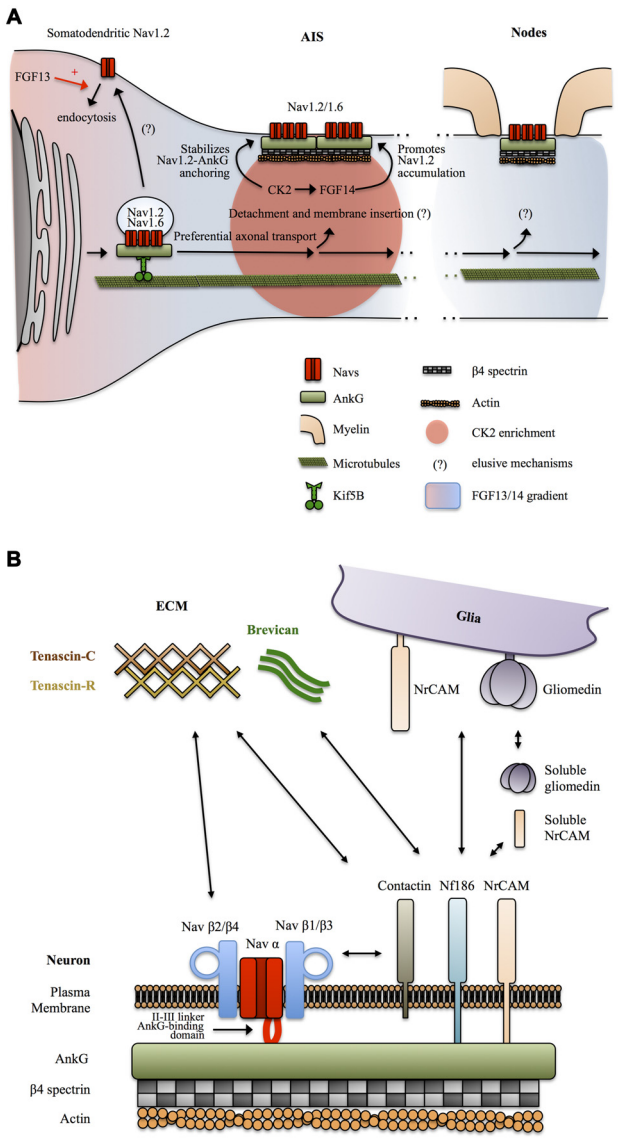

FIGURE 3 | Mechanisms targeting Nav channels to the axon.
(A) Preferential axonal transport and membrane insertion. Nav1.2, and presumably Nav1.6, are preferentially transported to the axonal domain by Kif5B. This is mediated by ankyrin-G (AnkG) which acts as a cargo adaptor. Casein kinase 2 (CK2) concentrates at the AIS following Nav channels enrichment and stabilizes the anchoring of Nav1.2 by phosphorylating their AnkG-binding domain. A somatodendritic-axonal gradient of fibroblast growth factor 13 (FGF13) and FGF14 participates in defining a polarized distribution of Nav1.2. FGF13 increases the endocytosis of Nav1.2 whereas FGF14 promotes their accumulation at the level of the AIS in a CK2-dependent manner. **(B)** Anchoring partners of Nav channels. β auxiliary subunits support Nav subcellular localization and surface expression stability by mediating multiple interactions with neuronal and glial transmembrane proteins but also components of the extracellular matrix (ECM).

AnkG-binding domain by casein kinase 2 (CK2) which is enriched at the level of the AIS and nodes of Ranvier (Bréchet et al., 2008; Brachet et al., 2010). CK2 binds to the II-III intracellular loop of Navs. It was suggested that the enrichment of CK2 at the level of the AIS is actually a consequence of the dense concentration of Navs in this region (Hien et al., 2014). Non-canonical fibroblast growth factors (also called fibroblast growth factor homologous factors or intracellular fibroblast growth factor) FGF13 and FGF14 have recently been shown to be differentially expressed in hippocampal neurons in cultures and to be able to interact with the C-terminal domain of Nav1.2 channels. FGF13 promotes somatodendritic Nav1.2 channel endocytosis whereas FGF14 leads to their accumulation at the AIS (Pablo et al., 2016; **Figure 3A**). CK2 activity is required for the interaction between FGF14 and Nav1.2/Nav1.6 channels and also modulates Nav1.6 currents (Hsu et al., 2016). Interestingly, FGF14 is a target of Glycogen Synthase Kinase 3 (GSK3), an enzyme critically involved in neuronal polarity (Gärtner et al., 2006; Shavkunov et al., 2013). Altogether, these results indicate that Nav appearance at the AIS and in the somatodendritic domain is followed by post-translational mechanisms that stabilize Nav-AnkG complexes, maturate Nav kinetics and promote elimination of somatodendritic Navs, leading to further refinement of the polarized Navs distribution.

Sodium channels are also composed of transmembrane β subunits that associate with α subunits by covalent or non-covalent bonds and regulate surface expression and kinetics of Nav α subunits (Namadurai et al., 2015). Four β subunits β1, β2, β3 and β4 have been identified, with further complexity added by alternative splicing of β1 (Namadurai et al., 2015). These β subunits are structurally very close to the family of Cell Adhesions Molecules (CAMs; Srinivasan et al., 1998; Catterall, 2000; Chopra et al., 2007) and thus can link Nav channels with the extracellular space and mediate interactions with components of the ECM and with glia membrane proteins. β2 subunits are structurally close to the neurally expressed cell-adhesion protein contactin and can, like contactin, interact with tenascin C and R, proteins of the ECM, and promote surface expression of Nav1.2 (Srinivasan et al., 1998). Contactin has also been reported to directly bind Nav β1 and to co-localize with it at nodes in the CNS, during development, but also in the adult brain (Kazarinova-Noyes et al., 2001). The exact subcellular distribution and functions of tenascin C and R at the level of axonal domains are unknown. Tenascin C seems to be preferentially expressed during development, whereas tenascin R is also expressed during adulthood, both in an overall uniform extracellular manner (Gaal et al., 2015; Giblin and Midwood, 2015). One possibility is that tenascin C and R promote Nav channels, especially Nav1.2, surface expression during development and later in mature neurons define the uniform distribution of Nav1.2 in unmyelinated axons and unmyelinated tracks of myelinated axons. Overall, the composition of the ECM and its functional relevance is a relatively novel focus of research and definitive conclusions are still lacking. Clustering of Nav channels at mature AIS and nodes of Ranvier and perhaps as well in unmyelinated axons is most likely mediated by other CAMs. Indeed, Nav β1 and β3 subunits associate with NF186 (Ratcliffe et al., 2001), and NrCAM (McEwen and Isom, 2004) two CAMs expressed by neurons at the level of the AIS and nodes of Ranvier and

possessing an AnkG-binding intracellular domain (Hedstrom et al., 2007). Neuronal NrCAM and NF186 in turn interact with glia-expressed NrCAM and gliomedin (Feinberg et al., 2010). In addition NrCAM and gliomedin can be secreted in a cleaved soluble form by glia (Feinberg et al., 2010). Complex heterophilic and homophilic interactions of both NrCAM (Mauro et al., 1992) and NF186 (Liu et al., 2011) make the exact interaction mechanisms difficult to address, but it appears that multiple interactions between glia and neuronal cell adhesion molecules regulate the clustering of Nav channels at the level of the AIS and nodes of Ranvier trough binding of their β1 and β3 subunits with NF186 and NrCAM and further coupling to AnkG and βIV spectrin-associated actin cytoskeleton (Feinberg et al., 2010). In addition, NF186 interacts with ECM proteins enriched at the level of the AIS and nodes of Ranvier such as the microglia and astrocytes secreted protein brevican (Hedstrom et al., 2007; **Figure 3B**).

Kv Channels

Axonal Kv channels perform several functions such as restricting the propagation of excitation, regulating APs threshold, determining the temporal sharpness of APs generation, enhancing Nav channels availability during repetitive firing and control APs width and subsequent neurotransmitter release (Trimmer, 2015). In this review article, we will focus on Kv1, critical regulators of axonal excitability enriched at the level of the AIS and juxta-paranodes (JXPN) of myelinated axons (**Figures 1**, **4**), which have been extensively studied and exhibit axonal targeting mechanisms that differ from Nav channels.

The Voltage-Gated Kv1 Channel

Distribution of Kv1 channel in the axon

Various distributions of Kv1 α subunits have been reported in the literature and may vary depending on cell types, dynamic regulatory states but also by sample preparation itself, which has been shown to determine the extent of Kv1 labeling (Trimmer, 2015). Kv1.1 and Kv1.2 are prominently found at the distal AIS of multiple neuronal types and at JXPN in myelinated axonal fibers (Rasband et al., 2001; Poliak et al., 2003; Inda et al., 2006; Kole et al., 2007; Van Wart et al., 2007; Ogawa and Rasband, 2008; Ogawa et al., 2010; Duflocq et al., 2011). At the AIS, Kv1.1 and Kv1.2 expression overlaps with those of Nav1.6 channels (Inda et al., 2006; Kole et al., 2007; Van Wart et al., 2007; Lorincz and Nusser, 2008; Duflocq et al., 2011). The picture for Kv1.4 is less clear. They seem to be preferentially localized at presynapses (Trimmer, 2015) even though they have been shown to co-localize with Kv1.1 and Kv1.2 at the level of the AIS (Ogawa and Rasband, 2008) and to be punctually found at JXPN (Rasband et al., 2001). Kv1.4 channels do not show a strong axonal targeting signal and their expression at the level of the AIS and JXPN might depend on its assembly in Kv1.2-subunit-containing heteromers (Manganas and Trimmer, 2000; Jenkins et al., 2011). Kv1.1 and Kv1.2 mediate low-threshold, slow delayed rectifier currents (Higgs and Spain, 2011) whereas Kv1.4 mediates a fast activating and fast inactivating A-type current (Carrasquillo et al., 2012). The differences between Kv1.1/1.2 and Kv1.4 and the apparent higher association of Kv1.1/1.2 with advanced excitability-related characteristics such as Nav1.6-based AIS and saltatory conduction trough nodes of Ranvier can be explained by the fact that Kv1.4 seems to be an evolutionary ancient member of the Kv1 family (Huang et al., 2014). Finally, heteromeric assembly of Kv1 subunits and β subunits determine the surface expression, subcellular distribution (Li et al., 2000; Manganas and Trimmer, 2000; Jenkins et al., 2011) and kinetics properties of Kv1 complexes (Guan et al., 2006). Kv1.1 and Kv1.2 are highly co-localized at the AIS and nodes of Ranvier, suggesting that the functionally relevant Kv1 complexes in these locations are composed of Kv1.1 and Kv1.2 heteromers, possibly also including Kv1.4 subunits (**Figures 1**, **4**).

Targeting Kv1 to the axon

Kv1 channels appear much later in the axon during development as compared to Nav-AnkG complexes (Gu et al., 2006) and Kv1 α subunits do not contain an AnkG binding domain, relying therefore on different mechanisms than Nav channels for their proper axonal targeting.

Various mechanisms have been shown to promote ER exit and surface expression of Kv1 channels (Lai and Jan, 2006). Interestingly, Kv1 exhibit subunit-dependent trafficking properties. Kv1.1 is mostly ER-retained, Kv1.4 is strongly surface expressed but lacks a specific axonal targeting signal whereas Kv1.2 is intermediate, equally ER retained and surface expressed but has the highest specificity for the axonal domain and its surface expression is strongly dependent on co-expression of the Kvβ2 subunit (Li et al., 2000; Manganas and Trimmer, 2000; Tiffany et al., 2000; Manganas et al., 2001; Campomanes et al., 2002; Gu et al., 2003; Jenkins et al., 2011). In neurons, functionally expressed Kv1 channels complexes are mostly, if not all, formed of heteromers that are assembled early in the ER (Shi et al., 1996; Manganas and Trimmer, 2000; Manganas et al., 2001). Thus, enrichment of Kv1 at different subcellular localizations of the axon can be the result of Kv1 α subunits heteromeric assembly combining the ER exit signal from Kv1.4, the axonal targeting signal from Kv1.2 and an unclear role of Kv1.1. In addition, Kv1.4 could further enhance surface expression of Kv1 heteromers by molecularly masking the ER retention signals of the other Kv1 subunits following tetramerization (Manganas and Trimmer, 2000).

Even though Kv α subunits can assemble into functional channels, Kv1 channels *in vivo* are composed of transmembrane Kv α subunits and cytosolic Kvβ subunits, associated in a stoichiometric manner with 4 α subunits—4 β subunits (Pongs and Schwarz, 2010). Kv α and β subunits are assembled early during biosynthesis in the ER (Nagaya and Papazian, 1997) by direct interaction of Kvβ subunits with the T1 tetramerization domain of Kv α subunits (Long et al., 2005). Kvβ subunits greatly extend the intracellular domain of Kv1 channels and provide an interface for intracellular protein binding (Pongs and Schwarz, 2010). They have multiple effects on Kv1 α subunits including regulation of intracellular trafficking, inactivation properties and kinetics (Pongs and Schwarz, 2010). Four Kvβ subunits

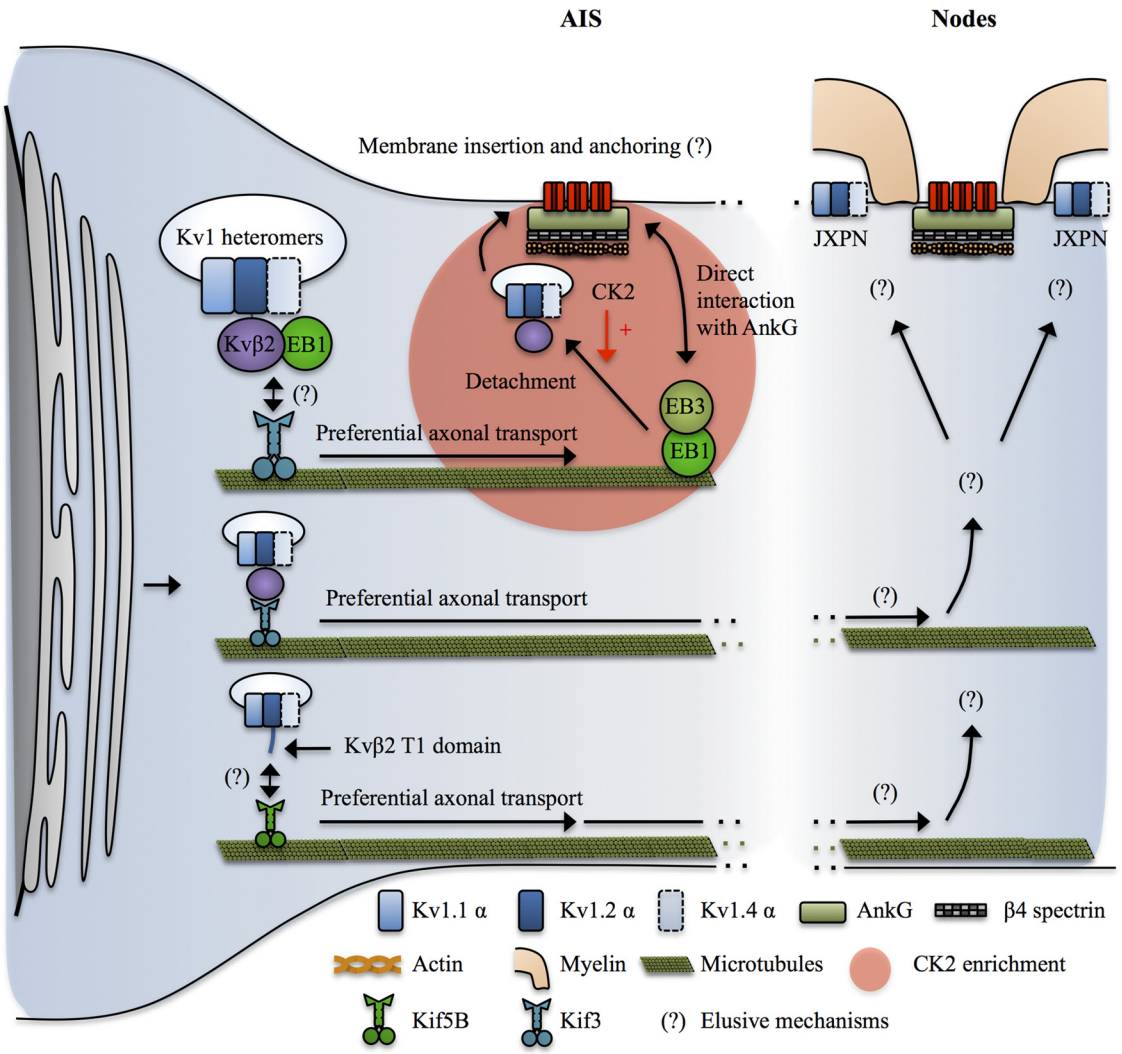

FIGURE 4 | Mechanisms targeting Kv1 channels to the axon. Kvβ2 mediates the axonal targeting of Kv1.2 and Kv1.2-containing heteromers by acting as a cargo adaptor, or a binding partner for an undetermined cargo adaptator for Kif3. Kif3 preferentially transports the Kv1.2/Kvβ2-containing complexes to the axon by a mechanism that requires EB1 in a yet unclear manner. At the level of the AIS, EB1 and EB3 form a complex that interacts with both microtubules and AnkG and possibly acts as a stop signal for the Kv1.2/Kvβ2-containing vesicles. CK2 then leads to release of the vesicle from the microtubules by phosphorylating Kvβ2 which causes its unbinding from EB1. How do the Kv1-containing vesicles recognize their destination site in distal axons and in nodal regions is not known. In addition, the mechanisms by which Kv1 channels get restricted to the juxta-paranodes (JXPN) remains elusive except for an important role of myelin and glial cells. In parallel Kif5B has also been implicated in transporting Kv1.1, Kv1.2 and Kv1.4 to the axon in a mechanism involving the T1 domain, possibly reflecting a similar cargo adaptor role of Kvβ2 interacting with Kv1.2 in this process.

have been identified, Kvβ1, Kvβ2, Kvβ3 and Kvβ4. Kvβ2 is the predominantly expressed isoform in the brain (Pongs and Schwarz, 2010) and seems to preferentially associate to Kv1.2 (Campomanes et al., 2002; Pongs and Schwarz, 2010).

Over the past 20 years, several studies have revealed that Kvβ2 and its interaction with Kv1.2 is a key upstream determinant of axonal targeting of Kv1 channels. As outlined above, Kv1.2 has a stronger axonal targeting signal than Kv1.1 and Kv1.4 (Gu et al., 2003; Jenkins et al., 2011). The axonal targeting of Kv1.2 and Kv1.2-containing Kv1 heteromers depends on the T1 tetramerization domain, but by a mechanism independent from the proper tetramerization of Kv1 α subunits (Gu et al., 2003). Kvβ2 knockout mice exhibit axon excitability-related impairments such as seizures and tremors (Connor et al., 2005). Kvβ2 subunits are expressed before Kv1 α subunits during development (Gu et al., 2003, 2006; Vacher et al., 2011) and Kvβ2 is required for the proper axonal targeting of Kv1.2 and Kv1.2-containing heteromers (Campomanes et al., 2002; Gu et al., 2006). Kvβ2 acts as a cargo adaptor, or a binding partner for a yet unidentified cargo adaptor, to link Kv1.2 and Kv1.2-containing heteromers with KiF3/kinesin II (Gu et al., 2006). Kvβ2/KiF3 mediated axonal targeting of Kv1.2 was dependent on the plus end tracking protein EB1. Indeed, EB1 and Kvβ2 were shown to be associated and to move together along the axon

in live-imaging (Gu et al., 2006). The exact role of EB1 was not directly assessed but it could reflect the fact that Kvβ2-Kv1.2 cargos are tethered on short microtubules polymers by EB1, which are subsequently transported by KiF3 moving along stable, long microtubules (Dent and Baas, 2014). Another possibility is that EB1 is important to signal to the KiF3-Kv1 complex that they reached destination. Indeed, it was shown that EB1 and EB3 interact with AnkG and stabilize both the AIS and microtubules, suggesting that they participate in establishing stable microtubules routes leading to the AIS (Leterrier et al., 2011). Consequently, AIS-enriched kinases such as CK2 would lead to detachment of the cargo vesicle from EB1 and the microtubules (Vacher et al., 2011) prior to membrane insertion. Note that this mechanism can explain the enrichment of Kv1 at the AIS, where Kv1.1, 1.2 and 1.4 colocalize with Nav channels, but at first sight it cannot apply in the nodal region where AnkG-Nav complexes and Kv1 are segregated in different regions, the node and the JXPN respectively. In parallel, KiF5B/kinesin I has been implicated in mediating the axonal transport of Kv1.1, 1.2 and 1.4 (Rivera et al., 2007; **Figure 4**).

Finally, the complete mechanisms leading to release of Kv1-containing cargoes at specific locations along the axon, particularly in the nodal regions, and their tethering and stabilization at the plasma membrane are not yet understood (**Figure 4**). Conflicting results have been reported in the literature and the mechanisms might vary between the AIS and the distal myelinated parts, and also between the CNS and the PNS and furthermore among cell types (Buffington and Rasband, 2011; Vacher and Trimmer, 2012; Buttermore et al., 2013; Chang and Rasband, 2013; Trimmer, 2015; Jones and Svitkina, 2016). In addition, the deciphering of nodal Kv1 targeting mechanisms is hampered by the difficulty to properly stain its various molecular partners, possibly reflecting the intense crowding of interacting molecules in these areas (Buffington and Rasband, 2011; Trimmer, 2015). However, the restriction of Kv1 expression at the level of the JXPN appears to critically depend upon myelination and on the integrity of the boundaries formed by the paranodal domain and glia-neuron septate junctions (Boyle et al., 2001; Ishibashi et al., 2002; Poliak et al., 2003; Traka et al., 2003).

The Voltage-Gated Kv2 Channel

Two isoforms of Kv2 channels exist, Kv2.1 and Kv2.2 (Trimmer, 2015). Kv2.1 has been recently studied at the level of the AIS of various neurons, including hippocampal principal cells and interneurons, where they form clusters devoid of AnkG staining and segregated from Nav1.6 and Kv1.2 (Johnston et al., 2008; Sarmiere et al., 2008; King et al., 2014; Kirizs et al., 2014). Kv2.1 clusters are distributed relatively uniformly along the AIS but show a different phosphorylation profile in the somatodendritic and proximal AIS as compared with the distal, Nav1.6- and Kv1-enriched, AIS (King et al., 2014) suggesting compartmentalization of their function between these two domains. They associate with cisternal organelles in close vicinity of GABAergic synapses, suggesting that they are implicated in mediating perisomatic inhibition induced changes in axonal excitability (King et al., 2014). In terms of number, Kv2.1 is predominant in the somatodendritic domain (see above). Kv2.2 has been reported to be concentrated at the level of the AIS of MNTB neurons but in a non-clustered distribution, and to support the high frequency firing typical of these neurons (Johnston et al., 2008). Kv2.2 channels have so far not been extensively studied.

Changes in functional distribution of axonal Nav and Kv1 channels in physiological contexts

Mechanisms determining the precise patterning of Nav and Kv1 channels at excitable domains of the axon such as the AIS and nodal regions are tightly intermingled with those defining the organization of these structures. Thus, changes in Nav and Kv1 functional distributions in the axon are mostly related to the reorganization of the AIS and nodes of Ranvier (Normand and Rasband, 2015; Yamada and Kuba, 2016).

The plasticity of axonal excitable domains is a relatively recently appreciated phenomenon (Ford et al., 2015; Yamada and Kuba, 2016). The AIS is indeed a highly dynamic structure and both its length (and the corresponding number of Nav and Kv channels) and its relative position to the soma can be modulated in an activity-dependent manner (Grubb et al., 2011; Yamada and Kuba, 2016). These changes strongly affect the excitability of neurons (Yamada and Kuba, 2016). This plasticity of the AIS allows neurons to finely adjust their firing according to their excitatory and inhibitory inputs in physiological but also in pathological conditions (Grubb et al., 2011; Yamada and Kuba, 2016).

Also the composition and functional state of VGCs within the AIS can be subject to modulation. In the avian cochlear nucleus, an enlargement of the AIS following experimental deprivation of auditory inputs is accompanied by a decrease in Kv1 channels, further increasing neuronal excitability (Kuba et al., 2015). Moreover, chronic depolarization of dentate gyrus granule cells induces both AIS shortening and dephosphorylation of Nav channels, with opposite effects on cells excitability (Evans et al., 2015). Recent evidence suggests that nodes of Ranvier are similarly subject to activity dependent changes of their structural and molecular properties (Ford et al., 2015).

Thus, contrary to what was assumed for a long time, excitable domains of axons and the polarized functional distribution of VGCs in these subcellular compartments are highly plastic and further support the elaborated electrogenic properties of neurons and the robust homeostatic balancing abilities of brain networks. The mechanisms involved in these phenomena are only starting to be explored and are likely a result of a complex cross-talk between genetic programs, cell to cell adhesion signals and activity-dependent calcium pathways (Grubb et al., 2011; Susuki and Kuba, 2016; Yamada and Kuba, 2016).

Alterations in Nav and Kv channels polarity in pathological conditions

As mentioned above, trafficking and targeting of VGCs are crucial phenomena ensuring a correct processing and integration of electrical signals. Functional alterations or mislocalization of ion channels might thus deeply change the computational

properties of a neuron explaining why ion channels deregulations have been observed in several pathologies.

A significant number of studies associate Kv4.2 channels with epilepsy (Bernard et al., 2004; Lugo et al., 2008; Monaghan et al., 2008). Kv4.2-mediated A-type current in CA1 pyramidal cells is reduced after brain injury, most likely explaining the neuronal hyperexcitability observed in epileptic brain (Bernard et al., 2004). In a pilocarpine-induced model of temporal lobe epilepsy the expression pattern of Kv4.2 as well as KChIP2 was altered in response to seizure. The relatively uniform distribution along dendrites of dentate granule cells was shifted to the distal part of the dendrite, whereas the expression of both proteins was deeply reduced along the CA1 pyramidal cells (Monaghan et al., 2008). However, mechanisms underlying the redistribution of the channel along dendrites in pathology are not yet known. The dynamic changes of Kv4.2 channel and its accessory subunits after seizure seem to be a complex phenomenon. In another study from Su et al. (2008) lithium-pilocarpine induced seizures first upregulated the expression of Kv4.2 and KChIP1 along the dendrites of CA1 pyramidal cells, whereas the chronic period was associated with a downregulation of the Kv complex. Traumatic brain injury, a factor associated with the development of epilepsy, also has been shown to diminish Kv4.2 channel expression as well as the Ia current in CA1 pyramidal cells for several weeks after injury (Lei et al., 2012). Determining precisely if and how trafficking or internalization of the Kv4.2 channels at the surface membrane is affected in epilepsy could provide further hints for the understanding of the establishment of the proximodistal gradient.

Ion channel auxiliary subunits seem to be critical for the development of pathologies. Indeed, the Kv2.1 channel auxiliary subunit AMIGO has been shown to be an integral part of the Kv2.1 channel complex (Peltola et al., 2011), and knockout of the AMIGO-encoding gene leads to reduced whole-brain expression of the Kv2.1 channel (Peltola et al., 2016). AMIGO knockout animals display electrophysiological and behavioral features similar to those observed in schizophrenia (Peltola et al., 2016). Interestingly, recent work also points to the involvement of the Kv2.1 channel in the hyperexcitability observed in a mouse model of Alzheimer's disease (Frazzini et al., 2016). In this model, activation of glutamate receptors leads to the overproduction of Reactive Oxygen Species (ROS) promoting clusterization of Kv2.1 channels in hippocampal neurons. The increase of non-conducting, clustered, Kv2.1 channels makes cells more excitable by changing their firing behavior normally controlled by single Kv2.1 channels (Frazzini et al., 2016).

Within the past decade, the auxiliary subunit DPP6, also called DPPX, has been associated with encephalitis (Boronat et al., 2013; Piepgras et al., 2015). A report from Boronat et al. (2013) has found that patients with encephalitis accompanied by seizure display an autoimmune disorder characterized by the production of anti-DPPX antibodies (Boronat et al., 2013). The altered expression of the auxiliary subunit DPPX caused by the autoimmune reaction could explain the development of seizures on these patients suffering from encephalitis.

Even though alteration of surface localization of ion channels has been mainly associated with pathophysiological conditions, it also has been reported that Kv2.1 channel modulation might underlie neuroprotective mechanisms during ischemia (Misonou et al., 2004, 2005a, 2006, 2008). Kainate-induced seizures induce the redistribution of Kv2.1 channels from clusters to a diffuse single-channel localization along the plasma membrane of pyramidal neurons (Misonou et al., 2004). This declusterization occurs upon calcium influx-mediated activation of calcineurin that dephosphorylates two serine residues (S563 and S603; **Figure 2C**) of Kv2.1 channels (Misonou et al., 2004). During brain hypoxia/ischemia, calcineurin-dependent dephosphorylation of non-conductive Kv2.1 channel (Misonou et al., 2005a) releases them from clusters, providing a quick and adaptive mechanism allowing neuron to suppress hyperexcitability caused by brain injury (Misonou et al., 2005a), a process that appears to be dependent on neuroglia interaction (Misonou et al., 2008). This potential neuroprotective effect of Kv2.1 channel declustering in the regulation of membrane excitability has been shown to be bidirectional, as suppression of neuronal activity potentiate Kv2.1 phosphorylation and cluster formation (Misonou et al., 2006). Activity-dependent regulation of Kv2.1 channel organization at the plasma membrane level is an excellent example of how ion channel localization might be a crucial component determining the computational properties of a neuron, and how dynamic regulation of channels at the surface is an key mechanism that allows the cell to adapt to its environment.

In pathological contexts, altering the proper distribution and function of Nav and Kv channels in axons has multiple effects on axonal excitability and nervous system function. It is generally difficult to segregate the functional impact of alterations of VGCs localized at the level of nodal regions from those at the level of the AIS because of redundancy in the targeting mechanisms of these channels in these subcellular compartments, as noted previously. In other words, impairment of proper functional expression of VGCs at AIS are often paralleled by defects of the channels at nodes of Ranvier, and reciprocally (Arancibia-Carcamo and Attwell, 2014).

Typically, disrupting Nav channels enrichment and clustering at the AIS and nodes leads to hypoexcitability responsible for various cognitive disorders such as schizophrenia, depression, bipolar disorders and autism (Buffington and Rasband, 2011; Arancibia-Carcamo and Attwell, 2014; Normand and Rasband, 2015; Griggs et al., 2017). In addition, and correlating with the predominant localization of Nav1.1 in the AIS of GABAergic neurons (Ogiwara et al., 2007; Lorincz and Nusser, 2008; Catterall et al., 2010; Tian et al., 2014), the loss of proper localization and function of Nav1.1 is considered to be a factor for the onset of epilepsy caused by a disruption of the inhibitory balance in the brain (Catterall et al., 2010).

The impact of abnormal Kv distribution, particularly Kv1 channels, can lead to failure of axonal conduction because of their stabilizing effects on membrane potential and their effects

on Nav channels availability (Trimmer, 2015). In parallel, it is often associated with hyperexcitability syndroms such as epilepsy and ataxia (Buffington and Rasband, 2011; Arancibia-Carcamo and Attwell, 2014; Trimmer, 2015).

Disruption of AIS and nodal structures and proper Nav and Kv localization along the axon is also a hallmark of neurodegenerative diseases such as multiple sclerosis, and axonal injury (Smith, 2007; Buffington and Rasband, 2011; Arancibia-Carcamo and Attwell, 2014; Normand and Rasband, 2015; Griggs et al., 2017). At the nodes of Ranvier, loss of Nav1.2 and Nav1.6 clustering are hallmarks of axonal degeneration (Smith, 2007). In addition, Nav1.2 and Nav1.6 spread expression and up-regulated activity can lead to further axonal damage. Indeed, the increased entry of sodium in the challenged axon can reverse the activity of Na+/Ca2+ exchangers, which will cause toxic accumulation of calcium in the cytoplasm (Smith, 2007).

Multiple pathological mechanisms can lead to impairment of normal AIS and nodes organization and the functional distribution of Nav and Kv channels along the axon (Buffington and Rasband, 2011; Normand and Rasband, 2015; Clark et al., 2016; Griggs et al., 2017). Mutations affecting the cytoskeletal organization typical of these structures, notably AnkG are implicated in a broad range of cognitive disorders (Normand and Rasband, 2015). Altered functions of proteins mediating cell to cell adhesion signaling at the level of the AIS and nodal regions such as Caspr2, but also deficits in myelination in general, are other important pathological factors (Buffington and Rasband, 2011; Arancibia-Carcamo and Attwell, 2014; Griggs et al., 2017). Also auto-immune inflammatory responses can lead to proteolysis of Navs, Kvs and AIS and node components (Griggs et al., 2017).

Finally, in parallel to the identification of β subunits as important regulators of Nav channels targeting and conductance, β subunits are increasingly implicated in Nav channelopathies and emerge as novel pharmacological targets (O'Malley and Isom, 2015). The role of Kv1 β subunits in diseases is less studied than for Nav channels but loss-of-function mutations of Kv1 β2 has been described as an important risk factor for epilepsy (Villa and Combi, 2016).

CONCLUDING REMARKS

Proper expression, segregated distribution and the functional state of Nav and Kv channel isoforms at axonal and somatodendritic domains, and within its subcellular compartments, are critical determinants of the electrogenic properties of a neuron as illustrated by the multiple pathologies associated with Nav and Kv channels (Smith, 2007; Mantegazza et al., 2010; Catterall, 2012; Savio-Galimberti et al., 2012; Shah and Aizenman, 2014; O'Malley and Isom, 2015; Kruger and Isom, 2016; Villa and Combi, 2016). The contribution of their multiple isoforms within single neurons but also among cell types remains to be elucidated (Vacher et al., 2008; Narayanan and Johnston, 2012; Nusser, 2012; Trimmer, 2015). It will also be interesting to determine how the Nav and Kv channel isoforms expression and functional distribution are selected by cell fate and environment and if common rules exist between channel expression, firing properties and neuronal function (Nusser, 2012).

As illustrated in this review article, the mechanisms leading to the multi-layered polarized organization of neuronal VGCs are complex and comprise regulation of biosynthesis, intracellular trafficking, surface expression and biophysical properties. The trafficking pathways mediating the transport of newly synthesized Nav and Kv channels to their specific neuronal compartments are only starting to be unraveled (Gasser et al., 2012; Su et al., 2013; Barry et al., 2014; Akin et al., 2015). In addition, the signaling pathways mediating the detachment of the cargo vesicles from the cytoskeletal tracks and subsequent membrane insertion at specific locations are mostly unknown (Jones and Svitkina, 2016). However, the principles underlying the distribution and targeting of Nav and Kv channels might help us to unravel the mechanisms of polarized distribution of the many other ion channels present in axons and dendrites.

AUTHOR CONTRIBUTIONS

All authors contributed to the conception, drafting and critical revision of the article.

ACKNOWLEDGMENTS

Supported by the WGL (Pakt f. Forschung 2015), LIN (LIN Special Project), DFG Kr1879 5-1 7 6-1, SFB TPB8, BMBF "Energi"FKZ: 01GQ1421B and EU-JPND - STAD. The publication of this article was funded by the Open Access fund of the Leibniz Association.

REFERENCES

Adams, J. P., Anderson, A. E., Varga, A. W., Dineley, K. T., Cook, R. G., Pfaffinger, P. J., et al. (2000). The A-type potassium channel Kv4.2 is a substrate for the mitogen-activated protein kinase ERK. *J. Neurochem.* 75, 2277–2287. doi: 10.1046/j.1471-4159.2000.0752277.x

Akin, E. J., Solé, L., Dib-Hajj, S. D., Waxman, S. G., and Tamkun, M. M. (2015). Preferential targeting of $Na_v1.6$ voltage-gated Na^+ Channels to the axon initial segment during development. *PLoS One* 10:e0124397. doi: 10.1371/journal.pone.0124397

Akin, E. J., Solé, L., Johnson, B., Beheiry, M. E., Masson, J.-B., Krapf, D., et al. (2016). Single-molecule imaging of $Na_v1.6$ on the surface of hippocampal neurons reveals somatic nanoclusters. *Biophys. J.* 111, 1235–1247. doi: 10.1016/j.bpj.2016.08.016

An, W. F., Bowlby, M. R., Betty, M., Cao, J., Ling, H. P., Mendoza, G., et al. (2000). Modulation of A-type potassium channels by a family of calcium sensors. *Nature* 403, 553–556. doi: 10.1038/35000592

Anderson, A. E., Adams, J. P., Qian, Y., Cook, R. G., Pfaffinger, P. J., and Sweatt, J. D. (2000). Kv4.2 phosphorylation by cyclic AMP-dependent protein kinase. *J. Biol. Chem.* 275, 5337–5346. doi: 10.1074/jbc.275.8.5337

Antonucci, D. E., Lim, S. T., Vassanelli, S., and Trimmer, J. S. (2001). Dynamic localization and clustering of dendritic Kv2.1 voltage-dependent potassium

channels in developing hippocampal neurons. *Neuroscience* 108, 69–81. doi: 10.1016/s0306-4522(01)00476-6

Arancibia-Carcamo, I. L., and Attwell, D. (2014). The node of Ranvier in CNS pathology. *Acta Neuropathol.* 128, 161–175. doi: 10.1007/s00401-014-1305-z

Bähring, R., Dannenberg, J., Peters, H. C., Leicher, T., Pongs, O., and Isbrandt, D. (2001). Conserved Kv4 N-terminal domain critical for effects of Kv channel-interacting protein 2.2 on channel expression and gating. *J. Biol. Chem.* 276, 23888–23894. doi: 10.1074/jbc.m101320200

Bao, L. (2015). Trafficking regulates the subcellular distribution of voltage-gated sodium channels in primary sensory neurons. *Mol. Pain* 11:61. doi: 10.1186/s12990-015-0065-7

Barry, J., Gu, Y., Jukkola, P., O'Neill, B., Gu, H., Mohler, P. J., et al. (2014). Ankyrin-G directly binds to kinesin-1 to transport voltage-gated Na^+ channels into axons. *Dev. Cell* 28, 117–131. doi: 10.1016/j.devcel.2013.11.023

Beck, H., and Yaari, Y. (2008). Plasticity of intrinsic neuronal properties in CNS disorders. *Nat. Rev. Neurosci.* 9, 357–369. doi: 10.1038/nrn2371

Bernard, C., Anderson, A., Becker, A., Poolos, N. P., Beck, H., and Johnston, D. (2004). Acquired dendritic channelopathy in temporal lobe epilepsy. *Science* 305, 532–535. doi: 10.1126/science.1097065

Black, J. A., Renganathan, M., and Waxman, S. G. (2002). Sodium channel $Na_v1.6$ is expressed along nonmyelinated axons and it contributes to conduction. *Mol. Brain Res.* 105, 19–28. doi: 10.1016/s0169-328x(02)00385-6

Boiko, T., Rasband, M. N., Levinson, S. R., Caldwell, J. H., Mandel, G., Trimmer, J. S., et al. (2001). Compact myelin dictates the differential targeting of two sodium channel isoforms in the same axon. *Neuron* 30, 91–104. doi: 10.1016/s0896-6273(01)00265-3

Boiko, T., Van Wart, A., Caldwell, J. H., Levinson, S. R., Trimmer, J. S., and Matthews, G. (2003). Functional specialization of the axon initial segment by isoform-specific sodium channel targeting. *J. Neurosci.* 23, 2306–2313.

Boronat, A., Gelfand, J. M., Gresa-Arribas, N., Jeong, H.-Y., Walsh, M., Roberts, K., et al. (2013). Encephalitis and antibodies to dipeptidyl-peptidase-like protein-6, a subunit of Kv4.2 potassium channels. *Ann. Neurol.* 73, 120–128. doi: 10.1002/ana.23756

Boyle, M. E., Berglund, E. O., Murai, K. K., Weber, L., Peles, E., and Ranscht, B. (2001). Contactin orchestrates assembly of the septate-like junctions at the paranode in myelinated peripheral nerve. *Neuron* 30, 385–397. doi: 10.1016/s0896-6273(01)00296-3

Brachet, A., Leterrier, C., Irondelle, M., Fache, M.-P., Racine, V., Sibarita, J.-B., et al. (2010). Ankyrin G restricts ion channel diffusion at the axonal initial segment before the establishment of the diffusion barrier. *J. Cell Biol.* 191, 383–395. doi: 10.1083/jcb.201003042

Bréchet, A., Fache, M.-P., Brachet, A., Ferracci, G., Baude, A., Irondelle, M., et al. (2008). Protein kinase CK2 contributes to the organization of sodium channels in axonal membranes by regulating their interactions with ankyrin G. *J. Cell Biol.* 183, 1101–1114. doi: 10.1083/jcb.200805169

Brette, R. (2013). Sharpness of spike initiation in neurons explained by compartmentalization. *PLoS Comput. Biol.* 9:e1003338. doi: 10.1371/journal.pcbi.1003338

Buffington, S. A., and Rasband, M. N. (2011). The axon initial segment in nervous system disease and injury. *Eur. J. Neurosci.* 34, 1609–1619. doi: 10.1111/j.1460-9568.2011.07875.x

Burbidge, S. A., Dale, T. J., Powell, A. J., Whitaker, W. R. J., Xie, X. M., Romanos, M. A., et al. (2002). Molecular cloning, distribution and functional analysis of the $NA_V1.6$. Voltage-gated sodium channel from human brain. *Mol. Brain Res.* 103, 80–90. doi: 10.1016/s0169-328x(02)00188-2

Buttermore, E. D., Thaxton, C. L., and Bhat, M. A. (2013). Organization and maintenance of molecular domains in myelinated axons. *J. Neurosci. Res.* 91, 603–622. doi: 10.1002/jnr.23197

Caldwell, J. H., Schaller, K. L., Lasher, R. S., Peles, E., and Levinson, S. R. (2000). Sodium channel $Na_v1.6$ is localized at nodes of ranvier, dendrites, and synapses. *Proc. Natl. Acad. Sci. U S A* 97, 5616–5620. doi: 10.1073/pnas.090034797

Campomanes, C. R., Carroll, K. I., Manganas, L. N., Hershberger, M. E., Gong, B., Antonucci, D. E., et al. (2002). Kvβ subunit oxidoreductase activity and Kv1 potassium channel trafficking. *J. Biol. Chem.* 277, 8298–8305. doi: 10.1074/jbc.m110276200

Carrasquillo, Y., Burkhalter, A., and Nerbonne, J. M. (2012). A-type K^+ channels encoded by Kv4.2, Kv4.3 and Kv1.4 differentially regulate intrinsic excitability of cortical pyramidal neurons. *J. Physiol.* 590, 3877–3890. doi: 10.1113/jphysiol.2012.229013

Catterall, W. A. (2000). From ionic currents to molecular mechanisms: the structure and function of voltage-gated sodium channels. *Neuron* 26, 13–25. doi: 10.1016/S0896-6273(00)81133-2

Catterall, W. A. (2012). Voltage-gated sodium channels at 60: structure, function and pathophysiology. *J. Physiol.* 590, 2577–2589. doi: 10.1113/jphysiol.2011.224204

Catterall, W. A., Kalume, F., and Oakley, J. C. (2010). $Na_v1.1$ channels and epilepsy. *J. Physiol.* 588, 1849–1859. doi: 10.1113/jphysiol.2010.187484

Chang, K.-J., and Rasband, M. N. (2013). Excitable domains of myelinated nerves: axon initial segments and nodes of Ranvier. *Curr. Top. Membr.* 72, 159–192. doi: 10.1016/B978-0-12-417027-8.00005-2

Chen, X., and Johnston, D. (2006). Voltage-gated ion channels in dendrites of hippocampal pyramidal neurons. *Pflugers Arch.* 453, 397–401. doi: 10.1007/s00424-006-0097-y

Chen, Y., Yu, F. H., Sharp, E. M., Beacham, D., Scheuer, T., and Catterall, W. A. (2008). Functional properties and differential neuromodulation of $Na_v1.6$ channels. *Mol. Cell. Neurosci.* 38, 607–615. doi: 10.1016/j.mcn.2008.05.009

Chen, X., Yuan, L.-L., Zhao, C., Birnbaum, S. G., Frick, A., Jung, W. E., et al. (2006). Deletion of Kv4.2 gene eliminates dendritic A-type K^+ current and enhances induction of long-term potentiation in hippocampal CA1 pyramidal neurons. *J. Neurosci.* 26, 12143–12151. doi: 10.1523/JNEUROSCI.2667-06.2006

Chopra, S. S., Watanabe, H., Zhong, T. P., and Roden, D. M. (2007). Molecular cloning and analysis of zebrafish voltage-gated sodium channel beta subunit genes: implications for the evolution of electrical signaling in vertebrates. *BMC Evol. Biol.* 7:113. doi: 10.1186/1471-2148-7-113

Chu, P.-J., Rivera, J. F., and Arnold, D. B. (2006). A role for Kif17 in transport of Kv4.2. *J. Biol. Chem.* 281, 365–373. doi: 10.1074/jbc.m508897200

Clark, K. C., Josephson, A., Benusa, S. D., Hartley, R. K., Baer, M., Thummala, S., et al. (2016). Compromised axon initial segment integrity in EAE is preceded by microglial reactivity and contact. *Glia* 64, 1190–1209. doi: 10.1002/glia.22991

Connor, J. X., McCormack, K., Pletsch, A., Gaeta, S., Ganetzky, B., Chiu, S.-Y., et al. (2005). Genetic modifiers of the Kvβ2-null phenotype in mice. *Genes Brain Behav.* 4, 77–88. doi: 10.1111/j.1601-183x.2004.00094.x

Cummins, T. R., Sheets, P. L., and Waxman, S. G. (2007). The roles of sodium channels in nociception: implications for mechanisms of pain. *Pain* 131, 243–257. doi: 10.1016/j.pain.2007.07.026

Dent, E. W., and Baas, P. W. (2014). Microtubules in neurons as information carriers. *J. Neurochem.* 129, 235–239. doi: 10.1111/jnc.12621

Deutsch, E., Weigel, A. V., Akin, E. J., Fox, P., Hansen, G., Haberkorn, C. J., et al. (2012). Kv2.1 cell surface clusters are insertion platforms for ion channel delivery to the plasma membrane. *Mol. Biol. Cell* 23, 2917–2929. doi: 10.1091/mbc.e12-01-0047

Du, J., Haak, L. L., Phillips-Tansey, E., Russell, J. T., and McBain, C. J. (2000). Frequency-dependent regulation of rat hippocampal somato-dendritic excitability by the K^+ channel subunit Kv2.1. *J. Physiol.* 522, 19–31. doi: 10.1111/j.1469-7793.2000.t01-2-00019.xm

Duflocq, A., Chareyre, F., Giovannini, M., Couraud, F., and Davenne, M. (2011). Characterization of the axon initial segment (AIS) of motor neurons and identification of a para-AIS and a juxtapara-AIS, organized by protein 4.1B. *BMC Biol.* 9:66. doi: 10.1186/1741-7007-9-66

Duflocq, A., Le Bras, B., Bullier, E., Couraud, F., and Davenne, M. (2008). $Na_v1.1$ is predominantly expressed in nodes of Ranvier and axon initial segments. *Mol. Cell. Neurosci.* 39, 180–192. doi: 10.1016/j.mcn.2008.06.008

Dulla, C. G., and Huguenard, J. R. (2009). Who let the spikes out? *Nat. Neurosci.* 12, 959–960. doi: 10.1038/nn0809-959

Evans, M. D., Dumitrescu, A. S., Kruijssen, D. L. H., Taylor, S. E., and Grubb, M. S. (2015). Rapid modulation of axon initial segment length influences repetitive spike firing. *Cell Rep.* 13, 1233–1245. doi: 10.1016/j.celrep.2015.09.066

Fache, M.-P., Moussif, A., Fernandes, F., Giraud, P., Garrido, J. J., and Dargent, B. (2004). Endocytotic elimination and domain-selective tethering constitute a potential mechanism of protein segregation at the axonal initial segment. *J. Cell Biol.* 166, 571–578. doi: 10.1083/jcb.200312155

Feinberg, K., Eshed-Eisenbach, Y., Frechter, S., Amor, V., Salomon, D., Sabanay, H., et al. (2010). A glial signal consisting of gliomedin and NrCAM clusters axonal Na^+ channels during the formation of nodes of Ranvier. *Neuron* 65, 490–502. doi: 10.1016/j.neuron.2010.02.004

Feinshreiber, L., Singer-Lahat, D., Ashery, U., and Lotan, I. (2009). Voltage-gated potassium channel as a facilitator of exocytosis. *Ann. N Y Acad. Sci.* 1152, 87–92. doi: 10.1111/j.1749-6632.2008.03997.x

Feinshreiber, L., Singer-Lahat, D., Friedrich, R., Matti, U., Sheinin, A., Yizhar, O., et al. (2010). Non-conducting function of the Kv2.1 channel enables it to recruit vesicles for release in neuroendocrine and nerve cells. *J. Cell Sci.* 123, 1940–1947. doi: 10.1242/jcs.063719

Ford, M. C., Alexandrova, O., Cossell, L., Stange-Marten, A., Sinclair, J., Kopp-Scheinpflug, C., et al. (2015). Tuning of Ranvier node and internode properties in myelinated axons to adjust action potential timing. *Nat. Commun.* 6:8073. doi: 10.1038/ncomms9073

Fourie, C., Li, D., and Montgomery, J. M. (2014). The anchoring protein SAP97 influences the trafficking and localisation of multiple membrane channels. *Biochim. Biophys. Acta* 1838, 589–594. doi: 10.1016/j.bbamem.2013.03.015

Fox, P. D., Haberkorn, C. J., Akin, E. J., Seel, P. J., Krapf, D., and Tamkun, M. M. (2015). Induction of stable ER-plasma-membrane junctions by Kv2.1 potassium channels. *J. Cell Sci.* 128, 2096–2105. doi: 10.1242/jcs.166009

Fox, P. D., Haberkorn, C. J., Weigel, A. V., Higgins, J. L., Akin, E. J., Kennedy, M. J., et al. (2013a). Plasma membrane domains enriched in cortical endoplasmic reticulum function as membrane protein trafficking hubs. *Mol. Biol. Cell* 24, 2703–2713. doi: 10.1091/mbc.E12-12-0895

Fox, P. D., Loftus, R. J., and Tamkun, M. M. (2013b). Regulation of Kv2.1 K^+ conductance by cell surface channel density. *J. Neurosci.* 33, 1259–1270. doi: 10.1523/JNEUROSCI.3008-12.2013

Frazzini, V., Guarnieri, S., Bomba, M., Navarra, R., Morabito, C., Mariggiò, M. A., et al. (2016). Altered Kv2.1 functioning promotes increased excitability in hippocampal neurons of an Alzheimer's disease mouse model. *Cell Death Dis.* 7:e2100. doi: 10.1038/cddis.2016.18

Freeman, S. A., Desmazières, A., Fricker, D., Lubetzki, C., and Sol-Foulon, N. (2016). Mechanisms of sodium channel clustering and its influence on axonal impulse conduction. *Cell. Mol. Life Sci.* 73, 723–735. doi: 10.1007/s00018-015-2081-1

Frick, A., Magee, J., and Johnston, D. (2004). LTP is accompanied by an enhanced local excitability of pyramidal neuron dendrites. *Nat. Neurosci.* 7, 126–135. doi: 10.1038/nn1178

Gaal, B., Jóhannesson, E. Ö., Dattani, A., Magyar, A., Wéber, I., and Matesz, C. (2015). Modification of tenascin-R expression following unilateral labyrinthectomy in rats indicates its possible role in neural plasticity of the vestibular neural circuit. *Neural Regen. Res.* 10, 1463–1470. doi: 10.4103/1673-5374.165517

Gardoni, F., Mauceri, D., Marcello, E., Sala, C., Di Luca, M., and Jeromin, A. (2007). SAP97 directs the localization of Kv4.2 to spines in hippocampal neurons: regulation by CaMKII. *J. Biol. Chem.* 282, 28691–28699. doi: 10.1074/jbc.m701899200

Garrido, J. J., Fernandes, F., Giraud, P., Mouret, I., Pasqualini, E., Fache, M. P., et al. (2001). Identification of an axonal determinant in the C-terminus of the sodium channel $Na_v1.2$. *EMBO J.* 20, 5950–5961. doi: 10.1093/emboj/20.21.5950

Garrido, J. J., Giraud, P., Carlier, E., Fernandes, F., Moussif, A., Fache, M.-P., et al. (2003). A targeting motif involved in sodium channel clustering at the axonal initial segment. *Science* 300, 2091–2094. doi: 10.1126/science.1085167

Gärtner, A., Huang, X., and Hall, A. (2006). Neuronal polarity is regulated by glycogen synthase kinase-3 (GSK-3β) independently of Akt/PKB serine phosphorylation. *J. Cell Sci.* 119, 3927–3934. doi: 10.1242/jcs.03159

Gasser, A., Ho, T. S.-Y., Cheng, X., Chang, K.-J., Waxman, S. G., Rasband, M. N., et al. (2012). An ankyrinG-binding motif is necessary and sufficient for targeting $Na_v1.6$ sodium channels to axon initial segments and nodes of Ranvier. *J. Neurosci.* 32, 7232–7243. doi: 10.1523/JNEUROSCI.5434-11.2012

Giblin, S. P., and Midwood, K. S. (2015). Tenascin-C: form versus function. *Cell Adh. Migr.* 9, 48–82. doi: 10.4161/19336918.2014.987587

Golding, N. L., and Spruston, N. (1998). Dendritic sodium spikes are variable triggers of axonal action potentials in hippocampal CA1 pyramidal neurons. *Neuron* 21, 1189–1200. doi: 10.1016/s0896-6273(00)80635-2

Gong, B., Rhodes, K. J., Bekele-Arcuri, Z., and Trimmer, J. S. (1999). Type I and type II Na^+ channel α-subunit polypeptides exhibit distinct spatial and temporal patterning, and association with auxiliary subunits in rat brain. *J. Comp. Neurol.* 412, 342–352. doi: 10.1002/(SICI)1096-9861(19990920)412:2<342::AID-CNE11>3.3.CO;2-U

Griggs, R. B., Yermakov, L. M., and Susuki, K. (2017). Formation and disruption of functional domains in myelinated CNS axons. *Neurosci. Res.* 116, 77–87. doi: 10.1016/j.neures.2016.09.010

Grubb, M. S., Shu, Y., Kuba, H., Rasband, M. N., Wimmer, V. C., and Bender, K. J. (2011). Short- and long-term plasticity at the axon initial segment. *J. Neurosci.* 31, 16049–16055. doi: 10.1523/JNEUROSCI.4064-11.2011

Gu, C., Jan, Y. N., and Jan, L. Y. (2003). A conserved domain in axonal targeting of Kv1 (Shaker) voltage-gated potassium channels. *Science* 301, 646–649. doi: 10.1126/science.1086998

Gu, C., Zhou, W., Puthenveedu, M. A., Xu, M., Jan, Y. N., and Jan, L. Y. (2006). The microtubule plus-end tracking protein EB1 is required for Kv1 voltage-gated K^+ channel axonal targeting. *Neuron* 52, 803–816. doi: 10.1016/j.neuron.2006.10.022

Guan, D., Lee, J. C. F., Tkatch, T., Surmeier, D. J., Armstrong, W. E., and Foehring, R. C. (2006). Expression and biophysical properties of Kv1 channels in supragranular neocortical pyramidal neurones. *J. Physiol.* 571, 371–389. doi: 10.1113/jphysiol.2005.097006

Hammond, R. S., Lin, L., Sidorov, M. S., Wikenheiser, A. M., and Hoffman, D. A. (2008). Protein kinase a mediates activity-dependent Kv4.2 channel trafficking. *J. Neurosci.* 28, 7513–7519. doi: 10.1523/JNEUROSCI.1951-08.2008

Häusser, M., Spruston, N., and Stuart, G. J. (2000). Diversity and dynamics of dendritic signaling. *Science* 290, 739–744. doi: 10.1126/science.290.5492.739

Hedstrom, K. L., Ogawa, Y., and Rasband, M. N. (2008). AnkyrinG is required for maintenance of the axon initial segment and neuronal polarity. *J. Cell Biol.* 183, 635–640. doi: 10.1083/jcb.200806112

Hedstrom, K. L., Xu, X., Ogawa, Y., Frischknecht, R., Seidenbecher, C. I., Shrager, P., et al. (2007). Neurofascin assembles a specialized extracellular matrix at the axon initial segment. *J. Cell Biol.* 178, 875–886. doi: 10.1083/jcb.200705119

Hien, Y. E., Montersino, A., Castets, F., Leterrier, C., Filhol, O., Vacher, H., et al. (2014). CK2 accumulation at the axon initial segment depends on sodium channel Na_v1. *FEBS Lett.* 588, 3403–3408. doi: 10.1016/j.febslet.2014.07.032

Higgs, M. H., and Spain, W. J. (2011). Kv1 channels control spike threshold dynamics and spike timing in cortical pyramidal neurones. *J. Physiol.* 589, 5125–5142. doi: 10.1113/jphysiol.2011.216721

Hildebrandt, M., Reutter, W., Arck, P., Rose, M., and Klapp, B. F. (2000). A guardian angel: the involvement of dipeptidyl peptidase IV in psychoneuroendocrine function, nutrition and immune defence. *Clin. Sci. (Lond)* 99, 93–104. doi: 10.1042/cs19990368

Hoffman, D. A., Magee, J. C., Colbert, C. M., and Johnston, D. (1997). K^+ channel regulation of signal propagation in dendrites of hippocampal pyramidal neurons. *Nature* 387, 869–875. doi: 10.1038/43119

Holmqvist, M. H., Cao, J., Hernandez-Pineda, R., Jacobson, M. D., Carroll, K. I., Sung, M. A., et al. (2002). Elimination of fast inactivation in Kv4 A-type potassium channels by an auxiliary subunit domain. *Proc. Natl. Acad. Sci. U S A* 99, 1035–1040. doi: 10.1073/pnas.022509299

Hsu, W.-C. J., Scala, F., Nenov, M. N., Wildburger, N. C., Elferink, H., Singh, A. K., et al. (2016). CK2 activity is required for the interaction of FGF14 with voltage-gated sodium channels and neuronal excitability. *FASEB J.* 30, 2171–2186. doi: 10.1096/fj.201500161

Hu, W., Tian, C., Li, T., Yang, M., Hou, H., and Shu, Y. (2009). Distinct contributions of $Na_v1.6$ and $Na_v1.2$ in action potential initiation and backpropagation. *Nat. Neurosci.* 12, 996–1002. doi: 10.1038/nn.2359

Huang, Q., Wu, Y., Wei, X., He, W., Liu, X., and Ye, J. (2014). Evolutionary analysis of voltage-gated potassium channels by Bayes method. *J. Mol. Neurosci.* 53, 41–49. doi: 10.1007/s12031-013-0192-4

Inda, M. C., DeFelipe, J., and Muñoz, A. (2006). Voltage-gated ion channels in the axon initial segment of human cortical pyramidal cells and their

relationship with chandelier cells. *Proc. Natl. Acad. Sci. U S A* 103, 2920–2925. doi: 10.1073/pnas.0511197103

Ishibashi, T., Dupree, J. L., Ikenaka, K., Hirahara, Y., Honke, K., Peles, E., et al. (2002). A myelin galactolipid, sulfatide, is essential for maintenance of ion channels on myelinated axon but not essential for initial cluster formation. *J. Neurosci.* 22, 6507–6514.

Jenkins, P. M., McIntyre, J. C., Zhang, L., Anantharam, A., Vesely, E. D., Arendt, K. L., et al. (2011). Subunit-dependent axonal trafficking of distinct α heteromeric potassium channel complexes. *J. Neurosci.* 31, 13224–13235. doi: 10.1523/JNEUROSCI.0976-11.2011

Jensen, C. S., Watanabe, S., Rasmussen, H. B., Schmitt, N., Olesen, S.-P., Frost, N. A., et al. (2014). Specific sorting and post-Golgi trafficking of dendritic potassium channels in living neurons. *J. Biol. Chem.* 289, 10566–10581. doi: 10.1074/jbc.M113.534495

Jerng, H. H., Pfaffinger, P. J., and Covarrubias, M. (2004). Molecular physiology and modulation of somatodendritic A-type potassium channels. *Mol. Cell. Neurosci.* 27, 343–369. doi: 10.1016/j.mcn.2004.06.011

Johnston, W. L., Dyer, J. R., Castellucci, V. F., and Dunn, R. J. (1996). Clustered voltage-gated Na^+ channels in Aplysia axons. *J. Neurosci.* 16, 1730–1739.

Johnston, J., Griffin, S. J., Baker, C., Skrzypiec, A., Chernova, T., and Forsythe, I. D. (2008). Initial segment Kv2.2 channels mediate a slow delayed rectifier and maintain high frequency action potential firing in medial nucleus of the trapezoid body neurons. *J. Physiol.* 586, 3493–3509. doi: 10.1113/jphysiol.2008.153734

Jones, S. L., and Svitkina, T. M. (2016). Axon initial segment cytoskeleton: architecture, development, and role in neuron polarity. *Neural Plast.* 2016:6808293. doi: 10.1155/2016/6808293

Kazarinova-Noyes, K., Malhotra, J. D., McEwen, D. P., Mattei, L. N., Berglund, E. O., Ranscht, B., et al. (2001). Contactin associates with Na^+ channels and increases their functional expression. *J. Neurosci.* 21, 7517–7525.

Kerti, K., Lorincz, A., and Nusser, Z. (2012). Unique somato-dendritic distribution pattern of Kv4.2 channels on hippocampal CA1 pyramidal cells. *Eur. J. Neurosci.* 35, 66–75. doi: 10.1111/j.1460-9568.2011.07907.x

Kim, J., and Hoffman, D. A. (2008). Potassium channels: newly found players in synaptic plasticity. *Neuroscientist* 14, 276–286. doi: 10.1177/1073858408315041

Kim, Y., Hsu, C.-L., Cembrowski, M. S., Mensh, B. D., and Spruston, N. (2015). Dendritic sodium spikes are required for long-term potentiation at distal synapses on hippocampal pyramidal neurons. *Elife* 4:06414. doi: 10.7554/eLife.06414

Kim, J., Jung, S.-C., Clemens, A. M., Petralia, R. S., and Hoffman, D. A. (2007). Regulation of dendritic excitability by activity-dependent trafficking of the A-type K^+ channel subunit Kv4.2 in hippocampal neurons. *Neuron* 54, 933–947. doi: 10.1016/j.neuron.2007.05.026

Kim, J., Nadal, M. S., Clemens, A. M., Baron, M., Jung, S.-C., Misumi, Y., et al. (2008). Kv4 accessory protein DPPX (DPP6) is a critical regulator of membrane excitability in hippocampal CA1 pyramidal neurons. *J. Neurophysiol.* 100, 1835–1847. doi: 10.1152/jn.90261.2008

Kim, J., Wei, D.-S., and Hoffman, D. A. (2005). Kv4 potassium channel subunits control action potential repolarization and frequency-dependent broadening in rat hippocampal CA1 pyramidal neurones. *J. Physiol.* 569, 41–57. doi: 10.1113/jphysiol.2005.095042

King, A. N., Manning, C. F., and Trimmer, J. S. (2014). A unique ion channel clustering domain on the axon initial segment of mammalian neurons. *J. Comp. Neurol.* 522, 2594–2608. doi: 10.1002/cne.23551

Kirizs, T., Kerti-Szigeti, K., Lorincz, A., and Nusser, Z. (2014). Distinct axo-somato-dendritic distributions of three potassium channels in CA1 hippocampal pyramidal cells. *Eur. J. Neurosci.* 39, 1771–1783. doi: 10.1111/ejn.12526

Kole, M. H. P., Letzkus, J. J., and Stuart, G. J. (2007). Axon initial segment Kv1 channels control axonal action potential waveform and synaptic efficacy. *Neuron* 55, 633–647. doi: 10.1016/j.neuron.2007.07.031

Kole, M. H. P., and Stuart, G. J. (2008). Is action potential threshold lowest in the axon? *Nat. Neurosci.* 11, 1253–1255. doi: 10.1038/nn.2203

Kruger, L. C., and Isom, L. L. (2016). Voltage-gated Na^+ channels: not just for conduction. *Cold Spring Harb. Perspect. Biol.* 8:a029264. doi: 10.1101/cshperspect.a029264

Krzemien, D. M., Schaller, K. L., Levinson, S. R., and Caldwell, J. H. (2000). Immunolocalization of sodium channel isoform NaCh6 in the nervous system. *J. Comp. Neurol.* 420, 70–83. doi: 10.1002/(SICI)1096-9861(20000424)420:1<70::AID-CNE5>3.3.CO;2-G

Kuba, H., Yamada, R., Ishiguro, G., and Adachi, R. (2015). Redistribution of Kv1 and Kv7 enhances neuronal excitability during structural axon initial segment plasticity. *Nat. Commun.* 6:8815. doi: 10.1038/ncomms9815

Lai, H. C., and Jan, L. Y. (2006). The distribution and targeting of neuronal voltage-gated ion channels. *Nat. Rev. Neurosci.* 7, 548–562. doi: 10.1038/nrn1938

Lei, Z., Deng, P., Li, J., and Xu, Z. C. (2012). Alterations of A-type potassium channels in hippocampal neurons after traumatic brain injury. *J. Neurotrauma* 29, 235–245. doi: 10.1089/neu.2010.1537

Lemaillet, G., Walker, B., and Lambert, S. (2003). Identification of a conserved ankyrin-binding motif in the family of sodium channel α subunits. *J. Biol. Chem.* 278, 27333–27339. doi: 10.1074/jbc.m303327200

Leterrier, C., Vacher, H., Fache, M.-P., d'Ortoli, S. A., Castets, F., Autillo-Touati, A., et al. (2011). End-binding proteins EB3 and EB1 link microtubules to ankyrin G in the axon initial segment. *Proc. Natl. Acad. Sci. U S A* 108, 8826–8831. doi: 10.1073/pnas.1018671108

Lewis, T. L. Jr., Mao, T., Svoboda, K., and Arnold, D. B. (2009). Myosin-dependent targeting of transmembrane proteins to neuronal dendrites. *Nat. Neurosci.* 12, 568–576. doi: 10.1038/nn.2318

Li, D., Takimoto, K., and Levitan, E. S. (2000). Surface expression of Kv1 channels is governed by a C-terminal motif. *J. Biol. Chem.* 275, 11597–11602. doi: 10.1074/jbc.275.16.11597

Lim, S. T., Antonucci, D. E., Scannevin, R. H., and Trimmer, J. S. (2000). A novel targeting signal for proximal clustering of the Kv2.1 K^+ channel in hippocampal neurons. *Neuron* 25, 385–397. doi: 10.1016/s0896-6273(00)80902-2

Lin, L., Sun, W., Kung, F., Dell'Acqua, M. L., and Hoffman, D. A. (2011). AKAP79/150 impacts intrinsic excitability of hippocampal neurons through phospho-regulation of A-type K^+ channel trafficking. *J. Neurosci.* 31, 1323–1332. doi: 10.1523/JNEUROSCI.5383-10.2011

Lindia, J. A., Köhler, M. G., Martin, W. J., and Abbadie, C. (2005). Relationship between sodium channel $Na_v1.3$ expression and neuropathic pain behavior in rats. *Pain* 117, 145–153. doi: 10.1016/j.pain.2005.05.027

Liu, H., Focia, P. J., and He, X. (2011). Homophilic adhesion mechanism of neurofascin, a member of the L1 family of neural cell adhesion molecules. *J. Biol. Chem.* 286, 797–805. doi: 10.1074/jbc.M110.180281

Liu, C., Tan, F. C. K., Xiao, Z.-C., and Dawe, G. S. (2015). Amyloid precursor protein enhances $Na_v1.6$ sodium channel cell surface expression. *J. Biol. Chem.* 290, 12048–12057. doi: 10.1074/jbc.M114.617092

Long, S. B., Campbell, E. B., and Mackinnon, R. (2005). Crystal structure of a mammalian voltage-dependent Shaker family K^+ channel. *Science* 309, 897–903. doi: 10.1126/science.1116269

Lorincz, A., and Nusser, Z. (2008). Cell-type-dependent molecular composition of the axon initial segment. *J. Neurosci.* 28, 14329–14340. doi: 10.1523/JNEUROSCI.4833-08.2008

Lorincz, A., and Nusser, Z. (2010). Molecular identity of dendritic voltage-gated sodium channels. *Science* 328, 906–909. doi: 10.1126/science.1187958

Losonczy, A., and Magee, J. C. (2006). Integrative properties of radial oblique dendrites in hippocampal CA1 pyramidal neurons. *Neuron* 50, 291–307. doi: 10.1016/j.neuron.2006.03.016

Losonczy, A., Makara, J. K., and Magee, J. C. (2008). Compartmentalized dendritic plasticity and input feature storage in neurons. *Nature* 452, 436–441. doi: 10.1038/nature06725

Lugo, J. N., Barnwell, L. F., Ren, Y., Lee, W. L., Johnston, L. D., Kim, R., et al. (2008). Altered phosphorylation and localization of the A-type channel, Kv4.2 in status epilepticus. *J. Neurochem.* 106, 1929–1940. doi: 10.1111/j.1471-4159.2008.05508.x

Lugo, J. N., Brewster, A. L., Spencer, C. M., and Anderson, A. E. (2012). Kv4.2 knockout mice have hippocampal-dependent learning and memory deficits. *Learn. Mem.* 19, 182–189. doi: 10.1101/lm.023614.111

Luján, R. (2010). Organisation of potassium channels on the neuronal surface. *J. Chem. Neuroanat.* 40, 1–20. doi: 10.1016/j.jchemneu.2010.03.003

Magee, J. C., and Johnston, D. (2005). Plasticity of dendritic function. *Curr. Opin. Neurobiol.* 15, 334–342. doi: 10.1016/j.conb.2005.05.013

Manganas, L. N., and Trimmer, J. S. (2000). Subunit composition determines Kv1 potassium channel surface expression. *J. Biol. Chem.* 275, 29685–29693. doi: 10.1074/jbc.M005010200

Manganas, L. N., Wang, Q., Scannevin, R. H., Antonucci, D. E., Rhodes, K. J., and Trimmer, J. S. (2001). Identification of a trafficking determinant localized to the Kv1 potassium channel pore. *Proc. Natl. Acad. Sci. U S A* 98, 14055–14059. doi: 10.1073/pnas.241403898

Mantegazza, M., Curia, G., Biagini, G., Ragsdale, D. S., and Avoli, M. (2010). Voltage-gated sodium channels as therapeutic targets in epilepsy and other neurological disorders. *Lancet Neurol.* 9, 413–424. doi: 10.1016/S1474-4422(10)70059-4

Mauro, V. P., Krushel, L. A., Cunningham, B. A., and Edelman, G. M. (1992). Homophilic and heterophilic binding activities of Nr-CAM, a nervous system cell adhesion molecule. *J. Cell Biol.* 119, 191–202. doi: 10.1083/jcb.119.1.191

McEwen, D. P., and Isom, L. L. (2004). Heterophilic interactions of sodium channel β1 subunits with axonal and glial cell adhesion molecules. *J. Biol. Chem.* 279, 52744–52752. doi: 10.1074/jbc.M405990200

Misonou, H., Menegola, M., Mohapatra, D. P., Guy, L. K., Park, K.-S., and Trimmer, J. S. (2006). Bidirectional activity-dependent regulation of neuronal ion channel phosphorylation. *J. Neurosci.* 26, 13505–13514. doi: 10.1523/JNEUROSCI.3970-06.2006

Misonou, H., Mohapatra, D. P., Menegola, M., and Trimmer, J. S. (2005a). Calcium- and metabolic state-dependent modulation of the voltage-dependent Kv2.1 channel regulates neuronal excitability in response to ischemia. *J. Neurosci.* 25, 11184–11193. doi: 10.1523/JNEUROSCI.3370-05.2005

Misonou, H., Mohapatra, D. P., and Trimmer, J. S. (2005b). Kv2.1: a voltage-gated k^+ channel critical to dynamic control of neuronal excitability. *Neurotoxicology* 26, 743–752. doi: 10.1016/j.neuro.2005.02.003

Misonou, H., Mohapatra, D. P., Park, E. W., Leung, V., Zhen, D., Misonou, K., et al. (2004). Regulation of ion channel localization and phosphorylation by neuronal activity. *Nat. Neurosci.* 7, 711–718. doi: 10.1038/nn1260

Misonou, H., Thompson, S. M., and Cai, X. (2008). Dynamic regulation of the Kv2.1 voltage-gated potassium channel during brain ischemia through neuroglial interaction. *J. Neurosci.* 28, 8529–8538. doi: 10.1523/JNEUROSCI.1417-08.2008

Mohapatra, D. P., Siino, D. F., and Trimmer, J. S. (2008). Interdomain cytoplasmic interactions govern the intracellular trafficking, gating, and modulation of the Kv2.1 channel. *J. Neurosci.* 28, 4982–4994. doi: 10.1523/JNEUROSCI.0186-08.2008

Monaghan, M. M., Menegola, M., Vacher, H., Rhodes, K. J., and Trimmer, J. S. (2008). Altered expression and localization of hippocampal A-type potassium channel subunits in the pilocarpine-induced model of temporal lobe epilepsy. *Neuroscience* 156, 550–562. doi: 10.1016/j.neuroscience.2008.07.057

Murakoshi, H., and Trimmer, J. S. (1999). Identification of the Kv2.1 K^+ channel as a major component of the delayed rectifier K^+ current in rat hippocampal neurons. *J. Neurosci.* 19, 1728–1735.

Nadal, M. S., Ozaita, A., Amarillo, Y., Vega-Saenz de Miera, E., Ma, Y., Mo, W., et al. (2003). The CD26-related dipeptidyl aminopeptidase-like protein DPPX is a critical component of neuronal A-type K^+ channels. *Neuron* 37, 449–461. doi: 10.1016/s0896-6273(02)01185-6

Nagaya, N., and Papazian, D. M. (1997). Potassium channel α and β subunits assemble in the endoplasmic reticulum. *J. Biol. Chem.* 272, 3022–3027. doi: 10.1074/jbc.272.5.3022

Namadurai, S., Yereddi, N. R., Cusdin, F. S., Huang, C. L. H., Chirgadze, D. Y., and Jackson, A. P. (2015). A new look at sodium channel β subunits. *Open Biol.* 5:140192. doi: 10.1098/rsob.140192

Narayanan, R., and Johnston, D. (2012). Functional maps within a single neuron. *J. Neurophysiol.* 108, 2343–2351. doi: 10.1152/jn.00530.2012

Neishabouri, A., and Faisal, A. A. (2014). Saltatory conduction in unmyelinated axons: clustering of Na^+ channels on lipid rafts enables micro-saltatory conduction in C-fibers. *Front. Neuroanat.* 8:109. doi: 10.3389/fnana.2014.00109

Nestor, M. W., and Hoffman, D. A. (2012). Differential cycling rates of Kv4.2 channels in proximal and distal dendrites of hippocampal CA1 pyramidal neurons. *Hippocampus* 22, 969–980. doi: 10.1002/hipo.20899

Normand, E. A., and Rasband, M. N. (2015). Subcellular patterning: axonal domains with specialized structure and function. *Dev. Cell* 32, 459–468. doi: 10.1016/j.devcel.2015.01.017

Nusser, Z. (2012). Differential subcellular distribution of ion channels and the diversity of neuronal function. *Curr. Opin. Neurobiol.* 22, 366–371. doi: 10.1016/j.conb.2011.10.006

O'Connell, K. M. S., Loftus, R., and Tamkun, M. M. (2010). Localization-dependent activity of the Kv2.1 delayed-rectifier K^+ channel. *Proc. Natl. Acad. Sci. U S A* 107, 12351–12356. doi: 10.1073/pnas.1003028107

O'Connell, K. M. S., Rolig, A. S., Whitesell, J. D., and Tamkun, M. M. (2006). Kv2.1 potassium channels are retained within dynamic cell surface microdomains that are defined by a perimeter fence. *J. Neurosci.* 26, 9609–9618. doi: 10.1523/JNEUROSCI.1825-06.2006

Ogawa, Y., Oses-Prieto, J., Kim, M. Y., Horresh, I., Peles, E., Burlingame, A. L., et al. (2010). ADAM22, a Kv1 channel-interacting protein, recruits membrane-associated guanylate kinases to juxtaparanodes of myelinated axons. *J. Neurosci.* 30, 1038–1048. doi: 10.1523/JNEUROSCI.4661-09.2010

Ogawa, Y., and Rasband, M. N. (2008). The functional organization and assembly of the axon initial segment. *Curr. Opin. Neurobiol.* 18, 307–313. doi: 10.1016/j.conb.2008.08.008

Ogiwara, I., Miyamoto, H., Morita, N., Atapour, N., Mazaki, E., Inoue, I., et al. (2007). $Na_v1.1$ localizes to axons of parvalbumin-positive inhibitory interneurons: a circuit basis for epileptic seizures in mice carrying an Scn1a gene mutation. *J. Neurosci.* 27, 5903–5914. doi: 10.1523/JNEUROSCI.5270-06.2007

O'Malley, H. A., and Isom, L. L. (2015). Sodium channel β subunits: emerging targets in channelopathies. *Annu. Rev. Physiol.* 77, 481–504. doi: 10.1146/annurev-physiol-021014-071846

Pablo, J. L., Wang, C., Presby, M. M., and Pitt, G. S. (2016). Polarized localization of voltage-gated Na^+ channels is regulated by concerted FGF13 and FGF14 action. *Proc. Natl. Acad. Sci. U S A* 113, E2665–2674. doi: 10.1073/pnas.1521194113

Patino, G. A., and Isom, L. L. (2010). Electrophysiology and beyond: multiple roles of Na^+ channel β subunits in development and disease. *Neurosci. Lett.* 486, 53–59. doi: 10.1016/j.neulet.2010.06.050

Peltola, M. A., Kuja-Panula, J., Lauri, S. E., Taira, T., and Rauvala, H. (2011). AMIGO is an auxiliary subunit of the Kv2.1 potassium channel. *EMBO Rep.* 12, 1293–1299. doi: 10.1038/embor.2011.204

Peltola, M. A., Kuja-Panula, J., Liuhanen, J., Võikar, V., Piepponen, P., Hiekkalinna, T., et al. (2016). AMIGO-Kv2.1 potassium channel complex is associated with schizophrenia-related phenotypes. *Schizophr. Bull.* 42, 191–201. doi: 10.1093/schbul/sbv105

Piepgras, J., Höltje, M., Michel, K., Li, Q., Otto, C., Drenckhahn, C., et al. (2015). Anti-DPPX encephalitis. *Neurology* 85, 890–897. doi: 10.1212/WNL.0000000000001907

Poliak, S., Salomon, D., Elhanany, H., Sabanay, H., Kiernan, B., Pevny, L., et al. (2003). Juxtaparanodal clustering of Shaker-like K^+ channels in myelinated axons depends on Caspr2 and TAG-1. *J. Cell Biol.* 162, 1149–1160. doi: 10.1083/jcb.200305018

Pongs, O., and Schwarz, J. R. (2010). Ancillary subunits associated with voltage-dependent K^+ channels. *Physiol. Rev.* 90, 755–796. doi: 10.1152/physrev.00020.2009

Puthussery, T., Venkataramani, S., Gayet-Primo, J., Smith, R. G., and Taylor, W. R. (2013). $Na_v1.1$ channels in axon initial segments of bipolar cells augment input to magnocellular visual pathways in the primate retina. *J. Neurosci.* 33, 16045–16059. doi: 10.1523/JNEUROSCI.1249-13.2013

Ramakrishnan, N. A., Drescher, M. J., and Drescher, D. G. (2012). The SNARE complex in neuronal and sensory cells. *Mol. Cell. Neurosci.* 50, 58–69. doi: 10.1016/j.mcn.2012.03.009

Rasband, M. N., Park, E. W., Vanderah, T. W., Lai, J., Porreca, F., and Trimmer, J. S. (2001). Distinct potassium channels on pain-sensing neurons. *Proc. Natl. Acad. Sci. U S A* 98, 13373–13378. doi: 10.1073/pnas.231376298

Ratcliffe, C. F., Westenbroek, R. E., Curtis, R., and Catterall, W. A. (2001). Sodium channel β1 and β3 subunits associate with neurofascin through their extracellular immunoglobulin-like domain. *J. Cell Biol.* 154, 427–434. doi: 10.1083/jcb.200102086

Remy, S., Beck, H., and Yaari, Y. (2010). Plasticity of voltage-gated ion channels in pyramidal cell dendrites. *Curr. Opin. Neurobiol.* 20, 503–509. doi: 10.1016/j.conb.2010.06.006

Ren, X., Hayashi, Y., Yoshimura, N., and Takimoto, K. (2005). Transmembrane interaction mediates complex formation between peptidase homologues and

Kv4 channels. *Mol. Cell. Neurosci.* 29, 320–332. doi: 10.1016/j.mcn.2005.02.003

Rhodes, K. J., Carroll, K. I., Sung, M. A., Doliveira, L. C., Monaghan, M. M., Burke, S. L., et al. (2004). KChIPs and Kv4 α subunits as integral components of A-type potassium channels in mammalian brain. *J. Neurosci.* 24, 7903–7915. doi: 10.1523/JNEUROSCI.0776-04.2004

Rios, J. C., Rubin, M., St Martin, M., Downey, R. T., Einheber, S., Rosenbluth, J., et al. (2003). Paranodal interactions regulate expression of sodium channel subtypes and provide a diffusion barrier for the node of Ranvier. *J. Neurosci.* 23, 7001–7011.

Rivera, J. F., Ahmad, S., Quick, M. W., Liman, E. R., and Arnold, D. B. (2003). An evolutionarily conserved dileucine motif in Shal K^+ channels mediates dendritic targeting. *Nat. Neurosci.* 6, 243–250. doi: 10.1038/nn0803-899a

Rivera, J., Chu, P.-J., Lewis, T. L. Jr., and Arnold, D. B. (2007). The role of Kif5B in axonal localization of Kv1 K^+ channels. *Eur. J. Neurosci.* 25, 136–146. doi: 10.1111/j.1460-9568.2006.05277.x

Rush, A. M., Dib-Hajj, S. D., and Waxman, S. G. (2005). Electrophysiological properties of two axonal sodium channels, $Na_v1.2$ and $Na_v1.6$, expressed in mouse spinal sensory neurones. *J. Physiol.* 564, 803–815. doi: 10.1113/jphysiol.2005.083089

Sarmiere, P. D., Weigle, C. M., and Tamkun, M. M. (2008). The Kv2.1 K^+ channel targets to the axon initial segment of hippocampal and cortical neurons in culture and *in situ*. *BMC Neurosci.* 9:112. doi: 10.1186/1471-2202-9-112

Savio-Galimberti, E., Gollob, M. H., and Darbar, D. (2012). Voltage-gated sodium channels: biophysics, pharmacology, and related channelopathies. *Front. Pharmacol.* 3:124. doi: 10.3389/fphar.2012.00124

Scannevin, R. H., Murakoshi, H., Rhodes, K. J., and Trimmer, J. S. (1996). Identification of a cytoplasmic domain important in the polarized expression and clustering of the Kv2.1 K^+ channel. *J. Cell Biol.* 135, 1619–1632. doi: 10.1083/jcb.135.6.1619

Schrader, L. A., Ren, Y., Cheng, F., Bui, D., Sweatt, J. D., and Anderson, A. E. (2009). Kv4.2 is a locus for PKC and ERK/MAPK cross-talk. *Biochem. J.* 417, 705–715. doi: 10.1042/BJ20081213

Segev, I., and Rall, W. (1998). Excitable dendrites and spines: earlier theoretical insights elucidate recent direct observations. *Trends Neurosci.* 21, 453–460. doi: 10.1016/s0166-2236(98)01327-7

Shah, N. H., and Aizenman, E. (2014). Voltage-gated potassium channels at the crossroads of neuronal function, ischemic tolerance, and neurodegeneration. *Transl. Stroke Res.* 5, 38–58. doi: 10.1007/s12975-013-0297-7

Shavkunov, A. S., Wildburger, N. C., Nenov, M. N., James, T. F., Buzhdygan, T. P., Panova-Elektronova, N. I., et al. (2013). The fibroblast growth factor 14·voltage-gated sodium channel complex is a new target of glycogen synthase kinase 3 (GSK3). *J. Biol. Chem.* 288, 19370–19385. doi: 10.1074/jbc.M112.445924

Shi, G., Nakahira, K., Hammond, S., Rhodes, K. J., Schechter, L. E., and Trimmer, J. S. (1996). β subunits promote K^+ channel surface expression through effects early in biosynthesis. *Neuron* 16, 843–852. doi: 10.1016/s0896-6273(00)80104-x

Shibata, R., Misonou, H., Campomanes, C. R., Anderson, A. E., Schrader, L. A., Doliveira, L. C., et al. (2003). A fundamental role for KChIPs in determining the molecular properties and trafficking of Kv4.2 potassium channels. *J. Biol. Chem.* 278, 36445–36454. doi: 10.1074/jbc.M306142200

Smith, K. J. (2007). Sodium channels and multiple sclerosis: roles in symptom production, damage and therapy. *Brain Pathol.* 17, 230–242. doi: 10.1111/j.1750-3639.2007.00066.x

Spruston, N. (2008). Pyramidal neurons: dendritic structure and synaptic integration. *Nat. Rev. Neurosci.* 9, 206–221. doi: 10.1038/nrn2286

Srinivasan, J., Schachner, M., and Catterall, W. A. (1998). Interaction of voltage-gated sodium channels with the extracellular matrix molecules tenascin-C and tenascin-R. *Proc. Natl. Acad. Sci. U S A* 95, 15753–15757. doi: 10.1073/pnas.95.26.15753

Stuart, G. J., and Spruston, N. (2015). Dendritic integration: 60 years of progress. *Nat. Neurosci.* 18, 1713–1721. doi: 10.1038/nn.4157

Su, T., Cong, W. D., Long, Y. S., Luo, A. H., Sun, W. W., Deng, W. Y., et al. (2008). Altered expression of voltage-gated potassium channel 4.2 and voltage-gated potassium channel 4-interacting protein, and changes in intracellular calcium levels following lithium-pilocarpine-induced status epilepticus. *Neuroscience* 157, 566–576. doi: 10.1016/j.neuroscience.2008.09.027

Su, Y.-Y., Ye, M., Li, L., Liu, C., Pan, J., Liu, W.-W., et al. (2013). KIF5B promotes the forward transport and axonal function of the voltage-gated sodium channel $Na_v1.8$. *J. Neurosci.* 33, 17884–17896. doi: 10.1523/JNEUROSCI.0539-13.2013

Südhof, T. C. (2013). Neurotransmitter release: the last millisecond in the life of a synaptic vesicle. *Neuron* 80, 675–690. doi: 10.1016/j.neuron.2013.10.022

Sun, W., Maffie, J. K., Lin, L., Petralia, R. S., Rudy, B., and Hoffman, D. A. (2011). DPP6 establishes the A-Type K^+ current gradient critical for the regulation of dendritic excitability in CA1 hippocampal neurons. *Neuron* 71, 1102–1115. doi: 10.1016/j.neuron.2011.08.008

Sun, Q., Srinivas, K. V., Sotayo, A., and Siegelbaum, S. A. (2014). Dendritic Na^+ spikes enable cortical input to drive action potential output from hippocampal CA2 pyramidal neurons. *Elife* 3:04551. doi: 10.7554/eLife.04551

Susuki, K., and Kuba, H. (2016). Activity-dependent regulation of excitable axonal domains. *J. Physiol. Sci.* 66, 99–104. doi: 10.1007/s12576-015-0413-4

Takigawa, T., and Alzheimer, C. (2003). Interplay between activation of GIRK current and deactivation of I_h modifies temporal integration of excitatory input in CA1 pyramidal cells. *J. Neurophysiol.* 89, 2238–2244. doi: 10.1152/jn.00957.2002

Tamkun, M. M., O'connell, K. M. S., and Rolig, A. S. (2007). A cytoskeletal-based perimeter fence selectively corrals a sub-population of cell surface Kv2.1 channels. *J. Cell Sci.* 120, 2413–2423. doi: 10.1242/jcs.007351

Tian, C., Wang, K., Ke, W., Guo, H., and Shu, Y. (2014). Molecular identity of axonal sodium channels in human cortical pyramidal cells. *Front. Cell. Neurosci.* 8:297. doi: 10.3389/fncel.2014.00297

Tiffany, A. M., Manganas, L. N., Kim, E., Hsueh, Y. P., Sheng, M., and Trimmer, J. S. (2000). PSD-95 and SAP97 exhibit distinct mechanisms for regulating K^+ channel surface expression and clustering. *J. Cell Biol.* 148, 147–158. doi: 10.1083/jcb.148.1.147

Traka, M., Goutebroze, L., Denisenko, N., Bessa, M., Nifli, A., Havaki, S., et al. (2003). Association of TAG-1 with Caspr2 is essential for the molecular organization of juxtaparanodal regions of myelinated fibers. *J. Cell Biol.* 162, 1161–1172. doi: 10.1083/jcb.200305078

Trimmer, J. S. (1991). Immunological identification and characterization of a delayed rectifier K^+ channel polypeptide in rat brain. *Proc. Natl. Acad. Sci. U S A* 88, 10764–10768. doi: 10.1073/pnas.88.23.10764

Trimmer, J. S. (2015). Subcellular localization of K^+ channels in mammalian brain neurons: remarkable precision in the midst of extraordinary complexity. *Neuron* 85, 238–256. doi: 10.1016/j.neuron.2014.12.042

Trimmer, J. S., and Rhodes, K. J. (2004). Localization of voltage-gated ion channels in mammalian brain. *Annu. Rev. Physiol.* 66, 477–519. doi: 10.1146/annurev.physiol.66.032102.113328

Truchet, B., Manrique, C., Sreng, L., Chaillan, F. A., Roman, F. S., and Mourre, C. (2012). Kv4 potassium channels modulate hippocampal EPSP-spike potentiation and spatial memory in rats. *Learn. Mem.* 19, 282–293. doi: 10.1101/lm.025411.111

Vacher, H., Mohapatra, D. P., and Trimmer, J. S. (2008). Localization and targeting of voltage-dependent ion channels in mammalian central neurons. *Physiol. Rev.* 88, 1407–1447. doi: 10.1152/physrev.00002.2008

Vacher, H., and Trimmer, J. S. (2012). Trafficking mechanisms underlying neuronal voltage-gated ion channel localization at the axon initial segment. *Epilepsia* 53, 21–31. doi: 10.1111/epi.12032

Vacher, H., Yang, J.-W., Cerda, O., Autillo-Touati, A., Dargent, B., and Trimmer, J. S. (2011). Cdk-mediated phosphorylation of the Kvβ2 auxiliary subunit regulates Kv1 channel axonal targeting. *J. Cell Biol.* 192, 813–824. doi: 10.1083/jcb.201007113

Van Wart, A., Trimmer, J. S., and Matthews, G. (2007). Polarized distribution of ion channels within microdomains of the axon initial segment. *J. Comp. Neurol.* 500, 339–352. doi: 10.1002/cne.21173

van Welie, I., van Hooft, J. A., and Wadman, W. J. (2004). Homeostatic scaling of neuronal excitability by synaptic modulation of somatic hyperpolarization-activated Ih channels. *Proc. Natl. Acad. Sci. U S A* 101, 5123–5128. doi: 10.1073/pnas.0307711101

Vardjan, N., Jorgacevski, J., and Zorec, R. (2013). Fusion pores, SNAREs, and exocytosis. *Neuroscientist* 19, 160–174. doi: 10.1177/1073858412461691

Varga, A. W., Anderson, A. E., Adams, J. P., Vogel, H., and Sweatt, J. D. (2000). Input-specific immunolocalization of differentially phosphorylated Kv4.2 in the mouse brain. *J. Neurosci.* 7, 321–332.

Varga, A. W., Yuan, L.-L., Anderson, A. E., Schrader, L. A., Wu, G.-Y., Gatchel, J. R., et al. (2004). Calcium-calmodulin-dependent kinase II modulates Kv4.2 channel expression and upregulates neuronal A-type potassium currents. *J. Neurosci.* 24, 3643–3654. doi: 10.1523/JNEUROSCI.0154-04.2004

Vernon, J., Irvine, E. E., Peters, M., Jeyabalan, J., and Giese, K. P. (2016). Phosphorylation of K^+ channels at single residues regulates memory formation. *Learn. Mem.* 23, 174–181. doi: 10.1101/lm.040816.115

Villa, C., and Combi, R. (2016). Potassium channels and human epileptic phenotypes: an updated overview. *Front. Cell. Neurosci.* 10:81. doi: 10.3389/fncel.2016.00081

Watanabe, S., Hoffman, D. A., Migliore, M., and Johnston, D. (2002). Dendritic K^+ channels contribute to spike-timing dependent long-term potentiation in hippocampal pyramidal neurons. *Proc. Natl. Acad. Sci. U S A* 99, 8366–8371. doi: 10.1073/pnas.122210599

Weber, J. P., Andrásfalvy, B. K., Polito, M., Magó, Á., Ujfalussy, B. B., and Makara, J. K. (2016). Location-dependent synaptic plasticity rules by dendritic spine cooperativity. *Nat. Commun.* 7:11380. doi: 10.1038/ncomms11380

Westenbroek, R. E., Merrick, D. K., and Catterall, W. A. (1989). Differential subcellular localization of the R_I and R_{II} Na^+ channel subtypes in central neurons. *Neuron* 3, 695–704. doi: 10.1016/0896-6273(89)90238-9

Wimmer, V. C., Reid, C. A., So, E. Y.-W., Berkovic, S. F., and Petrou, S. (2010). Axon initial segment dysfunction in epilepsy. *J. Physiol.* 588, 1829–1840. doi: 10.1113/jphysiol.2010.188417

Wu, L., Nishiyama, K., Hollyfield, J. G., and Wang, Q. (2002). Localization of $Na_v1.5$ sodium channel protein in the mouse brain. *Neuroreport* 13, 2547–2551. doi: 10.1097/00001756-200212200-00033

Xu, M., Gu, Y., Barry, J., and Gu, C. (2010). Kinesin I transports tetramerized Kv3 channels through the axon initial segment via direct binding. *J. Neurosci.* 30, 15987–16001. doi: 10.1523/JNEUROSCI.3565-10.2010

Yamada, R., and Kuba, H. (2016). Structural and Functional plasticity at the axon initial segment. *Front. Cell. Neurosci.* 10:250. doi: 10.3389/fncel.2016.00250

Zagha, E., Ozaita, A., Chang, S. Y., Nadal, M. S., Lin, U., Saganich, M. J., et al. (2005). DPP10 modulates Kv4-mediated A-type potassium channels. *J. Biol. Chem.* 280, 18853–18861. doi: 10.1074/jbc.M410613200

Zeng, S., and Tang, Y. (2009). Effect of clustered ion channels along an unmyelinated axon. *Phys. Rev. E Stat. Nonlin. Soft Matter Phys.* 80:021917. doi: 10.1103/physreve.80.021917

Conflict of Interest Statement: The authors declare that the research was conducted in the absence of any commercial or financial relationships that could be construed as a potential conflict of interest.

Advantages of publishing in Frontiers

OPEN ACCESS
Articles are free to read for greatest visibility and readership

FAST PUBLICATION
Around 90 days from submission to decision

HIGH QUALITY PEER-REVIEW
Rigorous, collaborative, and constructive peer-review

TRANSPARENT PEER-REVIEW
Editors and reviewers acknowledged by name on published articles

Frontiers
Avenue du Tribunal-Fédéral 34
1005 Lausanne | Switzerland

Visit us: www.frontiersin.org
Contact us: info@frontiersin.org | +41 21 510 17 00

REPRODUCIBILITY OF RESEARCH
Support open data and methods to enhance research reproducibility

DIGITAL PUBLISHING
Articles designed for optimal readership across devices

FOLLOW US
@frontiersin

IMPACT METRICS
Advanced article metrics track visibility across digital media

EXTENSIVE PROMOTION
Marketing and promotion of impactful research

LOOP RESEARCH NETWORK
Our network increases your article's readership